

University of St Andrews



Full metadata for this thesis is available in
St Andrews Research Repository
at:

<http://research-repository.st-andrews.ac.uk/>

This thesis is protected by original copyright

" A STUDY OF ION-
MOLECULE REACTIONS IN THE
GAS PHASE USING A TRIPLE
QUADRUPOLE MASS SPECTROMETER
AND A QUINQUA QUADRUPOLE
MASS SPECTROMETER. "

A THESIS SUBMITTED BY

GEORGE STEWART WALKER

FOR THE DEGREE OF Ph. D.
AT THE UNIVERSITY OF ST ANDREWS
JANUARY 1989



MASS SPECTROMETER. II
AND A QUINODA QUADRUPOLE
QUADRUPOLE MASS SPECTROMETER
GAS BEAM USING A TRIPLE
MOLECULAR BEAMS IN THE
A STUDY OF ION-

A PARIS CENTER IN

GEORGE STEWART WALLER

TH 1884

FOR THE DEGREE OF PH.D.
AT THE UNIVERSITY OF CALIFORNIA
JANUARY 1984



DECLARATION

I, George Stewart Walker, hereby certify that this thesis has been composed by myself, that it is a record of my own work, and that it has not been accepted in partial or complete fulfilment of any other degree or professional qualification.

Signed *G Stewart Walker*

Date *12/1/89*

I was admitted to the Faculty of Science of the University of St Andrews under Ordinance General No 12 on 9th October 1979 and as a candidate for the degree of Ph.D. on 1st October 1985.

Signed

Date 12/1/89...

DECLARATION

I hereby certify that the candidate has
fulfilled the conditions of the Resolution and
Regulations appropriate to the Degree of Ph.D.

Signature of Supervisor

Date 12/1/89....

In submitting this thesis to the University of St Andrews I understand that I am giving permission for it to be made available for use in accordance with the regulations of the University Library for the time being in force, subject to any copyright vested in the work not being affected thereby. I also understand that the title and abstract will be published, and that a copy of the work may be made and supplied to any bona fide library or research worker.

ACKNOWLEDGEMENTS

I am indebted to Professor The Lord Tedder for all his advice and encouragement throughout the duration of my research under his supervision. I wish to thank Professor D. Cole-Hamilton and Professor J.M Tedder for allowing me to use the facilities of the chemistry department. I am also indebted to the S.E.R.C. and B.P. Research for funding this work.

I would like to thank the people who have helped in this project. Mr. J. Rennie, Chief Technician, and Mr. J. Ward, Chief Electrician, have been invaluable to the successful development of the quinquapole mass spectrometer. Mr. C. Smith the glass blower who has built a technically difficult, but aesthetically pleasing, gas line for the quinquapole mass spectrometer.

I am indebted to Dr. S.R. Wade, my industrial supervisor, for his guidance and encouragement and I wish to thank him and all others, including Mrs. Smith, who made my time at B.P. Research so stimulating and fruitful.

I would like to thank Françoise van Tiggelin, an undergraduate student from Belgium, who spent one month

working on the reaction of methyl cations with chloromethane - and Jane Hollis, undergraduate student from St. Andrews, for her synthesis of fluoromethane that was used in the subsequent investigations.

I would like to thank my mother, and chemistry teacher, and father for encouraging me to develop my interest in science.

Mere words can not convey my thanks to my wife, Adele, who has been my support and companion.

CONTENTS

DECLARATIONS	i - iv
ACKNOWLEDGEMENTS	v - vi
TITLE PAGE	
CONTENTS PAGE	1 - 3
ABSTRACT	4
INTRODUCTION AND LITERATURE REVIEW	5 - 21
CHAPTER ONE :- EXPERIMENTAL CHAPTER	22 - 42
THE TRIPLE QUADRUPOLE MASS SPECTROMETER AND THE QUINQUA QUADRUPOLE MASS SPECTROMETER	
CHAPTER TWO :- PROTONATION OF ALKANES.	
LITERATURE REVIEW	43 - 67
RESULTS	68 - 97
DISCUSSION	98 - 142

CHAPTER THREE :- INVESTIGATION OF THE MECHANISMS

INVOLVED IN MOBIL'S

METHANOL-TO-GASOLINE REACTION.

LITERATURE REVIEW	143 - 160
RESULTS	161 - 176
DISCUSSION	177 - 218

REACTIONS OF METHANOL AND

DIMETHYL ETHER. FORMATION OF

METHYL OXONIUM, DIMETHYL OXONIUM

AND TRIMETHYL OXONIUM IONS.

REACTIONS OF HIGHER ALCOHOLS.

FORMATION OF HYDROGEN BRIDGED ADDUCTS.

DIRECT INVESTIGATIONS OF MECHANISMS

PROPOSED IN THE LITERATURE.

CHAPTER FOUR :- REACTIONS OF HALOGENOMETHANES.

LITERATURE REVIEW	219 - 232
RESULTS	233 - 265
DISCUSSION	266 - 291

FORMATION OF METHYL HALONIUM

AND DIMETHYL HALONIUM IONS.

COMPARISON OF REACTIONS OF CH_3X WHERE $\text{X} = \text{OH}, \text{Cl}, \text{F}, \text{Br}$ AND I .

CHAPTER FIVE :- SYNTHESIS OF ZSM-5 CATALYST	292 - 328
REACTIONS OF CH ₃ Cl, C ₂ H ₅ Cl AND CH ₃ Br IN A SMALL SCALE FIXED-BED REACTOR.	
OVERALL DISCUSSION AND CONCLUSIONS FROM CHAPTERS THREE, FOUR AND FIVE.	329 - 338
CHAPTER SIX :- THE CONSTRUCTION AND COMMISSIONING OF A QUINQUA QUADRUPOLE MASS SPECTROMETER.	339 - 405
APPENDIX A :- PHOTOGRAPHS OF THE QUINQUA QUADRUPOLE MASS SPECTROMETER.	406 - 410
APPENDIX B :- INDEX OF TABLES, FIGURES, GRAPHS AND DIAGRAMS.	411 - 415
REFERENCES.	416 - 431

ABSTRACT

The triple quadrupole mass spectrometer was used to study the reactions of ions and molecules in the gas phase. Two specific areas of research were investigated. The first involved the reaction of various protonating ions with methane, ethane, propane, n-butane, iso-butane, n-pentane, iso-pentane and neo-pentane. The alkonium ions, $C_nH_{2n+3}^+$, were observed for $n=1,2$ and 3 . The alkonium ions of $n>3$ were too unstable to be observed under the experimental conditions but their formation was deduced by consideration of the fragmentation patterns that were obtained. The second area involved investigations into the gas phase reactions of methanol and the halogenomethanes. This was undertaken in an attempt to investigate the reaction mechanisms that might be operating in the production of hydrocarbons from methanol or a halogenomethane over ZSM-5 catalyst as pioneered by Mobil. This work was coupled with investigations carried out at B.P. Research Centre, London, using a small scale fixed-bed reactor. A unifying mechanism was produced that could account for the reactions of all CH_3X over ZSM-5, where $X= OH, F, Cl, Br$ and I .

The quinquadrupole mass spectrometer was set up and commissioned to allow the work on sequential ion/molecule reactions to be extended. The results reported were relevant to each section of the research on the triple quadrupole mass spectrometer .

INTRODUCTION

INTRODUCTION

The work presented in this thesis covers three areas of research. An introduction and literature review will be presented at the start of each section. A general introduction and review of the study of ion-molecule reactions in mass spectrometers is presented here.

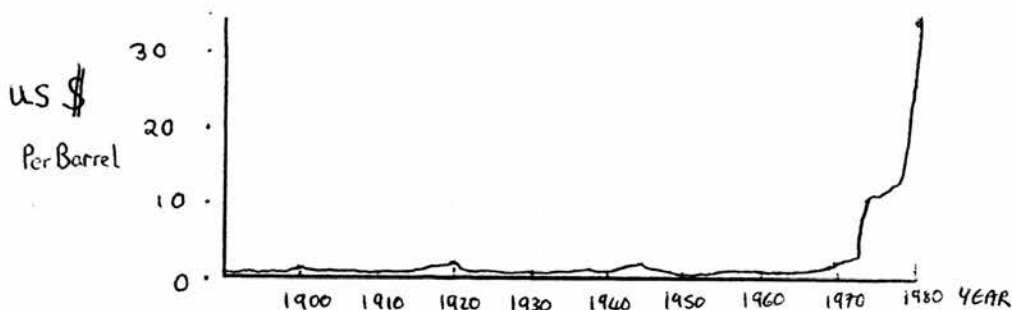
The first area concerns the protonation of alkanes, the detection of $C_nH_{2n+3}^+$ ions and the fragmentation patterns produced by these ions. This is covered in chapter two.

The second area deals with an investigation of the reactions of ions from methanol with methanol and ions from halogenomethanes with halogenomethanes as an attempt to investigate the mechanisms involved in the formation of hydrocarbons in the reaction of methanol or halogenomethanes over ZSM-5, and other, catalysts. This includes work carried out at B.P. Research Centre, Sunbury-on-Thames, London as part of a CASE Scholarship. This work is contained in chapters three, four and five. The work reported in chapters two to five was carried out in the first two years of research.

The third area involved the construction and commissioning of a quinquapole mass spectrometer

with a view to extending the work reported in chapters two to five. This represents one and a half years' work and is reported in chapter six.

The research can be put into context by considering the extent of research on alternative means of hydrocarbon production between 1973 and the present day. Graph 1, reproduced from reference 1, indicates the dramatic increase in oil prices from 1973.



With the increase in oil prices it is even more important that catalytic cracking of heavy oil should be efficient. To this end a thorough understanding of the mechanisms involved in the process are required. The work reported in chapter two was initially concerned with investigating a proposed mechanism of catalytic cracking. After the oil embargo of 1973 much research was initiated into alternative methods of producing hydrocarbons. The most successful of these was the Mobil methanol-to-gasoline, MTG, process developed by Chang and Silvestri.² A further increase in oil prices in 1979, as a result of the drop in oil production caused by the Iranian Revolution, increased the demand for alternative sources. In 1979 Mobil and the New Zealand Government signed an

agreement whereby a full scale commercial plant would be built to convert natural gas from the Maui gas field to gasoline in a fixed-bed reactor.³ The natural gas would be converted to methanol, by the ICI low pressure process,^{4,5} and thence into gasoline to provide one third of New Zealand's consumption.

A fluid-bed reactor was designed and scaled up to a full scale industrial plant in West Germany by Mobil, Uhde GmbH, Union Rheinische Braunkohlen Kraftstoff AG and the U.S. and German governments.⁶ In 1987 this plant was reported to be ready for full scale operation.

Much research was done in this period to investigate the mechanisms operating in the MTG process. A review of the research done to 1983 was published by Chang.⁷ A more detailed discussion of the previous work will be presented in the introduction to chapters three to five.

It was with this background that the present work reported in chapters three to five was started.



However, as graph 2 shows, the cost of oil has fallen since this research was started to such an extent that research of this nature is no longer of such immediate priority to industrial concerns. A high

proportion of papers that have appeared in the recent literature are written in Russian and Chinese. This is indicative of the continued importance that these countries place on developing these processes and the lessening of interest in other countries. Russia has enormous gas reserves - 43% of the world's known reserves. A large proportion of this gas is in remote unpopulated regions of the USSR where the demand for gas is minimal. If this gas could be converted into gasoline it could then be transported to regions of higher demand with greater ease than the transportation of gas.

In New Zealand the Maui full scale plant went into production in 1986 converting 155,000m³/h of natural gas to 4400t/d of methanol. The methanol is converted into 1665t/d of gasoline. This is equivalent to 0.57 million tonnes per annum - one seventh of New Zealand's consumption of oil in 1986. Because of the fall in world oil prices the gasoline produced in this way is not economically viable, but as the New Zealand government was committed to buying the gas from the gas field and it was surplus to needs, the plant is still in operation.

The short term prospects for the development of the MTG process are limited because of economic constraints to the plant in New Zealand that is operational and developments in countries where because of particular factors - such as Russia and South Africa - the production of indigenous gasoline is desired.

The long term prospects for the MTG process depend on the fluctuations in oil prices and in the eventual

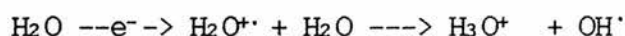
need for an alternative feedstock when oil reserves are exhausted. On consideration of the consumption of oil to the end of 1986 BP¹ calculate that oil will last for another 33 years at present rates of consumption.

Natural gas reserves would last for 59 years. Methanol can be obtained from renewable sources - fermentation of bio-matter⁸ or from the reaction of carbon monoxide, carbon dioxide and hydrogen over palladium catalysts for example.⁹ The long term prospects for the MTG process are good, and so further investigations of the mechanisms of the reactions are warranted.

LITERATURE REVIEW - THE STUDY OF ION-MOLECULE REACTIONS
IN MASS SPECTROMETERS

LITERATURE REVIEW - THE STUDY OF ION-MOLECULE REACTIONS
IN MASS SPECTROMETERS

Ion molecule reactions have been observed in the ionisation chamber of mass spectrometers since the early days of mass spectrometry. Ions are produced by electron-bombardment of gas molecules ¹⁰ in the ionisation chamber. At high pressures the ions can collide and react with neutral molecules of the same species. An example of this was given in the formation of H₃O⁺ ions from the electron bombardment of water. ¹¹



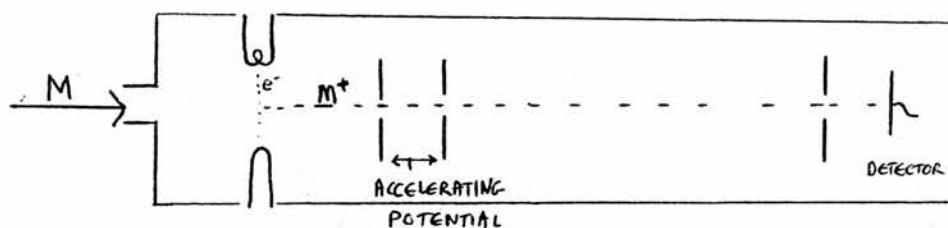
The reaction of methane ions with methane has been extensively studied using a high pressure ion source leading into a conventional magnetic sector mass spectrometer.¹²

By putting a mixture of molecules into the ionisation chamber of a mass spectrometer the study of ion-molecule reactions between ions of one compound and neutrals of a different compound could be studied. This crude technique was utilized by Munson and Field to investigate the reactions of CH₅⁺ and C₂H₅⁺ ions with a variety of other molecules.¹³

TIME-OF-FLIGHT MASS SPECTROMETRY

The pulsed time-of-flight mass spectrometer ^{14,15} separates ions of different mass to charge ratio on the basis of the different velocities of ions under the influence of an accelerating voltage. Gaseous molecules

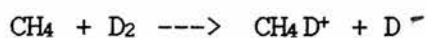
are ionised by a pulse of electrons and then accelerated into a drift tube by a pulsed voltage. In the drift tube the ions are accelerated to uniform kinetic energy between two plates. As $k.e. = \frac{1}{2}mv^2$ and all ions have the same kinetic energy then $v_n = (2k.e./m_n)^{\frac{1}{2}}$ the velocity of an ion n is inversely proportional to the square root of its mass to charge ratio. A detector at the far end of a field-free flight tube detects the arrival of the different ions at different times. As the difference in the time of arrival of successive peaks is very short - of the order of 10^{-7} s - many advances in the detectors and analysers have been made.¹⁶



Ion-molecule reactions have been studied using time-of-flight mass spectrometers.^{17,18,19} The advantages that this system has over other mass spectrometers are :-

- the reactions are occurring in a field free region
- the velocity of the ions can be adjusted and
- the ability to measure and alter time as a variable makes the system ideal for the study of reaction kinetics.

Using a time-of-flight mass spectrometer the reaction of methane with deuterium was observed.¹⁷



ION CYCLOTRON RESONANCE MASS SPECTROMETRY

Ion cyclotron resonance mass spectrometers operate on the basis of the cyclotron resonance frequency, ω_c , of ions which is independent of the velocity of the ions.²⁰

$$\omega_c = \frac{B}{m/e}$$

where ω_c is the cyclotron resonance frequency, B is the magnetic field, and m/e is the mass to charge ratio of the ions. Ions are formed by electron bombardment at one end of a uniform magnetic field. The application of a small electric field perpendicular to the magnetic field makes the ions drift down the system into the resonance cell. The resonance cell has an alternating electric field applied perpendicular to the magnetic field. When the frequency of the alternating field, ω_a , is equal to the resonance frequency of an ion then the ion absorbs energy. The absorption of energy alters the Q-factor of the oscillator and the detection of this produces a signal for each value of mass to charge ratio. The other ions reach a detector at the extreme end of the tube and are detected to give the total ion current. By adjusting the values of the various fields the ions can be retained in the chamber for long periods of time and therefore given long path lengths. This makes the ion cyclotron resonance mass spectrometer ideally suited to the study of ion-molecule reactions.²¹ Other techniques, such as double resonance²² and pulsing techniques²³ have enabled I.C.R. mass spectrometers to be used for the identification of reaction sequences, evaluation of thermodynamic data, energy dependence of rate constants

and determination of ion structure.

TANDEM MASS SPECTROMETERS

Tandem mass spectrometers have two mass spectrometers - the first one to select an ion - a reaction chamber into which the neutral gas to be reacted can be injected - and a second mass spectrometer to analyse the ions produced in the reaction of the ion with the neutral molecule.^{24,25,26} A tandem mass spectrometer, that has been used in the department in St. Andrews, is represented in figure 1.

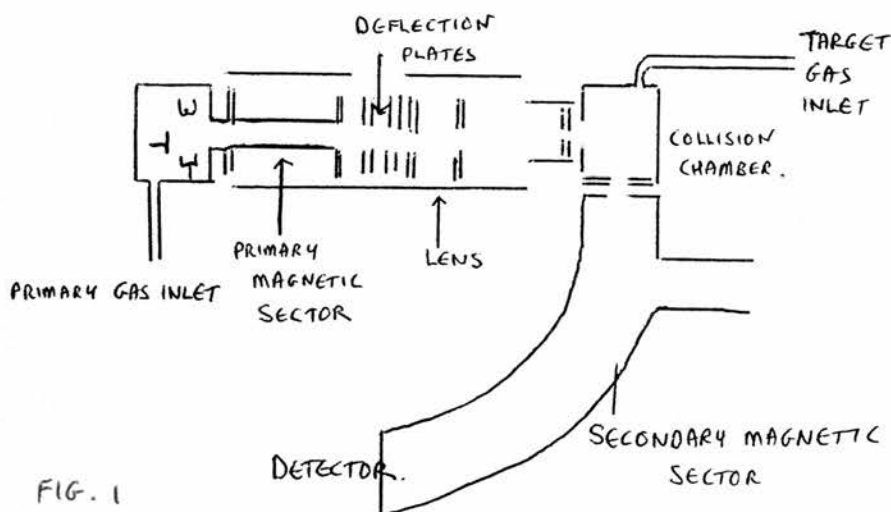
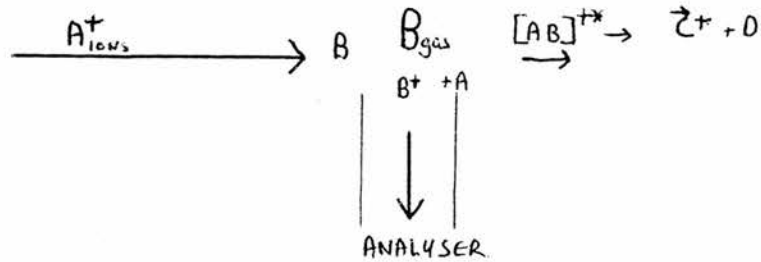


FIG. 1

As a result of the geometry of this system the analysing mass spectrometer tended to favour the detection of charge exchange products over the products of ion-molecule reactions. The primary ions had velocity perpendicular to the axis of the analysing mass spectrometer. In an ion-molecule reaction that involves a collision and the formation of an addition complex the product ions would have momentum that would take them out of the area within which the second mass spectrometer

would attract them. Ions formed by a simple charge transfer reaction, especially if electron tunnelling had occurred, would not have momentum to take them out of the catchment area of the second mass spectrometer.

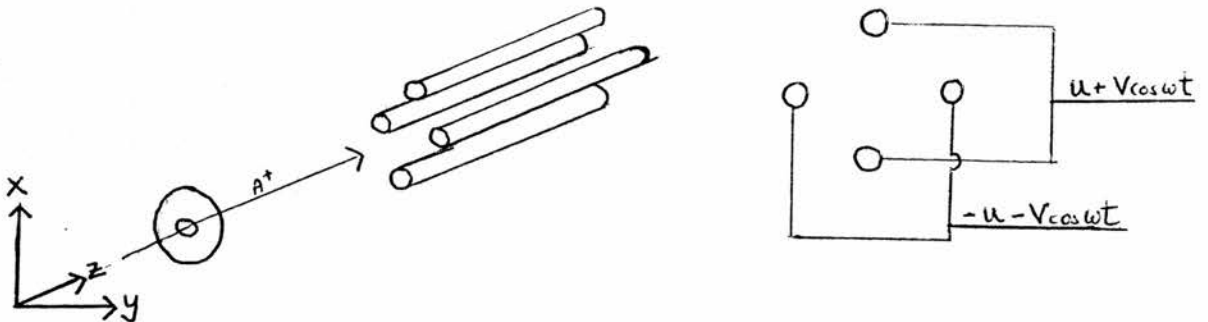


The tandem mass spectrometer has been used to study charge exchange reactions. 27-35

QUADRUPOLE MASS SPECTROMETERS

THE QUADRUPOLE

The quadrupole mass filter was first proposed by W. Paul and M. Reather in 1953.^{36,37} Ions are formed in an ion source and repelled through a series of plates into the quadrupole. The quadrupole consists of four hyperbolic rods which are precisely parallel to each other.



It has been found that circular rods can also be used. A direct current voltage U and an oscillating radio frequency voltage V are applied to opposite pairs of rods. One pair of rods has a combined voltage $U + V\cos\omega t$. The other pair has a voltage of $-U - V\cos\omega t$. The mathematics that describes the behaviour of ions under the influence of the fields in the quadrupole are very complex. For a full description refer to references.³⁸⁻⁴¹ Very much simplified the equations describing the motion in the three axis z - in the axis down the centre of the rods and x and y perpendicular to the centre of the rods - can be expressed as :-

$$m \frac{d^2 x}{dt^2} = eE_x = - \frac{2e}{r^2} (U + V\cos\omega t) x$$

$$m \frac{d^2 y}{dt^2} = eE_y = - \frac{2e}{r^2} (U + V\cos\omega t) y$$

$$m \frac{d^2 z}{dt^2} = eE_z = 0$$

where r_0 = the field radius = half the distance between a pair of rods.

ω = frequency of the R.F. signal

The ions describe a complex trajectory through the rods. For one value of U and V and ω only one mass of ion will have a stable trajectory that allows it to get to the end of the rods without hitting the rods or going through the gaps between rods. If the D.C. to R.F. ratio is retained constant whilst the voltages are increased ions of successively higher mass to charge ratio will get

to the end of the quadrupole. If a detector is placed at the end of the rods a spectrum can be obtained in this way. Under these conditions the quadrupole is operating as a mass analyser. If the voltages were set so that only one ion was allowed to pass through the rods the quadrupole would be operating as a mass filter. If the quadrupole is only given a R.F. voltage all ions will have a stable trajectory and will pass through the quadrupole. This is described as Total Ion Mode. This diversity of operation modes enables the quadrupole mass spectrometer to be utilized in multiple quadrupole mass spectrometers.

The disadvantages of quadrupole mass spectrometers are :

- they have only a limited mass range in which the ions are stable - this has been increased in recent years.
- they do not resolve ions at the higher mass end of the range as efficiently as those of lower mass. This leads to artificial enhancement of low mass to charge ions.

The advantages of a quadrupole mass spectrometer are

- it can scan very fast in comparison to a magnetic field mass spectrometer where fast scanning causes perturbations of the field.⁴²

- it is very compact - the rods are between 0.1 and 0.3 metres long - and they have no magnets.
- they do not discriminate ions by their energy but purely by their mass to charge ratio.

They have therefore found a diversity of uses in G.C.M.S., mobile and compact M.S.⁴³ and G.C.M.S.⁴⁴ - as

in experiments in the space shuttle⁴⁵ - and in multiple mass spectrometers where having large magnetic sectors at 90° angles to each other would be a disadvantage.

TRIPLE QUADRUPOLE MASS SPECTROMETERS

The triple quadrupole mass spectrometer consists of three quadrupole mass spectrometers in series. Ions are formed by electron bombardment in the ionisation chamber and repelled into the first quadrupole. This is operated as a mass filter to select one mass of ion. These ions are fed into the second quadrupole which is operated on radio frequency only to allow all ions to pass through into the third quadrupole. A target molecule can be allowed to flow into the second quadrupole which acts as a reaction chamber. The ions produced in the reaction of the primary ion with the neutral molecule are separated by the third quadrupole which operates as a mass analyser. The ions are detected and a spectrum recorded on a chart recorder.

The advantages of a multiple quadrupole system are that the gases in the source and in the reaction chamber can be kept apart by physical barriers and differential pumping. Unlike time-of-flight and ion cyclotron resonance mass spectrometers where all the ions are present the triple quadrupole mass spectrometer is totally selective and only ions of one mass to charge ratio are present in the reaction chamber. There is therefore more scope for investigating the reactions of specific ions with a different molecule. This was

utilized in the work to be reported to investigate the reaction pathways of ion-molecule reactions using isotopically labelled primary ions or neutral molecules in the knowledge that there would be no mixing of the gases in the system.

Many studies of ion-molecule reactions have been done using triple quadrupole mass spectrometers.⁴⁶⁻⁵⁵

Ion trapping techniques have been reported for a triple quadrupole mass spectrometer.⁵⁶

QUINQUA QUADRUPOLE MASS SPECTROMETER

The quinquadrupole mass spectrometer has been developed as a logical extension to the triple quadrupole. It will be discussed in detail in Chapters One and Six. No publications on the developments of quinquadrupole mass spectrometers by other researchers have been found.

OTHER TECHNIQUES

Various other techniques have been reported. They include Fourier-transform mass spectrometry⁵⁷, laser photofragmentation⁵⁸, molecular beam techniques⁵⁹, photoionization⁶⁰, hybrid magnet/quadrupole mass spectrometry⁶¹, radiolysis⁶², monopole mass spectrometry⁶³ and electrostatic octopole focusing of a quadrupole mass spectrometer⁶⁴.

General reviews of interest for more than one of the above sections are to be found in references 65 to 70.

The properties of the multiple quadrupole mass spectrometers make them ideally suited to investigations of reaction mechanisms in the gas phase. Previous work at this department has shown that ions can be separated in the first quadrupole and fired into a neutral gas in the second quadrupole. The ions produced in the reaction of this ion with the neutral can be detected by scanning the third quadrupole.⁴⁶⁻⁵³ It was the intention of this research to utilize this feature of the triple quadrupole mass spectrometer and to advance the technique on the quinquadrupole mass spectrometer to investigate the mechanisms of the reactions involved in the catalytic cracking of hydrocarbons and the production of hydrocarbons from methanol or halogenomethanes.

CHAPTER ONE

EXPERIMENTAL CHAPTER

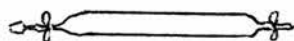
CHAPTER ONEEXPERIMENTAL CHAPTERSAMPLE PREPARATION

The method employed in preparing samples of chemicals was the same for both mass spectrometers.

GASEOUS SAMPLES

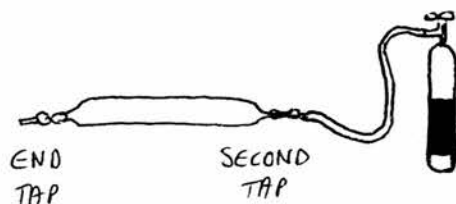
Gaseous samples were introduced into the mass spectrometer by means of glass tubes which were filled with gas and connected by means of a greased quickfit sintered glass coupling. This was done in a fume cupboard whenever possible and on all occasions when a noxious gas was used.

Gas tubes were of various volumes. For the triple quadrupole mass spectrometer the tubes were not interchangeable. The primary gas tube was 480mm long and 44mm³ in volume. The target gas tube was 300mm long and had a volume of 21mm³. The tubes for the quinquadrupole mass spectrometer were interchangeable and had the following dimensions:- length = 301mm and volume = 30mm³ , length = 310mm and volume = 29mm³ and length = 400mm and volume = 80mm³.



Gas bottles were fitted with a regulator valve to which a piece of rubber tubing was attached. The other end of the

tubing was placed over the other end of the gas tube.



The taps on the gas tube were opened. Gas was allowed to flow through the tube flushing out the air that was in it. Simultaneously, the end tap on the gas tube and the gas flow regulator were closed. The second tap on the gas tube was closed to seal the tube. The tube was disconnected from the gas bottle. The connector was greased and placed on the glass line at the appropriate point. The air that was trapped between the last tap on the glass line and the tap of the glass tube was pumped away.

When the whole glass line was re-evacuated that section of the line was disconnected from the pumps. The first tap of the glass tube was opened allowing the sample gas to flow through the section of the glass line up to the mass spectrometer inlet valve.

LIQUID SAMPLES

Small amounts - 1mm^3 of liquid were placed in a tube or a small round bottomed flask with an appropriate quickfit connector. The connector was greased and connected to the appropriate part of the glass line.

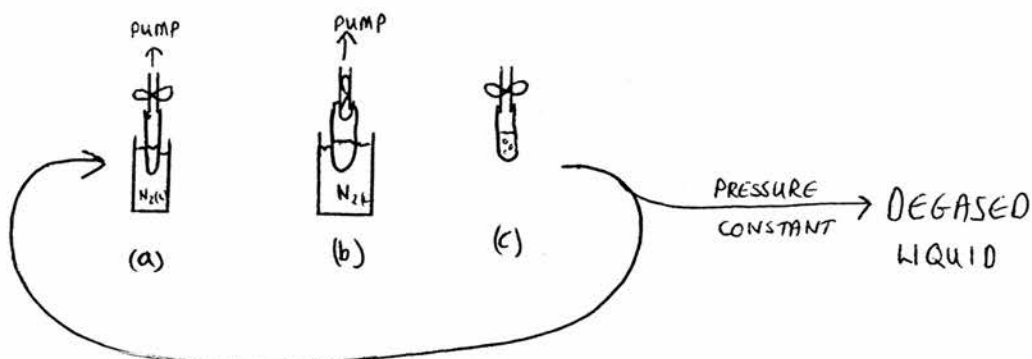
(a) The liquid sample was frozen by placing a dewar of liquid nitrogen round it.

(b) When the liquid was frozen the tap connecting the tube

to the glass line was opened allowing the air to be pumped out.

(c) The tap was shut and the liquid allowed to thaw.

Bubbles of trapped gas escaped from the thawing liquid.

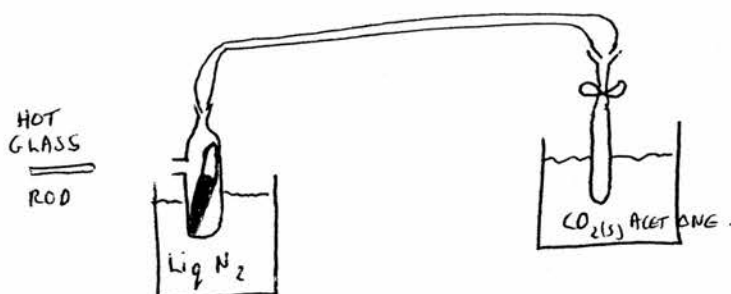


The liquid was refrozen (a). The tap was opened to pump away the released gas (b). This degassing process was repeated until the pressure remained constant - indicating that no further gas was being released from the liquid. The liquid was then allowed to thaw. If the liquid was slow to thaw the tube could be heated by hand or with a small hair dryer.

The two exceptions to this general pattern were for bromomethane liquid and gaseous samples contained within 1 litre glass containers such as quadruply deuterated methane and the noble gases Neon and Xenon. The flasks had a built-in glass sampling tube. The flask was connected to the line and the connector pumped out. A sample of gas was let into the sampler tube by opening tap 2 with tap 1 closed. This sample of gas was then allowed into the glass line by closing tap 2 and opening tap 1.



Because bromomethane has a boiling point of 5°C and its vapour is caustic ⁷¹ special handling techniques were adopted. Bromomethane was contained within a sealed vial. The vial was scratched with a glass cutter and placed inside a specially built glass tube with an opening on the side.



The tube containing the bromomethane vial was frozen in liquid nitrogen and connected through a glass line to a glass tube with a tap. This was all contained within a fume cupboard. A hot tipped glass rod was inserted into the opening at the side so that the vial cracked. The glass rod was withdrawn and the opening sealed up as quickly as possible. The liquid nitrogen was removed from around the bromomethane to allow it to vaporize. Bromomethane vapour evaporated from the first tube and was seen to condense in the second tube which was cooled in acetone and solid CO_2 . When it was thought that all the bromomethane in the connecting tube had been condensed the tap on the second tube was closed and it was disconnected from the connecting tube. The second tube was fitted to the glass line of the

triple quadrupole mass spectrometer and degassed in the same way as described above. When the experiments with bromomethane were completed the bromomethane was frozen in the second tube and the tube was heated and sealed. Throughout these operations thick rubber gloves were worn.

REAGENTS

All gases and liquids used were commercially available as indicated in the list, with the exception of fluoromethane, which was prepared by Jane Hollis using the method of Kamm and Marvel ⁷². All gases and liquids were used without further purification.

GASES

MONO METHYLAMINE	99 %	BDH (AIR PRODUCTS LIMITED)
METHANE	ULTRA HIGH PURITY	UCAR (UNION CARBIDE)
ETHANE	99%	BDH (AIR PRODUCTS LIMITED)
ETHENE	99 %	B.O.C.
PROPANE	99.5%	BDH (AIR PRODUCTS LIMITED)
n-BUTANE	99 %	BDH (AIR PRODUCTS LIMITED)
ISOBUTANE	99 %	BDH (AIR PRODUCTS LIMITED)
PENTANE	99 %	BDH (AIR PRODUCTS LIMITED)
ISOPENTANE	99 %	BDH (AIR PRODUCTS LIMITED)
NEOPENTANE	99 %	BDH (AIR PRODUCTS LIMITED)
DIMETHYL ETHER	UNKNOWN PURITY	B.O.C.
CHLOROMETHANE	99.8 %	BDH (AIR PRODUCTS LIMITED)
IODOMETHANE	UNKNOWN PURITY	UNKNOWN SOURCE
NEON	C.P. GRADE	B.O.C.
ARGON	99.997%	BDH (AIR PRODUCTS LIMITED)
NITROUS OXIDE	ZERO GRADE	UNKNOWN SOURCE

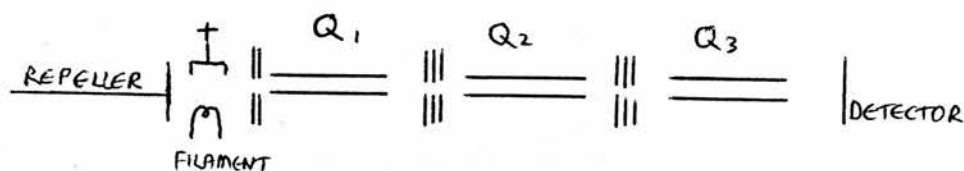
LIQUIDS

METHANOL	> 99 %	KOCH-LIGHT LABORATORIES.
D ₄ -METHANOL	99.5% D	ALDRICH CHEMICAL CO.
ETHANOL	-	LABORATORY REAGENT
DI-ISO-PROPYL ETHER	-	BDH
PROPAN-2-OL	-	LABORATORY REAGENT
BROMOMETHANE	-	FISONS LABORATORY REAGENT

THE TRIPLE QUADRUPOLE MASS SPECTROMETER

The triple quadrupole mass spectrometer used in the present work was built from the component parts of three V.G. Micromass mass spectrometers. It was constructed in this department with the assistance of a representative of V.G. Micromass.⁴⁸ It is portrayed in figures 1.1 and 1.2.

The triple quadrupole mass spectrometer comprises of three sets of quadrupole rods in series. Between each set of rods are placed lens and focus plates.



A standard tungsten filament produces electrons which are attracted across the ionisation chamber by a positively charged plate on the opposite side. The energy of the electrons is governed by the charge on the positive plate.

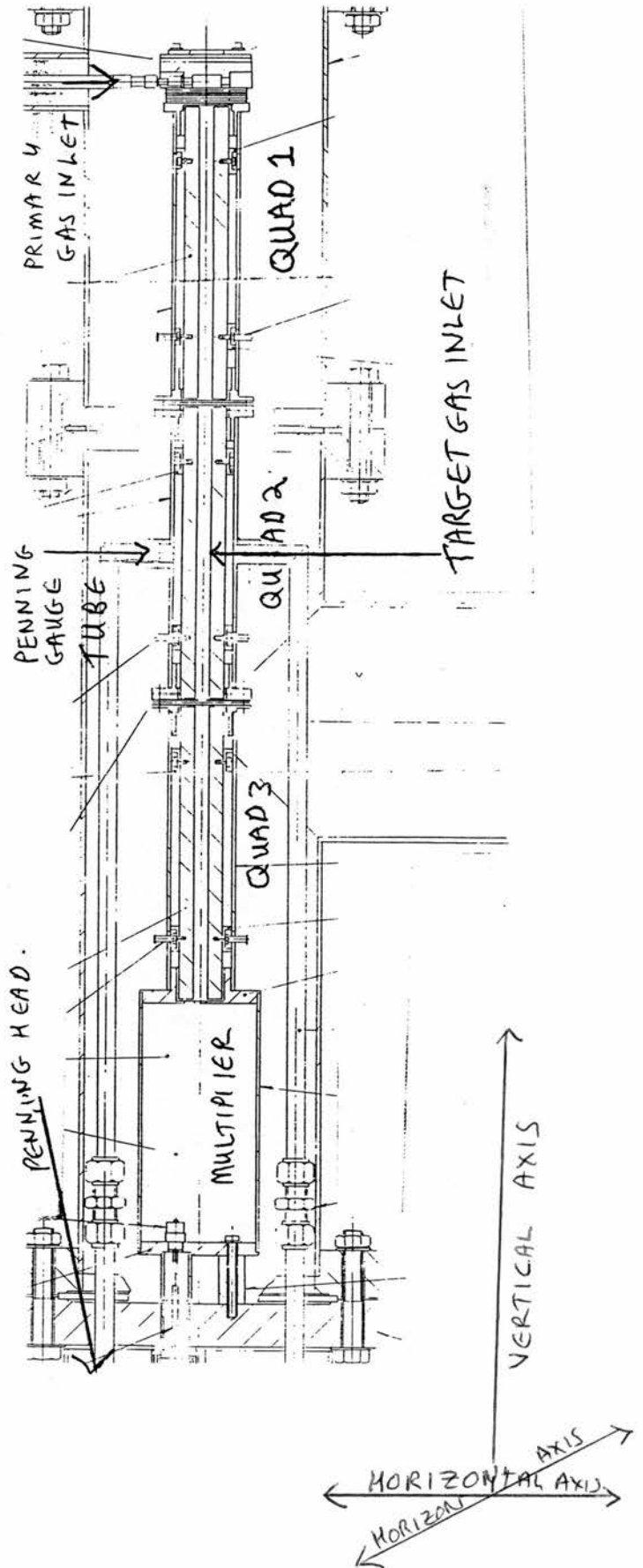
The primary gas is bled into the ionisation chamber at a 90° angle to the axis of the quadrupoles.

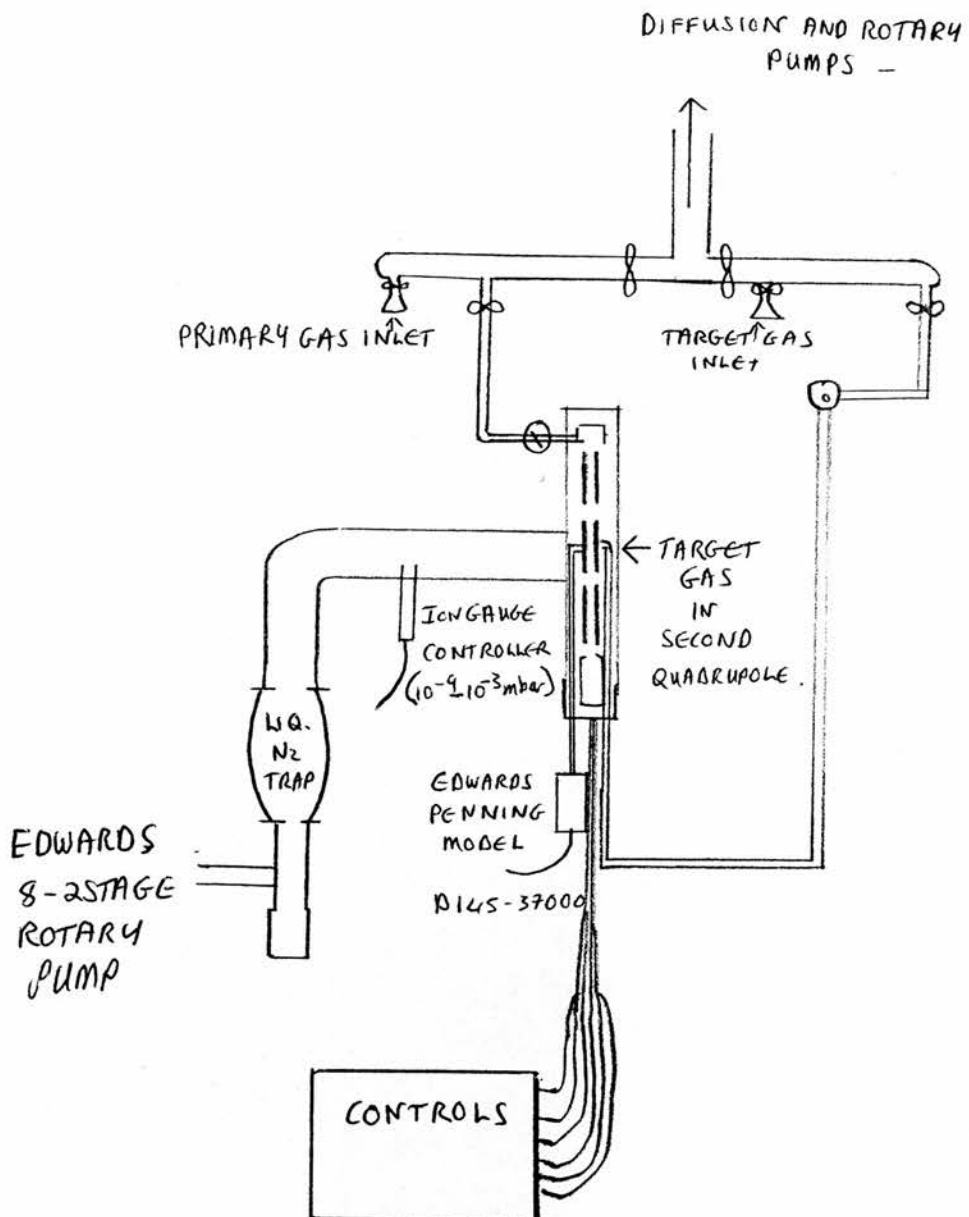
Ions formed by electron bombardment are driven into the first quadrupole by the differential pressure between the ionisation chamber and the quadrupoles and by the repeller plate to which is applied a positive voltage.

51

INTERIOR OF TRIPLE QUADRUPOLE
MASS SPECTROMETER

FIG. 1.1





CONTROLS, PUMPS AND GAS-LINE
FOR THE TRIPLE QUADRUPOLE
MASS SPECTROMETER.

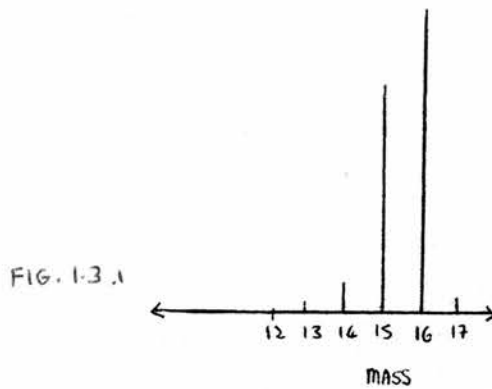
FIG. 1-2

OPERATION

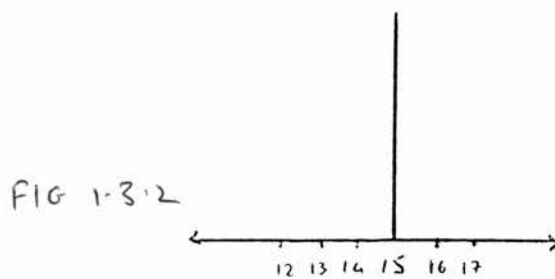
The first quadrupole was operated as a mass analyser. The second and third quadrupoles operated on R.F. signal only, which maintained all ions to pass through to the detector.

Operating in this way a mass spectrum of the ions in the first quadrupole could be obtained by scanning the first quadrupole.

For example an automatic scan of methane would produce a spectrum as in figure 1.3.1

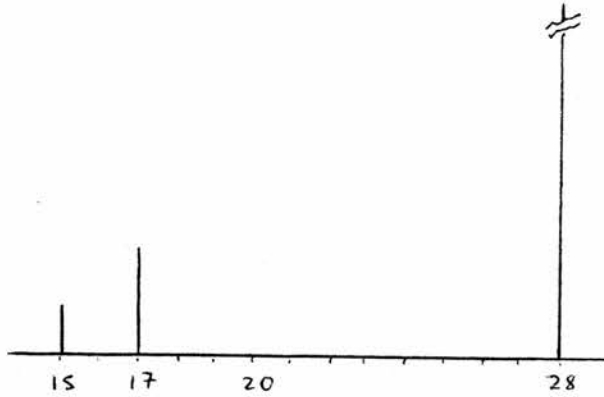


The first quadrupole was then set to manual scan and the mass adjusted until it was in line with the top of the peak of the ion to be selected. This could be monitored on the chart recorder or the oscilloscope. The first quadrupole was now acting as a mass filter and only allowing ions of one mass through to the second quadrupole. By putting the third quadrupole to mass and scanning it, the size and purity of the ion from quadrupole one could be monitored.



A target gas was now admitted into the second quadrupole mass spectrometer at a pressure of around 1×10^{-5} torr. The third quadrupole was scanned with the detector current at 10^{-9} A to detect any secondary ions present. For example, if the primary ion was CH_2N^+ and the secondary gas was methane, the secondary ions produced would be CH_5^+ and CH_3^+ .

FIG. 1-3-3



If the peak for the primary ion was too high for the chart recorder, then it could be reduced by increasing the current amplitude.

The pressure of target gas was increased stepwise and the spectrum re-run. The relative amounts of secondary ions at various pressures could be obtained. At higher pressures the secondary ions reacted with the target gas to produce tertiary ions.

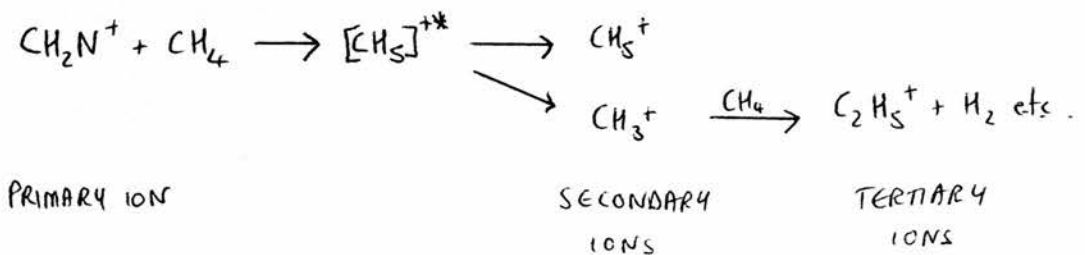


FIG 1-3-4

PRESSURE MEASUREMENT

The pressure of gas in the quadrupoles was measured by two gauges. An ionisation gauge was positioned in the outlet from the casing to the diffusion pump. This gauge gave a reading of the pressure in this region of the mass spectrometer when the primary gas had been introduced. This is recorded in the tables of data as Initial Ion Gauge Pressure. A Penning Head was positioned outside the casing with a long thin metal tube going into the casing and pointing into the centre of the second quadrupole. As a consequence of being directly opposite the inlet for the target gas this gauge was more sensitive to the pressure of target gas than to the pressure of the primary gas. When target gas was admitted to the quadrupoles the pressure reading on both gauges increased. These readings are recorded in the tables of data as Ion Gauge Pressure and Penning Pressure. When graphs of ion abundance against pressure were plotted it was the Penning Pressure that was used for the x-axis as it gave a better indication of the change in the target gas pressure.

The ionisation gauge was not close enough to give an accurate reading of the pressure in the second quadrupole. The penning head was also quite far away and connected by a thin tube which would reduce the accuracy of the pressure reading. Although neither of these pressure measuring devices gave an accurate reading of the pressure in the reaction region they did give the change in pressure within an experiment.

An attempt to rectify this problem was made when the quinquadrupole mass spectrometer was built by placing three penning heads directly above the quadrupoles so that the pressure in the immediate vicinity of the quadrupoles could be measured. This caused different problems as will be discussed in chapter six.

The pressure measurements indicated in the tables of data are best regarded as an indication of the relative pressures.

DATA

The amount of each ion was measured by measuring the peak height, the current and the voltage on the chart recorder.

$$[\text{CH}_3^+] = \text{Peak Height} \times \text{Current} \times \text{Voltage}$$

for example = 10 x 3 x 10⁻⁹ x 1 = [3x10⁻⁸]

$$[\text{CH}_5^+] = \text{Peak Height} \times \text{Current} \times \text{Voltage}$$

 = 20 x 3 x 10⁻⁹ x 1 = [6x10⁻⁸]

$$[\text{CH}_2\text{N}^+] = \text{Peak Height} \times \text{Current} \times \text{Voltage}$$

 = 100 x 1 x 10⁻⁷ x 1 = [1x10⁻⁵]

The percentage of each ions as a fraction of the total amount of ions was calculated.

$$\% \text{ Total Ion flux CH}_5^+ = \left(\frac{[\text{CH}_5^+]}{[\text{CH}_3^+] + [\text{CH}_5^+] + [\text{CH}_2\text{N}^+]} \right) \times 100$$

$$\% \text{ Total Ion flux CH}_3^+ = \left(\frac{[\text{CH}_3^+]}{\text{Total Ion flux}} \right) \times 100$$

In General :-

$$\% \text{ Total Ion flux for Ion X} = \left(\frac{\text{Flux of Ion X}}{\text{Total Ion Flux}} \right) \times 100$$

The percentage of Ion Flux for each secondary ion as a percentage of the total amount of product ions was calculated from the general equation.

% Secondary Ion flux for Ion X =

$$\left(\frac{\text{Flux of Ion X}}{\text{Total Flux of all secondary ions}} \right) \times 100$$

The results from a series of scans at increasing pressures of target gas were calculated and tabulated using programmes written specifically for this purpose.

The percentage of each secondary ion was tabulated at each set of pressures.

% SECONDARY ION FLUX

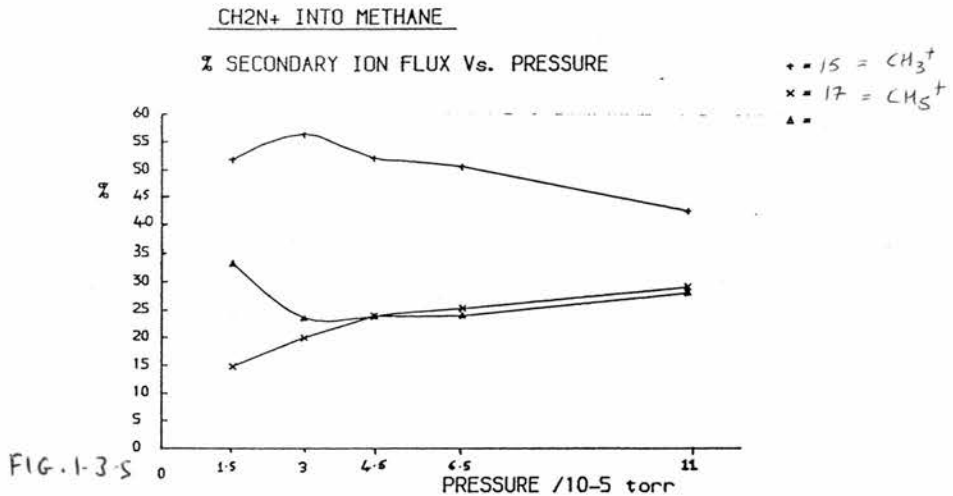
	PRESSURES in torr			m/e		
	INITIAL ION	ION	PENNING	15	17	29
	GAUGE	GAUGE	GAUGE			
(A)	7.5x10 ⁻⁷	1.5x10 ⁻⁶	1.5x10 ⁻⁵	51.85	14.81	33.33
(B)	7.5x10 ⁻⁷	2.3x10 ⁻⁶	3.0x10 ⁻⁵	56.36	20.00	23.64
(C)	7.5x10 ⁻⁷	3.0x10 ⁻⁶	4.5x10 ⁻⁵	52.11	23.94	23.94
(D)	7.5x10 ⁻⁷	3.4x10 ⁻⁶	6.4x10 ⁻⁵	50.63	25.32	24.05
(E)	7.5x10 ⁻⁷	4.5x10 ⁻⁵	1.1x10 ⁻⁴	42.72	29.13	28.16

The amount of each ion as a percentage of the total ion current was also tabulated at each set of pressures.

% TOTAL ION FLUX

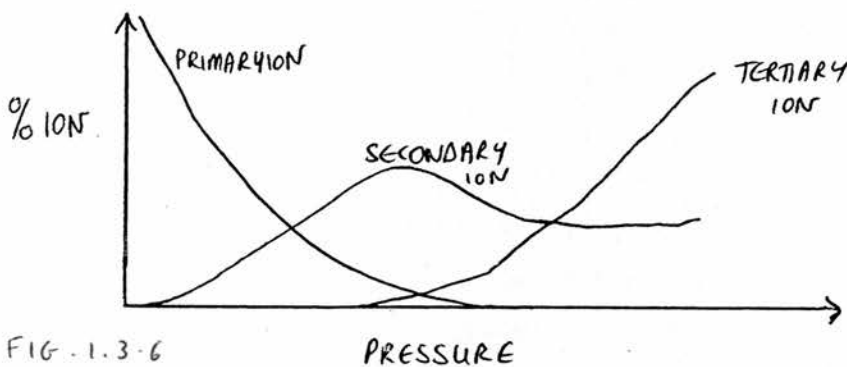
	PRESSURE in torr			m/e			
	INITIAL ION	ION	PENNING	15	17	28	29
	GAUGE	GAUGE	GAUGE				
	7.5x10 ⁻⁷	1.5x10 ⁻⁶	1.5x10 ⁻⁵	0.24	0.07	99.53	0.16
	7.5x10 ⁻⁷	2.3x10 ⁻⁶	3.0x10 ⁻⁵	0.58	0.21	98.97	0.24
	7.5x10 ⁻⁷	3.0x10 ⁻⁶	4.5x10 ⁻⁵	0.74	0.34	98.57	0.34
	7.5x10 ⁻⁷	3.4x10 ⁻⁶	6.4x10 ⁻⁵	0.82	0.41	98.38	0.39
	7.5x10 ⁻⁷	4.5x10 ⁻⁵	1.1x10 ⁻⁴	1.07	0.73	97.49	0.71

A graph of the secondary ion flux against pressure, as measured by the penning gauge head, was plotted.



This allows the relationship between each secondary ion to be studied.

For example - as the pressure of target gas increased, the amount of unreacted primary ion decreased and the total amount of secondary ions increased. If a secondary ion reacted with target molecule to produce a tertiary the proportion of secondary ion would diminish as the amount of tertiary ion increased.



In some instances the experiments were repeated using a higher pressure of primary ion. In others it was expedient to reduce the pressure of both gases in an attempt to identify the first ions produced.

NOVEL EXPERIMENTAL TECHNIQUES

1) In some experiments, most noticeably those involving the reaction of methyleneaminylinium ions, CH_2N^+ , with methane, the repeller voltage was adjusted to study the effect of altering the translational energy of the primary ion.

With the repeller plate at zero voltage the ions will have mean translational energy T_{e0} . By applying a negative potential the ions would be retarded and have a translational energy less than T_{e0} . By applying a positive potential to the plate the ions would be repelled down the axis of the quadrupoles with an additional translational energy $T_{e0} + T$.

This experiment will be discussed in more detail on page 108.

2) ION-MOLECULE REACTIONS WITHIN THE IONISATION CHAMBER TO PRODUCE UNUSUAL PRIMARY IONS

Rudimentary studies of ion-molecular reactions within the ionisation chamber of a conventional mass spectrometer were discussed earlier. This technique was used on the triple quadrupole to imitate the quinquadrupole mass spectrometer.

A mixture of gases was added to the ionisation chamber at high pressures. The ions produced were separated by scanning the first quadrupole. For example, dimethyl ether and methanol were fed into the ionisation chamber. An ion of mass 61 was observed. This was thought to be due to trimethyl oxonium ions. These ions were separated from the first quadrupole and put into another gas in the second

quadrupole. In this way, the reactions of an ion that could only be formed by an ion-molecule reaction could be studied in a triple quadrupole mass spectrometer. This technique has a very limited scope, but was used in a couple of experiments as a prelude to a full study of these ions in the quinquadrupole mass spectrometer.

THE QUINQUA QUADRUPOLE MASS SPECTROMETER

The quinquadrupole will be discussed in full in chapter six.

The preparation of gaseous and liquid samples for the quinquadrupole mass spectrometer was exactly the same as for the triple quadrupole mass spectrometer.

As a result of having two mass filtering quadrupoles and two target gases a new nomenclature for the gases and ions is needed to differentiate clearly between them. The following nomenclature has been adopted in the present research.

α -primary gas was bled into the ionisation chamber produced α -primary ions which reacted with the α -target gas in the second quadrupole to produce α -secondary ions. If α -secondary ions reacted with α -target gas the ions produced were α -tertiary ions.

One of the α -secondary ions was selected from the third quadrupole and put into a β -target gas in the fourth quadrupole. The ions produced are β -secondary and β -tertiary ions.

The introduction of sample gases was different. There are three inlets. The α -primary gas is bled into the ionisation chamber from a vent at the end of the filament cage.

The α -target gas was bled into the chamber at a point on the casing in line with the second quadrupole.

The β -target gas was bled into the chamber at a point on the casing in line with the fourth quadrupole.

These inlets are indicated on the schematic diagram of the quinquadrupole mass spectrometer in figures 1.4 and 1.5.

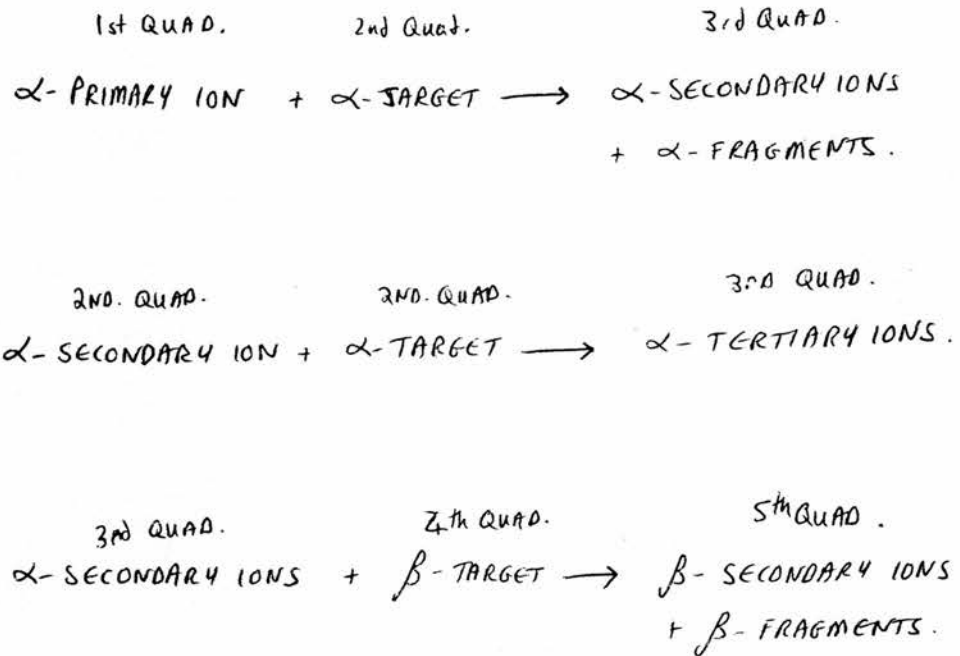
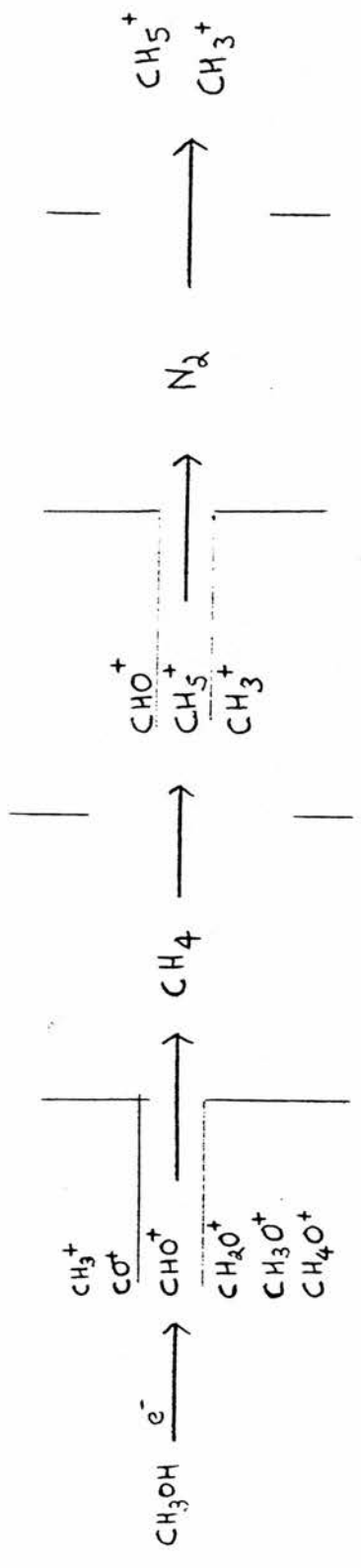
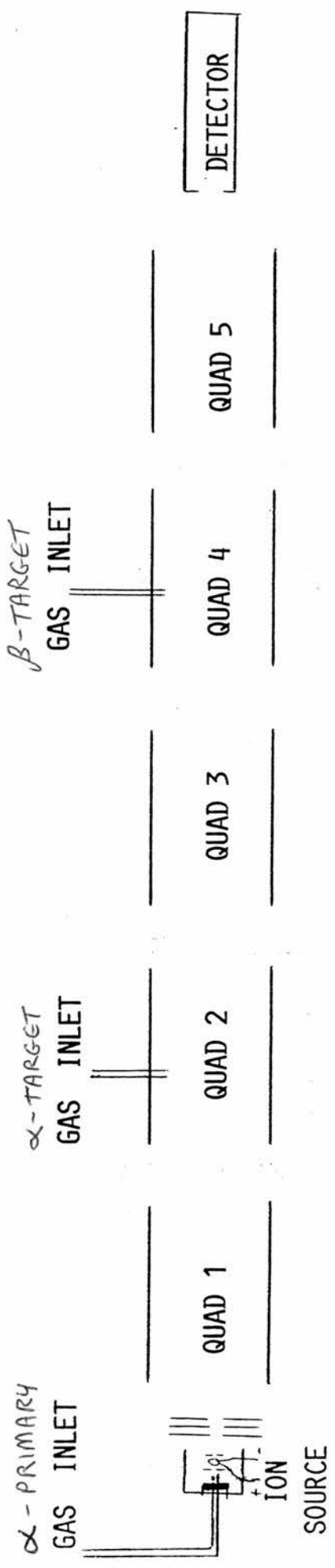


FIG. 1.4

SCHEMATIC DIAGRAM AND OPERATIONS OF THE
QUINQUAQUADRUPOLE MASS SPECTROMETER



CHAPTER TWOPROTONATION OF ALKANES

CHAPTER TWOGUIDE TO CONTENTS:-

INTRODUCTION AND LITERATURE SURVEY

PROTONATION OF ALKANES TO FORM $C_nH_{2n+3}^+$ IONS

CATALYTIC CRACKING OF HYDROCARBONS.

HYPERCOORDINATED CARBOCATIONS AS INTERMEDIATES

STRUCTURE OF HYPERCOORDINATED CARBOCATIONS

SELF PROTONATION REACTION

PROTONATING PRIMARY IONS

 CH_2OH^+ , CHO^+ , $CH_2NH_2^+$, CH_2N^+ , $C_2H_3^+$, $C_2H_5^+$

REACTIONS WITH METHANE, ETHANE, PROPANE, BUTANES

AND PENTANES.

REACTIONS OF CH_5^+ .

CONCLUSION

INTRODUCTION

Carbocations can be classified into two groups.

1) Trivalent-tricoordinate carbenium ions - of which the methenium ion, CH_3^+ , is the simplest example. These, so called classical carbenium ions, are consistent with the existing theory of two centre - two electron bonds.

2) Hypercoordinate carbonium ions - of which the methonium ion, CH_5^+ , is the simplest example. These nonclassical carbocations cannot be fully described by two centre -two electron bonds. The term hypercoordinate carbons, sometimes abbreviated to hypercarbon, is used to indicate that one carbon is coordinated to five or more atoms.

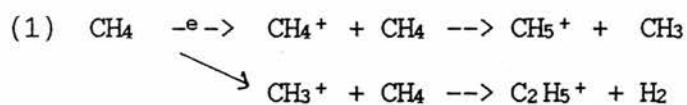
Much research has been done into the trivalent carbenium ions ⁷³ but relatively little into the hypercoordinate carbocations. This research will be reviewed.

CH_5^+ METHONIUM

Munson and Field studied the reactions of CH_5^+ because the "system was complex enough to show some interesting chemistry but simple enough that they felt able to describe it reasonably well".^{12,13}

The aim of their research, which was sponsored by Esso, was to investigate the reactions and properties of gaseous ions as a guide to reactive intermediates in the gaseous and liquid phases.

Operating their mass spectrometer at a pressure of a few torr they observed CH_5^+ and C_2H_5^+ ions as the main product ions from the electron impact of methane at high pressures. ¹²



They found that if a mixture of methane and a small amount of another material (usually less than 1% to 99% methane) was admitted to the ionisation chamber the reactions of CH_5^+ and C_2H_5^+ with the other material could be studied. This was a very crude way of studying ion molecular reactions. It was not possible to distinguish between the products of the reactions of the two main species which limits the value of the work they reported.

Reactions of $\text{CH}_5^+/\text{C}_2\text{H}_5^+$ with n-hexadecane at 1 torr pressure yielded a series of ions as depicted in fig.2.1.

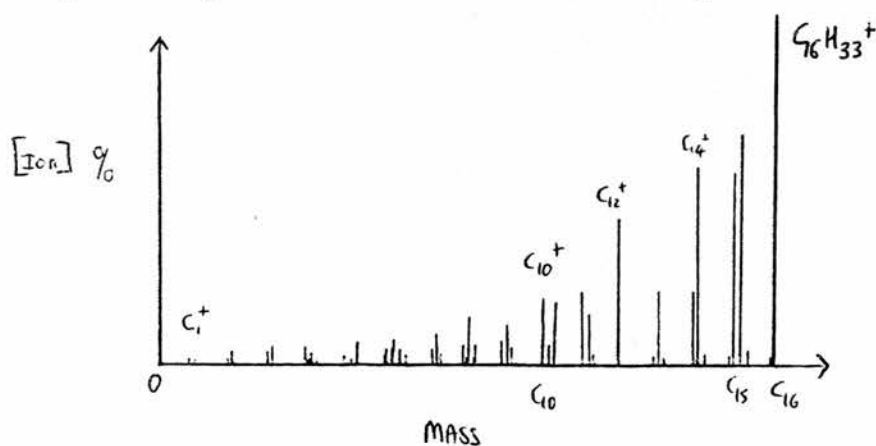
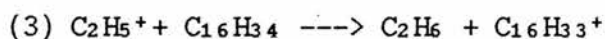
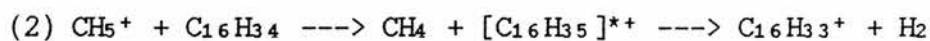


FIG 2.1

It was thought that this involved protonation of the alkane followed by fragmentation to a series of alkyl ions and that it could represent the mechanism of catalytic cracking. The predominant ion was $C_{16}H_{33}^+$ but it could not be ascertained if it was formed by protonation of n-hexadecane by CH_5^+ followed by loss of H_2 (2) or by hydride abstraction by $C_2H_5^+$ (3).



They did, however, postulate that the protonation of the alkane did occur and that this could be representative of the mechanism of catalytic cracking where the alkane is protonated from a very strong Brønsted acid site on the catalyst surface. ⁷⁴

In contrast to the mass spectrometer used by Field and Munson it is possible with a multiple sector instrument such as the triple quadrupole mass spectrometer to separate CH_5^+ from the other ions from methane and put it into an alkane in the second quadrupole and determine the products from this reaction in isolation from other reactions.

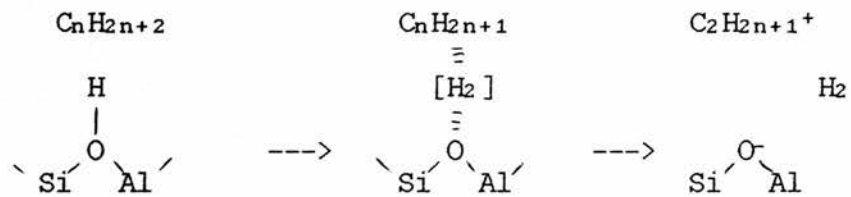
Corma and Wojciechowski in a recent review of catalytic cracking discussed this proposal.⁷⁵ It is generally agreed that the initial event in catalytic cracking of paraffins is the formation of a carbocation. The four hypotheses that have been postulated are summarised below.

The carbocation ion is formed by :-

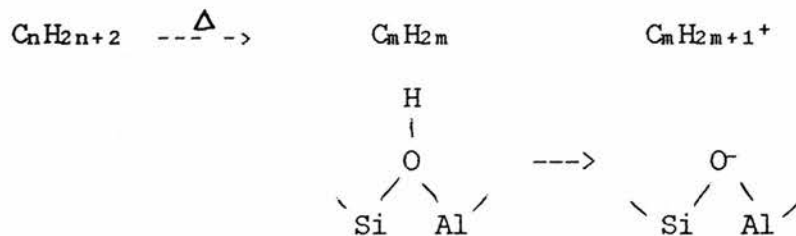
1) abstraction of a hydride ion on a Lewis acid site.⁷⁶⁻⁷⁸



2) abstraction of a hydride ion on a Brønsted acid site with the formation of hydrogen.⁷⁹



3) absorption of thermally produced olefins on Brønsted acid sites.⁸⁰



4) addition of a proton from a Brønsted acid site on the catalyst to the alkane producing a penta-coordinate carbon atom. ⁷⁹



They went on to say that "the hypothesis that addition of a proton to a carbon leading to a penta-coordinated carbonium appears to have little support at present." That notwithstanding, this was the mechanism that the present work was intended to investigate.

Recently research in penta-coordinate carbonium ions has been advanced by the study of reactions in superacid mediums. ⁸¹ Most noticeable is the work of Olah et al in which methane in a superacid matrix (4) was studied by Electron Spectroscopy for Chemical Analysis (ESCA). ⁸²

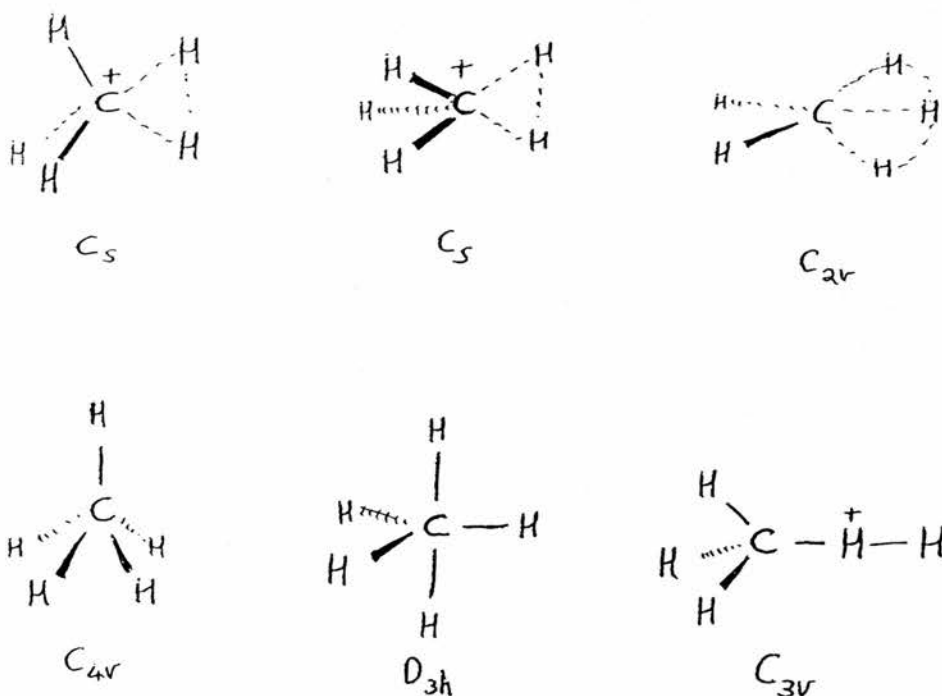
(4) $\text{CH}_4 + \text{FSO}_3\text{H}/\text{SbF}_5 \text{ ----> } (\text{CH}_5^+ \text{ FSO}_3^-)/\text{SbF}_5$

The amount of CH_5^+ produced in this way is very small and can only be detected because the unreacted methane is so insoluble in superacids at -180°C that under 10^{-9} torr vacuum it is virtually all pumped away leaving the methonium ions trapped in the superacid matrices. The presence of CH_5^+ ions was detected by the ESCA shift.

STRUCTURE OF METHONIUM IONS

The possible structures of the methonium ion have always been hotly debated. The recent advances that have allowed spectroscopic observations - ^{13}C NMR and ESCA - and better Quantum mechanical calculations have rekindled the arguments in the literature. For methonium the possibilities are best identified by their symmetry groups.

The methonium ion could be considered to be a carbon equally bonded to five hydrogens. This would have spherical symmetry. If the bonding was not equivalent to all hydrogens then four alternative structures could be drawn. They are represented below as C_s of which there are two forms, C_{2v} , C_{4v} (which is a square-pyramid) and D_{3h} (which is a trigonal-bipyramid). Alternatively CH_5^+ could be considered to be a methane molecule in which the tetrahedral arrangement has been retained in as far as is possible with a proton attached to one hydrogen. This would have C_{3v} symmetry. ^{83,84,85}



ESCA investigations have revealed that the 1s carbon binding energy indicates that the positive charge is spread over the hydrogens rather than being centred on the carbon. ⁸⁶

The trigonal bipyramidal structure (D_{3h}) had been favoured by early quantum calculations which were done at a very crude level (CNDO/2). ⁸⁷ Olah argued against this because, as each of the hydrogens would possess a positive charge, +0.1856 for the equatorial hydrogens and +0.3310 for the axial hydrogens, with the carbon carrying a negative charge of -0.2189, this would require that dehydrogenation should be a slow reaction ; which was not borne out by experimental observations. Further calculations indicated that the energy of this structure would be -5.48eV whilst that for the structure in which three of the hydrogens retain their normal position and the other two are equivalent (C_s) has a lower energy of

-5.84eV. The same calculations also showed that the structure in which the methane retains its tetrahedral symmetry with the additional hydrogen bonded to only one of the hydrogens would only have an energy lower than that of the fragments, CH_3^+ and H_2 , if the $\text{H}\cdots\text{H}$ distance was less than 0.75 \AA . As the normal H-H bond length is 0.749 \AA it is very unlikely that this requirement for stability would ever be achieved and so Olah suggested that this structure could be discounted. ⁸⁸⁻⁹¹

This argument is not conclusive as the margin of error in the quantum mechanical calculations is probably larger than the margin of change in the length of the $\text{H}\cdots\text{H}$ bond that would result in this structure being stable. The difference between the normal bond length and the minimum size that the $\text{H}\cdots\text{H}$ bond would need to be to be stable according to the quantum mechanical calculations is 0.001 \AA , a mere error of $\pm 0.13 \%$.

The most recent quantum mechanical calculations using MP3/6.31G*+ZPE have also favoured the C_s structure, having found that it is $3.7 \text{ kcal mol}^{-1}$ more stable than the C_{4v} structure and $11.7 \text{ kcal mol}^{-1}$ more stable than the D_{3h} structure. ^{85,92}

The consensus in the literature is one of accepting the structure with C_s symmetry. Three standard sp^3 hybridised orbitals of the carbon are envisaged as overlapping with three hydrogen $1s$ orbitals in standard

two centre, two electron bonds to form three C-H bonds that are slightly longer than the C-H bonds in methane - 1.185 Å.⁹² The fourth sp^3 orbital of the carbon interacts with a $1s-1s$ bond between the two remaining hydrogens in a three centred, two electron bond. Fig 2.2 This is pictorially represented as three standard C-H bonds and one triangular dotted line centered between the three atoms involved in the bond. Fig 2.3 This is described as being the result of protonation of a C-H bond.⁹³

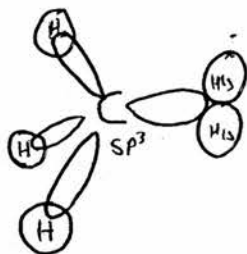


FIG - 2 - 2

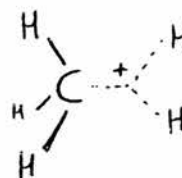


FIG - 2 - 3

Table 2.1 gives the energies of the CH₅⁺ structures relative to the lowest C_s configuration found by using the 6-311G** basis set and MP2/6-31G* optimized geometries.⁸⁵

TABLE 2.1

structure	HF	MP2	MP3	MP4(SDQ)
C_s	0.0	0.0	0.0	0.0
C_s	0.1	0.1	0.1	0.1
C_{2v}	3.0	0.6	0.9	1.1
C_{4v}	7.5	2.8	3.2	3.7
D_{3h}	16.4	10.8	11.2	11.7

An indication of the structures of the alkonium ions in the gas phase might be obtained from mass spectral studies by considering the fragments produced from the alkonium ions. Taking the methonium ion as an example an experiment could be devised for the quinquadrupole mass spectrometer in which methane is deuterated to produce CH_4D^+ in the second quadrupole. This ion would then be separated from the other ions and put into an inert gas in the fourth quadrupole. By considering the relative amounts of the two fragments - CH_3^+ and CH_2D^+ - that would be analysed in the fifth quadrupole an indication of the structure of the ion might be found. If CH_5^+ had a structure such that each hydrogen was equivalent then it would be expected that the ratio of CH_3^+ to CH_2D^+ would be of the order of 1:4. If, in the other extreme, the structure was that in which the additional proton was attached in a H-H bond then, provided there had been no H/D exchange, it would be expected that the only fragment would be CH_3^+ .

Allowance must be made for correction to the ratios of CH_2D^+ and CH_3^+ to allow for the kinetic isotope effect and H/D exchange.

This experiment was attempted on the quinquapole mass spectrometer and is discussed in chapter 6, page 399.

There has also been interest in postulating the involvement of protonated alkanes as intermediates in solution phase chemistry. The acid catalysed isomerisation of n-butane to iso-butane as represented in Fig 2.4, is a typical example.

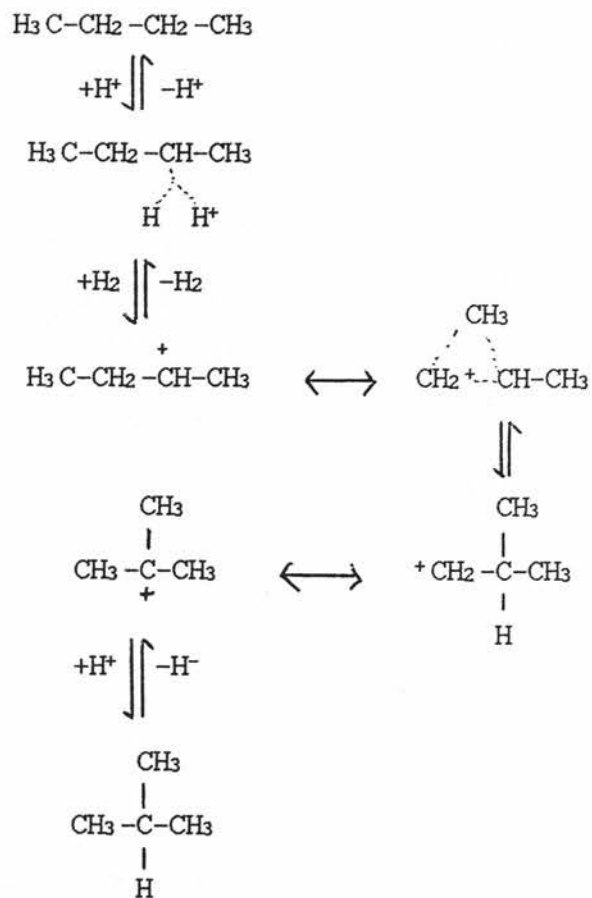
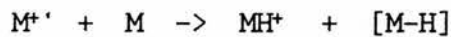


Fig. 2.4

The reactions that have been studied for this work involve the reaction of the following ions with methane. $\text{CH}_4^+ + \text{CH}_4$, $\text{CH}_5^+ + \text{CH}_4$, $\text{CH}_2\text{OH}^+ + \text{CH}_4$, $\text{CH}_2^{18}\text{OH}^+ + \text{CH}_4$, $\text{CHO}^+ + \text{CH}_4$, $\text{CH}^{18}\text{O}^+ + \text{CH}_4$, $\text{CDO}^+ + \text{CH}_4$, $\text{CH}_2\text{NH}_2^+ + \text{CH}_4$, $\text{CH}_2\text{N}^+ + \text{CH}_4$, $\text{C}_2\text{H}_5^+ + \text{CH}_4$, $\text{C}_2\text{H}_3^+ + \text{CH}_4$, $\text{C}_3\text{H}_3^+ + \text{CH}_4$, $\text{C}_3\text{H}_5^+ + \text{CH}_4$ and $\text{C}_3\text{H}_7^+ + \text{CH}_4$. Each of these will be discussed in the discussion. The previous work reported on specific ions will be discussed here.

CH_4^+

The self protonation reaction can occur for many gases.



Abramson and Futrell^{95,96} used a tandem mass spectrometer to investigate the reaction $\text{CD}_4^+ + \text{CH}_4$. They observed that the amount of $[\text{CH}_4\text{D}]^+$ was twice the amount of $[\text{CD}_4\text{H}]^+$ which indicated that the transfer tended to be from the ion to the neutral molecule (5) rather than the other way round (6).



That they did not observe any doubly exchanged ions i.e. CH_3D_2^+ or CH_2D_3^+ indicated that under their experimental conditions a collision complex, if formed at

all, was not sufficiently long-lived for isotopic exchange to occur.

Rate constants for the self-protonation reactions that are relevant to the present work are presented in table 2.2. ⁹⁷

TABLE 2.2 For reaction $M^+ + M \rightarrow MH^+ + [M-H]^+$

$$\text{Reaction Rate} = k_r [M^+][M]$$

M	$k_{\text{react}} / \text{cm}^3 \text{ molecule}^{-1} \text{ sec}^{-1} \times 10^9$
CH ₄	1.11
CH ₃ Cl	1.53
CH ₃ OH	2.53

CHO⁺

CHO⁺ has been used as a parent ion in various studies of ion/molecular reactions. Investigation of the interconversion of the two structures for this ion, CHO⁺ and COH⁺, led to the conclusion that the majority of ions present in the electron impact spectrum of methanol are of the CHO⁺ structure. ^{98,99} Gardner and Vinckier used a specially designed radial-electric-field fast flow reactor to isolate the CHO⁺ formed by chemi-ionisation of acetylene and oxygen atoms at room temperature which were then reacted with acetylene, C₂N₂, i-C₄H₁₀, NH₃, (CH₃)₂O, (CH₃)₂CO, ethylene oxide and CH₃CN to provide experimental rate constants. ¹⁰⁰ In all cases except i-C₄H₁₀ the protonated target ion was the main reaction

product. In the case of $i\text{-C}_4\text{H}_{10}$ the ions produced were fragments of $[\text{C}_4\text{H}_{11}]^{*+}$.

Futrell, Abramson, Bhattacharya and Tiernan ¹⁰¹, using a tandem mass spectrometer, studied the proton-transfer reactions from CHO^+ and CDO^+ to methane, ethane and the simple alkanes propane, butane, pentane and hexane. They concluded from consideration of the translational energy dependence of the reaction that the mechanism did not involve an intermediate complex $[\text{CHO}-\text{CH}_4]^{*+}$ but rather that the proton was "stripped" by the methane acting as a Brønsted base. By considering the extent of dissociation of CH_5^+ to CH_3^+ and H_2 with CHO^+ ions from source molecules they concluded that the CHO^+ from acetaldehyde had the lowest internal energy and therefore produced the CH_5^+ ion that was most stable. It should be noted that applying the same argument to the values that were reported later in the same paper for the protonation of ethane does not produce the same conclusion as can be seen from the table below.

Table 2.3

SOURCE MOLECULE	$\text{CH}_3^+ / \text{CH}_5^+$	$\text{C}_2\text{H}_5^+ / \text{C}_2\text{H}_7^+$
CH_3CHO	0.05	0.724
HCHO	0.23	-
HCOOH	0.27	0.369
CH_3OH	0.34	0.369

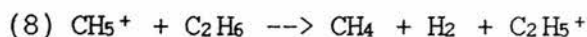
These values indicate that the CH_5^+ that is produced from the reaction of CHO^+ from acetaldehyde is the least

likely to fragment to CH_3^+ and H_2 whereas of the ions used to protonate ethane those which were made from acetaldehyde caused the maximum fragmentation. This is an inconsistency in the reported work.

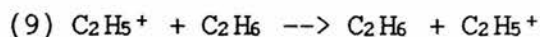
In the work to be reported here the interest was in comparing different protonating ions rather than comparing the same ion from different source molecules. The CHO^+ ion that was used was derived from methanol because deuterated methanol was available to hand and so direct comparison could be made between the reactions of CHO^+ and CDO^+ . (Apart from the fact that acetaldehyde is a volatile (B.P.= 21°C), explosive, cancer causing liquid its deuterated form costs £145.00 for 5ml. whereas deuterated methanol costs £35.00 for 5ml. It is also difficult to degas properly and it attacks the grease used on the taps.)

C_2H_7^+ ETHONIUM

Munson and Field ^{12,13} studied the gaseous ionic reactions of CH_5^+ and C_2H_5^+ with ethane in mixtures of 1% ethane to 99% methane at pressures as high as 2 torr. They observed what they took to be two reactions. Simple proton-transfer (7) to give C_2H_7^+ ions and dissociative proton-transfer (8) to give C_2H_5^+ .



It should be noted that C_2H_5^+ is also a reactant ion and could produce C_2H_5^+ ions by a hydride abstraction reaction (9) which could not be distinguished from the parent C_2H_5^+ ions.



Futrell, Abramson, Bhattacharya and Tiernan¹⁰¹ studied the formation of C_2H_7^+ by proton-transfer reactions from CHO^+ and CH_2N^+ ions. The C_2H_7^+ ion was observed in good yields - up to 42% with respect to the ethyl carbocation - C_2H_5^+ . Experiments using deuterated ethane were also done in an attempt to investigate the importance of the hydride abstraction reaction in the production of the C_2H_5^+ ion.

Reaction of CHO^+ with C_2D_6 would produce $\text{C}_2\text{D}_6\text{H}^+$ ions if a simple proton-transfer reaction occurred. This would, if it was long-lived enough to rearrange, give ethyl ion fragments of two types - C_2D_5^+ and $\text{C}_2\text{D}_4\text{H}^+$. If a hydride abstraction reaction occurred the product would be C_2D_5^+ and this would result in an imbalance in the proportions of the two ethyl ion peaks. By measuring the amount of each ion it was hoped that an estimate could be made of the importance of the hydride abstraction reaction. As can be seen from the data in table 2.4 the ratio of C_2D_5^+ to $\text{C}_2\text{D}_4\text{H}^+$ was 1:1 in all experiments from which they concluded that the hydride

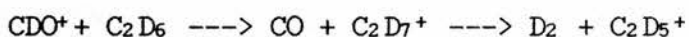
abstraction reaction was not playing a major role in the formation of the ethyl ions. The total amount of ethyl ions formed could therefore be taken as an indication of the extent of fragmentation of the ethonium ions. They did not report any C₁ fragment ions.

Table 2.4

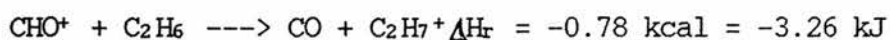
RATIO OF $C_2D_5^+ : C_2D_4H^+$ FROM PROTONATION OF ETHANE

Source	Ion	$C_2D_5^+$	$C_2D_4H^+$	Ratio
CH ₃ CHO	CHO ⁺	0.29	0.29	1:1
CH ₃ OH	CHO ⁺	0.37	0.36	1:1
HCO ₂ H	CHO ⁺	0.36	0.37	1:1
CH ₃ NH ₂	CH ₂ N ⁺	0.48	0.48	1:1
HCO ₂ H	HCO ₂ ⁺	0.36	0.34	1:1

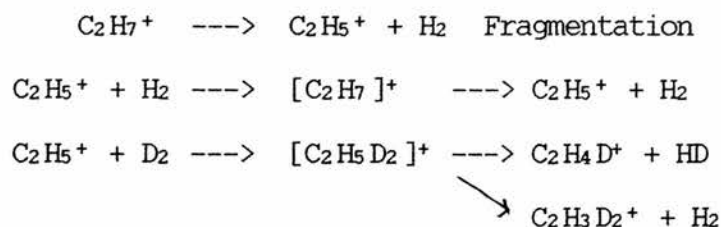
Smith and Futrell¹⁰² used a tandem-ICR mass spectrometer to study the effect of internal energy on the formation and decomposition of $C_2H_nD_m^+$ (where $n+m=7$). They found that the more energetic reactant ions such as ArD^+ or D_3^+ gave rise to fragmentation products of $C_2D_5^+$ and $C_2D_3^+$ whereas the less energetic ions, CDO^+ or N_2D^+ , only gave rise to $C_2D_5^+$ fragment ions.



The reaction of CHO^+ and ethane was found to be exothermic.



An attempt to form the $C_2H_7^+$ ion by combining the fragments $C_2H_5^+$ and H_2 failed because the complex thus formed had enough energy to fragment. However, product ions with a scrambled deuterium/hydrogen content indicated that some transitory complex had been formed.



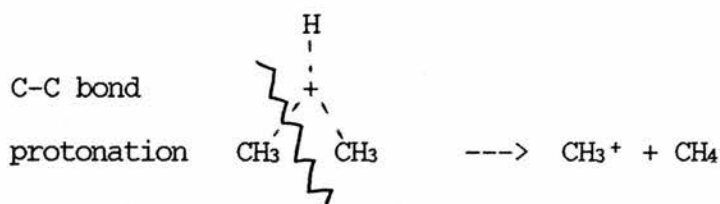
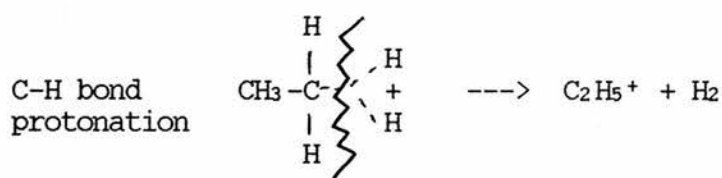
Kebarle and Hiraoka ^{103,104} studied the equilibrium of the reaction $\text{C}_2\text{H}_5^+ + \text{H}_2 = \text{C}_2\text{H}_7^+$ at 1-5 torr and temperatures between -160 and +200°C using a pulsed electron beam high pressure ion source mass spectrometer. Their kinetic and equilibrium results led them to conclude that there were two isomeric forms of C_2H_7^+ ions - C_2H_7^+ (a) which is the least stable of the two and has been assigned structure (a) by Raghavachari and co-workers ⁹² after quantum mechanical molecular orbital calculations and C_2H_7^+ (b) which has been assigned structure (b) and is of lower energy than the (a) isomer.



Isomer (b) corresponds to protonation of the C-C bond whereas isomer (a) could be considered to be the result of protonation of a C-H bond.

With methane the only fragment that was observed in our experiments was to CH_3^+ and H_2 . (It should, however, be noted in passing that a recent paper ¹⁰⁵ reported the observation of the fragmentation of CH_5^+ to CH_4^{++} and H by collision with O_2 . This was detected in the CAD/MIKE spectrum of the reaction of CH_5^+ with O_2 .)

With the protonation of ethane there are now two routes that the ethonium might take to fragment. This has been considered as the protonation and subsequent cleavage of a C-H bond and the protonation and subsequent cleavage of a C-C bond. ¹⁰⁶



Olah, who has been concerned with the formation of hypercarbon species in superacid mediums has reported that ethane underwent C-C bond protolysis in preference to C-H bond cleavage by a factor of between 8:1 to 15:1. This was detected by measuring the ratios of $\text{CH}_4:\text{H}_2$ in the gaseous products of the reaction of ethane with HF-SbF_5 (1:1) SO_2ClF . ¹⁰⁷ If the MO calculations are applicable to the superacid medium then this would lead us to suggest that the ethonium ion is adopting the structure (b) C_2H_7^+ in the superacid medium so that when it cleaves it is a C-C bond that cleaves. The results of our gas phase experiments should allow comparison with these results and the gas phase fragmentation of C_2H_7^+ ions.

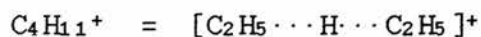
HIGHER ALKONIUM IONS

The higher alkonium ions have been postulated from theoretical considerations and as reaction intermediates. Observations in the gas phase by high pressure mass spectrometry of $C_3H_9^+$ ions have recently been reported.

92,103,108,109

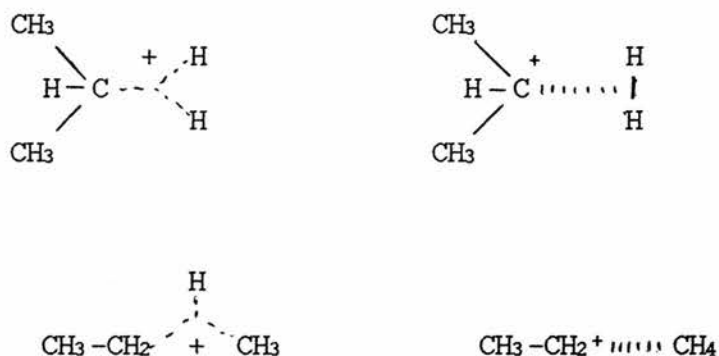
Olah, and others, working in superacid mediums have produced evidence for the existence of these ions in solution by considering the fragmentation pathways. They have not observed the ions. The fragmentation products of the higher alkanes tend to require the cleavage of a C-C bond. Olah takes this as being evidence of an increasing tendency for the higher protonated alkanes to form C-H-C three centre, two electron bonds.

In the gas phase the observation of an ion having the required mass for a protonated alkane might not be indicative that the ion is of the same form as a lower protonated alkane but that at the high pressures that these ions were observed there may be the formation of ion clusters. ¹⁰³



The question now arises as to whether these can be considered to be protonated alkanes or an ion cluster of two ethyl groups and a proton.

Kebarle and Hiraoka produced heats of formation and possible structures for protonated propane and butane but did not conclude whether they were observing the actual protonated propane or a close complex between $C_2H_5^+$ and CH_4 or $C_3H_7^+$ and H_2 as the two structures that they derived were very close in energy and geometry to these ion complexes. ¹¹⁰



These ions, $C_3H_9^+$ etc, have not previously been observed at the pressures at which the present work was done.

On considering the work that had previously been done it was felt that the protonation of alkanes could be restudied using the multiple quadrupole mass spectrometers to advance the understanding of the earlier reports, to investigate the formation and reaction of $C_nH_{2n+1}^+$ ions at lower pressures than had previously been studied and to investigate the hypothesis of their involvement in catalytic cracking.

RESULTS

<u>METHANE</u>	<u>PAGE</u>
Initial reaction of methane $\text{CH}_4^+ + \text{CH}_4$	70
Reaction of labelled $\text{CH}_2^{18}\text{OH}^+$ at low pressure	71
Reaction of $\text{CH}_2^{18}\text{OH}^+$ repeated at higher pressure	72
Reaction of $\text{CHO}^+ + \text{CH}_4$	73
Reaction of $\text{CH}_2\text{NH}_2^+ + \text{CH}_4$	74
Reaction of $\text{CH}_2\text{N}^+ + \text{CH}_4$	75
Reaction of $\text{C}_2\text{H}_3^+ + \text{CH}_4$	76
Reaction of $\text{C}_2\text{H}_5^+ + \text{CH}_4$	77
<u>ETHANE</u>	
Reaction of $\text{CHO}^+ + \text{C}_2\text{H}_6$	78
Reaction of $\text{CH}_2\text{N}^+ + \text{C}_2\text{H}_6$ at 10^{-5} and 10^{-4} torr	79 +80
Reaction of $\text{C}_2\text{H}_3^+ + \text{C}_2\text{H}_6$	81
Reaction of $\text{C}_2\text{H}_5^+ + \text{C}_2\text{H}_6$	82
Reaction of $\text{C}_2\text{H}_6^+ + \text{C}_2\text{H}_6$:- Main Peaks > 1%	83
Minor Peaks < 1%	84
<u>PROPANE</u>	
Reaction of $\text{CHO}^+ + \text{C}_3\text{H}_8$ at 10^{-5} and 10^{-4} torr	85 + 86
Reaction of $\text{CH}_2\text{N}^+ + \text{C}_3\text{H}_8$	87
Reaction of $\text{C}_2\text{H}_3^+ + \text{C}_3\text{H}_8$	88
Reaction of $\text{C}_2\text{H}_5^+ + \text{C}_3\text{H}_8$	89

BUTANE

Reaction of CH_2N^+ + Iso-Butane	90
Reaction of CH_2N^+ + n-Butane	91
Fragmentation of C_4H_9^+ by C.I.D. in N_2	92

PENTANE

Reaction of CH_2N^+ + n-Pentane	93
Reaction of CH_2N^+ + Iso-Pentane	94
Reaction of CH_2N^+ + Neo-Pentane	95

ADDITIONAL EXPERIMENTS

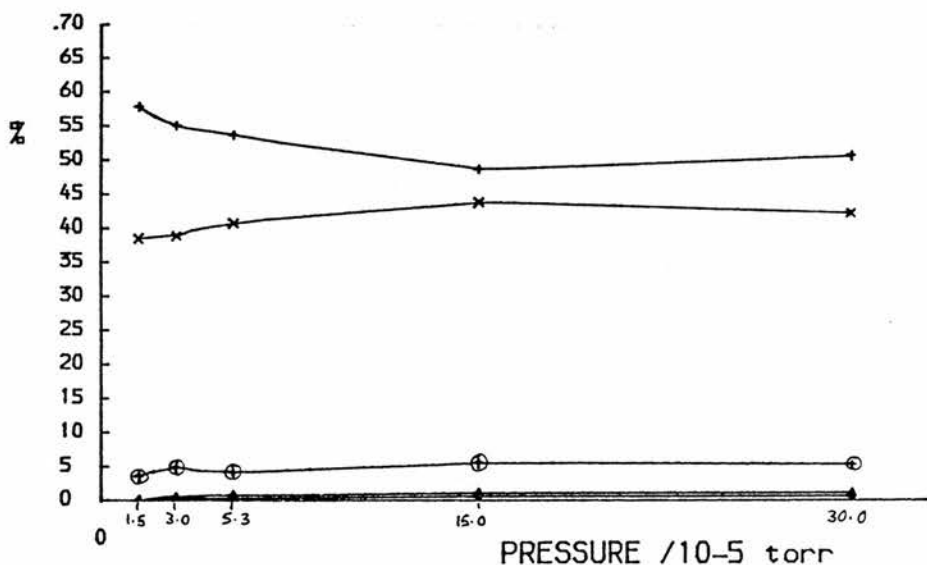
Reaction of CH_5^+ + C_2H_6	96
Reaction of CH_3^+ + CH_4	97

CH₄⁺ into CH₄

15 = CH₃⁺ 27 = C₂H₃⁺
 16 = CH₄⁺ 28 = C₂H₄⁺
 17 = CH₅⁺ 29 = C₂H₅⁺

CH₄⁺ INTO METHANE

% SECONDARY ION FLUX Vs. PRESSURE



+ = 15
 x = 17
 Δ = 27
 ◊ = 28
 ⊕ = 29

% SECONDARY ION FLUX

	PRESSURES in torr			m/e				
	INITIAL ION	ION	PENNING	15	17	27	28	29
	GAUGE	GAUGE	GAUGE					
(A)	7.5×10 ⁻⁸	7.5×10 ⁻⁷	1.5×10 ⁻⁵	57.83	38.55	0.00	0.00	3.61
(B)	7.5×10 ⁻⁸	1.5×10 ⁻⁶	3.0×10 ⁻⁵	55.05	39.02	0.70	0.35	4.88
(C)	7.5×10 ⁻⁸	2.3×10 ⁻⁶	5.3×10 ⁻⁵	53.66	40.80	0.89	0.44	4.21
(D)	7.5×10 ⁻⁸	4.5×10 ⁻⁶	1.5×10 ⁻⁴	48.67	43.81	1.24	0.73	5.55
(E)	7.5×10 ⁻⁸	6.0×10 ⁻⁶	3.0×10 ⁻⁴	50.68	42.23	1.18	0.68	5.24

% TOTAL ION FLUX

	PRESSURES in torr			m/e					
	INITIAL ION	ION	PENNING	15	16	17	27	28	29
	GAUGE	GAUGE	GAUGE						
	7.5×10 ⁻⁸	7.5×10 ⁻⁷	1.5×10 ⁻⁵	0.55	99.04	0.37	0.00	0.00	0.03
	7.5×10 ⁻⁸	1.5×10 ⁻⁶	3.0×10 ⁻⁵	1.46	97.35	1.04	0.02	0.01	0.13
	7.5×10 ⁻⁸	2.3×10 ⁻⁶	5.3×10 ⁻⁵	2.01	96.26	1.53	0.03	0.02	0.16
	7.5×10 ⁻⁸	4.5×10 ⁻⁶	1.5×10 ⁻⁴	7.43	84.73	6.69	0.19	0.11	0.85
	7.5×10 ⁻⁸	6.0×10 ⁻⁶	3.0×10 ⁻⁴	2.88	94.32	2.40	0.07	0.04	0.30

$^{18}\text{CH}_2\text{OH}^+$ into CH_4

$$17 = \text{CH}_5^+$$

$$31 = \text{CHO}^+$$

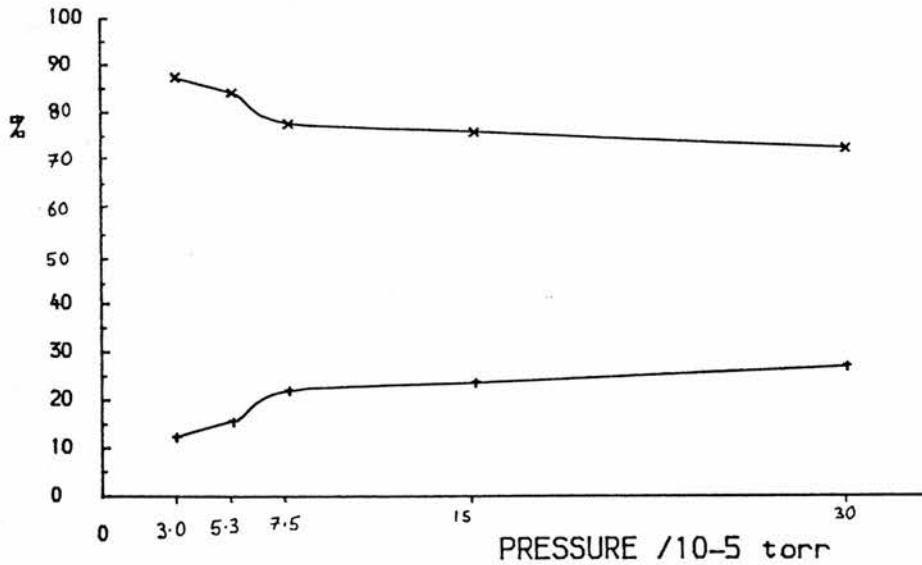
$$33 = \text{CH}_2^{18}\text{OH}^+$$

 CH_2OH^+ INTO METHANE

% SECONDARY ION FLUX Vs. PRESSURE

+ = 17

x = 31

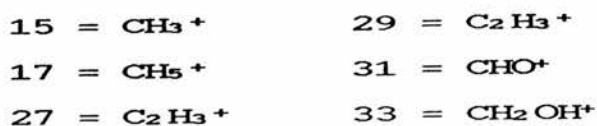


% SECONDARY ION FLUX

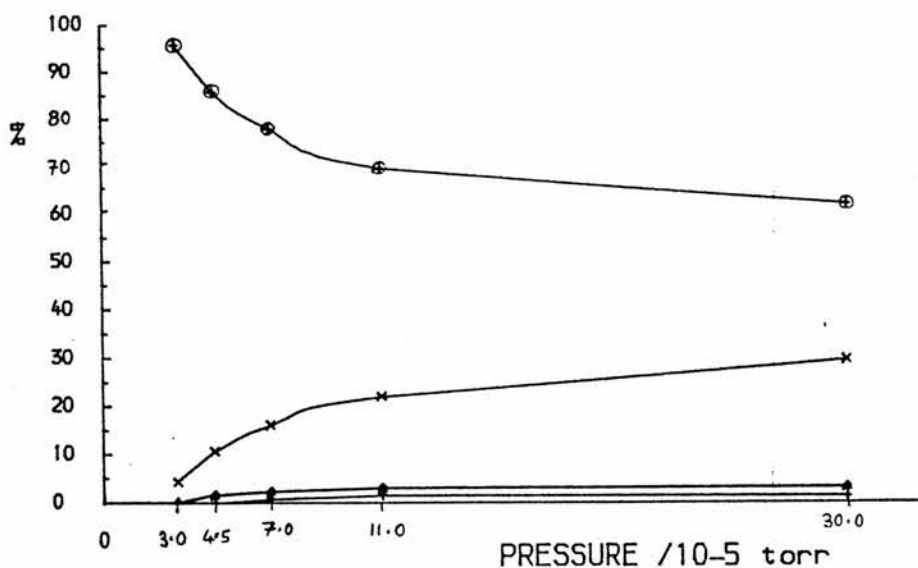
	PRESSURES in torr			m/e	
	INITIAL ION	ION	PENNING	17	31
	GAUGE	GAUGE	GAUGE		
(A)	7.5×10^{-8}	1.5×10^{-6}	3.0×10^{-5}	12.50	87.50
(B)	7.5×10^{-8}	3.0×10^{-6}	5.3×10^{-5}	15.79	84.21
(C)	7.5×10^{-8}	3.0×10^{-6}	7.5×10^{-5}	22.22	77.78
(D)	7.5×10^{-8}	3.8×10^{-6}	1.5×10^{-4}	23.81	76.19
(E)	7.5×10^{-8}	6.8×10^{-6}	3.0×10^{-4}	27.27	72.73

% TOTAL ION FLUX

	PRESSURES in torr			m/e		
	INITIAL ION	ION	PENNING	17	31	33
	GAUGE	GAUGE	GAUGE			
	7.5×10^{-8}	1.5×10^{-6}	3.0×10^{-5}	0.07	0.52	99.41
	7.5×10^{-8}	3.0×10^{-6}	5.3×10^{-5}	0.12	0.65	99.23
	7.5×10^{-8}	3.0×10^{-6}	7.5×10^{-5}	0.16	0.55	99.29
	7.5×10^{-8}	3.8×10^{-6}	1.5×10^{-4}	0.21	0.68	99.11
	7.5×10^{-8}	6.8×10^{-6}	3.0×10^{-4}	0.35	0.93	98.72

 $^{18}\text{CH}_2\text{OH}^+$ INTO METHANE

% SECONDARY ION FLUX Vs. PRESSURE



% SECONDARY ION FLUX

	PRESSURE in torr			m/e				
	INITIAL ION	ION	PENNING	15	17	27	29	31
	GAUGE	GAUGE	GAUGE					
(A)	7.5×10^{-7}	1.5×10^{-6}	3.0×10^{-5}	0.00	4.35	0.00	0.00	95.65
(B)	7.5×10^{-7}	2.3×10^{-6}	4.5×10^{-5}	0.00	10.71	1.79	1.79	85.71
(C)	7.5×10^{-7}	3.0×10^{-6}	6.8×10^{-5}	0.81	16.26	2.44	2.44	78.05
(D)	7.5×10^{-7}	3.8×10^{-6}	1.1×10^{-4}	1.59	22.22	3.17	3.17	69.84
(E)	7.5×10^{-7}	6.8×10^{-6}	3.0×10^{-4}	1.35	29.73	3.38	3.38	62.16

% TOTAL ION FLUX

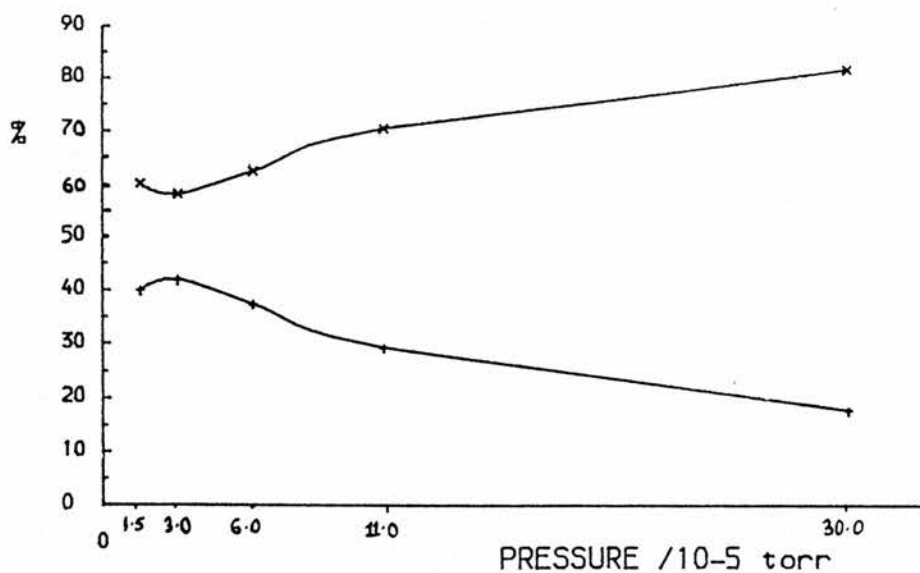
	PRESSURES in torr			m/e					
	INITIAL ION	ION	PENNING	15	17	27	29	31	33
	GAUGE	GAUGE	GAUGE						
	7.5×10^{-7}	1.5×10^{-6}	3.0×10^{-5}	0.00	0.02	0.00	0.00	0.50	99.48
	7.5×10^{-7}	2.3×10^{-6}	4.5×10^{-5}	0.00	0.08	0.01	0.01	0.63	99.27
	7.5×10^{-7}	3.0×10^{-6}	6.8×10^{-5}	0.01	0.14	0.02	0.02	0.66	99.15
	7.5×10^{-7}	3.8×10^{-6}	1.1×10^{-4}	0.01	0.21	0.03	0.03	0.65	99.06
	7.5×10^{-7}	6.8×10^{-6}	3.0×10^{-4}	0.02	0.46	0.05	0.05	0.96	98.46

CHO⁺ into CH₄15 = CH₃⁺17 = CH₅⁺CHO⁺ INTO METHANE

% SECONDARY ION FLUX Vs. PRESSURE

+ = 15

x = 17



% SECONDARY ION FLUX

	PRESSURES in torr			m/e	
	INITIAL ION	ION	PENNING	15	17
	GAUGE	GAUGE	GAUGE		
(A)	7.5x10 ⁻⁷	1.5x10 ⁻⁶	1.5x10 ⁻⁵	40.00	60.00
(B)	7.5x10 ⁻⁷	2.3x10 ⁻⁶	3.0x10 ⁻⁵	41.94	58.06
(C)	7.5x10 ⁻⁷	3.8x10 ⁻⁶	6.0x10 ⁻⁵	37.50	62.50
(D)	7.5x10 ⁻⁷	5.3x10 ⁻⁶	1.1x10 ⁻⁴	29.41	70.59
(E)	7.5x10 ⁻⁷	1.5x10 ⁻⁵	3.0x10 ⁻⁴	17.86	82.14

% TOTAL ION FLUX

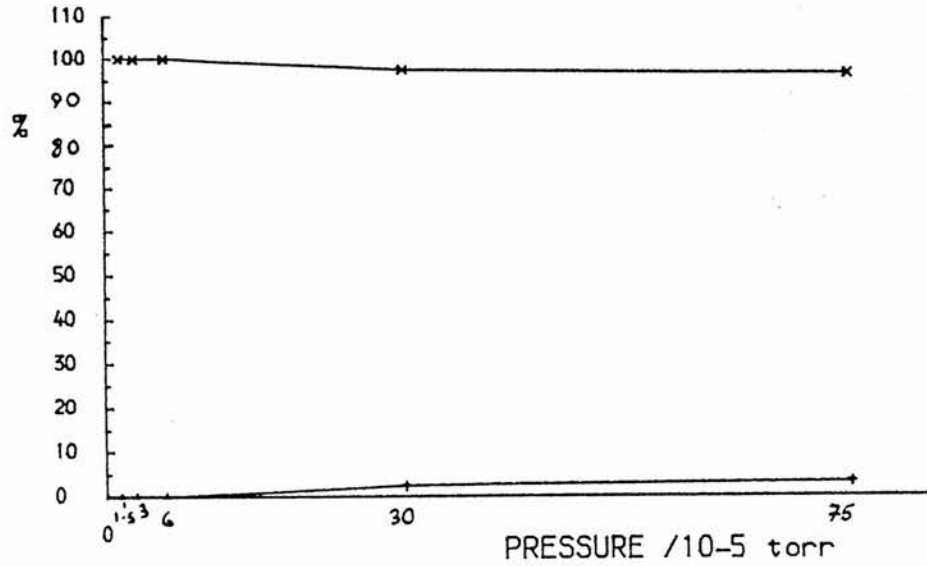
	PRESSURES in torr			m/e		
	INITIAL ION	ION	PENNING	15	17	29
	GAUGE	GAUGE	GAUGE			
	7.5x10 ⁻⁷	1.5x10 ⁻⁶	1.5x10 ⁻⁵	0.07	0.11	99.82
	7.5x10 ⁻⁷	2.3x10 ⁻⁶	3.0x10 ⁻⁵	0.27	0.37	99.37
	7.5x10 ⁻⁷	3.8x10 ⁻⁶	6.0x10 ⁻⁵	0.41	0.68	98.90
	7.5x10 ⁻⁷	5.3x10 ⁻⁶	1.1x10 ⁻⁴	0.55	1.31	98.15
	7.5x10 ⁻⁷	1.5x10 ⁻⁵	3.0x10 ⁻⁴	0.95	4.36	94.70

CH₂NH₂⁺ into CH₄17 = CH₅⁺28 = CH₂N⁺30 = CH₂NH₂⁺CH₂NH₂⁺ INTO METHANE

% SECONDARY ION FLUX Vs. PRESSURE

+ = 17

x = 28



% SECONDARY ION FLUX

	PRESSURES in torr			m/e	
	INITIAL ION	ION	PENNING	17	28
	GAUGE	GAUGE	GAUGE		
(A)	7.5x10 ⁻⁷	1.5x10 ⁻⁶	1.5x10 ⁻⁵	0.00	00.00
(B)	7.5x10 ⁻⁷	2.3x10 ⁻⁶	3.0x10 ⁻⁵	0.00	00.00
(C)	7.5x10 ⁻⁷	3.0x10 ⁻⁶	6.0x10 ⁻⁵	0.00	00.00
(D)	7.5x10 ⁻⁷	7.5x10 ⁻⁶	3.0x10 ⁻⁴	2.52	97.48
(E)	7.5x10 ⁻⁷	1.5x10 ⁻⁵	7.5x10 ⁻⁴	3.33	96.67

% TOTAL ION FLUX

	PRESSURES in torr			m/e		
	INITIAL ION	ION	PENNING	17	28	30
	GAUGE	GAUGE	GAUGE			
	7.5x10 ⁻⁷	1.5x10 ⁻⁶	1.5x10 ⁻⁵	0.00	0.41	99.59
	7.5x10 ⁻⁷	2.3x10 ⁻⁶	3.0x10 ⁻⁵	0.00	0.44	99.56
	7.5x10 ⁻⁷	3.0x10 ⁻⁶	6.0x10 ⁻⁵	0.00	0.51	99.49
	7.5x10 ⁻⁷	7.5x10 ⁻⁶	3.0x10 ⁻⁴	0.02	0.71	99.27
	7.5x10 ⁻⁷	1.5x10 ⁻⁵	7.5x10 ⁻⁴	0.03	0.85	99.12

CH₂N⁺ into CH₄

15 = CH₃⁺

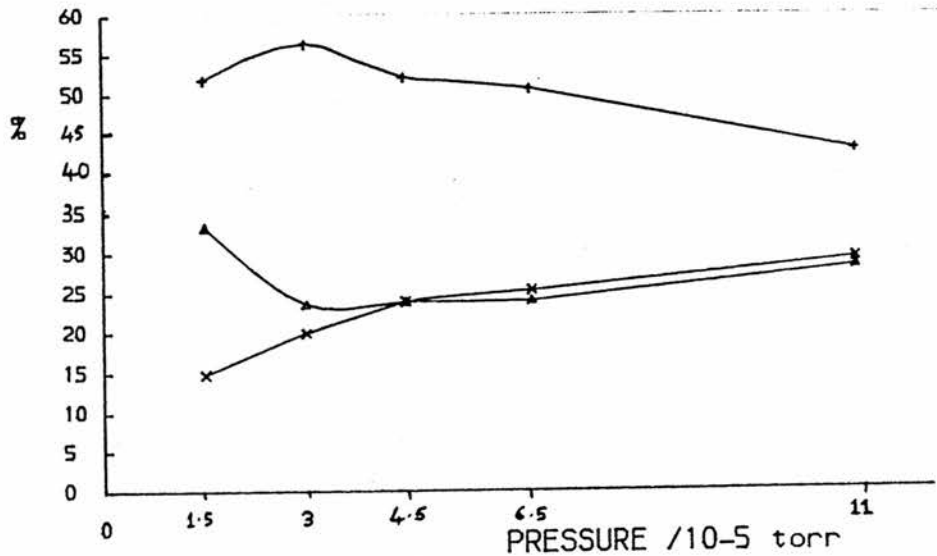
28 = CH₂N⁺

17 = CH₅⁺

29 = C₂H₅⁺

CH₂N⁺ INTO METHANE

% SECONDARY ION FLUX Vs. PRESSURE



+ = 15
x = 17
Δ = 29

% SECONDARY ION FLUX

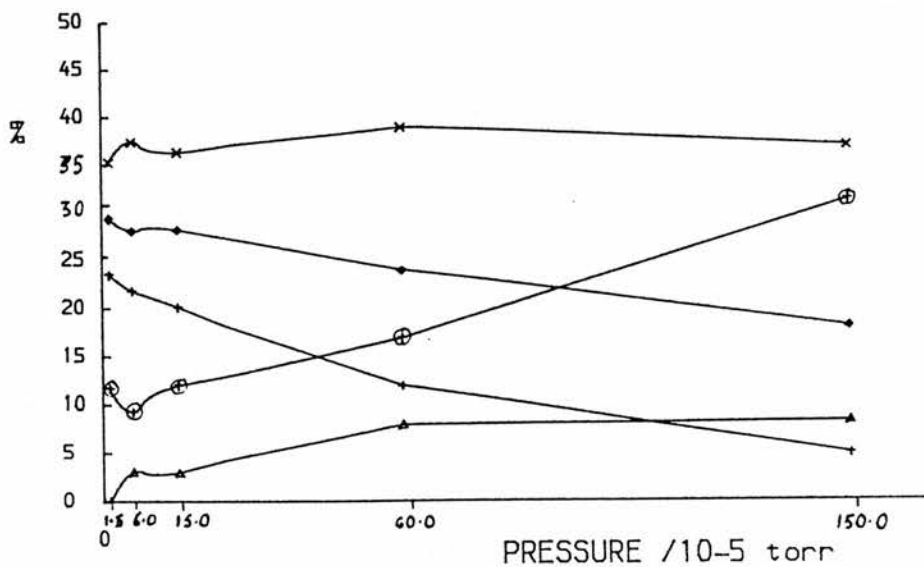
	PRESSURES in torr			m/e		
	INITIAL ION	ION	PENNING			
	GAUGE	GAUGE	GAUGE	15	17	29
(A)	7.5x10 ⁻⁷	1.5x10 ⁻⁶	1.5x10 ⁻⁵	51.85	14.81	33.33
(B)	7.5x10 ⁻⁷	2.3x10 ⁻⁶	3.0x10 ⁻⁵	56.36	20.00	23.64
(C)	7.5x10 ⁻⁷	3.0x10 ⁻⁶	4.5x10 ⁻⁵	52.11	23.94	23.94
(D)	7.5x10 ⁻⁷	3.4x10 ⁻⁶	6.4x10 ⁻⁵	50.63	25.32	24.05
(E)	7.5x10 ⁻⁷	4.5x10 ⁻⁵	1.1x10 ⁻⁴	42.72	29.13	28.16

% TOTAL ION FLUX

	PRESSURE in torr			m/e			
	INITIAL ION	ION	PENNING				
	GAUGE	GAUGE	GAUGE	15	17	28	29
	7.5x10 ⁻⁷	1.5x10 ⁻⁶	1.5x10 ⁻⁵	0.24	0.07	99.53	0.16
	7.5x10 ⁻⁷	2.3x10 ⁻⁶	3.0x10 ⁻⁵	0.58	0.21	98.97	0.24
	7.5x10 ⁻⁷	3.0x10 ⁻⁶	4.5x10 ⁻⁵	0.74	0.34	98.57	0.34
	7.5x10 ⁻⁷	3.4x10 ⁻⁶	6.4x10 ⁻⁵	0.82	0.41	98.38	0.39
	7.5x10 ⁻⁷	4.5x10 ⁻⁵	1.1x10 ⁻⁴	1.07	0.73	97.49	0.71

C₂H₃⁺ into CH₄15 = CH₃⁺ 29 = C₂H₅⁺17 = CH₅⁺ 39 = C₃H₃⁺27 = C₂H₃⁺ 41 = C₃H₅⁺C₂H₃⁺ INTO METHANE

% SECONDARY ION FLUX Vs. PRESSURE



% SECONDARY ION FLUX

	PRESSURE in torr			m/e				
	INITIAL ION	ION	PENNING	15	17	29	39	41
	GAUGE	GAUGE	GAUGE					
(A)	7.5×10 ⁻⁷	1.5×10 ⁻⁶	1.5×10 ⁻⁵	23.53	35.29	0.00	29.41	11.76
(B)	7.5×10 ⁻⁷	3.8×10 ⁻⁶	6.0×10 ⁻⁵	21.88	37.50	3.13	28.13	9.38
(C)	7.5×10 ⁻⁷	6.0×10 ⁻⁶	1.5×10 ⁻⁴	20.20	36.36	3.03	28.28	12.12
(D)	7.5×10 ⁻⁷	1.5×10 ⁻⁵	6.0×10 ⁻⁴	12.00	39.00	8.00	24.00	17.00
(E)	7.5×10 ⁻⁷	3.0×10 ⁻⁵	1.5×10 ⁻³	4.90	37.06	8.39	18.18	31.47

% TOTAL ION FLUX

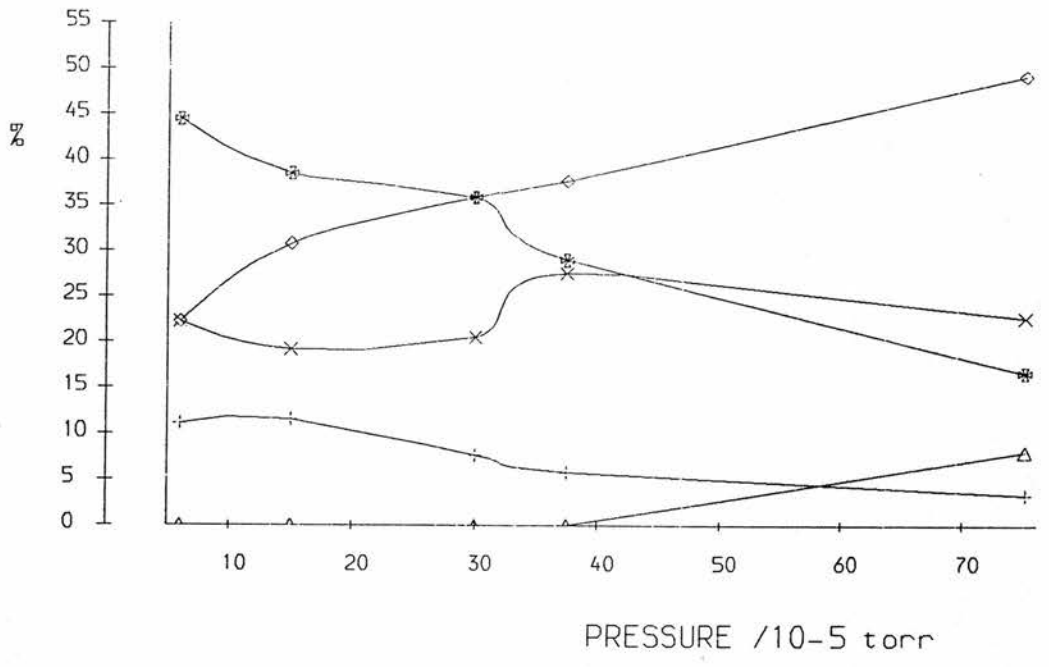
	PRESSURES in torr			m/e					
	INITIAL ION	ION	PENNING	15	17	27	29	39	41
	GAUGE	GAUGE	GAUGE						
	7.5×10 ⁻⁷	1.5×10 ⁻⁶	1.5×10 ⁻⁵	0.03	0.05	99.86	0.00	0.04	0.02
	7.5×10 ⁻⁷	3.8×10 ⁻⁶	6.0×10 ⁻⁵	0.15	0.26	99.29	0.02	0.20	0.07
	7.5×10 ⁻⁷	6.0×10 ⁻⁶	1.5×10 ⁻⁴	0.27	0.49	98.64	0.04	0.38	0.16
	7.5×10 ⁻⁷	1.5×10 ⁻⁵	6.0×10 ⁻⁴	0.73	2.39	93.88	0.49	1.47	1.04
	7.5×10 ⁻⁷	3.0×10 ⁻⁵	1.5×10 ⁻³	0.90	6.83	81.58	1.55	3.35	5.80

C₂H₅⁺ into CH₄

- 15 = CH₃⁺ 29 = C₂H₅⁺
- 17 = CH₅⁺ 39 = C₃H₃⁺
- 27 = C₂H₃⁺ 41 = C₃H₅⁺

C₂H₅⁺ INTO METHANE

% SECONDARY ION FLUX V.S. PRESSURE



- + = 15
- x = 17
- Δ = 39
- \diamond = 41
- * = 43

% SECONDARY ION FLUX

	PRESSURES in torr			m/e				
	INITIAL ION	ION	PENNING					
	GAUGE	GAUGE	GAUGE	15	17	39	41	43
(A)	7.5x10 ⁻⁷	2.3x10 ⁻⁶	6.0x10 ⁻⁵	11.11	22.22	0.00	22.22	44.44
(B)	7.5x10 ⁻⁷	3.8x10 ⁻⁶	1.5x10 ⁻⁴	11.54	19.23	0.00	30.77	38.46
(C)	7.5x10 ⁻⁷	7.5x10 ⁻⁶	3.0x10 ⁻⁴	7.69	20.51	0.00	35.90	35.90
(D)	7.5x10 ⁻⁷	1.5x10 ⁻⁵	3.8x10 ⁻⁴	5.80	27.54	0.00	37.68	28.99
(E)	7.5x10 ⁻⁷	2.3x10 ⁻⁵	7.5x10 ⁻⁴	3.33	22.67	8.00	49.33	16.67

% TOTAL ION FLUX

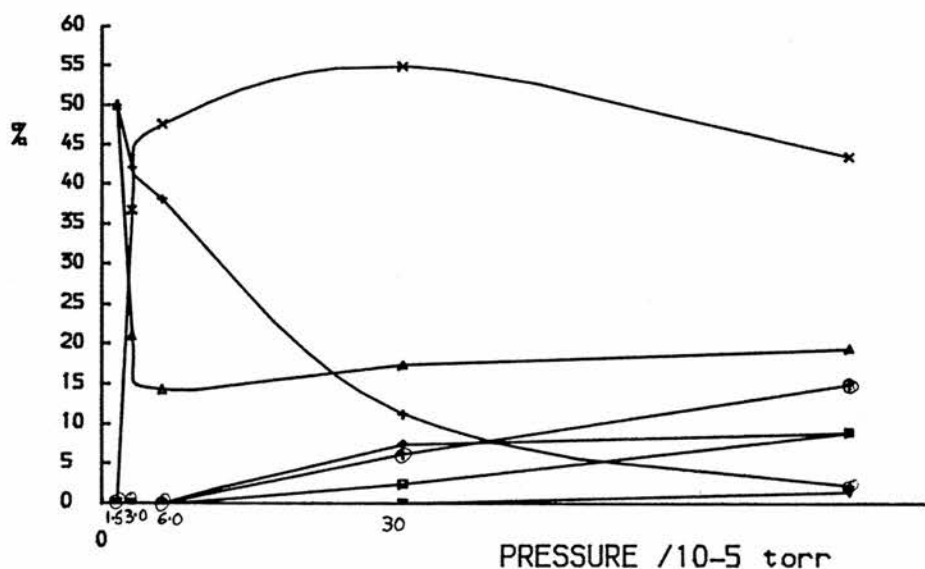
	PRESSURES in torr			m/e					
	INITIAL ION	ION	PENNING						
	GAUGE	GAUGE	GAUGE	15	17	29	39	41	43
	7.5x10 ⁻⁷	2.3x10 ⁻⁶	6.0x10 ⁻⁵	0.01	0.02	99.91	0.00	0.02	0.04
	7.5x10 ⁻⁷	3.8x10 ⁻⁶	1.5x10 ⁻⁴	0.03	0.05	99.74	0.00	0.08	0.10
	7.5x10 ⁻⁷	7.5x10 ⁻⁶	3.0x10 ⁻⁴	0.03	0.08	99.61	0.00	0.14	0.14
	7.5x10 ⁻⁷	1.5x10 ⁻⁵	3.8x10 ⁻⁴	0.04	0.19	99.31	0.00	0.26	0.20
	7.5x10 ⁻⁷	2.3x10 ⁻⁵	7.5x10 ⁻⁴	0.05	0.34	98.50	0.12	0.74	0.25

CHO⁺ into C₂H₆

15 = CH ₃ ⁺	31 = C ₂ H ₇ ⁺	55 = C ₄ H ₇ ⁺
27 = C ₂ H ₃ ⁺	41 = C ₃ H ₅ ⁺	57 = C ₄ H ₉ ⁺
29 = C ₂ H ₅ ⁺	43 = C ₃ H ₇ ⁺	

CHO⁺ INTO ETHANE

% SECONDARY ION FLUX Vs. PRESSURE



% SECONDARY ION FLUX

PRESSURES In torr			m/e							
INITIAL ION GAUGE	ION GAUGE	PENNING GAUGE	15	27	31	41	43	55	57	
(A)	7.5×10 ⁻⁷	1.5×10 ⁻⁶	1.5×10 ⁻⁵	50.00	0.00	50.00	0.00	0.00	0.00	0.00
(B)	7.5×10 ⁻⁷	2.3×10 ⁻⁶	3.0×10 ⁻⁵	42.11	36.84	21.05	0.00	0.00	0.00	0.00
(C)	7.5×10 ⁻⁷	5.3×10 ⁻⁶	6.0×10 ⁻⁵	38.10	47.62	14.29	0.00	0.00	0.00	0.00
(D)	7.5×10 ⁻⁷	1.5×10 ⁻⁵	3.0×10 ⁻⁴	11.25	55.00	17.50	7.50	6.25	0.00	2.50
(E)	7.5×10 ⁻⁷	3.0×10 ⁻⁵	7.5×10 ⁻⁴	2.26	43.61	19.55	9.02	15.04	1.50	9.02

% TOTAL ION FLUX

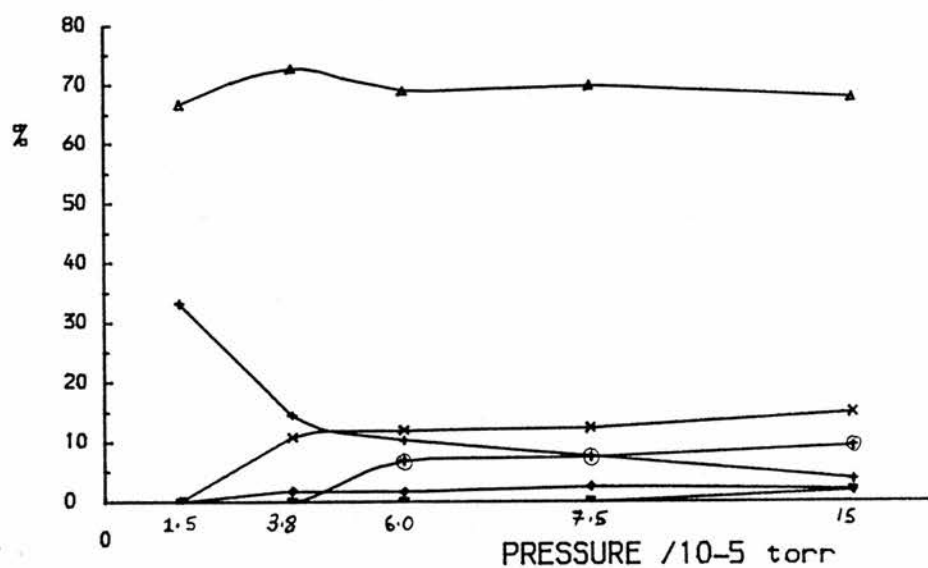
PRESSURES In torr			m/e							
INITIAL ION GAUGE	ION GAUGE	PENNING GAUGE	15	27	29	31	41	43	55	57
7.5×10 ⁻⁷	1.5×10 ⁻⁶	1.5×10 ⁻⁵	0.03	0.00	99.94	0.03	0.00	0.00	0.00	0.00
7.5×10 ⁻⁷	2.3×10 ⁻⁶	3.0×10 ⁻⁵	0.06	0.06	99.85	0.03	0.00	0.00	0.00	0.00
7.5×10 ⁻⁷	5.3×10 ⁻⁶	6.0×10 ⁻⁵	0.14	0.18	99.63	0.05	0.00	0.00	0.00	0.00
7.5×10 ⁻⁷	1.5×10 ⁻⁵	3.0×10 ⁻⁴	0.33	1.60	97.09	0.51	0.22	0.18	0.00	0.07
7.5×10 ⁻⁷	3.0×10 ⁻⁵	7.5×10 ⁻⁴	0.12	2.29	94.75	1.03	0.47	0.79	0.08	0.47

CH₂N⁺ into C₂H₆

15 = CH ₃ ⁺	29 = C ₂ H ₅ ⁺	43 = C ₃ H ₇ ⁺
26 = C ₂ H ₂ ⁺	31 = C ₂ H ₇ ⁺	
28 = CH ₂ N ⁺	41 = C ₃ H ₅ ⁺	

CH₂N⁺ INTO ETHANE

% SECONDARY ION FLUX Vs. PRESSURE



% SECONDARY ION FLUX

	PRESSURES in torr			m/e					
	INITIAL ION	ION	PENNING	15	26	29	31	41	43
	GAUGE	GAUGE	GAUGE						
(A)	7.5×10 ⁻⁷	1.5×10 ⁻⁶	1.5×10 ⁻⁵	33.33	0.00	66.67	0.00	0.00	0.00
(B)	7.5×10 ⁻⁷	3.8×10 ⁻⁶	3.8×10 ⁻⁵	14.55	10.91	72.73	1.82	0.00	0.00
(C)	7.5×10 ⁻⁷	6.0×10 ⁻⁶	6.0×10 ⁻⁵	10.34	12.07	68.97	1.72	6.90	0.00
(D)	7.5×10 ⁻⁷	7.5×10 ⁻⁶	9.8×10 ⁻⁵	7.50	12.50	70.00	2.50	7.50	0.00
(E)	7.5×10 ⁻⁷	1.5×10 ⁻⁵	1.5×10 ⁻⁴	3.77	15.09	67.92	1.89	9.43	1.89

% TOTAL ION FLUX

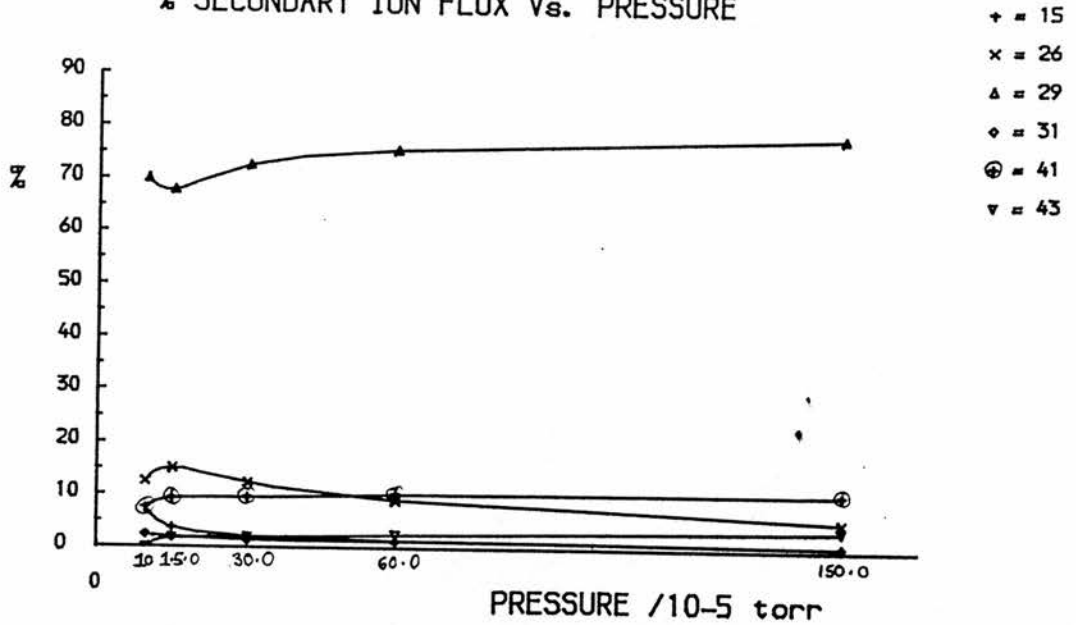
	PRESSURES in torr			m/e						
	INITIAL ION	ION	PENNING	15	26	28	29	31	41	43
	GAUGE	GAUGE	GAUGE							
	7.5×10 ⁻⁷	1.5×10 ⁻⁶	1.5×10 ⁻⁵	0.02	0.00	99.94	0.04	0.00	0.00	0.00
	7.5×10 ⁻⁷	3.8×10 ⁻⁶	3.8×10 ⁻⁵	0.04	0.03	99.71	0.21	0.01	0.00	0.00
	7.5×10 ⁻⁷	6.0×10 ⁻⁶	6.0×10 ⁻⁵	1.97	2.30	80.92	13.16	0.33	1.32	0.00
	7.5×10 ⁻⁷	7.5×10 ⁻⁶	9.8×10 ⁻⁵	0.08	0.13	98.94	0.74	0.03	0.08	0.00
	7.5×10 ⁻⁷	1.5×10 ⁻⁵	1.5×10 ⁻⁴	0.06	0.25	98.34	1.13	0.03	0.16	0.03

CH₂N⁺ into C₂H₆

15 = CH₃⁺ 29 = C₂H₅⁺ 43 = C₃H₇⁺
 26 = C₂H₂⁺ 31 = C₂H₇⁺
 28 = CH₂N⁺ 41 = C₃H₅⁺

CH₂N⁺ INTO ETHANE

% SECONDARY ION FLUX Vs. PRESSURE



% SECONDARY ION FLUX

	PRESSURES in torr			m/e					
	INITIAL ION	ION	PENNING	15	26	29	31	41	43
	GAUGE	GAUGE	GAUGE						
(A)	7.5×10 ⁻⁷	7.5×10 ⁻⁶	9.8×10 ⁻⁵	7.50	12.50	70.00	2.50	7.50	0.00
(B)	7.5×10 ⁻⁷	1.5×10 ⁻⁵	1.5×10 ⁻⁴	3.77	15.09	67.92	1.89	9.43	1.89
(C)	7.5×10 ⁻⁷	1.9×10 ⁻⁵	3.0×10 ⁻⁴	2.05	12.33	72.60	1.37	9.59	2.05
(D)	7.5×10 ⁻⁷	3.0×10 ⁻⁵	6.0×10 ⁻⁴	1.28	8.97	75.64	1.28	10.26	2.56
(E)	7.5×10 ⁻⁷	3.8×10 ⁻⁵	1.5×10 ⁻³	0.77	5.38	78.46	0.77	10.77	3.85

% TOTAL ION FLUX

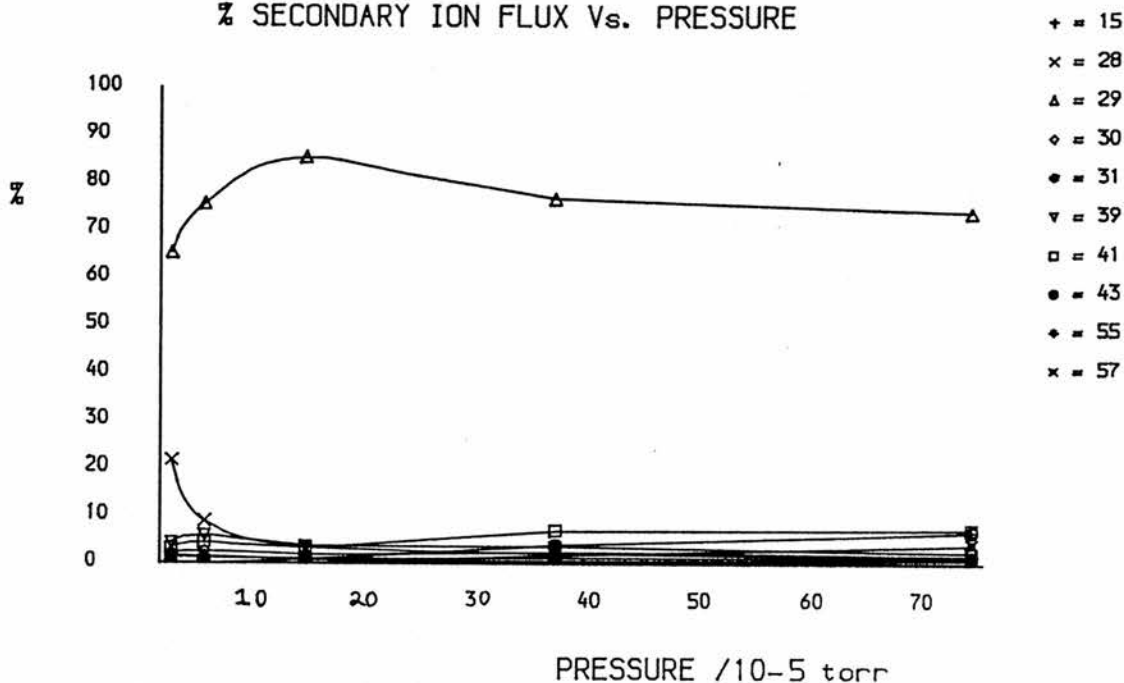
	PRESSURES in torr			m/e						
	INITIAL ION	ION	PENNING	15	26	28	29	31	41	43
	GAUGE	GAUGE	GAUGE							
	7.5×10 ⁻⁷	7.5×10 ⁻⁶	9.8×10 ⁻⁵	0.08	0.13	98.94	0.74	0.03	0.08	0.00
	7.5×10 ⁻⁷	1.5×10 ⁻⁵	1.5×10 ⁻⁴	0.06	0.25	98.34	1.13	0.05	0.16	0.03
	7.5×10 ⁻⁷	1.9×10 ⁻⁵	3.0×10 ⁻⁴	0.07	0.41	96.64	2.44	0.05	0.32	0.07
	7.5×10 ⁻⁷	3.0×10 ⁻⁵	6.0×10 ⁻⁴	0.08	0.53	94.05	4.50	0.08	0.61	0.15
	7.5×10 ⁻⁷	3.8×10 ⁻⁵	1.5×10 ⁻³	0.09	0.62	88.50	9.03	0.09	1.24	0.44

C₂H₃⁺ into C₂H₆

15 = CH ₃ ⁺	30 = C ₂ H ₆ ⁺	43 = C ₃ H ₇ ⁺
27 = C ₂ H ₃ ⁺	31 = C ₂ H ₇ ⁺	55 = C ₄ H ₇ ⁺
28 = C ₂ H ₄ ⁺	39 = C ₃ H ₃ ⁺	57 = C ₄ H ₉ ⁺
29 = C ₂ H ₅ ⁺	41 = C ₃ H ₅ ⁺	

C₂H₃⁺ INTO C₂H₆

% SECONDARY ION FLUX Vs. PRESSURE



% SECONDARY ION FLUX

	PRESSURES In torr			m/e									
	INITIAL ION GAUGE	ION GAUGE	PENNING GAUGE	15	28	29	30	31	39	41	43	55	57
(A)	7.5×10 ⁻⁷	1.5×10 ⁻⁶	3.0×10 ⁻⁵	1.63	21.74	65.22	2.17	1.63	4.35	3.26	0.00	0.00	0.00
(B)	7.5×10 ⁻⁷	3.8×10 ⁻⁶	6.0×10 ⁻⁵	1.48	8.89	75.56	2.59	1.11	5.93	4.44	0.00	0.00	0.00
(C)	7.5×10 ⁻⁷	7.5×10 ⁻⁶	1.5×10 ⁻⁴	0.70	3.26	85.34	1.86	0.93	3.72	3.26	0.93	0.00	0.00
(D)	7.5×10 ⁻⁷	1.9×10 ⁻⁵	3.8×10 ⁻⁴	0.41	2.17	76.71	2.44	1.35	3.52	7.04	3.93	0.54	1.90
(E)	7.5×10 ⁻⁷	3.0×10 ⁻⁵	7.5×10 ⁻⁴	0.16	1.23	73.95	1.73	1.15	2.38	7.40	6.82	0.99	4.19

% TOTAL ION FLUX

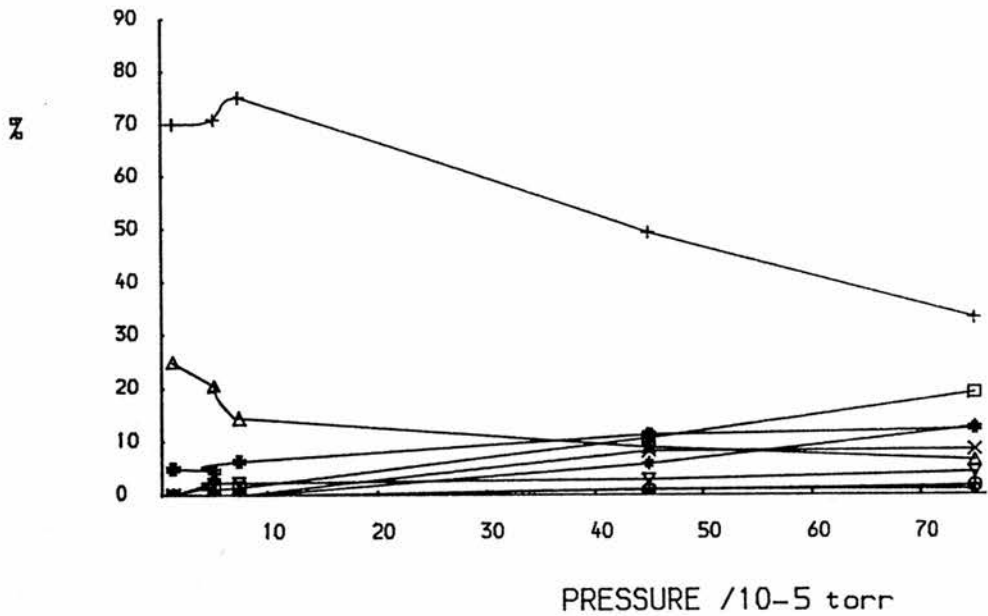
	PRESSURES In torr			m/e										
	INITIAL ION GAUGE	ION GAUGE	PENNING GAUGE	15	27	28	29	30	31	39	41	43	55	57
	7.5×10 ⁻⁷	1.5×10 ⁻⁶	3.0×10 ⁻⁵	0.02	98.86	0.25	0.74	0.02	0.02	0.05	0.04	0.00	0.00	0.00
	7.5×10 ⁻⁷	3.8×10 ⁻⁶	6.0×10 ⁻⁵	0.04	97.37	0.23	1.99	0.07	0.03	0.16	0.12	0.00	0.00	0.00
	7.5×10 ⁻⁷	7.5×10 ⁻⁶	1.5×10 ⁻⁴	0.09	86.56	0.44	11.47	0.25	0.13	0.50	0.44	0.13	0.00	0.00
	7.5×10 ⁻⁷	1.9×10 ⁻⁵	3.8×10 ⁻⁴	0.13	68.42	0.68	24.23	0.77	0.43	1.11	2.22	1.24	0.17	0.60
	7.5×10 ⁻⁷	3.0×10 ⁻⁵	7.5×10 ⁻⁴	0.09	44.27	0.69	41.22	0.96	0.64	1.33	4.12	3.80	0.55	2.34

C₂H₅⁺ into C₂H₆

- | | | |
|---|---|---|
| 27 = C ₂ H ₃ ⁺ | 31 = C ₂ H ₇ ⁺ | 43 = C ₃ H ₇ ⁺ |
| 28 = C ₂ H ₄ ⁺ | 41 = C ₃ H ₅ ⁺ | 55 = C ₄ H ₇ ⁺ |
| 29 = C ₂ H ₅ ⁺ | 42 = C ₃ H ₆ ⁺ | 57 = C ₄ H ₉ ⁺ |
| 30 = C ₂ H ₆ ⁺ | | |

C₂H₅⁺ INTO C₂H₆

% SECONDARY ION FLUX Vs. PRESSURE



- + = 27
- x = 28
- Δ = 30
- ◇ = 31
- = 41
- ∇ = 42
- = 43
- = 55
- ◆ = 57

% SECONDARY ION FLUX

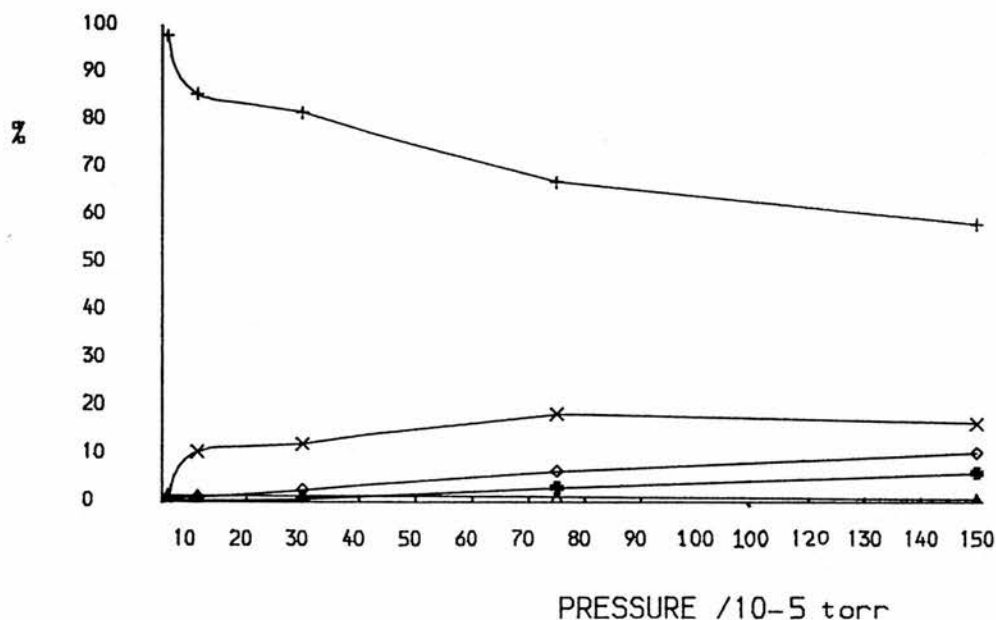
PRESSURES in torr			m/e									
INITIAL ION GAUGE	ION GAUGE	PENNING GAUGE	27	28	30	31	41	42	43	55	57	
(A)	7.5x10 ⁻⁷	1.5x10 ⁻⁶	1.5x10 ⁻⁵	70.00	0.00	25.00	0.00	5.00	0.00	0.00	0.00	0.00
(B)	7.5x10 ⁻⁷	3.0x10 ⁻⁶	5.3x10 ⁻⁵	70.86	0.00	20.57	0.00	4.57	2.29	1.71	0.00	0.00
(C)	7.5x10 ⁻⁷	4.5x10 ⁻⁶	7.5x10 ⁻⁵	75.20	0.00	14.40	0.00	6.40	2.40	1.60	0.00	0.00
(D)	7.5x10 ⁻⁷	2.3x10 ⁻⁵	4.5x10 ⁻⁴	49.38	8.40	8.89	1.23	11.36	2.96	10.86	0.99	5.93
(E)	7.5x10 ⁻⁷	3.0x10 ⁻⁵	7.5x10 ⁻⁴	33.21	8.57	6.43	1.07	12.50	4.29	19.29	1.79	12.86

% TOTAL ION FLUX

PRESSURES in torr			m/e									
INITIAL ION GAUGE	ION GAUGE	PENNING GAUGE	27	28	29	30	31	41	42	43	55	57
7.5x10 ⁻⁷	1.5x10 ⁻⁶	1.5x10 ⁻⁵	0.86	0.00	98.77	0.31	0.00	0.06	0.00	0.00	0.00	0.00
7.5x10 ⁻⁷	3.0x10 ⁻⁶	5.3x10 ⁻⁵	1.32	0.00	98.13	0.38	0.00	0.09	0.04	0.03	0.00	0.00
7.5x10 ⁻⁷	4.5x10 ⁻⁶	7.5x10 ⁻⁵	97.20	2.11	0.00	0.40	0.00	0.18	0.07	0.04	0.00	0.00
7.5x10 ⁻⁷	2.3x10 ⁻⁵	4.5x10 ⁻⁴	7.68	1.31	84.45	1.38	0.19	1.77	0.46	1.69	0.15	0.92
7.5x10 ⁻⁷	3.0x10 ⁻⁵	7.5x10 ⁻⁴	7.27	1.88	78.13	1.41	0.23	2.73	0.94	4.22	0.39	2.81

C₂H₆⁺ into C₂H₆ MAIN PEAKS

28 = C₂H₄⁺ 31 = C₂H₇⁺
 29 = C₂H₅⁺ 42 = C₃H₆⁺
 30 = C₂H₆⁺ 43 = C₃H₇⁺

C₂H₆⁺ INTO C₂H₆ MAIN PEAKS% SECONDARY ION FLUX Vs. PRESSURE% SECONDARY ION FLUX

	PRESSURES in torr			m/e				
	INITIAL ION	ION	PENNING	28	29	31	42	43
	GAUGE	GAUGE	GAUGE					
(A)	7.5×10 ⁻⁷	2.3×10 ⁻⁶	6.0×10 ⁻⁵	97.82	0.00	1.25	0.62	0.31
(B)	7.5×10 ⁻⁷	4.5×10 ⁻⁶	1.1×10 ⁻⁴	85.49	10.58	1.44	1.12	0.32
(C)	7.5×10 ⁻⁷	1.5×10 ⁻⁵	3.0×10 ⁻⁴	81.53	12.23	1.40	2.62	0.70
(D)	7.5×10 ⁻⁷	3.0×10 ⁻⁵	7.5×10 ⁻⁴	66.95	18.47	0.97	6.51	3.05
(E)	7.5×10 ⁻⁷	4.5×10 ⁻⁵	1.5×10 ⁻³	58.22	16.53	0.66	10.33	6.20

% TOTAL ION FLUX

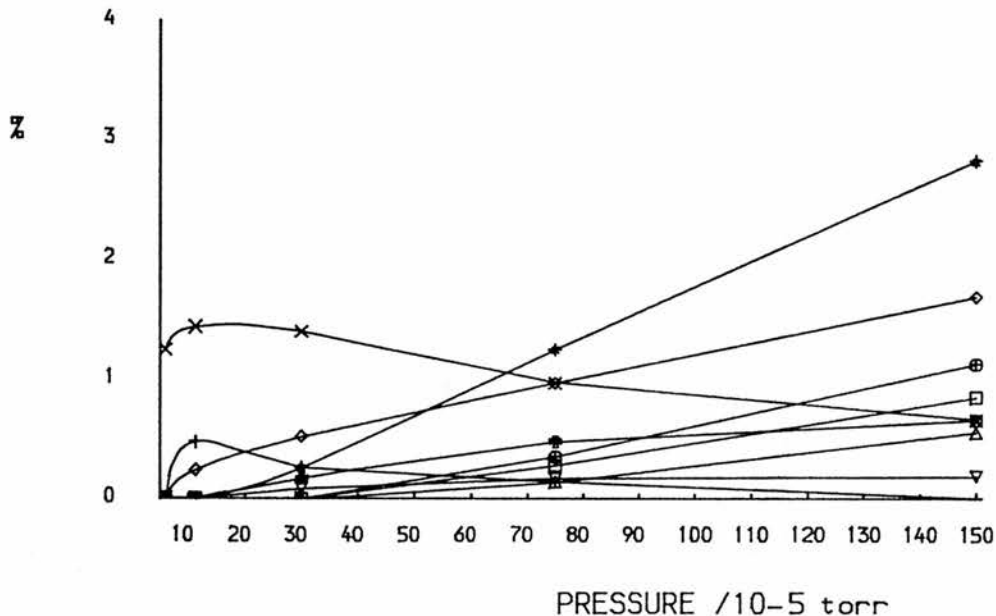
	PRESSURES in torr			m/e					
	INITIAL ION	ION	PENNING	28	29	30	31	42	43
	GAUGE	GAUGE	GAUGE						
	7.5×10 ⁻⁷	2.3×10 ⁻⁶	6.0×10 ⁻⁵	6.13	0.00	93.73	0.08	0.04	0.02
	7.5×10 ⁻⁷	4.5×10 ⁻⁶	1.1×10 ⁻⁴	12.24	1.51	85.68	0.21	0.16	0.05
	7.5×10 ⁻⁷	1.5×10 ⁻⁵	3.0×10 ⁻⁴	32.43	4.86	60.22	0.56	1.04	0.28
	7.5×10 ⁻⁷	3.0×10 ⁻⁵	7.5×10 ⁻⁴	53.39	14.73	20.25	0.77	5.19	2.43
	7.5×10 ⁻⁷	4.5×10 ⁻⁵	1.5×10 ⁻³	53.96	15.32	7.31	0.61	9.57	5.74

C₂H₆⁺ into C₂H₆ MINOR PEAKS

- 15 = CH₃⁺ 41 = C₃H₅⁺ 55 = C₄H₇⁺
- 30 = C₂H₆⁺ 44 = C₃H₈⁺ 56 = C₄H₈⁺
- 31 = C₂H₇⁺ 45 = C₃H₉⁺ 57 = C₄H₉⁺
- 39 = C₃H₃⁺

C₂H₆⁺ INTO C₂H₆ MINOR PEAKS

% SECONDARY ION FLUX Vs. PRESSURE



% SECONDARY ION FLUX

PRESSURES In torr			m/e								
INITIAL ION GAUGE	ION GAUGE	PENNING GAUGE	15	31	39	41	44	45	55	56	57
(A)	7.5x10 ⁻⁷	2.3x10 ⁻⁶	6.0x10 ⁻⁵	0.00	1.25	0.00	0.00	0.00	0.00	0.00	0.00
(B)	7.5x10 ⁻⁷	4.5x10 ⁻⁶	1.1x10 ⁻⁴	0.48	1.44	0.00	0.24	0.00	0.00	0.00	0.00
(C)	7.5x10 ⁻⁷	1.5x10 ⁻⁵	3.0x10 ⁻⁴	0.26	1.40	0.00	0.52	0.17	0.09	0.00	0.26
(D)	7.5x10 ⁻⁷	3.0x10 ⁻⁵	7.5x10 ⁻⁴	0.14	0.97	0.14	0.97	0.48	0.17	0.28	0.35
(E)	7.5x10 ⁻⁷	4.5x10 ⁻⁵	1.5x10 ⁻³	0.00	0.66	0.56	1.69	0.66	0.19	0.85	1.13

% TOTAL ION FLUX

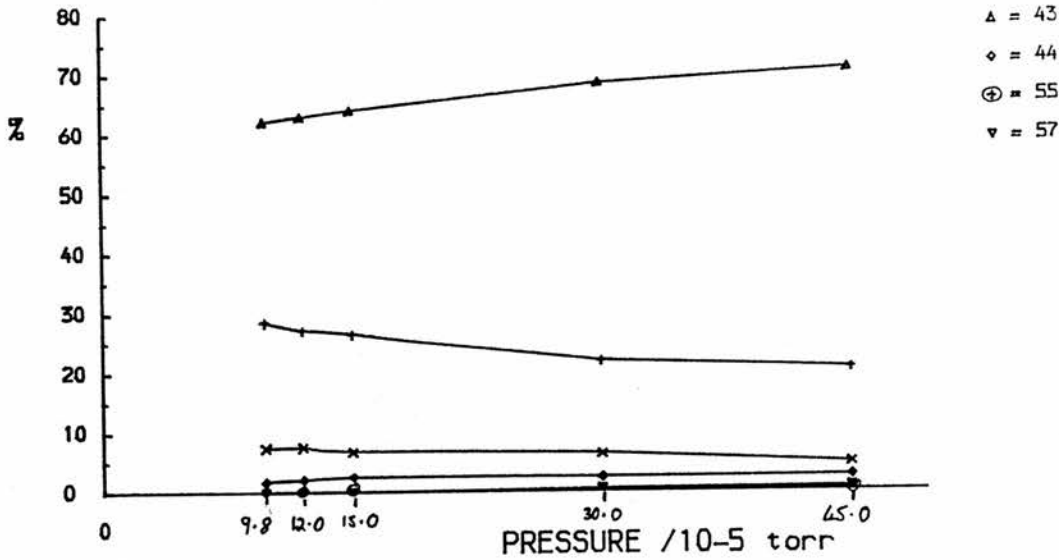
PRESSURES In torr			m/e									
INITIAL ION GAUGE	ION GAUGE	PENNING GAUGE	15	30	31	39	41	44	45	55	56	57
7.5x10 ⁻⁷	2.3x10 ⁻⁶	6.0x10 ⁻⁵	0.00	93.73	0.08	0.00	0.00	0.00	0.00	0.00	0.00	0.00
7.5x10 ⁻⁷	4.5x10 ⁻⁶	1.1x10 ⁻⁴	0.07	85.68	0.21	0.00	0.03	0.00	0.00	0.00	0.00	0.00
7.5x10 ⁻⁷	1.5x10 ⁻⁵	3.0x10 ⁻⁴	0.10	60.22	0.56	0.00	0.21	0.07	0.03	0.00	0.00	0.10
7.5x10 ⁻⁷	3.0x10 ⁻⁵	7.5x10 ⁻⁴	0.11	20.25	0.77	0.11	0.77	0.39	0.14	0.22	0.28	0.99
7.5x10 ⁻⁷	4.5x10 ⁻⁵	1.5x10 ⁻³	0.00	7.31	0.61	0.52	1.57	0.61	0.17	0.78	1.04	2.61

CHO⁺ into C₃H₈

- 27 = C₂H₃⁺ 43 = C₃H₇⁺ 55 = C₄H₇⁺
 29 = C₂H₅⁺ 44 = C₃H₈⁺ 57 = C₄H₉⁺
 41 = C₃H₅⁺

CHO⁺ INTO PROPANE

% SECONDARY ION FLUX Vs. PRESSURE



% SECONDARY ION FLUX

PRESSURES in torr			m/e					
INITIAL ION GAUGE	ION GAUGE	PENNING GAUGE	27	41	43	44	55	57
(A) 7.5x10 ⁻⁷	7.5x10 ⁻⁶	9.8x10 ⁻⁵	28.57	7.45	62.11	1.86	0.00	0.00
(B) 7.5x10 ⁻⁷	1.1x10 ⁻⁵	1.2x10 ⁻⁴	27.17	7.61	63.04	2.17	0.00	0.00
(C) 7.5x10 ⁻⁷	1.5x10 ⁻⁵	1.5x10 ⁻⁴	26.50	6.84	64.10	2.56	0.00	0.00
(D) 7.5x10 ⁻⁷	2.3x10 ⁻⁵	3.0x10 ⁻⁴	21.90	6.33	68.61	2.43	0.24	0.49
(E) 7.5x10 ⁻⁷	2.6x10 ⁻⁵	4.5x10 ⁻⁴	20.65	4.73	70.97	2.58	0.43	0.65

% TOTAL ION FLUX

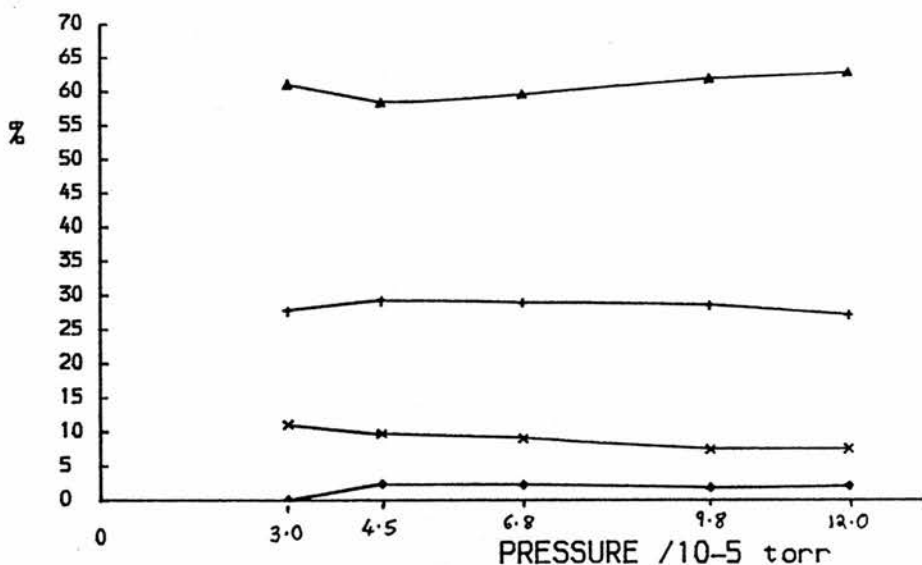
PRESSURES in torr			m/e						
INITIAL ION GAUGE	ION GAUGE	PENNING GAUGE	27	29	41	43	44	55	57
7.5x10 ⁻⁷	7.5x10 ⁻⁶	9.8x10 ⁻⁵	0.65	97.71	0.17	1.42	0.04	0.00	0.00
7.5x10 ⁻⁷	1.1x10 ⁻⁵	1.2x10 ⁻⁴	0.73	97.31	0.20	1.69	0.06	0.00	0.00
7.5x10 ⁻⁷	1.5x10 ⁻⁵	1.5x10 ⁻⁴	0.97	96.32	0.25	2.36	0.09	0.00	0.00
7.5x10 ⁻⁷	2.3x10 ⁻⁵	3.0x10 ⁻⁴	1.92	91.21	0.56	6.03	0.21	0.02	0.04
7.5x10 ⁻⁷	2.6x10 ⁻⁵	4.5x10 ⁻⁴	2.36	88.56	0.54	8.12	0.30	0.05	0.07

CHO⁺ into C₃H₈

27 = C₂H₃⁺ 43 = C₃H₇⁺
 28 = CHO⁺ 44 = C₃H₈⁺
 41 = C₃H₅⁺

CHO⁺ INTO PROPANE

% SECONDARY ION FLUX Vs. PRESSURE



+ = 27
 x = 41
 Δ = 43
 ◊ = 44

% SECONDARY ION FLUX

	PRESSURES in torr			m/e			
	INITIAL ION	ION	PENNING	27	41	43	44
	GAUGE	GAUGE	GAUGE				
(A)	7.5×10 ⁻⁷	3.8×10 ⁻⁶	3.0×10 ⁻⁵	27.78	11.11	61.11	0.00
(B)	7.5×10 ⁻⁷	6.0×10 ⁻⁶	4.5×10 ⁻⁵	29.27	9.76	58.54	2.44
(C)	7.5×10 ⁻⁷	7.5×10 ⁻⁶	6.8×10 ⁻⁵	28.96	9.05	59.73	2.26
(D)	7.5×10 ⁻⁷	7.5×10 ⁻⁶	9.8×10 ⁻⁵	28.57	7.45	62.11	1.86
(E)	7.5×10 ⁻⁷	1.1×10 ⁻⁵	1.2×10 ⁻⁴	27.17	7.61	63.04	2.17

% TOTAL ION FLUX

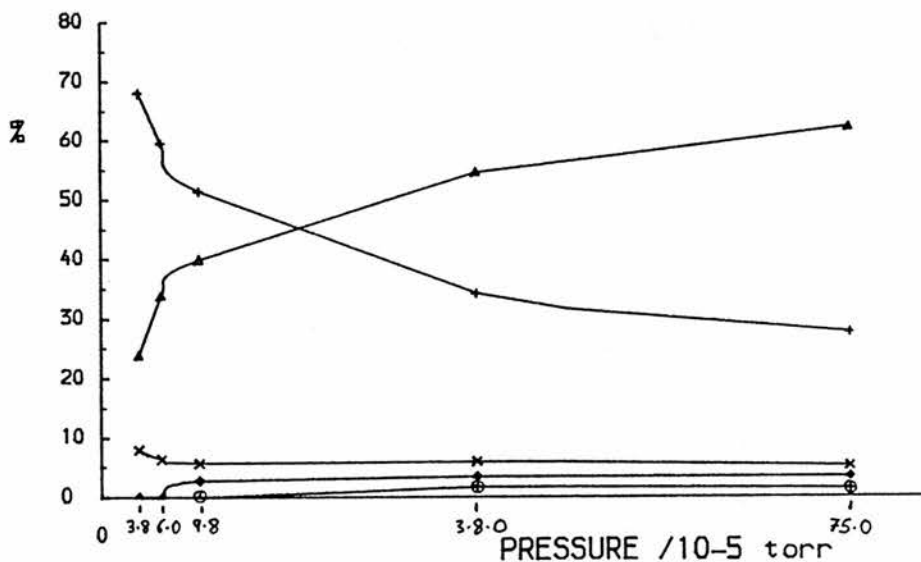
	PRESSURES in torr			m/e				
	INITIAL ION	ION	PENNING	27	29	41	43	44
	GAUGE	GAUGE	GAUGE					
	7.5×10 ⁻⁷	3.8×10 ⁻⁶	3.0×10 ⁻⁵	0.13	99.55	0.05	0.28	0.00
	7.5×10 ⁻⁷	6.0×10 ⁻⁶	4.5×10 ⁻⁵	0.31	98.93	0.10	0.62	0.03
	7.5×10 ⁻⁷	7.5×10 ⁻⁶	6.8×10 ⁻⁵	0.43	98.50	0.14	0.89	0.03
	7.5×10 ⁻⁷	7.5×10 ⁻⁶	9.8×10 ⁻⁵	0.65	97.71	0.17	1.42	0.04
	7.5×10 ⁻⁷	1.1×10 ⁻⁵	1.2×10 ⁻⁴	0.73	97.31	0.20	1.69	0.06

CH₂N⁺ into C₃H₈

28 = CH₂N⁺ 43 = C₃H₇⁺
 29 = C₂H₅⁺ 44 = C₃H₈⁺
 41 = C₃H₅⁺ 55 = C₄H₇⁺

CH₂N⁺ INTO PROPANE

% SECONDARY ION FLUX Vs. PRESSURE



% SECONDARY ION FLUX

	PRESSURES in torr			m/e				
	INITIAL ION	ION	PENNING	29	41	43	44	55
	GAUGE	GAUGE	GAUGE					
(A)	7.5×10 ⁻⁷	3.0×10 ⁻⁶	3.8×10 ⁻⁵	68.00	8.00	24.00	0.00	0.00
(B)	7.5×10 ⁻⁷	6.0×10 ⁻⁶	6.0×10 ⁻⁵	59.57	6.38	34.04	0.00	0.00
(C)	7.5×10 ⁻⁷	9.8×10 ⁻⁶	9.8×10 ⁻⁵	51.43	5.71	40.00	2.86	0.00
(D)	7.5×10 ⁻⁷	2.3×10 ⁻⁵	3.8×10 ⁻⁴	34.19	5.98	54.70	3.42	1.71
(E)	7.5×10 ⁻⁷	6.0×10 ⁻⁵	7.5×10 ⁻⁴	27.71	5.19	62.34	3.46	1.30

% TOTAL ION FLUX

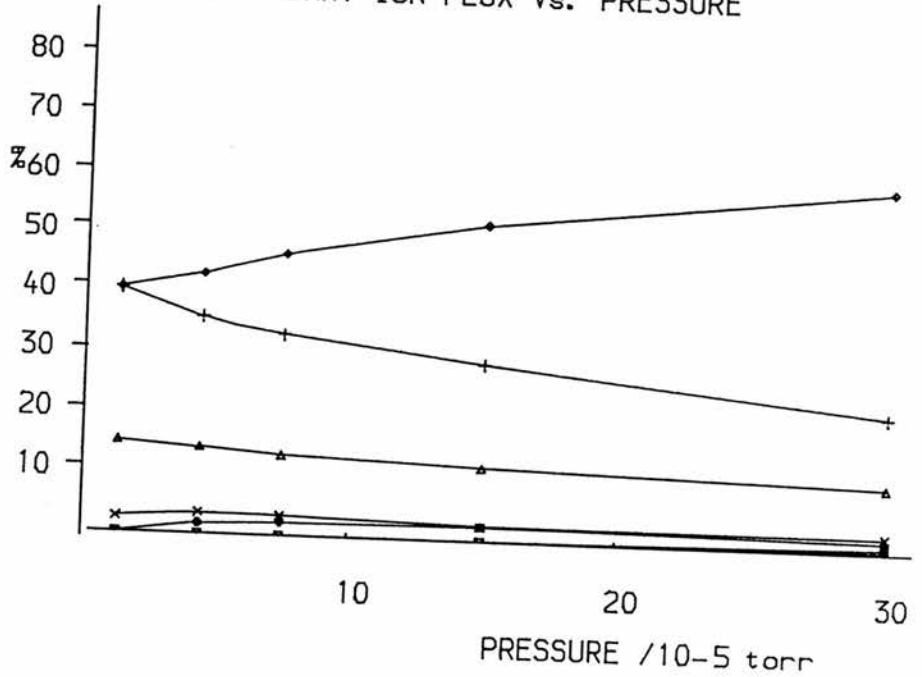
	PRESSURES in torr			m/e					
	INITIAL ION	ION	PENNING	28	29	41	43	44	55
	GAUGE	GAUGE	GAUGE						
	7.5×10 ⁻⁷	3.0×10 ⁻⁶	3.8×10 ⁻⁵	99.61	0.26	0.03	0.09	0.00	0.00
	7.5×10 ⁻⁷	6.0×10 ⁻⁶	6.0×10 ⁻⁵	99.13	0.52	0.06	0.30	0.00	0.00
	7.5×10 ⁻⁷	9.8×10 ⁻⁶	9.8×10 ⁻⁵	98.39	0.83	0.09	0.65	0.05	0.00
	7.5×10 ⁻⁷	2.3×10 ⁻⁵	3.8×10 ⁻⁴	94.29	1.95	0.34	3.12	0.20	0.10
	7.5×10 ⁻⁷	6.0×10 ⁻⁵	7.5×10 ⁻⁴	88.99	3.05	0.57	6.86	0.38	0.14

C₂H₃⁺ into C₃H₈

- 27 = C₂H₃⁺ 41 = C₃H₅⁺ 55 = C₄H₇⁺
 29 = C₂H₅⁺ 43 = C₃H₇⁺ 57 = C₄H₉⁺
 39 = C₃H₃⁺ 44 = C₃H₈⁺

C₂H₃⁺ INTO PROPANE

% SECONDARY ION FLUX Vs. PRESSURE



% SECONDARY ION FLUX

PRESSURES in torr			m/e							
INITIAL ION GAUGE	ION GAUGE	PENNING GAUGE	29	39	41	43	44	55	57	
(A)	7.5x10 ⁻⁷	2.3x10 ⁻⁶	1.5x10 ⁻⁵	41.03	2.56	15.38	41.03	0.00	0.00	0.00
(B)	7.5x10 ⁻⁷	5.3x10 ⁻⁶	4.5x10 ⁻⁵	36.36	3.64	14.55	43.64	1.82	0.00	0.00
(C)	7.5x10 ⁻⁷	7.5x10 ⁻⁶	7.5x10 ⁻⁵	33.71	3.37	13.48	47.19	2.25	0.00	0.00
(D)	7.5x10 ⁻⁷	1.5x10 ⁻⁵	1.5x10 ⁻⁴	29.63	2.47	12.35	53.09	2.47	0.00	0.00
(E)	7.5x10 ⁻⁷	2.3x10 ⁻⁵	3.0x10 ⁻⁴	22.62	2.71	10.86	60.63	1.81	0.45	0.90

% TOTAL ION FLUX

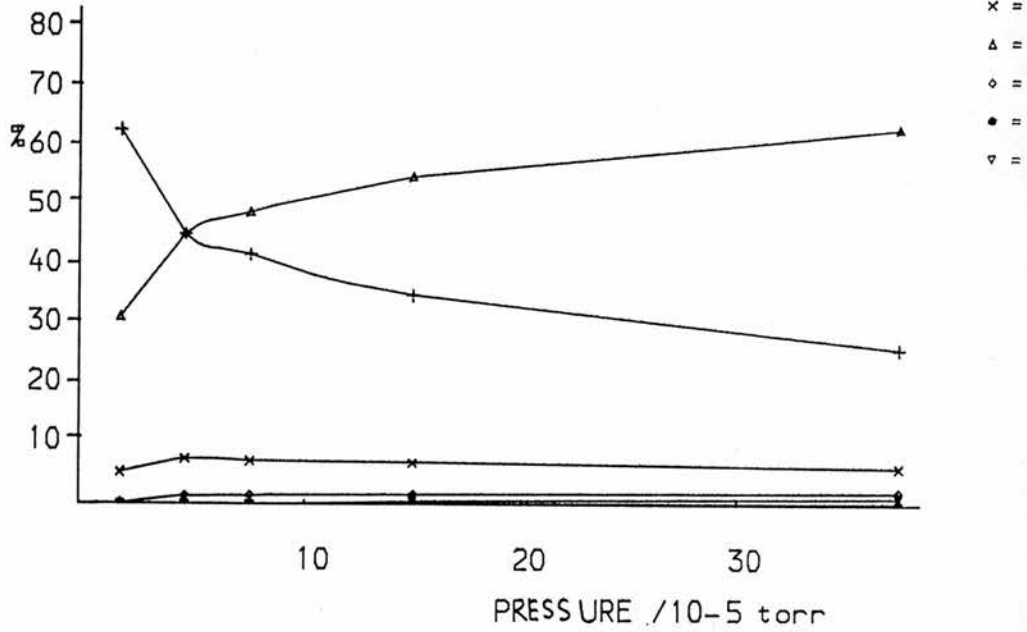
PRESSURES in torr			m/e								
INITIAL ION GAUGE	ION GAUGE	PENNING GAUGE	27	29	39	41	43	44	55	57	
7.5x10 ⁻⁷	2.3x10 ⁻⁶	1.5x10 ⁻⁵	99.57	0.18	0.01	0.07	0.18	0.00	0.00	0.00	
7.5x10 ⁻⁷	5.3x10 ⁻⁶	4.5x10 ⁻⁵	98.68	0.48	0.05	0.19	0.58	0.02	0.00	0.00	
7.5x10 ⁻⁷	7.5x10 ⁻⁶	7.5x10 ⁻⁵	97.39	0.88	0.09	0.35	1.23	0.06	0.00	0.00	
7.5x10 ⁻⁷	1.5x10 ⁻⁵	1.5x10 ⁻⁴	93.91	1.80	0.15	0.75	3.23	0.15	0.00	0.00	
7.5x10 ⁻⁷	2.3x10 ⁻⁵	3.0x10 ⁻⁴	89.48	2.38	0.29	1.14	6.38	0.19	0.05	0.10	

C₂H₅⁺ into C₃H₈

27 = C₂H₃⁺ 43 = C₃H₇⁺ 55 = C₄H₇⁺
 29 = C₂H₅⁺ 44 = C₃H₈⁺ 57 = C₄H₉⁺
 41 = C₃H₅⁺

C₂H₅⁺ INTO PROPANE

% SECONDARY ION FLUX Vs. PRESSURE



% SECONDARY ION FLUX

	PRESSURES in torr			m/e					
	INITIAL ION	ION	PENNING	27	41	43	44	55	57
	GAUGE	GAUGE	GAUGE						
(A)	7.5x10 ⁻⁷	1.5x10 ⁻⁶	1.5x10 ⁻⁵	63.16	5.26	31.58	0.00	0.00	0.00
(B)	7.5x10 ⁻⁷	4.5x10 ⁻⁶	4.5x10 ⁻⁵	45.50	7.58	45.50	1.42	0.00	0.00
(C)	7.5x10 ⁻⁷	7.5x10 ⁻⁶	7.5x10 ⁻⁵	42.05	7.18	49.23	1.54	0.00	0.00
(D)	7.5x10 ⁻⁷	1.5x10 ⁻⁵	1.5x10 ⁻⁴	35.16	6.92	55.33	1.73	0.29	0.58
(E)	7.5x10 ⁻⁷	3.0x10 ⁻⁵	3.8x10 ⁻⁴	26.23	6.19	63.75	2.19	0.36	1.28

% TOTAL ION FLUX

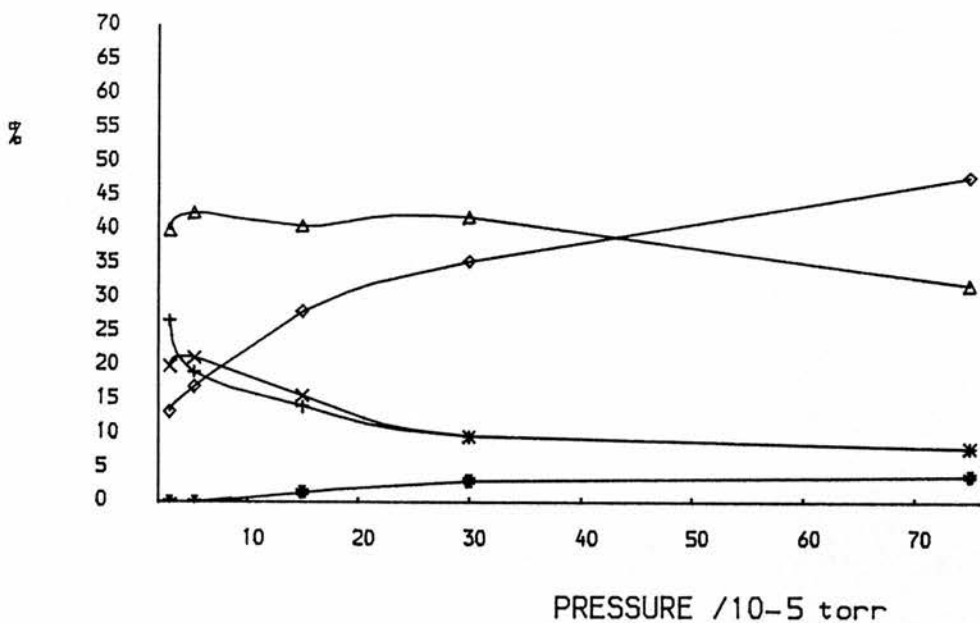
	PRESSURES in torr			m/e						
	INITIAL ION	ION	PENNING	27	29	41	43	44	55	57
	GAUGE	GAUGE	GAUGE							
	7.5x10 ⁻⁷	1.5x10 ⁻⁶	1.5x10 ⁻⁵	0.13	99.80	0.01	0.06	0.00	0.00	0.00
	7.5x10 ⁻⁷	4.5x10 ⁻⁶	4.5x10 ⁻⁵	0.58	98.73	0.10	0.58	0.02	0.00	0.00
	7.5x10 ⁻⁷	7.5x10 ⁻⁶	7.5x10 ⁻⁵	1.17	97.21	0.20	1.37	0.04	0.00	0.00
	7.5x10 ⁻⁷	1.5x10 ⁻⁵	1.5x10 ⁻⁴	2.23	93.67	0.44	3.50	0.11	0.02	0.04
	7.5x10 ⁻⁷	3.0x10 ⁻⁵	3.8x10 ⁻⁴	3.77	85.61	0.89	9.17	0.31	0.05	0.18

CH₂N⁺ into iso-C₄H₁₀

28 = CH₂N⁺ 41 = C₃H₅⁺ 57 = C₄H₉⁺
 29 = C₂H₅⁺ 43 = C₃H₇⁺ 58 = C₄H₁₀⁺

CH₂N⁺ INTO Iso-C₄H₁₀

% SECONDARY ION FLUX Vs. PRESSURE



% SECONDARY ION FLUX

	PRESSURES in torr			m/e				
	INITIAL ION	ION	PENNING	29	41	43	57	58
	GAUGE	GAUGE	GAUGE					
(A)	7.5×10 ⁻⁷	5.3×10 ⁻⁵	3.0×10 ⁻⁵	26.67	20.00	40.00	13.33	0.00
(B)	7.5×10 ⁻⁷	7.5×10 ⁻⁶	5.3×10 ⁻⁵	19.15	21.28	42.55	17.02	0.00
(C)	7.5×10 ⁻⁷	2.3×10 ⁻⁵	1.5×10 ⁻⁴	14.06	15.63	40.63	28.13	1.56
(D)	7.5×10 ⁻⁷	3.0×10 ⁻⁵	3.0×10 ⁻⁴	9.68	9.68	41.94	35.48	3.23
(E)	7.5×10 ⁻⁷	5.3×10 ⁻⁴	7.5×10 ⁻⁴	8.00	8.00	32.00	48.00	4.00

% TOTAL ION FLUX

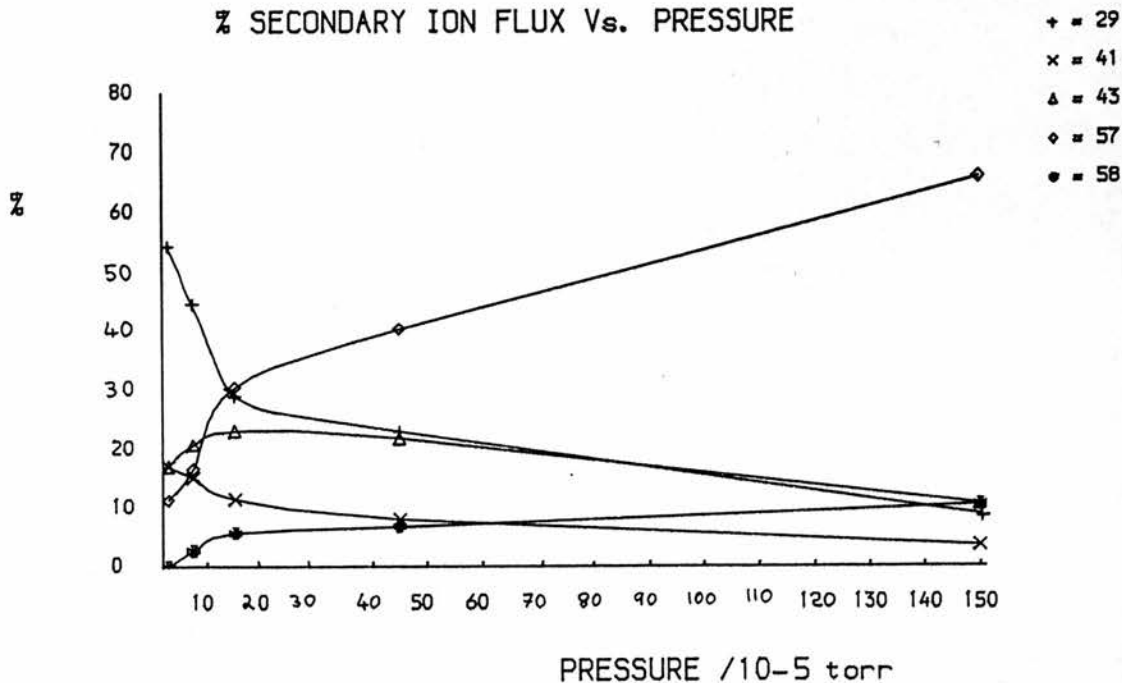
	PRESSURES in torr			m/e					
	INITIAL ION	ION	PENNING	28	29	41	43	57	58
	GAUGE	GAUGE	GAUGE						
	7.5×10 ⁻⁷	5.3×10 ⁻⁵	3.0×10 ⁻⁵	99.47	0.14	0.11	0.21	0.07	0.00
	7.5×10 ⁻⁷	7.5×10 ⁻⁶	5.3×10 ⁻⁵	98.89	0.21	0.24	0.47	0.19	0.00
	7.5×10 ⁻⁷	2.3×10 ⁻⁵	1.5×10 ⁻⁴	96.90	0.44	0.48	1.26	0.87	0.05
	7.5×10 ⁻⁷	3.0×10 ⁻⁵	3.0×10 ⁻⁴	94.16	0.56	0.56	2.45	2.07	0.19
	7.5×10 ⁻⁷	5.3×10 ⁻⁴	7.5×10 ⁻⁴	87.56	1.00	1.00	3.98	5.97	0.50

CH₂N⁺ into n-C₄H₁₀

28 = CH₂N⁺ 41 = C₃H₅⁺ 57 = C₄H₉⁺
 29 = C₂H₅⁺ 43 = C₃H₇⁺ 58 = C₄H₁₀⁺

CH₂N⁺ INTO n-C₄H₁₀

% SECONDARY ION FLUX Vs. PRESSURE



% SECONDARY ION FLUX

	PRESSURES in torr			m/e				
	INITIAL ION	ION	PENNING	29	41	43	57	58
	GAUGE	GAUGE	GAUGE					
(A)	7.5×10 ⁻⁷	3.8×10 ⁻⁶	3.0×10 ⁻⁵	54.29	17.14	17.14	11.43	0.00
(B)	7.5×10 ⁻⁷	6.8×10 ⁻⁶	7.5×10 ⁻⁵	44.44	15.28	20.83	16.67	2.78
(C)	7.5×10 ⁻⁷	2.3×10 ⁻⁵	1.5×10 ⁻⁴	28.99	11.59	23.19	30.43	5.80
(D)	7.5×10 ⁻⁷	3.0×10 ⁻⁵	4.5×10 ⁻⁴	22.99	8.05	21.84	40.23	6.90
(E)	7.5×10 ⁻⁷	7.5×10 ⁻⁵	1.5×10 ⁻³	8.93	3.57	10.71	66.07	10.71

% TOTAL ION FLUX

	PRESSURES in torr			m/e					
	INITIAL ION	ION	PENNING	28	29	41	43	57	58
	GAUGE	GAUGE	GAUGE						
	7.5×10 ⁻⁷	3.8×10 ⁻⁶	3.0×10 ⁻⁵	99.53	0.26	0.08	0.08	0.05	0.00
	7.5×10 ⁻⁷	6.8×10 ⁻⁶	7.5×10 ⁻⁵	98.81	0.53	0.18	0.25	0.20	0.03
	7.5×10 ⁻⁷	2.3×10 ⁻⁵	1.5×10 ⁻⁴	95.69	1.25	0.50	1.00	1.31	0.25
	7.5×10 ⁻⁷	3.0×10 ⁻⁵	4.5×10 ⁻⁴	91.19	2.03	0.71	1.93	3.55	0.61
	7.5×10 ⁻⁷	7.5×10 ⁻⁵	1.5×10 ⁻³	62.16	3.38	1.35	4.05	25.00	4.05

29 = C₂H₅⁺

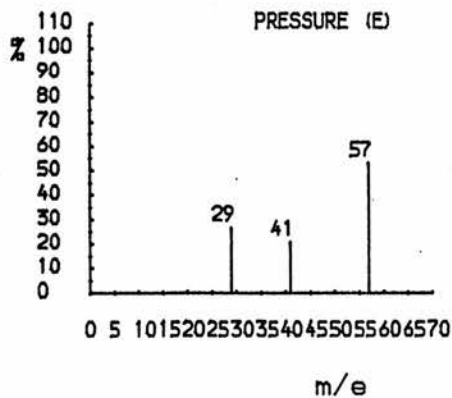
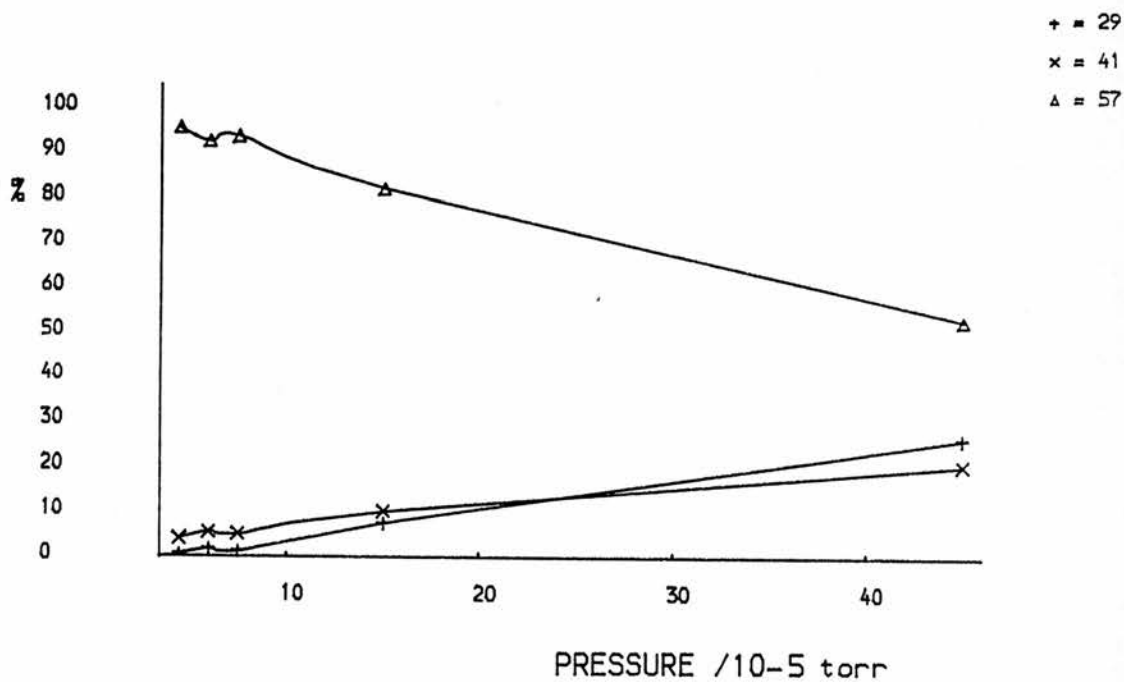
41 = C₃H₅⁺

57 = C₄H₉⁺

C₄H₉⁺ INTO N₂ (CID)

	PRESSURES in torr			m/e		
	INITIAL ION	ION	PENNING	29	41	57
	GAUGE	GAUGE	GAUGE			
(A)	3.8x10 ⁻⁶	3.8x10 ⁻⁶	4.5x10 ⁻⁵	0.51	4.06	95.43
(B)	3.8x10 ⁻⁶	4.5x10 ⁻⁶	6.0x10 ⁻⁵	1.89	5.66	92.45
(C)	3.8x10 ⁻⁶	4.5x10 ⁻⁶	7.5x10 ⁻⁵	1.28	5.12	93.61
(D)	3.8x10 ⁻⁶	6.0x10 ⁻⁶	1.5x10 ⁻⁴	7.69	10.26	82.05
(E)	3.8x10 ⁻⁶	1.5x10 ⁻⁵	4.5x10 ⁻⁴	26.47	20.59	52.94

C₄H₉⁺ INTO N₂ (CID)

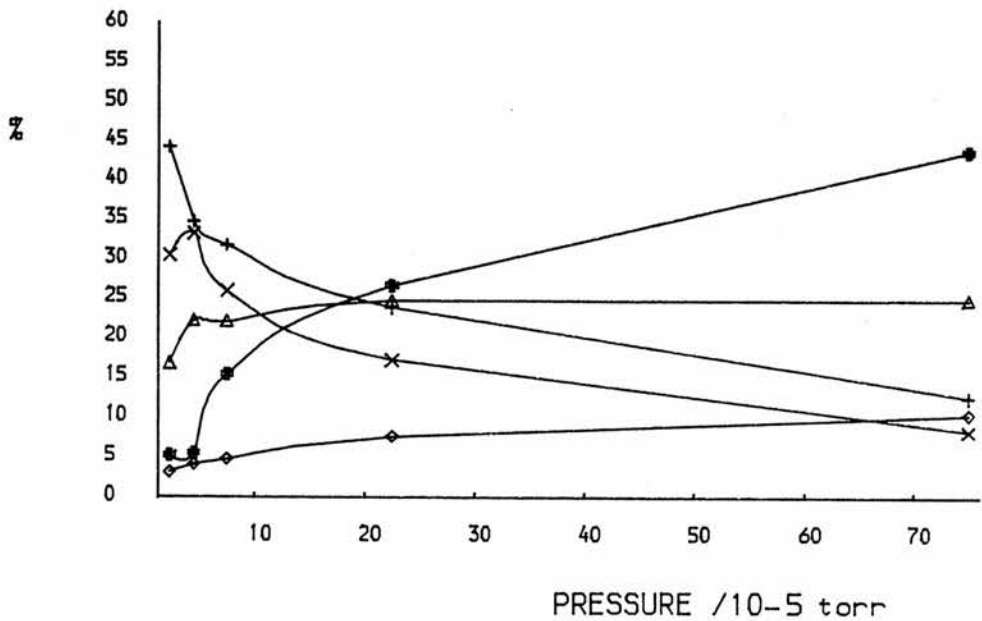


CH₂N⁺ into n-C₅H₁₂

28 = CH₂N⁺ 41 = C₃H₅⁺ 57 = C₄H₉⁺
 29 = C₂H₅⁺ 43 = C₃H₇⁺ 71 = C₅H₁₁⁺

CH₂N⁺ INTO n-PENTANE

% SECONDARY ION FLUX Vs. PRESSURE



% SECONDARY ION FLUX

PRESSURES in torr			m/e					
INITIAL ION GAUGE	ION GAUGE	PENNING GAUGE	29	41	43	57	71	
(A)	7.5×10 ⁻⁷	3.8×10 ⁻⁶	2.3×10 ⁻⁵	44.21	30.53	16.84	3.16	5.26
(B)	7.5×10 ⁻⁷	7.5×10 ⁻⁶	4.5×10 ⁻⁵	34.72	33.33	22.22	4.17	5.56
(C)	7.5×10 ⁻⁷	1.5×10 ⁻⁵	7.5×10 ⁻⁵	31.73	25.96	22.12	4.81	15.38
(D)	7.5×10 ⁻⁷	3.0×10 ⁻⁵	2.3×10 ⁻⁴	23.81	17.14	24.76	7.62	26.67
(E)	7.5×10 ⁻⁷	6.0×10 ⁻⁴	7.5×10 ⁻⁴	12.50	8.33	25.00	10.42	43.75

% TOTAL ION FLUX

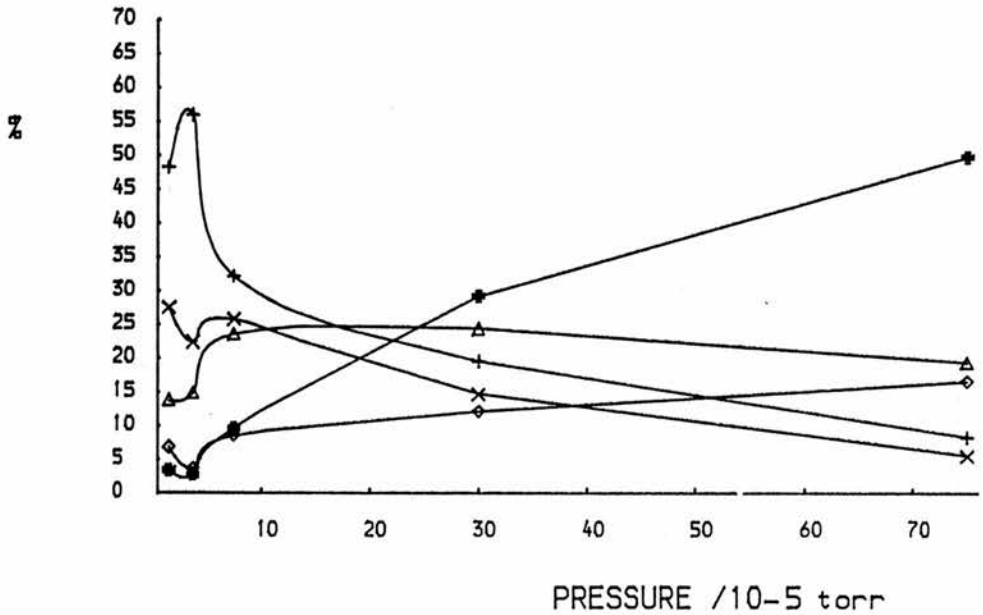
PRESSURES in torr			m/e					
INITIAL ION GAUGE	ION GAUGE	PENNING GAUGE	28	29	41	43	57	71
7.5×10 ⁻⁷	3.8×10 ⁻⁶	2.3×10 ⁻⁵	99.14	0.38	0.26	0.14	0.03	0.05
7.5×10 ⁻⁷	7.5×10 ⁻⁶	4.5×10 ⁻⁵	98.55	0.50	0.48	0.32	0.06	0.08
7.5×10 ⁻⁷	1.5×10 ⁻⁵	7.5×10 ⁻⁵	96.42	1.14	0.93	0.79	0.17	0.55
7.5×10 ⁻⁷	3.0×10 ⁻⁵	2.3×10 ⁻⁴	90.78	2.20	1.58	2.28	0.70	2.46
7.5×10 ⁻⁷	6.0×10 ⁻⁴	7.5×10 ⁻⁴	81.40	2.33	1.55	4.65	1.94	8.14

CH₂N⁺ into iso-C₅H₁₂

28 = CH₂N⁺ 41 = C₃H₅⁺ 57 = C₄H₉⁺
 29 = C₂H₅⁺ 43 = C₃H⁺ 71 = C₅H₁₁⁺

CH₂N⁺ INTO ISO-C₅H₁₂

% SECONDARY ION FLUX Vs. PRESSURE



% SECONDARY ION FLUX

	PRESSURES in torr			m/e				
	INITIAL ION	ION	PENNING					
	GAUGE	GAUGE	GAUGE	29	41	43	57	71
(A)	7.5×10 ⁻⁷	2.3×10 ⁻⁶	1.5×10 ⁻⁵	48.28	27.59	13.79	6.90	3.45
(B)	7.5×10 ⁻⁷	6.8×10 ⁻⁶	3.8×10 ⁻⁵	56.07	22.43	14.95	3.74	2.80
(C)	7.5×10 ⁻⁷	1.5×10 ⁻⁵	7.5×10 ⁻⁵	32.26	25.81	23.66	8.60	9.68
(D)	7.5×10 ⁻⁷	3.0×10 ⁻⁵	3.0×10 ⁻⁴	19.51	14.63	24.39	12.20	29.27
(E)	7.5×10 ⁻⁷	6.0×10 ⁻⁵	7.5×10 ⁻⁴	8.33	5.56	19.44	16.67	50.00

% TOTAL ION FLUX

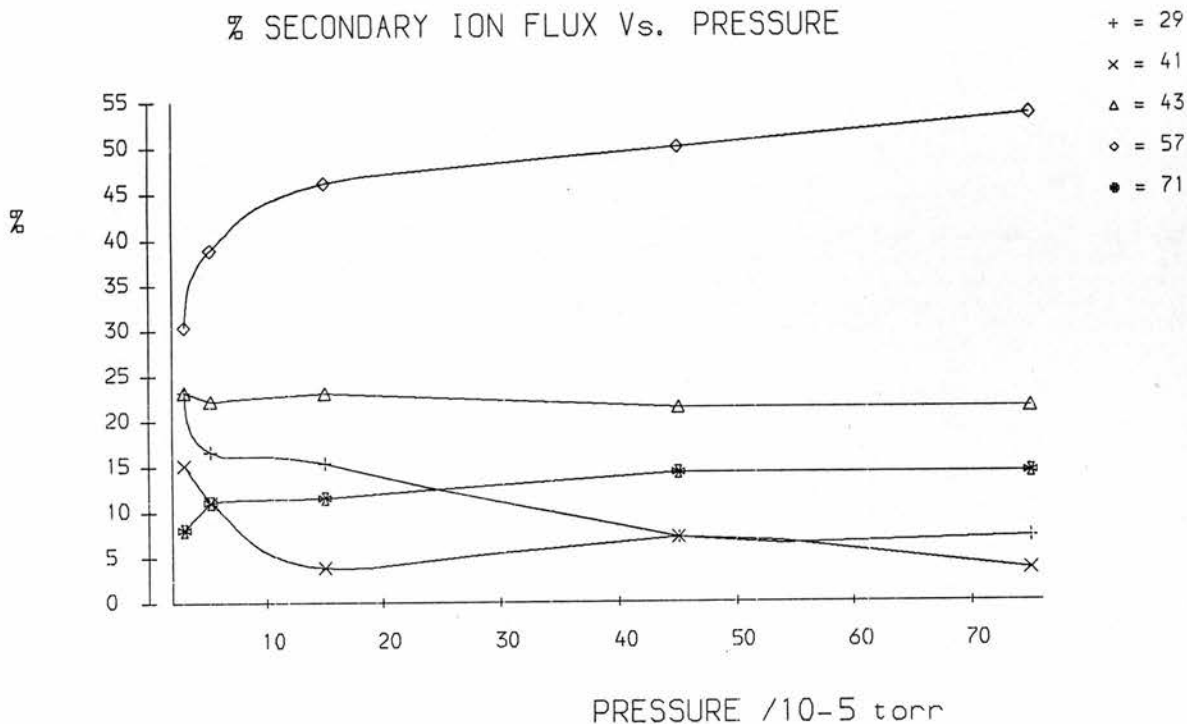
	PRESSURES in torr			m/e					
	INITIAL ION	ION	PENNING						
	GAUGE	GAUGE	GAUGE	28	29	41	43	57	71
	7.5×10 ⁻⁷	2.3×10 ⁻⁶	1.5×10 ⁻⁵	99.57	0.21	0.12	0.06	0.03	0.01
	7.5×10 ⁻⁷	6.8×10 ⁻⁶	3.8×10 ⁻⁵	98.94	0.59	0.24	0.16	0.04	0.03
	7.5×10 ⁻⁷	1.5×10 ⁻⁵	7.5×10 ⁻⁵	97.29	0.88	0.70	0.64	0.23	0.26
	7.5×10 ⁻⁷	3.0×10 ⁻⁵	3.0×10 ⁻⁴	90.70	1.81	1.36	2.27	1.13	2.72
	7.5×10 ⁻⁷	6.0×10 ⁻⁵	7.5×10 ⁻⁴	82.18	1.49	0.99	3.47	2.97	8.91

CH₂N⁺ into neo-C₅H₁₂

28 = CH₂N⁺ 41 = C₃H₅⁺ 57 = C₄H₉⁺
 29 = C₂H₅⁺ 43 = C₃H⁺ 71 = C₅H₁₁⁺

CH₂N⁺ INTO Neo-C₅H₁₂

% SECONDARY ION FLUX Vs. PRESSURE



% SECONDARY ION FLUX

PRESSURES In torr			m/e					
INITIAL ION GAUGE	ION GAUGE	PENNING GAUGE	29	41	43	57	71	
(A)	7.5×10 ⁻⁷	4.5×10 ⁻⁶	3.0×10 ⁻⁵	23.21	15.18	23.21	30.36	8.04
(B)	7.5×10 ⁻⁷	7.5×10 ⁻⁶	5.3×10 ⁻⁵	16.67	11.11	22.22	38.89	11.11
(C)	7.5×10 ⁻⁷	1.5×10 ⁻⁵	1.5×10 ⁻⁴	15.38	3.85	23.08	46.15	11.54
(D)	7.5×10 ⁻⁷	3.8×10 ⁻⁵	4.5×10 ⁻⁴	7.14	7.14	21.43	50.00	14.29
(E)	7.5×10 ⁻⁷	4.5×10 ⁻⁵	7.5×10 ⁻⁴	7.15	3.55	21.45	53.55	14.30

% TOTAL ION FLUX

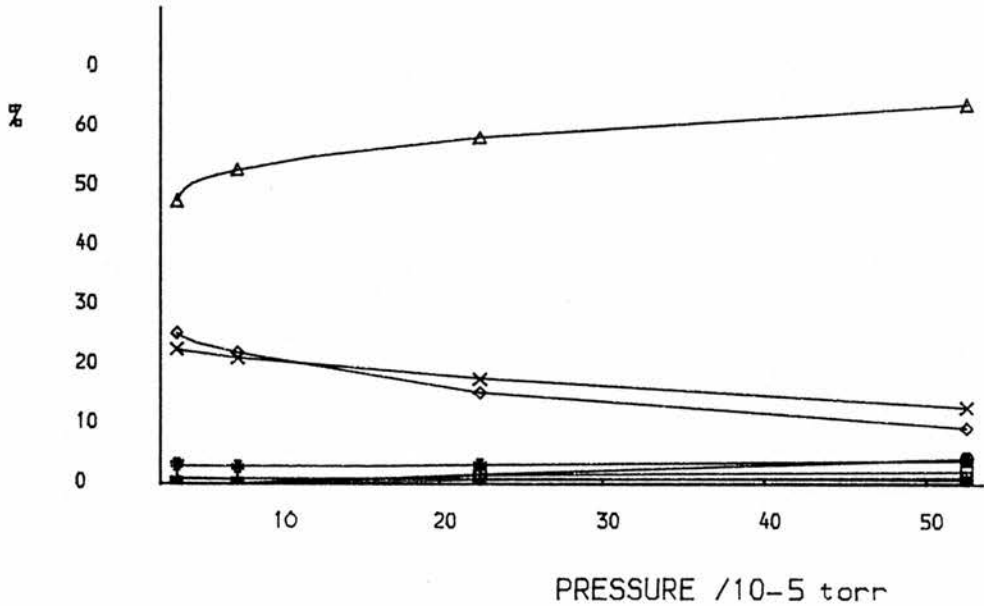
PRESSURES In torr			m/e					
INITIAL ION GAUGE	ION GAUGE	PENNING GAUGE	28	29	41	43	57	71
7.5×10 ⁻⁷	4.5×10 ⁻⁶	3.0×10 ⁻⁵	98.88	0.26	0.17	0.26	0.34	0.09
7.5×10 ⁻⁷	7.5×10 ⁻⁶	5.3×10 ⁻⁵	97.84	0.36	0.24	0.48	0.84	0.24
7.5×10 ⁻⁷	1.5×10 ⁻⁵	1.5×10 ⁻⁴	95.06	0.76	0.19	1.14	2.28	0.57
7.5×10 ⁻⁷	3.8×10 ⁻⁵	4.5×10 ⁻⁴	86.28	0.98	0.98	2.94	6.86	1.96
7.5×10 ⁻⁷	4.5×10 ⁻⁵	7.5×10 ⁻⁴	80.28	1.41	0.70	4.23	10.56	2.82

CH₅⁺ into C₂H₆

17 = CH₅⁺ 30 = C₂H₆⁺ 43 = C₃H₇⁺
 27 = C₂H₃⁺ 31 = C₂H₇⁺ 44 = C₃H₈⁺
 28 = C₂H₄⁺ 41 = C₃H₅⁺ 45 = C₃H₉⁺
 29 = C₂H₅⁺ 42 = C₃H₆⁺

CH₅⁺ INTO C₂H₆

% SECONDARY ION FLUX Vs. PRESSURE



+ = 27
 x = 28
 Δ = 29
 ◇ = 30
 ● = 31
 ∇ = 41
 □ = 42
 ● = 43
 ◆ = 44
 x = 45

% SECONDARY ION FLUX

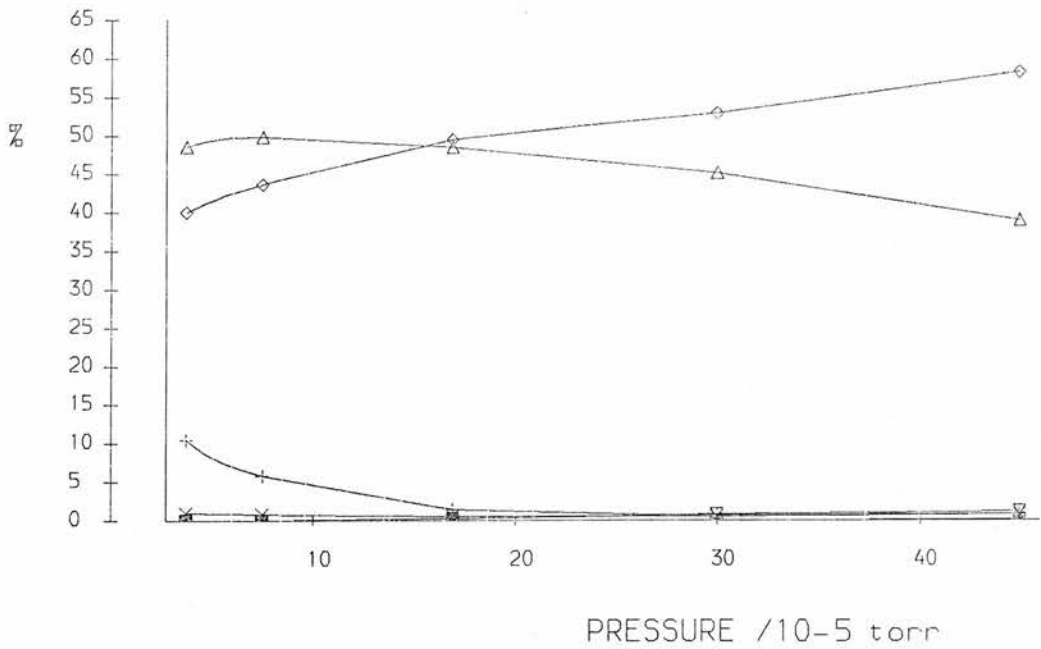
PRESSURES in torr			m/e										
INITIAL ION GAUGE	ION GAUGE	PENNING GAUGE	27	28	29	30	31	41	42	43	44	45	
(A)	1.5×10 ⁻⁵	1.5×10 ⁻⁵	3.8×10 ⁻⁵	1.08	22.70	47.57	25.41	3.24	0.00	0.00	0.00	0.00	0.00
(B)	1.5×10 ⁻⁵	1.7×10 ⁻⁵	7.5×10 ⁻⁵	0.89	21.22	52.87	22.11	2.90	0.00	0.00	0.00	0.00	0.00
(C)	1.5×10 ⁻⁵	2.3×10 ⁻⁵	2.3×10 ⁻⁴	0.91	17.64	58.41	15.36	3.30	0.80	1.59	1.71	0.17	0.11
(D)	1.5×10 ⁻⁵	3.8×10 ⁻⁵	5.3×10 ⁻⁴	0.83	12.93	64.15	9.52	4.14	1.24	2.28	4.45	0.36	0.10

% TOTAL ION FLUX

PRESSURES in torr			m/e										
INITIAL ION GAUGE	ION GAUGE	PENNING GAUGE	17	27	28	29	30	31	41	42	43	44	45
1.5×10 ⁻⁵	1.5×10 ⁻⁵	3.8×10 ⁻⁵	98.39	0.02	0.37	0.77	0.41	0.05	0.00	0.00	0.00	0.00	0.00
1.5×10 ⁻⁵	1.7×10 ⁻⁵	7.5×10 ⁻⁵	95.16	0.04	1.03	2.56	1.07	0.14	0.00	0.00	0.00	0.00	0.00
1.5×10 ⁻⁵	2.3×10 ⁻⁵	2.3×10 ⁻⁴	83.66	0.15	2.88	9.54	2.51	0.54	0.13	0.26	0.28	0.03	0.02
1.5×10 ⁻⁵	3.8×10 ⁻⁵	5.3×10 ⁻⁴	65.06	0.29	4.52	22.41	3.33	1.45	0.43	0.80	1.55	0.13	0.04

CH₃⁺ INTO CH₄

% SECONDARY ION FLUX Vs. PRESSURE



% SECONDARY ION FLUX

	PRESSURES in torr			m/e							
	INITIAL ION	ION	PENNING	16	17	27	29	39	41	42	43
	GAUGE	GAUGE	GAUGE								
(A)	7.5×10 ⁻⁷	1.5×10 ⁻⁶	3.8×10 ⁻⁵	10.48	0.95	48.57	40.00	0.00	0.00	0.00	0.00
(B)	7.5×10 ⁻⁷	3.0×10 ⁻⁶	7.5×10 ⁻⁵	5.79	0.77	49.81	43.63	0.00	0.00	0.00	0.00
(C)	7.5×10 ⁻⁷	4.5×10 ⁻⁶	1.7×10 ⁻⁴	1.43	0.48	48.45	49.40	0.00	0.24	0.00	0.00
(D)	7.5×10 ⁻⁷	1.7×10 ⁻⁵	3.0×10 ⁻⁴	0.68	0.54	45.13	52.89	0.00	0.75	0.00	0.00
(E)	7.5×10 ⁻⁷	1.7×10 ⁻⁵	4.5×10 ⁻⁴	0.75	0.75	38.97	58.19	0.06	1.16	0.06	0.06

CH₃⁺ INTO CH₄

% TOTAL ION FLUX

	PRESSURES in torr			m/e								
	INITIAL ION	ION	PENNING	15	16	17	27	29	39	41	42	43
	GAUGE	GAUGE	GAUGE									
	7.5×10 ⁻⁷	1.5×10 ⁻⁶	3.8×10 ⁻⁵	98.95	0.11	0.01	0.51	0.42	0.00	0.00	0.00	0.00
	7.5×10 ⁻⁷	3.0×10 ⁻⁶	7.5×10 ⁻⁵	97.41	0.15	0.02	1.29	1.13	0.00	0.00	0.00	0.00
	7.5×10 ⁻⁷	4.5×10 ⁻⁶	1.7×10 ⁻⁴	95.81	0.06	0.02	2.03	2.07	0.00	0.01	0.00	0.00
	7.5×10 ⁻⁷	1.7×10 ⁻⁵	3.0×10 ⁻⁴	85.31	0.10	0.08	6.63	7.77	0.00	0.11	0.00	0.00
	7.5×10 ⁻⁷	1.7×10 ⁻⁵	4.5×10 ⁻⁴	82.73	0.13	0.13	6.73	10.05	0.01	0.20	0.01	0.01

DISCUSSION

1 METHANE

REACTIONS OF METHANE

CH₄⁺ INTO METHANE

This reaction has been extensively studied^{12,13,95,96} in conventional mass spectrometers using pressures between millitorrs and a few hundred torrs. At high pressures the main product ions were CH₅⁺, mass=17, and C₂H₅⁺ mass=29. The results reported here were carried out at lower pressures - around 10⁻⁶ to 10⁻⁴ torr. The initial results indicate that the main product ions were CH₃⁺ (mass=15) ≈50% which decreased with increasing pressure, CH₅⁺ (mass=17) ≈40% which increased with increasing pressure and a trio of tertiary ions C₂H₃⁺ (mass=27) ≈1%, C₂H₄⁺ (mass=28) ≈0.7% and C₂H₅⁺ (mass=29) ≈5% which all increased with increasing pressure. The peaks of mass=15 and 17 were difficult to separate from the enormous primary peak of mass=16 which was at best a factor of 13 and at worst a factor of 270 times bigger than the CH₅⁺ peak. As a consequence the results from this experiment are not very accurate and so this was not found to be a good way to produce the CH₅⁺ ion for subsequent reactions in the quinquadrupole mass spectrometer.

In the triple quadrupole mass spectrometer this self protonation reaction can be used to form MH^+ in the ionisation chamber if the pressure of M is raised sufficiently high. Gas M is fed into the ionisation chamber where electron bombardment produces M^+ . If sufficient M molecules are present the self-ionisation reaction can produce MH^+ which can be isolated in the first quadrupole and put into a target gas in the second quadrupole. In this way the reactions of protonated molecules can be studied with only three quadrupoles. Care must be taken because using this method will not produce a pure MH^+ ion peak as any isotope of M which is one mass unit heavier will also be part of the signal that would be put into the second quadrupole. For methane the amount of the ion peak that was due to the isotope of CH_4^+ was quantitatively assessed.

CH₄⁺ (isotope)/CH₅⁺ Ratio

When methane was put into the ionisation chamber and analysed through the first quadrupole peaks were obtained at 16 and 17. The large peak at 16 was due to the parent CH₄⁺. The peak at 17 could be due to CH₅⁺ or due to the isotope peak of CH₄⁺. (¹³CH₄⁺ or CH₃D⁺).

To investigate if it was justified to use the peak at 17 as CH₅⁺ in the subsequent experiments the peaks at 16 and 17 were measured at a series of pressures. The height of the peak at 17 that would be expected to be due to the isotopes can be calculated from the equation 2.1 and the height of the 16 peak. Comparison of the height due to the isotope and the actual height obtained for the peak at 17 enabled the amount of CH₅⁺ to be estimated.

It can be seen from the graph of peak height against pressure that up until 1×10^{-6} mbar the peak at 17 is the same height as would be predicted as an isotope peak.

For example:-

At 5×10^{-7} mbar the peak at 16 is 9.9×10^{-5} units high

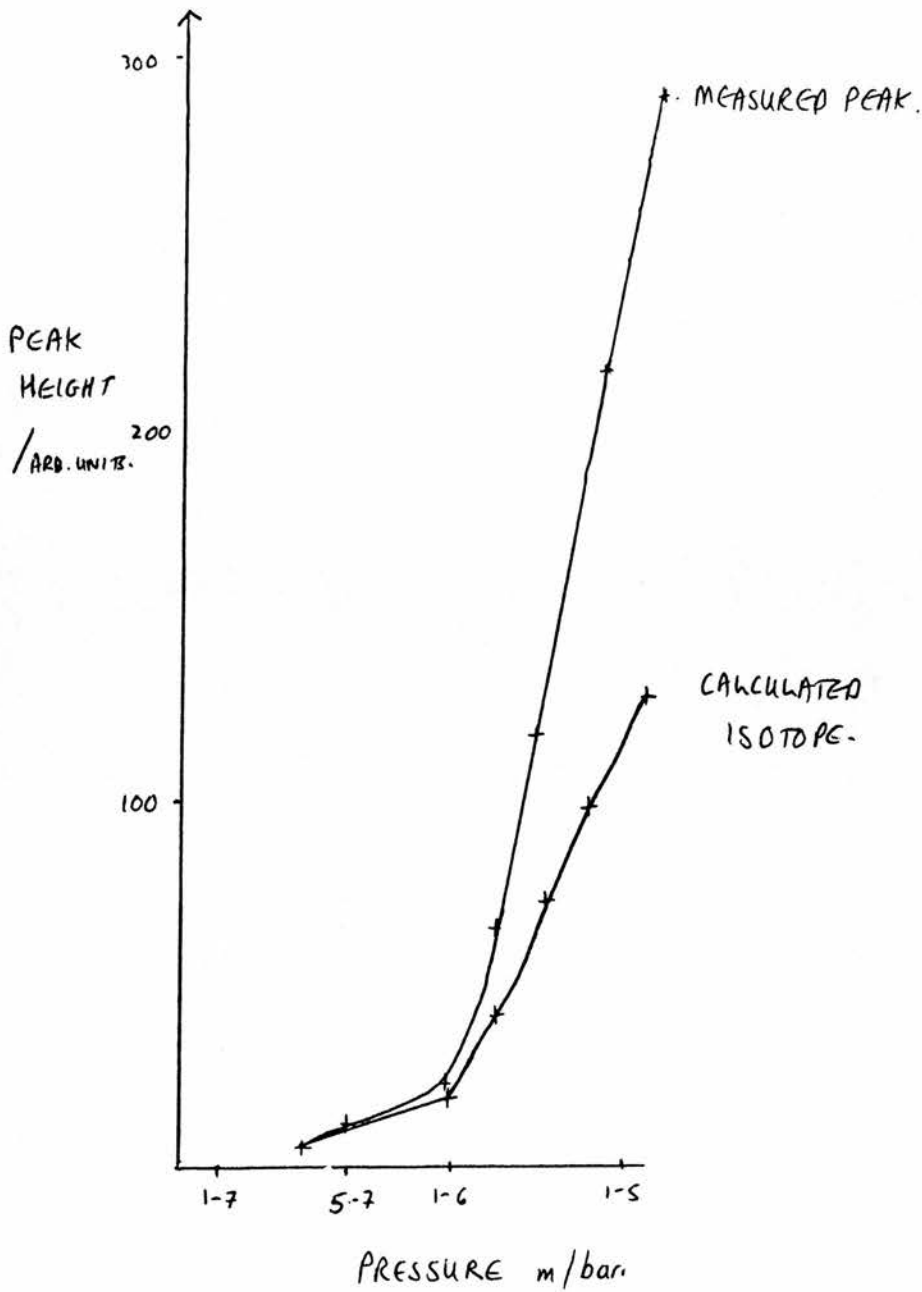
$$\text{Eq. 2.1} \quad \frac{M+1}{M} = \frac{(1.1 \times C + 0.01 \times H)}{100}$$

$$\Rightarrow \frac{M+1}{9.9 \times 10^{-5}} = \frac{1.1 + 0.04}{100} = 0.0114$$

$$M+1 = 9.9 \times 10^{-5} \times 0.0114 = 1.1 \times 10^{-6}$$

GRAPH 2.1

PEAK HEIGHT AGAINST PRESSURE FOR THE
CALCULATED ISOTOPE PEAK AND THE MEASURED PEAK OF MASS 17



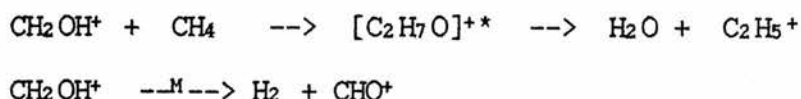
The peak at 17 measures 1.2×10^{-6} from which it can be deduced that the peak at 17 is just the isotope peak of 16.

As the pressure increases above 5×10^{-7} mbar the 'isotope' and the experimental peak diverge so that at a pressure of 2.5×10^{-5} mbar the isotope can only account for one quarter of the total peak height. It follows that the other three quarters must be due to CH_5^+ ions.

With methane at a pressure at or above 1×10^{-5} mbar the peak of mass 17 could be justifiably taken as being mostly CH_5^+ . This method of forming CH_5^+ was used in a couple of reactions. Only one comprehensive result is reported in the tables in the results section - page 96. This is because the high pressure of methane gas that was required to obtain a satisfactory signal of CH_5^+ ion meant that the pressure was already so high that there was little range left for varying the pressure of the target gas. The results from these experiments tend therefore to be qualitative rather than quantitative.

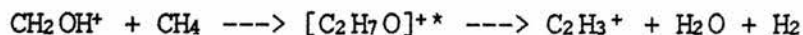
CH_2OH^+ INTO CH_4

CH_2OH^+ (from methanol) was reacted with methane. The main product ion was of mass 29 and could have been due to C_2H_5^+ or to the fragmentation of the primary ion to CHO^+ .

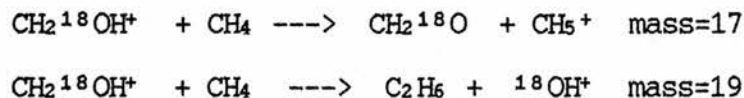


The experiment was repeated using $\text{CH}_2^{18}\text{OH}^+$ ions from ^{18}O labelled methanol to distinguish between these possibilities. If the ion of mass 29 in the non labelled experiment was CHO^+ then it would now give a peak of mass 31 CH^{18}O^+ , whereas C_2H_5^+ would remain of mass 29. The results as tabulated in the results section indicate that between 98 and 95% of the peak was due to the fragment CHO^+ and only the remaining 2 to 5% was due to the formation of C_2H_5^+ .

The ion of mass 27 was thought to be due to the fragmentation of the C_2H_5^+ ion to $\text{C}_2\text{H}_3^+ + \text{H}_2$ or due to the loss of H_2O and H_2 from the adduct $[\text{C}_2\text{H}_7\text{O}]^+$.



A peak of mass 17 was observed and the reaction of $\text{CH}_2^{18}\text{OH}^+$ was used to confirm that it was due to CH_5^+ and not due to OH^+ .



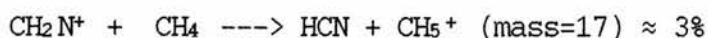
CH_5^+ accounted for at most 30% of the product ions and only 2% of the product ion was CH_3^+ .

CHO⁺ INTO CH₄

CHO⁺ when reacted with methane produced only CH₅⁺ and CH₃⁺ ions. The CH₅⁺ ion amounted for 82% of the product ions. No ion of mass 16 was obtained because the ionisation potential of the CHO⁺ ion is too low for charge exchange to take place. This was therefore found to be a good way of forming large amounts of CH₅⁺ ion in good purity and without any adjacent peaks to interfere with its isolation. There is however one drawback to using this reaction as a route to forming CH₅⁺ in the third quadrupole of a quinquadrupole mass spectrometer and that is that the source of the CHO⁺ ion, methanol, has a tendency to condense as it is admitted through the needle valve because of the cooling effect of the change in pressure. The condensed methanol blocks the fine needle valve and cuts the supply of primary ion. This causes the flux of the primary ion to fluctuate. That is why in the later experiments CH₂N⁺ ions were used as the protonating primary ion in preference to CHO⁺ ions.

CH₂NH₂⁺ INTO CH₄

CH₂NH₂⁺ from methylamine was reacted with methane but only produced CH₂N⁺ ion as a fragment analogous to the CHO⁺ ion in the methanol system. A very small peak of mass 17 was observed at high pressures - 5×10^{-4} torr. This could have been CH₅⁺ as a tertiary ion formed by the reaction of CH₂N⁺ with methane.

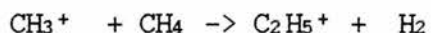
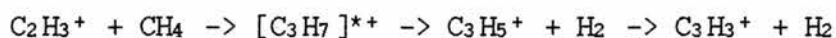
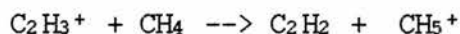


CH₂N⁺ INTO CH₄

The reaction of CH₂N⁺ with methane produced three ions. One of mass 29 which was shown by labelled methanol to be C₂H₅⁺ and is a common ion formed from the reactions of CH₃⁺ and or CH₅⁺ with methane. The associated ion of C₂H₃⁺ was not detected because it was covered by the large primary ion signal of mass 28. The other two ions were CH₅⁺ and CH₃⁺. In this system CH₃⁺ was the largest peak accounting for over 50% of the secondary ion current. However as the pressure increased the amount of CH₅⁺ increased and the amount of CH₃⁺ decreased. This was seen to be the case in all of the reactions and will be discussed later. (page 108)

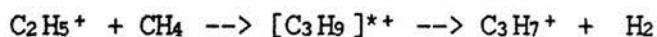
C₂H₃⁺ INTO CH₄

C₂H₃⁺ (from ethane) was reacted with methane and, in addition to the proton-transfer reaction, the other ions produced were C₂H₅⁺ (mass=29), C₃H₃⁺ (mass=39) and C₃H₅⁺ (mass=41) which were probably formed by successive oligomerisation reactions.



C₂H₅⁺ INTO CH₄

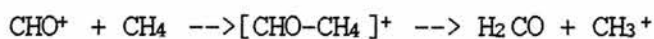
The ions produced when C₂H₅⁺ was reacted with CH₄ were identical to those produced with C₂H₃⁺ and the quantities of each ion were very similar except for the ion C₃H₇⁺ (mass=43) which was obtained by loss of H₂ from the addition complex [C₃H₉]⁺⁺ .



The conclusions that can be drawn from this section are as follows.

- A) All the primary ions that were investigated, except CH₂NH₂⁺, protonated methane to produce CH₅⁺ ions of various strengths and various stabilities.
- B) CHO⁺ produced the largest amount of CH₅⁺ but its tendency to condense in the needle valve made it difficult to maintain a constant flux of primary ions.
- C) CH₂N⁺, although not producing as large a proportion of CH₅⁺ as CHO⁺, did have the advantage of being produced from a gas which was easier to handle than methanol.
- D) C₂H₃⁺ and C₂H₅⁺ were not very satisfactory ions for the production of CH₅⁺ because unlike CH₂N⁺ and CHO⁺, these carbocations form addition complexes with the methane and can condense to produce a range of C_nH_m⁺ ions (where n=2 and m=3 or 5 or n=3 and m=3,5 or 7) which reduces the yield of CH₅⁺ ions.
- E) It has not been possible to investigate an interesting competing reaction that could lead to the production of CH₃⁺ ions. Ions such as CHO⁺ and CH₂N⁺ could react with

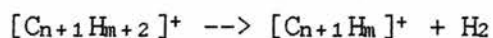
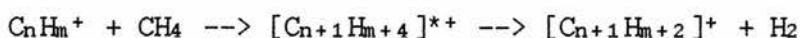
methane either to donate a proton or to abstract a hydride ion.



No experiment has been found that could investigate this unequivocally.

The overall conclusion is that it is possible to use the reactions investigated to produce a strong signal of pure CH_5^+ ions using the first three quadrupoles of a quinquadrupole mass spectrometer so that it could be isolated and the chemistry and reactions of CH_5^+ studied using the fourth and fifth quadrupoles.

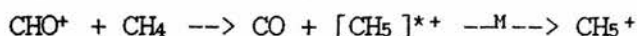
Two points of interest that arose in these investigations were investigated further. The first was the relationship between CH_5^+ and CH_3^+ ions which being one of parent ion to fragment ion could be studied by altering the excess energy of the CH_5^+ ion. The second point was the formation of C_{n+1} ions from the addition with elimination reactions of C_nH_m^+ ions and methane.



This second point will be discussed in the overall conclusion on page 334.

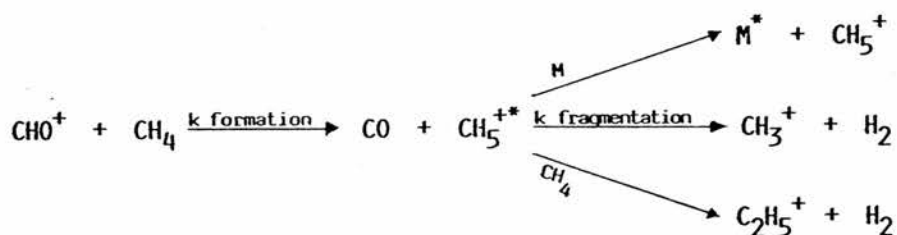


The variations of the size of these ion peaks with pressure would suggest a reaction mechanism with CH_3^+ as a fragment of CH_5^+ .



As the pressure increases the amount of $[\text{CH}_5]^{*+}$ that will be collision stabilised to CH_5^+ will increase and the amount of fragmentation to $\text{CH}_3^+ + \text{H}_2$ will diminish so that the ratio of $[\text{CH}_5^+]/[\text{CH}_3^+]$ will increase. This was found to be so in all the experiments done. It was decided to investigate this fragmentation reaction to see how altering the internal energy of the primary ion would alter the amount of fragmentation.

CH_5^+ ions can be produced in a triple quadrupole mass spectrometer. Once they are formed three things can occur. The CH_5^+ ion can fragment to $\text{CH}_3^+ + \text{H}_2$, or they could react with another molecule of methane to produce C_2H_m^+ ions or they can be collision stabilised by collision with methane. These are depicted in the diagram below.



By keeping the pressure of methane low the reaction to form C_2H_m^+ ions can be reduced to such an extent that

it cannot be detected. The absence of peaks of mass 27,29,39 and 41 can be verified throughout the subsequent experiments to check that these reactions have been effectively eliminated.

The stabilization reaction cannot be measured, but by keeping the pressure constant it can be assumed that this reaction is constant and can be incorporated in the 'rate of formation' of CH_5^+ .

Under conditions of low, constant pressure the amount of fragmentation of CH_5^+ to CH_3^+ can be observed as the translational energy of the primary ion was altered. This was done by altering the potential on the repeller plate in the ion source which imparts translational energy to the primary ions.

The results are presented in two forms - $[\text{CH}_5^+]$ and $[\text{CH}_3^+]$ as a percentage of the total secondary ion flux

$$[\text{CH}_5^+] \% = [\text{CH}_5^+] / ([\text{CH}_3^+] + [\text{CH}_5^+]) \times 100$$

$$[\text{CH}_3^+] \% = [\text{CH}_3^+] / ([\text{CH}_3^+] + [\text{CH}_5^+]) \times 100$$

and the ratio of fragment ion to parent ion.

$$[\text{CH}_3^+] / [\text{CH}_5^+]$$

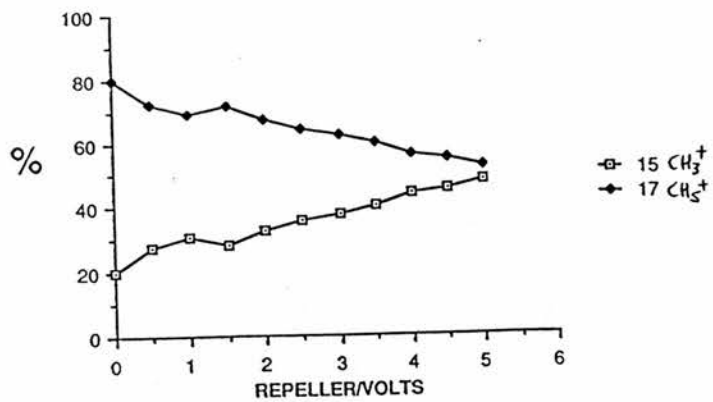
In both cases this compensates for the increase in the total flux of ions when the potential of the repeller is increased and allows comparison of the ratios of the ions.

With the repeller at zero - that is when no additional translation energy has been imparted to the primary ions - CH_5^+ accounts for some 80% of the ions and there is only 20% fragmentation. As the translational

energy is increased the amount of fragmentation increases - the CH_5^+ is being destabilized. The ratio of fragment ion to parent ion was plotted against increasing energy to yield a straight line. This experiment was repeated using CDO^+ and using CH_2N^+ as the primary ions. The results are similar except there is less of a destabilizing effect on increasing the energy of CH_2N^+ as the primary ion and more of a destabilizing effect with CDO^+ . This can be seen in the different gradients of the graphs of the ratio of the ions.

SECONDARY ION PERCENTAGE (%)
AGAINST REPELLER (VOLTS)

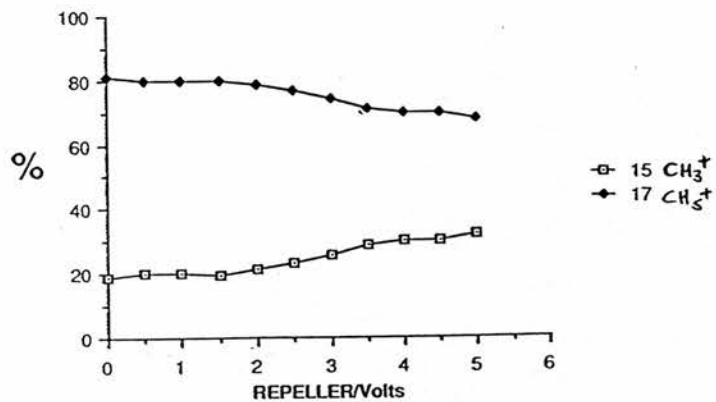
"CHO+ into CH4"



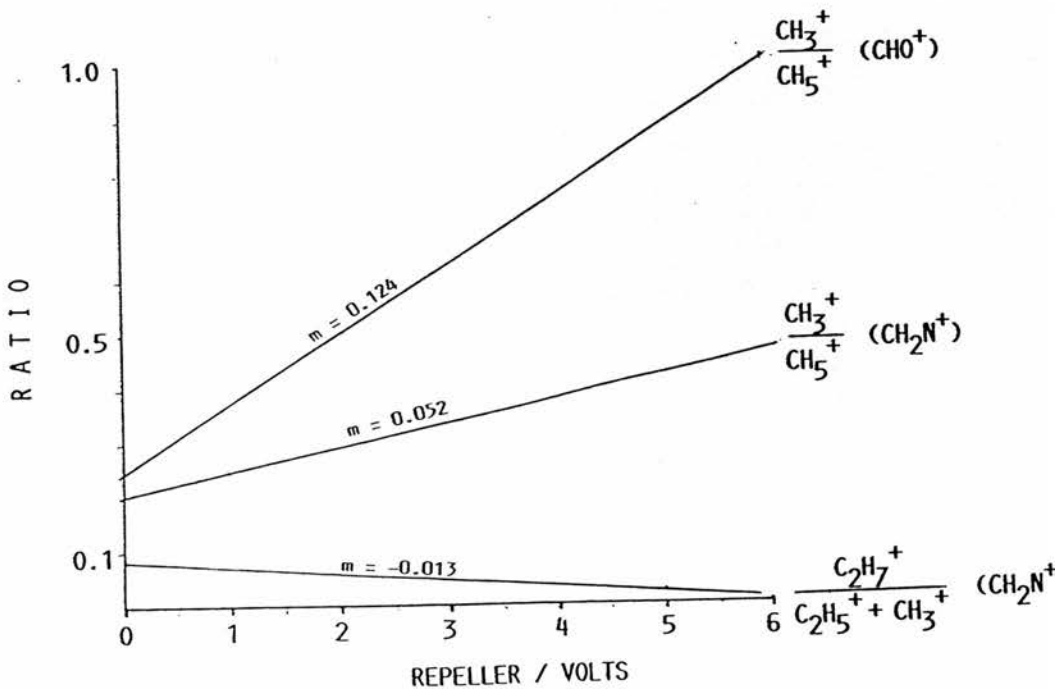
CH₂N⁺ INTO CH₄

SECONDARY ION PERCENTAGE (%)
AGAINST REPELLER (VOLTS)

"CH₂N+ into CH₄"



RATIO OF $\text{CH}_3^+ / \text{CH}_5^+$
AGAINST REPELLER (VOLTS)



To compare the results it was decided to extrapolate each graph to the point at which the ratio of fragment to parent ion would be 1:1 which could be seen as the energy that was needed to be imparted to the CH_5^+ ions to cause 50% of the ions formed to fragment. It could also be said that this was the energy at which the rate of fragmentation of CH_5^+ was one half of the rate of formation of CH_5^+ . From least squares linear regression analysis $[\text{CH}_3^+] = [\text{CH}_5^+]$ when the repeller would be set to + 3.9 V for CDO^+ , + 5.9 V for CHO^+ ion and + 15.5 V for CH_2N^+ .

The difference in additional translational energy that is required to destabilize the CH_5^+ ions to the same extent is an indication of the initial energy of the primary ions. The difference between CDO^+ and CHO^+ is not very large and may be within experimental error.

The difference between CHO^+ and CH_2N^+ ions is much more marked. CH_2N^+ requires much more additional energy to cause the same degree of fragmentation as CHO^+ . This would suggest, in direct contrast with the results reported by Futrell and co-workers¹⁰¹ which are replicated in table 2.5, that the CH_2N^+ ion can produce CH_5^+ ions with less excess internal energy than those produced by CHO^+ ions.

TABLE 2.5

SOURCE	ION	RATIO CH ₃ ⁺ /CH ₅ ⁺	RATIO CH ₃ ⁺ /CH ₅ ⁺
CH ₃ OH	CHO ⁺	0.34	0.34
CH ₃ NH ₂	CH ₂ N ⁺	0.46	0.23

REF. 101 PRESENT RESULTS

Two possible explanations can be given for this.

1) CH₂N⁺ has more vibrational modes to dissipate the excess energy than CHO⁺. Therefore the amount of energy transferred with the proton would be less with CH₂N⁺ than with CHO⁺.

2) The non-linear CH₂N⁺ is more stabilized by the various pole bias and focus potentials than the linear CHO⁺ ion as it passes through the quadrupole system.

No further conclusion can be drawn in this issue without further work being done but it is interesting to note that this could be an indication of a fundamental difference between the results of a tandem mass spectrometer and a triple quadrupole mass spectrometer.

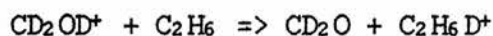
2 ETHANE

REACTIONS OF ETHANE

Not all the primary ions that were used to protonate methane were suitable for studying the protonation of ethane because their mass would coincide with an important peak.

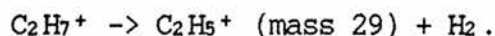
CH_2OH^+ (mass 31) would be indistinguishable from C_2H_7^+ (mass 31).

CD_2OD^+ (mass 34) would fragment to CDO^+ (mass 32) which would mask any $\text{C}_2\text{H}_6\text{D}^+$ (mass 32) that was produced.



$\text{CH}_2^{18}\text{OH}^+$ (mass 33) would fragment to CH^{18}O^+ (mass 31) which would mask C_2H_7^+ (mass 31).

CHO^+ (mass 29) would cover the main fragment ion of C_2H_7^+



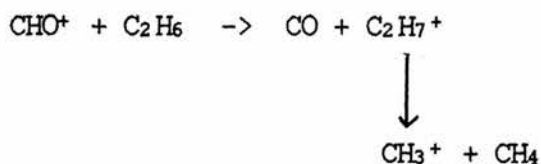
CH^{18}O^+ (mass 31) would coincide with C_2H_7^+ (mass 31).

CDO^+ (mass 30) would not coincide with any major ion exactly but the large size of peak would make it difficult to accurately see the small peaks of C_2H_5^+ (mass 29) and C_2H_7^+ (mass 31).

Therefore only the following ions CHO^+ , CH_2N^+ , C_2H_3^+ and C_2H_5^+ were reacted with ethane.

CHO⁺ INTO ETHANE

The reaction of CHO⁺ ion with ethane only produced two ions at low pressures - the C₂H₇⁺ ion and the fragment CH₃⁺.



It is not possible to discuss the flux of these ions as there is no indication of the other product ions at C₂H₅⁺ (mass 29) because it coincides with the parent ion.

At higher pressures ions of mass 41, 43, 55 and 57 become important. They will be discussed later.

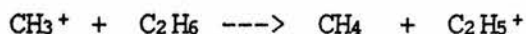
CH₂N⁺ INTO ETHANE

The reaction of CH₂N⁺ with ethane produced a spectrum of ions which were almost identical to those produced from the reaction of CHO⁺ with ethane. The only differences were that a peak of mass 26 C₂H₂⁺ was observed and that whereas with CHO⁺ the C₂H₅⁺ fragment ions could not be distinguished from the parent ion with CH₂N⁺ as the primary ion the C₂H₅⁺ ion could be seen but the C₂H₃⁺ fragment could not be seen. This means that the relative ratio of fragments cannot be calculated.

C₂H₃⁺ INTO ETHANE and C₂H₅⁺ INTO ETHANE

These reactions, which both produced C₂H₇⁺, are complicated by the subsequent reactions of the other major ions with ethane. The reactions of these other major ions, CH₃⁺, C₂H₃⁺ and C₂H₅⁺, with ethane were investigated.

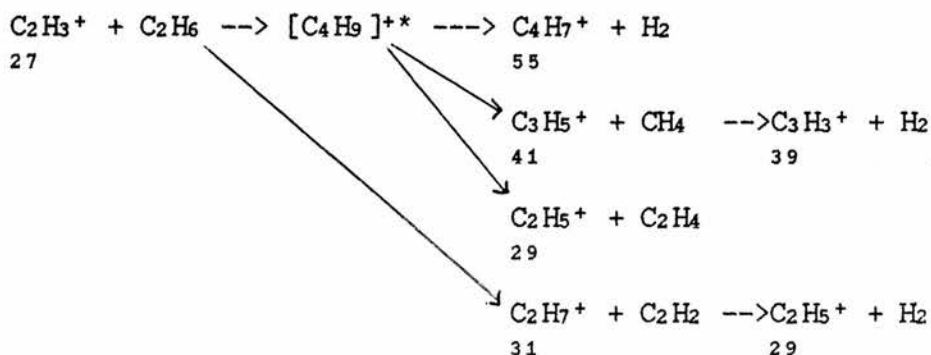
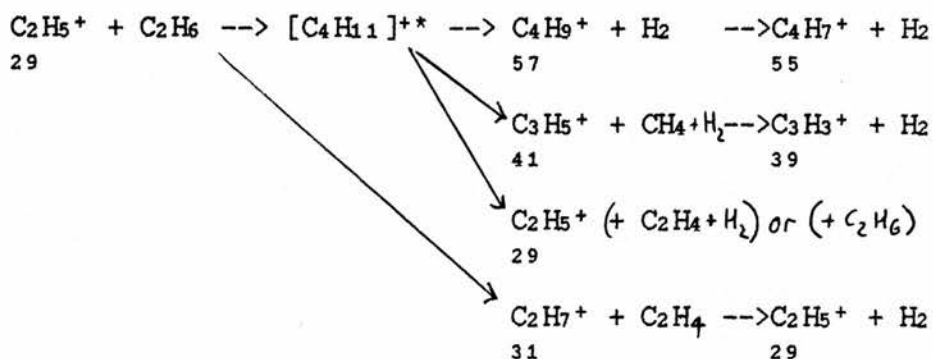
The reaction of CH₃⁺ with ethane has been studied in the triple quadrupole mass spectrometer. Mitchell and Tedder ^{49,111} stated that the initial process in the reaction of CH₃⁺ ions with ethane was a hydride abstraction reaction to give C₂H₅⁺. This work was not repeated.



The reactions of the other dominant ions C₂H₃⁺ and C₂H₅⁺ were studied in an ion cyclotron resonance mass spectrometer by Kim, Anicich and Huntress. ¹¹²

These reactions were studied in the triple quadrupole mass spectrometer under the same conditions as the protonation experiments to see if the reaction pathways to the higher alkyl ions could be determined.

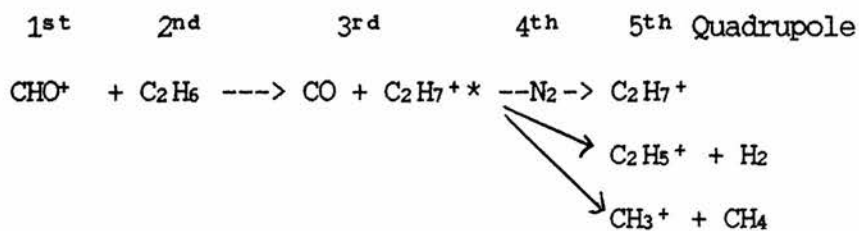
The reaction of C₂H₃⁺ with ethane produced C₂H₅⁺ (mass 29), C₃H₅⁺ (mass=41) and C₄H₇⁺ (mass=55). The reaction of C₂H₅⁺ with ethane also produced C₄H₉⁺ ions (mass=57).



C₂H₆⁺ INTO C₂H₆

This reaction was done and the self protonation reaction was observed. There were many other reactions, producing minor ions which could be accounted for from the reactions of C₂H₅⁺ and C₂H₃⁺ with ethane.

Collision induced fragmentation of C₂H₇⁺ is needed to study the ratio of the fragment products accurately. This could be done using the quinquadrupole mass spectrometer.



STRUCTURE AND FRAGMENTATION OF C₂H₇⁺

The possible structures and fragmentation routes are probably connected.

Protonation of a C-H bond, as represented in fig. 2.5, would favour the cleavage of this C-H bond to produce C₂H₅⁺ and H₂.

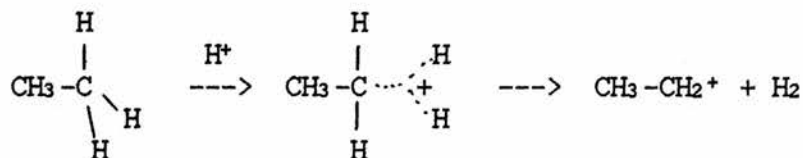


Fig. 2.5

As in methane each hydrogen in ethane is equivalent and so equally likely to be protonated. Protonation of the C-C bond would result in the structure represented in figure 2.6, and might lead to C-C bond cleavage and the formation of CH₃⁺ and methane.

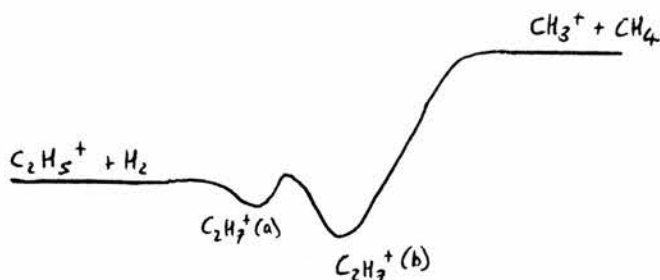


Fig. 2.6

Our results which indicate an overwhelming preference for C-H bond cleavage are in direct contrast to those of Olah¹⁰⁷. This is probably due to the fact that in the present experiment C₂H₇⁺ ions were in the gas phase whereas in Olah's case they were solvated in superacid solutions. In the gas phase reactions ethonium ions could be in an excited state. Ethonium ions in solution are solvated and could be held in the most stable form which has been shown to be the C-C bridged ethane which would be more likely to fragment with C-C

bond cleavage. The results of Kebarle ¹⁰³ obtained at a higher pressure and lower temperature than our experiments suggested that the activation energy required for the $C_2H_7^+$ ion to fragment to CH_3^+ and CH_4 is greater than that required for fragmentation to $C_2H_5^+$ and H_2 .

Fig. 2.7



CONCLUSIONS

Ethane can be protonated by CHO^+ , CH_2N^+ , $C_2H_3^+$ or $C_2H_5^+$ ions. $C_2H_7^+$ ions formed in this way tend to fragment with loss of H_2 to give $C_2H_5^+$ ions rather than with loss of CH_4 to give CH_3^+ ions. This suggests that initial protonation is on a C-H bond so that the ions have the less stable form (a). The $C_2H_7^+$ ion either does not have the energy to rearrange and fragment with the cleavage of a C-C bond or it is not stable long enough for the rearrangement to take place before it fragments. Although this gives an indication of the structure and stability of the $C_2H_7^+$ ions that have fragmented it does not mean that the $C_2H_7^+$ ions that do not fragment and are therefore detected in the mass spectrometer are of the same structure. They may well be of the more stable structure (b) which would account for them being stable enough to be isolated at the end of the quadrupole.

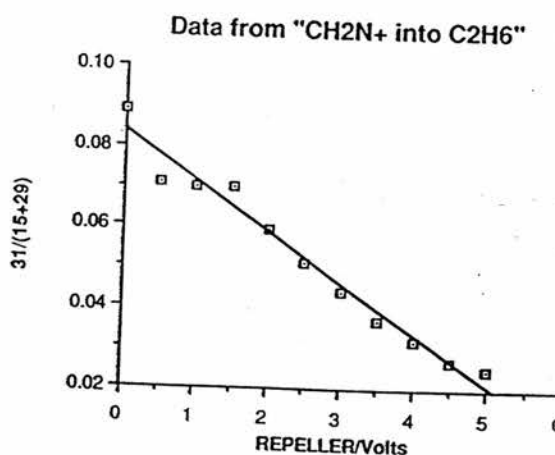
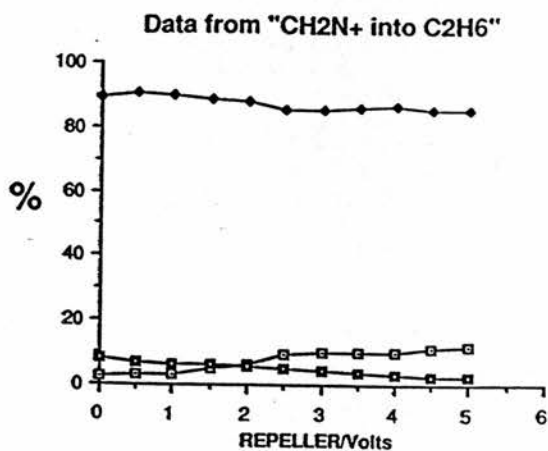
These ions are the ions that would be isolated in the third quadrupole for further reaction in the fourth quadrupole of the quinquadrupole mass spectrometer. This means that nothing definite can be concluded about the structure of the ethonium ions that are stable enough to be detected in the third quadrupole. This could be investigated further in the quinquadrupole mass spectrometer.

The effects of altering the translational energy of the primary ion on the fragmentation reactions of $C_2H_7^+$ ions indicates that the $C_2H_7^+$ ion is much more unstable and will fragment much more readily than the CH_5^+ ion. This is in complete agreement with all previous investigations.

CH₂N⁺ INTO C₂H₆

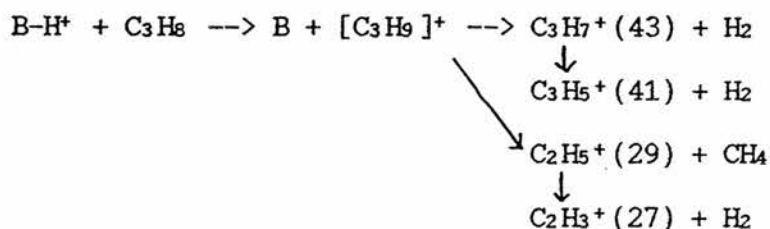
SECONDARY ION
PERCENTAGE (%)
AGAINST REPELLER (VOLTS)

RATIO OF
[C₂H₇⁺]/[CH₃⁺]+[C₂H₅⁺]
AGAINST REPELLER (VOLTS)



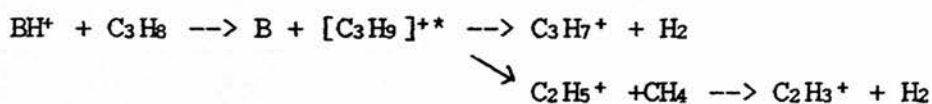
3 PROPANE

The reactions of propane fit into a general reaction scheme.

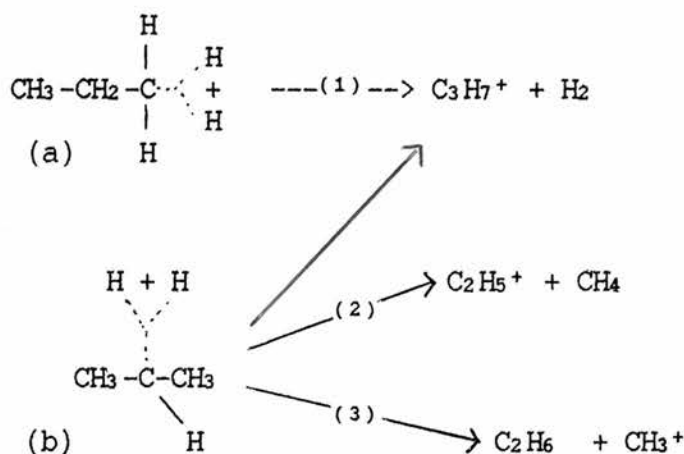


CHO⁺ INTO C₃H₈

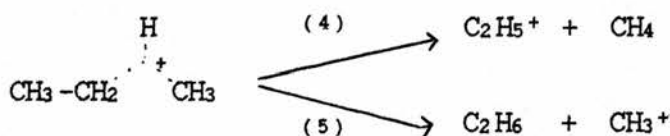
No C₃H₉⁺ ions were observed. The major products C₃H₇⁺ (43) and C₂H₅⁺ (29) (which was inferred by the presence of C₂H₃⁺) and C₂H₃⁺ (27) suggest that the propane has been protonated to C₃H₉⁺, but being unstable it fragments readily.



Protonation of a C-H bond could result in two structures, (a) and (b), fragmentation of which could lead to C₃H₇⁺ + H₂ or C₂H₅⁺ + CH₄ or C₂H₆ + CH₃⁺. No CH₃⁺ ions were observed so pathway (3) can be discounted.



Protonation of a C-C bond would give one structure which on fragmentation could either give CH_4 and C_2H_5^+ (4) or CH_3^+ and C_2H_6 (5) as the products. That no CH_3^+ was observed indicates that of fragmentation routes (4) is totally dominant.



CH_2N^+ INTO PROPANE

No C_3H_9^+ ion was observed. The fragment ions C_3H_8^+ (mass 44), C_3H_7^+ (mass 43), C_3H_5^+ (mass 41) and C_2H_5^+ (mass 29) were observed. The fragment C_2H_3^+ (mass 27) which had been observed in the reaction of CHO^+ with propane was not observed because it was under the tail of the large primary ion of mass 28. It is therefore not possible to compare the relative proportions of the fragment products.

C₂H₃⁺ INTO PROPANE AND C₂H₅⁺ INTO PROPANE

The only difference between the products of these two reactions is the appearance of C₃H₃⁺ with C₂H₃⁺ but not with C₂H₅⁺ as the primary ion.

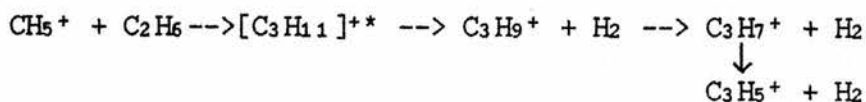
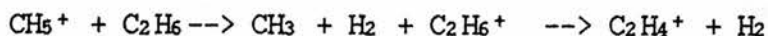
CH₅⁺ INTO C₂H₆

The reaction of CH₅⁺ into ethane was achieved by raising the pressure of methane in the ionisation chamber of the triple quadrupole mass spectrometer until the self-protonation reaction was substantial enough to produce CH₅⁺ in the first quadrupole as described earlier (page 99).

The experiment was done because the results from the reaction of a protonating ion with an alkane to form the protonated alkane showed that for alkanes above ethane the protonated ion had too much energy and so fragmented instantaneously. It was felt that if a 'softer' way of protonating an alkane could be found then they would be more stable. One way of achieving this would be to react CH₅⁺ with ethane to form the addition complex [C₃H₁₁]⁺⁺. This complex would have excess energy and would fragment. It was hoped that it would fragment with the loss of H₂ to leave C₃H₉⁺ with less energy than it would have had it been formed by direct protonation. If this did occur then it might be stable enough to be detected.

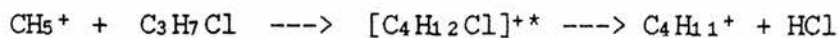
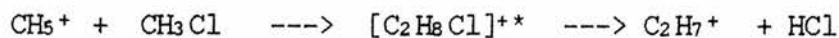
The results from this experiment indicate that ethane has been protonated by the methonium ion. The peak height of 31 must be corrected for the isotope of C₂H₆⁺. Even so it is clear that the ethonium ion has been formed. The other main ions are the fragments of

the ethonium ion $C_2H_5^+$ and $C_2H_3^+$, the ethane ion and its fragments and the fragment products of the addition complex $[C_2H_6-CH_5^+]^*$.



The $C_3H_9^+$ ion has indeed been formed in this way.

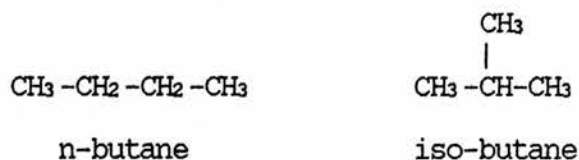
A series of reactions were done to see if this process could be used to form other protonated alkanes, some of which used chlorinated reagents to enhance the stability of the leaving neutral.



No alkonium ions of one carbon more than the target gas were observed in these experiments.

HIGHER ALKANES

Butane is the first alkane for which there are isomeric forms to be considered.



The following questions are raised:-

- 1) Are the protonated isomers of different stabilities ?
- 2) If so do the protonated isomers rearrange to the most stable form ?
- 3) Can this be detected by considering the fragments produced from the different isomers ?

4 BUTANE

With n-butane there are two possibilities for H-C bond protonation, α -H-C protonation and β -H-C protonation.

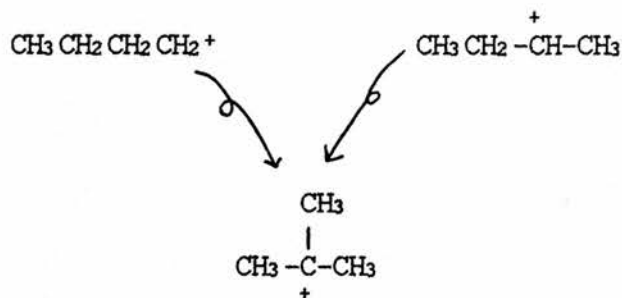


α -C-H Bond Protonation

β -Bond Protonation

A purely statistical approach would suggest that the ratio of fragments would be 6:4 = 3:2 in favour of α -protonation and subsequent H₂ loss to give the primary

carbocation rather than the secondary carbocation that would result from the β -protonation. If this were the case could this be detected or would both carbocations rearrange to the most stable tertiary ion ?



C-C bond protonation would give rise to two possible ions - α -C-C bond protonation (a) and β -C-C bond protonation (b).



Fragmentation would lead to $\text{C}_3\text{H}_7^+ + \text{CH}_4$ from α -protonation (no $\text{CH}_3^+ + \text{C}_3\text{H}_8$ was observed) or $\text{C}_2\text{H}_5^+ + \text{C}_2\text{H}_6$ from β -protonation. A purely statistical approach would give twice as much α -C-C protonation fragments as β -H-C protonation fragments.

The results from our experiments are presented in Table 2.6 in the form of percentage of the total of the ions that were C_2 , C_3 or C_4 fragments which could arise from β -C-C cleavage, α -C-C cleavage or α and β C-H cleavage respectively.

Table 2.6

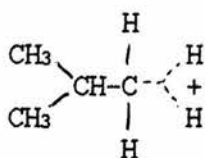
Penning Pressure 10^{-5} torr	Total $C_2H_5^+$	Total $C_3H_m^+$	Total $C_4H_9^+$	(m = 3 or 5)
3.0	55	35	12	
7.5	45	37	18	
15	30	34	32	
45	24	34	40	
150	8	14	68	

These results indicate that the fragmentation pattern does not follow a simple statistical relationship. There may be routes to the fragment ions other than the simple ones indicated above. At low pressures there is much more fragmentation to $C_2H_5^+$ ions than to $C_3H_m^+$ (where $n=3$ and 5) and $C_4H_9^+$ ions. But as the pressure increases the relative values of the ions are inverted so that at the highest pressure investigated the most abundant fragment ion is $C_4H_9^+$.

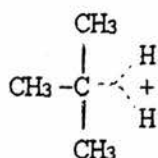
The only appreciable difference in the fragments of iso-butane is that there are considerably less $C_2H_5^+$ ions obtained with the iso-butane reaction than were obtained with n-butane. This is not at all surprising on

considering the possible structures and fragmentation routes of iso-butane.

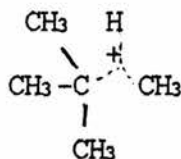
There are two forms of H-C bond to protonate. α -Protonation of the nine equivalent methyl hydrogens and β -H-C protonation of the methine hydrogen. There is only one kind of C-H bond to protonate and cleave and this would give $C_3H_7^+$ and CH_4 as the product of C-C bond cleavage.



α -H-C Bond Protonation

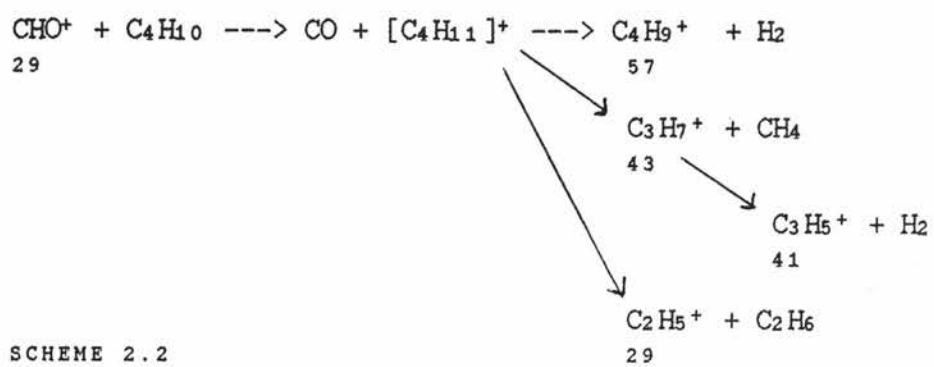


β -H-C Bond Protonation



C-C Bond Protonation

That any $C_2H_5^+$ ions were observed at all is indicative that there is rearrangement of some sort occurring. That the ratio of fragments from the two isomers is not the same indicates that the two isomers are not rearranging into the same intermediate stage before fragmentation occurs. It would be interesting to continue these investigations using the quinquadrupole mass spectrometer to isolate these ions in the third quadrupole and by collision induced fragmentation in the

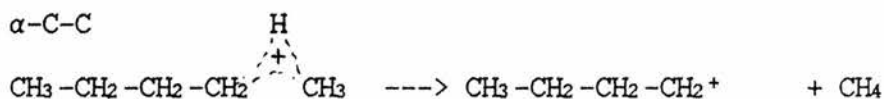
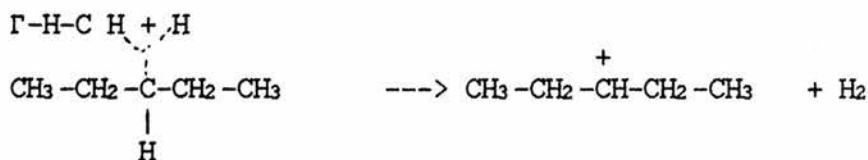
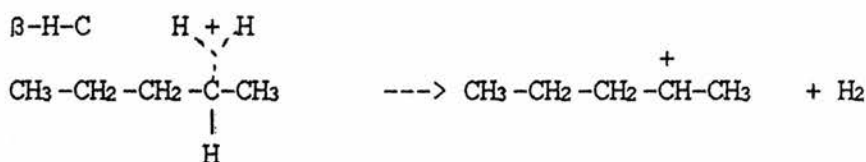
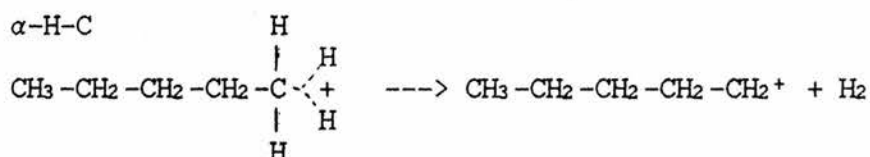


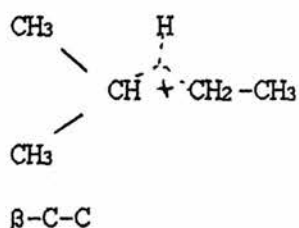
SCHEME 2.2

5 PENTANE

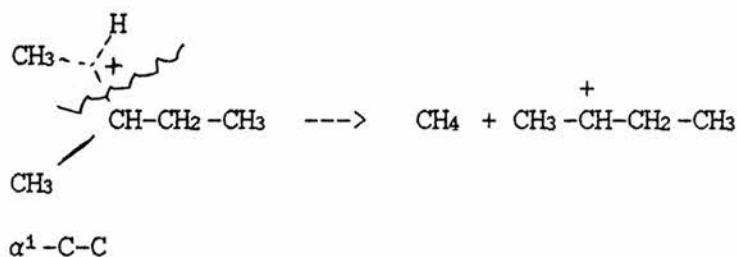
No protonated pentane, $C_5H_{13}^+$, was observed from the reactions of any of the isomers of pentane. The three isomers of pentane offer more scope for studying the relationship between structure and fragmentation routes.

n-pentane has six α -H-C bonds, four β -H-C bonds and two Γ -H-C bonds. α -C-C bond protonation and β -C-C bond protonation are statistically of equal weight. Cleavage of the α -C-C bond would produce $C_4H_9^+ + CH_4$ (no $CH_3^+ + C_4H_{10}$ was observed) and cleavage of the β -C-C bond would produce either $C_2H_5^+ + C_3H_8$ or $C_3H_7^+ + C_2H_6$ as the initial fragment ions.

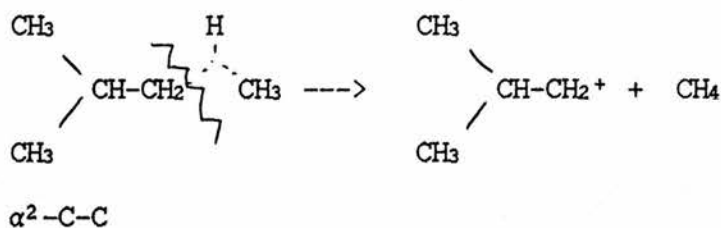




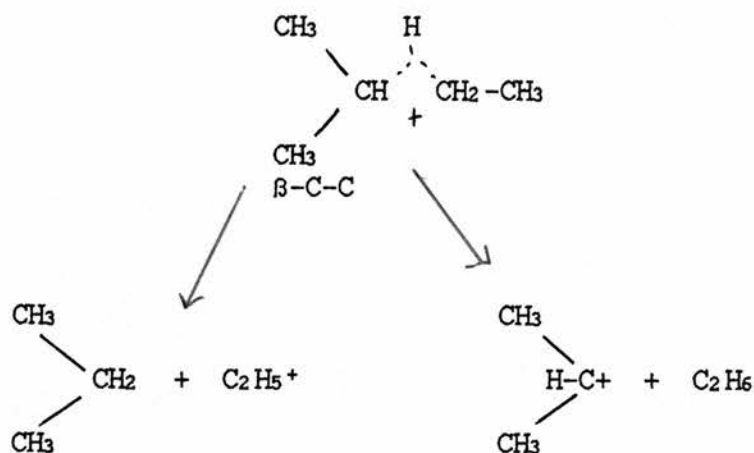
Cleavage of the protonated $\alpha^1\text{-C-C}$ bond would produce methane and a linear secondary butyl carbocation as the initial fragment ion. This could subsequently rearrange or fragment further.



Cleavage of the protonated $\alpha^2\text{-C-C}$ bond would initially produce $(\text{CH}_3)_2\text{-CH-CH}_2^+$ as the fragment ion.



Cleavage of the $\beta\text{-C-C}$ bond could produce C_2H_5^+ and C_3H_6 or C_2H_6 and C_3H_7^+ initially in the form of a secondary propyl carbocation which would be stabilized by the electron repelling effect of the methyl groups.

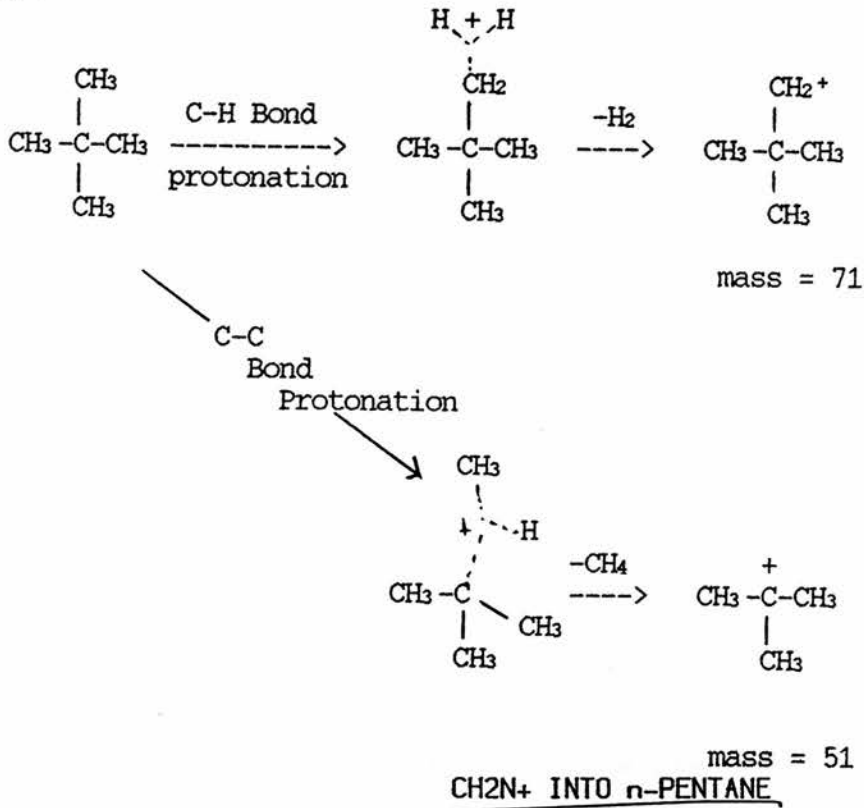


With there being so much scope for rearrangement and/or further fragmentation it is meaningless to consider the proportion of fragments in a statistical way.

Neo-pentane is a very interesting structure for considering protonation and fragmentation. If this is a valid approach to consider that protonation and fragmentation can be modelled by considering C-H and C-C bond protonation and cleavage then neo-pentane would initially form only two species as it has only one type of C-H bond and one type of C-C bond to be protonated.

C-H bond protonation followed by loss of H_2 , where both hydrogens come from the same carbon as there are no β -hydrogens for α - β dehydrogenation to occur, would give an ion of mass 71.

C-C bond protonation and cleavage would produce methane and the stable tertiary butyl carbocation of mass 57.



TABLES 2.7 AND 2.8

% SECONDARY ION FLUX

PRESSURES in torr			m/e				
INITIAL ION GAUGE	ION GAUGE	PENNING GAUGE	29	41	43	57	71
7.5×10 ⁻⁷	3.8×10 ⁻⁶	2.3×10 ⁻⁵	44.21	30.53	16.84	3.16	5.26
7.5×10 ⁻⁷	7.5×10 ⁻⁶	4.5×10 ⁻⁵	34.72	33.33	22.22	4.17	5.56
7.5×10 ⁻⁷	1.5×10 ⁻⁵	7.5×10 ⁻⁵	31.73	25.96	22.12	4.81	15.38
7.5×10 ⁻⁷	3.0×10 ⁻⁵	2.3×10 ⁻⁴	23.81	17.14	24.76	7.62	26.67
7.5×10 ⁻⁷	6.0×10 ⁻⁴	7.5×10 ⁻⁴	12.50	8.33	25.00	10.42	43.75

CH₂N⁺ INTO ISO-C₅H₁₂

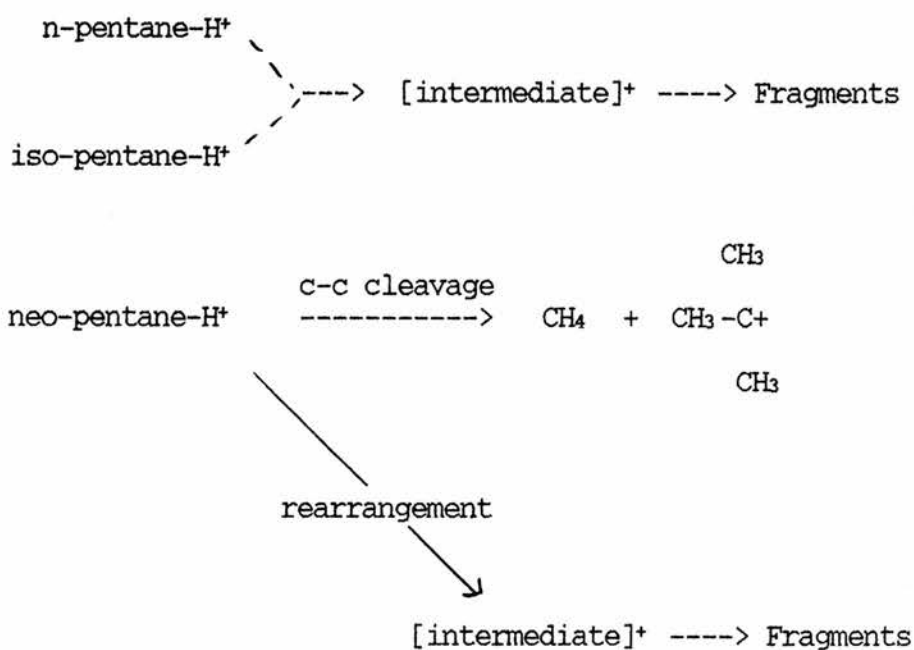
% SECONDARY ION FLUX

PRESSURES in torr			m/e				
INITIAL ION GAUGE	ION GAUGE	PENNING GAUGE	29	41	43	57	71
7.5×10 ⁻⁷	2.3×10 ⁻⁶	1.5×10 ⁻⁵	48.28	27.59	13.79	6.90	3.45
7.5×10 ⁻⁷	6.8×10 ⁻⁶	3.8×10 ⁻⁵	56.07	22.43	14.95	3.74	2.80
7.5×10 ⁻⁷	1.5×10 ⁻⁵	7.5×10 ⁻⁵	32.26	25.81	23.66	8.60	9.68
7.5×10 ⁻⁷	3.0×10 ⁻⁵	3.0×10 ⁻⁴	19.51	14.63	24.39	12.20	29.27
7.5×10 ⁻⁷	6.0×10 ⁻⁵	7.5×10 ⁻⁴	8.33	5.56	19.44	16.67	50.00

Considering the results, as shown in tables 2.7 and 2.8, it was found that the pattern of ions produced from n- and iso- pentane were, to all intents and purposes, identical. $C_2H_5^+$ (29) and $C_3H_n^+$ (where $n=3$ or 5)(39,41) are very large at low pressures but diminish as the pressure increases and as $C_4H_9^+$ (57) and $C_5H_{11}^+$ (71) become more important. That the patterns are identical suggests that both protonated n- and iso- pentane fragment through a common intermediate structure.

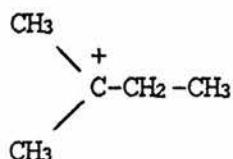
Neo-pentane gives a totally different pattern of ions. That any $C_2H_5^+$ and $C_3H_n^+$ ($n=3$ or 5) ions are seen indicates that rearrangement is occurring - perhaps through the same intermediate structure as the n- and iso- isomers. That there is so little $C_5H_{11}^+$ suggests that the loss of H_2 from $C_5H_{13}^+$ involves an α - β dehydration step. By far the major product at all pressures is the stabilized butyl ion in considerably larger amounts than either of the other isomers.

The results from this section could be represented by a series of competing pathways.



The products from neo-pentane are dominated by the C-C bond cleavage because the resultant tertiary carbocation is stabilized by three methyl groups. This is in accord with results from investigations using a tandem mass spectrometer. ¹⁰¹

It is suggested that the common intermediate ion that the protonated n-pentane and protonated iso-pentane fragment through is the tertiary pentyl ion.



Dehydrogenation of protonated neo-pentane would initially produce $(\text{CH}_3)_3\text{-C-CH}_2^+$ ions which could rearrange, as in figure 2.5, to give a tertiary carbocation which would be

identical to the ion produced from β^2 -dehydrogenation of iso-pentane. Rearrangement of n-pentane could also produce an ion of this structure. It might be concluded therefore that iso and n-pentane fragment primarily through this intermediate. Neo-pentane fragments through two routes - loss of methane to give the tertiary butyl carbocation or rearrangement through the common intermediate and subsequent fragmentation.

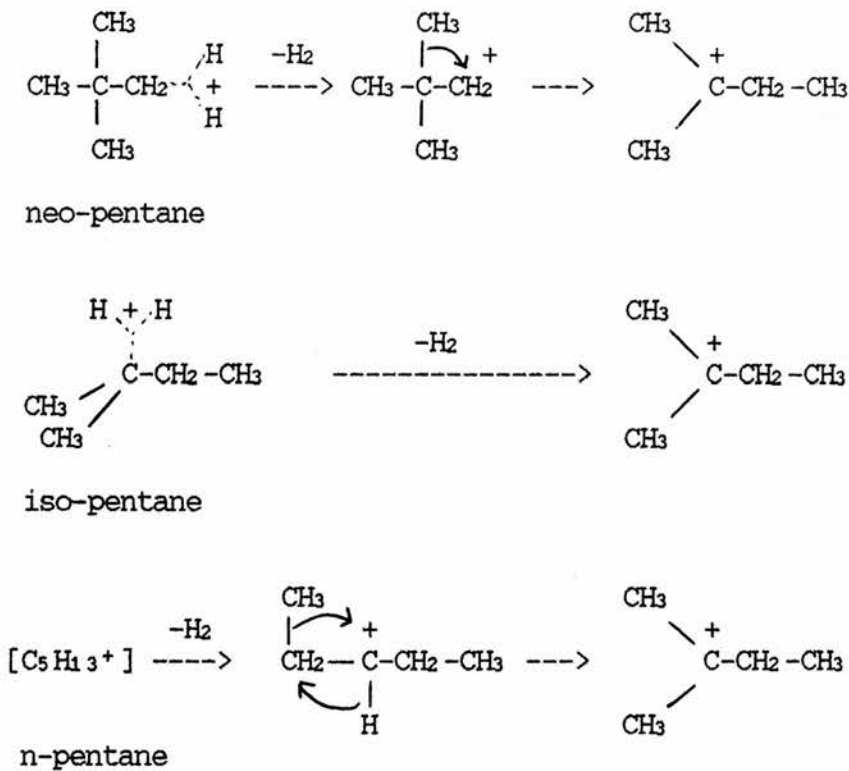
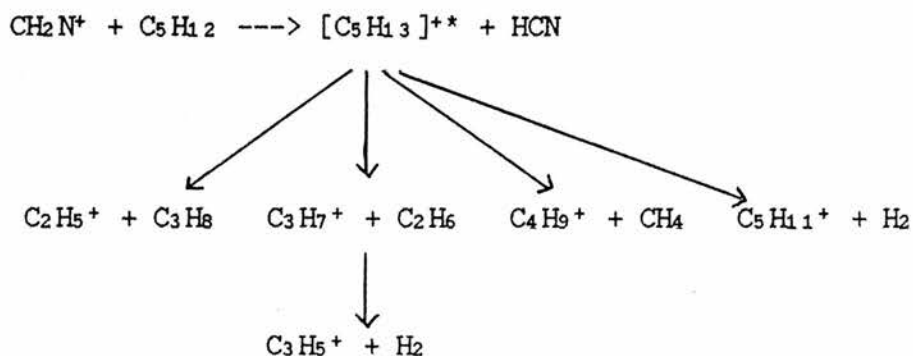


Fig. 2.5

The tertiary ion represented in figure 2.5 has been found to be the most stable of the isomeric forms ¹¹³ so it seems reasonable to suggest that this could be the common intermediate. ¹¹⁴

The fragmentation of the tertiary $C_5H_{11}^+$ ion that is reported in the literature to $C_3H_7^+$ in its tertiary form and C_2H_4 as the neutral fragment cannot account for the total fragmentation patterns obtained from the reaction of CH_2N^+ with the isomers of pentane but it could account for the formation of $C_5H_{11}^+$ and $C_3H_7^+$ ions from neo-pentane.

Further work would need to be done in order to provide evidence for the suggestion that emerges from consideration of these results that, as with the other alkanes studied, the ions produced can only be accounted for through the formation and fragmentation of $[C_5H_{13}]^+$ - protonated pentane as in scheme 2.3.



SCHEME 2.3

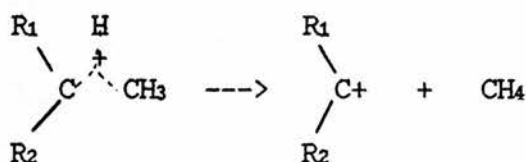
At this stage it was decided to delay further investigations of the protonation of alkanes and the matters raised in the results so far until the quinquapole mass spectrometer was working because this would allow much more scope for investigation of these problems.

OVERALL CONCLUSIONS

It can be concluded from the work done on the triple quadrupole mass spectrometer that alkanes can be protonated in the triple quadrupole mass spectrometer by reacting a protonating primary ion from the first quadrupole with the alkane in the second quadrupole. When the alkane was methane or ethane the alkonium ion was observed. For the alkanes from methane to pentane the fragments observed agree with the suggestion that the alkane was protonated but fragmented rapidly - either with or without rearrangement. The fragmentation patterns of alkyl ions have been extensively studied^{85,115-118} and are different from the patterns that were obtained in the present experiments. Unless these differences are due to the energy of the ions in the studies the fragmentation patterns that have been observed are the fragmentation patterns of the $C_nH_{2n+3}^+$ ions.

The implications of the results in the present work to the mechanisms of catalytic cracking were not considered as it was hoped to continue the work in the quinquadrupole mass spectrometer to obtain a better understanding of the mechanisms of fragmentation of higher hydrocarbons. The results that were obtained are in agreement with a study of protonation of n-hexane¹⁰⁶ in an ICR mass spectrometer. Protonation of an alkane can be considered to be either of a C-H bond or of a C-C

bond. An ion with a structure containing a protonated C-H bond is more likely to fragment with the loss of H₂ - where one of the hydrogens is the hydrogen that was added to the alkane. An ion with a structure containing a protonated C-C bond is more likely to fragment with the cleavage of the C-C bond to give a neutral saturated hydrocarbon and an alkyl ion. For all alkanes with a terminal C-C bond the cleavage of this bond will result in methane as the neutral in preference to methyl ion as the charged species.



providing that the following condition is met:-

- 1) R₁ and R₂ are not both H

Evidence for the rearrangement of ions has been found in the results of these experiments. This could be investigated further in the quinquadrupole mass spectrometer whereas combination of the use of isotopically labelled species and CID fragmentation of ions from the third quadrupole in the fourth quadrupole could advance the understanding of the mechanisms of fragmentation of protonated alkanes and associated ions.

CHAPTER THREE

INVESTIGATIONS OF THE MECHANISMS INVOLVED

IN MOBIL'S METHANOL-TO-GASOLINE REACTION

REACTIONS OF IONS FROM METHANOL WITH METHANOLSUMMARY

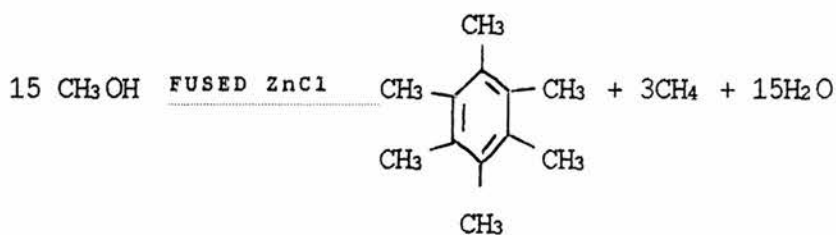
The triple quadrupole mass spectrometer was used to study the reactions between fragment ions of methanol with methanol.

The development of Mobil's Methanol-to-Gasoline (MTG) Process on an industrial scale has resulted in many investigations being undertaken into the mechanisms involved. The aim of the present work was to use the triple quadrupole mass spectrometer to investigate the mechanisms of reactions involving methanol in the gas phase.

A general review of zeolites and the mechanisms proposed to account for the formation of hydrocarbons from methanol is presented.

A full review of the history of hydrocarbon formation from methanol is given in reference 7. Only the major advances which lead to mechanistic considerations are reviewed here.

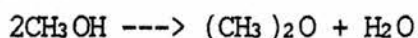
The conversion of methanol to hydrocarbons was first reported in 1880 by J.A. Lebel and W.H. Greene for the formation of hexamethylbenzene and methane by passing methanol over fused zinc chloride. ¹¹⁹



$$\Delta G_{600 \text{ K}} = -265.2 \text{ kcal/mol}$$

This reaction was thought to be condensation of carbene, $\text{CH}_2:$, to benzene followed by extensive methylation by Friedel-Craft reactions.

In 1928 H. Adkins and P.D. Perkins¹²⁰ reported the formation of ethene by reaction of methanol over Al_2O_3 . At temperatures between $300\text{--}350^\circ\text{C}$ dimethyl ether was quantitatively produced.



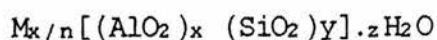
Above 350°C methane, ethene, carbon monoxide, carbon dioxide and hydrogen were produced. This was the first suggestion that dimethyl ether was an important intermediate and that ethene was the first hydrocarbon product to be formed.

The first report of methanol conversion over zeolites was that of Schwartz and Ciric¹²¹.

Methanol Decomposition over Metal
Cation-Exchanged Faujasites

Gaseous product composition (mol%)		
	REX	ZnX (9.46 wt% Zn)
H ₂	Trace	10.3
CH ₄	22.5	43.0
2 H ₄	24.5	17.0
C ₂ H ₆	2.7	2.9
C ₃ H ₆	10.8	9.2
C ₃ H ₈	4.4	-
C ₄ H ₈	8.0	7.8
i-C ₄ H ₁₀	13.9	4.0
i-C ₆ H ₁₂	6.2	-
Hexanes	4.3	2.0
Others	2.7	3.8

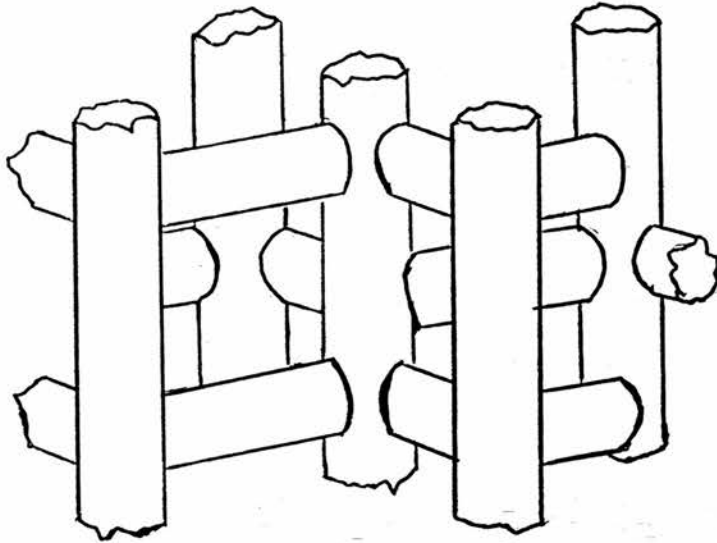
Zeolites are porous crystalline aluminosilicates with a three-dimensional framework in which AlO₄ and SiO₄ tetrahedra are interconnected by shared oxygen atoms ⁷. The charges on the lattice are balanced by cations Mⁿ⁺ to give the general equation



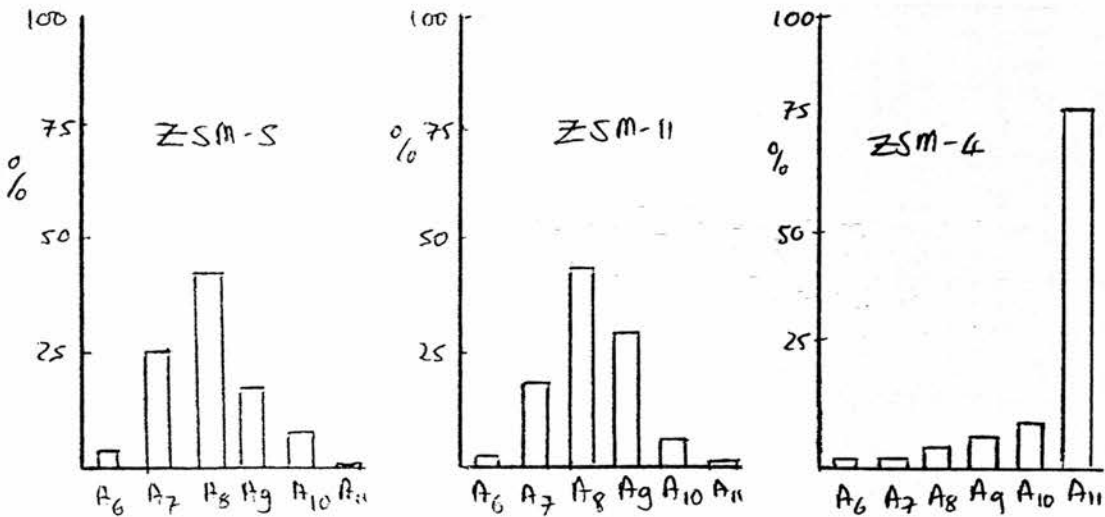
The synthetic zeolites have shape-selective catalytic properties. They have the ability to discriminate for reactant molecules and control the product selectivity. This has been attributed to the well-defined geometry of their pores, channels and cages.

ZSM-5 has orthorhombic symmetry $Pnma$ with cell parameters $a = 20.07$, $b = 19.92$, $c = 13.42$ Å. The channel system is portrayed in figure 3.1. The pores have the dimensions - 5.4 Å by 5.6 Å

Fig. 3.1



The typical product distributions from methanol conversion over ZSM-5, ZSM-11 and ZSM-4 are presented in tables 3.1 to 3.3. (A_n refers to number of carbons in the aromatic fractions.)



ZSM-5 is the most selective zeolite and also the most resilient to deactivation by coking.

ZSM-4 is a large pored zeolite having large supercages of around 13Å diameter and pores of ≈ 7.4 Å. This zeolite gave a predominantly C₁₁ aromatic product.

It was concluded that the distribution of products depends on the dimensions of the zeolite. Hydrocarbons above C₅ cannot move through small pore zeolites such as ZK-5 which has pore dimensions of 3.8Å by 5.2Å. The products from small pore zeolites are comprised of C₁ to C₅ hydrocarbons. Large pore zeolites allow formation of hydrocarbons up to C₁₁. A medium pore zeolite, such as ZSM-5, will favour the formation of molecules of C₈. The gasoline produced from the MTG reaction over ZSM-5 has a high octane rating. In the data presented in table 3.4 the synthetic gasoline has a higher octane rating than leaded commercial gasoline and so does not require the addition of anti-knocking agents. This is indicative of the selectivity that this catalyst has.

Table 3.4

Octane number of commercial gasoline and ZSM-5 gasoline.

	Commercial	ZSM-5
No Additives	83	93
Leaded	90	101

From reference 5

The consensus of recent research is that the product distribution is dependent on the shape and size of the catalyst pores.

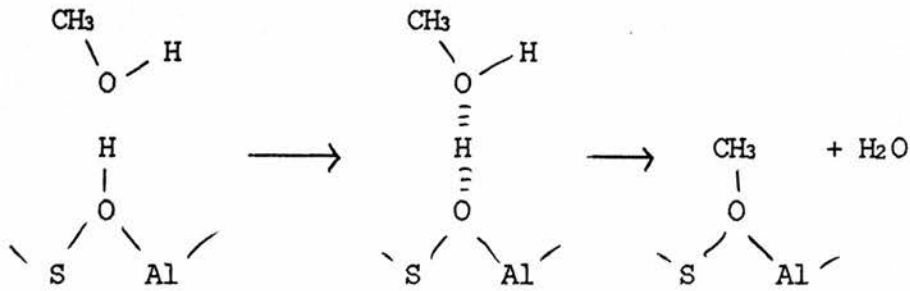
The formation of hydrocarbons from methanol is not restricted to zeolite catalysts. The production of ethene from methanol in 86% H₂SO₄ was reported by Dolgov¹²² and similar non zeolitic catalysts have been noted.⁷

MECHANISMS

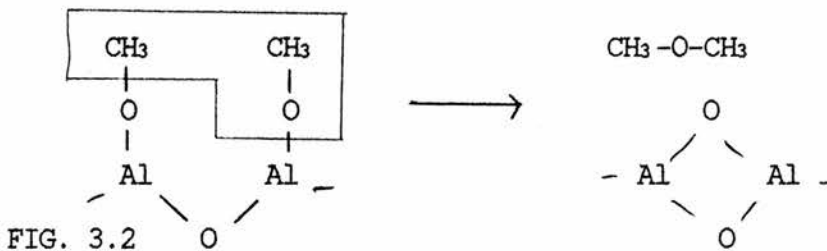
The mechanisms of the reaction occurring in the MTG process have been intensively studied.^{7,123,125,131} In the nine years up till 1985 when this present research was started, the mechanism of the initial C-C bond formation step had not been found. Now, three years later, in 1988, this is still an unsolved problem and is the subject of "ongoing controversy".¹²⁴ Chang claimed that there are now over twenty four mechanisms proposed in the literature.¹²⁵ Most of these mechanisms differ only in minor details. The main mechanisms are discussed.

REACTION MECHANISMS INVOLVING METHYL GROUPS

Formation of methyl groups on zeolite surfaces has been reported.¹²⁶



A study on Al_2O_3 as a simple oxide catalyst led Parera and Figoli¹²⁷ to propose that dimethyl ether was formed by combining two such methoxy groups as represented in fig 3.2.

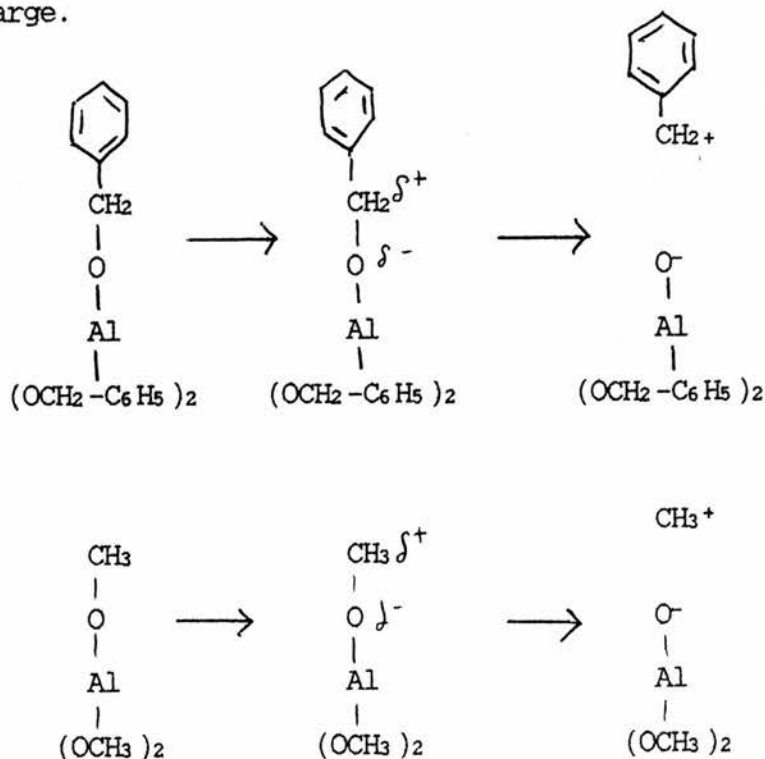


A mechanism proposed by Heiba and Landis involved liberation of methyl cations from surface methoxy groups.¹²⁸ They showed that the products of thermal analysis of aluminium alkoxides produce very similar products to the dehydration of methanol over aluminium oxide catalyst.

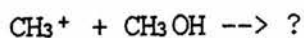
Table 3.5

	Al(OCH ₃) ₃ 385°C mol %	CH ₃ OH over Al ₂ O ₃ at 450°C 0.5 LHSV	(CH ₃) ₂ O over Al ₂ O ₃ at 450°C 0.5 LHSV
CH ₄	22.5	MAJOR	MAJOR
H ₂	35.2	MAJOR	MAJOR
CO	31.1	MAJOR	MAJOR
C ₂ H ₄	1.3	MINOR	MINOR
C ₃ H ₆	2.5	MINOR	MINOR
(CH ₃) ₂ O	7.1	MAJOR	-
Other	0.3	MINOR	MINOR

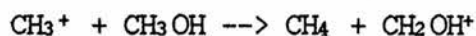
That Al(OCH₂-C₆H₅)₃ decomposed more readily than Al(OCH₃)₃ suggested that the cleavage of the C-O bond was a heterolytic process with carbon having a positive charge.



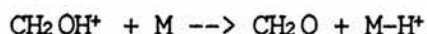
They proposed that the subsequent step would be reaction of CH₃⁺ on another methoxy group. This mechanism can be approximated by reacting methyl ions with methanol.



The reaction of methyl ions with methanol was discounted by Chang and Silvestri because they thought that the main reaction would be hydride abstraction to form methane and CH_2OH^+ .



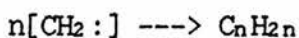
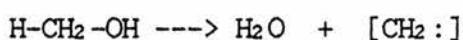
CH_2OH^+ could then deprotonate to form formaldehyde



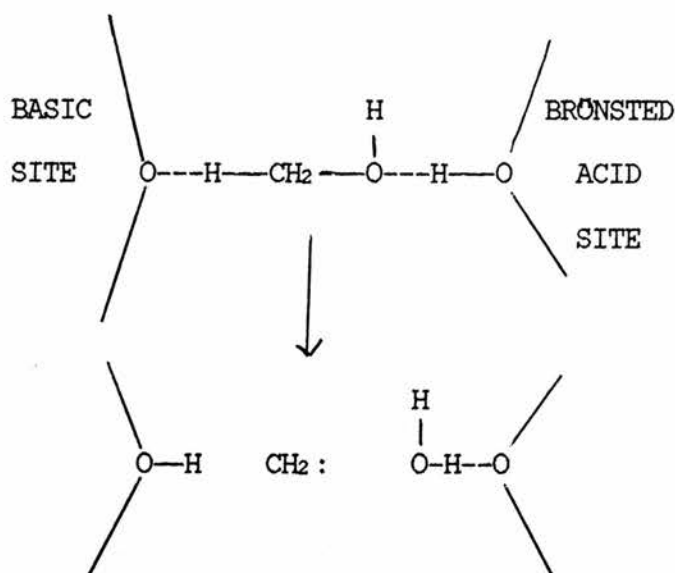
As methane is usually less than 1% of the products and formaldehyde is not observed, they concluded that this could not be occurring in the ZSM-5 catalyst.¹²⁹

CARBENE MECHANISMS

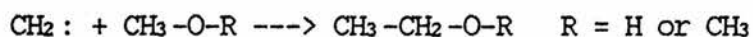
Mechanisms involving the formation of carbenes have been proposed.¹³⁰ Venuto and Landis¹³¹ proposed a mechanism involving α -elimination of water to form a carbene which would then polymerise to form olefins.



Chang and Silvestri¹³² suggested that this α -elimination could be facilitated by the concerted action of an acidic and a basic site on the catalyst.



The carbenes thus formed could either polymerise or insert into a C-O bond of methanol or dimethyl ether to form a C-C bond.



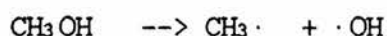
Support for the formation of carbenes was reported from investigations by ^{13}C N.M.R. techniques. A peak corresponding to $-\text{CH}_2-$ was observed in the ^{13}C N.M.R. spectra of methanol over HY Zeolite. ¹³³

A modified adsorbed carbene mechanism was proposed to account for the experimental observation of reactivity with respect to time of fresh ZSM-5 at temperatures below 250°C . ¹³⁴⁻¹³⁸

These mechanisms cannot be studied in a mass spectrometer.

FREE RADICAL MECHANISMS

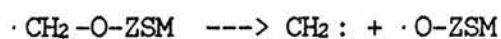
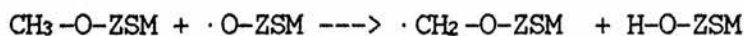
Zatorski and Krzyzanowski proposed a free radical mechanism in 1978 but did not provide experimental evidence.¹³⁹ Recent work has detected free radicals by ESR using α -phenyl-N-t-butylnitron as a spin trapping reagent. It was suggested that the radicals were formed by interaction of dimethyl ether with paramagnetic centres in the zeolite caused by solid-state defects. The combination of free radicals could produce the C-C bond formation step.¹⁴⁰



Hunter, Hutchings and Pickl carried out reactions with methanol and dimethyl ether over ZSM-5 in the presence of oxygen and nitric oxide as radical scavengers and concluded that free radicals were not present and were not involved in the mechanism of hydrocarbon formation.¹⁴¹

FREE RADICAL SCISSION TO CARBENES

It has also been proposed that a surface bound methoxy could react with a surface oxygen and form a carbene.¹⁴⁰



These mechanisms cannot be studied using a mass spectrometer.

CARBONIUM ION MECHANISM

The mechanisms that can be studied using a mass spectrometer are those involving carbonium ions. The species thought to be important in the reaction of methanol are protonated methanol, CH_3OH_2^+ , dimethyl ether CH_3OCH_3 , dimethyl oxonium ions $\text{CH}_3\text{OHCH}_3^+$ and trimethyl oxonium ions.

Investigations that support these reactions and investigations that provide evidence against these reactions have been reported. Van den Berg and co-workers have been the champion of the mechanisms involving oxonium ions.¹⁴² Support for these mechanisms have been reported by Gabelica, Perot and co-workers¹⁴³, Olah and co-workers¹⁴⁴ and others¹⁴⁵. Experimental evidence that disputes the involvement of oxonium ions has been reported.¹⁴⁶⁻¹⁴⁹

As specific mechanisms involving oxonium ions will be discussed in detail in the light of experiments to be reported, these mechanisms will not be discussed in detail at present.

The literature on gas phase reactions of methanol will now be reviewed.

LITERATURE REVIEW - METHANOL

Munson and Field, in 1966, had observed hydrated protons, $(\text{H}_2\text{O})_n\text{H}^+$, where $n=1,2,3$ or 4 .^{74,150,151} They went on to study the solvation of protons by oxygenated organic compounds. When gaseous methanol was admitted to their modified conventional mass spectrometer at a few tenths of a torr and 200°C mono-, di- and tri-solvated protons were observed. $(\text{CH}_3\text{OH})-\text{H}^+$, $(\text{CH}_3\text{OH})_2-\text{H}^+$ and $(\text{CH}_3\text{OH})_3-\text{H}^+$. In gaseous dimethyl ether only mono- and di- solvated protons were observed. $((\text{CH}_3)_2\text{O})-\text{H}^+$, $((\text{CH}_3)_2\text{O})_2-\text{H}^+$.

These results could be rationalised by considering the initial solvation of the proton forming a protonated oxonium species - H_3O^+ , CH_3OH_2^+ and $(\text{CH}_3)_2\text{OH}^+$. If each oxygen bound proton could bind to one additional molecule this would allow the formation of $(\text{H}_2\text{O})_n\text{H}^+$ where $n=1,2,3$ or 4 , $(\text{CH}_3\text{OH})_n-\text{H}^+$ where $n=1,2$ or 3 and $((\text{CH}_3)_2\text{O})_n-\text{H}^+$ where $n=1$ or 2 .

It was also shown that protonated dimethyl ether - the dimethyl oxonium ion - was a weaker acid than protonated methanol - the methyl oxonium ion - which was a weaker acid than protonated methanol - the oxonium ion. This would be expected from consideration of the inductive effect of methyl groups. Methyl groups repel electrons and stabilize a positive charge on an adjacent oxygen. Dimethyl oxonium ions having two electron repelling methyl groups will be less likely to lose the

proton than methyl oxonium with only one methyl group and the oxonium ions with no methyl groups.

Henis, in 1968, used ion-cyclotron resonance techniques to study ion-molecule reactions of methanol at around 1×10^{-6} torr and an electron energy of 70eV. ¹⁵² Using ion trapping techniques ions could be held for over 1 second - which is a long time in the time scale of ion-molecule reactions - and given a path length of close to 1 kilometre. These results indicated the importance of the methyl oxonium ion, CH_3OH_2^+ , and confirmed its structure as that represented in figure 3.2.2



Solvated protons of the type reported by Munson and Field were also observed and were assigned the structures as represented in figure 3.2.3

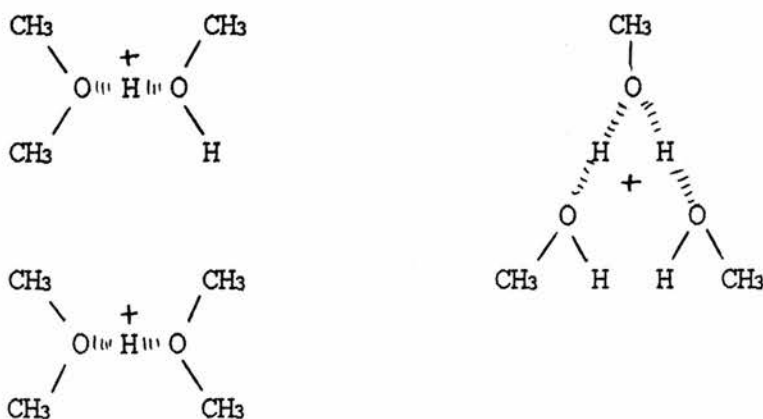
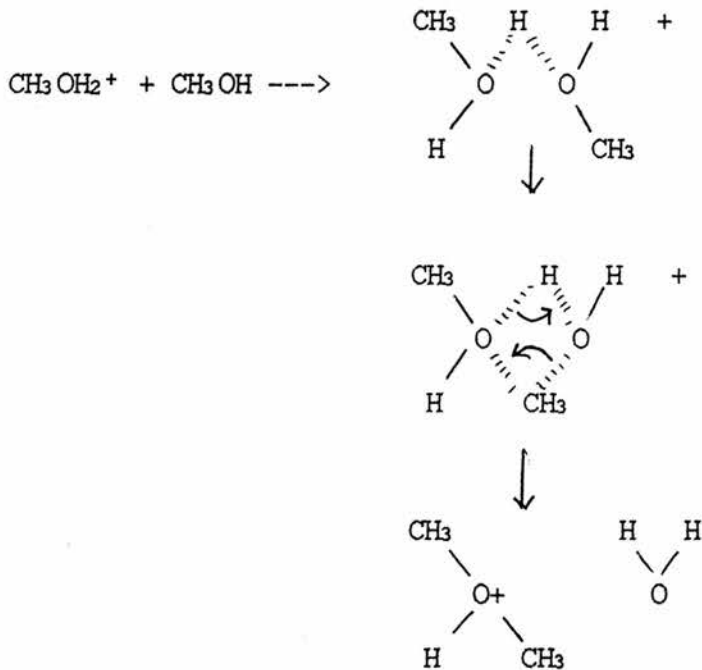


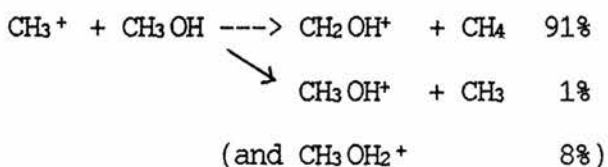
FIG. 3.2.3

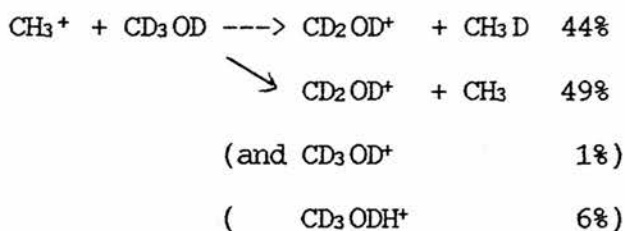
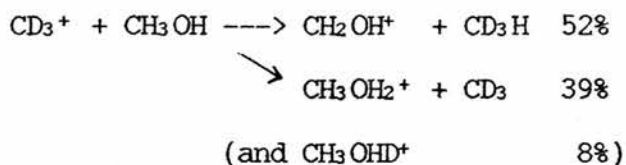
From the results of double resonance experiments Henis concluded that the dimethyl oxonium ions were formed by fragmentation of the addition complex of two methanol molecules and the solvated proton. The mechanism that he proposed involved a methyl group and a proton shifting from one oxygen to the other.



This mechanism will be discussed later in the light of the investigations undertaken in this work.

Tandem ion cyclotron resonance mass spectrometry was used to investigate the reactions of methyl ions and methanol by Smith and Futrell.¹⁵³ CH_3^+ and CD_3^+ ions were decelerated to an energy equivalent to $< 0.1\text{eV}$ and injected into the I.C.R. cell containing around 10^{-6} torr of methanol.





These results suggested that all ions occurred via fragmentation of an addition complex - $[\text{CH}_3\text{OH}-\text{CH}_3]^{+*}$. This adduct was not observed, which led to the estimation of its lifetime as less than 10^{-6} s.

The results reported here were done with ions of a higher energy.

In a series of papers from 1967 to 1984, Kebarle and co-workers investigated gas phase ion equilibria of the solvation of the hydrogen ion by water, methanol, dimethyl ether and other solvent molecules.¹⁵⁴⁻¹⁵⁹ They used a pulsed electron beam high pressure ion source mass spectrometer and operated at pressures of 10 to 250 mtorr of methanol in 4-5 torr of methane. They observed poly solvated protons of higher orders than those of earlier workers such as $(\text{CH}_3\text{OH})_n\text{-H}^+$ where $n = 1$ to 8.

The formation of adducts between CH_3OH_2^+ ions with certain compounds in which the hydrogen forms a hydrogen bond between the sample molecule and methanol were reported in ICR studies.¹⁶⁰

The present work was done at low pressures and used isotopically labelled molecules to aid the investigation of the mechanisms operating.

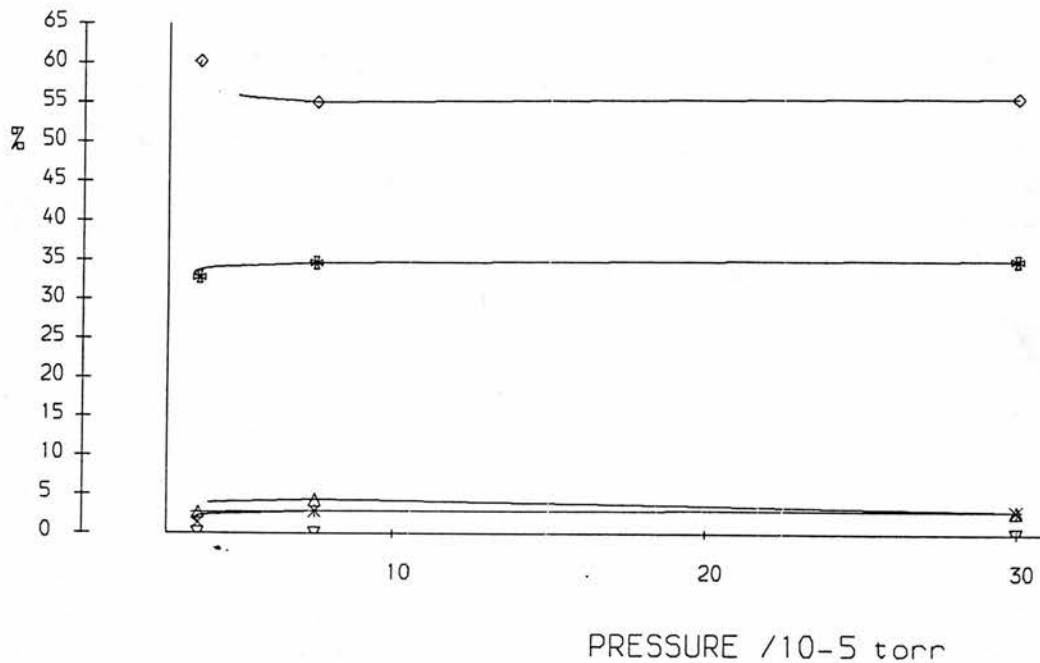
RESULTS

Owing to the high mass of some of the ions produced in these reactions, and problems with maintaining a constant pressure of the alcohols, many of the results in this section were qualitative. The experiments that produced enough results to tabulate are indicated below. A full account of the reactions and the identity of the ions produced is included in the discussion section.

<u>REACTION</u>	<u>PAGE</u>
Reaction of $\text{CH}_3^{18}\text{OH}^+ + \text{CH}_3^{16}\text{OH}$	162
Reaction of $\text{CH}_2\text{OH}^+ + \text{CH}_3\text{OH}$	163
Reaction of $\text{CHO}^+ + \text{CH}_3\text{OH}$	164
Reaction of $\text{CHO}^+ + \text{CD}_3\text{OD}$	165
Reaction of $\text{CH}_3^+ + \text{CH}_3\text{OH}$ at 10^{-7} and 10^{-6} torr	166 + 167
Reaction of $\text{CD}_3^+ + \text{CH}_3\text{OH}$ -major and minor ions	168 - 171
Reaction of $\text{CD}_3\text{OD}_2^+ + \text{CH}_3\text{OH}$	172 - 173
Reaction of $\overset{\text{H}}{\text{CH}_3\text{OCH}_3^+} + \text{CH}_3\text{OH}$	174
<u>ETHANOL</u>	
Reaction of $\text{CH}_3\text{OH}_2^+ + \text{CH}_3\text{CH}_2\text{OH}$	175
Reaction of $\text{C}_2\text{H}_5\text{OH}_2^+ + \text{CH}_3\text{CH}_2\text{OH}$	176

CH₃¹⁸OH+ INTO CH₃¹⁶OH

% SECONDARY ION FLUX Vs. PRESSURE



% SECONDARY ION FLUX

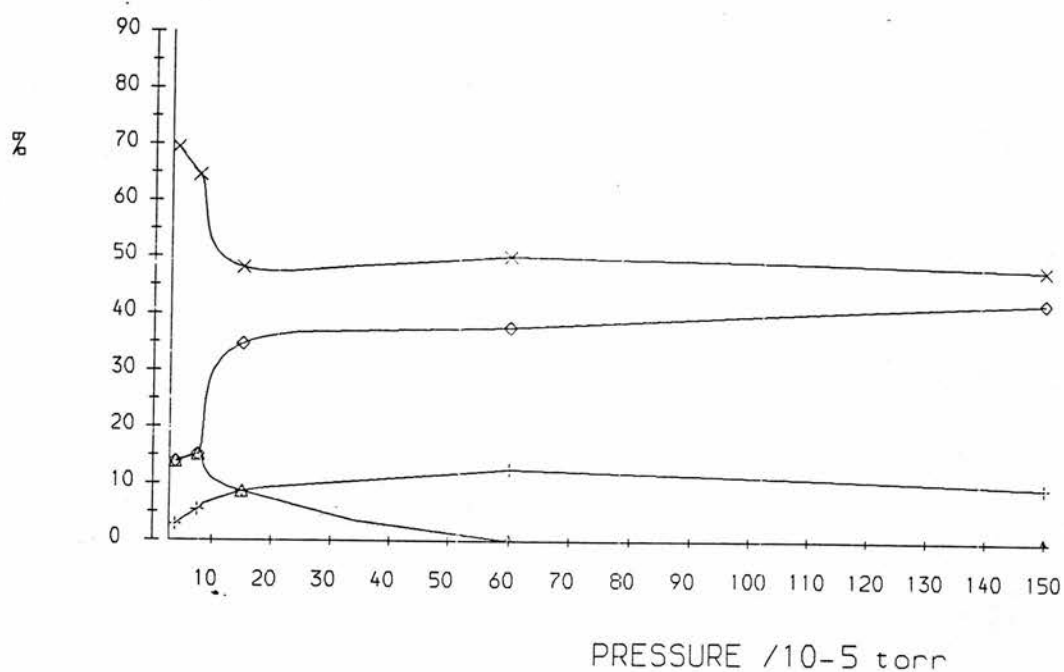
PRESSURES in torr			m/e						
INITIAL ION GAUGE	ION GAUGE	PENNING GAUGE	15	31	32	33	35	47	
(A)	7.5 × 10 ⁻⁷	2.3 × 10 ⁻⁶	3.8 × 10 ⁻⁵	2.74	1.37	2.74	60.27	32.88	0.00
(B)	7.5 × 10 ⁻⁷	3.8 × 10 ⁻⁶	7.5 × 10 ⁻⁵	2.90	2.90	4.35	55.07	34.78	0.00
(C)	7.5 × 10 ⁻⁷	7.5 × 10 ⁻⁶	3.0 × 10 ⁻⁴	2.94	2.94	2.94	55.89	35.29	0.00

% TOTAL ION FLUX

PRESSURES in torr			m/e						
INITIAL ION GAUGE	ION GAUGE	PENNING GAUGE	15	31	32	33	34	35	47
7.5 × 10 ⁻⁷	2.3 × 10 ⁻⁶	3.8 × 10 ⁻⁵	0.05	0.02	0.05	1.01	98.32	0.55	0.00
7.5 × 10 ⁻⁷	3.8 × 10 ⁻⁶	7.5 × 10 ⁻⁵	0.14	0.14	0.21	2.66	95.17	1.68	0.00
7.5 × 10 ⁻⁷	7.5 × 10 ⁻⁶	3.0 × 10 ⁻⁴	0.35	0.35	0.35	6.69	88.03	4.23	0.00

CH₂OH⁺ INTO CH₃OH

% SECONDARY ION FLUX Vs. PRESSURE

PRESSURE /10⁻⁵ torr

% SECONDARY ION FLUX

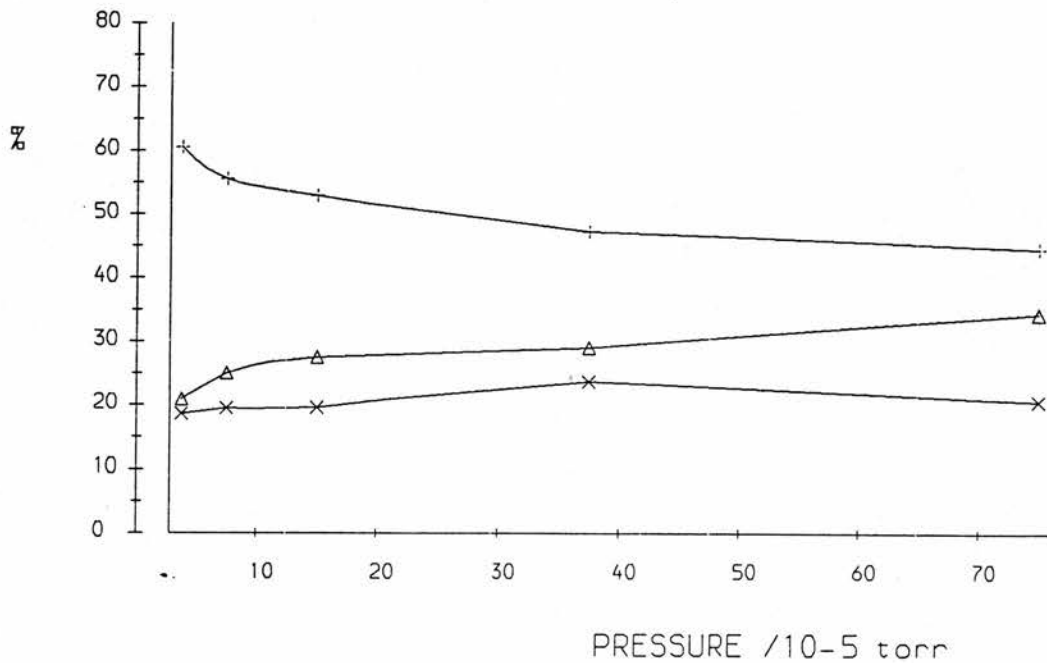
	PRESSURES in torr			m/e			
	INITIAL ION	ION	PENNING				
	GAUGE	GAUGE	GAUGE	15	29	32	33
(A)	7.5 × 10 ⁻⁷	1.5 × 10 ⁻⁶	3.8 × 10 ⁻⁵	2.78	69.44	13.89	13.89
(B)	7.5 × 10 ⁻⁷	1.9 × 10 ⁻⁶	7.5 × 10 ⁻⁵	5.38	64.52	15.05	15.05
(C)	7.5 × 10 ⁻⁷	3.8 × 10 ⁻⁶	1.5 × 10 ⁻⁴	8.65	48.08	8.65	34.62
(D)	7.5 × 10 ⁻⁷	7.5 × 10 ⁻⁶	6.0 × 10 ⁻⁴	12.50	50.00	0.00	37.50
(E)	7.5 × 10 ⁻⁷	2.3 × 10 ⁻⁵	1.5 × 10 ⁻³	9.62	48.08	0.00	42.31

% TOTAL ION FLUX

	PRESSURES in torr			m/e				
	INITIAL ION	ION	PENNING					
	GAUGE	GAUGE	GAUGE	15	29	31	32	33
	7.5 × 10 ⁻⁷	1.5 × 10 ⁻⁶	3.8 × 10 ⁻⁵	0.02	0.50	99.28	0.10	0.10
	7.5 × 10 ⁻⁷	1.9 × 10 ⁻⁶	7.5 × 10 ⁻⁵	0.05	0.60	99.07	0.14	0.14
	7.5 × 10 ⁻⁷	3.8 × 10 ⁻⁶	1.5 × 10 ⁻⁴	0.05	0.30	99.38	0.05	0.22
	7.5 × 10 ⁻⁷	7.5 × 10 ⁻⁶	6.0 × 10 ⁻⁴	0.40	1.60	96.81	0.00	1.20
	7.5 × 10 ⁻⁷	2.3 × 10 ⁻⁵	1.5 × 10 ⁻³	0.50	2.50	94.81	0.00	2.20

CHO⁺ INTO CH₃OH

% SECONDARY ION FLUX Vs. PRESSURE



% SECONDARY ION FLUX

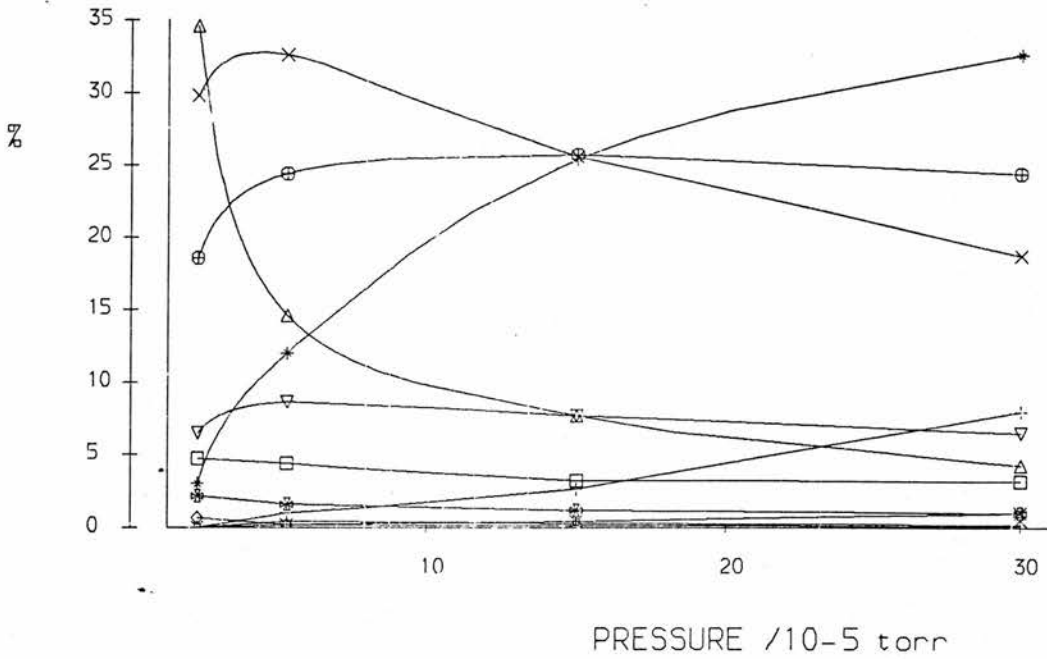
	PRESSURES in torr			m/e		
	INITIAL ION	ION	PENNING	15	31	33
	GAUGE	GAUGE	GAUGE			
(A)	7.5×10^{-6}	7.5×10^{-6}	3.8×10^{-5}	60.47	18.60	20.93
(B)	7.5×10^{-6}	1.1×10^{-5}	7.5×10^{-5}	55.56	19.44	25.00
(C)	7.5×10^{-6}	1.5×10^{-5}	1.5×10^{-4}	52.94	19.61	27.45
(D)	7.5×10^{-6}	1.9×10^{-5}	3.8×10^{-4}	47.31	23.66	29.03
(E)	7.5×10^{-6}	2.3×10^{-5}	7.5×10^{-4}	44.83	20.69	34.48

% TOTAL ION FLUX

	PRESSURES in torr			m/e			
	INITIAL ION	ION	PENNING	15	29	31	33
	GAUGE	GAUGE	GAUGE				
	7.5×10^{-6}	7.5×10^{-6}	3.8×10^{-5}	0.14	99.77	0.04	0.05
	7.5×10^{-6}	1.1×10^{-5}	7.5×10^{-5}	0.26	99.53	0.09	0.12
	7.5×10^{-6}	1.5×10^{-5}	1.5×10^{-4}	0.46	99.13	0.17	0.24
	7.5×10^{-6}	1.9×10^{-5}	3.8×10^{-4}	0.64	98.65	0.32	0.39
	7.5×10^{-6}	2.3×10^{-5}	7.5×10^{-4}	1.26	97.18	0.58	0.97

CHO+ INTO CD300

% SECONDARY ION FLUX Vs. PRESSURE



% SECONDARY ION FLUX

	PRESSURES In torr			m/e										
	INITIAL ION	ION	PENNING	17	18	30	31	33	34	36	37	38	53	54
	GAUGE	GAUGE	GAUGE											
(A)	7.5×10^{-7}	1.5×10^{-6}	2.3×10^{-5}	0.00	29.81	34.56	0.65	2.16	6.48	4.75	18.57	3.02	0.00	0.00
(B)	7.5×10^{-7}	1.9×10^{-6}	5.3×10^{-5}	0.40	32.60	14.60	0.20	1.60	8.60	4.40	24.40	12.00	0.20	1.00
(C)	7.5×10^{-7}	3.0×10^{-6}	1.5×10^{-4}	0.28	25.58	7.69	0.14	1.19	7.69	3.21	25.72	25.44	0.42	2.00
(D)	7.5×10^{-7}	4.5×10^{-6}	3.0×10^{-4}	0.18	18.82	4.28	0.09	0.98	6.48	3.18	24.44	32.63	0.98	7.00
(E)	7.5×10^{-7}	4.5×10^{-6}	3.0×10^{-4}	0.18	18.82	4.28	0.09	0.98	6.48	3.18	24.44	32.63	0.98	7.00

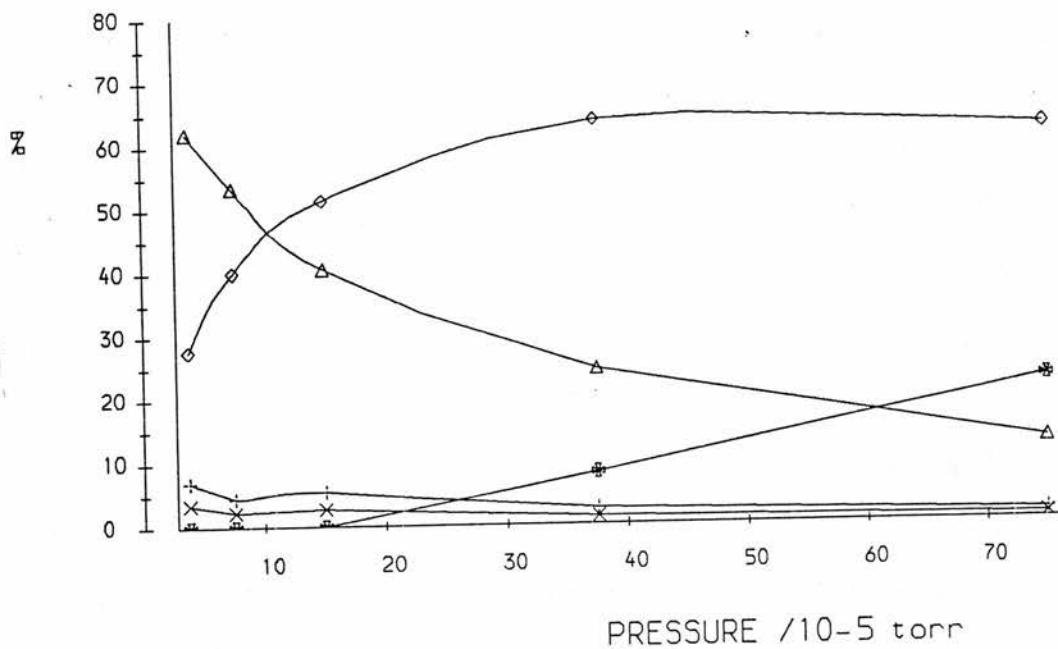
% TOTAL ION FLUX

	PRESSURES In torr			m/e											
	INITIAL ION	ION	PENNING	17	18	29	30	31	33	34	36	37	38	53	54
	GAUGE	GAUGE	GAUGE												
	7.5×10^{-7}	1.5×10^{-6}	2.3×10^{-5}	0.00	0.76	97.46	0.88	0.02	0.05	0.16	0.12	0.47	0.08	0.00	0.00
	7.5×10^{-7}	1.9×10^{-6}	5.3×10^{-5}	0.03	2.23	93.15	1.00	0.01	0.11	0.59	0.30	1.67	0.82	0.01	0.00
	7.5×10^{-7}	3.0×10^{-6}	1.5×10^{-4}	0.03	3.12	87.80	0.94	0.02	0.14	0.94	0.39	3.14	3.10	0.05	0.00
	7.5×10^{-7}	4.5×10^{-6}	3.0×10^{-4}	0.00	0.37	98.03	0.08	0.00	0.02	0.13	0.06	0.48	0.64	0.02	0.00
	7.5×10^{-7}	4.5×10^{-6}	3.0×10^{-4}	0.00	0.37	98.03	0.08	0.00	0.02	0.13	0.06	0.48	0.64	0.02	0.00

CH₃⁺ INTO CH₃OH

% SECONDARY ION FLUX Vs. PRESSURE

+ = 27-C₂H₅⁺
 x = 29-C₂H₃⁺
 CH₃⁺
 Δ = 31-CH₃⁺
 ○ = 33-CH₂⁺
 * = 47
 (CH₃)₂O⁺



% SECONDARY ION FLUX

	PRESSURES in torr			m/e				
	INITIAL ION	ION	PENNING	27	29	31	33	47
	GAUGE	GAUGE	GAUGE					
(A)	7.5 × 10 ⁻⁷	2.3 × 10 ⁻⁶	3.8 × 10 ⁻⁵	6.90	3.45	62.07	27.59	0.00
(B)	7.5 × 10 ⁻⁷	3.0 × 10 ⁻⁶	7.5 × 10 ⁻⁵	4.44	2.22	53.33	40.00	0.00
(C)	7.5 × 10 ⁻⁷	3.8 × 10 ⁻⁶	1.5 × 10 ⁻⁴	5.41	2.70	40.54	51.35	0.00
(D)	7.5 × 10 ⁻⁷	6.0 × 10 ⁻⁶	3.8 × 10 ⁻⁴	2.45	1.22	24.49	63.67	8.16
(E)	7.5 × 10 ⁻⁷	1.5 × 10 ⁻⁵	7.5 × 10 ⁻⁴	1.42	0.71	12.77	62.41	22.70

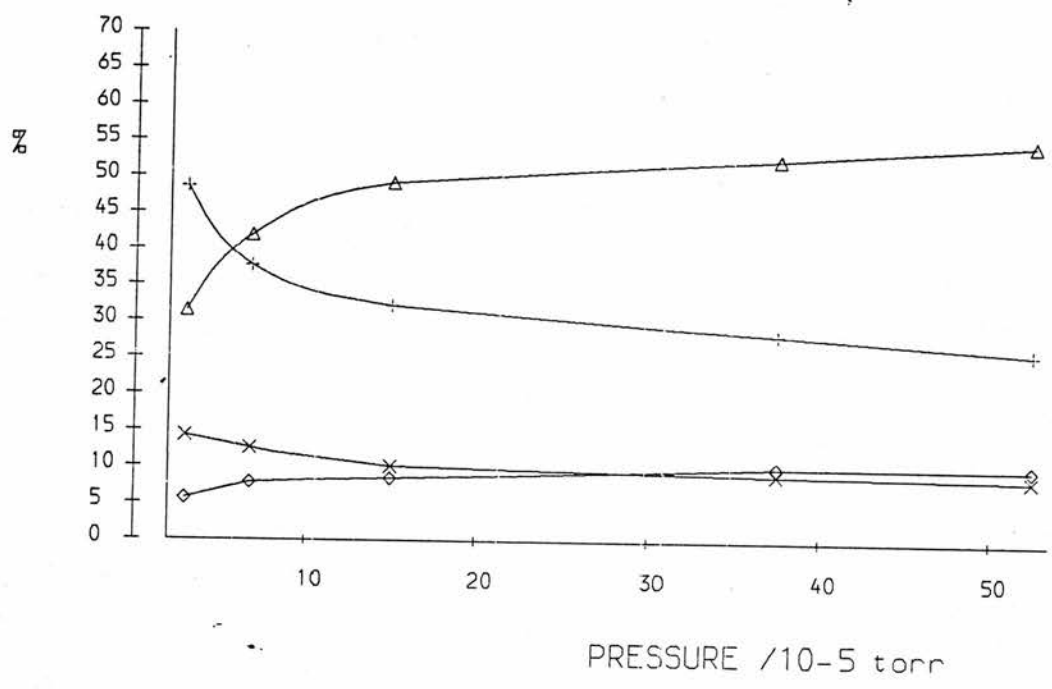
% TOTAL ION FLUX

	PRESSURES in torr			m/e					
	INITIAL ION	ION	PENNING	15	27	29	31	33	47
	GAUGE	GAUGE	GAUGE						
	7.5 × 10 ⁻⁷	2.3 × 10 ⁻⁶	3.8 × 10 ⁻⁵	99.32	0.05	0.02	0.42	0.19	0.00
	7.5 × 10 ⁻⁷	3.0 × 10 ⁻⁶	7.5 × 10 ⁻⁵	98.72	0.06	0.03	0.68	0.51	0.00
	7.5 × 10 ⁻⁷	3.8 × 10 ⁻⁶	1.5 × 10 ⁻⁴	97.58	0.13	0.07	0.98	1.24	0.00
	7.5 × 10 ⁻⁷	6.0 × 10 ⁻⁶	3.8 × 10 ⁻⁴	93.42	0.16	0.08	1.61	4.19	0.54
	7.5 × 10 ⁻⁷	1.5 × 10 ⁻⁵	7.5 × 10 ⁻⁴	81.32	0.26	0.13	2.38	11.66	4.24

CH₃⁺ INTO CH₃OH

% SECONDARY ION FLUX Vs. PRESSURE

+ = 27
 x = 29
 Δ = 31
 ◊ = 33



% SECONDARY ION FLUX

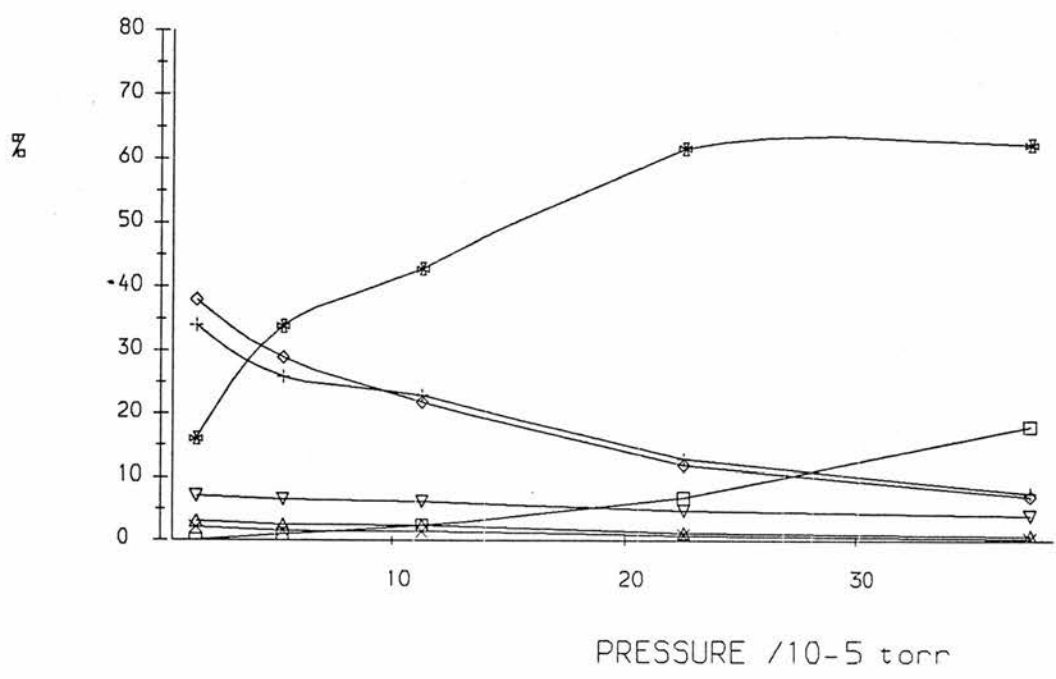
	PRESSURES in torr			m/e			
	INITIAL ION	ION	PENNING	27	29	31	33
	GAUGE	GAUGE	GAUGE				
(A)	7.5 × 10 ⁻⁶	1.1 × 10 ⁻⁵	3.0 × 10 ⁻⁵	48.57	14.29	31.43	5.71
(B)	7.5 × 10 ⁻⁶	1.1 × 10 ⁻⁵	6.8 × 10 ⁻⁵	37.70	12.57	41.88	7.85
(C)	7.5 × 10 ⁻⁶	1.1 × 10 ⁻⁵	1.5 × 10 ⁻⁴	32.20	10.17	49.15	8.47
(D)	7.5 × 10 ⁻⁶	1.5 × 10 ⁻⁵	3.8 × 10 ⁻⁴	28.28	9.09	52.53	10.10
(E)	7.5 × 10 ⁻⁶	1.9 × 10 ⁻⁵	5.3 × 10 ⁻⁴	26.09	8.70	55.07	10.14

% TOTAL ION FLUX

	PRESSURES in torr			m/e				
	INITIAL ION	ION	PENNING	15	27	29	31	33
	GAUGE	GAUGE	GAUGE					
	7.5 × 10 ⁻⁶	1.1 × 10 ⁻⁵	3.0 × 10 ⁻⁵	99.95	0.03	0.01	0.02	0.00
	7.5 × 10 ⁻⁶	1.1 × 10 ⁻⁵	6.8 × 10 ⁻⁵	99.91	0.03	0.01	0.04	0.01
	7.5 × 10 ⁻⁶	1.1 × 10 ⁻⁵	1.5 × 10 ⁻⁴	99.85	0.05	0.02	0.07	0.01
	7.5 × 10 ⁻⁶	1.5 × 10 ⁻⁵	3.8 × 10 ⁻⁴	99.74	0.07	0.02	0.14	0.03
	7.5 × 10 ⁻⁶	1.9 × 10 ⁻⁵	5.3 × 10 ⁻⁴	99.64	0.09	0.03	0.20	0.04

CO₃⁺ INTO CH₃OH

% SECONDARY ION FLUX Vs. PRESSURE

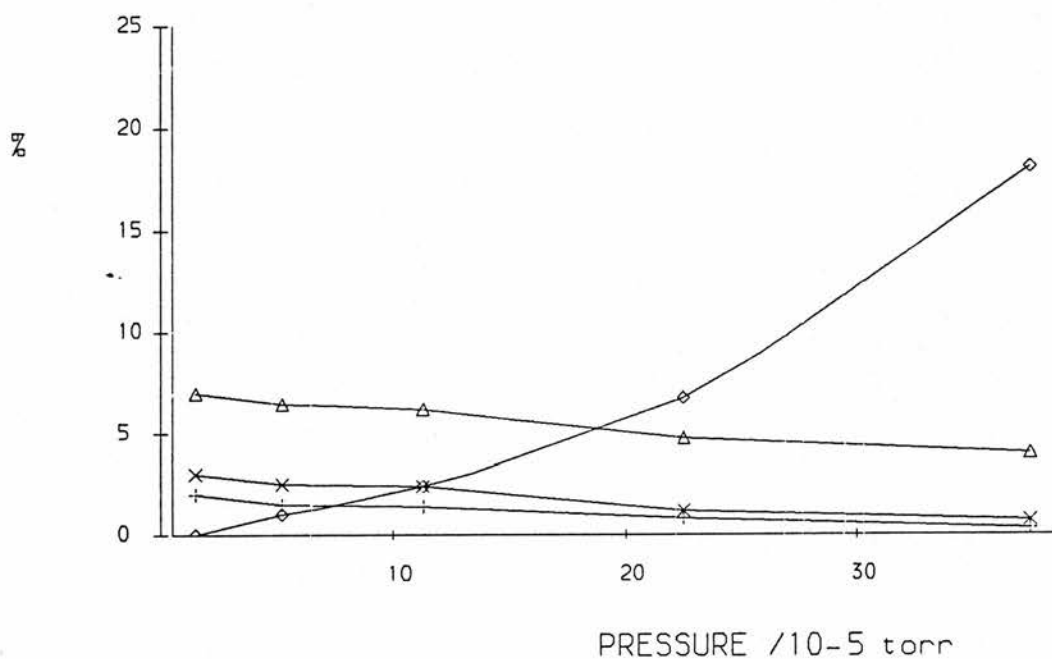


% TOTAL ION FLUX

PRESSURES in torr			m/e							
INITIAL ION GAUGE	ION GAUGE	PENNING GAUGE	15	18	28	29	31	33	34	4
7.5x10 ⁻⁷	1.5x10 ⁻⁶	1.5x10 ⁻⁵	0.58	98.31	0.03	0.05	0.64	0.27	0.12	0.0
7.5x10 ⁻⁷	2.3x10 ⁻⁶	5.3x10 ⁻⁵	0.51	98.03	0.03	0.05	0.57	0.67	0.13	0.0
7.5x10 ⁻⁷	3.0x10 ⁻⁶	1.1x10 ⁻⁴	0.55	97.61	0.03	0.06	0.52	1.02	0.15	0.0
7.5x10 ⁻⁷	4.5x10 ⁻⁶	2.3x10 ⁻⁴	0.52	95.98	0.03	0.05	0.48	2.48	0.19	0.2
7.5x10 ⁻⁷	7.5x10 ⁻⁶	3.8x10 ⁻⁴	0.59	92.21	0.02	0.05	0.55	4.86	0.31	1.4

CD3+ INTO CH3OH

% SECONDARY ION FLUX Vs. PRESSURE

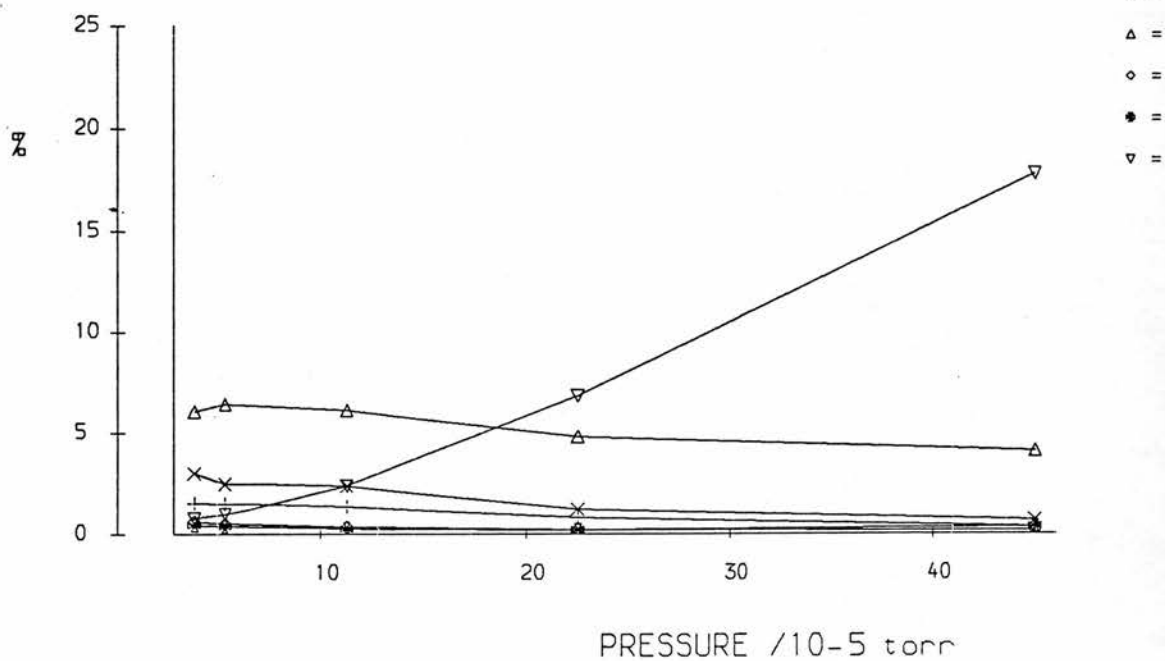


% SECONDARY ION FLUX

	PRESSURES in torr			m/e						
	INITIAL ION	ION	PENNING	15	28	29	31	33	34	47
	GAUGE	GAUGE	GAUGE							
(A)	7.5×10^{-7}	1.5×10^{-6}	1.5×10^{-5}	34.00	2.00	3.00	38.00	16.00	7.00	0.00
(B)	7.5×10^{-7}	2.3×10^{-6}	5.3×10^{-5}	25.87	1.49	2.49	28.86	33.83	6.47	1.00
(C)	7.5×10^{-7}	3.0×10^{-6}	1.1×10^{-4}	22.91	1.39	2.39	21.91	42.83	6.18	2.39
(D)	7.5×10^{-7}	4.5×10^{-6}	2.3×10^{-4}	12.92	0.80	1.19	11.93	61.63	4.77	6.78
(E)	7.5×10^{-7}	7.5×10^{-6}	3.8×10^{-4}	7.54	0.30	0.70	7.04	62.31	4.02	18.00

CD3+ Into CH3OH

% SECONDARY ION FLUX Vs. PRESSURE



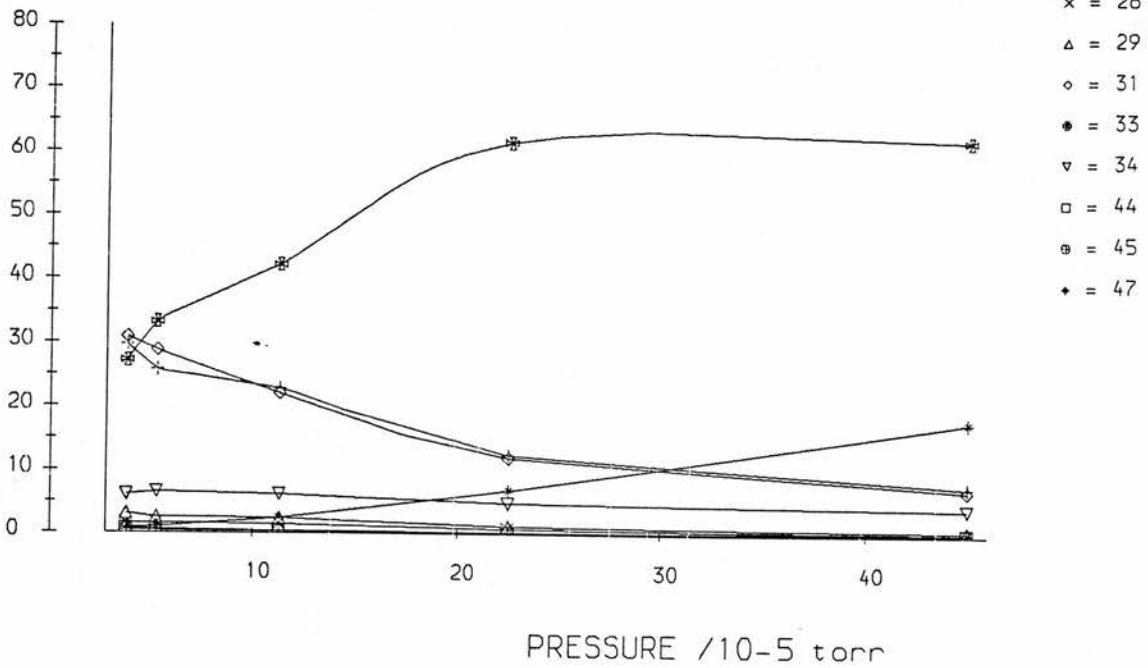
CD3+ Into CH3OH

% SECONDARY ION FLUX

	PRESSURES in torr			m/e								
	INITIAL ION GAUGE	ION GAUGE	PENNING GAUGE	15	28	29	31	33	34	44	45	47
(A)	7.5×10^{-7}	1.9×10^{-6}	3.8×10^{-5}	29.61	1.51	3.02	30.82	27.19	6.04	0.60	0.45	0.70
(B)	7.5×10^{-7}	2.3×10^{-6}	5.3×10^{-5}	25.77	1.49	2.48	28.75	33.21	6.44	0.50	0.37	0.99
(C)	7.5×10^{-7}	3.0×10^{-6}	1.1×10^{-4}	22.81	1.36	2.38	22.13	42.21	6.13	0.34	0.26	2.36
(D)	7.5×10^{-7}	4.5×10^{-6}	2.3×10^{-4}	12.43	0.80	1.20	12.03	61.50	4.81	0.20	0.20	6.82
(E)	7.5×10^{-7}	7.5×10^{-6}	4.5×10^{-4}	7.52	0.34	0.68	7.00	62.07	4.10	0.17	0.34	17.77

CD3+ Into CH3OH

% SECONDARY ION FLUX Vs. PRESSURE



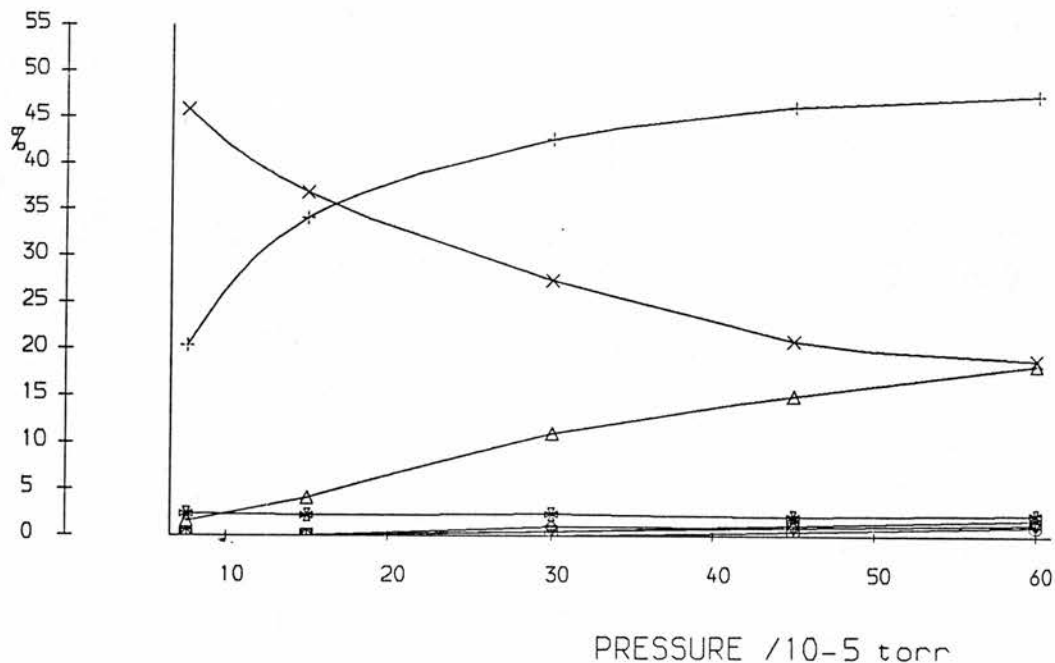
CD3+ Into CH3OH

% TOTAL ION FLUX

PRESSURES In torr			m/e									
INITIAL ION GAUGE	ION GAUGE	PENNING GAUGE	15	18	28	29	31	33	34	44	45	47
7.5x10 ⁻⁷	1.9x10 ⁻⁶	3.8x10 ⁻⁵	0.95	96.80	0.05	0.10	0.99	0.87	0.19	0.02	0.01	0.02
7.5x10 ⁻⁷	2.3x10 ⁻⁶	5.3x10 ⁻⁵	1.00	96.12	0.06	0.10	1.12	1.29	0.25	0.02	0.01	0.04
7.5x10 ⁻⁷	3.0x10 ⁻⁶	1.1x10 ⁻⁴	20.01	12.25	1.19	2.09	19.42	37.04	5.38	0.30	0.22	2.09
7.5x10 ⁻⁷	4.5x10 ⁻⁶	2.3x10 ⁻⁴	2.14	82.80	0.14	0.21	2.07	10.58	0.83	0.03	0.03	1.17
7.5x10 ⁻⁷	7.5x10 ⁻⁶	4.5x10 ⁻⁴	2.51	66.59	0.11	0.23	2.34	20.74	1.37	0.06	0.11	5.94

CD3OD2+ INTO CH3OH

% SECONDARY ION FLUX Vs. PRESSURE



% SECONDARY ION FLUX

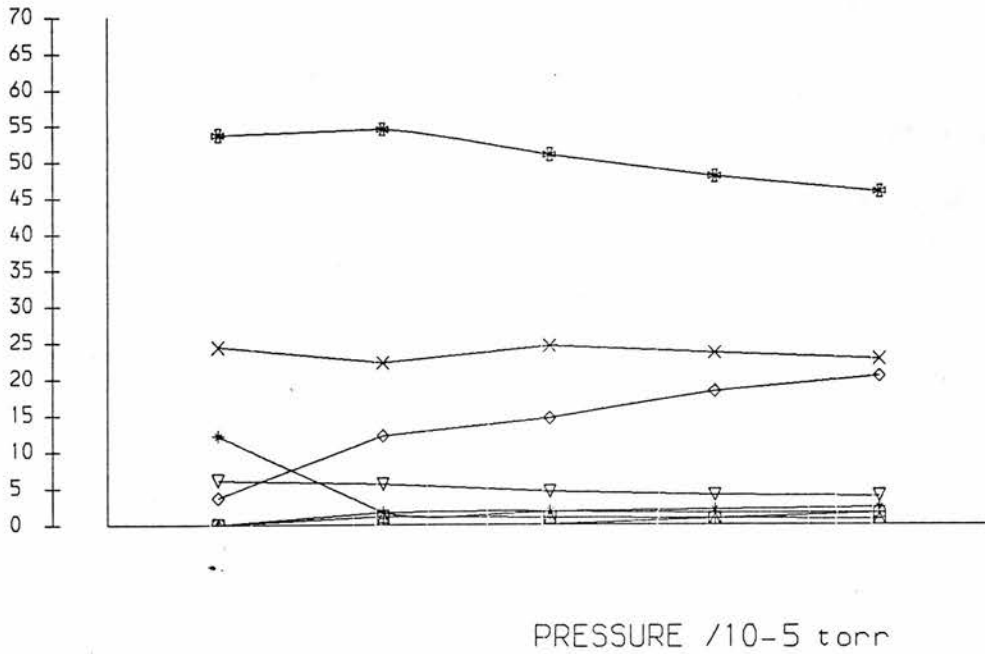
	PRESSURES in torr			m/e							
	INITIAL ION	ION	PENNING								
	GAUGE	GAUGE	GAUGE	33	34	47	48	50	59	65	79
(A)	3.8×10 ⁻⁶	6.8×10 ⁻⁶	7.5×10 ⁻⁵	20.39	45.88	1.57	0.00	2.35	0.00	0.00	0.00
(B)	3.8×10 ⁻⁶	7.5×10 ⁻⁶	1.5×10 ⁻⁴	34.07	36.81	4.12	0.00	2.20	0.00	0.00	0.00
(C)	3.8×10 ⁻⁶	1.1×10 ⁻⁵	3.0×10 ⁻⁴	42.62	27.40	11.01	0.94	2.34	0.47	0.47	0.00
(D)	3.8×10 ⁻⁶	1.1×10 ⁻⁵	4.5×10 ⁻⁴	46.14	20.91	15.00	0.91	2.05	0.91	1.14	0.45
(E)	3.8×10 ⁻⁶	1.5×10 ⁻⁵	6.0×10 ⁻⁴	47.45	18.88	18.37	1.28	2.30	1.28	1.79	1.02

% TOTAL ION FLUX

	PRESSURES in torr			m/e								
	INITIAL ION	ION	PENNING									
	GAUGE	GAUGE	GAUGE	33	34	38	47	48	50	59	65	79
	3.8×10 ⁻⁶	6.8×10 ⁻⁶	7.5×10 ⁻⁵	1.21	2.73	94.05	0.09	0.00	0.14	0.00	0.00	0.00
	3.8×10 ⁻⁶	7.5×10 ⁻⁶	1.5×10 ⁻⁴	4.45	4.81	86.93	0.54	0.00	0.29	0.00	0.00	0.00
	3.8×10 ⁻⁶	1.1×10 ⁻⁵	3.0×10 ⁻⁴	11.05	7.10	74.07	2.85	0.24	0.61	0.12	0.12	0.00
	3.8×10 ⁻⁶	1.1×10 ⁻⁵	4.5×10 ⁻⁴	15.94	7.23	65.45	5.18	0.31	0.71	0.31	0.39	0.16
	3.8×10 ⁻⁶	1.5×10 ⁻⁵	6.0×10 ⁻⁴	19.68	7.83	58.53	7.62	0.53	0.95	0.53	0.74	0.42

CD3OD2+ INTO CH3OH

% SECONDARY ION FLUX Vs. PRESSURE



- + = 15 = CH₃⁺
- x = 18 = CD₃⁺
- Δ = 31 = CH₂O⁺
- ◊ = 33 = CH₃OH⁺
- = 34 = CH₃OD⁺ + NO CD₃⁺
- ∇ = 35 = CD₃OH⁺
- = 39 = CH₃CO⁺
- ⊙ = 47 = CH₃^HOCH₃⁺
- * = 50 = CD₃^HOCH₃⁺

% SECONDARY ION FLUX

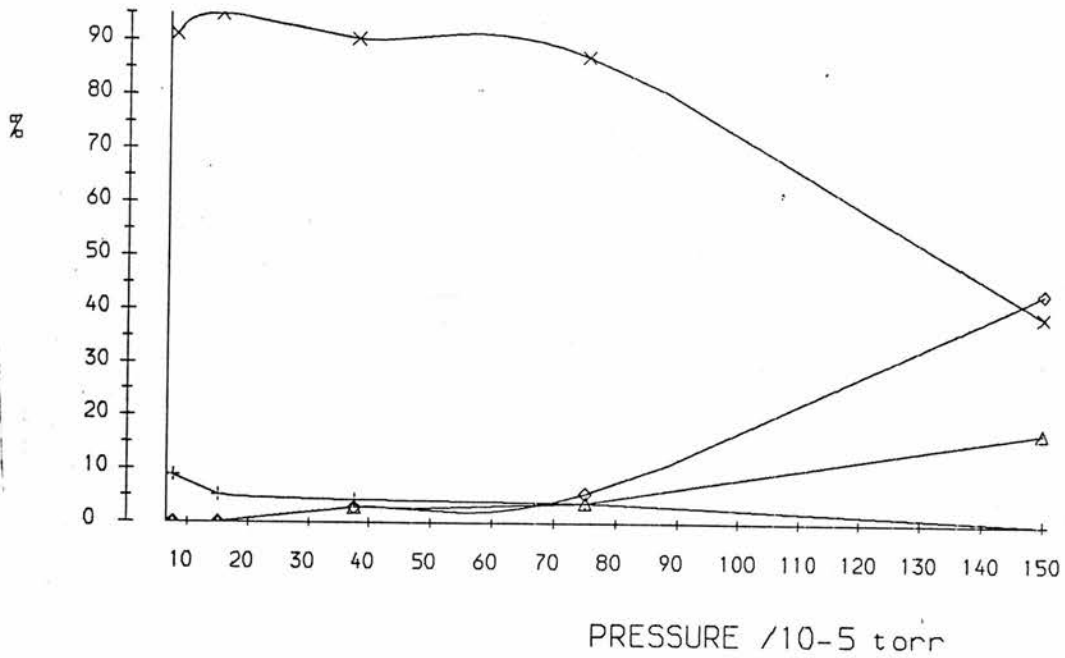
	PRESSURES in torr			m/e								
	INITIAL ION GAUGE	ION GAUGE	PENNING GAUGE	15	18	31	33	34	35	39	47	50
(A)	3.8x10 ⁻⁶	4.9x10 ⁻⁶	1.5x10 ⁻⁵	0.00	24.39	0.00	3.66	53.66	6.10	0.00	0.00	12.20
(B)	3.8x10 ⁻⁶	6.0x10 ⁻⁶	3.0x10 ⁻⁵	1.67	22.22	1.11	12.22	54.44	5.56	1.11	0.00	1.67
(C)	3.8x10 ⁻⁶	6.0x10 ⁻⁶	4.5x10 ⁻⁵	1.82	24.55	0.91	14.55	50.91	4.55	0.91	0.00	1.82
(D)	3.8x10 ⁻⁶	6.8x10 ⁻⁶	6.0x10 ⁻⁵	1.63	23.58	0.81	18.29	47.97	4.07	0.81	0.81	2.03
(E)	3.8x10 ⁻⁶	6.8x10 ⁻⁶	7.5x10 ⁻⁵	1.57	22.75	0.78	20.39	45.88	3.92	0.78	1.57	2.35

% TOTAL ION FLUX

	PRESSURES in torr			m/e									
	INITIAL ION GAUGE	ION GAUGE	PENNING GAUGE	15	18	31	33	34	35	38	39	47	50
	3.8x10 ⁻⁶	4.9x10 ⁻⁶	1.5x10 ⁻⁵	0.00	0.42	0.00	0.06	0.93	0.11	98.27	0.00	0.00	0.2
	3.8x10 ⁻⁶	6.0x10 ⁻⁶	3.0x10 ⁻⁵	0.07	0.89	0.04	0.49	2.19	0.22	95.98	0.04	0.00	0.0
	3.8x10 ⁻⁶	6.0x10 ⁻⁶	4.5x10 ⁻⁵	0.08	1.09	0.04	0.65	2.26	0.20	95.56	0.04	0.00	0.0
	3.8x10 ⁻⁶	6.8x10 ⁻⁶	6.0x10 ⁻⁵	0.08	1.22	0.04	0.95	2.49	0.21	94.82	0.04	0.04	0.1
	3.8x10 ⁻⁶	6.8x10 ⁻⁶	7.5x10 ⁻⁵	0.09	1.35	0.05	1.21	2.73	0.23	94.05	0.05	0.09	0.1

174

(CH₃)₂OH⁺ INTO CH₃OH
% SECONDARY ION FLUX Vs. PRESSURE



+ = 31 = CH₂⁺
x = 33 = CH₃⁺
Δ = 65 = (H₂O)⁺
o = 79 =
(CH₃OH)⁺H/O(CH₃)⁺

% SECONDARY ION FLUX

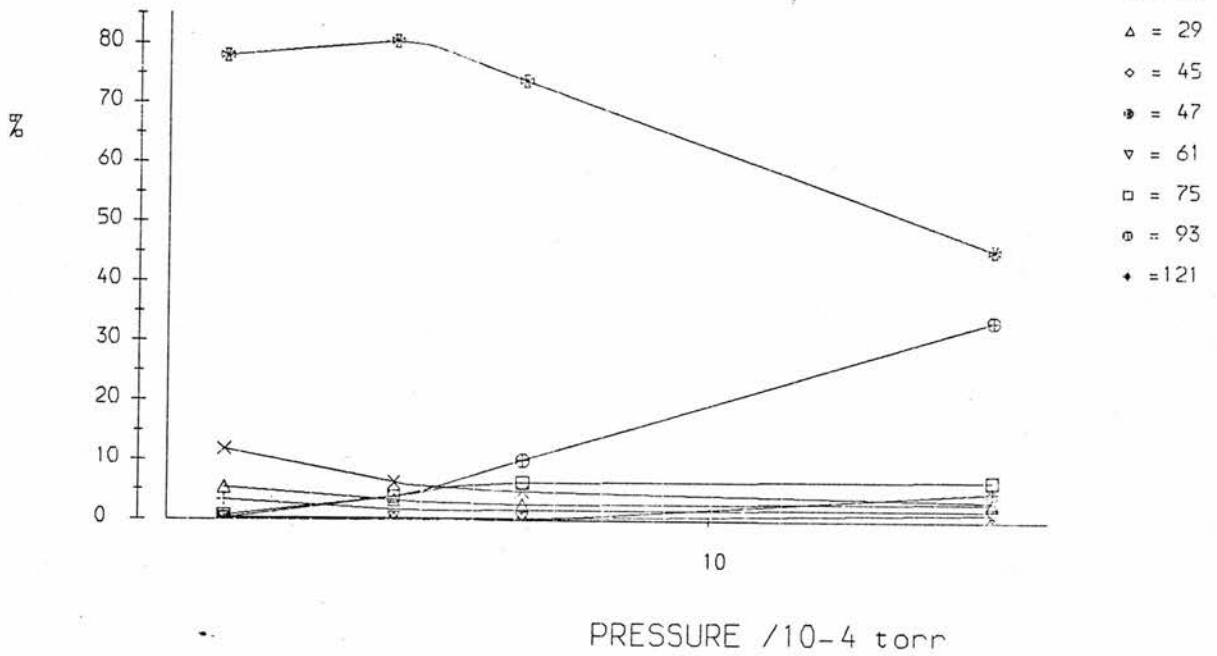
	PRESSURES in torr			m/e			
	INITIAL ION	ION	PENNING				
	GAUGE	GAUGE	GAUGE	31	33	65	79
(A)	3.8 × 10 ⁻⁶	5.3 × 10 ⁻⁵	7.5 × 10 ⁻⁵	8.82	91.18	0.00	0.00
(B)	3.8 × 10 ⁻⁶	6.8 × 10 ⁻⁵	1.5 × 10 ⁻⁴	5.08	94.92	0.00	0.00
(C)	3.8 × 10 ⁻⁶	1.1 × 10 ⁻⁵	3.8 × 10 ⁻⁴	4.17	90.28	2.78	2.78
(D)	3.8 × 10 ⁻⁶	1.5 × 10 ⁻⁵	7.5 × 10 ⁻⁴	3.70	87.04	3.70	5.56
(E)	3.8 × 10 ⁻⁶	3.0 × 10 ⁻⁵	1.5 × 10 ⁻³	0.00	39.13	17.39	43.48

% TOTAL ION FLUX

	PRESSURES in torr			m/e				
	INITIAL ION	ION	PENNING					
	GAUGE	GAUGE	GAUGE	31	33	47	65	79
	3.8 × 10 ⁻⁶	5.3 × 10 ⁻⁵	7.5 × 10 ⁻⁵	0.80	8.31	90.88	0.00	0.00
	3.8 × 10 ⁻⁶	6.8 × 10 ⁻⁵	1.5 × 10 ⁻⁴	1.02	19.11	79.86	0.00	0.00
	3.8 × 10 ⁻⁶	1.1 × 10 ⁻⁵	3.8 × 10 ⁻⁴	1.38	29.95	66.82	0.92	0.92
	3.8 × 10 ⁻⁶	1.5 × 10 ⁻⁵	7.5 × 10 ⁻⁴	1.31	30.72	64.71	1.31	1.96
	3.8 × 10 ⁻⁶	3.0 × 10 ⁻⁵	1.5 × 10 ⁻³	0.00	17.65	54.90	7.84	19.61

CH₃OH⁺ INTO C₂H₅OH

% SECONDARY ION FLUX Vs. PRESSURE



% SECONDARY ION FLUX

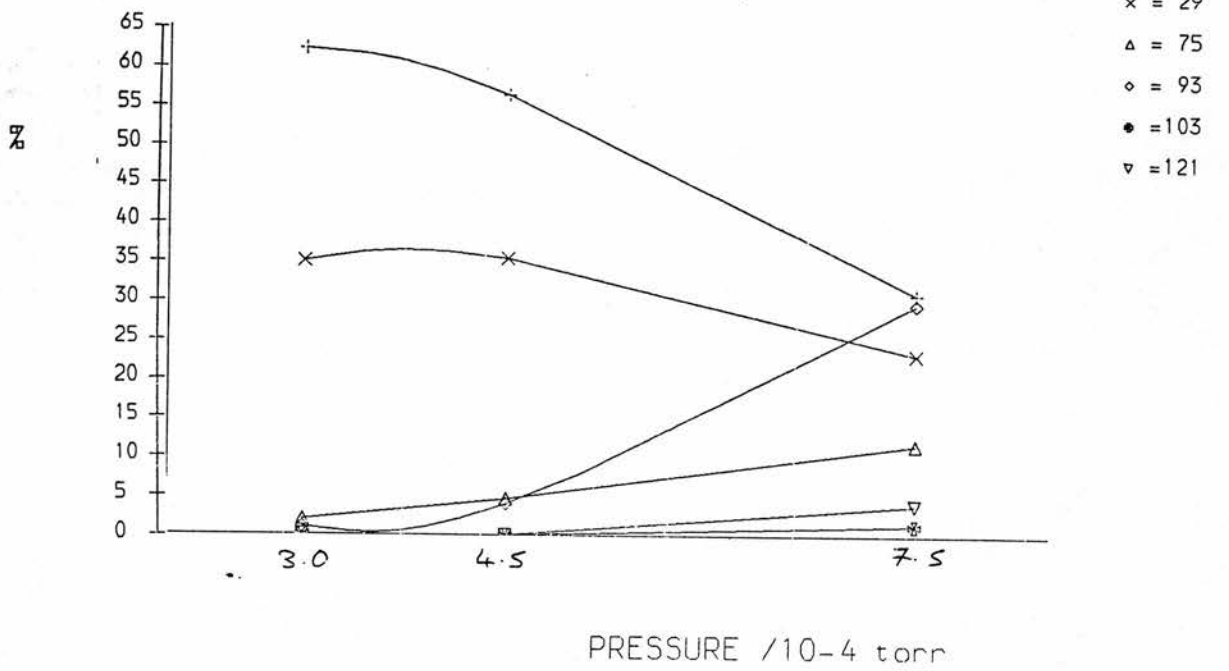
	PRESSURES In torr			m/e								
	INITIAL ION GAUGE	ION GAUGE	PENNING GAUGE	15	19	29	45	47	61	75	93	121
(A)	1.5 × 10 ⁻⁵	2.3 × 10 ⁻⁵	1.5 × 10 ⁻⁴	3.31	11.81	5.43	0.35	77.92	0.24	0.71	0.24	0.00
(B)	1.5 × 10 ⁻⁵	3.8 × 10 ⁻⁵	4.5 × 10 ⁻⁴	1.73	6.26	3.33	0.20	80.41	0.33	3.86	3.86	0.00
(C)	1.5 × 10 ⁻⁵	3.8 × 10 ⁻⁵	6.8 × 10 ⁻⁴	1.73	4.87	2.67	0.16	73.87	0.35	6.29	10.06	0.00
(D)	1.5 × 10 ⁻⁵	5.3 × 10 ⁻⁵	1.5 × 10 ⁻³	1.80	3.30	3.00	0.00	45.65	1.20	6.61	33.63	4.80
(E)	1.5 × 10 ⁻⁵	5.3 × 10 ⁻⁵	1.5 × 10 ⁻³	1.80	3.30	3.00	0.00	45.65	1.20	6.61	33.63	4.80

% TOTAL ION FLUX

	PRESSURES In torr			m/e									
	INITIAL ION GAUGE	ION GAUGE	PENNING GAUGE	15	19	29	33	45	47	61	75	93	121
	1.5 × 10 ⁻⁵	2.3 × 10 ⁻⁵	1.5 × 10 ⁻⁴	0.45	1.60	0.74	86.44	0.05	10.57	0.03	0.10	0.03	0.00
	1.5 × 10 ⁻⁵	3.8 × 10 ⁻⁵	4.5 × 10 ⁻⁴	0.70	2.53	1.34	59.67	0.08	32.43	0.13	1.56	1.56	0.00
	1.5 × 10 ⁻⁵	3.8 × 10 ⁻⁵	6.8 × 10 ⁻⁴	0.86	2.41	1.32	50.53	0.08	36.54	0.17	3.11	4.98	0.00
	1.5 × 10 ⁻⁵	5.3 × 10 ⁻⁵	1.5 × 10 ⁻³	1.39	2.55	2.32	22.74	0.00	35.27	0.93	5.10	25.99	3.71
	1.5 × 10 ⁻⁵	5.3 × 10 ⁻⁵	1.5 × 10 ⁻³	1.39	2.55	2.32	22.74	0.00	35.27	0.93	5.10	25.99	3.71

C₂H₅O₂⁺ INTO C₂H₅OH

% SECONDARY ION FLUX Vs. PRESSURE



% SECONDARY ION FLUX

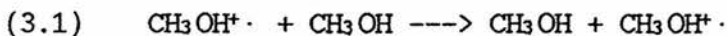
	PRESSURES in torr			m/e					
	INITIAL ION	ION	PENNING						
	GAUGE	GAUGE	GAUGE	1	29	75	93	103	121
(A)	7.5 × 10 ⁻⁶	1.5 × 10 ⁻⁵	3.0 × 10 ⁻⁴	62.14	34.95	1.94	0.97	0.00	0.00
(B)	7.5 × 10 ⁻⁶	2.3 × 10 ⁻⁵	4.5 × 10 ⁻⁴	56.21	35.29	4.58	3.92	0.00	0.00
(C)	7.5 × 10 ⁻⁶	3.0 × 10 ⁻⁵	7.5 × 10 ⁻⁴	30.77	23.08	11.54	29.49	1.28	3.85

% TOTAL ION FLUX

	PRESSURES in torr			m/e						
	INITIAL ION	ION	PENNING							
	GAUGE	GAUGE	GAUGE	1	29	47	75	93	103	121
	7.5 × 10 ⁻⁶	1.5 × 10 ⁻⁵	3.0 × 10 ⁻⁴	5.07	2.85	91.84	0.16	0.08	0.00	0.00
	7.5 × 10 ⁻⁶	2.3 × 10 ⁻⁵	4.5 × 10 ⁻⁴	7.25	4.55	87.10	0.59	0.51	0.00	0.00
	7.5 × 10 ⁻⁶	3.0 × 10 ⁻⁵	7.5 × 10 ⁻⁴	8.86	6.64	71.22	3.32	8.49	0.37	1.11

DISCUSSIONCH₃OH⁺ + CH₃OH

The reaction of methanol cations with methanol produced methanol cations by charge exchange (3.1) which was indistinguishable from the original ion except when the initial methanol ion or the neutral methanol was labelled.



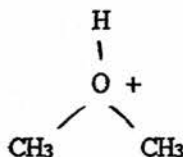
32

32

The secondary ions produced were CH₂OH⁺ (≈50%) and CH₃OH₂⁺ (≈50%) with the CH₃⁺ ion (maximum ≈2.5%) also present.

A peak of mass 47 was observed in low yields at higher pressures. This tertiary ion must come from the reaction of one of the ions CH₃OH₂⁺, CH₂OH⁺ or CH₃⁺ with methanol and could be the dimethyl oxonium ion - which could also be considered to be protonated dimethyl ether. (3.2) As dimethyl ether is an important intermediate in the proposed reaction pathways ¹⁴²⁻¹⁴⁵ this was investigated further.

(3.2)



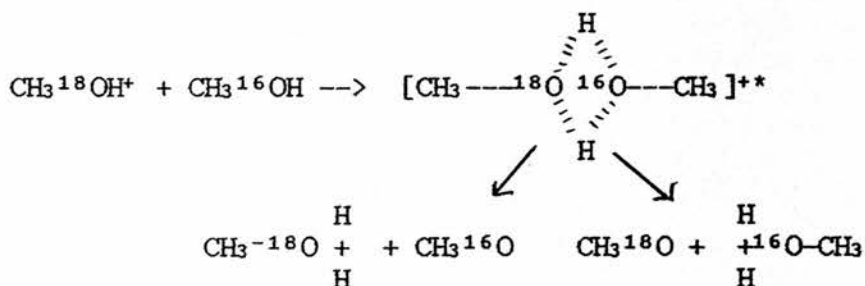
With the triple quadrupole mass spectrometer CH_2OH^+ , CHO^+ and CH_3^+ ions can be isolated and their individual reaction with methanol studied. These reactions are itemized below.



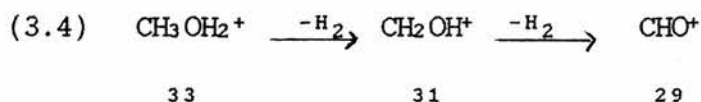
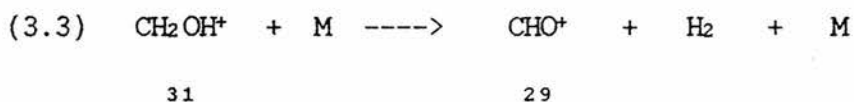
The use of ^{18}O labelled methanol to produce the methanol radical cation in the ion source enabled the reaction of methanol radical cation with methanol to be studied. It was found that the charge exchange reaction occurred to a maximum 5% of the product ions.



The other major ions produced were protonated ^{16}O methanol and protonated ^{18}O methanol. The large yield of $\text{CH}_3^{18}\text{OH}_2^+$ indicates that the self protonation of methanol occurs via an addition complex from which either the neutral or cationic methanol can cleave.

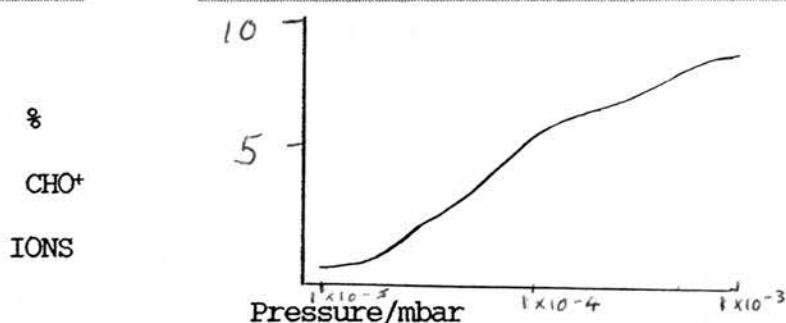


CH₂OH⁺ + CH₃OH There were two main reactions, protonation giving rise to ions of mass 33, and fragmentation giving rise to ions of mass 29. At low pressures the main ion was 29 and could have been due to the fragmentation of the primary ion (3.3) or due to the fragmentation of protonated methanol which at low pressures would readily fragment(3.4).



CH₂OH⁺ + Ne To test the hypothesis that the large amount of CHO⁺ (29) in this reaction was formed by collision induced fragmentation, an experiment was done in which the CH₂OH⁺ ion was separated in the first quadrupole and put into an inert gas, in this instance Neon, in the second quadrupole. The results as depicted in graph 3.1 indicate that this does indeed occur.

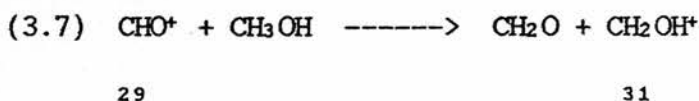
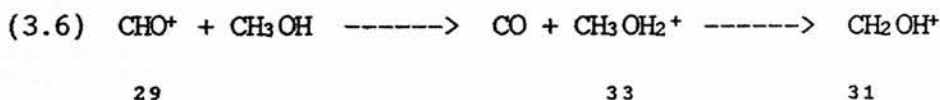
GRAPH 3.1 Amount of CHO^+ produced from $\text{CH}_2\text{OH}^+ + \text{N}_2$



$\text{CHO}^+ + \text{CH}_3\text{OH}$ The main reaction appears to be protonation (3.5), followed by fragmentation at low pressures and further reaction at higher pressures.



The main products at low pressures are CH_3^+ and CH_2OH^+ . CH_3^+ ions arise from fragmentation of CH_3OH_2^+ (3.5). There are two possible routes to CH_2OH^+ , (3.6) and (3.7), which labelling experiments cannot separate because of the extent of H/D scrambling that would occur.



If the CH_2OH^+ was all produced by hydride abstraction (3.7) it would be a secondary ion. If it were all produced by fragmentation of the CH_3OH_2^+ (3.6) then it would be a tertiary ion and it might be expected that a plot of ion

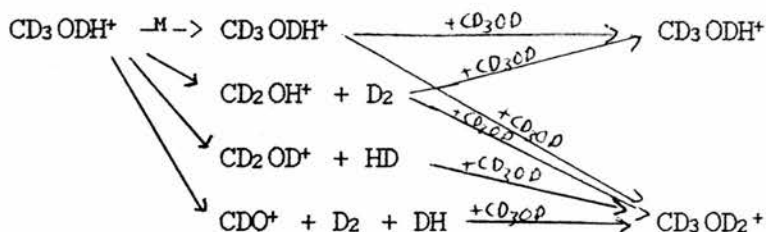
yield against pressure would show which order the ion had, and thereby which of these two routes were operating. But because CH_3OH_2^+ fragments readily to give CH_2OH^+ , no clear distinction could be found in the data.

The largest peak at higher pressures is due to CH_3OH_2^+ ions. The second most abundant ion has a mass of 47 and is the dimethyl oxonium ion. As both CH_3^+ and CH_3OH_2^+ are present in large amounts it is not possible to tell which of these two is the precursor of the ion of mass 47 at this stage.

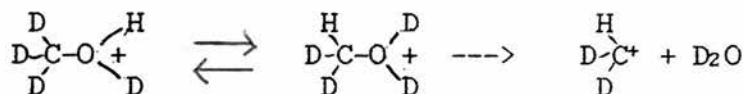


The ions produced in these isotopically labelled experiments served to indicate the mechanisms that were occurring after the methanol was protonated. As the conclusions to be drawn from both experiments are the same, only the reaction of CHO^+ with d_4 -methanol will be discussed in full.

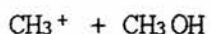
Protonation of deuterated methanol produced ions of mass 37 = CD_3ODH^+ (19%), 18 = CD_3^+ (30%) and 30 = C_2D_3^+ (35%). On increasing the pressure of d_4 -methanol CD_3OD_2^+ ions were observed and increased to become the largest proportion of product ions at the highest pressure. This was indicative of the subsequent reaction of CD_3ODH^+ , and its fragment ions, with d_4 -methanol.



As the pressure of methanol was increased ions of mass 17 appeared. These ions were thought to be formed by intramolecular H/D migration between the methyl deuteriums and the oxonium hydrogen followed by fragmentation with loss of D_2O .



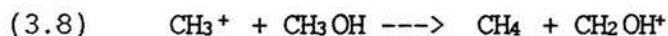
Dimethyl oxonium ions were observed at the higher pressures. The mass of the main dimethyl oxonium peak was 54, which indicated that it was totally deuterated - $(\text{CD}_3)_2\text{OD}^+$. A smaller ion of mass 53 indicated that some dimethyl oxonium ions with six deuteriums and one hydrogen had been formed. However, as CD_3^+ , CD_2H^+ , CD_3OD_2^+ and CD_3ODH^+ ions were all present, no mechanistic conclusions can be drawn from this.



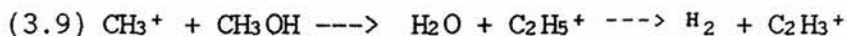
The initial products with this reaction were ions of mass 33, 31, 29 and 27.

The main one was CH_2OH^+ (31) produced by hydride abstraction from CH_3OH to give methane. (3.8) This reaction is thermodynamically very favorable and is known to occur.

153



It has been shown that the CH_2OH^+ ion can go on to produce CH_3OH_2^+ which would fragment to CH_2OH^+ and CHO^+ and CH_3^+ . This might suggest therefore that the ions are CH_2OH^+ of mass 31, CHO^+ of mass 29 and CH_3^+ of mass 15. However as the ion of mass 27 must be C_2H_3^+ the ion of mass 29 could be C_2H_5^+ . (3.9)



15

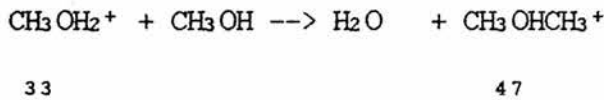
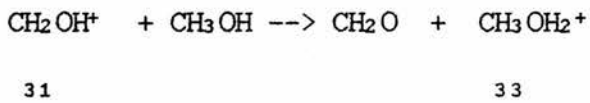
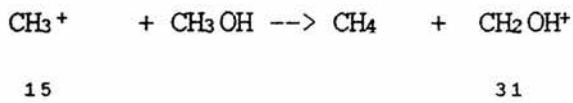
29

27

The experiment was repeated using labelled reactant and labelled neutral gas which elucidated the nature of these ions. This will be discussed later.

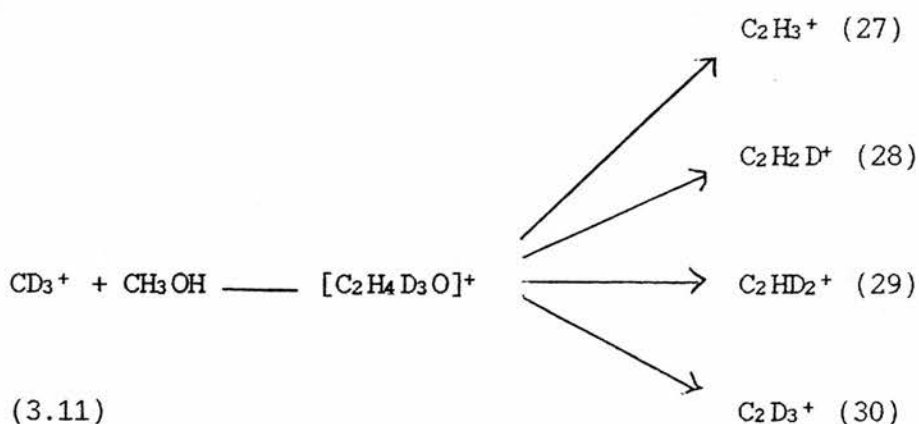
As the pressure increases the dominant ion is CH_3OH_2^+ which falls away when the ion of mass 47 appears.

The reaction sequence for the production of the ion of mass 47 would appear to be :-



(3.10)

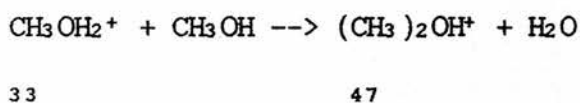
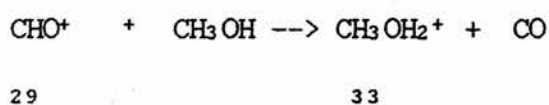
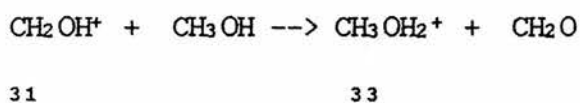
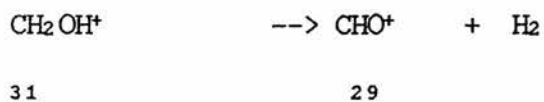
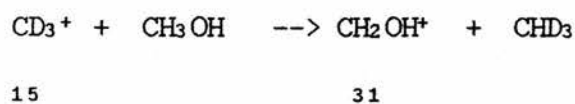
$\text{CD}_3^+ + \text{CH}_3\text{OH}$ To confirm these ideas the experiment was repeated using CD_3^+ . Any product incorporating the primary ion would move to a higher mass because of the deuterium in the ions. Any ion arising from the subsequent reaction of a methanol derived ion rather than from a combination of methanol and the primary ion would not contain any deuterium and the mass would not change. If the ion of mass 27 was due to C_2H_3^+ and arose from an addition complex then four ions might be formed.(3.11)



No ion of mass 27 was observed, therefore the C_2H_3^+ ion does not come from a reaction of methanol derived cations with methanol. Nor does it come from a reaction of the deuterated methyl ion with methanol in which all the deuteriums are lost from the methyl ion. No C_2D_3^+ was observed either, so a reaction in which all the hydrogens are lost from the methanol can be ruled out. The ion corresponding to that of mass 27 was found to have a mass of 28 and therefore contained a mixture of hydrogens from the neutral methanol and deuteriums from the methyl ion. The other ion that might have been expected, namely C_2HD_2^+ , would occur at mass 29 and would not be distinguishable from CHO^+ which would also be formed.

No ions corresponding to $\text{C}_2\text{H}_n\text{D}_m^+$ where $(n + m = 5)$ were observed.

The other ions observed did not incorporate deuterium.(3.12)

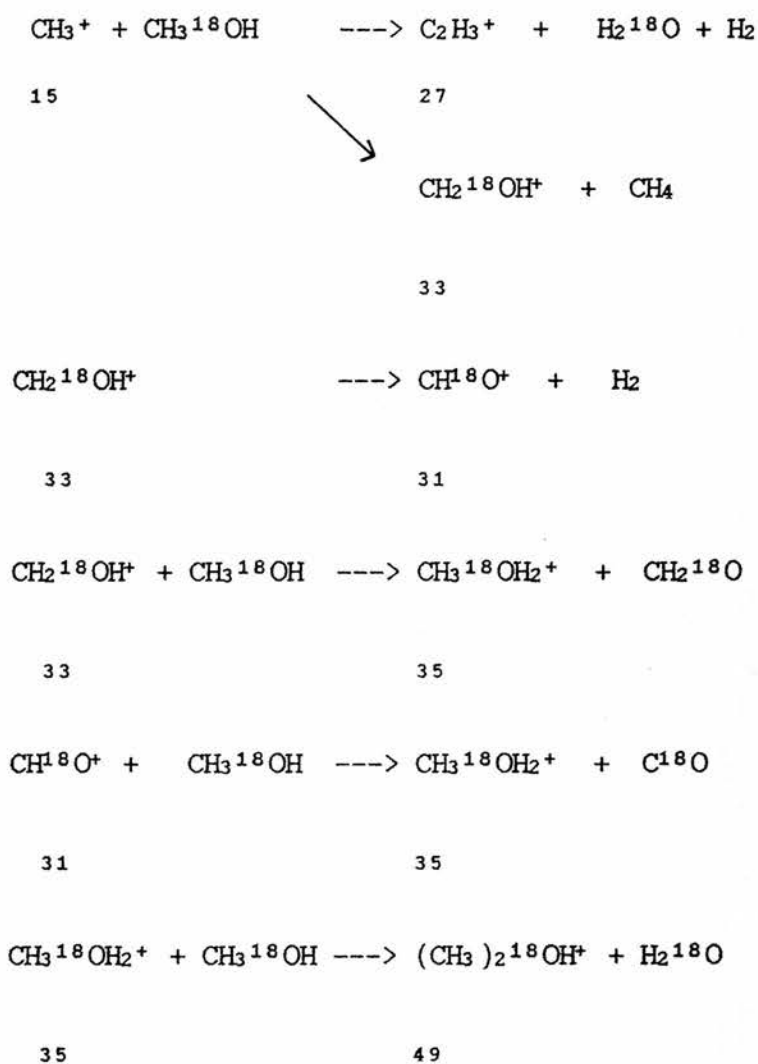


(3.12)

There were no dimethyl oxonium ions observed with a mass of 50 - containing three deuteriums. It can be concluded that the dimethyl oxonium ion is not formed from a direct adduct of the primary methyl ion with methanol.



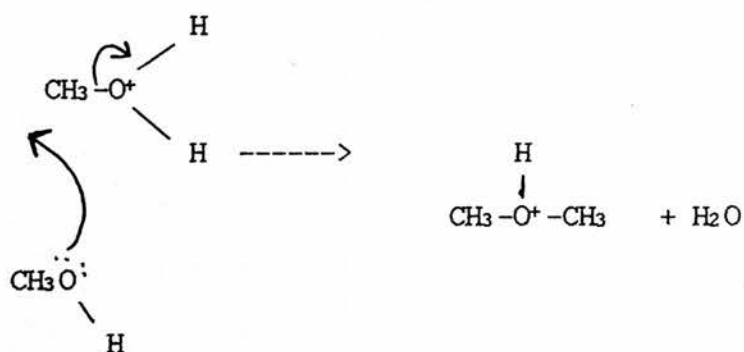
$\text{CH}_3^+ + \text{CH}_3^{18}\text{OH}$ Using oxygen-18 labelled methanol each ion's composition was confirmed.



CHO^+ was shown to be formed but no ion corresponding to C_2H_5^+ was found. It can be concluded, therefore, that under these conditions the ion of mass 29 that was observed in the non labelled experiment was CHO^+ .

Verification of the mechanism of $\text{CH}_3\text{OHCH}_3^+$ formation.

By considering the yield of ions in the preceding experiments it seems that protonated methanol, CH_3OH_2^+ , is a secondary ion, protonated dimethyl ether $(\text{CH}_3)_2\text{OH}^+$ is a tertiary ion and protonated methanol is a precursor of protonated dimethyl ether. Several isotopic labelled experiments were done with the triple quadrupole mass spectrometer to confirm the mechanism outlined below.



Protonated methanol was formed from the self-protonation reaction of methanol in the ionisation chamber at high pressures.

In the triple quadrupole mass spectrometer this self-protonation reaction can be used to form CH_3OH_2^+ in the ionisation chamber if the pressure of CH_3OH is raised sufficiently high. Methanol is fed into the ionisation chamber, where electron bombardment produces CH_3OH^+ . If sufficient CH_3OH molecules are present, the self-ionisation reaction can produce CH_3OH_2^+ which can be isolated in the first quadrupole and put into a target gas in the second

quadrupole. In this way the reactions of protonated methanol can be studied with only three quadrupoles. Care must be taken, because using this method will not produce a pure CH_3OH_2^+ ion peak as any isotope of methanol which is one mass unit heavier will also be part of the signal that would be put into the second quadrupole. For methanol the peak due to the isotope of CH_3OH^+ and the CH_3OH_2^+ was found to consist of 94% CH_3OH_2^+ at the lowest pressure and 99.7% CH_3OH_2^+ at the highest pressure measured.

TABLE 3.6

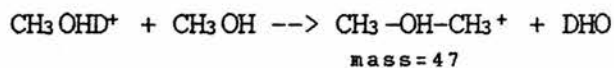
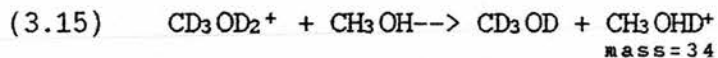
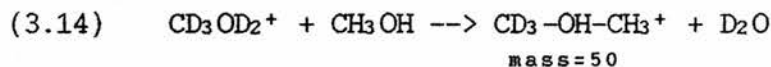
PRESSURE $\times 10^{-7}$ mbar	32 $\times 10^{-7}$	33 $\times 10^{-7}$	ISOTOPE '33'	33 - ISOTOPE $\times 10^{-7}$	CH_3OH_2^+ %
1	65	1.5	0.09	1.48	94.2
2.5	183	5	0.26	4.74	94.8
5	372	12	0.54	11.46	95.5
7.5	610	22.5	0.88	21.6	96.0
10	815	40	1.17	38.8	97.1
25	1690	150	2.43	147.6	98.4
50	2700	405	3.89	401	99.0
75	3420	615	4.92	610	99.2
100	4530	930	6.52	923	99.3
250	8100	2800	11.66	2788	99.6
500	11200	6100	16.13	6084	99.7

The peak at 33 was found to contain at least 94% protonated methanol and so this peak could justifiably be used for each of the following experiments.

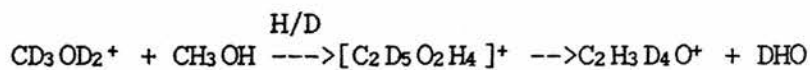
$\text{CD}_3\text{OD}_2^+ + \text{CH}_3\text{OH}$

Both $\text{CD}_3\text{OHCH}_3^+$ and $\text{CH}_3\text{OHCH}_3^+$ ions were formed. At low pressures the amount of the partially deuterated ion was greater than the non-deuterated ion, but $(\text{CH}_3)_2\text{OH}^+$ rose as the pressure increased to be a much larger proportion of the ions. This indicates that the ion with no deuteriums is

formed by the competing deuteration of methanol and subsequent reaction (3.15).

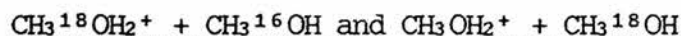
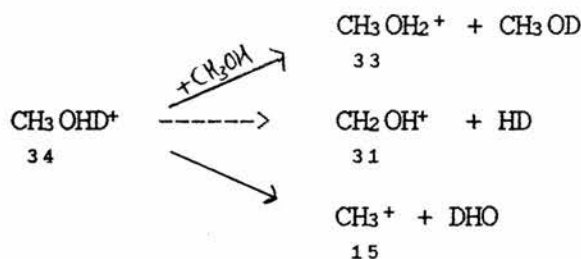
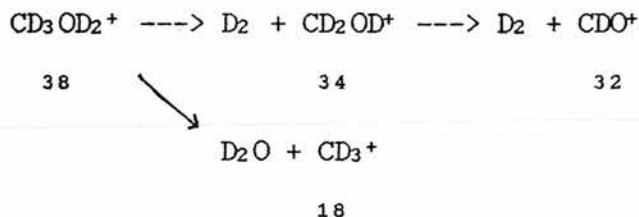


The presence of an ion of mass 48 indicates that H/D exchange is occurring.



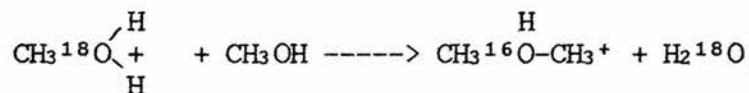
The formation of these three ions $[\text{C}_2\text{H}_n\text{D}_m\text{O}]^+$ (where $n = 4$ and $m = 3$, $n = 7$ and $m = 0$ or $n = 3$ and $m = 4$) would be consistent with the mechanism proposed but would not prove it conclusively.

The other ions produced are fragments of protonated or deuterated methanol.



The reaction of ^{18}O labelled methanol allows the source of the oxygen atom in the protonated dimethyl ether ion to be traced.

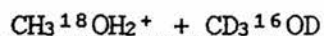
The reaction of ^{18}O labelled protonated methanol with ^{16}O methanol produced only ^{16}O in the protonated dimethyl ether (mass = 47).



In the reverse reaction in which $\text{CH}_3^{16}\text{OH}_2^+$ was reacted with ^{18}O methanol the protonated dimethyl ether contained only ^{18}O .

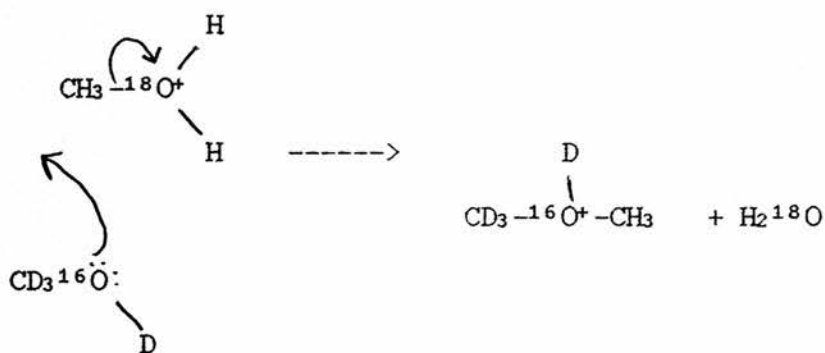


This showed that the oxygen in the protonated dimethyl ether comes exclusively from the neutral methanol. This is consistent with the mechanism proposed but did not prove it.

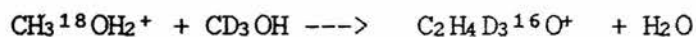


The definitive experiment was to react $\text{CH}_3^{18}\text{OH}_2^+$ ions with $\text{CD}_3^{16}\text{OD}$. Each methyl group, each oxygen and the protons on each oxygen could be traced in the reaction.

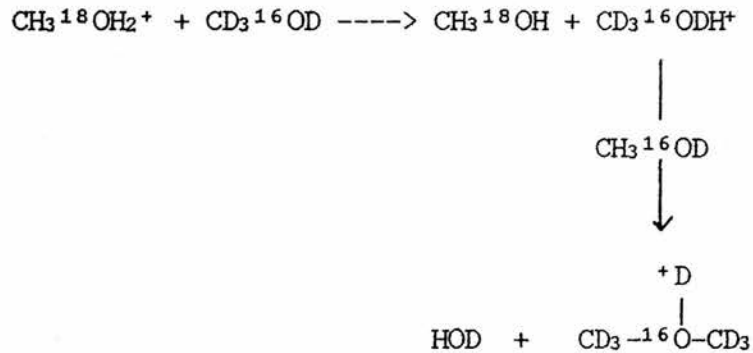
At low pressures the only protonated dimethyl ether ion observed had a mass of 51 which must be formed by the addition with elimination reaction.



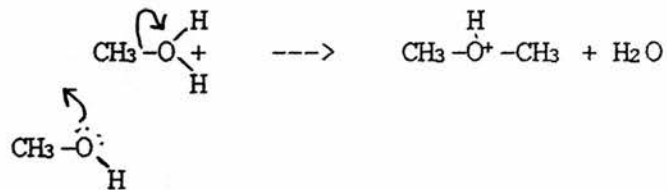
At higher pressures a very small peak of mass 50 was observed. This tertiary ion was the result of D/H exchange.



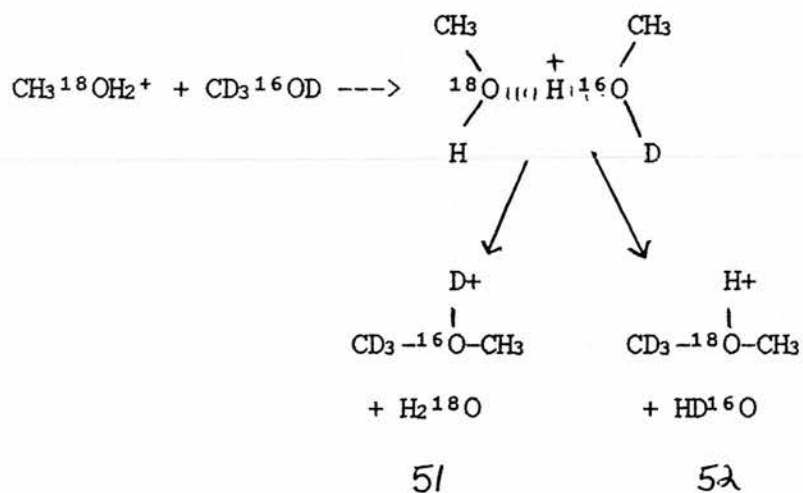
At the highest pressure used an ion of mass 54 was observed. This was due to the further reaction of $\text{CD}_3^{16}\text{ODH}^+$ which had been formed by protonation of $\text{CD}_3^{16}\text{OD}$ by $\text{CH}_3^{18}\text{OH}_2^+$.



All three of these ions can only be formed via the mechanism proposed below.



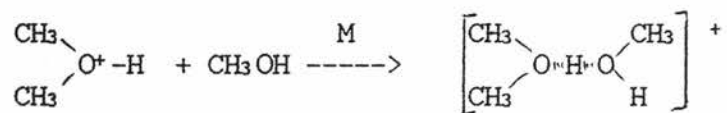
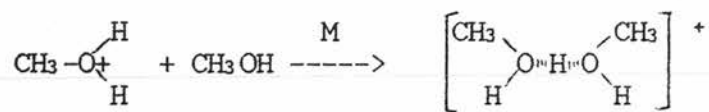
The symmetrical additional complex intermediate proposed by Henis ¹⁵² as an intermediate in the formation of dimethyl oxonium ions is not consistent with the results of these reactions and has been disproved.



The production of dimethyl oxonium ions by loss of water from a symmetrical addition complex would result in a mixture of isotopes from the methyloxonium ion and the neutral methanol. In each of the labelled reactions carried out in this investigation there was absolutely no mixing of isotopes.

The mechanism of Henis would predict that both of the ions of mass 51 and mass 52 would be formed. In our experiment only the ion of mass 51 was obtained. Only the mechanism proposed in this chapter can account for the results of all the experiments.

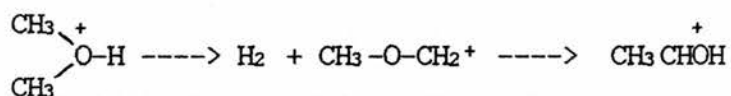
At high pressures collision stabilized adducts were observed.



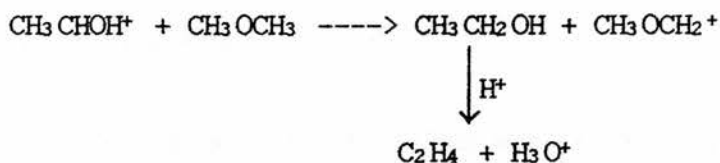
INVESTIGATION OF THE MECHANISMS INVOLVING REACTIONS OF
PROTONATED DIMETHYL ETHER

A route for the formation of protonated dimethyl ether from methanol having been established, an investigation of the reactions of protonated dimethyl ether was carried out.

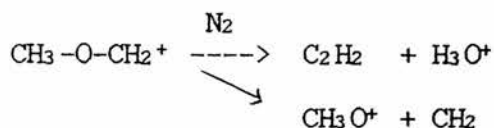
Van den Berg proposed a mechanism involving the rearrangement of a carboxonium ion. ¹⁶¹



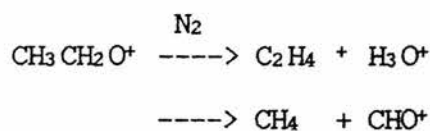
Subsequent hydride abstraction from dimethyl ether would result in ethanol and a carboxonium ion. Acid catalysed dehydration of ethanol would give ethene.



To test this mechanism in the gas phase, $\text{CH}_3\text{OCH}_2^+$ was separated from dimethyl ether in the first quadrupole of the triple quadrupole mass spectrometer. This ion was fed into an inert gas, nitrogen in this instance, in the second quadrupole and yielded ions of mass 19 and 31. These were thought to be due to the fragmentations to H_3O^+ and CH_3O^+ .

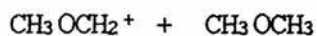


Comparison with the fragment pattern of $\text{CH}_3\text{CH}_2\text{O}^+$ was required. $\text{CH}_3\text{CH}_2\text{O}^+$ from ethanol produced ions of mass 29 and 19 due to the fragmentations to H_3O^+ and CHO^+ .



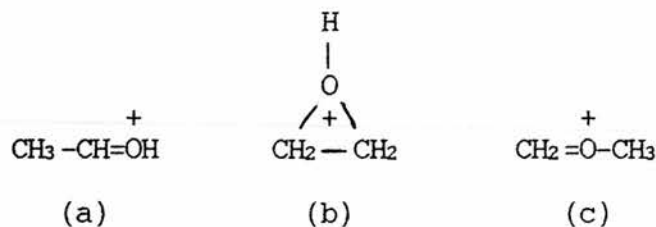
29

It was noted that no fragment of CH_3O^+ , mass = 31, was obtained from the fragmentation of the $\text{CH}_3\text{CH}_2\text{O}^+$ ion and no CHO^+ ion, mass = 29, was obtained from the fragmentation of the $\text{CH}_3\text{OCH}_2^+$ ion. This could be used as a diagnostic fragmentation in the quinquapole mass spectrometer to distinguish between these two forms of carboxonium cations.

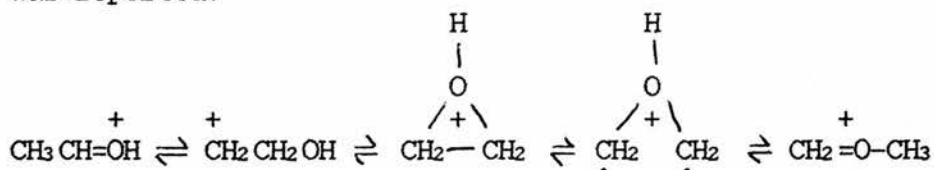


$\text{CH}_3\text{OCH}_2^+$ from dimethyl ether was reacted with dimethyl ether. No reaction was observed. The only ions observed had mass of 31 and 19 which were due to the fragmentation of $\text{CH}_3\text{OCH}_2^+$ ions. That no CHO^+ , mass = 29, was observed suggested that no rearrangement of the form suggested by Van den Berg had taken place.

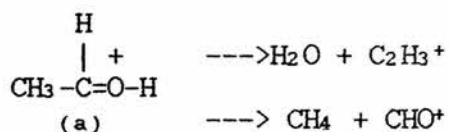
The structure and rearrangement of $C_2H_5O^+$ ions have been extensively studied.¹⁶²⁻¹⁶⁴ Three stable isomers have been identified.



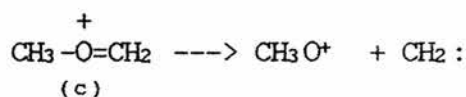
A mechanism for the interconversion of these isomers was reported.¹⁶⁵



The fragmentation of the two types of $C_2H_5O^+$ ion formed from ethanol and dimethyl ether in the triple quadrupole mass spectrometer indicates that the ion from ethanol has the form (a) and fragments with the loss of methane or loss of water.



$C_2H_5O^+$ ions from dimethyl ether have the form (c) and fragment to CH_3O^+ .



A potential energy diagram for the interconversion of $C_2H_5O^+$ ions has been constructed from consideration of various experimental results.¹⁶⁶⁻¹⁶⁹ It is reproduced in figure 3.3.

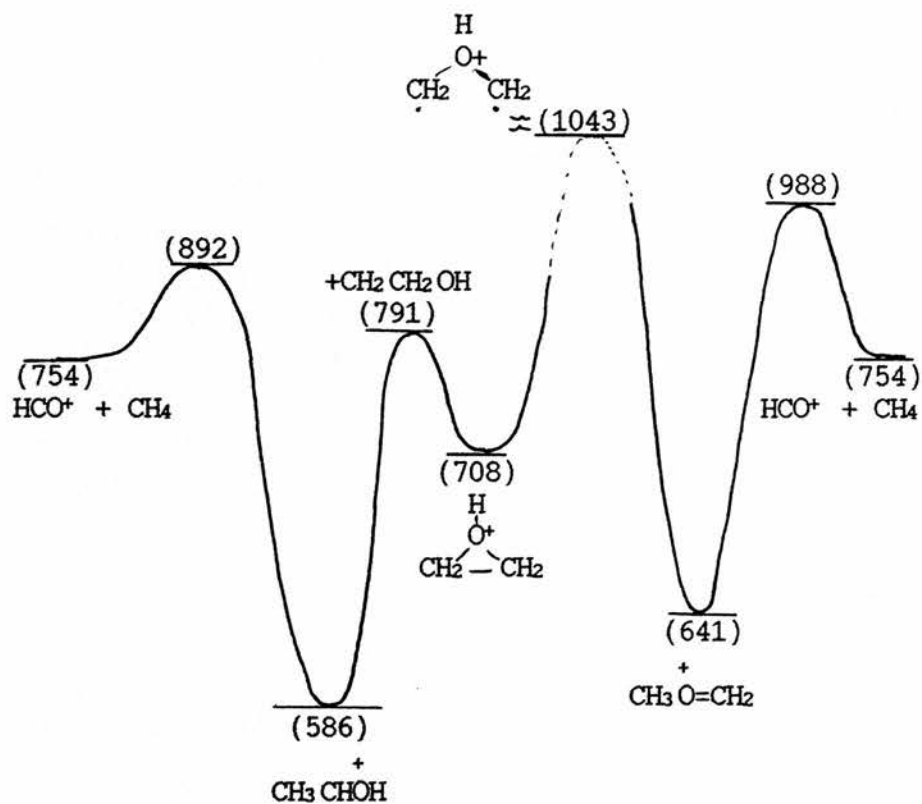
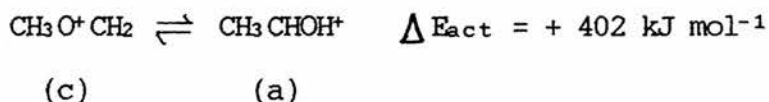


FIGURE 3.3

Potential Energy Diagram of Isomers of C₂H₅O⁺ Ions

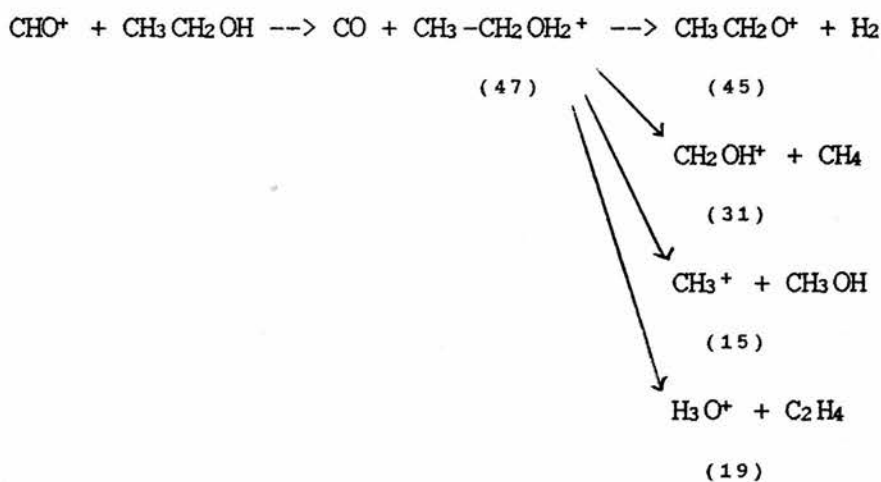
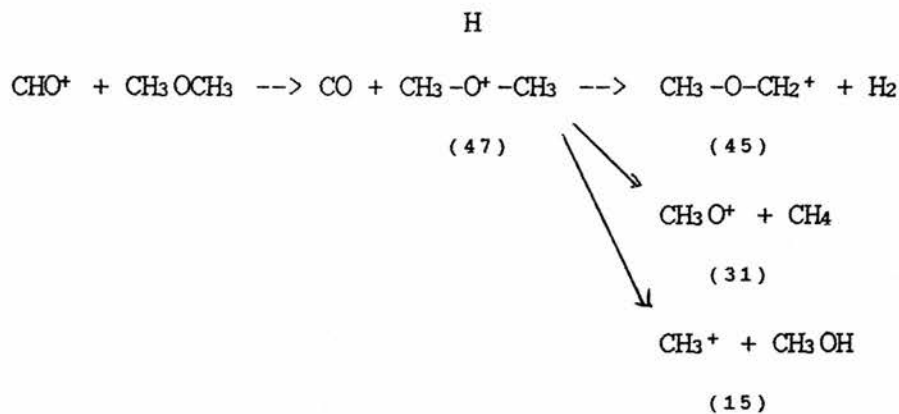
(Energy in kJ mol⁻¹)

That no CHO^+ ion is observed from the fragmentation of $\text{CH}_3\text{O}^+\text{CH}_2$ indicates that the $\text{CH}_3\text{O}^+\text{CH}_2$ ions in the mass spectrometer do not have enough energy to surmount the energy barrier to fragmentation. $E_{\text{act}} = 347 \text{ kJ mol}^{-1}$. Therefore, it follows, that they will not have enough energy to rearrange through the barrier to CH_3CHOH^+ .



This could explain why no rearrangement of the $\text{C}_2\text{H}_5\text{O}^+$ ions were observed in these experiments. It would not be valid to assume anything about the possible rearrangement of $\text{C}_2\text{H}_5\text{O}^+$ ions within a zeolite from the behaviour of ions in a triple quadrupole mass spectrometer.

Fragmentation of the protonated ethanol and protonated dimethyl ether ions were also studied and showed that these ions could be distinguished if formed in the quinquapole mass spectrometer. No fragment of mass 19 was formed from the dimethyl oxonium ion.



In all experiments done there was no indication that $\text{CH}_3\text{OCH}_2^+$ reacted with dimethyl ether or rearranged to $\text{CH}_3\text{CH}_2\text{O}^+$ and in so doing formed a C-C bond.

The most likely reaction for $\text{CH}_3\text{OCH}_2^+$ with CH_3OCH_3 would be hydride abstraction to form CH_3OCH_3 and $\text{CH}_3\text{OCH}_2^+$ - this would be indistinguishable without isotopically labelled dimethyl ether.



An alternative mechanism, also proposed by Van den Berg, and represented in fig. 3.4, involves the protonation of dimethyl ether by a Brønsted acid site to form the dimethyl oxonium ion, I. This subsequently reacts with another molecule of dimethyl ether to give the trimethyl oxonium ion II and methanol.

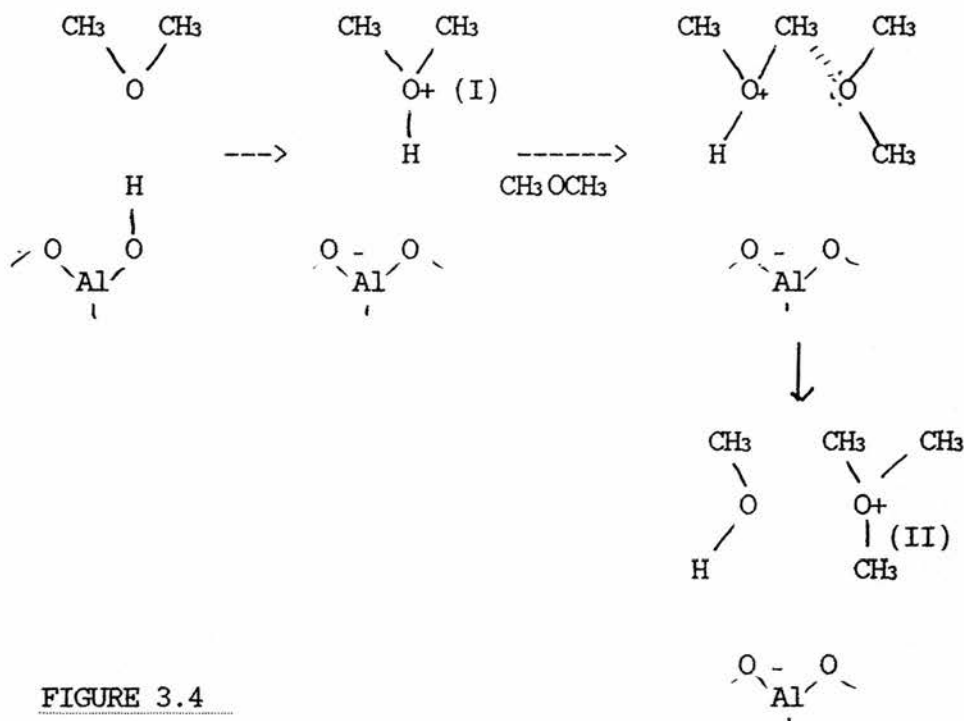
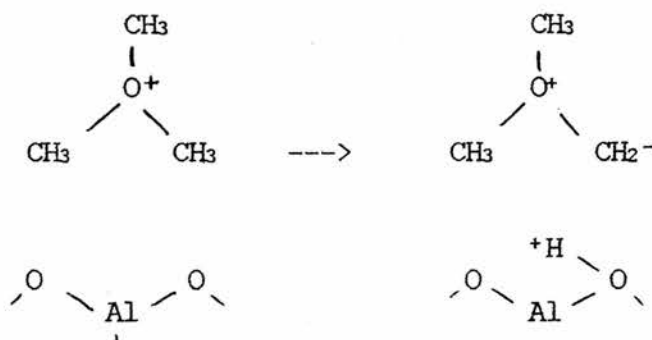


FIGURE 3.4

The trimethyl oxonium ion would then be deprotonated by a basic site on the catalyst to form the oxonium ylid $(\text{CH}_3)_2\text{O}^+\text{CH}_2^-$ as shown in fig. 3.5.

Fig. 3.5

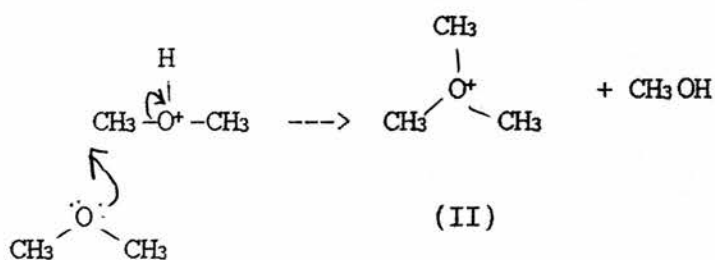


Cis-insertion of the carbenoid species into the adjacent C-O bond would result in the formation of a C-C bond. Fig 3.6.

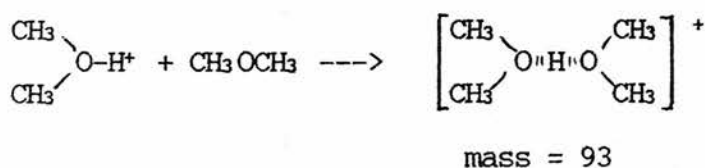


Fig. 3.6

To investigate this mechanism the dimethyl oxonium ion was reacted with dimethyl ether. Two interesting ions were formed. One of mass 61 was the trimethyl oxonium ion II. This was thought to be formed by the elimination of methanol from dimethyl oxonium ion. This reaction was further studied using the quinquadrupole mass spectrometer. The results of the experiment which confirm this mechanism are reported in chapter six.

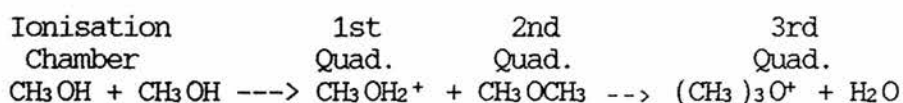


The other ion had a mass of 93 and was the adduct of methyl oxonium and a dimethyl ether molecule.



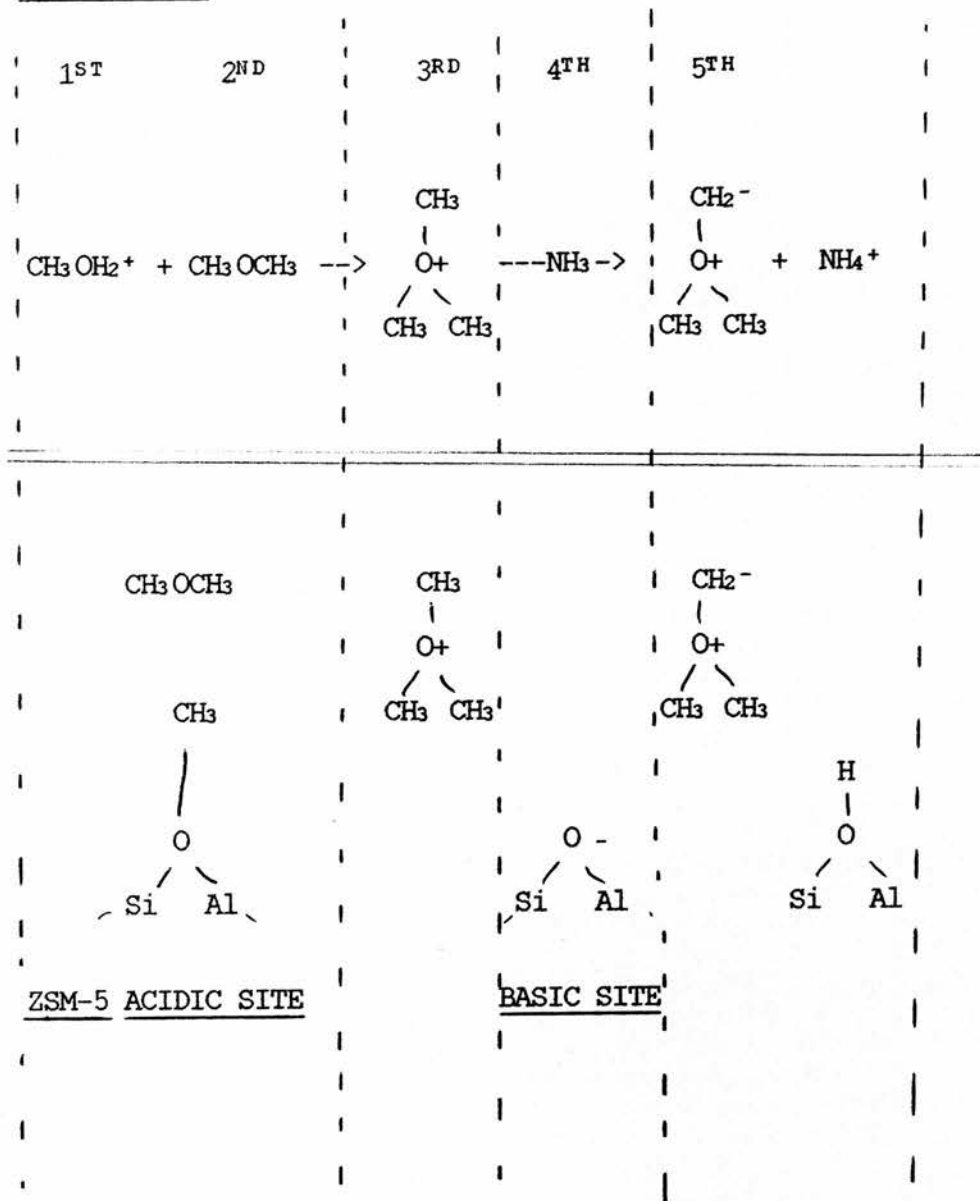
This indicates that the first part of this mechanism is feasible and can occur in the gas phase. To investigate the

next part of the mechanism the quinqa quadrupole could be used to full effect. The trimethyl oxonium ion could be formed in the second quadrupole from methylation of dimethyl ether by methyl oxonium ions formed by a self protonation reaction in the ionisation chamber.



The trimethyl oxonium ion could be separated in the third quadrupole and fed into a gaseous base in the fourth quadrupole. The oxonium ylid, $(\text{CH}_3)_2\text{O}^+\text{CH}_2^-$, would not be detected in the fifth quadrupole because it is neutral, but the presence of protonated base would indicate that the trimethyl oxonium ion had protonated the base. By using bases of decreasing basic strength the acidic strength of the trimethyl oxonium ion could be gauged.

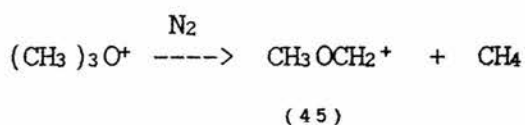
In effect the quinqa quadrupole mass spectrometer would be used to mimic the acidic sites of ZSM-5 in the second quadrupole and the basic sites in the fourth quadrupole.

QUADRUPOLES

An attempt was made to study the reaction of trimethyl oxonium ions with bases in the triple quadrupole mass spectrometer as a prelude to a full investigation using the quinquadrupole mass spectrometer. A mixture of methanol and dimethyl ether was fed into the ionisation chamber of the triple quadrupole mass spectrometer. An ion of mass 61 was observed in the first quadrupole at high pressure. This ion was separated and put into the second quadrupole which contained ammonia. The ions produced from this reaction were of mass 45, 32, 30 and 18. These were thought to be

mass 45 = $\text{CH}_3\text{OCH}_2^+$
 mass 32 = CH_3OH^+ or CH_3NH_3^+
 mass 30 = CH_2O^+ or CH_2NH_2^+
 and mass 18 = NH_4^+ .

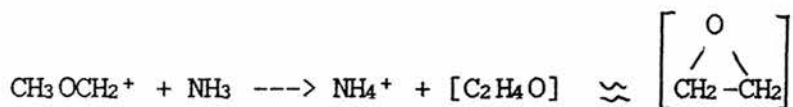
To ascertain if any of the product arose by fragmentation rather than reaction with the base, the experiment was repeated with the $(\text{CH}_3)_3\text{O}^+$ ion fed into nitrogen. An ion of mass 45 was observed.



This suggests that the $\text{CH}_3\text{OCH}_2^+$ ion arose from fragmentation of $(\text{CH}_3)_3\text{O}^+$ rather than a reaction with a base.

CH₃OCH₂⁺ into NH₃

CH₃OCH₂⁺ (from dimethyl ether) was reacted with ammonia in a separate experiment. Ions of mass 32, 30 and 18 were obtained.



18



32

30

It was not possible to have the trimethyl oxonium ion in isolation from the CH₃OCH₂⁺ ion because the former fragments so readily to the latter. As the fragment CH₃OCH₂⁺ cannot be separated from the trimethyl oxonium ion, it cannot be concluded whether the ions of 32, 30 and 18 arise from the reaction of trimethyl oxonium ions with ammonia or from the reaction of CH₃OCH₂⁺ with ammonia. This would have to be investigated further in the quinquapole mass spectrometer.

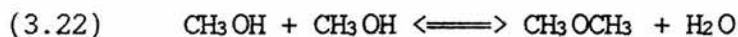
It should be noted that the presence of CH₃NH₃⁺ indicates that the ammonia has been methylated. This could also be investigated further. The effect of using different bases in this reaction has still to be investigated on the quinquapole mass spectrometer.

The conclusions that can be drawn from this section are

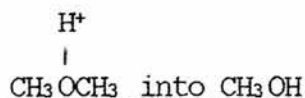
:-

- 1) the fragments of $\text{CH}_3\text{OCH}_2^+$ and $\text{CH}_3\text{CH}_2\text{O}^+$ can be distinguished in the quinquadropole mass spectrometer
- 2) as can the fragments of protonated dimethyl ether be distinguished from those of protonated ethanol.
- 3) no support for the rearrangement of $\text{CH}_3\text{-O-CH}_2^+$ to CH_3CHOH^+ has been found in this gas phase investigation, but it must be noted that the ions studied in this work are of low energy and would not have sufficient energy to surmount the activation energy barrier for this rearrangement.
- 4) the trimethyl oxonium ion can be formed in the gas phase in the manner specified by the mechanism of van den Berg.
Fig. 3.4.
- 5) the quinquadropole mass spectrometer could be used to study the reactions of acidic and basic mediums in sequence and could mimic the acidic and basic sites on a zeolite catalyst.

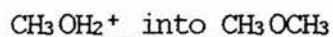
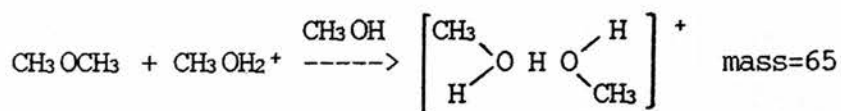
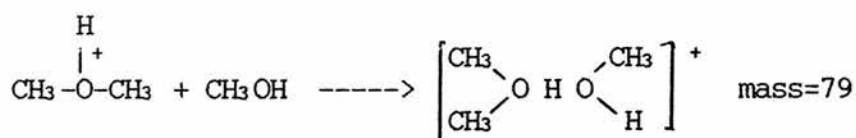
The mechanisms investigated so far have involved the reaction of an ion produced from dimethyl ether reacting with dimethyl ether. They have all assumed that the dehydration of methanol to dimethyl ether goes to completion before any hydrocarbon is formed. The dehydration reaction is, however, an equilibrium, so the importance of a small amount of methanol cannot be ruled out. Any reaction that involves methanol would upset the balance of the equilibrium and cause more methanol to be formed.



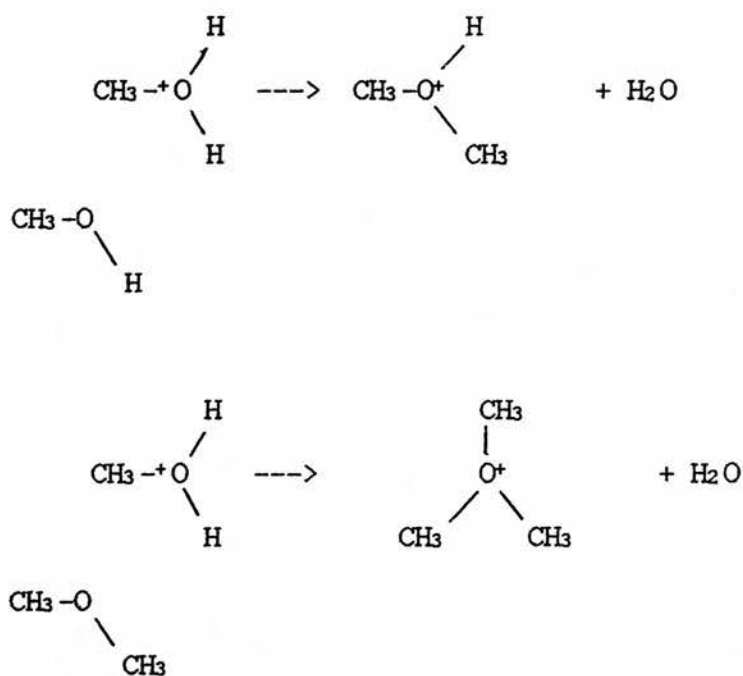
It could be argued that mechanisms involving the reaction of protonated dimethyl ether with dimethyl ether do not truly represent the conditions existing in the early stages of the reaction of methanol over ZSM-5 catalyst. Under the initial conditions a dimethyl oxonium ion would be much more likely to encounter a methanol molecule than a dimethyl ether molecule. The reactions of dimethyl oxonium with methanol and methyl oxonium with dimethyl ether were studied.



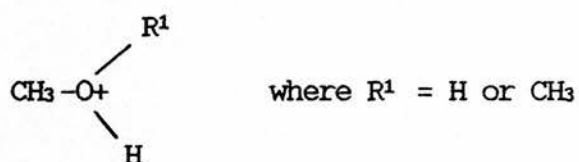
The reaction of $\text{CH}_3\text{OHCH}_3^+$ with CH_3OH produced protonated methanol, CH_3OH_2^+ (mass 33) and at high pressures two addition complexes - one of mass 79 which was the adduct of dimethyl oxonium and methanol and one of mass 65 due to the adduct of methyl oxonium with methanol.



The reaction of CH_3OH_2^+ with CH_3OCH_3 produced dimethyl oxonium ions, $\text{CH}_3\text{OHCH}_3^+$ mass 47, and an ion of mass 61 which was thought to be the trimethyl oxonium ion. This ion could be formed in a reaction analogous to that which produced dimethyl oxonium ion from CH_3OH_2^+ and CH_3OH .

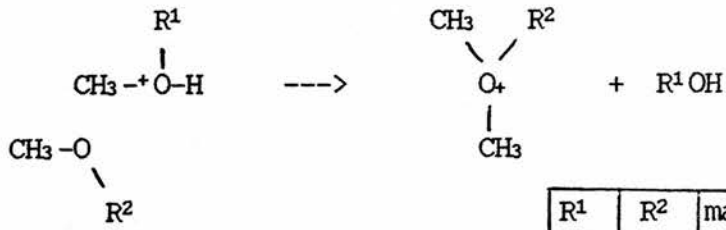


The reactions of protonated methanol and dimethyl ether ions - of the general formula



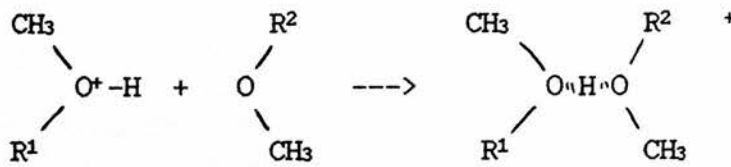
with methanol or dimethyl ether - expressed as $\text{CH}_3-\text{O}-\text{R}^2$ - can be summarised in the scheme below.

ELIMINATION OF R¹OH



R ¹	R ²	mass
H	H	47
H	CH ₃	61
CH ₃	H	47
CH ₃	CH ₃	61

FORMATION OF AN ADDUCT



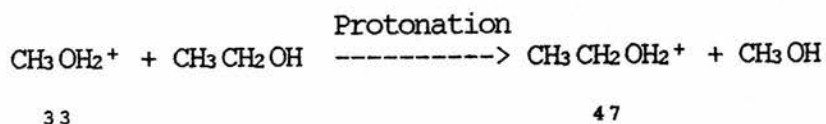
where

R ¹	R ²	mass
H	H	65
H	CH ₃	79
CH ₃	H	79
CH ₃	CH ₃	93

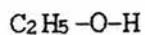
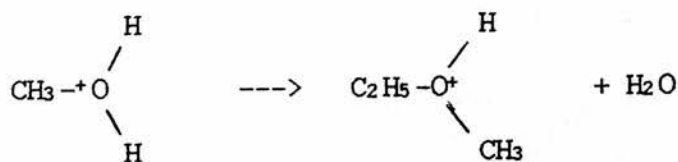
The reactions of higher analogues were studied.

ETHANOL

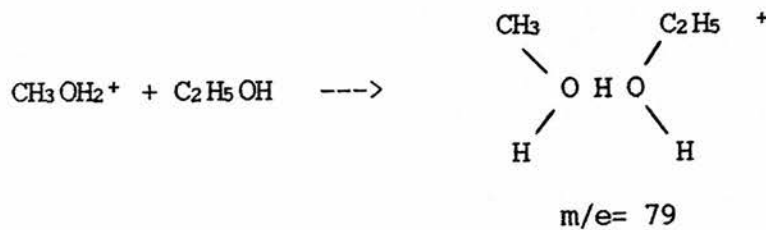
CH_3OH_2^+ reacted with ethanol in an analogous way to produce the following ions.



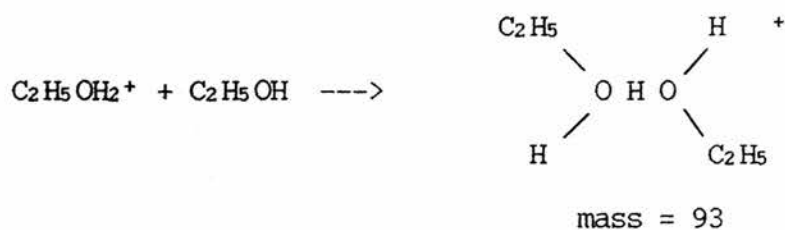
Addition-with-elimination of H_2O produced the methyl ethyl oxonium ion of mass 61.



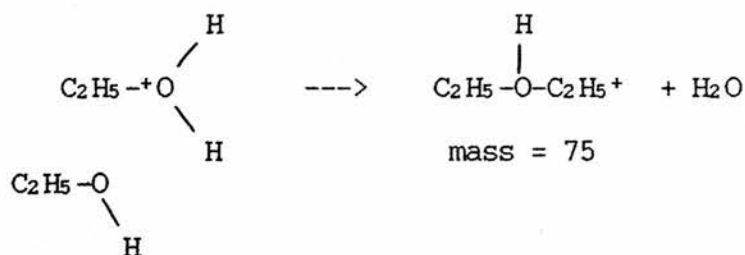
An adduct between methyl oxonium and ethanol was formed.



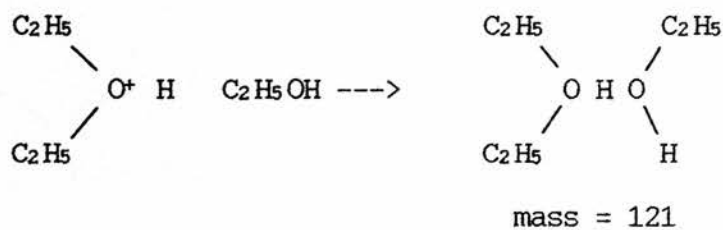
An adduct between ethyl oxonium and ethanol was formed.



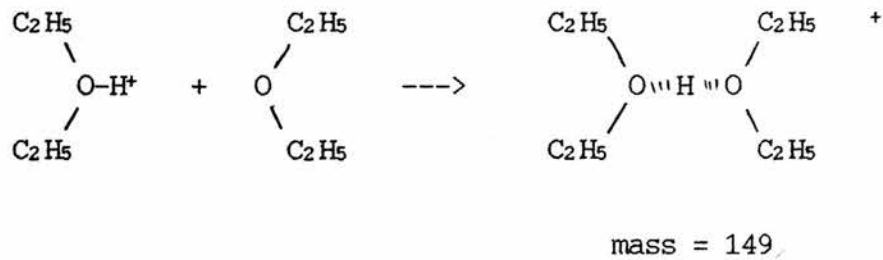
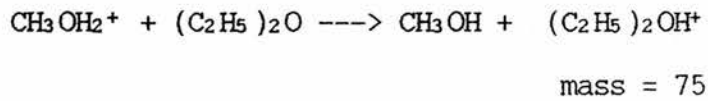
Addition-with-elimination of H_2O occurred between ethyl oxonium ion and ethanol to produce a diethyl oxonium ion.



This diethyl oxonium ion reacts further with ethanol to produce an adduct of mass 121 at high pressures.



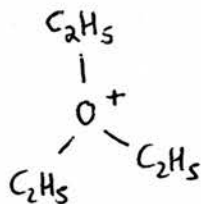
Methyl oxonium was reacted with diethyl ether and the addition complex of diethyl oxonium ions with diethyl oxonium ion was observed.



All combinations of addition complex with $\text{R} = \text{C}_2\text{H}_5$ had now been observed.

R ¹	R ²	R ³	R ⁴	mass
CH ₃	H	C ₂ H ₅	H	79
C ₂ H ₅	H	C ₂ H ₅	H	93
C ₂ H ₅	C ₂ H ₅	C ₂ H ₅	H	121
C ₂ H ₅	C ₂ H ₅	C ₂ H ₅	C ₂ H ₅	149

The triethyl oxonium ion was observed in small quantities.

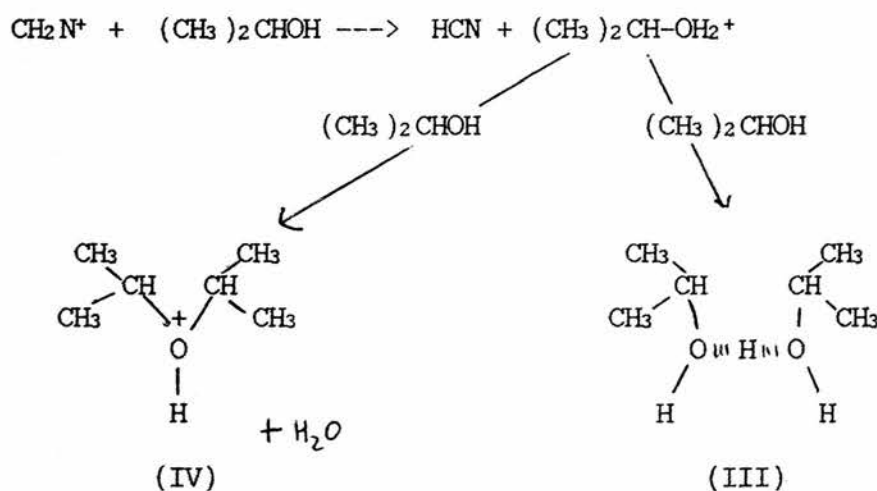


PROPANOL

Investigations of the reactions of propyl alcohol and propyl ether were limited because of the mass of the ions formed. The mass of the adduct between dipropyl oxonium ion and dipropyl ether was 205 a.m.u. which is at the maximum extreme of the range of the quadrupole mass spectrometer.

CH₂N⁺ INTO PROPAN-2-OL

The protonation of propan-2-ol produced ions of mass 61 - (CH₃)₂CH-OH₂⁺, mass 121 (III) and the diisopropyl oxonium ion (IV).



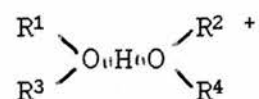
Protonation of diisopropyl ether produced the diisopropyl oxonium ion and the adduct of two diisopropyl

CONCLUSIONS

The reactions of methanol with ions from methanol have been studied. A mechanism for the formation of dimethyl oxonium ions from an addition with elimination reaction of methyl oxonium ions with methanol has been postulated. The use of selected isotopically labelled ions and neutrals has enabled the mechanism proposed by Henis to be disproved. The results of all experiments reported are consistent with the mechanism proposed in the present work.

A similar mechanism for the formation of trimethyl oxonium ions was proposed.

Adducts of all combinations of the general formula



where $\text{R}^1, \text{R}^2, \text{R}^3$ and R^4 can be any combination of

a) H, CH_3 , b) H, C_2H_5 or c) H, C_3H_7 were found.

No evidence to support the production of C-C bonded compounds from these dimethyl oxonium, trimethyl oxonium and adduct ions was found. The fragmentations and reactions of these ions could be investigated in the quinquadrupole mass spectrometer.

The production of C-C bonds in alkyl ions C_2H_3^+ and C_2H_5^+ was observed. They were formed by an addition with elimination reaction of a methyl cation and methanol. This will be discussed in the overall conclusion to chapters three to five on page 329.

CHAPTER FOURREACTIONS INVOLVING HALOGENOMETHANES

CHAPTER FOUR REACTIONS INVOLVING HALOGENOMETHANES

Having considered the mechanisms involving the reactions of methanol and dimethyl ether over an acidic catalyst, attention now turned to considering the reaction of chloromethane and other halogenomethanes over an acidic catalyst.

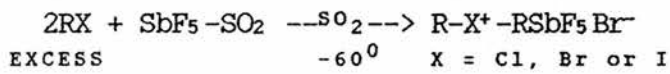
The aims of the work present here were :

- to investigate the reactions of ions from halogenomethanes in the gas phase in an attempt to find the pathway to the formation of methyl halonium and dimethyl halonium ions,
- to compare the reaction mechanisms of halogen containing ions with respect to the reactions of oxygen containing ions for considerations of the reaction mechanisms pertaining to the reactions of methanol and the halogenomethanes over ZSM-5 catalyst.

At the time of commencement of this study very little had been reported in the literature on the reactions of halogenomethanes over ZSM-5 catalyst.

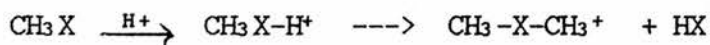
Alkyl halonium ions, $R-X-H^+$, and dialkyl halonium ions, R^1-X-R^2+ , had been observed as rearrangement products from electron impact mass spectrometer¹⁷⁰ and in ion cytotron studies of ion reactions.¹⁷¹

Dialkyl halonium ions had been formed in superacids as indicated by an additional nmr signal. ¹⁷²



Dimethyl and diethyl halonium ions, prepared in this way, were found to be effective alkylating agents in the solution phase. ¹⁷³⁻¹⁸⁰

A mechanism for the formation of dimethyl halonium ions was proposed. ¹⁷²



where X = Cl, Br or I

In 1985 a mechanism for the formation of ethene via the rearrangement of dimethyl halonium ions to methylhalonium methylides was proposed. ¹⁸¹ This is represented in figure 4.1.

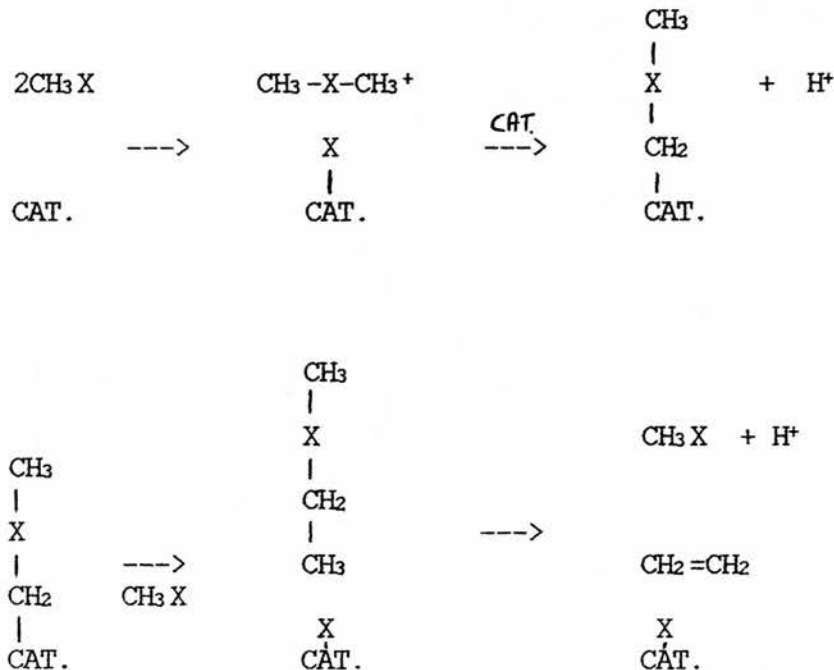


FIGURE 4.1

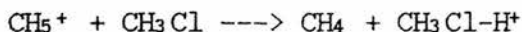
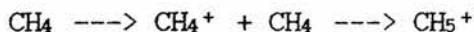
This mechanism could be important in the production of hydrocarbons from the reaction of halogenomethanes over ZSM-5 catalysts.

Gas phase studies of alkyl halonium ions have developed over the last twenty years. McAskill studied the energy dependence of ion-molecule reactions of methane ¹⁸² and halogenomethanes ¹⁸³⁻¹⁸⁵ using a high pressure ion cyclotron mass spectrometer. In addition to the ions of chloromethane - CH_2Cl^+ , CH_3Cl^+ and CH_3ClH^+ - condensation ions were observed. C_2H_3^+ and C_2H_5^+ were observed in very small quantities and an ion that was assigned the structure of protonated ethyl chloride - $\text{C}_2\text{H}_6\text{Cl}^+$ - was a tertiary ion. Similar results were reported for fluoromethane and the condensation ion, $\text{C}_2\text{H}_6\text{F}^+$, was described as protonated fluoroethane.

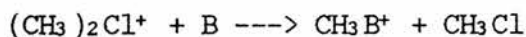
Kebarle and co-workers, in a series of papers from 1978 to 1986, have studied the gas phase binding energy and stability of chloronium ions from consideration of the gas phase equilibria. ¹⁸⁶⁻¹⁹² In all papers they considered the $\text{C}_2\text{H}_6\text{Cl}^+$ ion to be dimethyl chloronium rather than protonated chloromethane.



The chloronium ions were formed by electron bombardment of a mixture of methane at 4 torr and chloromethane at 0.1 torr.

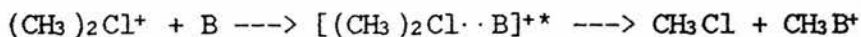
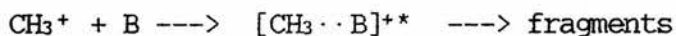


The dimethyl chloronium ions thus formed were used as gas phase alkylating agents. The molecule to be alkylated was added to the mixture of methane and chloromethane at a pressure of 0.001 torr.

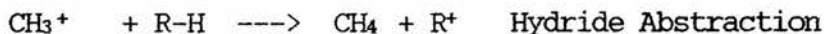


The advantages of using dimethyl chloronium ions over free methyl ions in ion-molecule reactions are twofold:-

1) methylation by dimethyl chloronium ions is a much milder form of methylation.



2) there are less side reactions with the dimethyl chloronium ion than with direct methyl ion reaction. Hydride abstraction which tends to occur with free methyl ions will not occur so readily with the dimethyl chloronium ions.

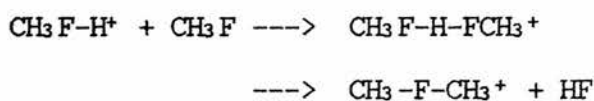


The reactions of methyl ions with many molecules have been studied. With the quinquadrupole mass

spectrometer the reactions of dimethyl chloronium ions as a methylating agent with many molecules could be studied.

Dimethyl iodonium ions have been used for gas phase methylation of organic functional groups. Dimethyl iodonium ions were formed by electron impact of iodomethane at 1 torr pressure. With the exceptions of aliphatic alcohols, benzene, anisole, furan and thiophene, all other compounds were methylated by dimethyl iodonium ions. ¹⁹³

In 1986 a report of dimethyl fluoronium ions in the gas phase was presented by McMahon and Kebarle. ¹⁹⁴ The proton bound dimer was also reported in this paper.



Reports of the reaction of chloromethane over ZSM-5 catalyst were very sparse at the commencement of the present work. In 1984 work had been reported by Romannikov and Ione ¹⁹⁵ and work had been done, but not reported, by employees of B.P.

A table of comparative yields for the reaction of methanol by Chang and chloromethane by Romannikov show the great degree of similarity between the two reactions.

TABLE 4.1 YIELD (wt%) OF HYDROCARBON REACTION PRODUCTS

Product	CH ₃ OH	CH ₃ Cl
Ethene	2.3	1.0
Propene	19.3	15.0
Butenes	7.0	7.0
Pentenes	0.5	2.5

$$P_{CH_3X} = 0.01 \times 10^5 \text{ Pa}$$

Ref. 7

Products	CH ₃ OH	CH ₃ Cl
Methane	0.1	0.1
Ethene	2.0	1.3
Ethane	0.1	0.3
Propene	-	1.9
Propane	28.9	11.2
Isobutane	-	9.5
n-Butane	10.4	4.5
Isopentane	-	2.1
n-Pentane	1.5	4.4
C ₆ Aliphatic	0.2	5.4
Benzene	0.2	0.2
Toluene	2.5	1.9
m-Xylene	20.3	13.6
o-Xylene	5.3	3.9
Pseudocumene	-	18.8
C ₁₀ Aromatic	27.5	15.3

$$P_{CH_3X} = 0.4 \times 10^5 \text{ Pa}$$

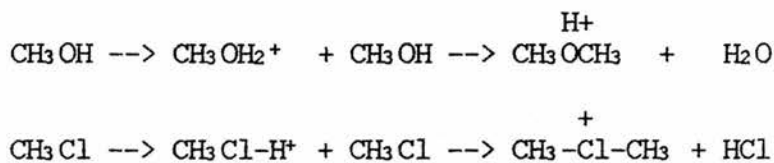
Ref. 195

They concluded that as the products obtained from chloromethane and methanol over the same catalysts, under the same reaction conditions, were similar, a common mechanism must be operating. Since the start of this work more reports have been presented in the literature. 196-199

The mechanisms proposed from considering the reactions of methanol must now be reconsidered to ascertain if they are compatible for methylchloride.

If dimethyl ether is the important intermediate in the conversion of methanol to hydrocarbons then the question arises of what is the key intermediate with chloromethane. There is no equivalent for dimethyl ether

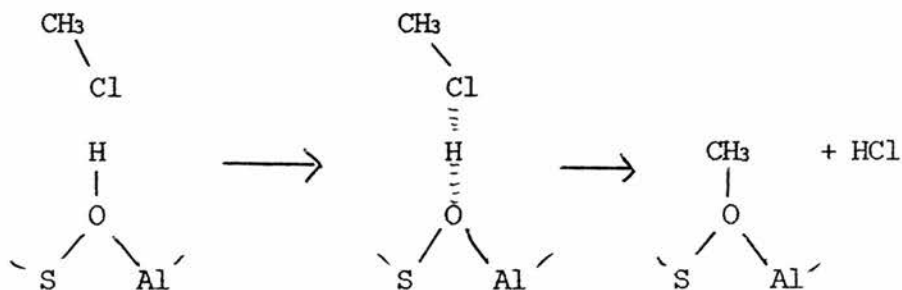
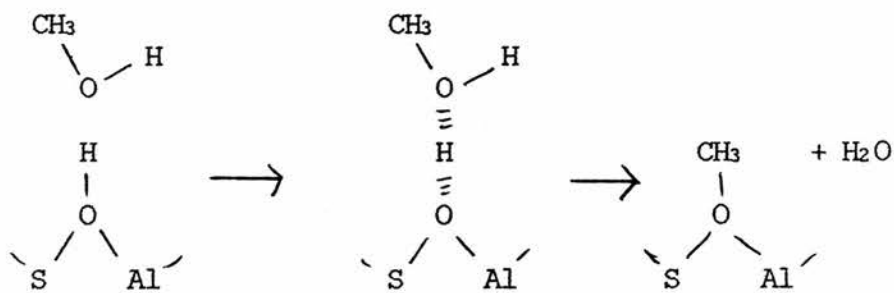
but there is a chlorine equivalent for the dimethyl oxonium ion, the dimethyl chloronium ion.



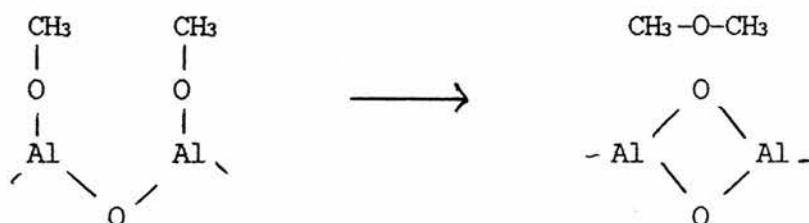
The work of this chapter is concerned with the search for a mechanism that can accommodate both reactants or an alternative mechanism.

REACTION MECHANISMS INVOLVING METHYL GROUPS

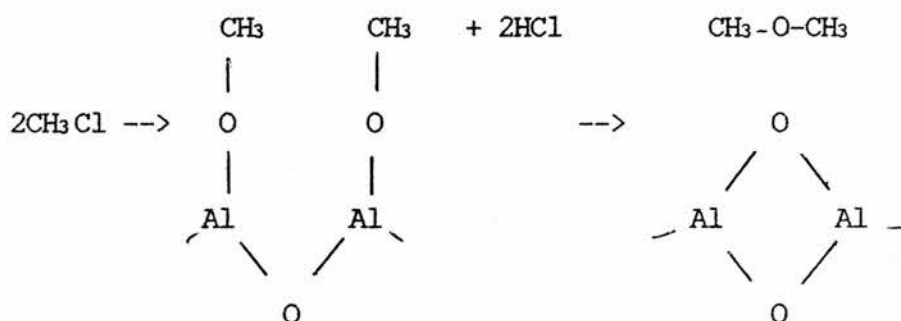
Formation of methyl groups on zeolite surfaces could be a step common to both reactants. Whatever the subsequent mechanism of hydrocarbon formation from bound methyl groups, both methanol and chloromethane precursors could form methyl groups on the zeolite.



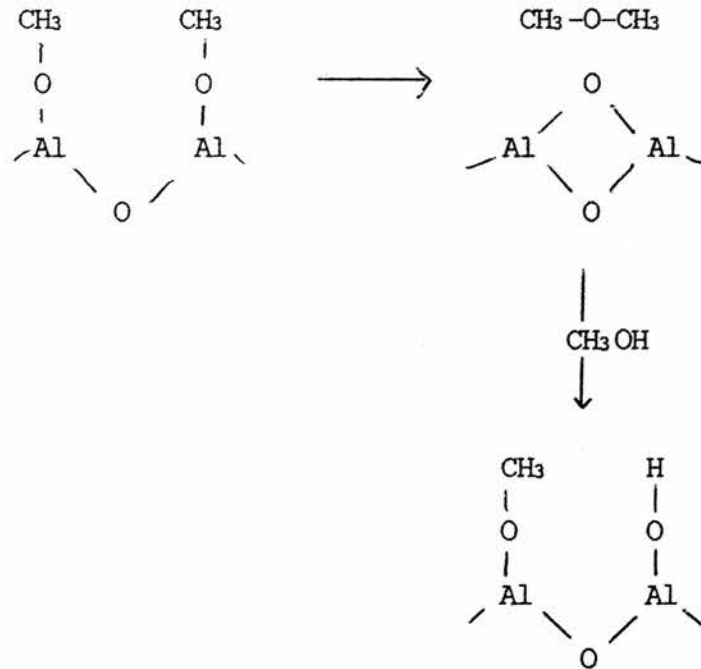
It was proposed that dimethyl ether was formed by combining two methoxy groups. ¹²⁷



The same mechanism could be proposed for the formation of dimethyl ether from chloromethane by combining two methoxy groups.

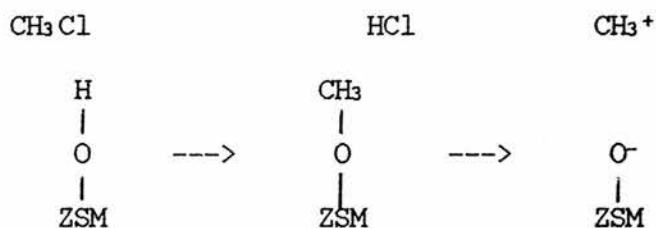
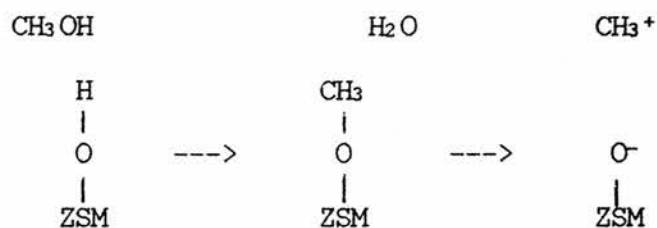


This mechanism could be applied to the reactions over ZSM-5 catalyst. However, this would deplete the surface oxygens of the catalyst. Methanol could replace the oxygens but chloromethane would not be able to replenish the oxygens, so this reaction would lead to depletion of the surface oxygens and to eventual collapse of the framework and loss of activity.



There is no indication that this loss of activity and structural collapse due to depletion of structural oxygens has been observed. It is known that chloromethane tends to deactivate the catalyst faster than methanol, but this is attributed to the larger amount of coking with chloromethane.¹⁹⁹ Furthermore, as dimethyl ether was not detected as a product when chloromethane was reacted over ZSM-5 catalyst - (see results in Chapter 5) - this mechanism can be ruled out.

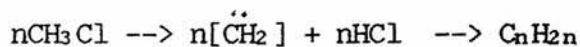
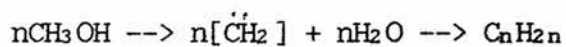
The mechanism proposed by Heiba and Landis which involved liberation of methyl cations from surface methoxy groups is viable for chloromethane. ¹²⁸



However, it has little support.

CARBENE MECHANISMS

Mechanisms involving the formation of carbenes are viable for chloromethane.



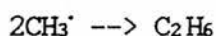
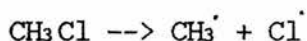
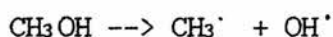
These mechanisms cannot be studied in a mass spectrometer.

FREE RADICAL MECHANISMS

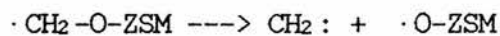
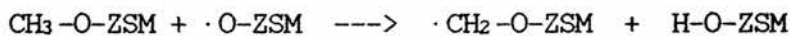
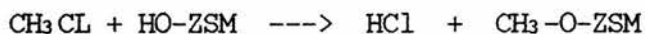
The free radical mechanisms proposed for methanol would apply equally well, if not better, to chloromethane.

FREE RADICAL COMBINATION

It has been proposed that the combination of free radicals could produce the C-C bond formation step. ¹⁴⁰

FREE RADICAL SCISSION TO CARBENES

It has also been proposed that a methyl radical could react with a surface oxygen and form a carbene. ¹⁴⁰



These mechanisms cannot be studied using a mass spectrometer.

CARBONIUM ION MECHANISM

The mechanisms that can be studied using a mass spectrometer are those involving carbonium ions. The species thought to be important in the reaction of methanol are protonated methanol, CH_3OH_2^+ , dimethyl ether CH_3OCH_3 , dimethyl oxonium ions $\text{CH}_3\text{OHCH}_3^+$ and trimethyl oxonium ions.

There is no analogue of dimethyl ether and trimethyl chloronium ions, but the analogues of the other species have been found in mass spectral studies. ^{182-192,194}

methanol species	chloromethane analogues
CH_3OH	CH_3Cl
$\begin{array}{c} + \text{H} \\ \\ \text{CH}_3 - \text{O} \\ \\ \text{H} \end{array}$	$\text{CH}_3 - \text{Cl} - \text{H}^+$
$\text{CH}_3 - \text{O} - \text{CH}_3$?
$(\text{CH}_3)_2 - \text{OH}^+$	$\text{CH}_3 - \text{Cl} - \text{CH}_3^+$
$\begin{array}{c} \text{CH}_3 \\ \\ \text{O}^+ \\ / \quad \backslash \\ \text{CH}_3 \quad \text{CH}_3 \end{array}$?

The experiments reported in this section were done with the following aims:

1. to study the reactions of chloromethane in the gas phase.
2. to produce at low pressure protonated chloromethane and dimethyl chloronium ions.
3. to identify the routes/mechanisms of formation of these ions.
4. to compare the reactions of fluoromethane, bromomethane and iodomethane.

RESULTS

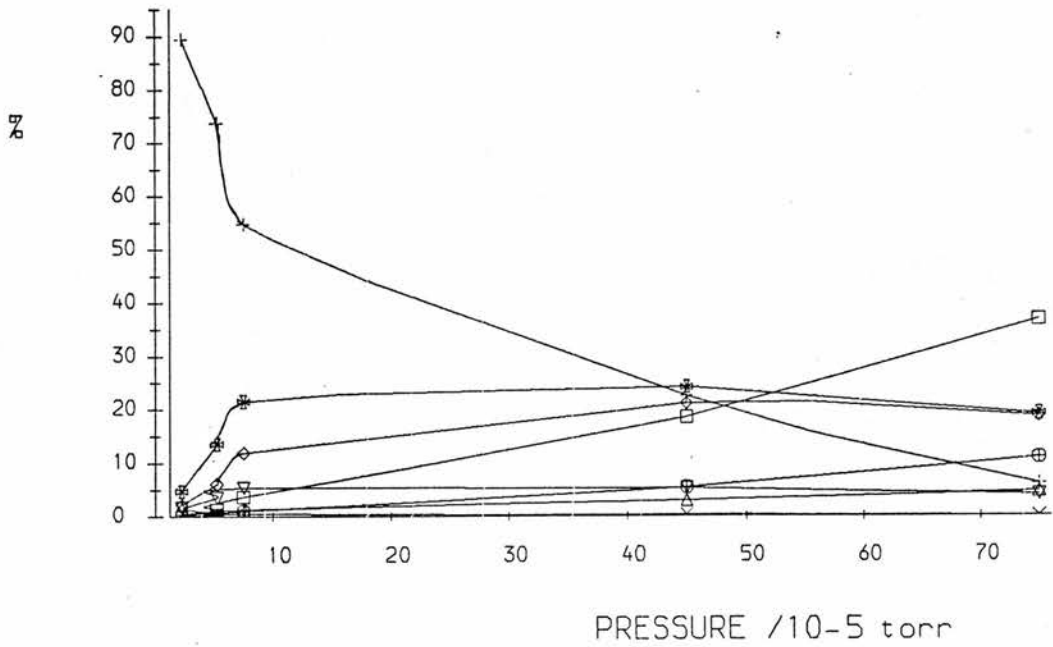
These results tables present the relative amount of each ion. The ions are represented by mass. The composition of each ion is discussed in the discussion.

<u>REACTION</u>	<u>PAGE</u>
Reaction of CH_2N^+ + CH_3Cl	234
Reaction of CDO^+ at two pressures	235 + 236
Reaction of CH_3^+ at 10^{-5} and 10^{-4} torr of CH_3Cl	237 + 238
Reaction of CD_3^+ at 10^{-7} and 10^{-6} torr of CD_3^+	239 + 240
Reaction of CH_3OH_2^+ + CH_3Cl	241
Reaction of CH_3OD_2^+ + CH_3Cl	242
Reaction of CH^{18}O^+ + CH_3F	244
Reaction of CH_2N^+ "	245
Reaction of CH_3^+ "	246 - 248
Reaction of CD_3^+ "	249 - 252
Reaction of CH_2F^+ + CH_3F to identify tertiary ions	253
Reaction of CH_2N^+ + CH_3Br	254
Reaction of CH_3^+ "	255
Reaction of CH_2N^+ + CH_3I	256 + 257
Reaction of CH_3^+ "	258 + 259
Reaction of CD_3^+ "	260 + 261
Reaction of C_2H_3^+ "	262 + 263
Reaction of C_2H_5^+ "	264
Reaction of $\text{CH}_3\text{Cl-H}^+$ + CH_3OCH_3	265

in the Quinqua Quadrupole Mass Spectrometer

CH₂N⁺ INTO CH₃CL

% SECONDARY ION FLUX Vs. PRESSURE



- + = 15 = CH₃⁺
- x = 16 = O⁺
- Δ = 32 = O₂⁺
- ◊ = 49 = CH₂⁺
- = 51 = CH₃⁺
- ∇ = 53 = C⁺
- ◻ = 65 = C₂⁺
- = 67 = C₂⁺

% SECONDARY ION FLUX

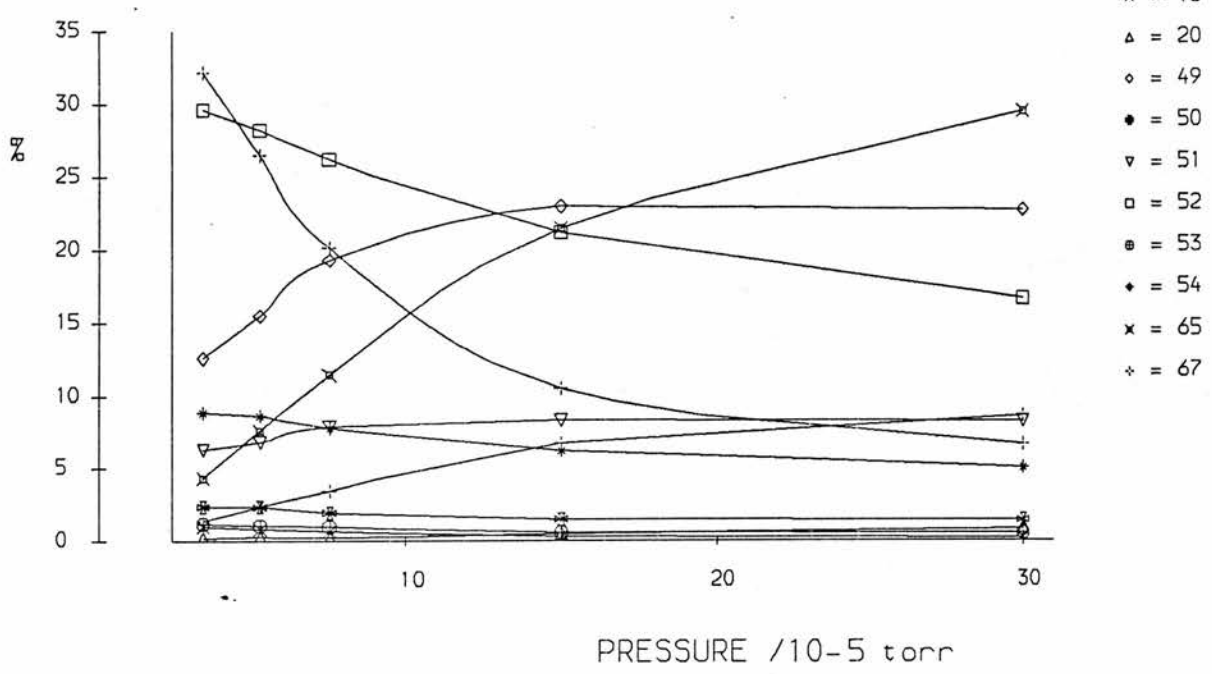
	PRESSURES In torr			m/e							
	INITIAL ION	ION	PENNING	15	16	32	49	51	53	65	67
	GAUGE	GAUGE	GAUGE								
(A)	7.5 × 10 ⁻⁷	3.0 × 10 ⁻⁶	2.3 × 10 ⁻⁵	89.42	0.53	1.59	2.12	4.76	1.59	0.00	0.00
(B)	7.5 × 10 ⁻⁷	6.0 × 10 ⁻⁶	5.3 × 10 ⁻⁵	73.73	0.78	0.39	6.11	13.65	3.64	1.30	0.30
(C)	7.5 × 10 ⁻⁷	7.5 × 10 ⁻⁶	7.5 × 10 ⁻⁵	54.73	0.44	1.26	11.91	21.52	5.40	3.70	1.00
(D)	7.5 × 10 ⁻⁷	2.3 × 10 ⁻⁵	4.5 × 10 ⁻⁴	22.47	0.22	2.98	21.02	24.15	5.22	18.52	5.40
(E)	7.5 × 10 ⁻⁷	4.5 × 10 ⁻⁵	7.5 × 10 ⁻⁴	6.03	0.00	4.57	18.64	19.08	4.02	36.73	10.90

% TOTAL ION FLUX

	PRESSURES In torr			m/e								
	INITIAL ION	ION	PENNING	15	16	28	32	49	51	53	65	67
	GAUGE	GAUGE	GAUGE									
	7.5 × 10 ⁻⁷	3.0 × 10 ⁻⁶	2.3 × 10 ⁻⁵	1.69	0.01	98.11	0.03	0.04	0.09	0.03	0.00	0.00
	7.5 × 10 ⁻⁷	6.0 × 10 ⁻⁶	5.3 × 10 ⁻⁵	5.67	0.06	92.31	0.03	0.47	1.05	0.28	0.10	0.03
	7.5 × 10 ⁻⁷	7.5 × 10 ⁻⁶	7.5 × 10 ⁻⁵	7.40	0.06	86.48	0.17	1.61	2.91	0.73	0.50	0.14
	7.5 × 10 ⁻⁷	2.3 × 10 ⁻⁵	4.5 × 10 ⁻⁴	6.03	0.06	73.17	0.80	5.64	6.48	1.40	4.97	1.45
	7.5 × 10 ⁻⁷	4.5 × 10 ⁻⁵	7.5 × 10 ⁻⁴	2.31	0.00	61.69	1.75	7.14	7.31	1.54	14.07	4.19

CDO+ INTO CH3Cl

% SECONDARY ION FLUX Vs. PRESSURE



% SECONDARY ION FLUX

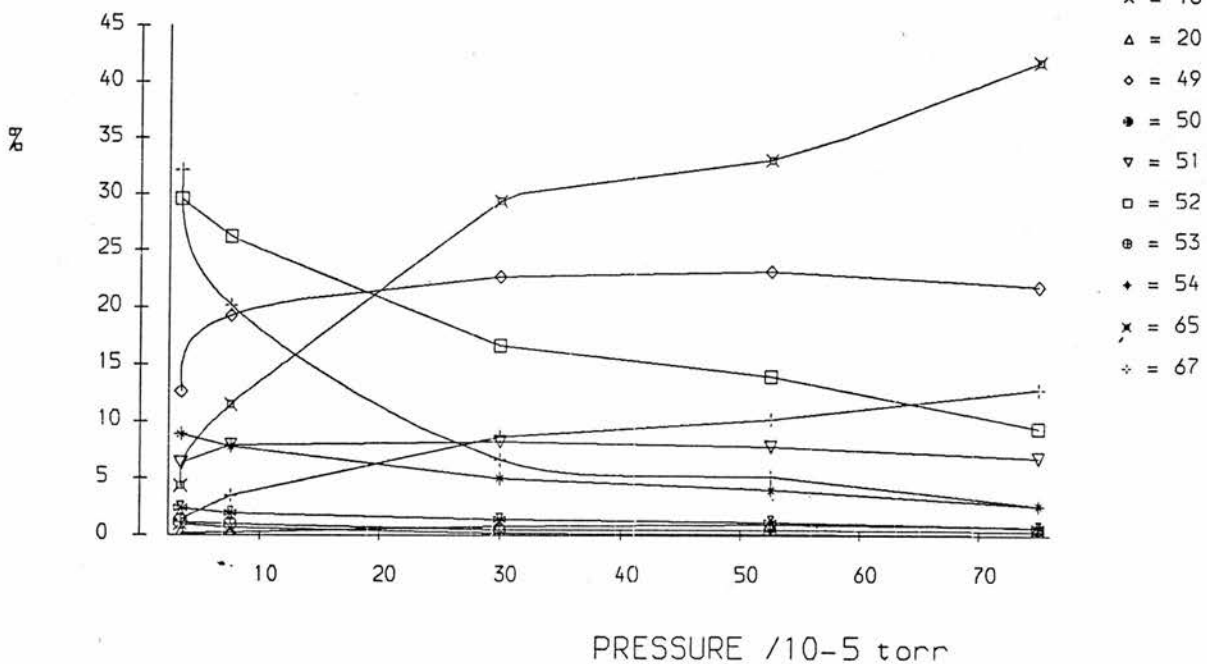
PRESSURES in torr			m/e											
INITIAL ION GAUGE	ION GAUGE	PENNING GAUGE	15	16	20	49	50	51	52	53	54	65	67	
(A)	7.5×10^{-7}	3.0×10^{-6}	3.4×10^{-5}	32.15	0.99	0.20	12.62	2.37	6.31	29.59	1.18	8.88	4.34	1.38
(B)	7.5×10^{-7}	4.5×10^{-6}	5.3×10^{-5}	26.47	0.79	0.26	15.47	2.36	6.82	28.18	1.05	8.65	7.60	2.36
(C)	7.5×10^{-7}	6.0×10^{-6}	7.5×10^{-5}	20.13	0.65	0.22	19.26	1.95	7.90	26.19	0.97	7.79	11.47	3.46
(D)	7.5×10^{-7}	1.1×10^{-5}	1.5×10^{-4}	10.53	0.28	0.46	22.90	1.48	8.31	21.14	0.55	6.19	21.42	6.74
(E)	7.5×10^{-7}	1.5×10^{-5}	3.0×10^{-4}	6.61	0.20	0.80	22.65	1.40	8.22	16.63	0.50	5.01	29.36	8.62

% TOTAL ION FLUX

PRESSURES in torr			m/e											
INITIAL ION GAUGE	ION GAUGE	PENNING GAUGE	15	16	20	30	49	50	51	52	53	54	65	67
7.5×10^{-7}	3.0×10^{-6}	3.4×10^{-5}	1.42	0.04	0.01	95.59	0.56	0.10	0.28	1.30	0.05	0.39	0.19	0.00
7.5×10^{-7}	4.5×10^{-6}	5.3×10^{-5}	2.03	0.06	0.02	92.34	1.18	0.18	0.52	2.16	0.08	0.66	0.58	0.18
7.5×10^{-7}	6.0×10^{-6}	7.5×10^{-5}	2.39	0.08	0.03	88.14	2.28	0.23	0.94	3.11	0.12	0.92	1.36	0.41
7.5×10^{-7}	1.1×10^{-5}	1.5×10^{-4}	2.70	0.07	0.12	74.31	5.88	0.38	2.13	5.43	0.14	1.59	5.50	1.73
7.5×10^{-7}	1.5×10^{-5}	3.0×10^{-4}	2.66	0.08	0.32	59.73	9.12	0.56	3.31	6.70	0.20	2.02	11.82	3.47

CDO+ INTO CH3CL

% SECONDARY ION FLUX Vs. PRESSURE



% SECONDARY ION FLUX

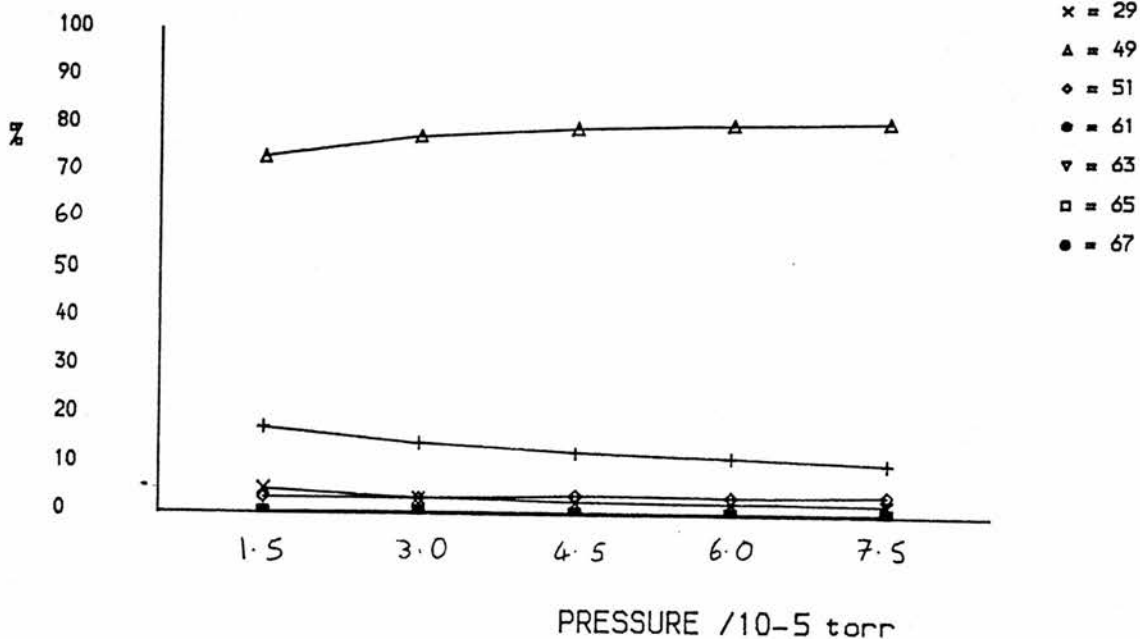
PRESSURES in torr			m/e											
INITIAL ION GAUGE	ION GAUGE	PENNING GAUGE	15	16	20	49	50	51	52	53	54	65	67	
(A)	7.5x10 ⁻⁷	3.0x10 ⁻⁶	3.4x10 ⁻⁵	32.15	0.99	0.20	12.62	2.37	6.31	29.59	1.18	8.88	4.34	1.36
(B)	7.5x10 ⁻⁷	6.0x10 ⁻⁶	7.5x10 ⁻⁵	20.13	0.65	0.22	19.26	1.95	7.90	26.19	0.97	7.79	11.47	3.46
(C)	7.5x10 ⁻⁷	1.5x10 ⁻⁵	3.0x10 ⁻⁴	6.61	0.20	0.80	22.65	1.40	8.22	16.63	0.50	5.01	29.36	8.62
(D)	7.5x10 ⁻⁷	1.5x10 ⁻⁵	5.3x10 ⁻⁴	5.19	0.12	0.94	23.14	1.18	7.79	13.93	0.47	4.01	33.06	10.15
(E)	7.5x10 ⁻⁷	2.3x10 ⁻⁵	7.5x10 ⁻⁴	2.64	0.00	0.75	21.89	0.75	6.79	9.43	0.38	2.64	41.89	12.83

% TOTAL ION FLUX

PRESSURES in torr			m/e												
INITIAL ION GAUGE	ION GAUGE	PENNING GAUGE	15	16	20	30	49	50	51	52	53	54	65	67	
7.5x10 ⁻⁷	3.0x10 ⁻⁶	3.4x10 ⁻⁵	1.42	0.04	0.01	95.59	0.56	0.10	0.28	1.30	0.05	0.39	0.19	0.01	
7.5x10 ⁻⁷	6.0x10 ⁻⁶	7.5x10 ⁻⁵	2.39	0.08	0.03	88.14	2.28	0.23	0.94	3.11	0.12	0.92	1.36	0.01	
7.5x10 ⁻⁷	1.5x10 ⁻⁵	3.0x10 ⁻⁴	2.66	0.08	0.32	59.73	9.12	0.56	3.31	6.70	0.20	2.02	11.82	3.01	
7.5x10 ⁻⁷	1.5x10 ⁻⁵	5.3x10 ⁻⁴	2.58	0.06	0.47	50.38	11.48	0.59	3.87	6.91	0.23	1.99	16.40	5.01	
7.5x10 ⁻⁷	2.3x10 ⁻⁵	7.5x10 ⁻⁴	1.97	0.00	0.56	25.35	16.34	0.56	5.07	7.04	0.28	1.97	31.27	9.01	

CH₃⁺ INTO CH₃CL (1)

% SECONDARY ION FLUX Vs. PRESSURE



% SECONDARY ION FLUX

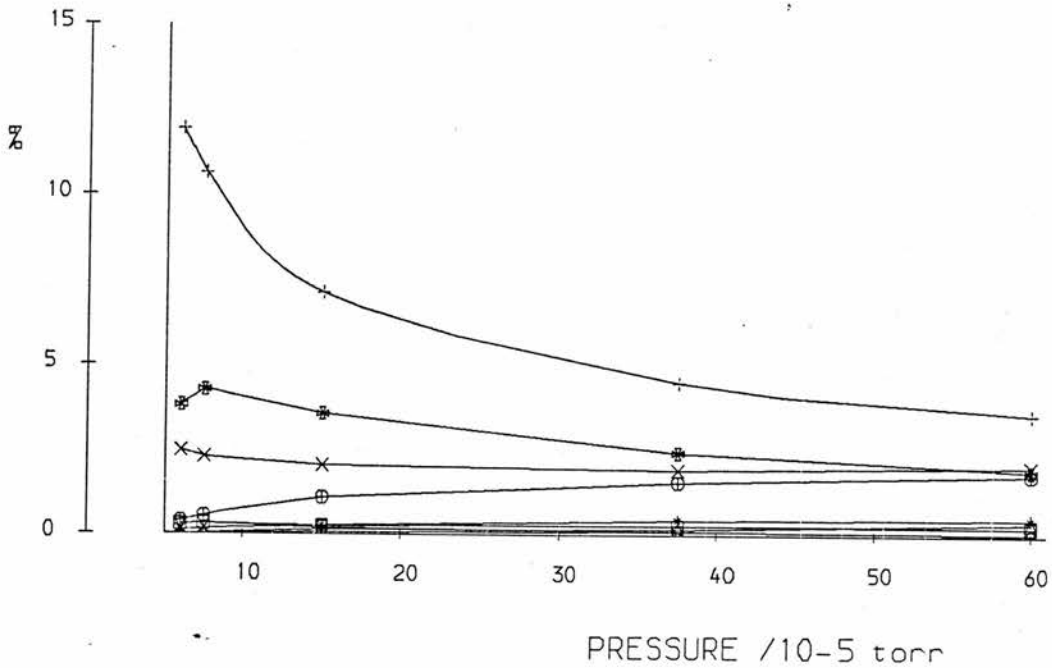
PRESSURES In torr			m/e							
INITIAL ION GAUGE	ION GAUGE	PENNING GAUGE	27	29	49	51	61	63	65	67
(A) 7.5x10 ⁻⁷	1.5x10 ⁻⁶	1.5x10 ⁻⁵	17.72	5.06	73.42	3.38	0.21	0.21	0.00	0.00
(B) 7.5x10 ⁻⁷	2.3x10 ⁻⁶	3.0x10 ⁻⁵	14.60	3.25	77.89	3.25	0.41	0.41	0.20	0.00
(C) 7.5x10 ⁻⁷	3.0x10 ⁻⁶	4.5x10 ⁻⁵	12.84	2.47	79.87	3.95	0.37	0.25	0.25	0.00
(D) 7.5x10 ⁻⁷	4.5x10 ⁻⁶	6.0x10 ⁻⁵	11.93	2.46	80.78	3.79	0.28	0.28	0.38	0.09
(E) 7.5x10 ⁻⁷	5.3x10 ⁻⁵	7.5x10 ⁻⁵	10.64	2.28	81.54	4.25	0.30	0.30	0.53	0.15

% TOTAL ION FLUX

PRESSURES In torr			m/e								
INITIAL ION GAUGE	ION GAUGE	PENNING GAUGE	15	27	29	49	51	61	63	65	67
7.5x10 ⁻⁷	1.5x10 ⁻⁶	1.5x10 ⁻⁵	99.68	0.06	0.02	0.23	0.01	0.00	0.00	0.00	0.00
7.5x10 ⁻⁷	2.3x10 ⁻⁶	3.0x10 ⁻⁵	99.27	0.11	0.02	0.57	0.02	0.00	0.00	0.00	0.00
7.5x10 ⁻⁷	3.0x10 ⁻⁶	4.5x10 ⁻⁵	98.61	0.18	0.03	1.11	0.06	0.01	0.00	0.00	0.00
7.5x10 ⁻⁷	4.5x10 ⁻⁶	6.0x10 ⁻⁵	97.76	0.27	0.06	1.81	0.09	0.01	0.01	0.01	0.00
7.5x10 ⁻⁷	5.3x10 ⁻⁵	7.5x10 ⁻⁵	96.71	0.35	0.08	2.68	0.14	0.01	0.01	0.02	0.01

CH₃⁺ INTO CH₃Cl (2)

% SECONDARY ION FLUX Vs. PRESSURE



- + = 27
- x = 29
- △ = 39
- ◊ = 41
- = 51
- ▼ = 62
- = 63
- = 65
- ◆ = 67

% SECONDARY ION FLUX

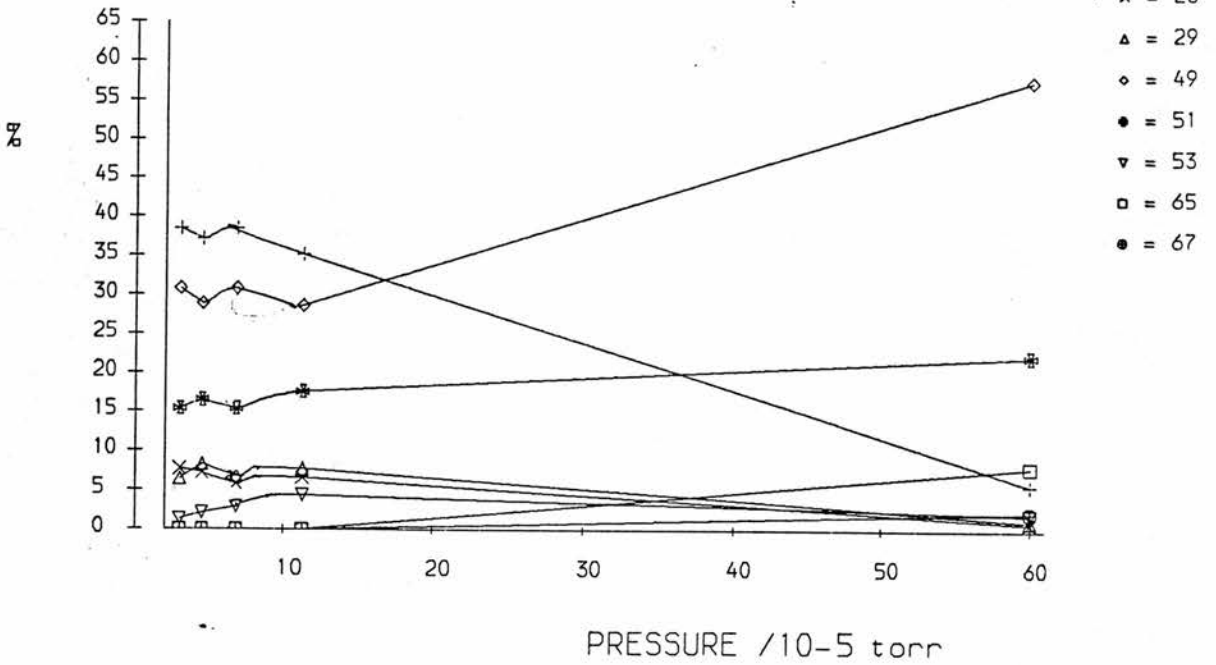
PRESSURES in torr			m/e										
INITIAL ION GAUGE	ION GAUGE	PENNING GAUGE	27	29	39	41	49	51	62	63	65	67	
(A)	7.5x10 ⁻⁷	4.5x10 ⁻⁶	6.0x10 ⁻⁵	11.93	2.46	0.00	0.00	80.78	3.79	0.28	0.28	0.38	0.00
(B)	7.5x10 ⁻⁷	5.3x10 ⁻⁵	7.5x10 ⁻⁵	10.64	2.28	0.00	0.00	81.54	4.25	0.30	0.30	0.53	0.00
(C)	7.5x10 ⁻⁷	7.5x10 ⁻⁶	1.5x10 ⁻⁴	7.10	2.03	0.13	0.06	85.36	3.55	0.19	0.25	1.08	0.00
(D)	7.5x10 ⁻⁷	1.5x10 ⁻⁵	3.8x10 ⁻⁴	4.49	1.90	0.17	0.09	88.61	2.42	0.09	0.26	1.55	0.00
(E)	7.5x10 ⁻⁷	2.3x10 ⁻⁵	6.0x10 ⁻⁴	3.57	2.02	0.36	0.06	89.54	1.90	0.06	0.24	1.78	0.00

% TOTAL ION FLUX

PRESSURES in torr			m/e										
INITIAL ION GAUGE	ION GAUGE	PENNING GAUGE	15	27	29	39	41	49	51	62	63	65	67
7.5x10 ⁻⁷	4.5x10 ⁻⁶	6.0x10 ⁻⁵	97.76	0.27	0.06	0.00	0.00	1.81	0.09	0.01	0.01	0.01	0.00
7.5x10 ⁻⁷	5.3x10 ⁻⁵	7.5x10 ⁻⁵	96.71	0.35	0.08	0.00	0.00	2.68	0.14	0.01	0.01	0.02	0.00
7.5x10 ⁻⁷	7.5x10 ⁻⁶	1.5x10 ⁻⁴	92.91	0.50	0.14	0.01	0.00	6.05	0.25	0.01	0.02	0.08	0.00
7.5x10 ⁻⁷	1.5x10 ⁻⁵	3.8x10 ⁻⁴	85.44	0.65	0.28	0.03	0.01	12.90	0.35	0.01	0.04	0.23	0.00
7.5x10 ⁻⁷	2.3x10 ⁻⁵	6.0x10 ⁻⁴	83.95	0.57	0.32	0.06	0.01	14.37	0.31	0.01	0.04	0.29	0.00

CO₃⁺ INTO CH₃Cl

% SECONDARY ION FLUX Vs. PRESSURE



% SECONDARY ION FLUX

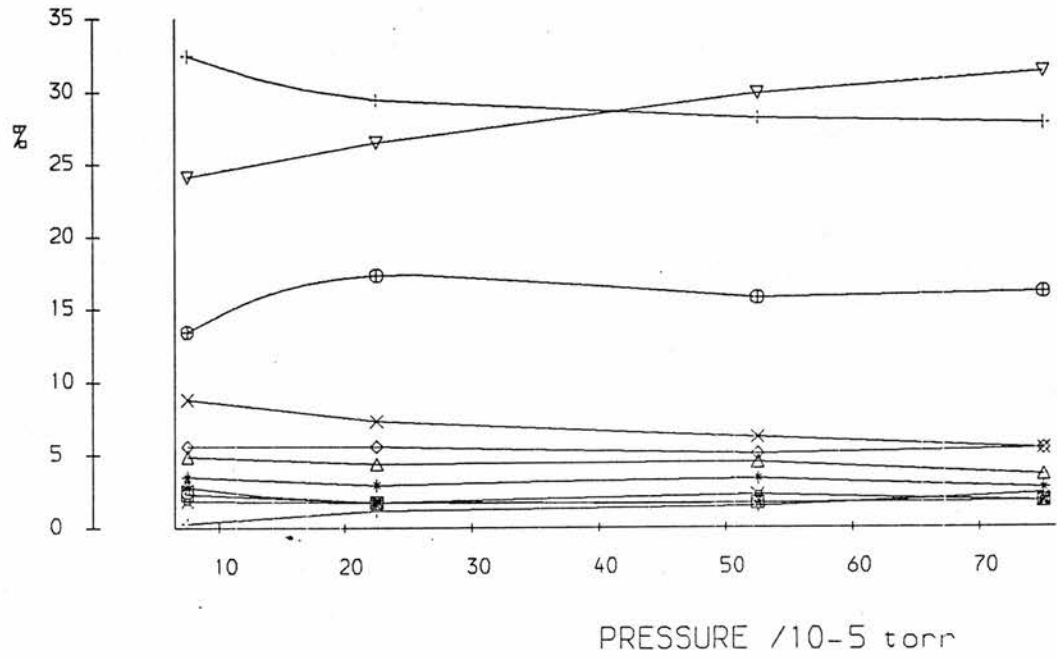
	PRESSURES in torr			m/e							
	INITIAL ION	ION	PENNING								
	GAUGE	GAUGE	GAUGE	15	28	29	49	51	53	65	67
(A)	7.5×10 ⁻⁷	1.5×10 ⁻⁶	3.0×10 ⁻⁵	38.46	7.69	6.41	30.77	15.38	1.28	0.00	0.00
(B)	7.5×10 ⁻⁷	3.0×10 ⁻⁶	4.5×10 ⁻⁵	37.11	7.22	8.25	28.87	16.49	2.06	0.00	0.00
(C)	7.5×10 ⁻⁷	4.5×10 ⁻⁶	6.8×10 ⁻⁵	38.46	5.77	6.73	30.77	15.38	2.88	0.00	0.00
(D)	7.5×10 ⁻⁷	7.5×10 ⁻⁶	1.1×10 ⁻⁴	35.16	6.59	7.69	28.57	17.58	4.40	0.00	0.00
(E)	7.5×10 ⁻⁷	6.0×10 ⁻⁵	6.0×10 ⁻⁴	5.71	0.86	1.14	57.71	22.29	2.00	8.00	2.29

% TOTAL ION FLUX

	PRESSURES in torr			m/e								
	INITIAL ION	ION	PENNING									
	GAUGE	GAUGE	GAUGE	15	18	28	29	49	51	53	65	67
	7.5×10 ⁻⁷	1.5×10 ⁻⁶	3.0×10 ⁻⁵	0.37	99.03	0.07	0.06	0.30	0.15	0.01	0.00	0.00
	7.5×10 ⁻⁷	3.0×10 ⁻⁶	4.5×10 ⁻⁵	0.53	98.57	0.10	0.12	0.41	0.24	0.03	0.00	0.00
	7.5×10 ⁻⁷	4.5×10 ⁻⁶	6.8×10 ⁻⁵	1.04	97.31	0.16	0.18	0.83	0.41	0.08	0.00	0.00
	7.5×10 ⁻⁷	7.5×10 ⁻⁶	1.1×10 ⁻⁴	0.02	99.95	0.00	0.00	0.01	0.01	0.00	0.00	0.00
	7.5×10 ⁻⁷	6.0×10 ⁻⁵	6.0×10 ⁻⁴	4.20	26.47	0.63	0.84	42.44	16.39	1.47	5.88	1.68

CD3+ INTO CH3CL

% SECONDARY ION FLUX V. PRESSURE



- + = 15
- x = 16
- Δ = 28
- ◊ = 29
- = 34
- ▽ = 49
- = 50
- ⊕ = 51
- ⊙ = 52
- × = 53
- ⋄ = 65

% SECONDARY ION FLUX

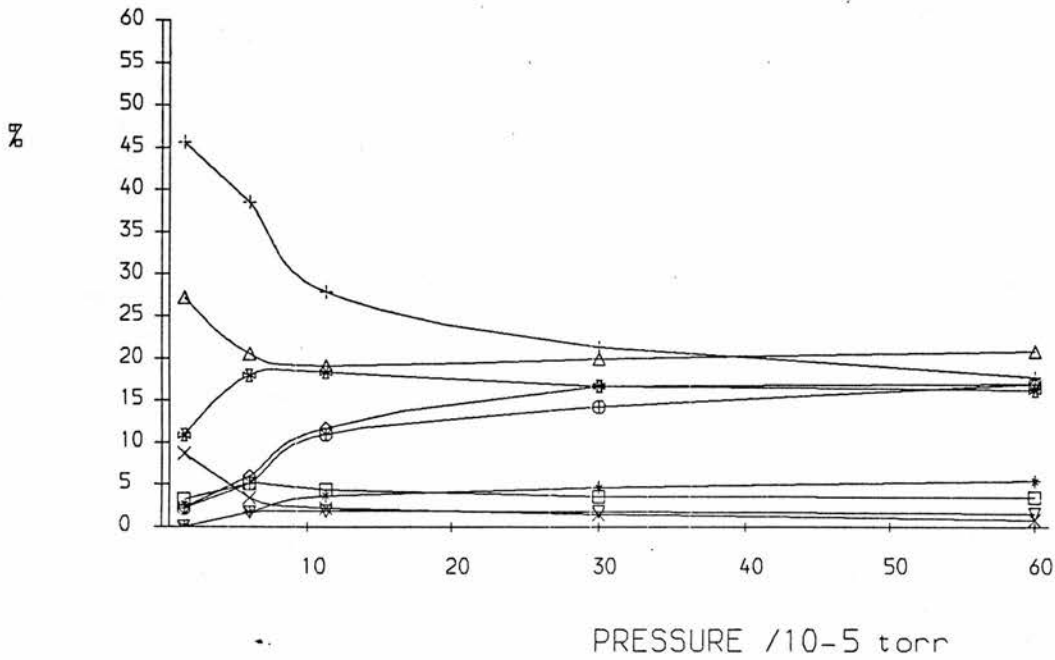
PRESSURES in torr			m/e											
INITIAL ION GAUGE	ION GAUGE	PENNING GAUGE	15	16	28	29	34	49	50	51	52	53	65	
(A)	7.5x10 ⁻⁶	1.1x10 ⁻⁵	7.5x10 ⁻⁵	32.47	8.81	4.87	5.57	2.78	24.12	2.32	13.45	3.48	1.86	0.16
(B)	7.5x10 ⁻⁶	1.5x10 ⁻⁵	2.3x10 ⁻⁴	29.41	7.35	4.41	5.59	1.76	26.47	1.76	17.35	2.94	1.76	1.16
(C)	7.5x10 ⁻⁶	1.9x10 ⁻⁵	5.3x10 ⁻⁴	28.15	6.19	4.50	5.07	1.69	29.84	1.69	15.77	3.38	2.25	1.16
(D)	7.5x10 ⁻⁶	2.3x10 ⁻⁵	7.5x10 ⁻⁴	27.78	5.38	3.58	5.38	1.79	31.36	1.79	16.13	2.69	1.79	2.16

% TOTAL ION FLUX

PRESSURES in torr			m/e											
INITIAL ION GAUGE	ION GAUGE	PENNING GAUGE	15	16	18	28	29	34	49	50	51	52	53	65
7.5x10 ⁻⁶	1.1x10 ⁻⁵	7.5x10 ⁻⁵	1.09	0.30	96.64	0.16	0.19	0.09	0.81	0.08	0.45	0.12	0.06	0.16
7.5x10 ⁻⁶	1.5x10 ⁻⁵	2.3x10 ⁻⁴	1.83	0.46	93.79	0.27	0.35	0.11	1.64	0.11	1.08	0.18	0.11	0.16
7.5x10 ⁻⁶	1.9x10 ⁻⁵	5.3x10 ⁻⁴	2.07	0.46	92.63	0.33	0.37	0.12	2.20	0.12	1.16	0.25	0.17	0.16
7.5x10 ⁻⁶	2.3x10 ⁻⁵	7.5x10 ⁻⁴	2.46	0.48	91.15	0.32	0.48	0.16	2.77	0.16	1.43	0.24	0.16	0.16

CH₃OH₂⁺ INTO CH₃Cl

% SECONDARY ION FLUX Vs. PRESSURE



% SECONDARY ION FLUX

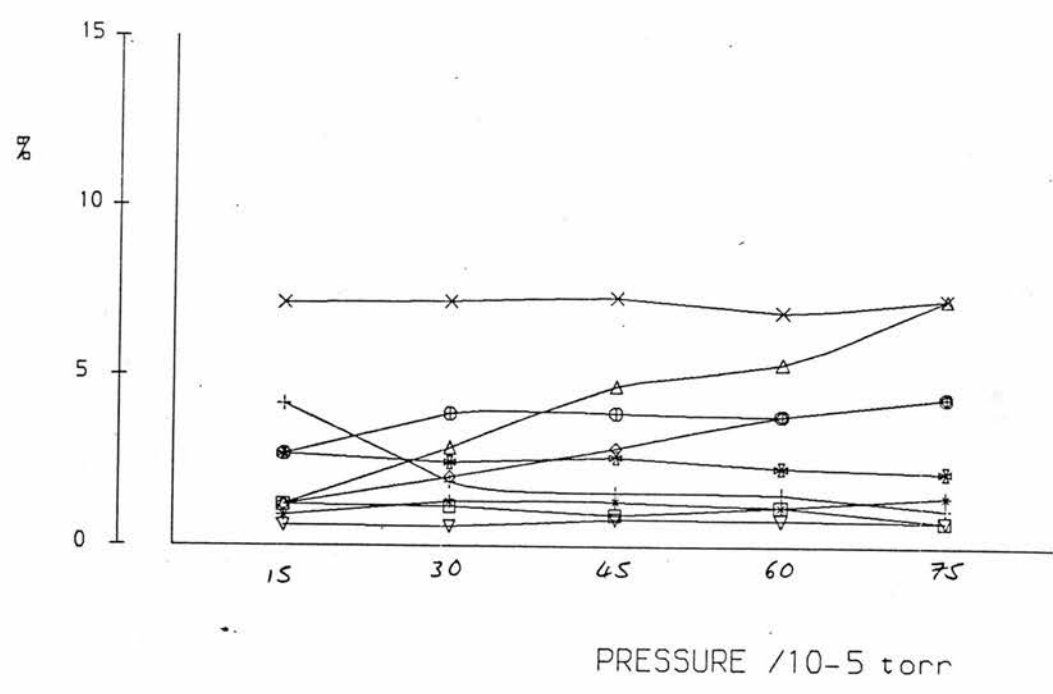
PRESSURES In torr			m/e									
INITIAL ION GAUGE	ION GAUGE	PENNING GAUGE	15	29	34	49	51	52	53	65	67	
(A)	7.5x10 ⁻⁷	4.5x10 ⁻⁶	1.5x10 ⁻⁵	45.65	8.70	27.17	2.17	10.87	0.00	3.26	2.17	0.00
(B)	7.5x10 ⁻⁷	7.5x10 ⁻⁶	6.0x10 ⁻⁵	38.46	3.42	20.51	5.98	17.95	1.71	5.13	5.13	1.71
(C)	7.5x10 ⁻⁷	1.1x10 ⁻⁵	1.1x10 ⁻⁴	27.84	2.20	19.05	11.72	18.32	1.83	4.40	10.99	3.66
(D)	7.5x10 ⁻⁷	1.5x10 ⁻⁵	3.0x10 ⁻⁴	21.28	1.42	19.86	16.67	16.67	1.77	3.55	14.18	4.61
(E)	7.5x10 ⁻⁷	1.5x10 ⁻⁵	6.0x10 ⁻⁴	17.76	0.77	20.85	16.99	16.22	1.54	3.47	16.99	5.41

% TOTAL ION FLUX

PRESSURES In torr			m/e									
INITIAL ION GAUGE	ION GAUGE	PENNING GAUGE	15	29	33	34	49	51	52	53	65	67
7.5x10 ⁻⁷	4.5x10 ⁻⁶	1.5x10 ⁻⁵	0.32	0.06	99.30	0.19	0.02	0.08	0.00	0.02	0.02	0.00
7.5x10 ⁻⁷	7.5x10 ⁻⁶	6.0x10 ⁻⁵	1.11	0.10	97.11	0.59	0.17	0.52	0.05	0.15	0.15	0.05
7.5x10 ⁻⁷	1.1x10 ⁻⁵	1.1x10 ⁻⁴	1.58	0.12	94.32	1.08	0.67	1.04	0.10	0.25	0.62	0.21
7.5x10 ⁻⁷	1.5x10 ⁻⁵	3.0x10 ⁻⁴	2.25	0.15	89.41	2.10	1.77	1.77	0.19	0.38	1.50	0.49
7.5x10 ⁻⁷	1.5x10 ⁻⁵	6.0x10 ⁻⁴	2.40	0.10	86.50	2.81	2.29	2.19	0.21	0.47	2.29	0.73

CD3OD2+ Into CH3Cl

% SECONDARY ION FLUX Vs. PRESSURE



% SECONDARY ION FLUX

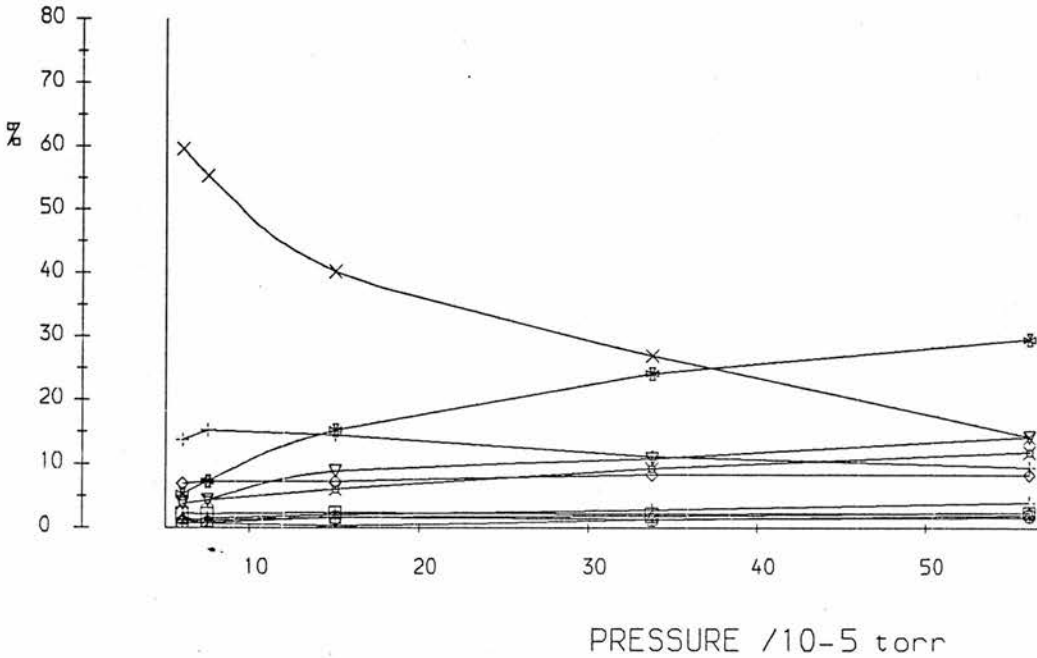
	PRESSURES in torr			m/e										
	INITIAL ION	ION	PENNING											
	GAUGE	GAUGE	GAUGE	15	18	34	36	49	51	52	53	54	68	70
(A)	7.5x10 ⁻⁶	7.5x10 ⁻⁶	1.5x10 ⁻⁵	7.12	71.22	4.15	7.12	1.19	1.19	2.67	0.59	1.19	2.67	0.8
(B)	7.5x10 ⁻⁶	7.5x10 ⁻⁶	3.0x10 ⁻⁵	12.32	64.47	1.86	7.16	2.87	2.01	2.44	0.57	1.15	3.87	1.2
(C)	7.5x10 ⁻⁶	7.5x10 ⁻⁶	4.5x10 ⁻⁵	13.26	60.86	1.56	7.28	4.68	2.86	2.60	0.78	0.91	3.90	1.3
(D)	7.5x10 ⁻⁶	7.5x10 ⁻⁶	6.0x10 ⁻⁵	13.74	59.54	1.53	6.87	5.34	3.82	2.29	0.76	1.15	3.82	1.1
(E)	7.5x10 ⁻⁶	1.1x10 ⁻⁵	7.5x10 ⁻⁵	15.27	55.27	1.09	7.27	7.27	4.36	2.18	0.73	0.73	4.36	1.4

% TOTAL ION FLUX

	PRESSURES in torr			m/e											
	INITIAL ION	ION	PENNING												
	GAUGE	GAUGE	GAUGE	15	18	34	36	38	49	51	52	53	54	68	70
	7.5x10 ⁻⁶	7.5x10 ⁻⁶	1.5x10 ⁻⁵	0.07	0.73	0.04	0.07	98.97	0.01	0.01	0.03	0.01	0.01	0.03	0.0
	7.5x10 ⁻⁶	7.5x10 ⁻⁶	3.0x10 ⁻⁵	0.28	1.47	0.04	0.16	97.73	0.07	0.05	0.06	0.01	0.03	0.09	0.0
	7.5x10 ⁻⁶	7.5x10 ⁻⁶	4.5x10 ⁻⁵	0.38	1.76	0.05	0.21	97.11	0.14	0.08	0.08	0.02	0.03	0.11	0.0
	7.5x10 ⁻⁶	7.5x10 ⁻⁶	6.0x10 ⁻⁵	0.50	2.17	0.06	0.25	96.36	0.19	0.14	0.08	0.03	0.04	0.14	0.0
	7.5x10 ⁻⁶	1.1x10 ⁻⁵	7.5x10 ⁻⁵	0.66	2.37	0.05	0.31	95.71	0.31	0.19	0.09	0.03	0.03	0.19	0.0

CD3002+ into CH3Cl

% SECONDARY ION FLUX Vs. PRESSURE



- + = 15 = CH₃⁺
- x = 18 = CO₃⁺
- Δ = 34 = CD₃O⁺
- ◊ = 36 = CD₃OO
- = 49 } CH₂Cl
- ∇ = 51 } CHCl
- ◻ = 52 } CH₃Cl
- ⊙ = 53 } CH₃Cl
- + = 54 = CH₃⁺
- x = 68 = CO₃Cl
- ◊ = 70 = CO₃Cl

% SECONDARY ION FLUX

	PRESSURES In torr			m/e										
	INITIAL ION	ION	PENNING	15	18	34	36	49	51	52	53	54	68	
	GAUGE	GAUGE	GAUGE											
(A)	7.5×10 ⁻⁶	7.5×10 ⁻⁶	6.0×10 ⁻⁵	13.74	59.54	1.53	6.87	5.34	3.82	2.29	0.76	1.15	3.82	1.
(B)	7.5×10 ⁻⁶	1.1×10 ⁻⁵	7.5×10 ⁻⁵	15.27	55.27	1.09	7.27	7.27	4.36	2.18	0.73	0.73	4.36	1.
(C)	7.5×10 ⁻⁶	1.5×10 ⁻⁵	1.5×10 ⁻⁴	14.48	40.21	1.61	7.24	15.28	8.85	2.41	1.61	0.27	6.03	2.
(D)	7.5×10 ⁻⁶	1.9×10 ⁻⁵	3.4×10 ⁻⁴	11.15	26.93	1.86	8.36	24.15	10.84	2.17	1.24	1.24	9.29	2.
(E)	7.5×10 ⁻⁶	2.3×10 ⁻⁵	5.6×10 ⁻⁴	9.49	14.23	2.37	8.30	29.64	14.23	2.37	1.98	1.58	11.86	3.

% TOTAL ION FLUX

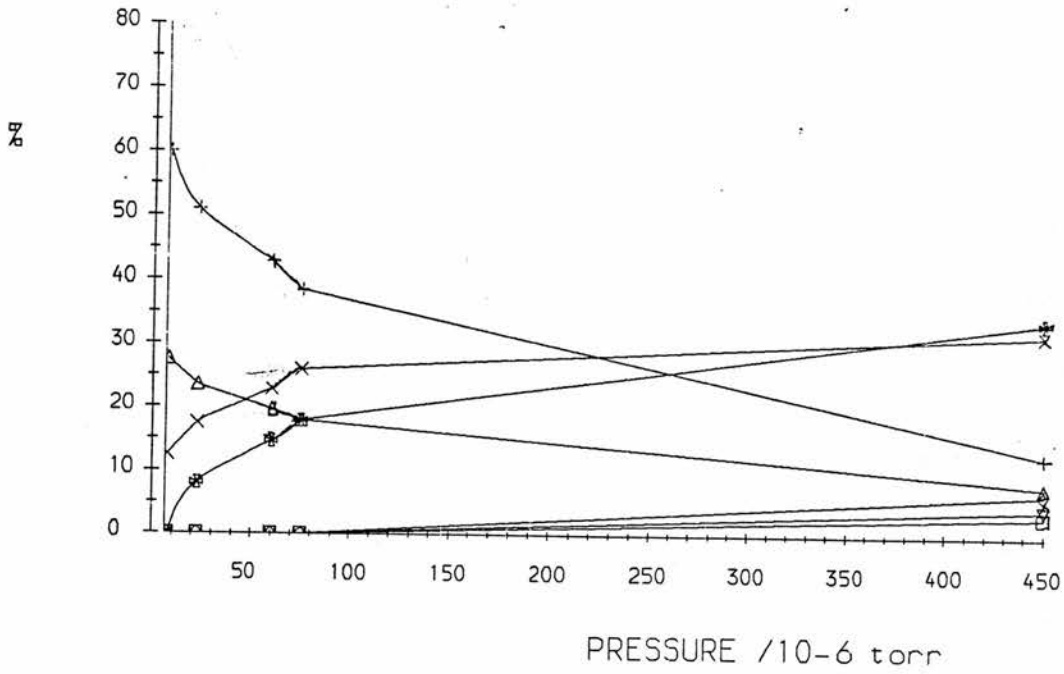
	PRESSURES In torr			m/e											
	INITIAL ION	ION	PENNING	15	18	34	36	38	49	51	52	53	54	68	
	GAUGE	GAUGE	GAUGE												
	7.5×10 ⁻⁶	7.5×10 ⁻⁶	6.0×10 ⁻⁵	0.50	2.17	0.06	0.25	96.36	0.19	0.14	0.08	0.03	0.04	0.14	0.
	7.5×10 ⁻⁶	1.1×10 ⁻⁵	7.5×10 ⁻⁵	0.66	2.37	0.05	0.31	95.71	0.31	0.19	0.09	0.03	0.03	0.19	0.
	7.5×10 ⁻⁶	1.5×10 ⁻⁵	1.5×10 ⁻⁴	1.16	3.21	0.13	0.58	92.02	1.22	0.71	0.19	0.13	0.02	0.48	0.
	7.5×10 ⁻⁶	1.9×10 ⁻⁵	3.4×10 ⁻⁴	1.19	2.88	0.20	0.89	89.32	2.58	1.16	0.23	0.13	0.13	0.99	0.
	7.5×10 ⁻⁶	2.3×10 ⁻⁵	5.6×10 ⁻⁴	1.37	2.05	0.34	1.20	85.57	4.28	2.05	0.34	0.29	0.23	1.71	0.

CH180+ INTO CH3F

244

% SECONDARY ION FLUX Vs. PRESSURE

- + = 15
- x = 33
- △ = 35
- = 45
- = 49
- ▽ = 51
- = 61



% SECONDARY ION FLUX

PRESSURES In torr			m/e							
INITIAL ION GAUGE	ION GAUGE	PENNING GAUGE	15	33	35	45	49	51	61	
(A)	7.5×10^{-7}	1.1×10^{-6}	7.5×10^{-6}	60.00	12.50	27.50	0.00	0.00	0.00	0.00
(B)	7.5×10^{-7}	1.9×10^{-6}	2.3×10^{-5}	51.01	17.45	23.49	0.00	8.05	0.00	0.00
(C)	7.5×10^{-7}	2.6×10^{-6}	6.0×10^{-5}	42.86	22.79	19.73	0.00	14.63	0.00	0.00
(D)	7.5×10^{-7}	3.0×10^{-6}	7.5×10^{-5}	38.40	25.87	17.87	0.00	17.87	0.00	0.00
(E)	7.5×10^{-7}	7.5×10^{-6}	4.5×10^{-4}	12.54	31.75	7.86	6.68	33.72	4.32	3.14

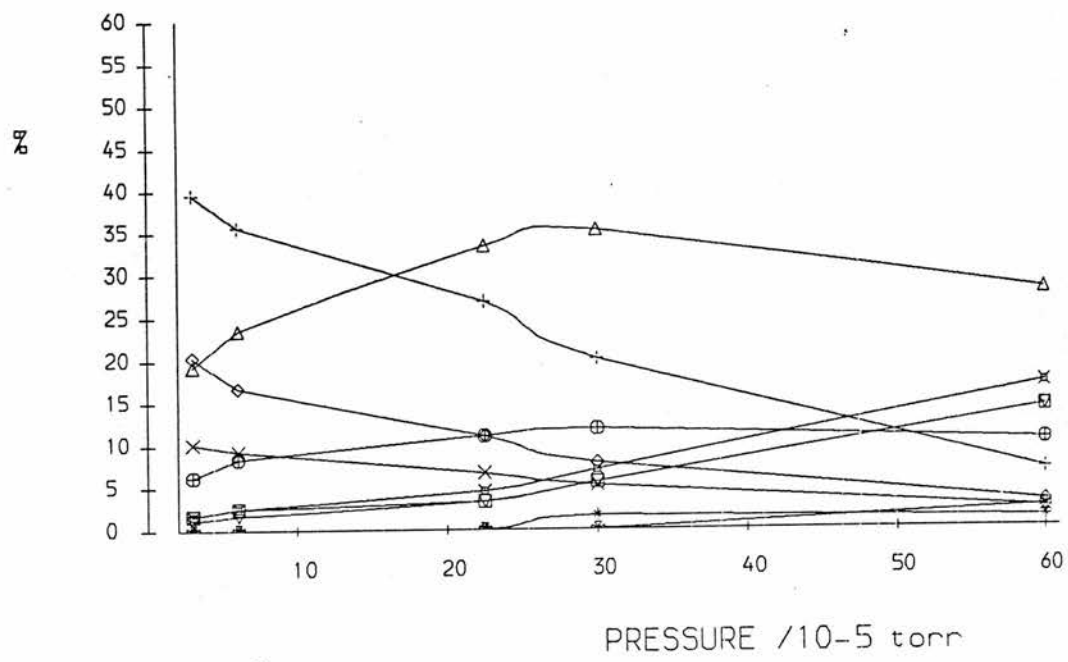
% TOTAL ION FLUX

PRESSURES In torr			m/e							
INITIAL ION GAUGE	ION GAUGE	PENNING GAUGE	15	31	33	35	45	49	51	61
7.5×10^{-7}	1.1×10^{-6}	7.5×10^{-6}	0.24	99.60	0.05	0.11	0.00	0.00	0.00	0.00
7.5×10^{-7}	1.9×10^{-6}	2.3×10^{-5}	0.76	98.51	0.26	0.35	0.00	0.12	0.00	0.00
7.5×10^{-7}	2.6×10^{-6}	6.0×10^{-5}	1.26	97.06	0.67	0.58	0.00	0.43	0.00	0.00
7.5×10^{-7}	3.0×10^{-6}	7.5×10^{-5}	1.44	96.25	0.97	0.67	0.00	0.67	0.00	0.00
7.5×10^{-7}	7.5×10^{-6}	4.5×10^{-4}	3.83	69.45	9.70	2.40	2.04	10.30	1.32	0.96

CH₂N⁺ INTO CH₃F

% SECONDARY ION FLUX Vs. PRESSURE

- + = 15
- x = 29
- △ = 33
- = 35
- = 42
- ▽ = 45
- = 47
- ⊙ = 49
- ◆ = 51
- × = 61



% SECONDARY ION FLUX

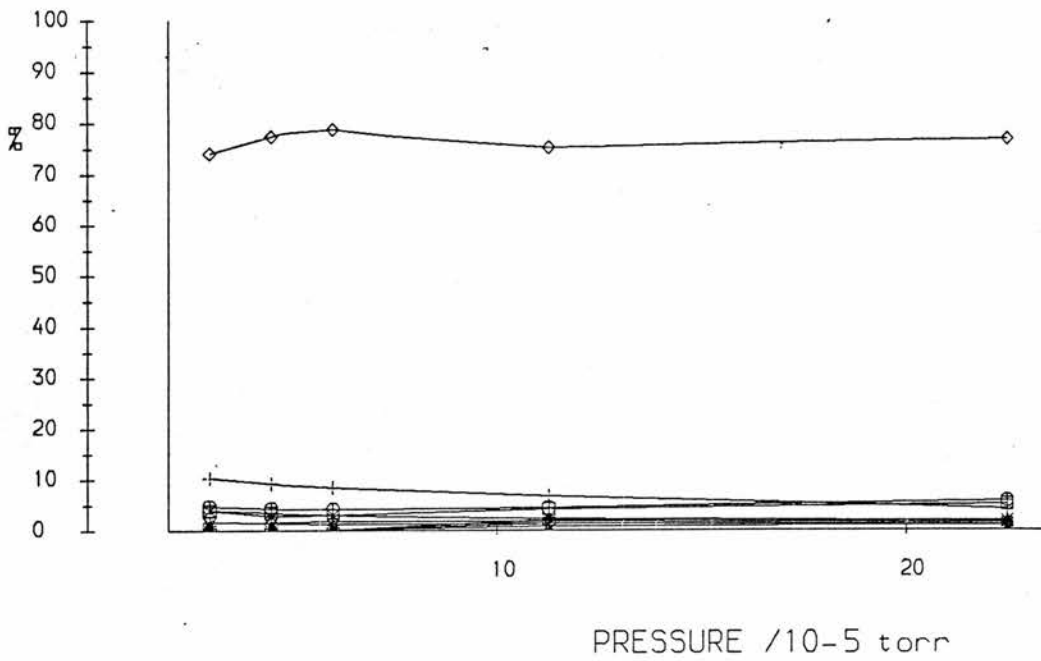
	PRESSURES in torr			m/e									
	INITIAL ION GAUGE	ION GAUGE	PENNING GAUGE	15	29	33	35	42	45	47	49	51	61
(A)	7.5 × 10 ⁻⁷	1.9 × 10 ⁻⁶	3.0 × 10 ⁻⁵	39.55	10.17	19.21	20.34	0.00	1.13	1.69	6.21	0.00	1.69
(B)	7.5 × 10 ⁻⁷	3.0 × 10 ⁻⁶	6.0 × 10 ⁻⁵	35.56	9.21	23.43	16.74	0.00	1.67	2.51	8.37	0.00	2.51
(C)	7.5 × 10 ⁻⁷	4.5 × 10 ⁻⁶	2.3 × 10 ⁻⁴	26.77	6.69	33.27	11.02	0.00	3.35	3.35	11.02	0.00	4.53
(D)	7.5 × 10 ⁻⁷	6.0 × 10 ⁻⁶	3.0 × 10 ⁻⁴	20.05	5.16	35.17	7.85	0.00	5.63	5.63	11.84	1.64	7.03
(E)	7.5 × 10 ⁻⁷	1.1 × 10 ⁻⁵	6.0 × 10 ⁻⁴	6.91	2.26	28.12	3.04	2.44	14.26	14.26	10.39	1.22	17.12

% TOTAL ION FLUX

	PRESSURES in torr			m/e										
	INITIAL ION GAUGE	ION GAUGE	PENNING GAUGE	15	28	29	33	35	42	45	47	49	51	61
	7.5 × 10 ⁻⁷	1.9 × 10 ⁻⁶	3.0 × 10 ⁻⁵	0.70	98.23	0.18	0.34	0.36	0.00	0.02	0.03	0.11	0.00	0.00
	7.5 × 10 ⁻⁷	3.0 × 10 ⁻⁶	6.0 × 10 ⁻⁵	0.85	97.61	0.22	0.56	0.40	0.00	0.04	0.06	0.20	0.00	0.00
	7.5 × 10 ⁻⁷	4.5 × 10 ⁻⁶	2.3 × 10 ⁻⁴	1.36	94.92	0.34	1.69	0.56	0.00	0.17	0.17	0.56	0.00	0.20
	7.5 × 10 ⁻⁷	6.0 × 10 ⁻⁶	3.0 × 10 ⁻⁴	1.71	91.47	0.44	3.00	0.67	0.00	0.48	0.48	1.01	0.14	0.60
	7.5 × 10 ⁻⁷	1.1 × 10 ⁻⁵	6.0 × 10 ⁻⁴	1.93	72.08	0.63	7.85	0.85	0.68	3.98	3.98	2.90	0.34	4.78

% SECONDARY ION FLUX Vs. PRESSURE

- + = 27
- x = 29
- Δ = 31
- ◊ = 33
- = 34
- ▽ = 35
- = 43
- ⊙ = 45
- ✦ = 47
- × = 49



% SECONDARY ION FLUX

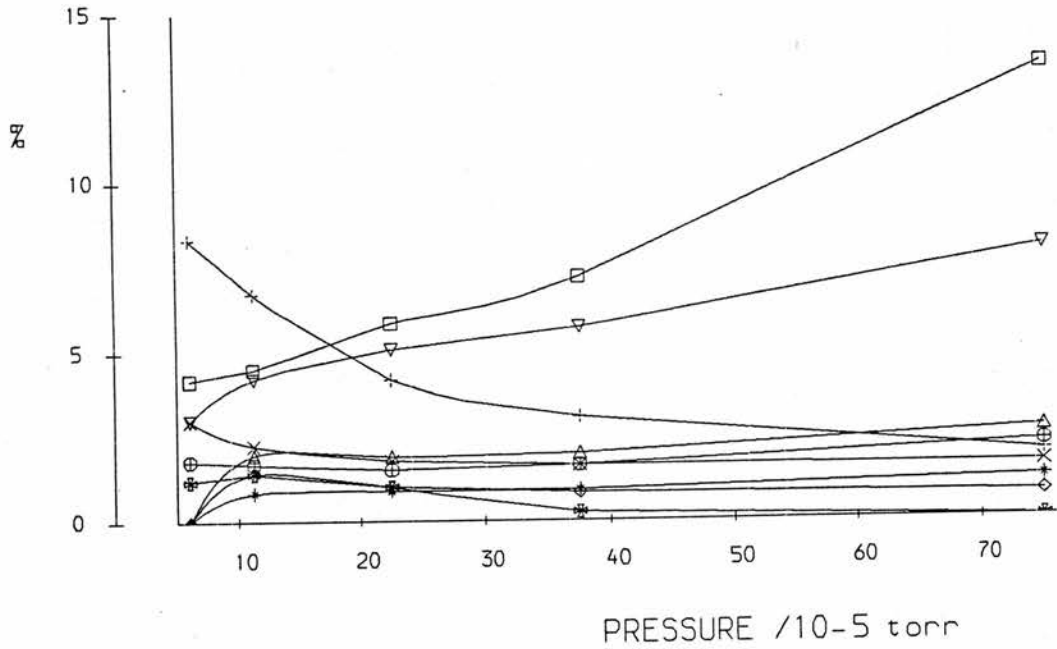
PRESSURES in torr			m/e									
INITIAL ION GAUGE	ION GAUGE	PENNING GAUGE	27	29	31	33	34	35	43	45	47	49
7.5x10 ⁻⁷	1.5x10 ⁻⁶	3.0x10 ⁻⁵	10.24	3.94	0.00	74.02	0.00	1.57	3.94	4.72	1.57	0.00
7.5x10 ⁻⁷	1.5x10 ⁻⁶	4.5x10 ⁻⁵	9.22	2.84	0.00	77.30	0.00	1.42	3.55	4.26	1.42	0.00
7.5x10 ⁻⁷	1.5x10 ⁻⁶	6.0x10 ⁻⁵	8.33	2.98	0.00	78.57	0.00	1.19	2.98	4.17	1.79	0.00
7.5x10 ⁻⁷	2.6x10 ⁻⁶	1.1x10 ⁻⁴	6.72	2.24	1.96	75.07	1.40	1.40	4.20	4.48	1.68	0.84
7.5x10 ⁻⁷	4.5x10 ⁻⁶	2.3x10 ⁻⁴	4.19	1.78	1.91	76.75	1.02	1.02	5.08	5.84	1.52	0.89

% TOTAL ION FLUX

PRESSURES in torr			m/e									
INITIAL ION GAUGE	ION GAUGE	PENNING GAUGE	15	27	29	31	33	34	35	43	45	47
7.5x10 ⁻⁷	1.5x10 ⁻⁶	3.0x10 ⁻⁵	98.73	0.13	0.05	0.00	0.94	0.00	0.02	0.05	0.06	0.02
7.5x10 ⁻⁷	1.5x10 ⁻⁶	4.5x10 ⁻⁵	98.59	0.13	0.04	0.00	1.09	0.00	0.02	0.05	0.06	0.02
7.5x10 ⁻⁷	1.5x10 ⁻⁶	6.0x10 ⁻⁵	98.32	0.14	0.05	0.00	1.32	0.00	0.02	0.05	0.07	0.03
7.5x10 ⁻⁷	2.6x10 ⁻⁶	1.1x10 ⁻⁴	96.43	0.24	0.08	0.07	2.68	0.05	0.05	0.15	0.16	0.06
7.5x10 ⁻⁷	4.5x10 ⁻⁶	2.3x10 ⁻⁴	92.10	0.33	0.14	0.15	6.07	0.08	0.08	0.40	0.46	0.12

CH3+ INTO CH3F

% SECONDARY ION FLUX Vs. PRESSURE



% SECONDARY ION FLUX

	PRESSURES in torr			m/e									
	INITIAL ION	ION	PENNING	27	29	31	33	34	35	43	45	47	49
	GAUGE	GAUGE	GAUGE										
(A)	7.5×10^{-7}	1.5×10^{-6}	6.0×10^{-5}	8.33	2.98	0.00	78.57	0.00	1.19	2.98	4.17	1.79	0.00
(B)	7.5×10^{-7}	2.6×10^{-6}	1.1×10^{-4}	6.72	2.24	1.96	75.07	1.40	1.40	4.20	4.48	1.68	0.84
(C)	7.5×10^{-7}	4.5×10^{-6}	2.3×10^{-4}	4.19	1.78	1.91	76.75	1.02	1.02	5.08	5.84	1.52	0.89
(D)	7.5×10^{-7}	6.8×10^{-6}	3.8×10^{-4}	3.06	1.65	1.98	76.80	0.83	0.25	5.70	7.18	1.65	0.91
(E)	7.5×10^{-7}	8.3×10^{-6}	7.5×10^{-4}	1.94	1.62	2.66	68.24	0.75	0.00	8.01	13.37	2.23	1.19

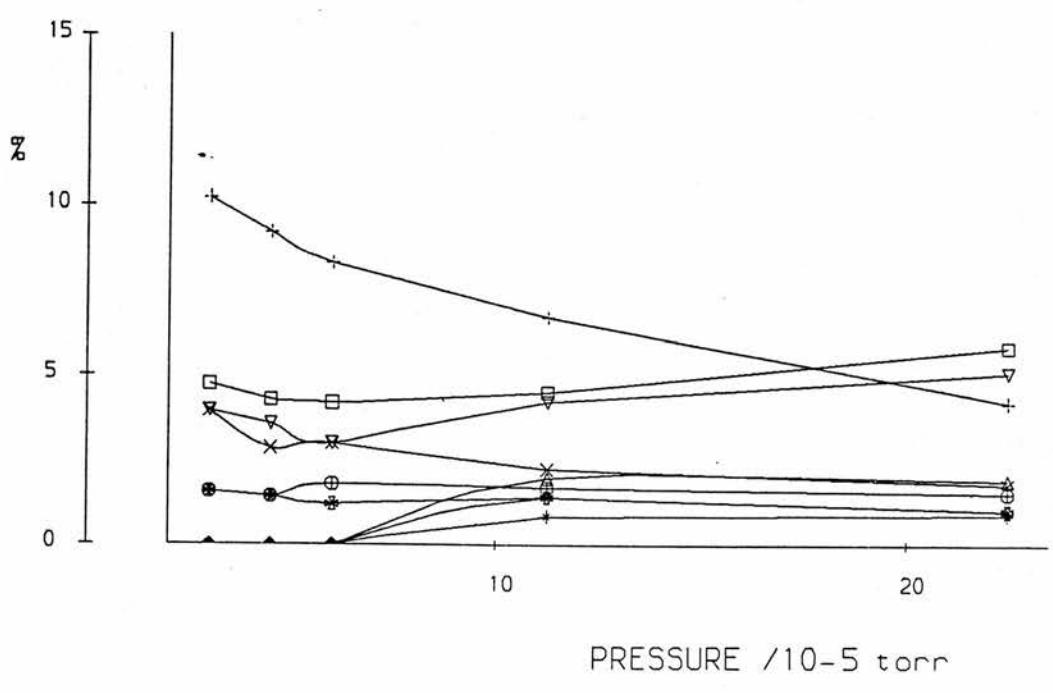
% TOTAL ION FLUX

	PRESSURES in torr			m/e										
	INITIAL ION	ION	PENNING	15	27	29	31	33	34	35	43	45	47	49
	GAUGE	GAUGE	GAUGE											
	7.5×10^{-7}	1.5×10^{-6}	6.0×10^{-5}	98.32	0.14	0.05	0.00	1.32	0.00	0.02	0.05	0.07	0.03	0.00
	7.5×10^{-7}	2.6×10^{-6}	1.1×10^{-4}	96.43	0.24	0.08	0.07	2.68	0.05	0.05	0.15	0.16	0.06	0.03
	7.5×10^{-7}	4.5×10^{-6}	2.3×10^{-4}	92.10	0.33	0.14	0.15	6.07	0.08	0.08	0.40	0.46	0.12	0.07
	7.5×10^{-7}	6.8×10^{-6}	3.8×10^{-4}	87.78	0.37	0.20	0.24	9.38	0.10	0.03	0.70	0.88	0.20	0.11
	7.5×10^{-7}	8.3×10^{-6}	7.5×10^{-4}	69.87	0.58	0.49	0.80	20.56	0.23	0.00	2.41	4.03	0.67	0.36

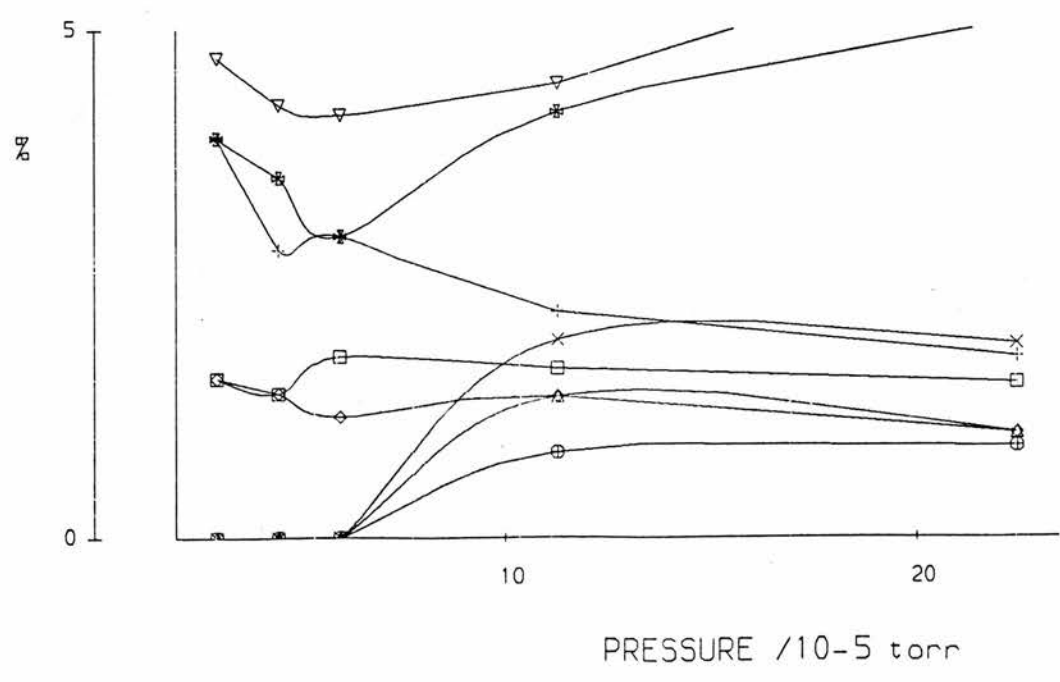
CH3+ INTO CH3F

% SECONDARY ION FLUX Vs. PRESSURE

- + = 27
- x = 29
- Δ = 31
- ◊ = 34
- = 35
- ▽ = 43
- = 45
- ⊗ = 47
- ◆ = 49



- Δ = 34
- ◊ = 35
- = 43
- ▽ = 45
- = 47
- ⊗ = 49



CD3+ INTO CH3F

% TOTAL ION FLUX

PRESSURES In torr			m/e										
INITIAL ION GAUGE	ION GAUGE	PENNING GAUGE	18	33	34	35	43	45	46	47	48	49	61
7.5×10^{-7}	3.4×10^{-6}	1.5×10^{-4}	98.16	0.91	0.00	0.07	0.00	0.05	0.00	0.00	0.00	0.00	0.00
7.5×10^{-7}	6.8×10^{-6}	2.3×10^{-4}	90.44	5.51	0.21	0.33	0.28	0.33	0.14	0.09	0.11	0.15	0.06
7.5×10^{-7}	1.1×10^{-5}	3.0×10^{-4}	82.26	9.05	0.33	0.60	1.02	1.66	0.21	0.27	0.43	0.33	0.34
7.5×10^{-7}	1.5×10^{-5}	4.5×10^{-4}	73.52	15.01	0.46	0.72	1.36	2.65	0.29	0.46	0.69	0.50	0.60
7.5×10^{-7}	1.5×10^{-5}	6.0×10^{-4}	56.67	20.77	0.68	1.02	3.33	7.08	0.49	1.02	1.40	0.81	1.44

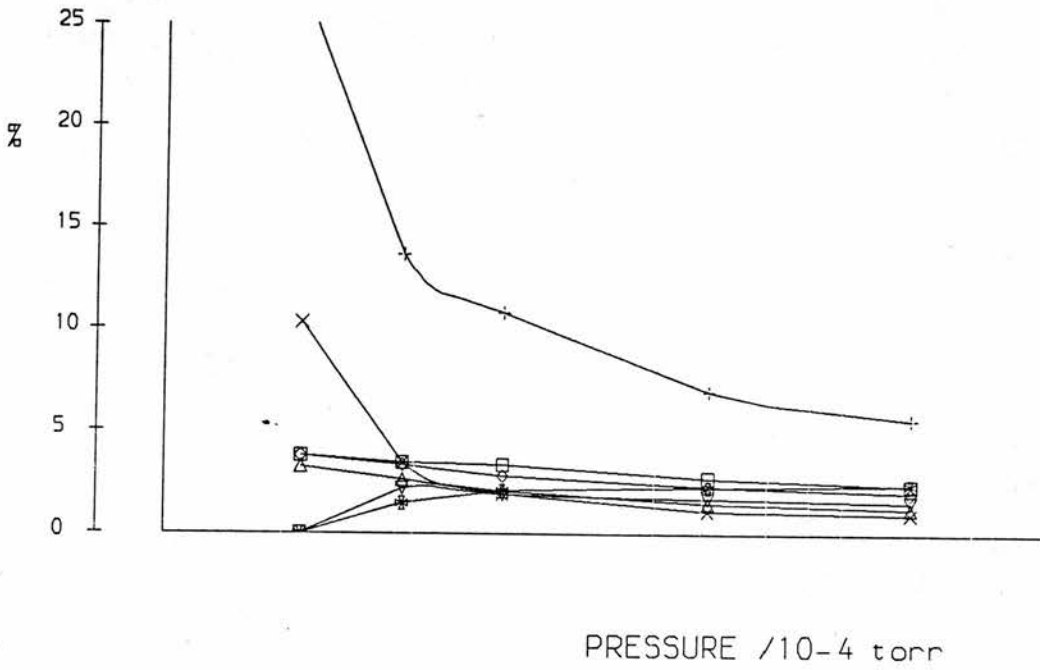
CD3+ INTO CH3F

% SECONDARY ION FLUX

PRESSURES In torr			m/e									
INITIAL ION GAUGE	ION GAUGE	PENNING GAUGE	33	34	35	43	45	46	47	48	49	61
(A) 7.5×10^{-7}	3.4×10^{-6}	1.5×10^{-4}	49.46	0.00	3.80	0.00	2.72	0.00	0.00	0.00	0.00	0.00
(B) 7.5×10^{-7}	6.8×10^{-6}	2.3×10^{-4}	57.65	2.20	3.46	2.94	3.46	1.47	0.94	1.15	1.57	0.63
(C) 7.5×10^{-7}	1.1×10^{-5}	3.0×10^{-4}	50.99	1.88	3.35	5.74	9.38	1.19	1.53	2.44	1.88	1.93
(D) 7.5×10^{-7}	1.5×10^{-5}	4.5×10^{-4}	56.70	1.72	2.72	5.13	10.00	1.11	1.72	2.61	1.88	2.26
(E) 7.5×10^{-7}	1.5×10^{-5}	6.0×10^{-4}	47.94	1.57	2.35	7.68	16.34	1.14	2.35	3.22	1.86	3.32

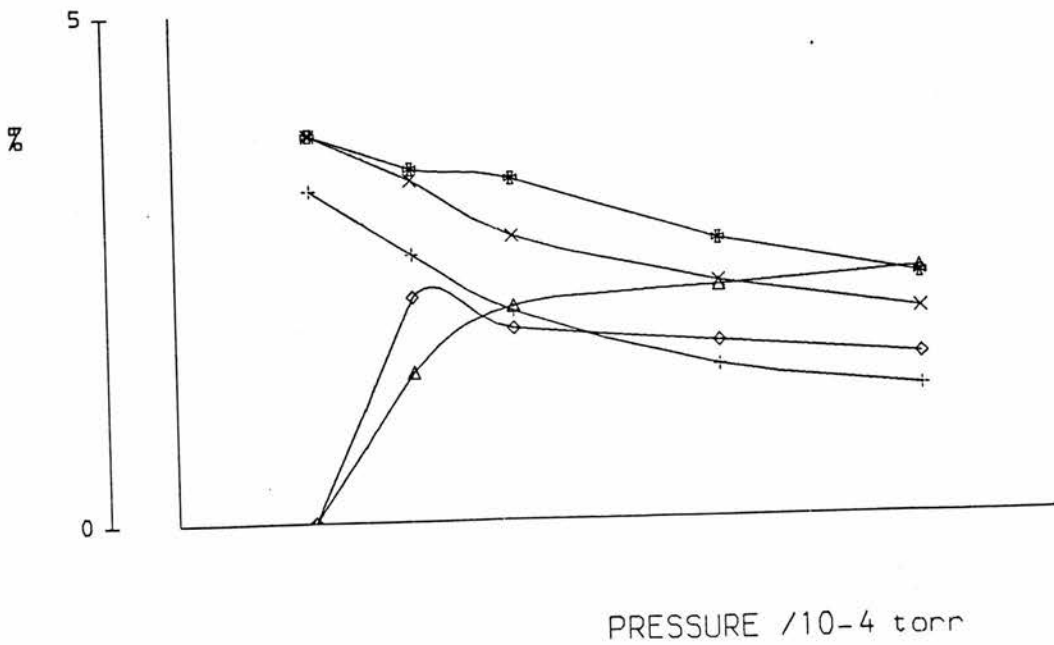
CD3+ INTO CH3F

% SECONDARY ION FLUX Vs. PRESSURE



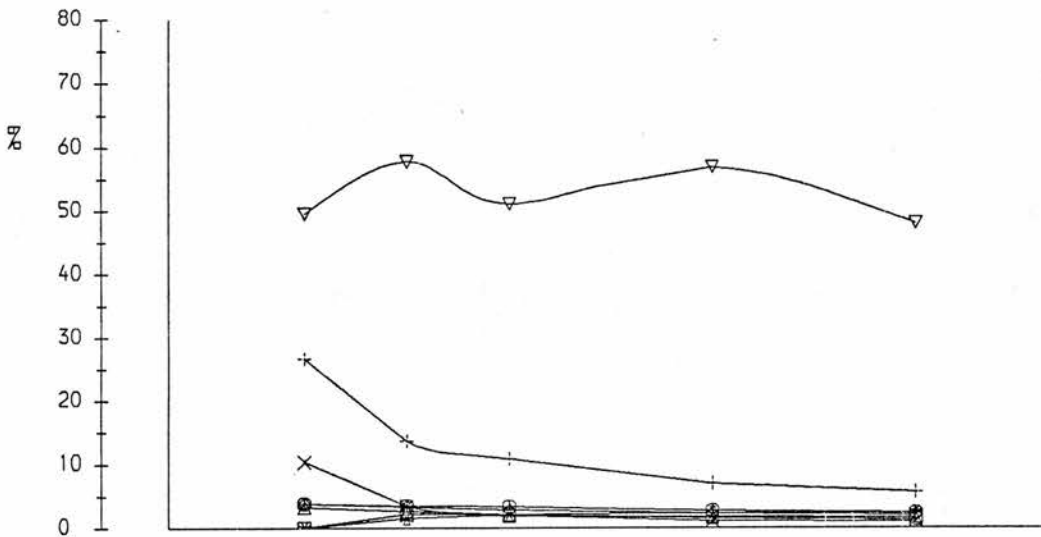
CD3+ INTO CH3F

% SECONDARY ION FLUX Vs. PRESSURE



CD3+ INTO CH3F

% SECONDARY ION FLUX Vs. PRESSURE



- + = 15
- x = 16
- Δ = 28
- ◇ = 29
- = 31
- ▽ = 33
- = 34
- e = 35

PRESSURE /10⁻⁴ torr

% SECONDARY ION FLUX

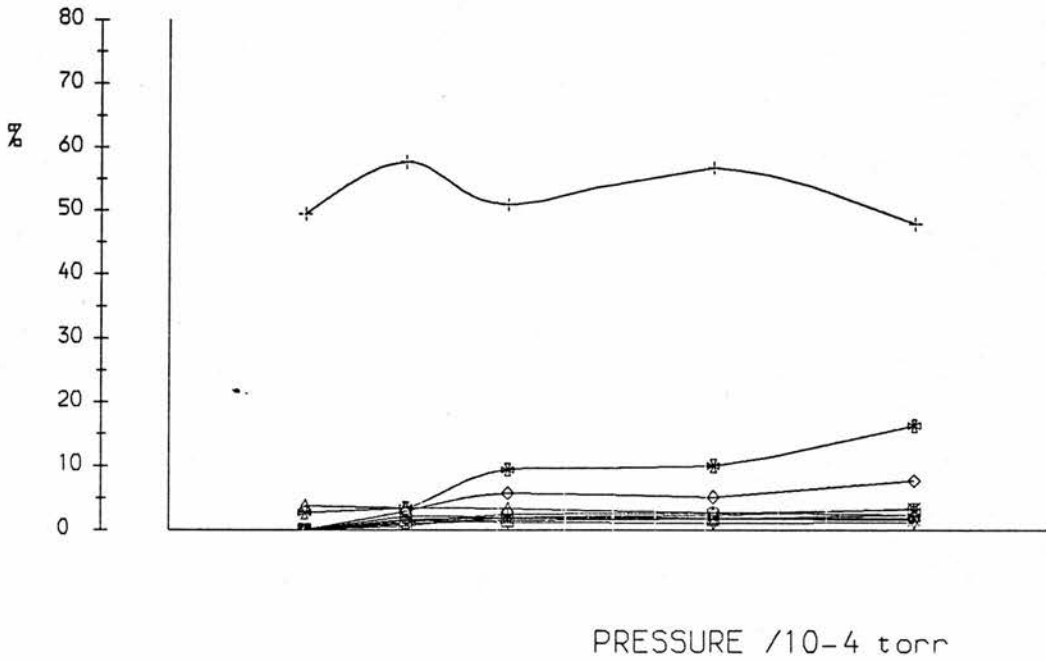
PRESSURES in torr			m/e								
INITIAL ION GAUGE	ION GAUGE	PENNING GAUGE	15	16	28	29	31	33	34	35	
(A)	7.5×10 ⁻⁷	3.4×10 ⁻⁶	1.5×10 ⁻⁴	26.63	10.33	3.26	3.80	0.00	49.46	0.00	3.80
(B)	7.5×10 ⁻⁷	6.8×10 ⁻⁶	2.3×10 ⁻⁴	13.63	3.46	2.62	3.35	1.47	57.65	2.20	3.46
(C)	7.5×10 ⁻⁷	1.1×10 ⁻⁵	3.0×10 ⁻⁴	10.80	1.93	2.05	2.79	2.10	50.99	1.88	3.35
(D)	7.5×10 ⁻⁷	1.5×10 ⁻⁵	4.5×10 ⁻⁴	6.97	1.11	1.49	2.30	2.26	56.70	1.72	2.72
(E)	7.5×10 ⁻⁷	1.5×10 ⁻⁵	6.0×10 ⁻⁴	5.57	0.99	1.26	2.01	2.40	47.94	1.57	2.35

% TOTAL ION FLUX

PRESSURES in torr			m/e									
INITIAL ION GAUGE	ION GAUGE	PENNING GAUGE	15	16	18	28	29	31	33	34	35	
7.5×10 ⁻⁷	3.4×10 ⁻⁶	1.5×10 ⁻⁴	0.49	0.19	98.16	0.06	0.07	0.00	0.91	0.00	0.07	
7.5×10 ⁻⁷	6.8×10 ⁻⁶	2.3×10 ⁻⁴	1.30	0.33	90.44	0.25	0.32	0.14	5.51	0.21	0.33	
7.5×10 ⁻⁷	1.1×10 ⁻⁵	3.0×10 ⁻⁴	1.92	0.34	82.26	0.36	0.49	0.37	9.05	0.33	0.49	
7.5×10 ⁻⁷	1.5×10 ⁻⁵	4.5×10 ⁻⁴	1.85	0.29	73.52	0.40	0.61	0.60	15.01	0.46	0.72	
7.5×10 ⁻⁷	1.5×10 ⁻⁵	6.0×10 ⁻⁴	2.41	0.43	56.67	0.55	0.87	1.04	20.77	0.68	1.04	

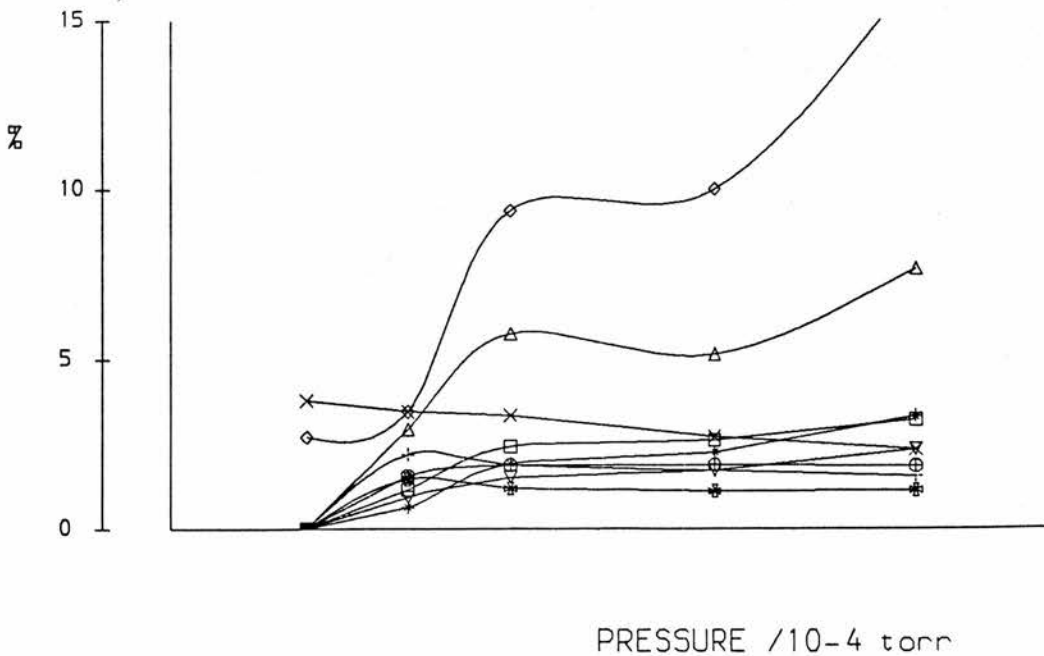
CD3+ INTO CH3F

% SECONDARY ION FLUX Vs. PRESSURE

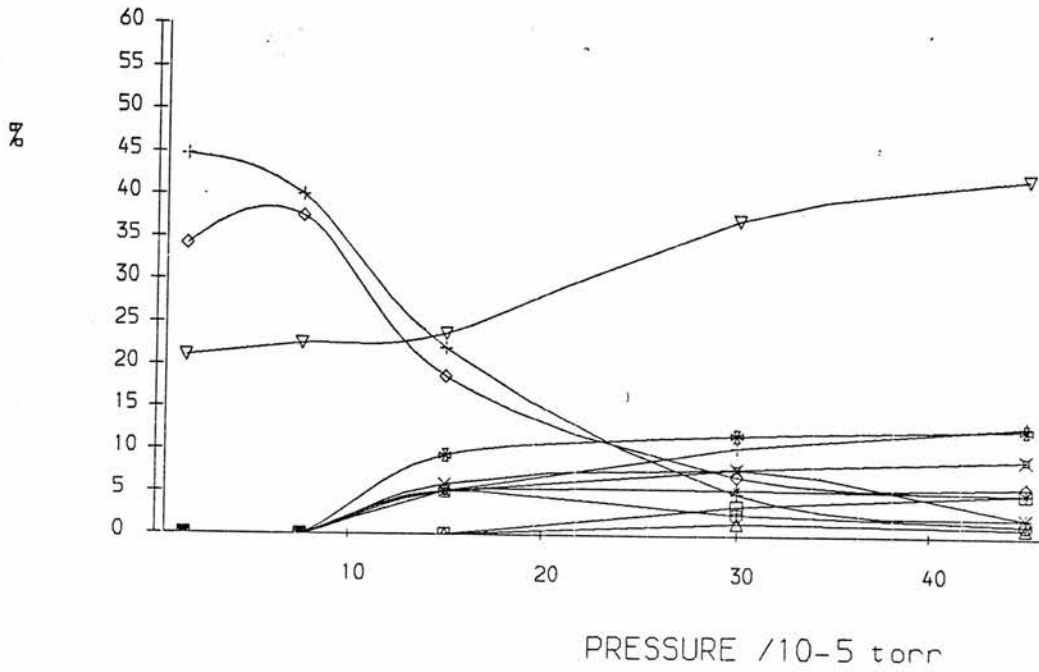


CD3+ INTO CH3F

% SECONDARY ION FLUX Vs. PRESSURE



% SECONDARY ION FLUX Vs. PRESSURE



% SECONDARY ION FLUX

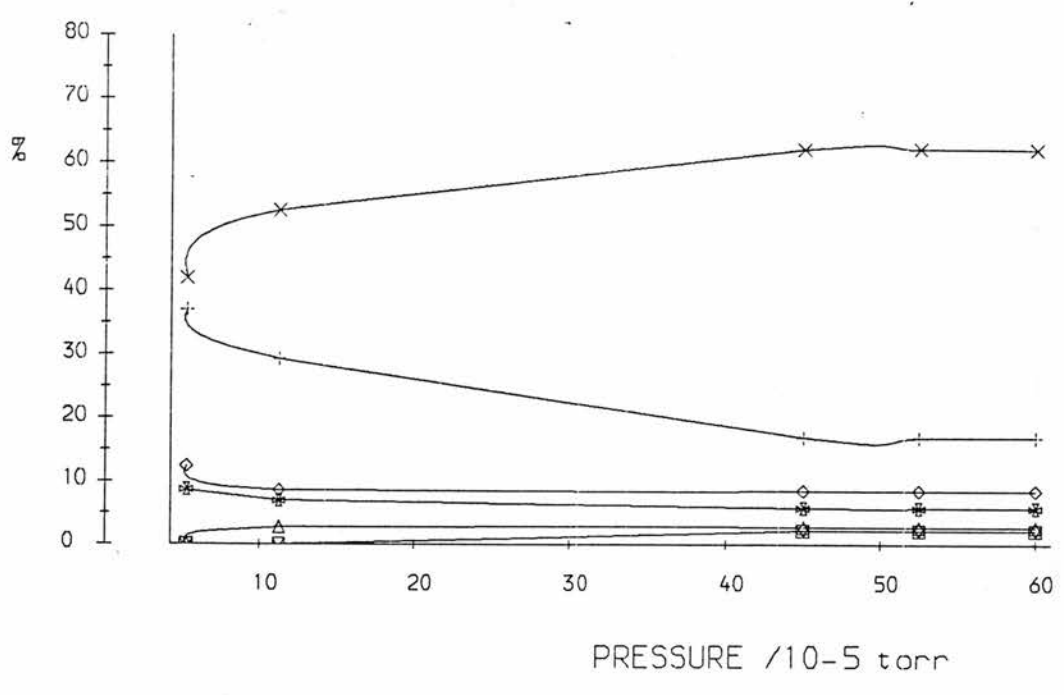
PRESSURES in torr			m/e										
INITIAL ION GAUGE	ION GAUGE	PENNING GAUGE	15	27	29	31	43	45	47	49	51	61	
(A)	7.5x10 ⁻⁷	1.1x10 ⁻⁶	1.5x10 ⁻⁵	44.74	0.00	0.00	34.21	0.00	21.05	0.00	0.00	0.00	0.00
(B)	7.5x10 ⁻⁷	3.0x10 ⁻⁶	7.5x10 ⁻⁵	40.00	0.00	0.00	37.50	0.00	22.50	0.00	0.00	0.00	0.00
(C)	7.5x10 ⁻⁷	4.5x10 ⁻⁶	1.5x10 ⁻⁴	22.03	5.93	0.00	18.64	9.32	23.73	0.00	5.08	5.08	5.08
(D)	7.5x10 ⁻⁷	7.5x10 ⁻⁶	3.0x10 ⁻⁴	4.94	7.88	1.47	6.94	11.88	37.12	3.47	2.54	5.47	7.88
(E)	7.5x10 ⁻⁷	1.1x10 ⁻⁵	4.5x10 ⁻⁴	2.18	2.18	1.06	5.80	12.73	42.17	5.12	1.43	5.12	9.11

% TOTAL ION FLUX

PRESSURES in torr			m/e											
INITIAL ION GAUGE	ION GAUGE	PENNING GAUGE	15	27	29	31	33	43	45	47	49	51	61	
7.5x10 ⁻⁷	1.1x10 ⁻⁶	1.5x10 ⁻⁵	0.17	0.00	0.00	0.13	99.62	0.00	0.08	0.00	0.00	0.00	0.00	0.00
7.5x10 ⁻⁷	3.0x10 ⁻⁶	7.5x10 ⁻⁵	0.16	0.00	0.00	0.15	99.60	0.00	0.09	0.00	0.00	0.00	0.00	0.00
7.5x10 ⁻⁷	4.5x10 ⁻⁶	1.5x10 ⁻⁴	0.26	0.07	0.00	0.22	98.82	0.11	0.28	0.00	0.06	0.06	0.06	0.00
7.5x10 ⁻⁷	7.5x10 ⁻⁶	3.0x10 ⁻⁴	0.37	0.60	0.11	0.53	92.41	0.90	2.82	0.26	0.19	0.42	0.60	0.00
7.5x10 ⁻⁷	1.1x10 ⁻⁵	4.5x10 ⁻⁴	0.37	0.37	0.18	0.98	83.07	2.15	7.14	0.87	0.24	0.87	1.54	2.00

CH₂N⁺ INTO CH₃Br

% SECONDARY ION FLUX Vs. PRESSURE



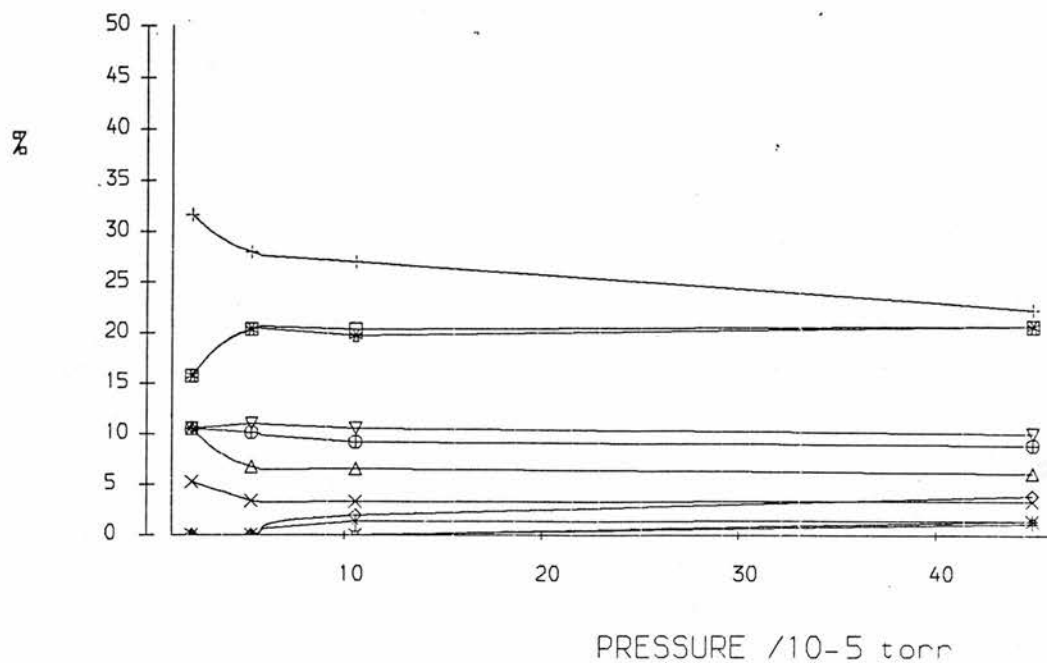
% SECONDARY ION FLUX

PRESSURES in torr			m/e							
INITIAL ION GAUGE	ION GAUGE	PENNING GAUGE	15	19	93	95	97	109	111	
(A)	7.5 × 10 ⁻⁷	1.9 × 10 ⁻⁶	5.3 × 10 ⁻⁵	37.04	41.98	0.00	12.35	8.64	0.00	0.00
(B)	7.5 × 10 ⁻⁷	3.8 × 10 ⁻⁶	1.1 × 10 ⁻⁴	29.26	52.66	2.66	8.51	6.91	0.00	0.00
(C)	7.5 × 10 ⁻⁷	7.5 × 10 ⁻⁶	4.5 × 10 ⁻⁴	16.84	62.11	2.74	8.42	5.68	2.11	2.11
(D)	7.5 × 10 ⁻⁷	1.5 × 10 ⁻⁵	5.3 × 10 ⁻⁴	16.84	62.11	2.74	8.42	5.68	2.11	2.11
(E)	7.5 × 10 ⁻⁷	2.3 × 10 ⁻⁵	6.0 × 10 ⁻⁴	16.84	62.11	2.74	8.42	5.68	2.11	2.11

% TOTAL ION FLUX

PRESSURES in torr			m/e							
INITIAL ION GAUGE	ION GAUGE	PENNING GAUGE	15	19	28	93	95	97	109	111
7.5 × 10 ⁻⁷	1.9 × 10 ⁻⁶	5.3 × 10 ⁻⁵	0.30	0.34	99.19	0.00	0.10	0.07	0.00	0.00
7.5 × 10 ⁻⁷	3.8 × 10 ⁻⁶	1.1 × 10 ⁻⁴	0.55	0.99	98.12	0.05	0.16	0.13	0.00	0.00
7.5 × 10 ⁻⁷	7.5 × 10 ⁻⁶	4.5 × 10 ⁻⁴	0.80	2.95	95.25	0.13	0.40	0.27	0.10	0.10
7.5 × 10 ⁻⁷	1.5 × 10 ⁻⁵	5.3 × 10 ⁻⁴	0.80	2.95	95.25	0.13	0.40	0.27	0.10	0.10
7.5 × 10 ⁻⁷	2.3 × 10 ⁻⁵	6.0 × 10 ⁻⁴	0.80	2.95	95.25	0.13	0.40	0.27	0.10	0.10

% SECONDARY ION FLUX Vs. PRESSURE



% SECONDARY ION FLUX

PRESSURES in torr			m/e										
INITIAL ION GAUGE	ION GAUGE	PENNING GAUGE	27	28	29	31	93	94	95	96	97	109	111
(A)	7.5 × 10 ⁻⁷	1.1 × 10 ⁻⁶	2.3 × 10 ⁻⁵	31.58	5.26	10.53	0.00	15.79	10.53	15.79	10.53	0.00	0.00
(B)	7.5 × 10 ⁻⁷	4.1 × 10 ⁻⁶	5.3 × 10 ⁻⁵	27.97	3.39	6.78	0.00	20.34	11.02	20.34	10.17	0.00	0.00
(C)	7.5 × 10 ⁻⁷	5.3 × 10 ⁻⁶	1.1 × 10 ⁻⁴	26.97	3.29	6.58	1.97	19.74	10.53	20.39	9.21	1.32	0.00
(D)	7.5 × 10 ⁻⁷	1.1 × 10 ⁻⁵	4.5 × 10 ⁻⁴	22.35	3.35	6.15	3.91	20.67	10.06	20.67	8.94	1.40	1.40
(E)	7.5 × 10 ⁻⁷	1.1 × 10 ⁻⁵	4.5 × 10 ⁻⁴	22.35	3.35	6.15	3.91	20.67	10.06	20.67	8.94	1.40	1.40

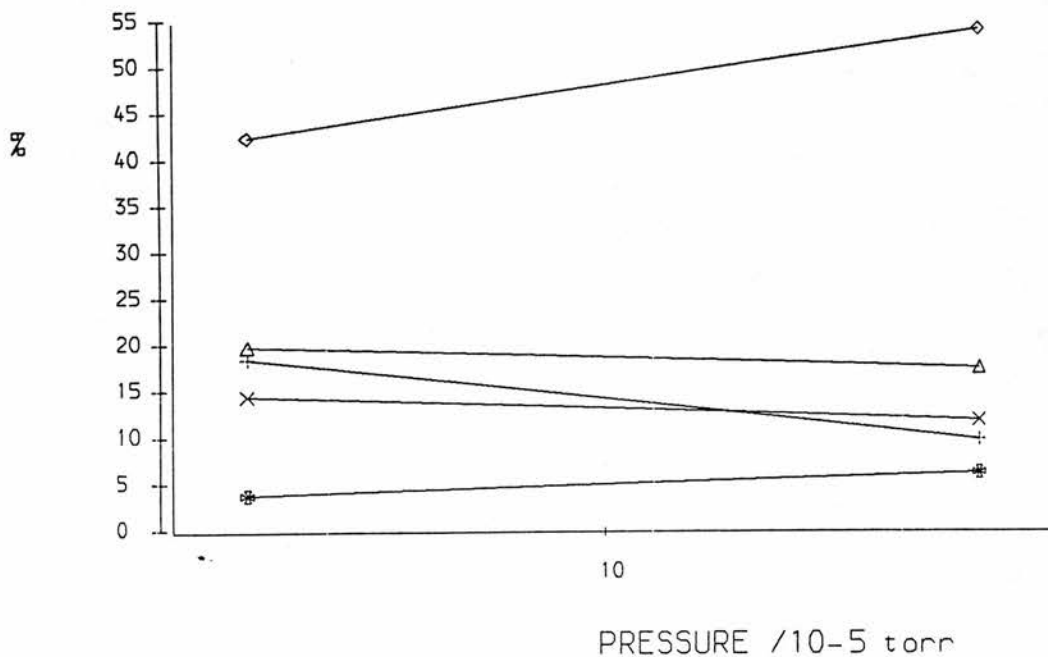
% TOTAL ION FLUX

PRESSURES in torr			m/e												
INITIAL ION GAUGE	ION GAUGE	PENNING GAUGE	15	27	28	29	31	93	94	95	96	97	109	111	
7.5 × 10 ⁻⁷	1.1 × 10 ⁻⁶	2.3 × 10 ⁻⁵	99.81	0.06	0.01	0.02	0.00	0.03	0.02	0.03	0.02	0.00	0.00	0.00	
7.5 × 10 ⁻⁷	4.1 × 10 ⁻⁶	5.3 × 10 ⁻⁵	98.83	0.33	0.04	0.08	0.00	0.24	0.13	0.24	0.12	0.00	0.00	0.00	
7.5 × 10 ⁻⁷	5.3 × 10 ⁻⁶	1.1 × 10 ⁻⁴	98.48	0.41	0.05	0.10	0.03	0.30	0.16	0.31	0.14	0.02	0.00	0.00	
7.5 × 10 ⁻⁷	1.1 × 10 ⁻⁵	4.5 × 10 ⁻⁴	96.41	0.80	0.12	0.22	0.14	0.74	0.36	0.74	0.32	0.05	0.05	0.04	
7.5 × 10 ⁻⁷	1.1 × 10 ⁻⁵	4.5 × 10 ⁻⁴	96.41	0.80	0.12	0.22	0.14	0.74	0.36	0.74	0.32	0.05	0.05	0.04	

CH₂N⁺ INTO CH₃I

% SECONDARY ION FLUX Vs. PRESSURE

+ = 15
 x = 127
 Δ = 142
 ◊ = 143
 ● = 157



% SECONDARY ION FLUX

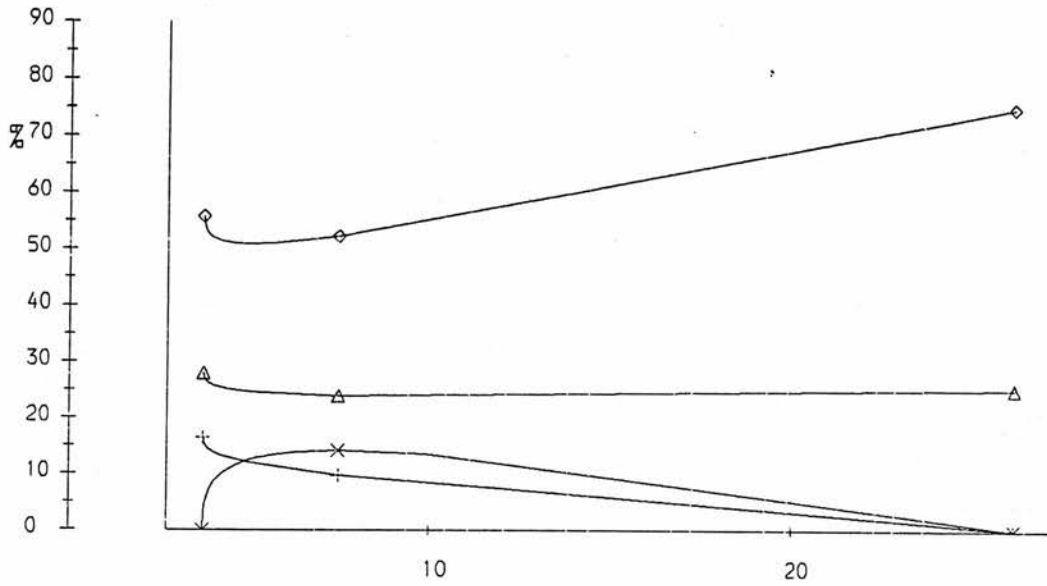
	PRESSURES in torr			m/e				
	INITIAL ION	ION	PENNING					
	GAUGE	GAUGE	GAUGE	15	127	142	143	157
(A)	7.5 × 10 ⁻⁶	1.5 × 10 ⁻⁵	5.3 × 10 ⁻⁵	18.67	14.67	20.00	42.67	4.00
(B)	7.5 × 10 ⁻⁶	2.3 × 10 ⁻⁵	1.5 × 10 ⁻⁴	9.86	11.97	17.61	54.23	6.34

% TOTAL ION FLUX

	PRESSURES in torr			m/e					
	INITIAL ION	ION	PENNING						
	GAUGE	GAUGE	GAUGE	15	28	127	142	143	157
	7.5 × 10 ⁻⁶	1.5 × 10 ⁻⁵	5.3 × 10 ⁻⁵	0.14	99.25	0.11	0.15	0.32	0.03
	7.5 × 10 ⁻⁶	2.3 × 10 ⁻⁵	1.5 × 10 ⁻⁴	0.14	98.57	0.17	0.25	0.77	0.09

CH₂N⁺ INTO CH₃I

% SECONDARY ION FLUX Vs. PRESSURE



+ = 15
x = 127
Δ = 142
◊ = 143

PRESSURE /10⁻⁵ torr

% SECONDARY ION FLUX

PRESSURES in torr			m/e			
INITIAL ION GAUGE	ION GAUGE	PENNING GAUGE	15	127	142	143
(A) 7.5×10 ⁻⁷	3.0×10 ⁻⁶	3.8×10 ⁻⁵	16.39	0.00	27.87	55.74
(B) 7.5×10 ⁻⁷	7.5×10 ⁻⁶	7.5×10 ⁻⁵	9.73	14.16	23.89	52.21
(C) 7.5×10 ⁻⁷	1.5×10 ⁻⁵	2.6×10 ⁻⁴	0.00	0.00	25.15	74.85

% TOTAL ION FLUX

PRESSURES in torr			m/e				
INITIAL ION GAUGE	ION GAUGE	PENNING GAUGE	15	28	127	142	143
7.5×10 ⁻⁷	3.0×10 ⁻⁶	3.8×10 ⁻⁵	0.10	99.39	0.00	0.17	0.34
7.5×10 ⁻⁷	7.5×10 ⁻⁶	7.5×10 ⁻⁵	0.11	98.87	0.16	0.27	0.59
7.5×10 ⁻⁷	1.5×10 ⁻⁵	2.6×10 ⁻⁴	0.00	98.37	0.00	0.41	1.22

CH3+ INTO CH3I

% SECONDARY ION FLUX

PRESSURES in torr			m/e											
INITIAL ION GAUGE	ION GAUGE	PENNING GAUGE	27	28	29	43	45	59	127	141	142	143	157	
(A)	7.5×10 ⁻⁶	7.5×10 ⁻⁶	2.3×10 ⁻⁵	11.37	0.84	3.37	0.42	0.00	0.00	0.42	4.00	77.26	1.05	1.26
(B)	7.5×10 ⁻⁶	1.1×10 ⁻⁵	6.8×10 ⁻⁵	5.55	0.47	1.15	0.73	0.21	0.64	0.21	4.22	77.77	1.41	7.64
(C)	7.5×10 ⁻⁶	2.3×10 ⁻⁵	2.3×10 ⁻⁴	2.87	0.00	0.56	2.07	0.61	1.93	0.00	3.95	57.10	1.32	29.59
(D)	7.5×10 ⁻⁶	3.0×10 ⁻⁵	1.5×10 ⁻³	2.19	0.00	0.00	5.11	1.46	3.65	0.00	3.28	14.96	0.00	69.34
(E)	7.5×10 ⁻⁶	3.0×10 ⁻⁵	1.5×10 ⁻³	2.19	0.00	0.00	5.11	1.46	3.65	0.00	3.28	14.96	0.00	69.34

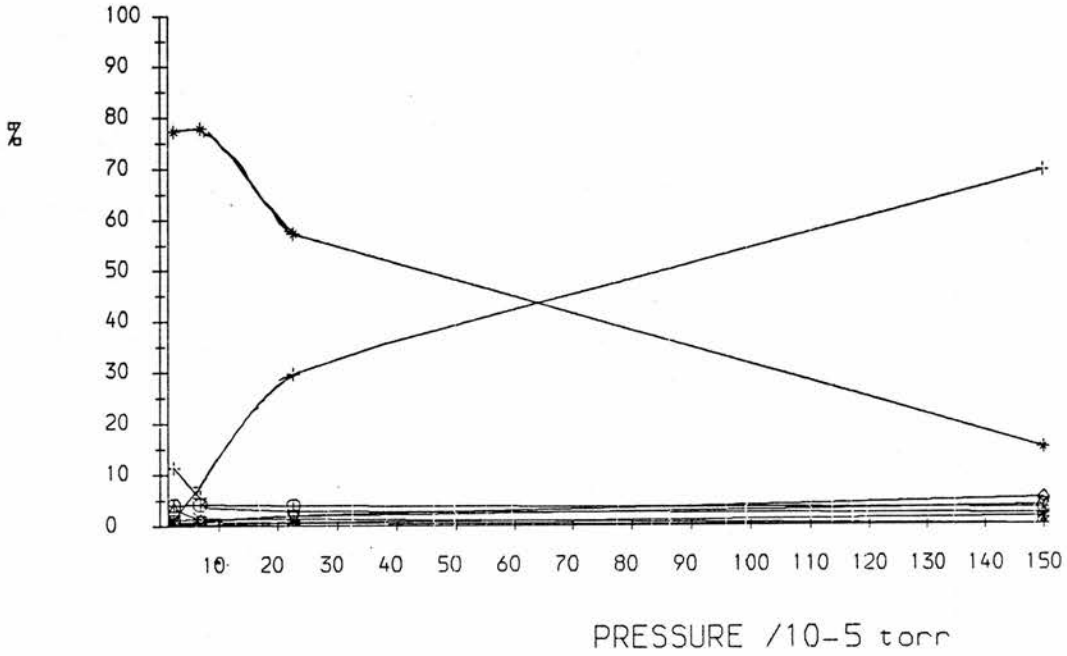
CH3+ INTO CH3I

% TOTAL ION FLUX

PRESSURES in torr			m/e											
INITIAL ION GAUGE	ION GAUGE	PENNING GAUGE	15	27	28	29	43	45	59	127	141	142	143	157
7.5×10 ⁻⁶	7.5×10 ⁻⁶	2.3×10 ⁻⁵	95.25	0.54	0.04	0.16	0.02	0.00	0.00	0.02	0.19	3.67	0.05	0.06
7.5×10 ⁻⁶	1.1×10 ⁻⁵	6.8×10 ⁻⁵	76.54	1.30	0.11	0.27	0.17	0.05	0.15	0.05	0.99	18.25	0.33	1.79
7.5×10 ⁻⁶	2.3×10 ⁻⁵	2.3×10 ⁻⁴	78.74	0.61	0.00	0.12	0.44	0.13	0.41	0.00	0.84	12.14	0.28	6.29
7.5×10 ⁻⁶	3.0×10 ⁻⁵	1.5×10 ⁻³	7.43	2.03	0.00	0.00	4.73	1.35	3.38	0.00	3.04	13.85	0.00	64.19
7.5×10 ⁻⁶	3.0×10 ⁻⁵	1.5×10 ⁻³	7.43	2.03	0.00	0.00	4.73	1.35	3.38	0.00	3.04	13.85	0.00	64.19

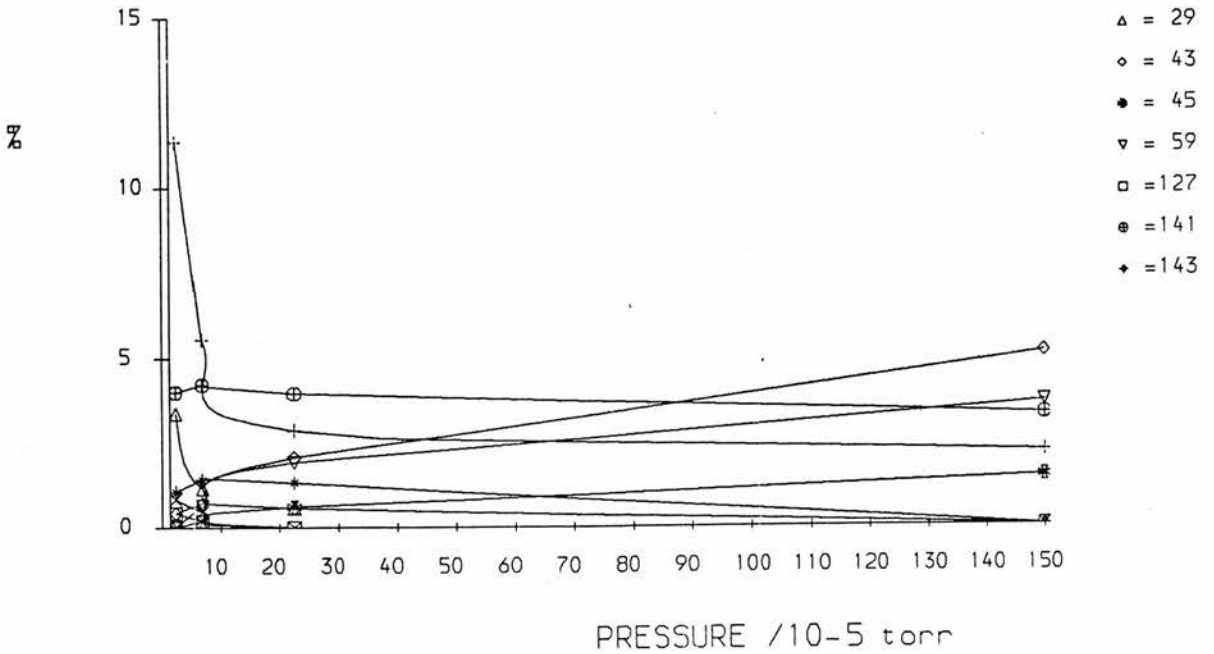
CH₃⁺ INTO CH₃I

% SECONDARY ION FLUX Vs. PRESSURE



CH₃⁺ INTO CH₃I

% SECONDARY ION FLUX Vs. PRESSURE



CD3+ INTO CH3I

% SECONDARY ION FLUX

PRESSURES in torr			m/e										
INITIAL ION GAUGE	ION GAUGE	PENNING GAUGE	15	28	29	30	33	34	37	127	141	157	
(A)	7.5×10^{-6}	1.1×10^{-5}	2.3×10^{-5}	5.30	1.41	2.12	1.77	4.24	3.18	1.06	0.71	79.51	0.71
(B)	7.5×10^{-6}	1.1×10^{-5}	6.0×10^{-5}	4.63	2.32	3.35	1.16	1.29	1.16	0.00	0.51	81.08	4.50
(C)	7.5×10^{-6}	1.9×10^{-5}	1.1×10^{-4}	0.00	0.00	0.00	0.00	0.00	0.00	0.00	0.00	87.72	12.28
(D)	7.5×10^{-6}	2.6×10^{-5}	3.0×10^{-4}	0.00	0.00	0.00	0.00	0.00	0.00	0.00	0.00	64.24	35.76
(E)	7.5×10^{-6}	2.6×10^{-5}	3.0×10^{-4}	0.00	0.00	0.00	0.00	0.00	0.00	0.00	0.00	64.24	35.76

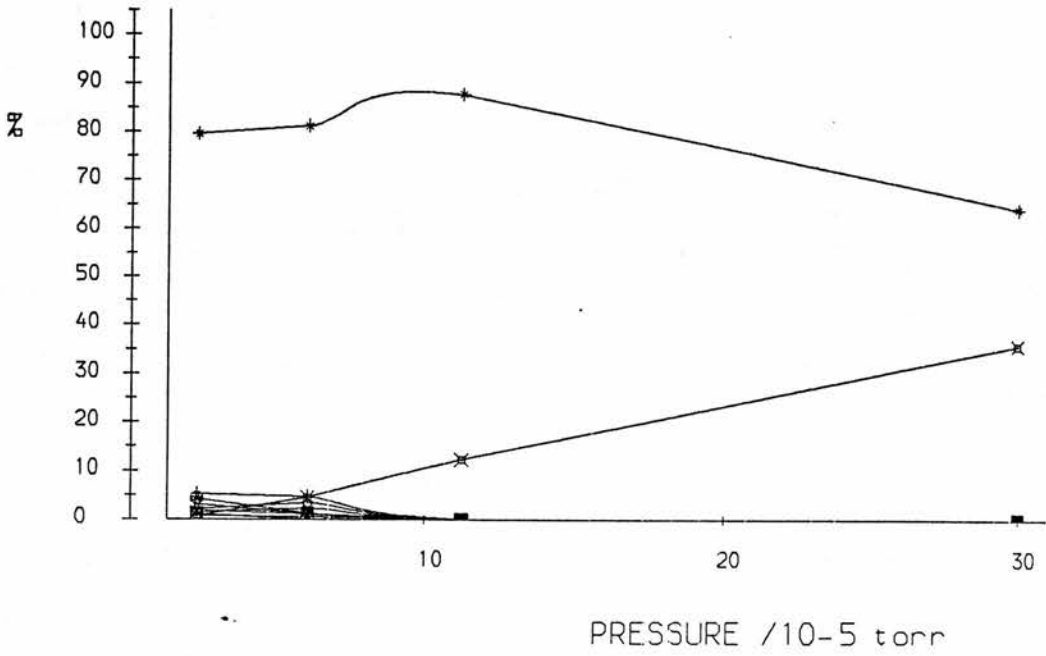
CD3+ INTO CH3I

% TOTAL ION FLUX

PRESSURES in torr			m/e											
INITIAL ION GAUGE	ION GAUGE	PENNING GAUGE	15	18	28	29	30	33	34	37	127	141	157	
	7.5×10^{-6}	1.1×10^{-5}	2.3×10^{-5}	0.15	97.17	0.04	0.06	0.05	0.12	0.09	0.03	0.02	2.25	0.02
	7.5×10^{-6}	1.1×10^{-5}	6.0×10^{-5}	0.36	92.23	0.18	0.26	0.09	0.10	0.09	0.00	0.04	6.30	0.35
	7.5×10^{-6}	1.9×10^{-5}	1.1×10^{-4}	0.00	86.56	0.00	0.00	0.00	0.00	0.00	0.00	0.00	11.79	1.65
	7.5×10^{-6}	2.6×10^{-5}	3.0×10^{-4}	0.00	83.53	0.00	0.00	0.00	0.00	0.00	0.00	0.00	10.58	5.89
	7.5×10^{-6}	2.6×10^{-5}	3.0×10^{-4}	0.00	0.00	0.00	0.00	0.00	0.00	0.00	0.00	10.58	5.89	83.53

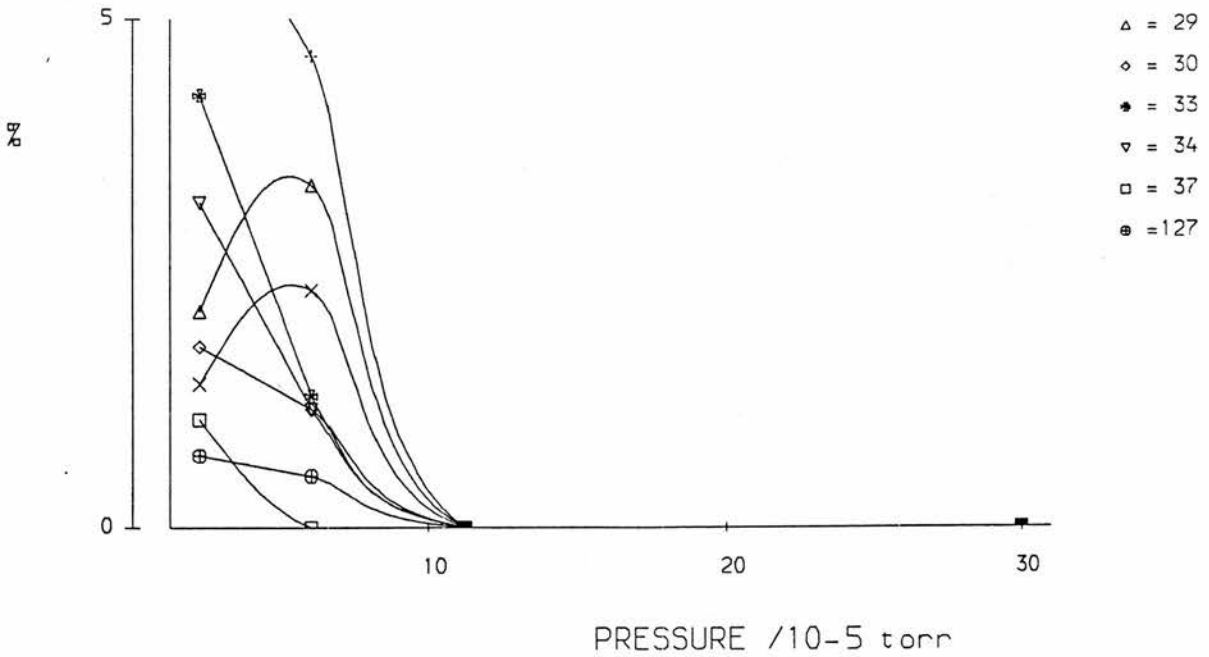
CD3+ INTO CH3I

% SECONDARY ION FLUX VS. PRESSURE



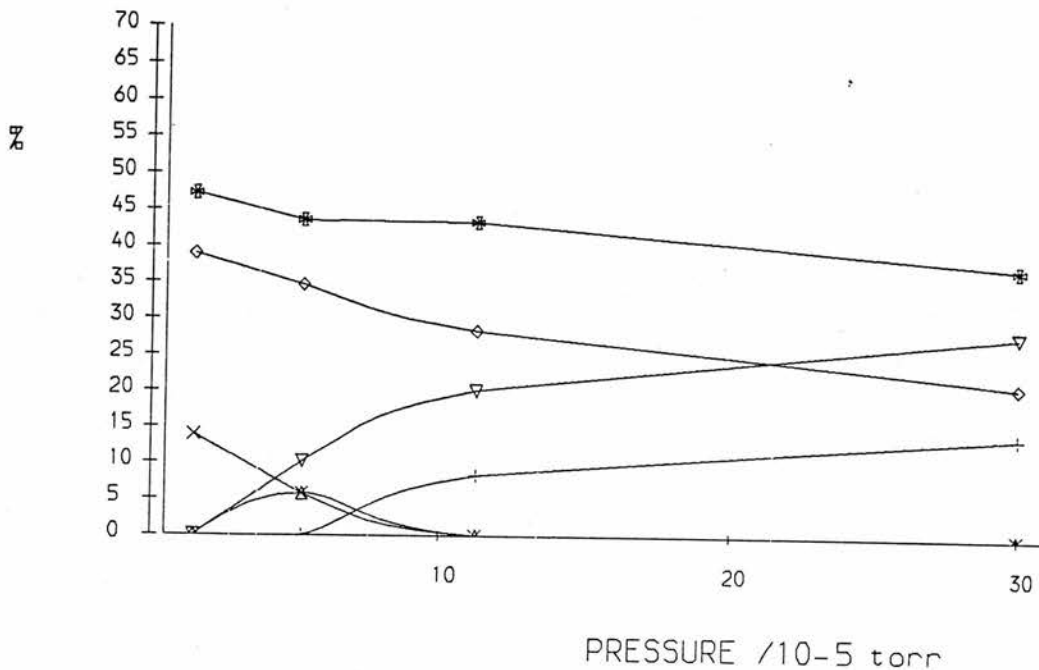
CD3+ INTO CH3I

% SECONDARY ION FLUX VS. PRESSURE



C2H3+ INTO CH3I

% SECONDARY ION FLUX Vs. PRESSURE



% SECONDARY ION FLUX

	PRESSURES in torr			m/e					
	INITIAL ION	ION	PENNING						
	GAUGE	GAUGE	GAUGE	45	127	141	142	143	157
(A)	7.5 × 10 ⁻⁷	1.1 × 10 ⁻⁶	1.5 × 10 ⁻⁵	0.00	13.89	0.00	38.89	47.22	0.00
(B)	7.5 × 10 ⁻⁷	5.3 × 10 ⁻⁶	5.3 × 10 ⁻⁵	0.00	5.77	5.77	34.65	43.57	10.24
(C)	7.5 × 10 ⁻⁷	3.0 × 10 ⁻⁵	1.1 × 10 ⁻⁴	8.31	0.00	0.00	28.34	43.32	20.03
(D)	7.5 × 10 ⁻⁷	1.5 × 10 ⁻⁵	3.0 × 10 ⁻⁴	13.96	0.00	0.00	20.94	37.18	27.92

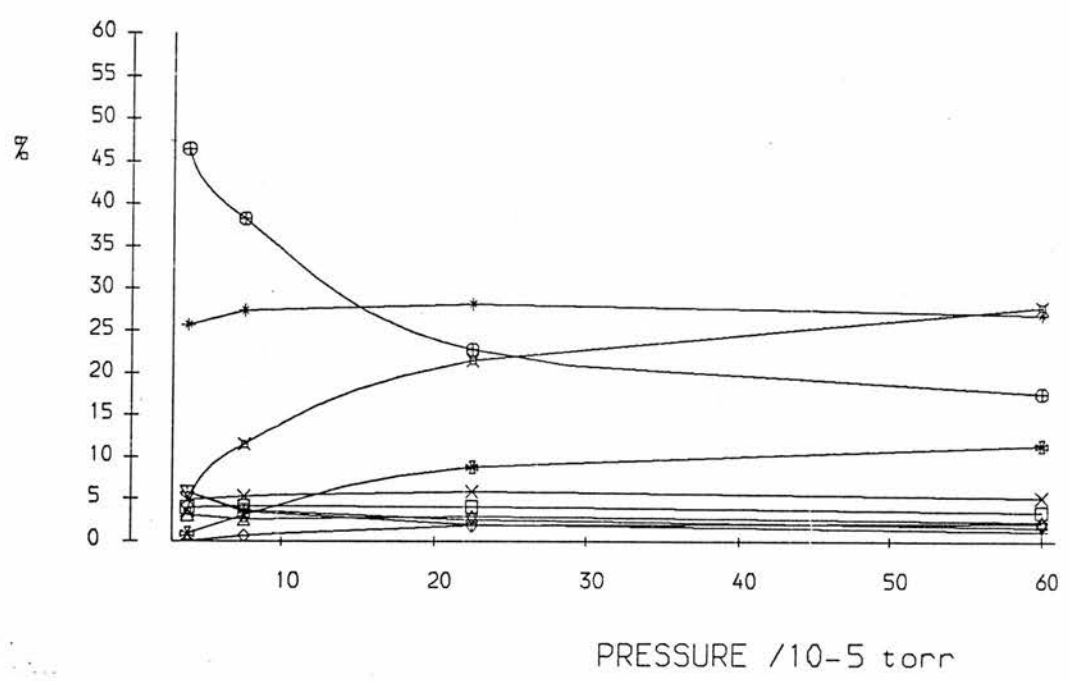
% TOTAL ION FLUX

	PRESSURES in torr			m/e						
	INITIAL ION	ION	PENNING							
	GAUGE	GAUGE	GAUGE	27	45	127	141	142	143	157
	7.5 × 10 ⁻⁷	1.1 × 10 ⁻⁶	1.5 × 10 ⁻⁵	99.28	0.00	0.10	0.00	0.28	0.34	0.00
	7.5 × 10 ⁻⁷	5.3 × 10 ⁻⁶	5.3 × 10 ⁻⁵	96.19	0.00	0.22	0.22	1.32	1.66	0.39
	7.5 × 10 ⁻⁷	3.0 × 10 ⁻⁵	1.1 × 10 ⁻⁴	93.26	0.56	0.00	0.00	1.91	2.92	1.35
	7.5 × 10 ⁻⁷	1.5 × 10 ⁻⁵	3.0 × 10 ⁻⁴	87.68	1.72	0.00	0.00	2.58	4.58	3.44

C2H3+ INTO CH3I

% SECONDARY ION FLUX Vs. PRESSURE

- + = 15 = CH₃⁺
- x = 37
- Δ = 39
- ◊ = 43
- = 45
- ▽ = 127 = I⁺
- ◻ = 141 = CH₂I⁺
- ⊖ = 142 = CH₃I⁺
- ◆ = 143 = CH₃IH⁺
- × = 157 = CH₃ICH₃⁺



% SECONDARY ION FLUX

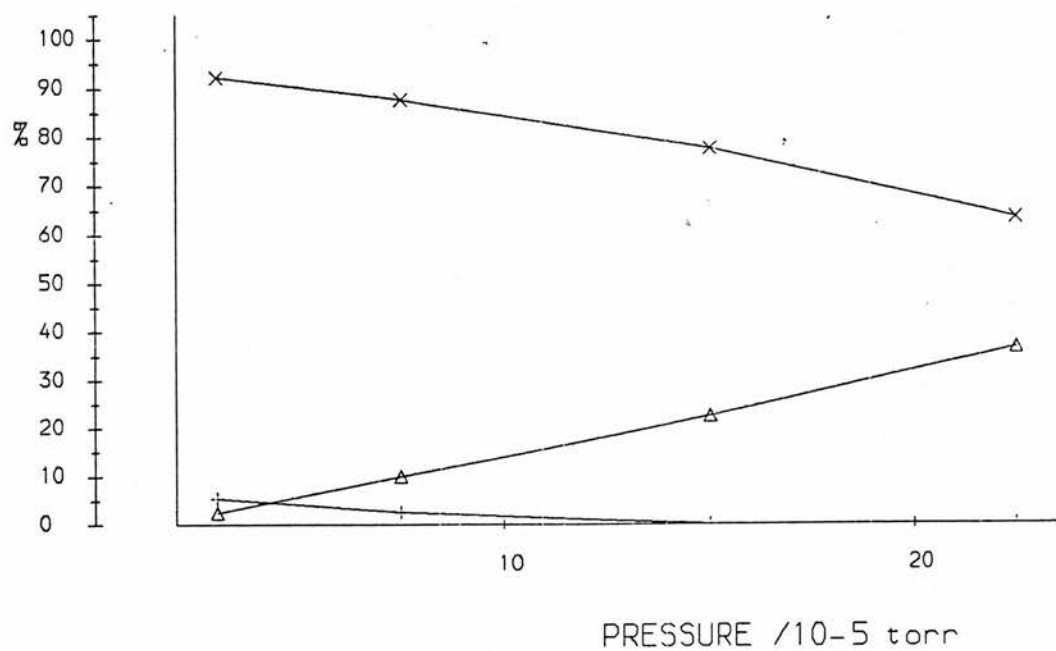
	PRESSURES in torr			m/e									
	INITIAL ION	ION	PENNING	15	37	39	43	45	127	141	142	143	157
	GAUGE	GAUGE	GAUGE										
(A)	7.5×10 ⁻⁶	7.5×10 ⁻⁶	3.8×10 ⁻⁵	5.75	4.87	3.10	0.00	0.88	5.75	3.98	46.46	25.66	3.54
(B)	7.5×10 ⁻⁶	1.5×10 ⁻⁵	7.5×10 ⁻⁵	3.52	5.28	2.56	0.64	3.04	3.68	4.16	38.24	27.36	11.52
(C)	7.5×10 ⁻⁶	2.3×10 ⁻⁵	2.3×10 ⁻⁴	1.92	5.85	2.88	1.82	8.73	2.50	4.03	22.74	28.12	21.40
(D)	7.5×10 ⁻⁶	3.0×10 ⁻⁵	6.0×10 ⁻⁴	1.17	5.21	2.33	2.21	11.41	1.72	3.50	17.61	26.99	27.85
(E)	7.5×10 ⁻⁶	3.0×10 ⁻⁵	6.0×10 ⁻⁴	1.17	5.21	2.33	2.21	11.41	1.72	3.50	17.61	26.99	27.85

% TOTAL ION FLUX

	PRESSURES in torr			m/e										
	INITIAL ION	ION	PENNING	15	27	37	39	43	45	127	141	142	143	157
	GAUGE	GAUGE	GAUGE											
	7.5×10 ⁻⁶	7.5×10 ⁻⁶	3.8×10 ⁻⁵	0.13	97.74	0.11	0.07	0.00	0.02	0.13	0.09	1.05	0.58	0.08
	7.5×10 ⁻⁶	1.5×10 ⁻⁵	7.5×10 ⁻⁵	0.22	93.75	0.33	0.16	0.04	0.19	0.23	0.26	2.39	1.71	0.72
	7.5×10 ⁻⁶	2.3×10 ⁻⁵	2.3×10 ⁻⁴	0.20	89.57	0.61	0.30	0.19	0.91	0.26	0.42	2.37	2.93	2.23
	7.5×10 ⁻⁶	3.0×10 ⁻⁵	6.0×10 ⁻⁴	0.19	83.70	0.85	0.38	0.36	1.86	0.28	0.57	2.87	4.40	4.54
	7.5×10 ⁻⁶	3.0×10 ⁻⁵	6.0×10 ⁻⁴	0.19	83.70	0.85	0.38	0.36	1.86	0.28	0.57	2.87	4.40	4.54

% SECONDARY ION FLUX Vs. PRESSURE

+ = 15 = CH₃⁺
 x = 143 = CH₃IH⁺
 Δ = 157 = (CH₃)₂I⁺



% SECONDARY ION FLUX

	PRESSURES in torr			m/e		
	INITIAL ION	ION	PENNING			
	GAUGE	GAUGE	GAUGE	15	143	157
(A)	7.5 × 10 ⁻⁶	1.1 × 10 ⁻⁵	3.0 × 10 ⁻⁵	5.41	92.19	2.40
(B)	7.5 × 10 ⁻⁶	1.5 × 10 ⁻⁵	7.5 × 10 ⁻⁵	2.51	87.62	9.87
(C)	7.5 × 10 ⁻⁶	1.9 × 10 ⁻⁵	1.5 × 10 ⁻⁴	0.00	77.55	22.45
(D)	7.5 × 10 ⁻⁶	2.3 × 10 ⁻⁵	2.3 × 10 ⁻⁴	0.00	63.37	36.63

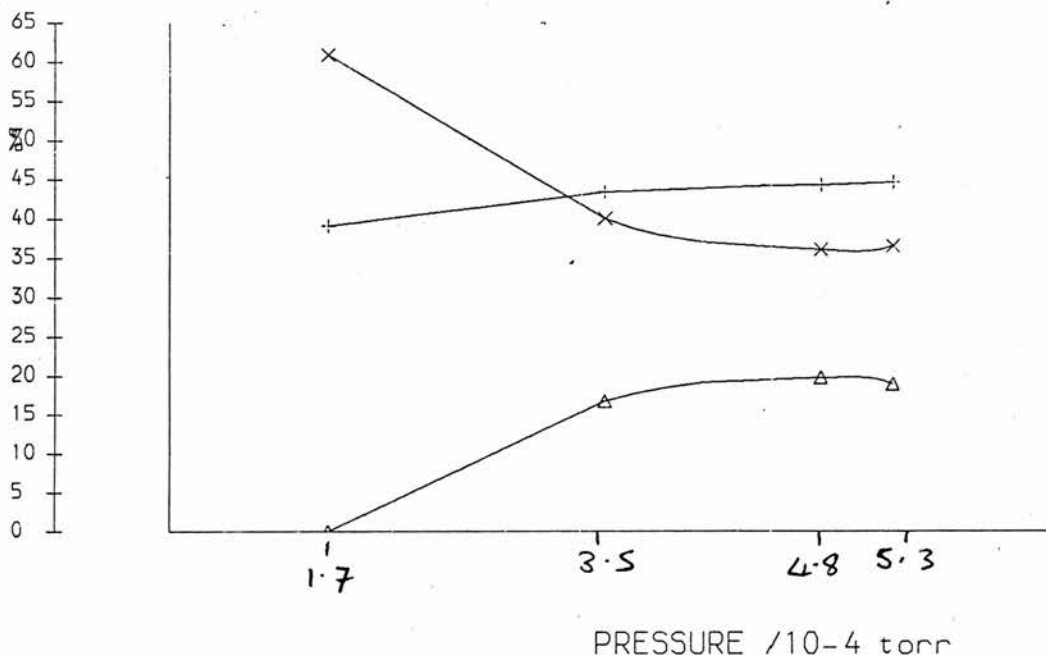
% TOTAL ION FLUX

	PRESSURES in torr			m/e			
	INITIAL ION	ION	PENNING				
	GAUGE	GAUGE	GAUGE	15	29	143	157
	7.5 × 10 ⁻⁶	1.1 × 10 ⁻⁵	3.0 × 10 ⁻⁵	0.18	96.67	3.07	0.08
	7.5 × 10 ⁻⁶	1.5 × 10 ⁻⁵	7.5 × 10 ⁻⁵	0.40	84.09	13.94	1.57
	7.5 × 10 ⁻⁶	1.9 × 10 ⁻⁵	1.5 × 10 ⁻⁴	0.00	73.54	20.52	5.94
	7.5 × 10 ⁻⁶	2.3 × 10 ⁻⁵	2.3 × 10 ⁻⁴	0.00	61.83	24.19	13.98

CH₃Cl⁺ + CH₃-O-CH₃ QUINQUA QUADRUPOLE²⁶⁵

% SECONDARY ION FLUX Vs. PRESSURE

+ = 45 C₂H₅O⁺
 x = 47 C₂H₄O⁺
 Δ = 61 (CH₃)₃O⁺



CH₃Cl⁺ + CH₃-O-CH₃

% SECONDARY ION FLUX

	PRESSURES in torr			m/e		
	1ST PENNING GAUGE	2ND PENNING GAUGE	3RD PENNING GAUGE	45	47	61
(A)	8.3 × 10 ⁻⁵	1.1 × 10 ⁻⁴	1.7 × 10 ⁻⁴	39.13	60.87	0.00
(B)	1.5 × 10 ⁻⁴	2.0 × 10 ⁻⁴	3.5 × 10 ⁻⁴	43.33	40.00	16.67
(C)	2.0 × 10 ⁻⁴	2.8 × 10 ⁻⁴	4.8 × 10 ⁻⁴	44.26	36.07	19.67
(D)	2.5 × 10 ⁻⁴	3.5 × 10 ⁻⁴	5.3 × 10 ⁻⁴	44.59	36.49	18.92
(E)	2.5 × 10 ⁻⁴	3.5 × 10 ⁻⁴	5.3 × 10 ⁻⁴	44.59	36.49	18.92

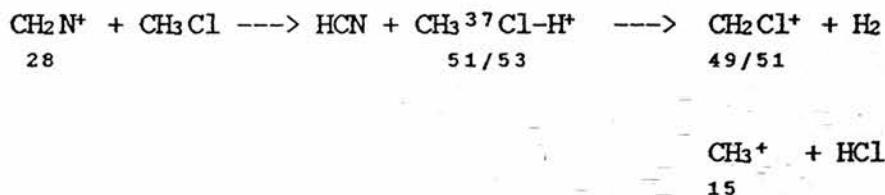
CH₃Cl⁺ + CH₃-O-CH₃

% TOTAL ION FLUX

	PRESSURES in torr			m/e			
	1ST PENNING GAUGE	2ND PENNING GAUGE	3RD PENNING GAUGE	45	47	51	61
	8.3 × 10 ⁻⁵	1.1 × 10 ⁻⁴	1.7 × 10 ⁻⁴	2.79	4.33	92.88	0.00
	1.5 × 10 ⁻⁴	2.0 × 10 ⁻⁴	3.5 × 10 ⁻⁴	19.26	17.78	55.56	7.41
	2.0 × 10 ⁻⁴	2.8 × 10 ⁻⁴	4.8 × 10 ⁻⁴	21.60	17.60	51.20	9.60
	2.5 × 10 ⁻⁴	3.5 × 10 ⁻⁴	5.3 × 10 ⁻⁴	22.92	18.75	48.61	9.72
	2.5 × 10 ⁻⁴	3.5 × 10 ⁻⁴	5.3 × 10 ⁻⁴	22.92	18.75	48.61	9.72

DISCUSSIONREACTIONS OF IONS WITH CHLOROMETHANECH₂N⁺ INTO CH₃Cl

The reaction of CH₂N⁺ with chloromethane produced ions of mass 15⁺ = CH₃⁺, 49 = CH₂³⁵Cl⁺, 51 = CH₃³⁵Cl-H⁺ and CH₂³⁷Cl⁺ and 53 = CH₃³⁷Cl-H⁺. These ions are consistent with protonation and fragmentation of chloromethane.

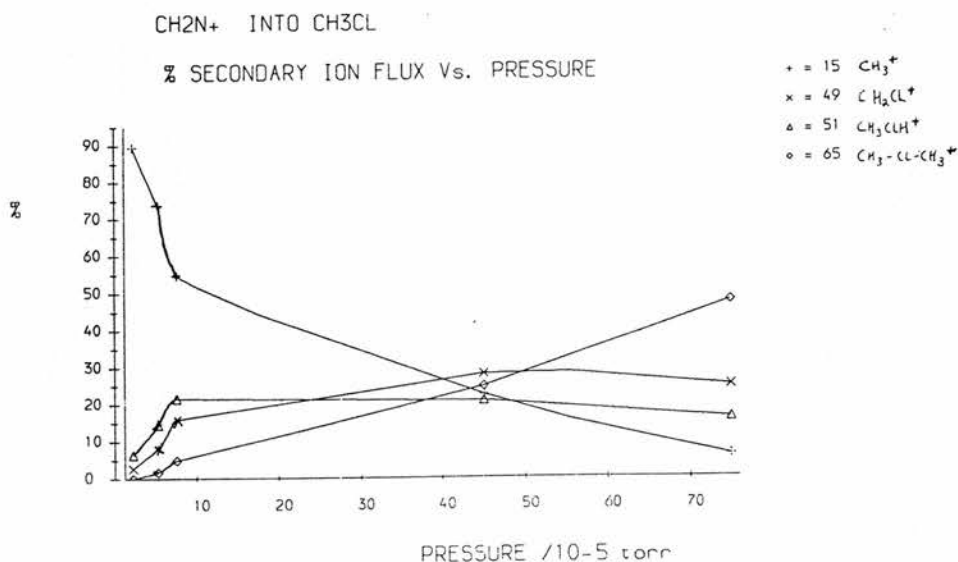


There is an overlap of the CH₂³⁷Cl⁺ and CH₃³⁵Cl-H⁺ peaks as the triple quadrupole cannot resolve to a fraction of a dalton. The values of intensity for each ion containing chlorine need to be corrected to take account of the isotope peak. The isotopes of chlorine are ³⁵Cl (75.53%) and ³⁷Cl (24.47%). The ion of mass 49 must have a companion peak of mass 51 which should be of about one third of the intensity. The ion of mass 53, being attributed to CH₃³⁷Cl-H⁺, must be one third of the peak of mass 51 due to the CH₃³⁵Cl-H⁺ ion. If the intensity of the peak of mass 49 is multiplied by 1.333 this should give the total intensity of the CH₂Cl⁺ ions. If the intensity of the peak of mass 53 is multiplied by 4 this should give the total intensity of CH₃Cl-H⁺ ions. This

was done for the results from all experiments. It was found that the total peak height calculated for the ions of mass 51 was very close to the actual measured peak height, and so this procedure was found to be a valid approach to distinguishing between the relative intensities of the overlapping peaks.

Ions of mass 65 and 67 were observed at higher pressures. The intensities of these peaks were combined to give a total intensity for the dimethyl chloronium ions.

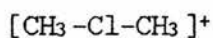
A graph of corrected values was plotted.



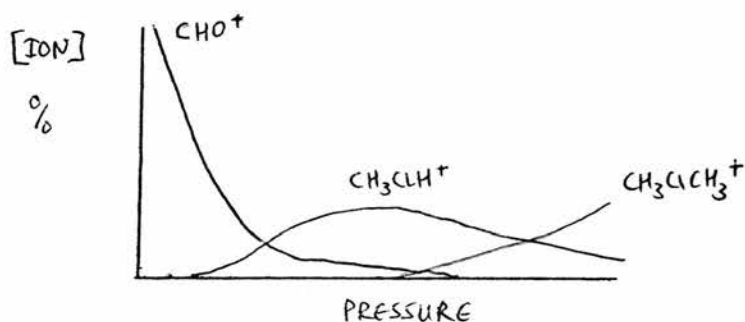
As the intensity of both CH₃⁺ and CH₃Cl-H⁺ ions decreases as the amount of CH₃-Cl-CH₃⁺ ions increases, it is not possible to identify which of these ions is the precursor of the dimethyl chloronium ions from this experiment.



The reaction of CDO^+ ions with chloromethane produced protonated chloromethane ions of mass 51 and 53 and at higher pressures ions of mass 65 and 67 which were identified as the isotopes of the dimethyl chloronium ion.



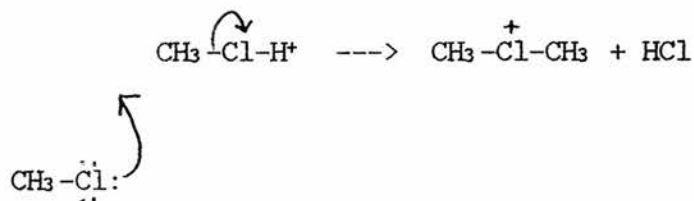
The dimethyl chloronium ions were always found to be of a higher order than the protonated chloromethane ions.



This would suggest that protonated chloromethane reacts with chloromethane to produce the dimethyl chloronium ion and hydrogen chloride.



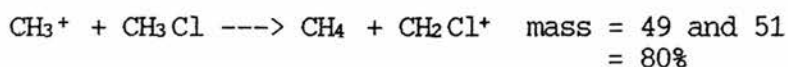
A mechanism similar to that proposed for the reaction of methyl oxonium ions with methanol can be proposed to account for this reaction.



Several reactions were undertaken in an attempt to prove this mechanism.

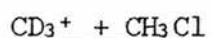


The dominant reaction is a hydride abstraction to form methane and CH₂Cl⁺ ions.

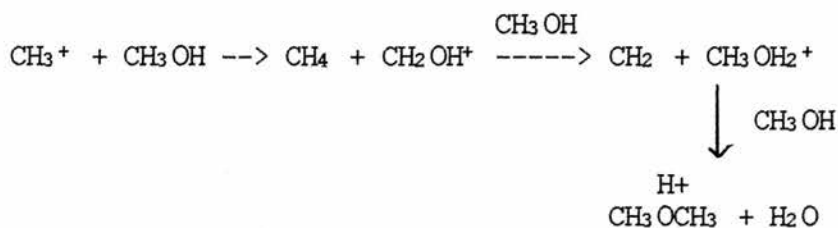


(A halide abstraction would not be observed because the product ion has the same mass as the primary ions.)

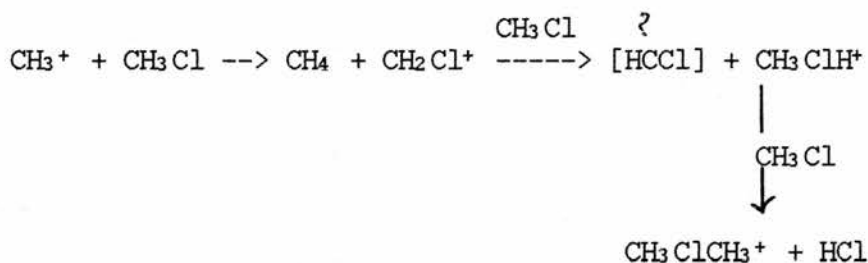
Also present were ions of mass 27 (C₂H₃⁺: max = 12%), 29 (C₂H₅⁺: max = 3%), 39 (C₃H₃⁺: max = 0.4%), 41 (C₃H₅⁺: max = 0.1%), 49 (CH₂Cl⁺: max = 90%), 51 (CH₃ClH⁺: max = 5%), 65 + 67 (C₂H₆Cl⁺: max = 2%). The pathways to these ions were investigated.



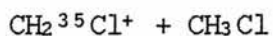
The reaction of CD₃⁺ with chloromethane did not produce any deuterated dimethyl chloronium ions, CD₃ClCH₃⁺. This indicates that dimethyl chloronium ions are not formed by direct addition of methyl cations with chloromethane. The largest ion was CH₂Cl⁺. By analogy with the methanol reaction the largest ion produced in the reaction of methyl cations was CH₂OH⁺. The CH₂OH⁺ ion then protonated methanol to give methyl oxonium ions and hence dimethyl oxonium ions.



An analogous mechanism for the reaction of chloromethane would require that the CH_2Cl^+ ion would protonate a chloromethane molecule. This reaction does not look favourable as the neutral produced would be $[\text{HCCl}]$.

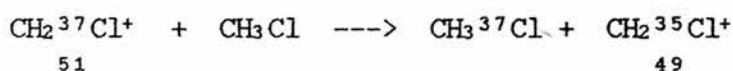
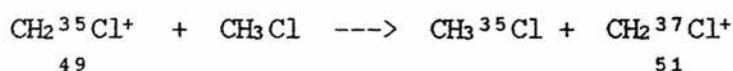


An experiment was done in which CH_2Cl^+ ions were separated from dichloromethane (a better source of the CH_2Cl^+ ion than CH_3Cl) and reacted with chloromethane in the second quadrupole.



This reaction produced only one ion of mass 51 which was due to hydride abstraction.

The reaction of the ^{37}Cl isotope produced a small peak of mass 49 indicating that a hydride abstraction reaction had taken place.



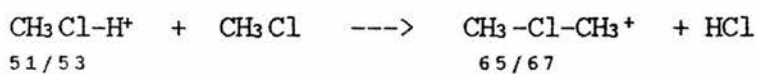
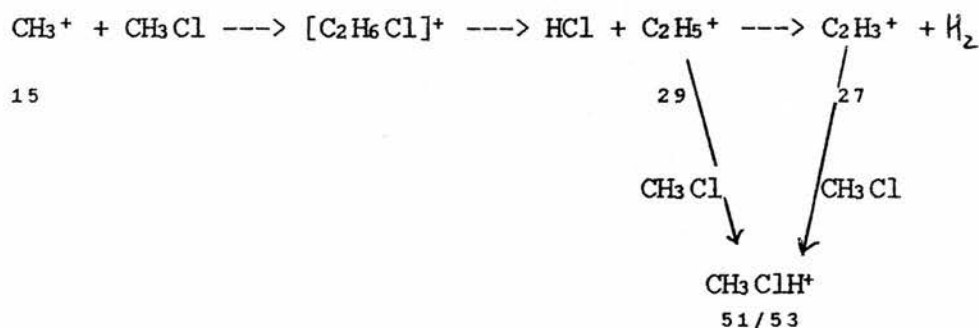
The elimination of this route to protonated chloromethane posed a couple of new questions.

1. How is the dimethyl chloronium ion produced in the reaction of methyl cation with chloromethane?

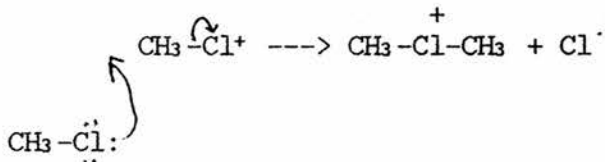
It was noticed that at low pressures the major ions were CH_2Cl^+ , C_2H_3^+ and C_2H_5^+ . CH_2Cl^+ has already been discounted as a precursor to methyl chloronium ions.

C_2H_3^+ and C_2H_5^+ are both known protonating ions.

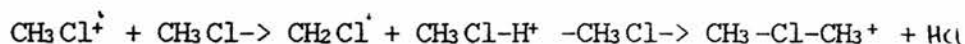
Experiments were carried out in which C_2H_5^+ ions from the electron bombardment of ethane and C_2H_3^+ , from ethene, were reacted with chloromethane. In both reactions methyl chloronium was the major ionic product at low pressures. Dimethyl chloronium ions were observed and became the largest product at the highest pressures. This leads to the conclusion that dimethyl chloronium ions are formed from the reaction of methyl cations with chloromethane by the route outlined below.



2) The second question that arose from this work centred round an alternative mechanism for the formation of dimethyl chloronium ions. During the initial investigations several experiments had been done in which a chemically unreactive ion, such as Xenon⁺, was passed into chloromethane. Charge exchange was a major reaction. In all experiments large amounts of dimethyl chloronium ions were observed. How were they being formed? Could the elimination of a chlorine atom from the reaction of chloromethane radical ion with chloromethane be responsible for the production of dimethyl chloronium ions?



To test this hypothesis chloromethane ions were reacted with chloromethane. The results from these experiments indicate that chloromethane ions can react with chloromethane molecules to produce methyl chloronium ions by a self-protonation reaction. (As discussed in Chapter 2 page 57) The methyl chloronium ions would then react with a chloronium molecule to form dimethyl chloronium ions and HCl.

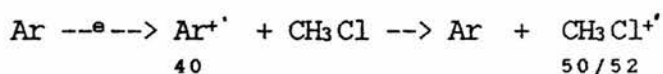


50/52

51/53

65/67

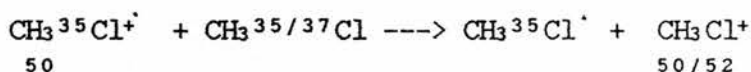
An experiment was done using the quinquapole mass spectrometer in which Argon ions were selected in the first quad and passed into chloromethane in the second quadrupole. Chloromethane ions were the major product - arising from charge exchange reactions.



40

50/52

The ion containing the ^{35}Cl isotope was selected from the third quadrupole and put into chloromethane in the fourth quadrupole. Ions of mass 50, 51, 52, 53, 65 and 67 were observed in the fifth quadrupole. The ions of mass 52 were formed by simple charge exchange reactions.

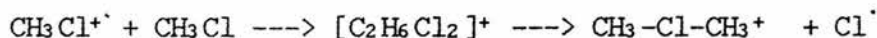


50

50/52

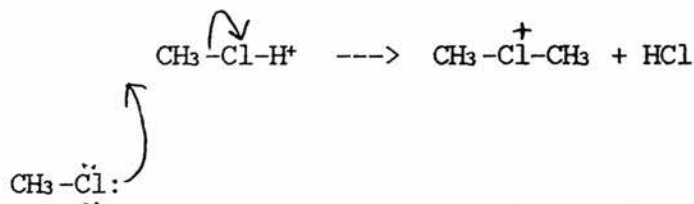
The ions of mass 51 and 53 were methyl chloronium ions formed by the self-protonation reaction. The dimethyl chloronium ions, 65 and 67, were only formed at high pressures and were thought to arise from the reaction of methyl chloronium ions with chloromethane. Because the reaction of chloromethane ions with chloromethane produces methyl chloronium ions, it is not possible, without using labelled chloromethane, to investigate the possible formation of dimethyl chloronium ions by elimination of a chlorine atom from the addition

complex of a chloronium ion with a chloromethane molecule.



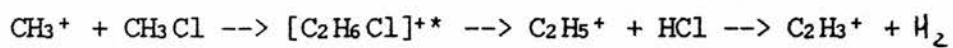
As there was no CD_3Cl or $^{13}\text{CH}_3\text{Cl}$ available in the department this was not investigated further.

The conclusions that can be drawn from this section are that the methyl chloronium ions, $\text{CH}_3\text{Cl}-\text{H}^+$, can be formed at the pressures studied. Dimethyl chloronium ions can also be formed. The formation of the dimethyl chloronium ions by loss of chlorine atom from a $[\text{C}_2\text{H}_6\text{Cl}_2]^+$ complex cannot be ruled out. The mechanism involving elimination of HCl from $\text{CH}_3\text{Cl}-\text{H}^+$ by addition of CH_3Cl has been shown to occur.

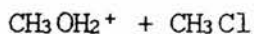


The formation of dimethyl chloronium ions in the reaction of methyl cations and chloromethane was attributed to the reaction of C_2H_n^+ ions ($n=3$ or 5) with chloromethane. That a C_2 species was a precursor to the formation of dimethyl chloronium ions would indicate that dimethyl chloronium ions could not be considered to be the precursor to C_2 species. The distribution of deuterium and hydrogen in the C_2 species when CD_3^+ ions were reacted with CH_3Cl would indicate that the C_2

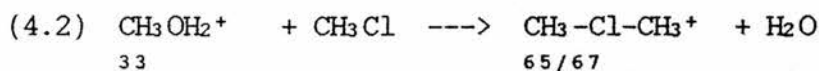
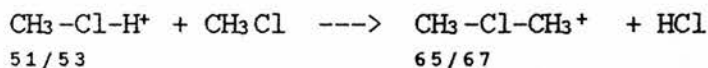
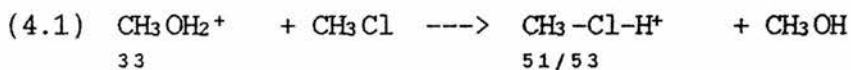
species arose from addition of the methyl cation with a chloromethane molecule with elimination of HCl. This is a mechanism that would be viable for both chloromethane and methanol.



REACTIONS OF METHYL OXONIUM IONS WITH CHLOROMETHANE



Methyl oxonium ions, formed by reaction within the ionisation chamber, were separated from the other ions in the first quadrupole and passed into chloromethane gas. The main products were methyl chloronium ions of mass 51 and 53, fragment ions of mass 49 and $51 - \text{CH}_2\text{Cl}^+$, and $15 - \text{CH}_3^+$. Dimethyl chloronium ions were observed at higher pressures. They could be formed by two routes.



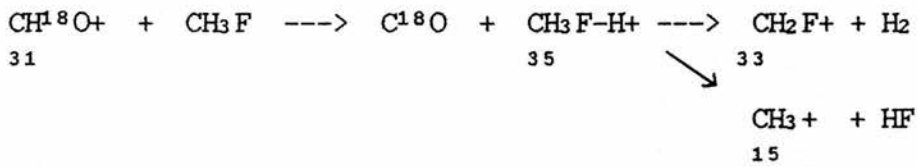
To investigate the two possible routes the reaction was repeated using deuterated methyl oxonium ions. If dimethyl chloronium ions were only formed by the reaction of methyl oxonium ions with chloromethane (4.2), then $\text{CD}_3\text{-Cl-CH}_3^+$ ions would be produced. If dimethyl chloronium ions were only formed via the reaction of methyl chloronium ions with chloromethane (4.1), then the $\text{CH}_3\text{-Cl-CH}_3^+$ dimethyl chloronium ions would be formed. That a mixture of ions of mass 65/67 and 68/70 were observed indicates that both routes are in operation.

REACTIONS OF IONS WITH FLUOROMETHANE

The reaction of CH^{18}O^+ , CH_2N^+ , CH_3^+ and CD_3^+ ions with fluoromethane were studied.

CH^{18}O^+

The products at low pressures were protonated fluoromethane $\text{CH}_3\text{F-H}^+$ (mass=35) and its fragment ions CH_2F^+ (mass=33) and CH_3^+ (mass=15).



As the pressure of fluoromethane was increased the dimethyl fluoronium ion was observed. Both CH_3^+ and $\text{CH}_3\text{F-H}^+$ ions diminish as the dimethyl fluoronium ions are formed so neither of the mechanisms in figure 4.2 can be ruled out at this stage.

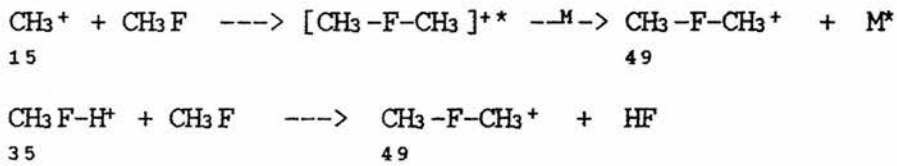
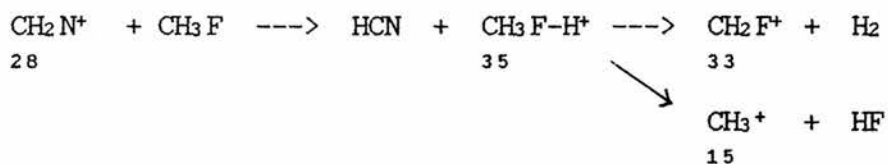


FIG 4.2.

Small peaks of mass 45, 51 and 61 were observed at the highest pressures. These will be discussed later.

CH₂N⁺

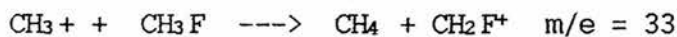
The ions produced from the reaction of CH₂N⁺ ions with fluoromethane were initially similar to those produced from the reaction of CHO⁺ ions with fluoromethane. The main products were protonated fluoromethane and its fragment ions. The tertiary dimethyl fluoronium ion (mass=49) CH₃-F-CH₃⁺ was also important.



In addition to the ions produced in the CHO⁺ reaction there were many more minor ions produced in the reaction of CH₂N⁺ ions. These include ions of mass 29, 45, 47, 51 and 61. These will be discussed later.

CH₃⁺

The main reaction of CH₃⁺ with fluoromethane was hydride abstraction to produce methane and the CH₂F⁺ ion.



The other ions had a mass of 27 and 29 which were due to C₂H₃⁺ and C₂H₅⁺ as was found to be the case with the reaction of the methyl carbocation with methanol and chloromethane.



where X = OH, Cl or F

Small amounts of other ions were observed. They were of masses :-

- 31 which was probably due to the further fragmentation of the CH_2F^+ ion to CF^+ and H_2 ,
- 34 which was due to charge exchange reaction CH_3F^+ ,
- 35 protonated fluoromethane $\text{CH}_3\text{F}-\text{H}^+$,
- 49 dimethyl fluoronium ion $(\text{CH}_3)_2-\text{F}^+$ and
- 43, 45 and 47 which will be discussed later.

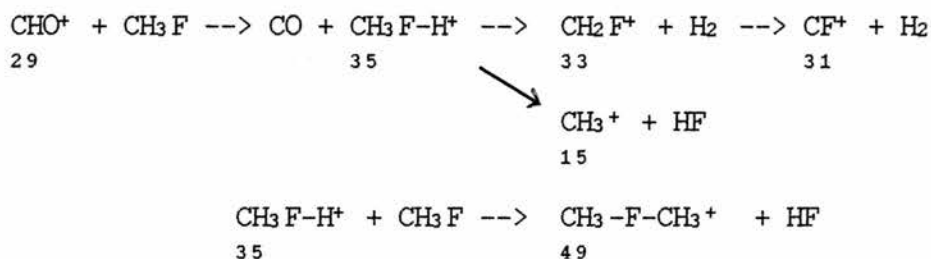
CD_3^+

The reaction of deuterated methyl cations with fluoromethane elucidated some of the mechanisms involved by indicating that the dimethyl fluoronium ions formed contained no deuterium. The direct addition of a methyl ion with fluoromethane to form dimethyl fluoronium ion as an adduct can be ruled out.

Of the minor ions small peaks of mass 48 and 46 occurred with the deuterated methyl reaction but not with the protonated methyl reaction. It should be noted that the pressure of fluoromethane in the two experiments was not identical. The deuterated methyl was reacted with a higher pressure of fluoromethane. It can be suggested that the additional ions formed in the deuterated methyl cation reaction were due to deuterium/hydrogen exchange occurring at the elevated pressure, and as such do not

give an indication of the mechanisms operating in the main reactions.

It can be concluded that the main reactions of fluoromethane are identical to those of chloromethane.



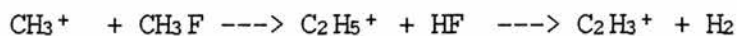
The main difference between the reactions of fluoromethane and chloromethane was that the CH_2F^+ ion reacts with CH_3F to produce some minor peaks whilst CH_2Cl^+ ions were effectively unreactive with CH_3Cl . (refer to page 270, chapter 4)

$\text{CH}_2\text{F}^+ + \text{CH}_3\text{F}$

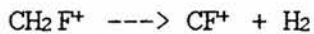
The reaction of CH_2F^+ ions with CH_3F produced many of the minor ions that had been present in the reactions previously discussed. The ion of mass 15, CH_3^+ , occurred as almost 50% of the ion products at low pressures. This would indicate that it was a secondary ion and could arise from a fluoride abstraction reaction.



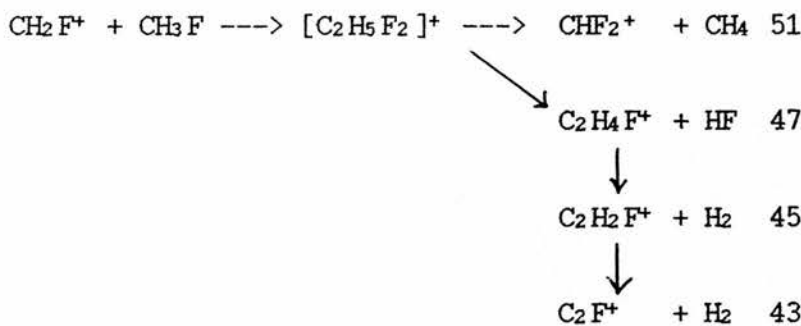
The CH_3^+ ions then react to form C_2H_5^+ (29) and C_2H_3^+ (27) ions as with chloromethane.



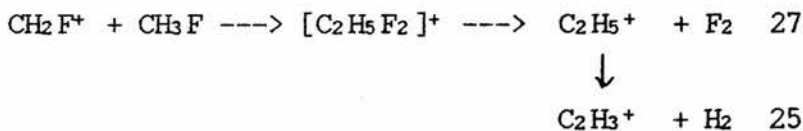
The ion of mass 31 arose from the fragmentation of the primary ion. It was a very important ion at the lower pressures but diminishes as the pressure increases.



A main ion which accounted for some 22% of the ions produced at the lowest pressure and increases to a maximum value of 43% as the pressure increases had a mass of 45. Other ions that were related to it were also formed by addition with elimination of the CH_2F^+ primary ion with a molecule of fluoromethane.

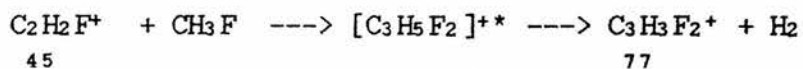
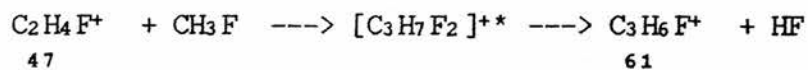


The loss of F_2 from this adduct could also be responsible for the ions of C_2H_5^+ and C_2H_3^+ .



Ions of mass 61 and 77 were formed at the higher pressures indicating that they were tertiary ions. They can be accounted for by the following reactions of

secondary ions with fluoromethane.



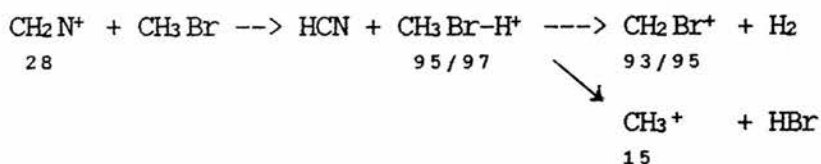
There may well be other routes to the production of these minor ions but as they were not important in the overall scheme they were not investigated further.

REACTIONS OF IONS WITH BROMOMETHANE

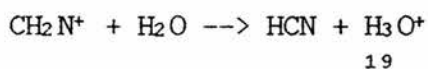
The reactions of ions with bromomethane were carried out with the additional safety precautions described in the experimental section. Because of the high reactivity of bromomethane vapour these reactions were kept to a minimum. Only two ions were used CH_2N^+ and CH_3^+ . The ions produced in these reactions fit into the same general pattern as had been found for the reactions of chloromethane and fluoromethane.

CH_2N^+ INTO CH_3Br

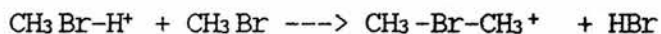
Protonation of bromomethane produced the methyl bromonium ions of masses 95 and 97 corresponding to the two isotopes of bromine - ^{79}Br (50.54%) and ^{81}Br (49.46%). These ions fragmented to CH_2Br^+ ions of mass 93 and 95 which overlapped. A fragment of mass 15, CH_3^+ , was also observed.



A significantly large amount of an ion of mass 19 was present at all pressures. It was thought that this was due to protonation of water which was present in the bromomethane sample.

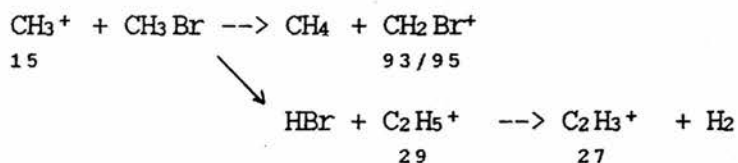


The dimethyl bromonium ions were observed at higher pressures at a 1:1 ratio.



CH₃⁺ into CH₃Br

The reaction of methyl cations with bromomethane produced analogous ions to the reaction of methyl cations with chloromethane. The main products were CH₂Br⁺ ions and C₂H_n⁺ ions (n=3,4 or 5).



Bromomethane radical cations were also present with masses of 94 and 96.

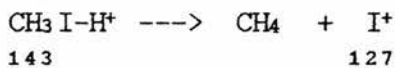
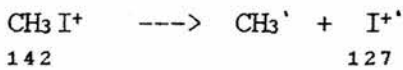
A small amount of methyl bromonium ions were observed as the pressure increased and, at the highest pressure, ions of mass 109 and 111 due to dimethyl bromonium ions were found.

REACTIONS OF IONS WITH IODOMETHANE

The reactions of iodomethane followed a similar pattern to fluoromethane and bromomethane with a few exceptions.

The $\text{CH}_3\text{I-H}^+$ ion was produced by the reaction of CH_2N^+ ions with iodomethane. A fragment ion of mass 15, CH_3^+ , was observed but no ion corresponding to CH_2I^+ was observed. All the other $\text{CH}_3\text{X-H}^+$ ions, where X= OH, F, Cl or Br, fragmented by loss of H_2 .

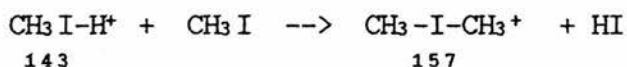
Also present in these reactions were the ions due to iodomethane radical cations and iodine cations. Iodine cations could arise from cleavage of the iodomethane cation or from elimination of methane from the methyl iodonium ions.



This reaction could be studied in the quinquapole mass spectrometer. If this reaction was repeated using the first three quadrupoles of the quinquapole mass spectrometer, then the iodomethane radical cation could then be separated and put into an inert collision gas in the fourth quadrupole. If iodine cations were observed it would indicate that they could arise from the fragmentation of CH_3I^+ ions. The ions

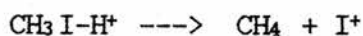
corresponding to methyl iodonium could then be separated and put into a gas in the fourth quadrupole to see if iodine cations were formed from the fragmentation of $\text{CH}_3\text{I-H}^+$ ions.

In the experiment that was carried out at a higher pressure the dimethyl iodonium ion of mass 157 was produced.



The products from the reaction of CH_3^+ and CD_3^+ ions were as for the other halides except that the iodomethane cation produced by charge exchange was the dominant ion. CH_2I^+ ions were also present as were C_2H_n^+ ions ($n=3,4$ or 5), $\text{CH}_3\text{I-H}^+$ and $\text{CH}_3\text{-I-CH}_3^+$ ions.

It should be noted that the large amount of iodomethane ions obtained in these experiments are not matched by a correspondingly large quantity of iodine cations. This would suggest that the I^+ ions observed arise from the rearrangement and fragmentation of the methyl iodonium ion.

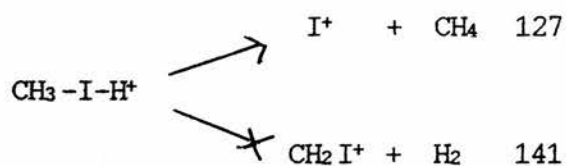


This rearrangement could be studied in the quinquadrupole mass spectrometer and if found to occur could explain the large quantities of methane that are formed

in the reaction of iodomethane over ZSM-5 catalyst.

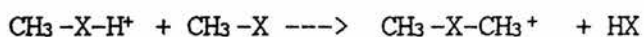
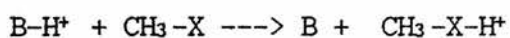
(Refer to chapter 5, page 325)

That no CH_2I^+ ions were observed as fragment ions from the methyl iodonium ions may imply nothing more than that there is a more energetically favourable fragmentation - such as the rearrangement and fragmentation to methane and the iodine cation.



CONCLUSIONS

The overall conclusion to be drawn from this chapter is that all the halogenomethane molecules can be protonated to form methyl halonium ions, $\text{CH}_3\text{X-H}^+$. These ions are thought to react further with another molecule of halogenomethane to produce dimethyl halonium ions.

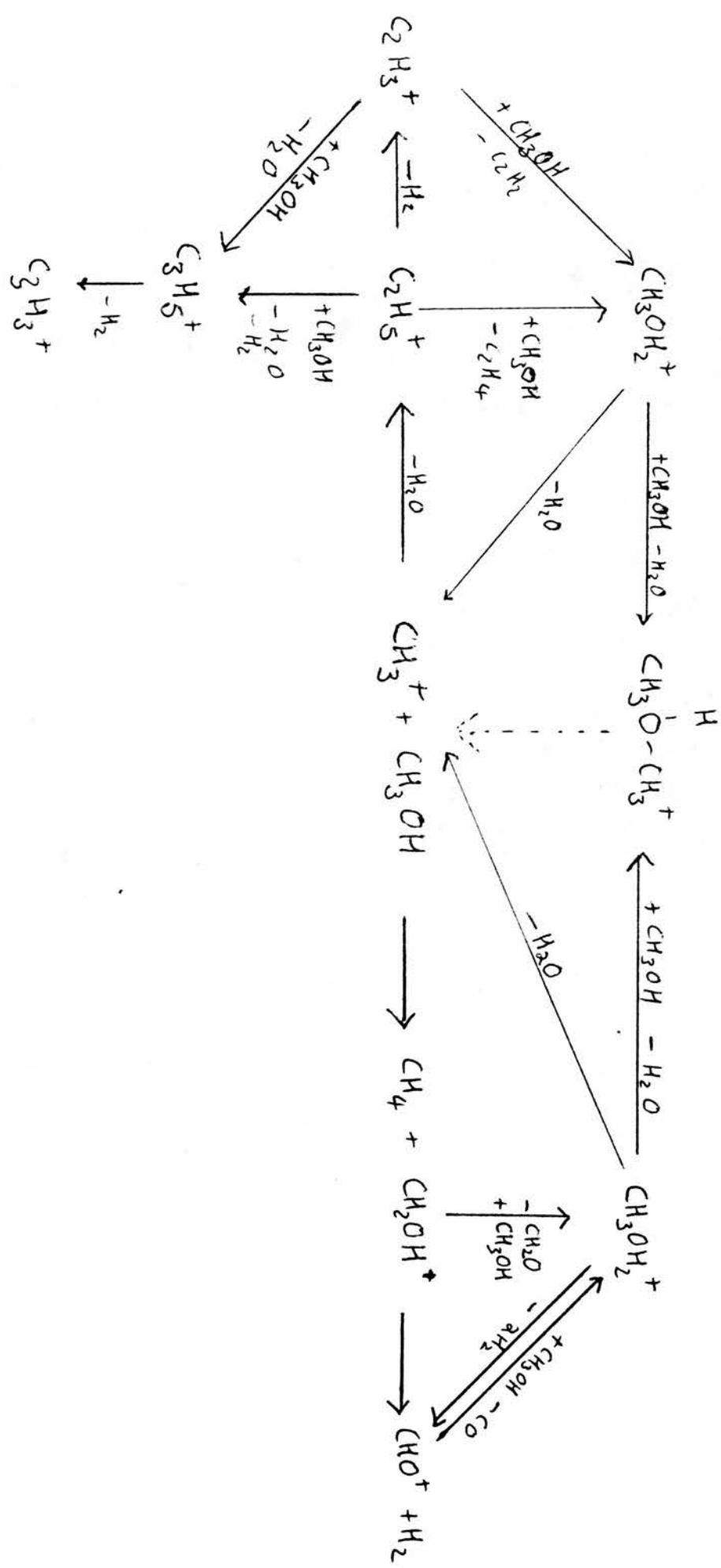


In this respect the reactions of the halogenomethane species were found to be identical to those of the oxonium ions discussed in chapter 3.

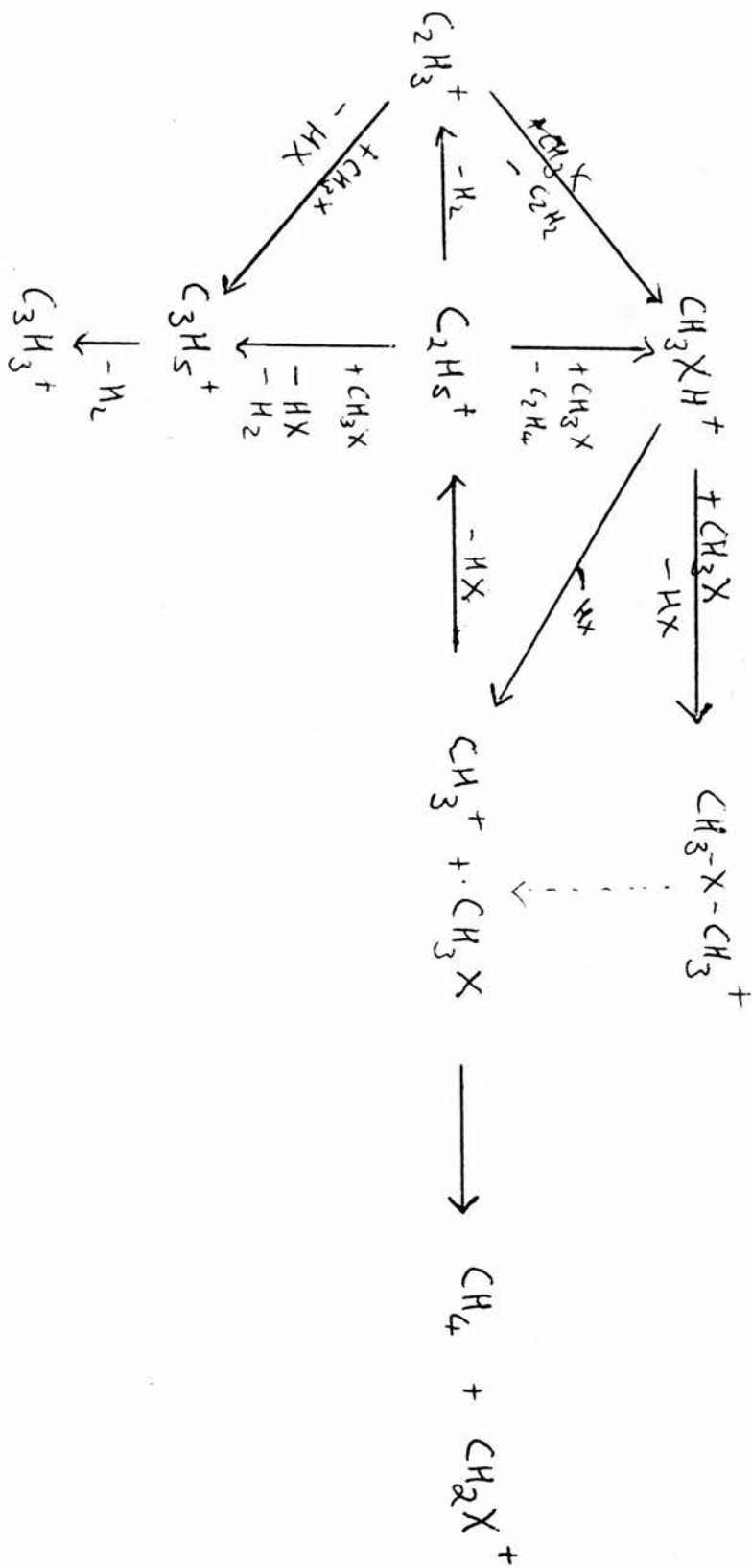
OVERALL CONCLUSIONS AT END OF CHAPTER 4.

The halogenomethane species differed from the oxonium species in one important respect. The reaction of methyl cations with the oxygen containing species could produce an oxonium ion. In this way dimethyl oxonium ions could be regarded as possible precursors to C₂ species. With the reaction of methyl cations with any of the halogenomethanes the dimethyl halonium ions that were formed could only be accounted for by a reaction involving C₂ species. This would suggest that the halonium ions were not a fundamental step in the production of the first C-C bond. The reactions represented in the diagrams 4.1 and 4.2 summarize the reaction pathways that were found to be operating. The minor reactions of the halogen containing ions have been omitted for clarity.

IN METHANOL



IN HALOGENOMETHANES.



CHAPTER FIVEHALOGENOMETHANE REACTIONS OVER ZSM-5

CHAPTER FIVE

CONTAINING WORK CARRIED OUT AT

B.P. RESEARCH CENTRE, SUNBURY-ON-THAMES, LONDON

BETWEEN 10th AND 29th MARCH 1988

UNDER THE SUPERVISION OF Dr. S. WADE.

CONTENTSZEOLITE SYNTHESIS

METHOD

EXPERIMENTAL APPARATUS

REAGENTS

ANALYSIS

ZEOLITE REACTION EXPERIMENTS

1) CH₃Cl

2) CH₃CH₂Cl

3) CH₃Br

RESULTSDISCUSSION

INTRODUCTION

The aim of the work reported in this chapter was to study the reactions of halogenomethanes over ZSM-5 catalyst in a small scale fixed bed reactor and to compare the products with those obtained from the reaction of methanol in previous investigations.

Previous reports of the reactions of chloromethane and iodomethane over ZSM-5 were referenced in the introductions to chapters three and four.¹⁹⁵⁻¹⁹⁹ No reports of the reactions of fluoromethane or bromomethane have been reported. It was hoped to study the reactions of all halogenomethanes over ZSM-5 so that direct comparisons could be made. However, at the time of these experiments, fluoromethane cost £1150.00 for a lecture bottle. As time did not permit the synthesis of fluoromethane by the method used in chapter four this reaction was not studied. Time did not allow the reaction of iodomethane to be studied. In the discussion the results from the reaction of iodomethane over ZSM-5 by Hunter and Hutchings¹⁴⁷⁻¹⁴⁸ will be used for comparison.

ZEOLITE SYNTHESIS

The aim was to synthesise two samples of H-ZSM-5 catalyst for the subsequent experiments. They would have Si:Al ratios of around 30:1 and 120:1 respectively. The silica used was in the form of Ludox, a commercially available aqueous colloidal suspension of silica (40% by weight). The aluminium was in the form of sodium aluminate. Tetra propyl ammonium hydroxide (TPA) was used as the template. On heating in the oven a hydrothermal synthesis of the zeolite occurs. This zeolite was then dried of excess water by heating it in an oven at 100°C. On heating at 550°C for 18 hours the propyl sidechains were burnt off. The sodium form of ZSM-5 in which the cation sites were occupied by sodium ions was produced. The sodium ions were exchanged for ammonium ions by washing the zeolite in solutions of ammonium nitrate. By this stage the zeolite was the ammonium form NH_4 -ZSM-5. On heating in an oven at 400°C the ammonia was driven off to yield the hydrogen form of the catalyst H-ZSM-5.

METHODGSW 1 Aiming for Si:Al ratio of 30:1

0.54g of sodium aluminate, 0.36g of sodium hydroxide and 17.95g of water were mixed in a beaker and stirred with a magnetic stirrer until all the aluminate had dissolved.

29.66g of SiO₂ Ludox (40% silica by weight in suspension), 33.52g of 20% tetra propyl ammonium hydroxide (TPA) and 17.95g of water were likewise mixed.

When homogeneous the ludox/TPA mixture was poured into the beaker containing sodium aluminate. A white coagulation appeared which became a white gel on stirring for 1½ hours. This gel was transferred to a bomb which was sealed with a greased top and placed in a rotisserie in an oven at 186°C for 67 hours and 39 minutes (3 days).

On removing the bomb from the oven it was quenched in cold water and opened. The zeolite was filtered at a Buchner funnel and washed with distilled water then dried in an oven at 100°C for 20 minutes and weighed. The sample was further dried in an oven at 40°C for 1½ hours and then at 100°C for 1 hour before being placed in a crucible and calcined in an oven at 550°C for 18½ hours.

The zeolite, after weighing, was stirred for 1 hour in a 0.1M ammonium nitrate solution. The partially exchanged zeolite was filtered and washed with distilled water. This exchange process was repeated three times. The fully exchanged zeolite was then dried in a furnace at 400°C for 15 3/4 hours. This produced the hydrogen form of the zeolite catalyst - H-ZSM-5.

This process was also done in tandem to produce a zeolite with a Si:Al ratio of around 120:1. All procedures were identical and all quantities the same except that 0.14g of sodium aluminate and 0.63g of sodium hydroxide were used.

The resultant zeolites are hereafter referred to by their BP reference numbers GSW 1 (Si:Al=30:1) and GSW 2 (Si:Al=120:1).

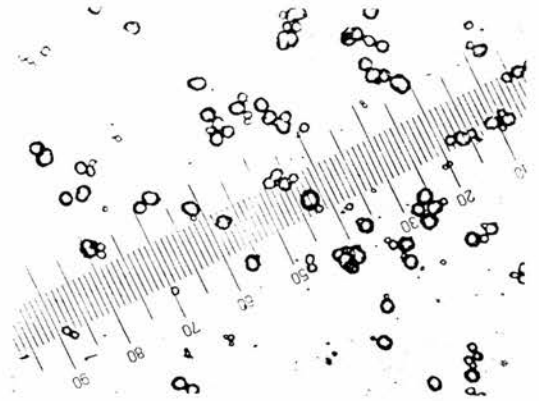
The zeolites were smeared onto a slide and photographed through a Dialux 20 (Leitz Wetzlar) magnifier with a WILD MPS II Camera attachment. The photographs show the crystals to have a high degree of uniformity in size.

Photograph 5.1 is GSW1 magnified by 320 times so that one division equals 5μ .

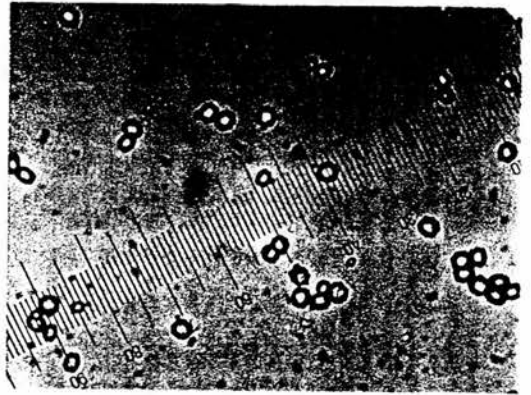
Photograph 5.2 is GSW2 also magnified by 320 times.

Photograph 5.3 is GSW2 magnified by 200 times so that one division equals 3μ .

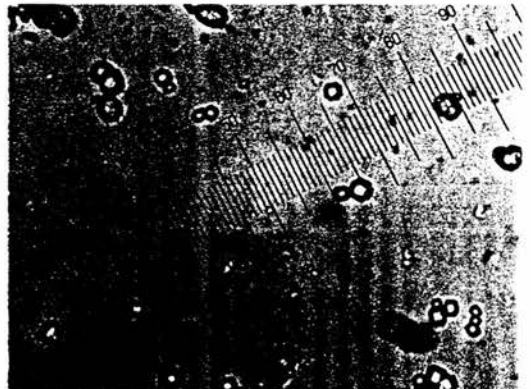
P. 5.3



P. 5.2



P. 5.1



EXPERIMENTAL APPARATUS

The Gas Chromatographs used in the following experiments had the following specifications.

G.C. No. 342824

Pye Unicam PU4500 Chromatograph by Philips with a PU4751 Valve Oven by Philips and a PU4810 Computing Integrator and both a Thermal Conductivity and a Flame Ionization Detector
The carrier was Helium and sample tubes were pressurised to 15lb/in²

Attenuation = 4 x 1

Temperatures:- Injector = 151°C

Detector = 122°C

Column = 99°C isothermal.

G.C. No. 348890

Pye Unicam PU4500 Chromatograph by Philips with a Flame ionisation detector and a PU4811 Computing Integrator by Philips.

The sample tube was pressurised to 10lb/in² with Argon

Attenuation = 64 x 10

Temperatures = Injector = 221°C

Detector = 270°C

Column = 111°C isothermal

Splitter vent = 50ml/min

Inlet pressure = 1.3 barg

Argon pressure = 7 psig

Both G.C.'s were equipped with a Valco multichannel valve system with multiple columns to facilitate separation of the wide range of reactant and product gases.

A diagram of the experimental rig is shown in diagram

5.2.

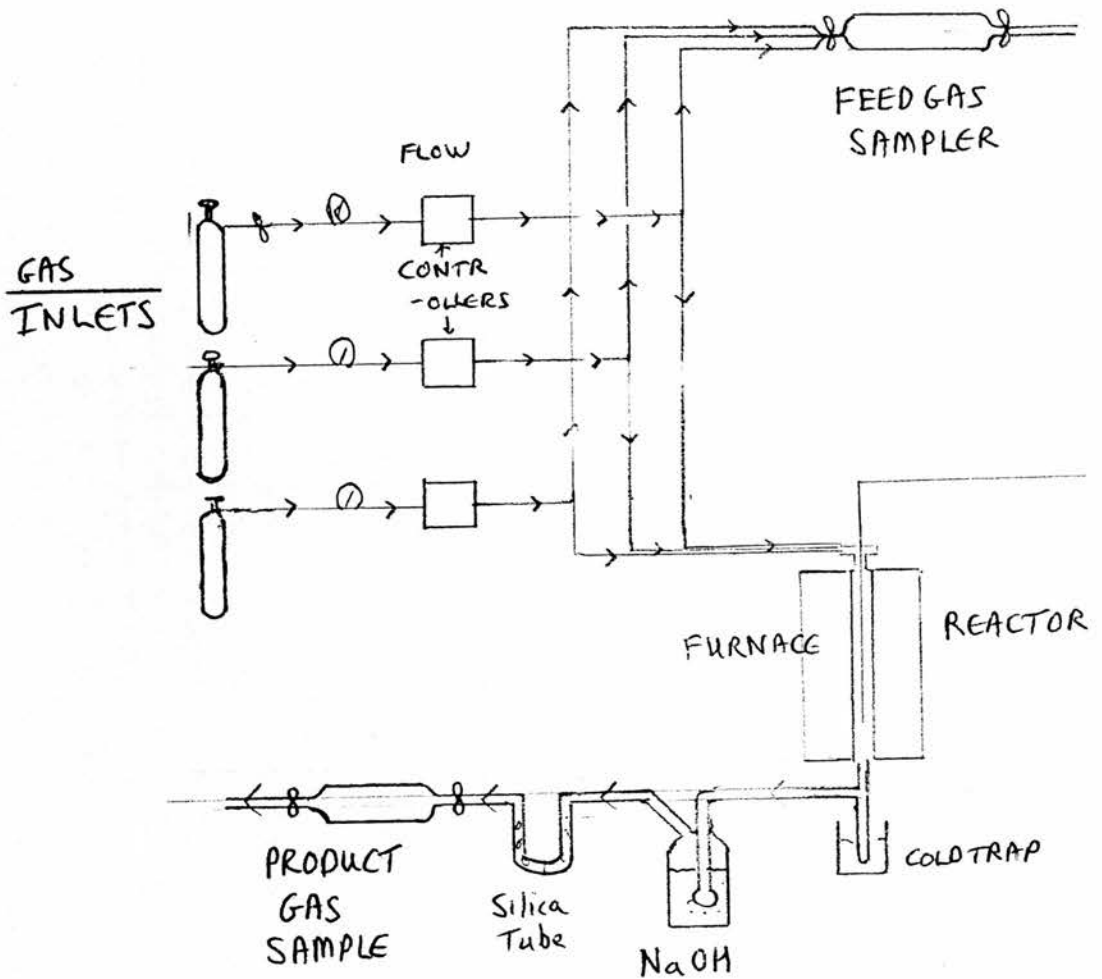


DIAGRAM 5.2

REAGENTS

Chloromethane was 99.5% pure (from B.O.C., 64 Longbridge Road, Barking, Essex.)

Bromomethane was unspecified purity (from Matheson.)

Chloroethane was 99.7% (from B.O.C., 64 Longbridge Road, Barking, Essex.)

Sodium aluminate was Technical grade (from BDH Chemicals Ltd, Poole.)

Sodium hydroxide was Analar Minimum assay 98.0% (from BDH as above.)

Tetra propyl ammonium hydroxide was from Fluka AG.

ANALYSIS

- a) X-Ray Diffraction for crystal structure
- b) X-Ray Fluorescence - Si/Al ratio
- c) Sodium analysis. Atomic absorption
- d) Coke analysis
- e) G.C.M.S. for product analysis

a) X-ray diffraction revealed that GSW1 was orthorhombic with 100% crystallinity. Fig.5.3 . GSW2 was monoclinic - which was distinguished by the split peak at 24.5° - and also 100% crystalline. Fig 5.4.

b) X-ray-Fluorescence showed GSW1 to have a Si to Al ratio of 42:1 and GSW2 to have a ratio of 170:1.

c) Atomic absorption analysis revealed that the sodium content of GSW1 was 7 p.p.m. and GSW2 was 227 p.p.m. Using the formula $\text{Si}_{(96-x)}\text{Al}_{(x)}\text{Na}_{(x)}\text{O}_{(192)}$ and the value of Si:Al of 42:1 for GSW1 and 170:1 for GSW2 and making the assumption that all Si and Al ions are in the crystal framework the full equation can be calculated.

FOR GSW1

$$\frac{\text{Total Silicon}}{\text{Total Aluminium}} = \frac{96-X}{X} = \frac{42}{1}$$

$$\Rightarrow 42X = 96-X$$

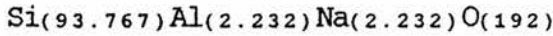
$$\Rightarrow 42X + X = 96$$

$$\Rightarrow 43X = 96$$

$$\Rightarrow X = 96/43$$

$$\Rightarrow X = 2.232$$

The full equation is therefore



Using this the initial percentage of sodium by weight can be determined.

$$\text{Si} = 28.08 \times 93.767 = 2632.98$$

$$\text{Al} = 26.98 \times 2.232 = 60.219$$

$$\text{Na} = 22.99 \times 2.232 = 51.314$$

$$\text{O} = 15.99 \times 192 = 3070.08$$

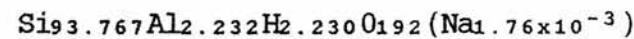
$$\underline{\underline{5814.59}}$$

$$\text{Maximum Sodium by weight} = \frac{51.314}{5814.6} = 8.825 \times 10^{-3} \times 100 = 8.825 \times 10^{-1} \%$$

$$\text{Analysed value} = 7 \text{ p.p.m.} \approx 7 \times 10^{-6} \times 100 = 7 \times 10^{-4} \%$$

$$\begin{aligned} \text{Percentage of acid sites occupied by sodium} &= \frac{7 \times 10^{-4}}{8.825 \times 10^{-1}} \times 100 = 0.079\% \end{aligned}$$

Full formula



Amount of Na remaining is negligible.

99.92% exchange completed

FOR GSW2

$$\frac{96-X}{X} = \frac{170}{1}$$

$$\Rightarrow 170X = 96-X$$

$$\Rightarrow 171X = 96$$

$$\Rightarrow X = \frac{96}{171} = 0.561$$

Initial equation = $\text{Si}_{(95.438)}\text{Al}_{(0.561)}\text{Na}_{(0.561)}\text{O}_{192}$

$$\text{Si} = 28.08 \times 95.438 = 2679.9$$

$$\text{Al} = 26.98 \times 0.561 = 15.136$$

$$\text{Na} = 22.99 \times 0.561 = 12.897$$

$$\text{O} = 15.99 \times 192 = 3070.08$$

$$\underline{\underline{5778.08}}$$

$$\begin{array}{l} \text{Maximum sodium} \\ \text{by weight} \end{array} = \frac{12.897}{5778.08} = 2.232 \times 10^{-3}$$

$$\text{Analysed value} = 227 \text{ p.p.m.} \approx 2.27 \times 10^{-4}$$

$$\begin{array}{l} \text{Percentage of} \\ \text{acid sites} \\ \text{occupied by} \\ \text{sodium} \end{array} \quad \frac{2.27 \times 10^{-4}}{2.232 \times 10^{-3}} = 10.17\%$$

\Rightarrow only 89.83% exchange completed.

Full formula = $\text{Si}_{(95.438)}\text{Al}_{(0.561)}\text{H}_{(0.504)}\text{Na}_{(0.057)}\text{O}_{(192)}$

This catalyst was not used in any of the subsequent experiments.

FOR GSW1/13

A sample of GSW1 was exchanged with NaCl. Sodium analysis showed 6100 p.p.m..

Maximum sodium by weight = 0.8825

Analysed value = 6100 p.p.m. = 6.1×10^{-3} = 0.61

Percentage of acid sites occupied by sodium = $\frac{0.61}{0.8825} \times 100 = 69\%$

Around 70% of acid sites are occupied by sodium ions.

Full formula =

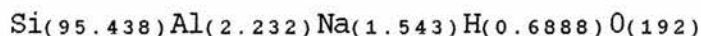


TABLE 5.1

	GSW1	GSW2	GSW1/13
Si:Al ratio	42	170	-
Na analysis	7 ppm	227 ppm	6100 ppm
Proportion of acid sites occupied by sodium	0.079%	10.18%	69.14%

d) Coke Analysis of Used Catalyst

GSW1 was found to have a total coking representing 1.97% of its total weight. 57% of the coke was carbon, 36% hydrogen and 7% nitrogen.

GSW13 was found to be coked to a larger extent 5.5% of which 86% was carbon, 13% hydrogen and 0.7% nitrogen.

GSW13 has a lower H to C ratio and subsequently has less $(CH)_n$ coke. GSW1 with a larger H to C ratio has a large amount of aromatic type $(CH)_n$ coke.

TABLE 5.2

COKE ANALYSIS

WEIGHT %		1 ST	2 ND	AVERAGE	MOLES	RATIO
GSW 1	C	1.12	1.11	1.12	0.093	1
	H	0.71	0.71	0.71	0.710	7.6
	N	0.14	0.14	0.14	0.011	-
GSW 13	C	4.77	4.69	4.73	0.394	1
	H	0.70	0.77	0.74	0.740	1.88
	N	0.04	0.03	0.04	0.003	-

The nitrogen content reported is an artifact of the analysis and does not indicate that the coke from the catalyst contains nitrogen.

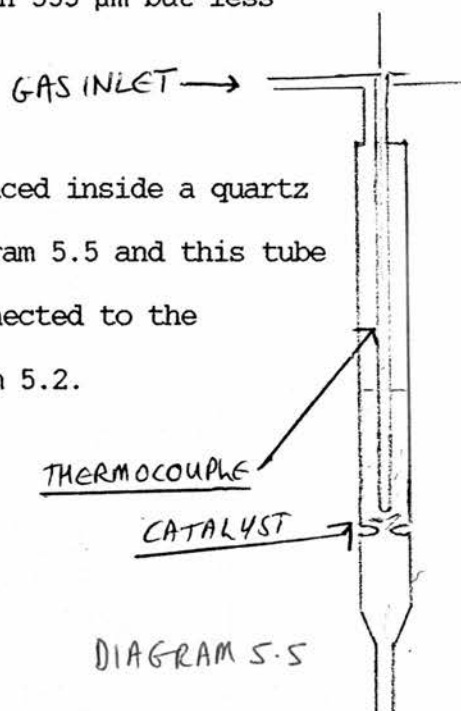
e) G.C.M.S. analysis of product gases

A sample of product gas was submitted to the analytical laboratories for G.C.M.S. analysis. The identification of the products was as listed in tables 5.4 and 5.5.

ZEOLITE REACTION EXPERIMENTS

GSW was pelleted in a Perkin Elmer 5 ton per inch diameter steel press and meshed between 600 μm mesh and 355 μm mesh steel framed laboratory test sieves. The catalyst was, therefore, greater than 355 μm but less than 600 μm in diameter.

5ml (3.28g) of catalyst was placed inside a quartz reactor tube as illustrated in diagram 5.5 and this tube was placed into the furnace and connected to the experimental apparatus as in diagram 5.2.

EXPERIMENT 1

The furnace was switched on and set to 300°C. N_2 was passed over the catalyst for 1½ hours. The gas flow was adjusted to give 10% CH_3Cl in 90% N_2 with a space velocity of $\approx 2000 \text{ h}^{-1}$ and a residence time of $\approx 1.8 \text{ s}$.

$$(\text{SPACE VELOCITY } (\text{h}^{-1})) = \frac{\text{flow rate at STP } (\text{ml h}^{-1})}{\text{volume of catalyst charge } (\text{ml})}$$

$$\text{RESIDENCE TIME } (\text{s}) = \frac{1}{\text{space velocity (in seconds}^{-1}\text{)}} \quad (\text{STP})$$

A sample of this initial gas was pressurised to 15 lb/in² with helium and injected onto G.C. 342824.

50 ml of 0.1m NaOH was placed in the acid scrubber with 4 drops of methyl orange indicator. HCl gas released from the reactor would bubble through the NaOH and be neutralised. This was done to protect the G.C. column.

The extent of reaction was determined both by back titration of the NaOH and by 'monitoring' the CH₃Cl/N₂ ratio from G.C.(342824) analysis of the product gases.

$$\text{Extent of reaction} = 100 - \frac{\text{Final amount of CH}_3\text{Cl}}{\text{Initial amount of CH}_3\text{Cl}} \times 100$$

OR

Extent of reaction = conversion of CH₃Cl to HCl.

It could be taken that the extent of reaction would be equivalent to the amount of HCl produced. This assumed that 1 mole of CH₃Cl reacted to produce 1 mole of HCl. This was a reasonable assumption as HCl was the only chlorine containing product detected. By backtitrating the remaining NaOH the amount of HCl produced could be determined and hence the amount of CH₃Cl that had reacted could be found.

This also assumed that all HCl formed in the reaction was neutralized in the NaOH which need not be the case as some HCl could be absorbed onto the catalyst

or bubble through the NaOH.

An alternative method was to subtract the amount of CH_3Cl in the gas flowing out of the reactor from the amount going in to give the amount of CH_3Cl that had reacted. This was a more accurate method but could not be completed until the gas samples had been processed. This could, depending on the queue for the G.C. machine, take anything up to three days. A compromise solution was to use the rough value from the titration of the acid scrubber as an immediate guide to the extent of reaction and to use the accurate G.C. value in the final calculations.

In each experiment a monitored flow of reactant gas was passed through the reactor for a recorded period of time - usually 30 minutes exactly. The experiment was run at temperatures of 250, 275, 300, 325 and 350°C.

The gaseous products were analysed by G.C. - all peaks were identified as alkanes or alkenes up to C_5 except for one peak at R.T.=6.35 which was not recognized. A gas sample was sent for G.C.M.S. analysis to determine what this peak was, to check the identification of the other products and to see if there was any chloroethane present. The results of this analysis were presented in the Analysis section.(page 312)

EXPERIMENT 2

In the meantime the rig was set up to feed a

chloroethane + N₂ mixture over the catalyst. This was done at temperatures of 250 and 275°C.

EXPERIMENT 3

The rig was set up to feed bromomethane and N₂ over the catalyst. The procedure was as for Experiment 1 and was repeated at temperatures of 250, 275, 300, 325 and 350°C.

The final weight of catalyst was 2.68g. The initial weight of catalyst was 2.88g. $\Rightarrow \Delta -0.20\text{g}$.

A sample of the used zeolite was submitted for coke analysis. See page 306.

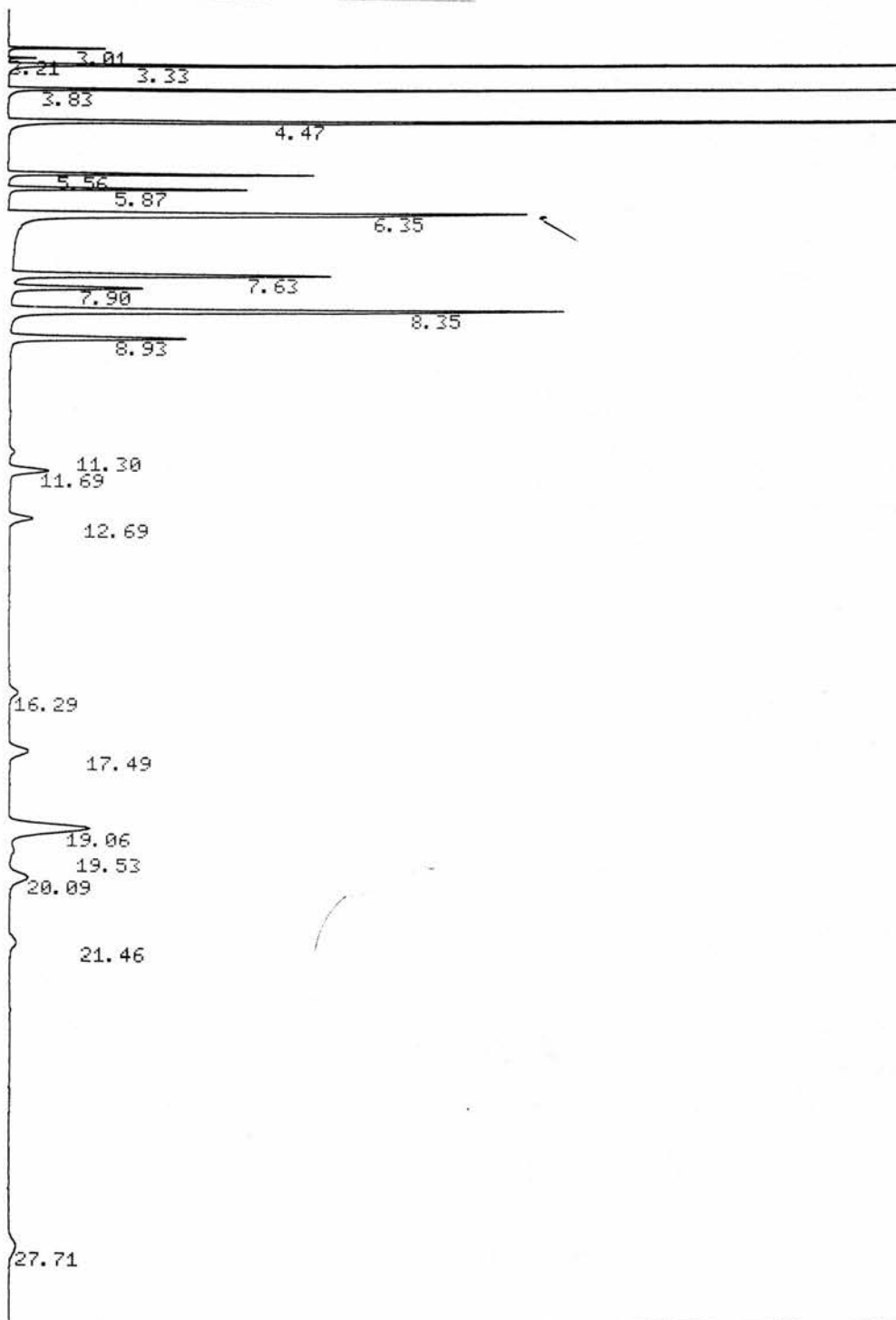
RESULTS

ZEOLITE REACTION EXPERIMENTS No. 1,2 AND 3

This section describes the procedure for obtaining the results from the first experiment with CH_3Cl . It also applies to the subsequent experiments where for CH_3Cl and HCl read CH_3Br and HBr respectively.

Samples of the initial gas and of the products were passed through two G.C.s. G.C. 342824 indicated the relative amounts of N_2 and CH_3Cl in the initial gas and the amount of N_2 , CH_3Cl and C_2 and C_3 hydrocarbons in the product gas. G.C. 348890 gave the relative amounts of alkane/alkenes from C_1 up to C_5 . Examples of traces from both G.C.'s are presented here as fig.5.5.

The C_3 values appeared on both traces and so were taken to calibrate the traces. The resulting values for each gas and the appropriate values for the variables were fed into a previously set up computer. The selectivity (%) with respect to carbon and percentage conversion for successive runs are presented in table 5.3 for chloromethane and table 5.4 for bromomethane.



NAME	CONC	RT	AREA	BC	RF
METHANE	0.023	3.01	3986	01	91617.
ETHANE	0.004	3.21	1054	01	180260.
ETHENE	0.343	3.33	114846	01	180260.
PROPANE	0.106	3.83	55710	01	281184.
PROPENE	0.367	4.47	180114	01	264550.
I C4	0.037	5.56	25741	01	374912.
N C4	0.029	5.87	20534	01	374912.
8	0.	6.35	92333	01	
T BUTENE	0.068	7.63	44693	08	357160.
N BUTENE	0.027	7.9	18329	05	357160.
I BUTENE	0.132	8.35	87741	01	357160.
C BUTENE	0.044	8.93	28851	01	357160.
13	0.	11.3	1125	01	
I C5	0.011	11.69	9575	01	468640.
N C5	0.007	12.69	6299	01	468640.
C5-	0.004	16.29	3315	01	450000.
C5-	0.009	17.49	7191	01	450000.
C5-	0.041	19.06	34532	02	450000.
C5-	0.002	19.53	1714	03	450000.
C5-	0.01	20.09	8051	01	450000.
C5-	0.003	21.46	2917	01	450000.
22	0.	27.71	4241	01	
TOTALS	1.267		752892		

FIGURE 5.3 X-RAY DIFFRACTION PATTERN FOR ZSM-5.

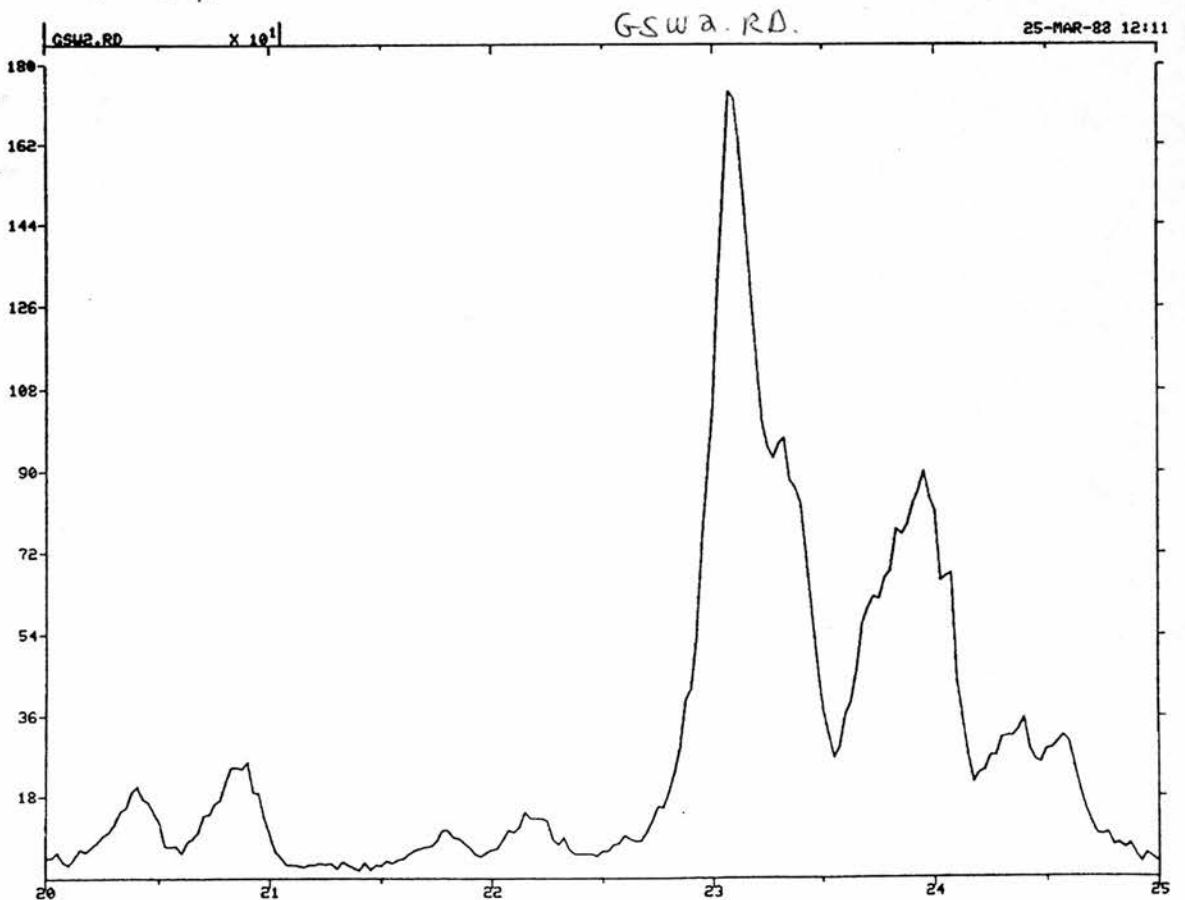
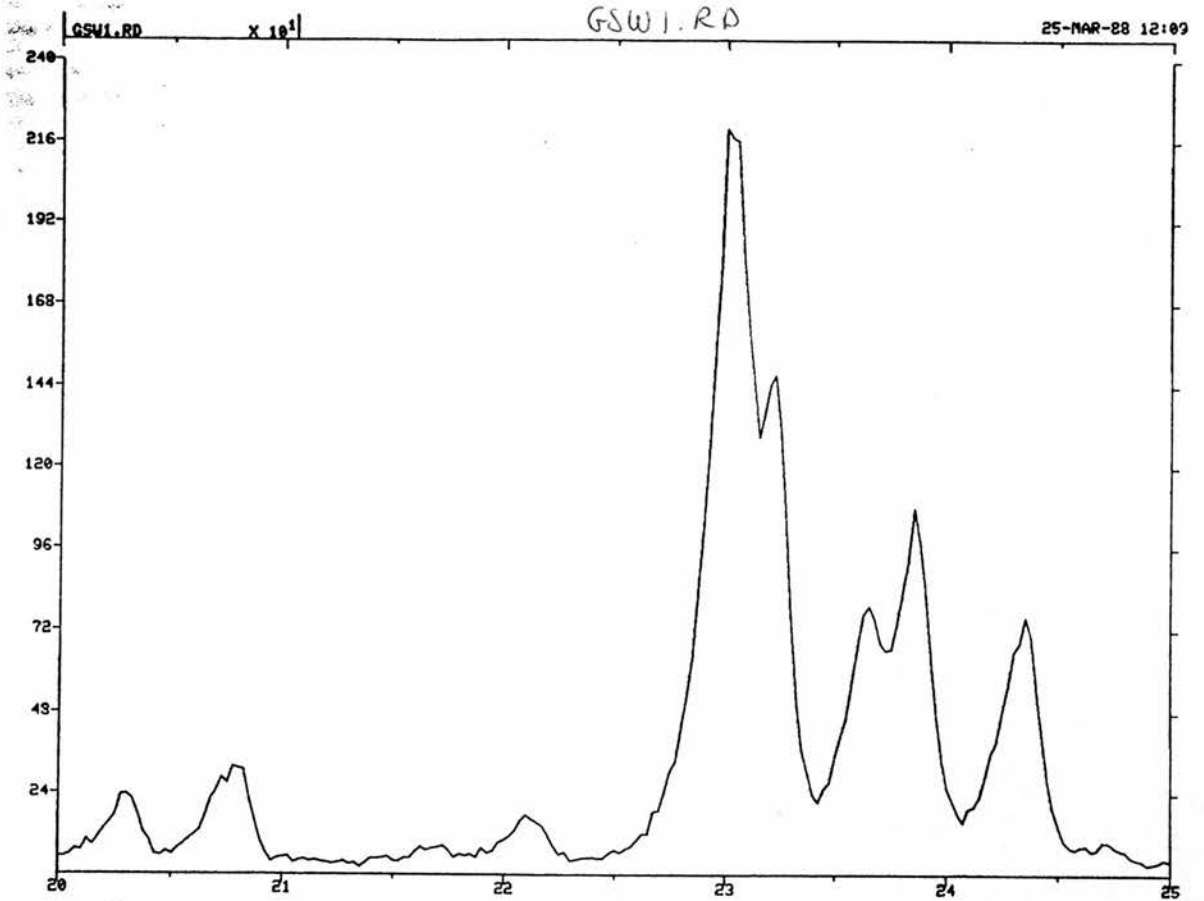


TABLE 5.3 CHLOROMETHANE

RESULTS SELECTIVITY OF PRODUCTS WITH RESPECT TO CARBON
 FOR THE REACTION OF CH₃Cl OVER ZSM-5 CATALYST

Temp °C	250	275	300	325	350
% Conv	6.78	8.74	13.51	22.43	31.63
Methane	0	0	0.19	0.31	0.63
Ethane	0	0	0	0.07	0.22
Ethene	1.60	5.90	8.95	12.88	18.89
Propane	1.21	1.56	4.83	6.00	8.76
Propene	19.85	22.40	30.40	27.26	30.34
C ₄	6.41	4.17	10.34	7.56	7.28
C ₄ =	51.34	37.76	31.89	32.38	22.35
C ₅	6.50	2.17	2.97	2.82	2.18
C ₅ =	13.06	26.02	10.14	10.74	9.1

TABLE 5.4 BROMOMETHANE

RESULTS SELECTIVITY OF PRODUCTS WITH RESPECT TO CARBON
 FOR THE REACTION OF CH₃Cl OVER ZSM-5 CATALYST

Temp	250	275	300	325	350°C
% Conv	8.65	12.22	14.73	19.99	32.33
Methane	0	0.33	0.81	0.81	1.61
Ethane	0	0	0	0	0.29
Ethene	6.17	4.77	10.30	11.90	19.85
Propane	2.10	3.99	7.32	7.26	12.62
Propene	32.40	44.19	48.78	41.13	37.55
C ₄	2.80	6.64	6.50	6.05	4.30
C ₄ =	37.59	23.48	19.51	25.81	17.41
C ₅	14.03	3.87	1.36	2.52	1.22
C ₅ =	4.9	12.72	5.42	4.53	5.14

DISCUSSION

The values that were of greatest interest in these experiments were the analytical conversions and the carbon selectivities.

CONVERSION

A table of conversion for each reaction gas against temperature show that in all cases the conversion increases as the temperature increases. It should be noted that the conversion for chloroethane is much greater than that for either of the halogenomethanes.

TABLE 5.5

CONVERSION WITH RESPECT TO CARBON AGAINST TEMPERATURE

REACTANT	250	275	300	325	350 °C
CH ₃ Cl	6.8	8.7	13.5	22.9	31.6
CH ₃ Br	8.7	12.2	14.73	20.0	32.3
C ₂ H ₅ Cl	18.1	23.8	-	-	-

CHLOROETHANE -EXPERIMENT 2

Experiment 2 was done to see if chloroethane could be considered an intermediate. One product from experiment 1 had not been identified by the G.C. and it was thought that it might be chloroethane. It has been

postulated that the route to C-C bond formation in reactions of methanol could involve the rearrangement of dimethyl ether to ethanol and the subsequent β -elimination of H₂O to form ethene.¹⁴² The products from the reaction of ethanol over ZSM-5 was identical to the products from methanol with the exception of the amounts of durene and ethylbenzenes that were formed.²⁰¹ Durene amounted to 58.8% of the aromatic products from methanol but only amounted to 0.9% of the aromatic products from ethanol. Ethylbenzenes amounted for 0.6% of the aromatics with methanol and 4.1% of the aromatics with ethanol. Never-the-less ethanol could still be considered an intermediate in these reactions.

An analagous reaction with chloromethane would produce chloroethane which would eliminate HCl to form ethene. Indeed the results from the reaction of chloroethane over ZSM-5 show ethene to be by far the major product \approx 90%. With only two results there is not enough data for a detailed comparison. This experiment was cut short because the G.C.M.S. analysis indicated that the amount of chloroethane in the chloromethane reaction product sample was only one part to ten thousand of chloromethane. The unidentified peak that might have been chloroethane was shown to be chloromethane. This finding, coupled to the striking difference in the product distribution between this reaction and that of chloromethane, lead to the conclusion that chloroethane is not an intermediate in the reaction on chloromethane

over ZSM-5.

CHLOROMETHANE AND BROMOMETHANE

EXPERIMENTS 1 AND 3

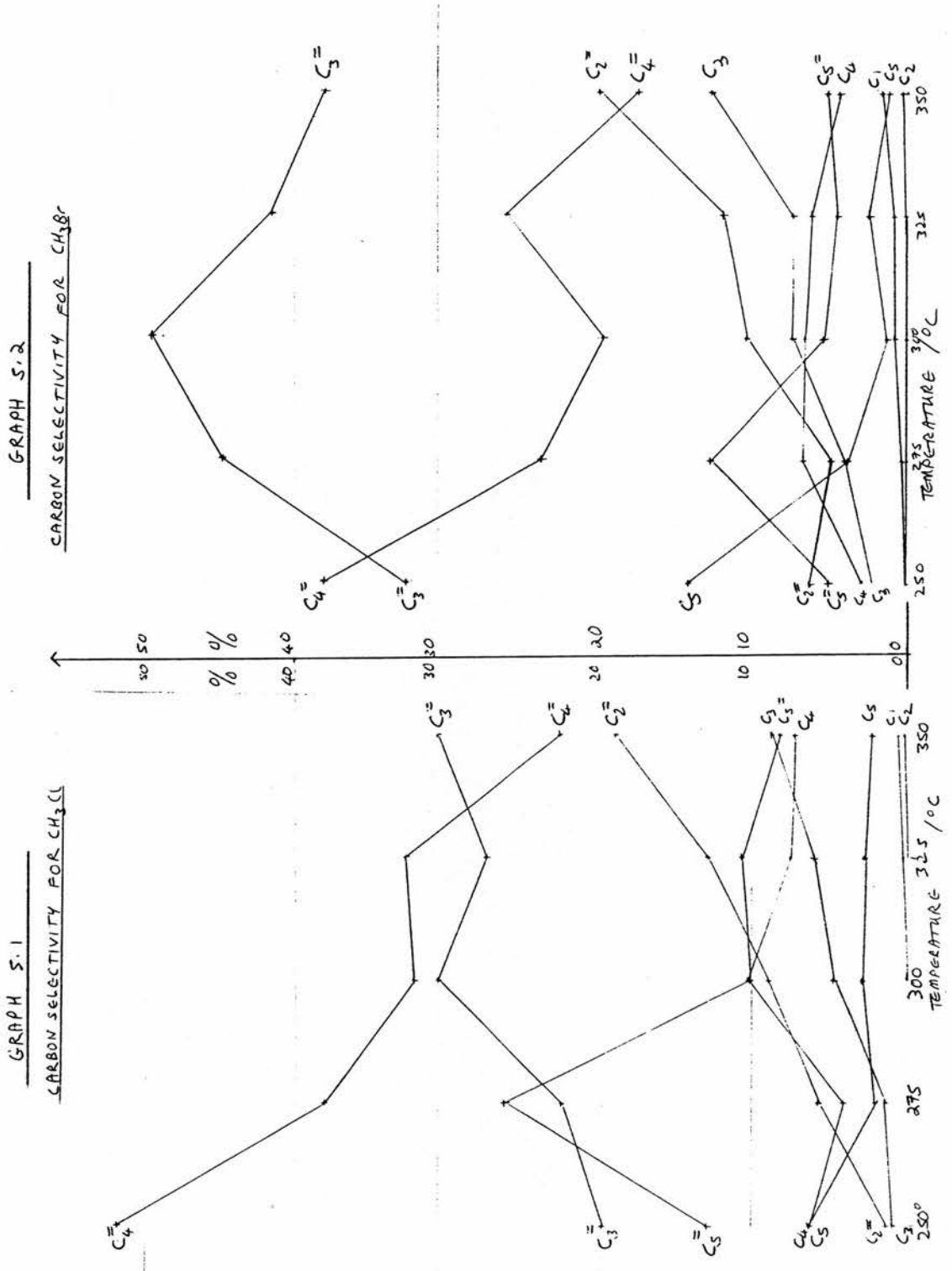
Selectivity

Graphs of selectivity of alkane and alkene for each carbon length against temperature were plotted. Graphs 5.1 and 5.2.

GRAPHS 5.1 AND 5.2

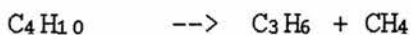
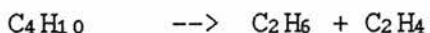
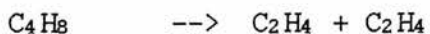
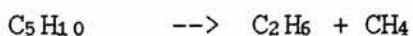
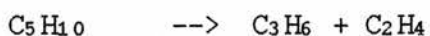
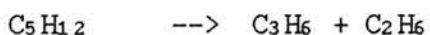
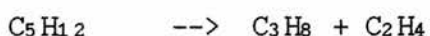
CARBON SELECTIVITY AGAINST TEMPERATURE/°C

FOR THE REACTION OF CH₃Cl AND CH₃Br OVER ZSM-5.



The results for CH_3Cl and CH_3Br were very similar. In both cases the biggest product at lowest temperature was the butenes - 51% with CH_3Cl and 38% with CH_3Br . As the temperature was raised the amount of this product diminished. The second most abundant compound with both reagents was propene which increased as temperature increased.

Ethene was very minor at low temperatures but rose as the temperature increased. Methane and ethane were very minor products increasing as temperature increased. Generally the trend was to get alkenes (C_3+C_4) at low temperatures and lower alkenes (C_2+C_3) and alkanes at higher temperatures. This, along with the appearance of methane and ethane, would suggest that the change in product distribution with increasing temperature could be explained by the cracking, either thermally or catalytically, of the large $\text{C}_4 + \text{C}_5$ products.



The main points of these investigations were:-

- i) To find if the products produced by CH_3Cl would be the same as those for CH_3OH and if not could the differences be used to indicate the mechanism involved in either or both of these reactions.
- ii) To find if CH_3Br produced the same products as CH_3Cl and again, to utilise any differences to elucidate the mechanisms.
- iii) To do these reactions under low temperature, high dilution conditions to see if the results could shed light on what the initial products of these reactions are.

Each of these points will be discussed separately.

- i) Other researchers have reported their findings in many publications. ^{7,195-199} The results of the present work have no products equivalent to the oxygen containing products from methanol. Apart from this difference it would be anticipated that having formed the initial hydrocarbon, from whatever reactant, the resultant reactions would not produce dissimilar products even if differences in rate of production and distribution of products did occur. The mechanism by which the first hydrocarbon is extended is generally thought to occur by methylation of an olefinic species. ^{200,201} This would

account for the proportions of methylated aromatics with methanol and ethylated aromatics with ethanol as reagent. This notion is upheld by these results. Having produced the first hydrocarbon it appears that subsequential reaction with CH_3X molecules, or the reactive species that these molecules become in the zeolite, will result in a series of hydrocarbons which are dependent more on the acidity of the zeolite, the temperature and the concentration of reactant rather than on the exact nature of the X moiety.

ii) To all intents and purposes quantity and distribution of products from chloromethane and bromomethane were identical. (Graphs 5.1 and 5.2). Therefore no difference could be used to aid the investigation of the mechanisms. It can be assumed that the same mechanism occurs in both reactions.

Results published for the reaction of iodomethane reactions differ in that they indicate a large quantity of methane produced.

TABLE 5.6 REACTION OF IODOMETHANE OVER ZSM-5

	W.H. S.V.	T/°c	Time on Line	Total conv.	Product selectivity			
					CH ₄	C ₂ H ₄	C ₃ H ₆	>C ₄
H-ZSM-5	0.8	250	60 m	0.02%	66.1	33.9	0	0
	0.8	250	100m	0.13%	7.0	44.1	32.5	16.4
Na-ZSM-5	0.1	250	15m	0.05	66.0	34.0	0	0
	0.1	300	90m	0.07	70.0	30.0	0	0

(from Reference 148)

This could be due to the radical cleavage of the C-I bond. Radical reaction of iodomethane could cause the splitting to I[·] and the methyl radical. Subsequent abstraction of a proton from another iodomethane molecule would result in the production of methane. As methane is unreactive over ZSM-5 this would result in an abnormally high yield of methane. The extent of radical formation of methane from a halogenamethane will depend on the halide. Iodomethane will split more readily than bromomethane and much more so than chloromethane.

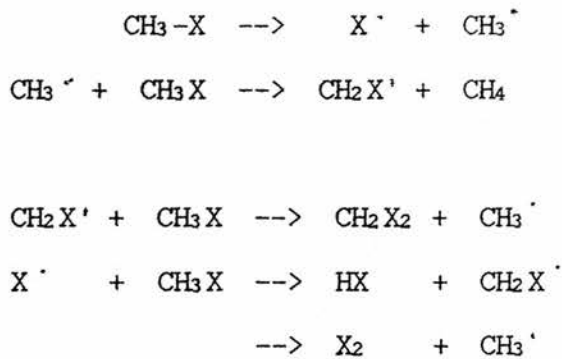


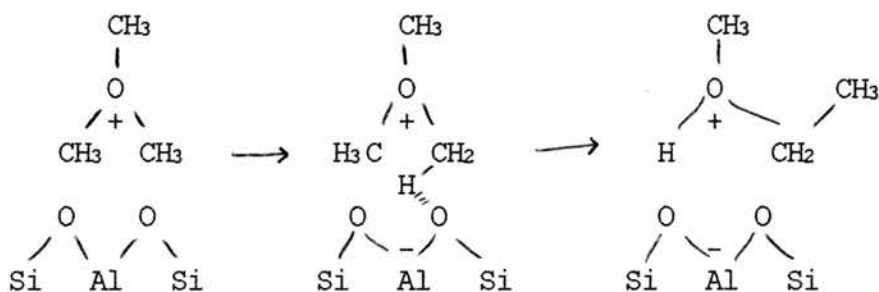
FIG 5.9

In the result presented here there was more methane produced from the bromomethane than from the chloromethane, but both are so minor that no conclusions should be drawn from this. Both halogenomethanes produce methane in quantities that could be accounted for by cracking of higher hydrocarbons.

An alternative route for the production of methane from iodomethane was suggested by the gas phase investigation of chapter four. It appeared that the iodomethonium ion, $\text{CH}_3\text{-I-H}^+$, rearranged and lost I^+ to give methane. This would support the postulation that the initial step in the reaction of CH_3X over ZSM-5 is protonation. This reaction would account for the high quantity of methane produced in the reaction of iodomethane over a ZSM-5 catalyst.

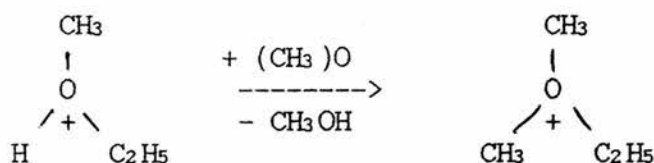
iii) The initial products

The initial hydrocarbon products for the reactions of methanol are thought to be ethene and/or propene. Various researchers have suggested that ethene is the first hydrocarbon formed in the reaction of methanol.^{7,203,204} Other workers have concluded from their results that propene is the first hydrocarbon formed.^{142,205} A compromise was attempted between the two groups of researchers when van den Berg¹⁴² proposed a dual mechanism to explain the production of ethene and propene as joint initial products and to account for the range of ratios of ethene to propene reported in the literature. Following on from the formation of trimethyl oxonium ions by the mechanism outlined in chapter three, page 203, they proposed that a Stevens type rearrangement could produce methylethyl oxonium ions.



From this stage two routes diverge. Hydration and loss of methanol would produce ethyl oxonium ions, $\text{CH}_3\text{CH}_2\text{-OH}_2^+$, which could cleave to form ethene and water with regeneration of the acidic site on the catalyst.

If the methylethyl oxonium reacted with dimethyl ether the dimethylethyl oxonium ion would be formed.



A Stevens type rearrangement of this ion would produce methylisopropyl oxonium ions which, if they reacted in the same way as the dimethylethyl oxonium ions, would produce propene as the first hydrocarbon.

If this is correct then the amount of ethene and propene formed initially will depend on the relative amounts of methanol, dimethyl ether and water present in the reaction mixture.

How this mechanism would apply to halonium ions is not clear. No halogen containing ions equivalent to the trialkyl oxonium ions were observed.

It was hoped by carrying out reactions under conditions of low conversion - low temperatures, low activity of zeolite and high dilution of reactant gas - that the initial hydrocarbon in the reaction of halogenomethanes might be detected.

If the propene was formed by methylation of ethene then propene would be of a higher order than the ethene and by considering the changes in production of ethene and propene as the temperature was increased it was hoped to detect this.

The results indicate that ethene is not a primary product but occurs by fragmentation of a higher

hydrocarbon. The ratio of ethene/propene was, therefore, just a function of the relative production of precursors and the relative extent of cracking.

At the lowest temperatures at which the reaction was tried the most abundant products were the butenes and the pentenes. They cannot be considered to be the first hydrocarbons formed but rather that they are formed by methylation of smaller hydrocarbons and cracking of larger hydrocarbons formed within the zeolite pores. This would suggest that the conditions were too severe for the initial products to be observed without further reaction occurring.

This serves to illustrate an important point in the attempted elucidation of reaction mechanisms from the observation of neutral products from a zeolite reaction bed. Under all conditions consideration must be given to the possible disguising of the true production of products by the kinetics of the reactions and the selectivity of the zeolite. In an experiment such as the one reported here which produced a large propene to ethene ratio in the early stages of the reaction it might be concluded that propene was the main product of the initial reaction. However, it would also be possible that ethene was the first hydrocarbon formed but the ethene molecule had a higher degree of absorption on to the zeolite than had propene. In this case ethene could be being formed in high yields but most of it remained bound in the zeolite. Only when it has been further methylated to propene with a lower binding energy does

the zeolite 'release' the product. The large amounts of propene produced might lead to the suggestion that propene was much more important than it really was. This notion, that the true importance of each compound might be being disguised, has been referred to as kinetic disguise of the product distribution.^{206,207} Applied to the results of the experiments undertaken for this investigation would mean that it could only be said that under the experimental conditions the main products released from the reactor vessel were C₃, C₄ and C₅ alkenes. Nothing could be stated about the initial hydrocarbon product.

OVERALL CONCLUSIONS TO CHAPTERS THREE, FOUR AND FIVE

The initial C-C bond formation step in the catalytic condensation of methanol to gasoline in the MTG process remains an enigma. The investigations of halogenomethane 'condensation' reactions over the same catalysts could aid in the understanding of the mechanisms.

The literature in recent years has been full of claim and counter claim as each proponent produced experimental results that supported their favoured mechanism and cast doubt on other mechanisms. The number and diversity of proposals produced and the general failure to confirm or repudiate any of them is indicative of the complexity of the problem.

Part of the problem has been that the mechanism, whatever it is, is operating within the confines of the zeolite channels. Experiments, such as those reported in chapter five, in which neutral reactants are fed in over a zeolite and neutral products are detected in the outflow are flawed. Any proposal drawn from consideration of the product distribution can only surmise what chemistry is occurring in between the gas inlet and the gas outlet.

It was with this problem in mind that the reactions were investigated in the multiple quadrupole mass spectrometers. Using the ability to form and select specific ions in isolation it was possible to study the reactions of the reactant species outwith the confines of the zeolite. Caution must be used in applying the

results in the gas phase to a consideration of the mechanisms in a zeolite. As was seen for example in the attempt to study the rearrangement reaction of $\text{CH}_3-\text{O}^+=\text{CH}_2$ ions to $\text{CH}_3\text{CHO}^+\text{H}$ the energy of the ions in the gas phase are not the same as in solution or absorbed phase. It must also be taken into account that in solution or absorbed phases there are steric factors and solvation effects that could play an important part in the reactions of ions in a zeolite. Rearrangements of trimethyl oxonium ions, for example, might take a different path under the influence of the zeolite to produce a C-C bond in a way that would not be observed in the gas phase.

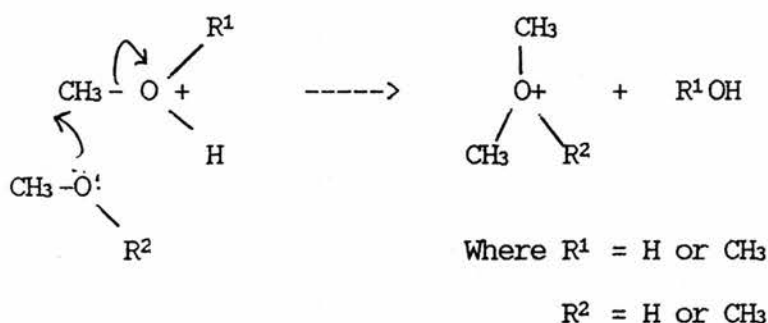
Two techniques that could provide information about the species that are present in the zeolite are ^{13}C nmr and Fourier Transform (Diffuse Reflectance) Infra Red - F.T.I.R. Both of these techniques have been used to investigate the species from methanol that were absorbed on aluminosilicate catalysts.²¹³⁻²¹⁵ An experiment was attempted, as part of the work at B.P. Research Centre, in which a sample of ZSM-5 was placed in a F.T.I.R. A laser was focused onto the surface of the zeolite at an angle such that the reflected rays were reflected to a detector. Chloromethane gas was admitted to the chamber. After a short time the gas was evacuated. It was hoped to detect the species that were absorbed onto the surface of the zeolite, and to monitor their reaction as the

temperature was increased. This would have given some information about the active species that occur with chloromethane over a ZSM-5 catalyst. This experiment did not work as no signal was detected. Owing to the heavy demands on the F.T.I.R. it was not possible to try this experiment more than once. It was hoped that the results from this experiment could go some way towards bridging the gap between the experiments that were studied in the gas-phase, where the ionic species and reaction mechanisms could be determined, but the zeolite was not involved, and the experiments in which the zeolite was playing it's part, but the active species could not be determined.

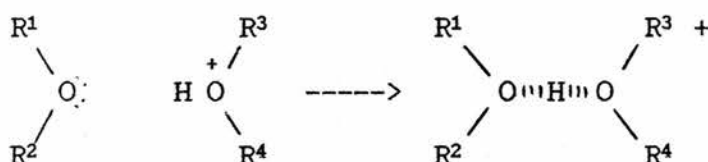
What then, can be concluded from the experiments undertaken in this research. It is beyond dispute that, whatever the mechanisms in operation, methanol, chloromethane, bromomethane and iodomethane react over ZSM-5 catalyst to produce alkane, alkene and aromatic hydrocarbons. The reaction of iodomethane over ZSM-5 could not be studied because of time constraints. The reaction of fluoromethane over ZSM-5 was not studied because of the expense of fluoromethane. The reaction of chloromethane and bromomethane over ZSM-5 were studied. Both reagents produced the same mixture of products in the range of temperatures studied. It was concluded that the same mechanism is operating for both these reagents.

Investigations in the gas phase confirmed that methyl oxonium, dimethyl oxonium and trimethyl oxonium ions could be formed in the gas phase from methanol in

'acidic' conditions. The mechanism that was proposed by Henis ¹⁵² to account for the formation of dimethyl oxonium ions from the reaction of methyl oxonium and methanol was disproved. An alternative mechanism was proposed and verified by a series of experiments using isotopically labelled reagents. This mechanism was extended to account for the formation of trimethyl oxonium ions and can be represented by the general scheme shown below.



Adducts of methanol, dimethyl ether and a proton were observed. These were thought to have the general structure as proposed and partially confirmed by Henis ¹⁵².



The analogues of the higher alcohols and ethers were found to form the same addition complexes.

The possible reaction mechanisms involving these intermediates were investigated as far as was possible in the triple quadrupole mass spectrometer. There was scope

There was no evidence from these investigations that any of the methyl oxonium ions or the methyl halonium ions rearranged to form an ion with a C-C bond. Indeed in the reactions of CH_3^+ with halogenomethanes, the only way to account for the formation of the methyl halonium ions was to consider that the halogenomethanes had been protonated by C_2H_5^+ or C_2H_3^+ ions that were formed by a different route.

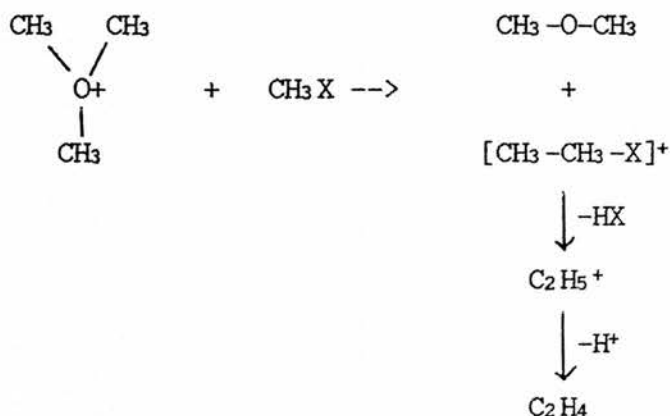
In the experiments with CH_3^+ ions reacting with CH_3X , where $\text{X} = \text{H}, \text{OH}, \text{F}, \text{Cl}, \text{Br}$ and I , it was noted that C_2H_5^+ and C_2H_3^+ ions had been formed at low pressures of target gas. Further investigation with CD_3^+ ions indicated that the C_2 ions were being formed by an addition with elimination reaction between methyl cations and CH_3X .



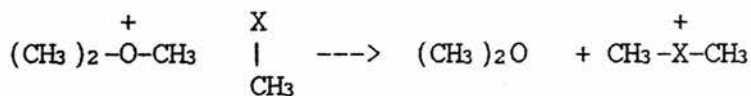
This 'methylation' reaction is applicable to, and was observed with, all CH_3X molecules that were investigated. This is directly relevant to the mechanisms that have been postulated for the zeolite reaction. It would seem that a mechanism of methylation could meet the requirements to satisfy the reactions of methanol and halogenomethanes. This mechanism does not require the rearrangement of C-O-C bonds to C-C-O bonds. It cannot be concluded from the gas phase studies what form the 'methylating' agent would have in the zeolite.

form the 'methylating' agent would have in the zeolite. It could be a 'free' methyl cation, or a + methoxy group bound to the zeolite surface, or it could be in the form of a gaseous or surface bound methylating ion, such as the methyl oxonium and methyl halonium ions.

In each of these cases the methylation of the carbon in the CH_3X , followed by elimination, would form a C-C bond. For example if trimethyl oxonium methylated a CH_3X molecule the following reaction pathway might be followed.



The C-C bond formation would occur if it was the C in CH_3X that was methylated. If the methylating agent methylated the X of CH_3X no new C-C bond would be formed but a new methylating agent would be formed.



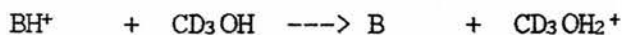
To summarise - methylation at the heteroatom position would result in the recreation of a methylating agent whilst methylation at the carbon with subsequent

elimination of HX would result in the formation of a C-C bond.

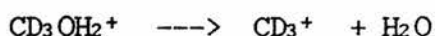
In this way it would not matter how much of the methylation would occur at the X end of the CH_3X molecule rather than at the carbon end. Methylation of the heteroatom would not diminish the eventual yield of hydrocarbons because each unsuccessful methylation would regenerate a methylating agent. Once the first olefins have been formed methylation of the olefins would produce a new C-C bond with each methylation. This would account for the reported autocatalysis of the reactions over ZSM-5. ⁷

The mechanisms that were observed in the gas-phase can be applied to explain the products detected over ZSM-5 by Nováková ²¹⁶ at low temperature and high dilution of methanol. It was reported that at low methanol concentrations the gaseous products from the reaction of CD_3OH over ZSM-5 were CD_4 and CD_2O . These products would be produced in the gas phase under conditions of low concentration. The stages in the reaction would be as follows.

1) Protonation of methanol, either by a gaseous acid or an acidic site on the zeolite.



2) Fragmentation of the protonated methanol to triply deuterated methyl cations and H₂O.



3) Hydride abstraction from a methanol molecule by the methyl cation to form methane and CD₂OH⁺.

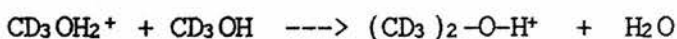


4) Loss of a proton, either to a molecule of methanol or to a basic site on the catalyst would produce formaldehyde.



At higher concentrations of methanol Nováková reported the formation of dimethyl ether at temperatures below 250°C.

In the gas phase results dimethyl oxonium ions were formed at higher concentrations of methanol. The protonated methanol, produced in the reactions as described for the low concentration of methanol, would react with a molecule of methanol to produce the dimethyl oxonium ion and water.



At temperatures above 370°C aromatics, alkanes and alkenes were produced.

The objection, of Chang and others, to formaldehyde, or CD₂OH⁺, as an intermediate in the reaction scheme on the ground that no formaldehyde was detected in the products can be dispelled by considering the behaviour of the CH₂OH⁺ ions in the gas phase. CH₂OH⁺ ion tends to

fragment with the loss of H_2 to become CHO^+ . Loss of a proton from this species, either by donation to another molecule, or to a basic site on the catalyst, would produce carbon monoxide which has been observed in most investigations.

The final conclusion, of the work in chapters three, four and five, is that the reaction mechanisms that have been found in the gas phase investigations by multiple quadrupole mass spectrometers correlate with this report of the neutral molecules obtained in the early stages of the reaction. The mechanism by which the first C-C bond cannot be unequivocally decided upon by the results of this investigation - indeed there may be more than one mechanism operating - but the results suggest that methylation, perhaps by a methyl oxonium or methyl halonium ion, is a strong contender.

CHAPTER SIX

THE CONSTRUCTION AND COMMISSIONING OF A QUINQUA

QUADRUPOLE MASS SPECTROMETER

CHAPTER SIXTHE CONSTRUCTION AND COMMISSIONING OF A QUINQUAQUADRUPOLE MASS SPECTROMETER

BASIC DESIGN.

VARIABLES:-

- 1) Electron Energy
- 2) Ion Energy
- 3) Pole Bias
- 4) Multiplier
- 5) Emission Control
- 6) Filament Current
- 7) Focus plates 1 and 2
- 8) ΔM
- 9) Resolution
- 10) D.C.:R.F. Ratio

MAIN MODIFICATIONS.

- 1) Replacing the wires supplying the quadrupoles.
- 2) Fitting liquid nitrogen traps between the pumps and the quadrupoles.
- 3) Removing the penning gauge heads away from the quadrupoles.
- 4) Redesigning the gas inlet.

RESULTS

- 1) Charge exchange reactions.
- 2) Protonation of methane.
- 3) Sequential ion/molecule reactions using all five quadrupoles.

THE QUINTA QUADRUPOLE MASS SPECTROMETER

The quinquadrupole mass spectrometer is the logical extension to the triple quadrupole mass spectrometer that is in operation. With the triple quadrupole mass spectrometer an ion from the first quadrupole can be selected and reacted with a neutral gas in the second quadrupole. The ions produced in this reaction can be detected by using the third quadrupole as a mass analyser. All that can be obtained from this is the mass to charge ratio of the ions and from this the composition of the ions can be calculated. The possible neutral fragment can be deduced to give a balanced equation. The structure of the ion and its reactivity can not be determined unequivocally. With the quinquadrupole mass spectrometer the ions that have been formed in the second quadrupole can be separated in the third quadrupole. These ions can then be put into another gas in the fourth quadrupole and the ions that are produced can be analysed in the fifth quadrupole. If an inert gas is placed in the fourth quadrupole then the ion from the third will fragment and by studying the fragments the structure of the ion can be determined. If a reactive gas was put into the fourth quadrupole then the reactivity of an ion that has been formed in the second quadrupole could be studied. This should enable the reactivity of novel ions that can only be produced by

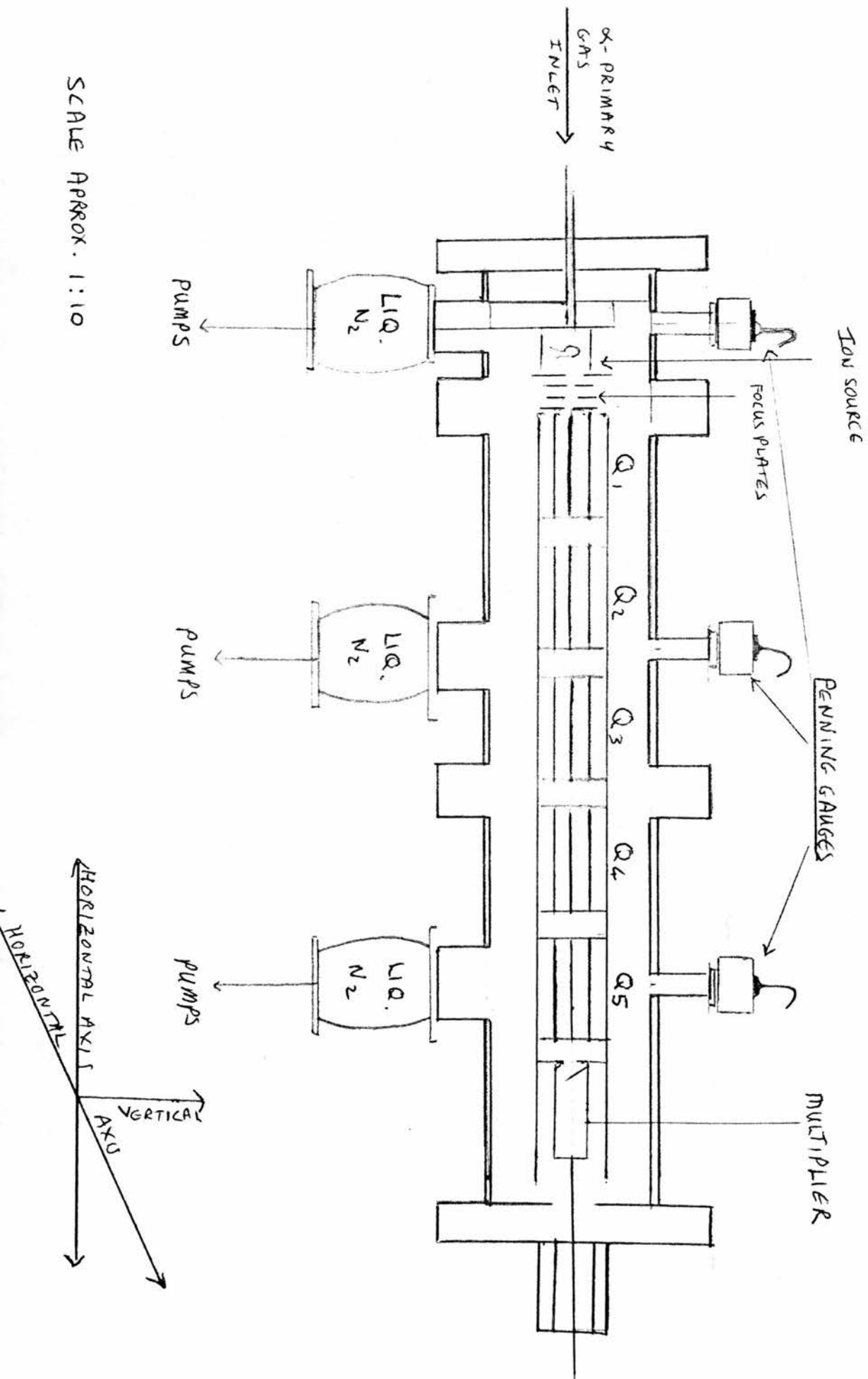
reacting an ion from the first quadrupole with a neutral in the second quadrupole to be studied.

The work in this chapter presents an overview of the main advances that have been made towards an understanding of the operation of the quinquadrupole mass spectrometer. Experiments to monitor the variables that effect the ion signal are discussed and the deficiencies that were observed are corrected by the main modifications that were made. The results of some experiments that were carried out using the modified quinquadrupole mass spectrometer are presented.

THE BASIC DESIGN

The quinquadrupole mass spectrometer was designed and built at the University of St. Andrews. The casing was milled at the workshops of La Trobe University, Bundoora, Victoria, Australia. The electronic circuits were built by Joe Ward of the Electronic Workshop from original designs and from considerations of the circuits of the triple quadrupole mass spectrometer. The essential features are portrayed in figure 6.1. The variables will be discussed in the next sections.

FIG. 6.1 THE QUINTUPLE QUADRUPOLE MASS SPECTROMETER



SCALE APPROX. 1:10

ION SOURCE

The source is a modification of a design from Prof. J.H. Lech, of the Department of Electrical Engineering and Electronics at the University of Liverpool, as described in the Ph.D. Thesis of A.E. Holme (1972) entitled 'The Quadrupole Mass Spectrometer.'²⁰⁸

Figure 6.2 shows the ion source configuration.

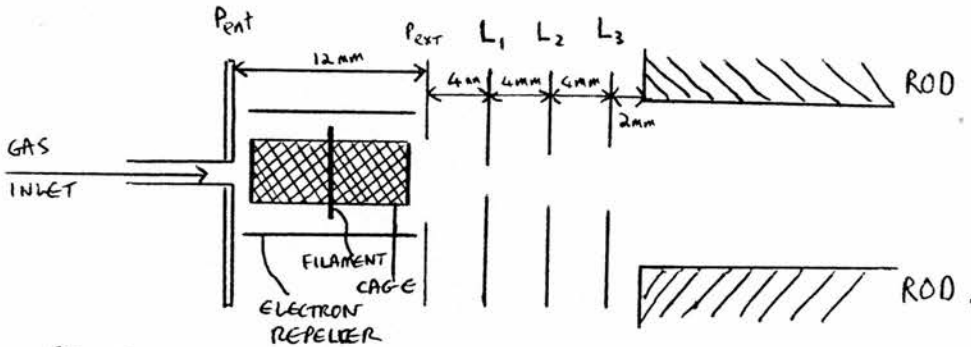


FIG. 6.2.1

The cage was made from 80% transmitting tungsten mesh on a stainless steel former 10mm long and with an internal diameter of 7mm. Outwith the cage lies the 10mm diameter ring shaped filament of 0.150mm diameter thoriated tungsten wire. This whole arrangement was enclosed within an horseshoe shaped electron repeller which was connected to the negative supply for the filament.

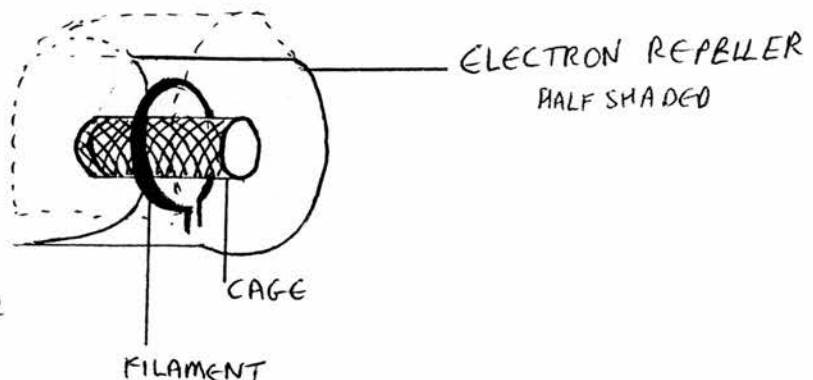


FIG. 6.2.2

ION ENERGY

The Ion Energy control alters the cage potential relative to ground between 0 and +30V. At various stages the size of signal obtained at different ion energies was studied. Typical values are presented in table 6.1. They indicate that as the ion energy increases the size of ion signal observed at the detector increases. A typical operating value at the onset of this work was 25V. This gives the ions their translational energy - the z component of their momentum. It would be desirable to reduce this value to slow down the ions and improve the resolution, but, under the initial operating conditions, it was found that if the Ion Energy was reduced the ion signal was not large enough to be detected.

TABLE 6.1

30/6/88

I.E. Volts	Signal Strength	I.E. Volts	Signal Strength	I.E. Volts	Signal Strength
12	0.0	16	10.0	23	210.0
12.125	0.0	17	27.0	24	340.0
12.25	0.065	18	73.0	25	640.0
12.5	0.09	19	146.0	26	1110.0
13	0.34	20	169.0	27	1530.0
14	1.05	21	175.0	28	1600.0
15	3.40	22	160.0	29	1900.0

ELECTRON ENERGY

The Electron Energy controls the potential between the cage and the filament from 20 to 75V - with a typical operating value of 70V. This accelerates the electrons into the centre of the source.

TABLE 6.2

ELECTRON ENERGY /VOLTS	SIGNAL SIZE
75	127
70	162
65	121
60	139
55	117
50	101
45	92
40	42
35	0
30	0
25	0
20	0

LENS PLATES

The lens plates were made of stainless steel and were 44.35mm. in diameter and 2.0mm. thick. The potential on Lens 1 is governed by Focus Control 1 and has a range of 0 to -150V. It has an aperture of 1.5mm.. The potential on Lens 2 is governed by Focus 2 and has a

range of - 75 to 0V. It has an aperture of 3.0mm.. Lens 3 is grounded and has an aperture of 5.4mm..

The lens system is portrayed in figure 6.2. The dimensions are as follows :-

Between ion source entrance plate, (P_{ent}) and the ion source exit plate, (P_{ext}) = 12.00mm.

Between P_{ent} and Lens 1, (L_1), = 4.00mm..

Between Lens 1, (L_1), and Lens 2, (L_2), = 4.00mm..

Between Lens 2, (L_2), and Lens 3, (L_3), = 4.00mm..

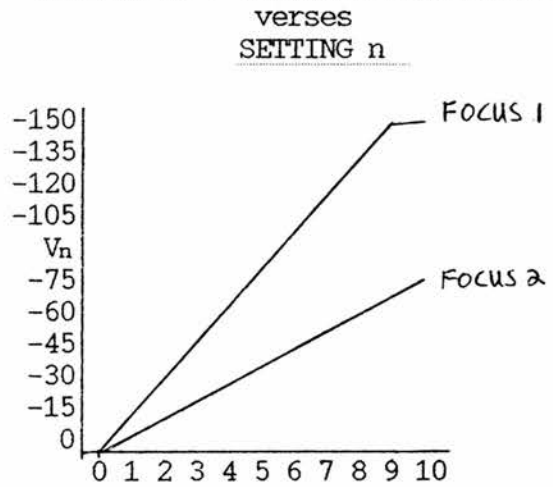
Between Lens 3, (L_3), and the first set of quads. = 2.00mm..

THE FOCUS PLATES

The focus controls were found to operate erratically. If the focus control was altered it had a dramatic effect. A large increase in the signal was detected but this subsided to its original value. Attempt to measure this effect quantitatively had failed. The voltage supplied to the plates was measured to see if it was erratic. Both focus plate supplies were found to be linear, static and imperturbable - they did not alter on altering the other variables.

TABLE 6.3

SETTING	FOCUS 1	FOCUS 2
n	V_n	V_n
0	0.00	0.00
1	-14.10	-6.86
2	-29.32	-13.94
3	-45.99	-20.29
4	-61.55	-28.36
5	-78.33	-37.16
6	-94.56	-45.63
7	-115.89	-53.95
8	-134.01	-62.14
9	-150.30	-70.32
10	-150.55	-74.37

GRAPH 6.1 FOCUS VOLTAGE / V_n 

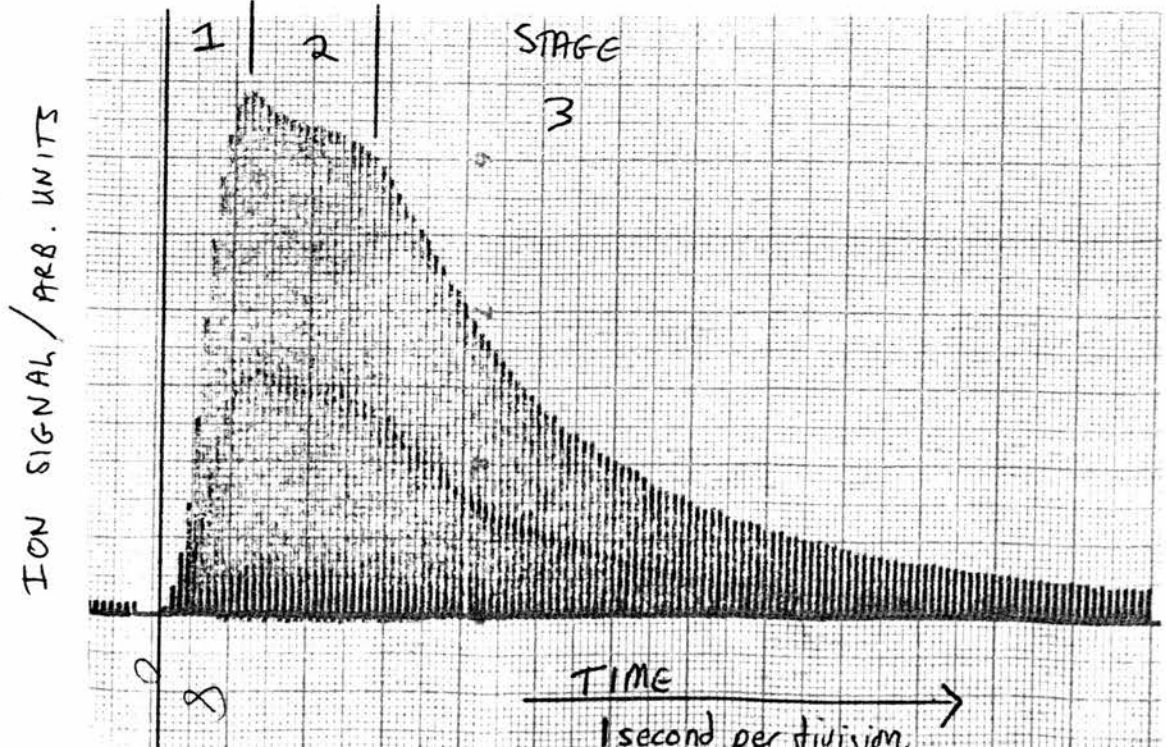
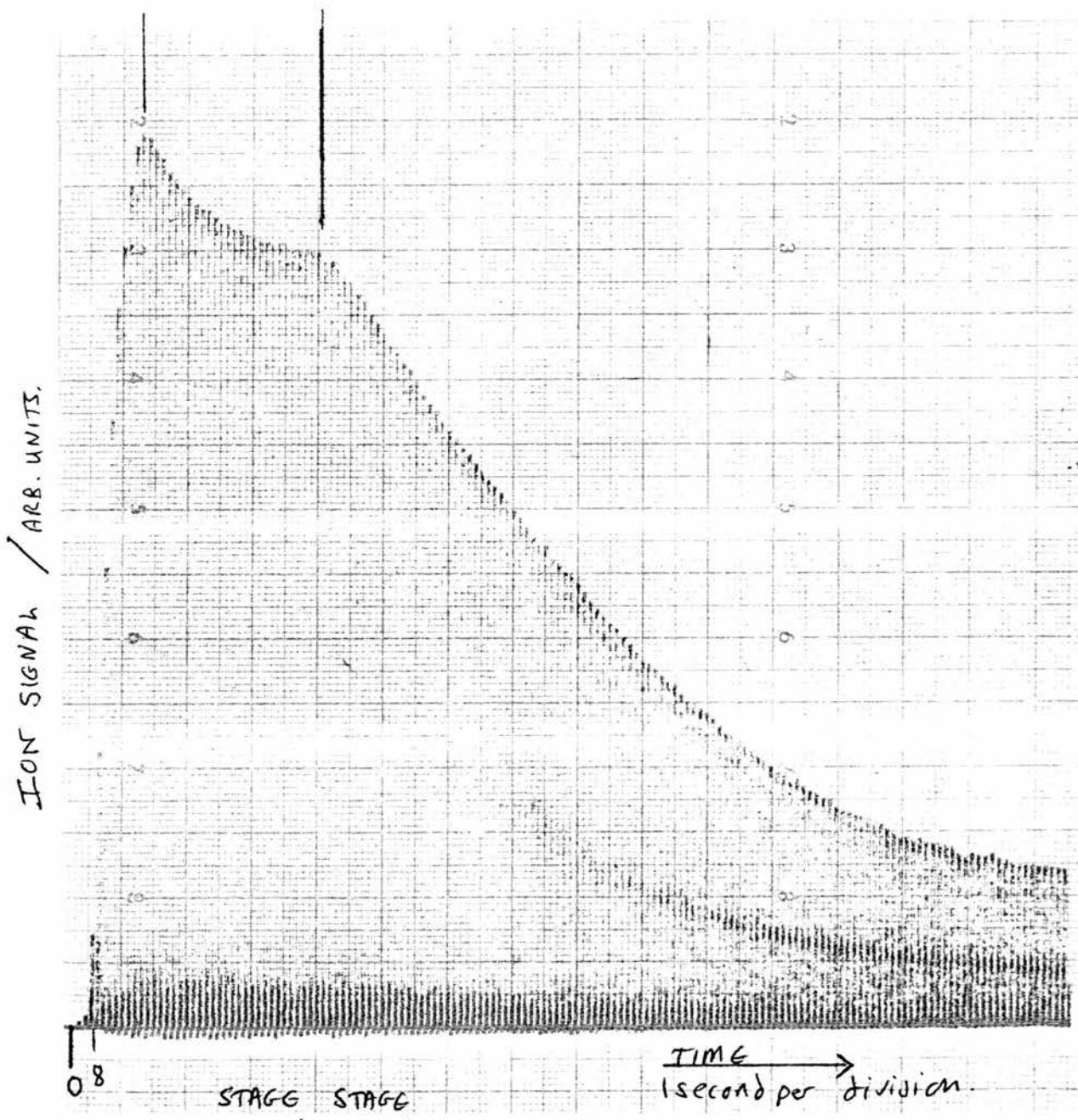
The voltage supplied to the plates remained constant as the signal fluctuated. The following copies of spectrum are non quantitative indications of the effect. They were obtained by setting the quadrupoles to repeatedly scan over a narrow mass range in which there were two main ions. By running the chart recorder at a speed such that the spectra come close together a general picture of the rise and fall of the signal can be gauged. They show that there are three stages in the effect:-

Stage one - immediately after the repeller voltage was increased the signal increases dramatically until it reached a maximum.

Stage two - after this maximum value was reached the signal diminished in a gradual exponential decay.

Stage three - in stage three the signal diminished in a much faster exponential decay until it eventually reached a minimum value.

REPETITIVE SCAN OF MASS 29+31 IONS



This process was repeated for each of the values of repeller. It was found that a stable maximum could be obtained by tuning the focus plates to a medium value. For focus 1 this was $n = 4 = -61.55V$ and for Focus 2 this was $n = 7 = -53.95V$. It was thought that this effect was probably due to the build up of charge on part of the ion source.

This dramatic increase in signal strength was utilised in an experiment that involved reacting a primary ion from the first quadrupole with a neutral gas in the second quadrupole and analysing the product ions in the fifth quadrupole. This experiment was set up but no product ions were detected despite attempts to maximising all variables. (If there is no product ion signal it is impossible to determine if the variables have been maximised.) The value of Focus 2 was then reduced to zero then put back up to 7. A large primary ion and product ion signal was obtained if the spectrum was recorded immediately after the focus was altered. After a time delay, equivalent to the time taken for the signal to diminish in the previous experiments, the spectrum contained a small primary ion signal and no product ions. It appears as if the ions were being pulsed down the quadrupoles. If the system had reached equilibrium then the size of signal was not large enough to detect any product ions. If the ion source was

perturbed by reducing the focus voltage to zero then raising it to -54V the size of signal increased dramatically but temporarily.

THE QUADRUPOLES

The rods in the quadrupoles are 120mm. long and have a diameter of 6.00mm. \pm 0.0025mm.. The longitudinal spacing between each set of rods is 4.00mm.. The internal spacing between rods in a set are such that the distance between the centre of each rod and the centre of the rods is 8.9063mm.. See figure 6.3. The minimum 'aperture' of the four rods is therefore 11.8126mm

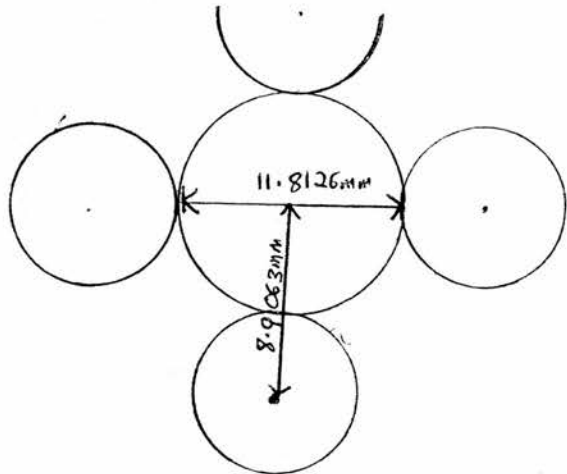


FIG. 6.3.

The first set of rods are placed flush with the ceramic butts on the third lens - that is 2mm. away from the last lens. The subsequent quadrupoles have their rods imbedded in a ceramic housing so that the separation between each set of rods is 4mm. There are no focusing plates between each set of rods. This is a matter of some debate. Some designers consider that having lenses

between each quadrupole is essential to the successful operation of the system.²⁰⁹ There are lenses in between the sets of quadrupoles in the triple quadrupole mass spectrometer but they were not found to have a beneficial effect. It was felt, however, that having constrictions between the quadrupoles in the quinquadrupole mass spectrometer would cut down the transmission of ions between the quadrupoles. Therefore to ensure maximum signal strength no lenses were fitted between the sets of rods in the quinquadrupole mass spectrometer. The question of whether placing plates between the rods in the quinquadrupole mass spectrometer would enhance the spectra or not has been raised several times throughout the commissioning of the mass spectrometer. That there was only four millimeters separation between the ends of each set of rods would make it difficult to insert plates in to the spectrometer. The quinquadrupole mass spectrometer that has been built in La Trobe University, in Australia, does have plates between each set of rods and has not produced strong ion signals at the detector. Generally it was felt that the time and effort that such a modification would require could not be justified by any deficiencies in the results obtained.

POLE BIAS

Each set of rods has a pole bias control which alters the potential of the rods with respect to ground. When set to 5.0 the pole bias is zero. At a higher setting the rods are given a negative bias which accelerates the ions through the quadrupole. At lower settings the poles have a positive bias which retards the ions.

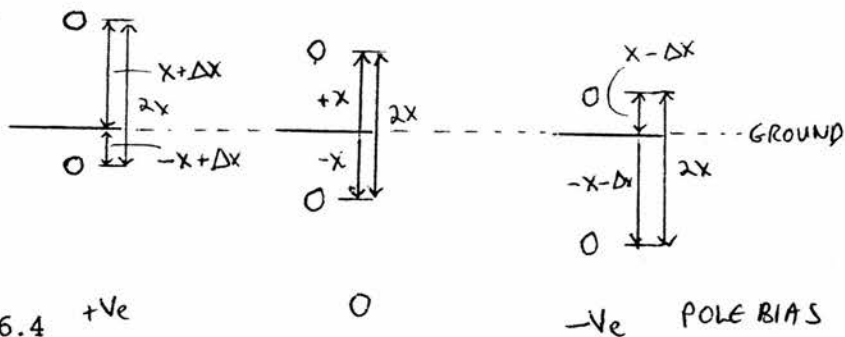


FIG. 6.4

The pole biases have to be adjusted in order to see ions at the successive quadrupoles. To enhance the signal of primary ion the pole bias of the first quadrupole must be high and negative. To detect a strong signal of the primary ion in the third quadrupole the pole biases of quadrupoles 1,2 and 3 must be large and negative. Once the primary ion has been observed in the third quadrupole and the target gas let into the second quadrupole the pole bias of the second quadrupole must be made positive in order to observe product ions in the third quadrupole. This is explicable by considering the effect of the pole biases on the ions. Having a negative pole bias on the first quadrupoles rods accelerates the ions through the quadrupoles and enhances the size of the signal. By making the pole bias of the second quadrupole positive the primary ions are retarded

and so have more chance of reacting with the gas in the second quadrupole. A negative pole bias in the third quadrupole helps separation of the ions.

The pole biases do not need to be constantly adjusted on the triple quadrupole. This is an additional complication to the operation of the quinquadrupole mass spectrometer and arises as a result of the necessity of keeping an ion signal in a stable trajectory through the intermediate quadrupoles.

THE MULTIPLIER

The multiplier on the quinquadrupole mass spectrometer is a AEM-2000 17 stage, off axis, multiplier bought from ETP PTY Limited. It works on the principle of deflecting the ions past a shield -this prevents the detector from seeing the emission from the filament- to the first stage. Ions hitting the plates cause electrons to be emitted which go on to hit the next plate, and so

on, increasing in intensity at each stage until the electrons are detected at the seventeenth stage. This is represented in figure 6.5.

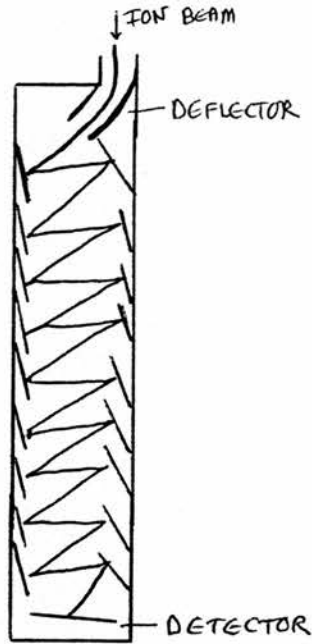


FIG 6.5

The experiment reported below was intended to check that the multiplier was working and to obtain some quantitative information on the improvement of signal-to-noise ratio that could be obtained by increasing the voltage supplied to the multiplier.

TABLE 6.4

VOLTAGE kV	PEAK HEIGHT	BACKGROUND NOISE	NOISE % SIGNAL
2.5	5700	1000	18
2.4	3900	500	13
2.3	3000	500	17
2.2	2000	300	15
2.1	1300	200	15
2.0	800	100	13
1.9	580	130	22
1.8	330	50	15
1.7	190	50	26
1.6	100	20	20
1.5	62	15	24
1.4	30	8	27
1.3	11	5	45

This table shows that although not completely linear the tendency is for the noise-to-signal level to decrease as the multiplier voltage is increased. The multiplier can be operated within the values 2.0 to 2.5 kV to maintain a good signal to noise ratio.

The signal should increase by a factor of ten when the multiplier voltage is increased from 2.0 to 2.5 kV. The results of the experiment which give an increase by a factor of 7 are in reasonable agreement.

It was concluded that the multiplier was working as it was designed to do.

EMISSION CONTROL

The emission current can vary between 0.0 and +0.5 mA. An experiment to monitor the change in size of an ion peak with respect to a change in the emission current has been repeated at several stages in the commissioning of the quinquapole mass spectrometer. The results from three such experiments which are representative of the three most common situations are shown here.

TABLE 6.5EXPERIMENT 1 27/1/1988

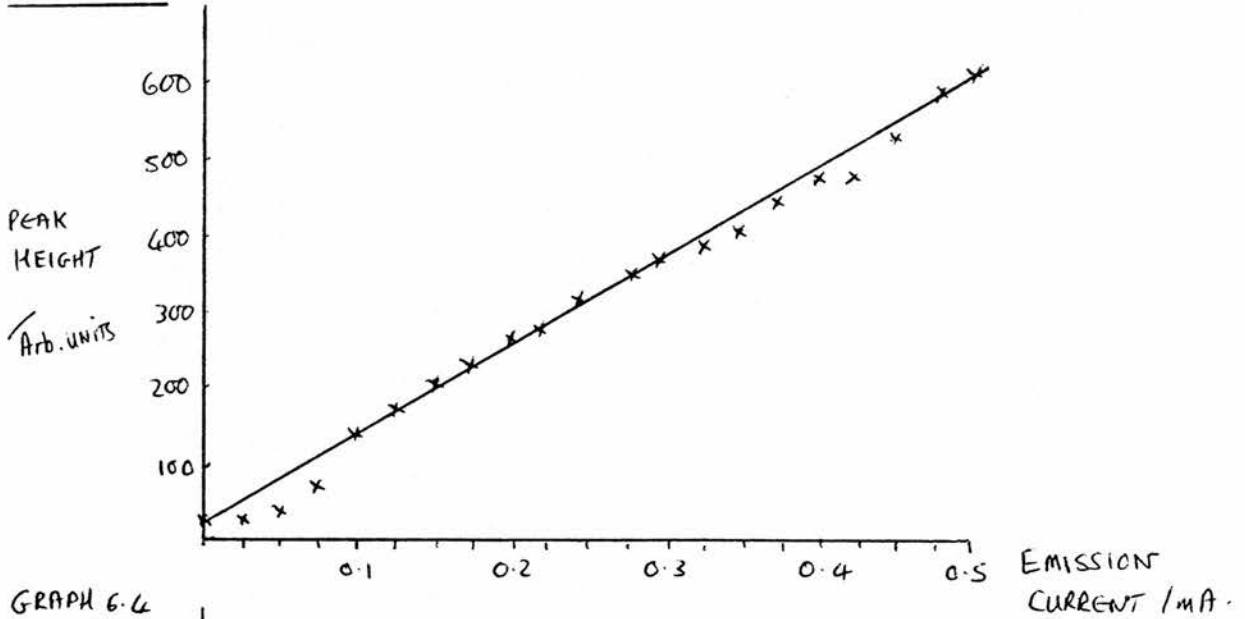
Emission Current/mA	Peak Height
0.0	27
0.025	26
0.05	29
0.075	69
0.1	139
0.125	170
0.15	210
0.175	235
0.2	270
0.225	280
0.25	320

Emission Current/mA	Peak Height
0.275	355
0.3	370
0.325	390
0.35	410
0.375	450
0.4	485
0.425	485
0.45	540
0.475	615
0.5	610

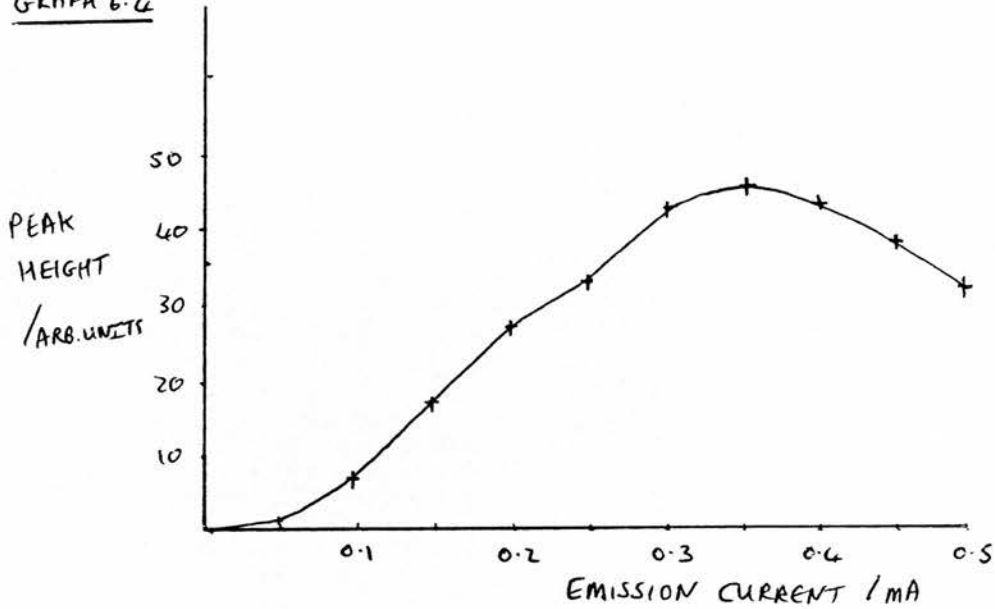
These results are plotted in Graph 6.2 and show a good linear relationship between the size of peak produced and the emission current.

The results obtained when the experiment was repeated on 30th May 1988 and 24th October 1988 are not in agreement with this finding. Graphs 6.3 and 6.4.

GRAPH 6.2



GRAPH 6.4



GRAPH 6.3

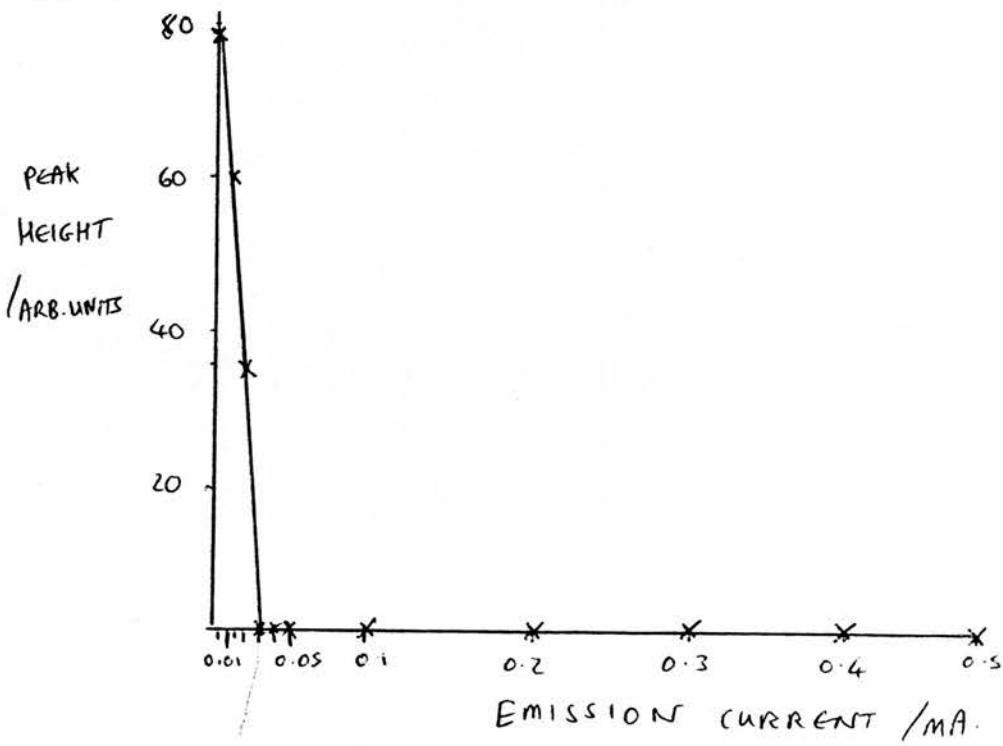


TABLE 6.6

EXPERIMENT 2 30/5/88

Emission Current/mA	Peak Height
0.00	79
0.01	60
0.02	35
0.03	0
0.04	0
0.05	0
"	"
"	"
"	"
0.45	0
0.50	0

TABLE 6.7

EXPERIMENT 3 24/10/88

Emission Current/mA	Peak Height
0.00	0
0.05	1
0.1	7
0.15	17
0.2	27
0.25	32
0.3	42
0.35	45
0.4	43
0.45	38
0.5	32

On 31st March a maximum was reached with the emission current at around 0.1mA. On 30th May 1988 the maximum was obtained when the emission current was 0.0mA. The results from experiment 1 are those of a perfect filament. The results represented by experiment 2, where the maximum signal was obtained at an intermediate value, are commonly found in other mass spectrometers and are thought to be due to a deposit building up on the filament. ²¹⁰

The results of the third experiment, in which the maximum signal was obtained with the emission set at zero can not be explained as easily. The emission control knob, the meter and the filament are all connected directly to the circuit supplying the current. It was not thought possible that the emission knob and meter could be reading a false value of the current supplied to the filament. After much thought, discussion and searching for possible explanations it was reluctantly

decided that the results of experiment 3 could not be explained but as the mass spectrometer seemed to work best with the emission control set at zero milliamps, the best thing to do was to continue to use it at that setting. A possible explanation for this strange behaviour has been found and will be discussed later in this chapter.

FILAMENT CURRENT

The filament current should be within the range 14-22 A. There is no way of directly controlling the filament current. It is a function of the emission setting. As the emission is altered the filament current is automatically adjusted to compensate. Theoretically the filament current will adapt to ensure that the emission setting is maintained.

Several diagnostics are associated with the behaviour of the filament current. If the filament is struggling to produce a current then the filament current will be very high - 22 A or above. If the ion source is at too high a pressure the filament current will fluctuate and the meter will be seen to oscillate. If the filament has gone then the filament current will read zero.

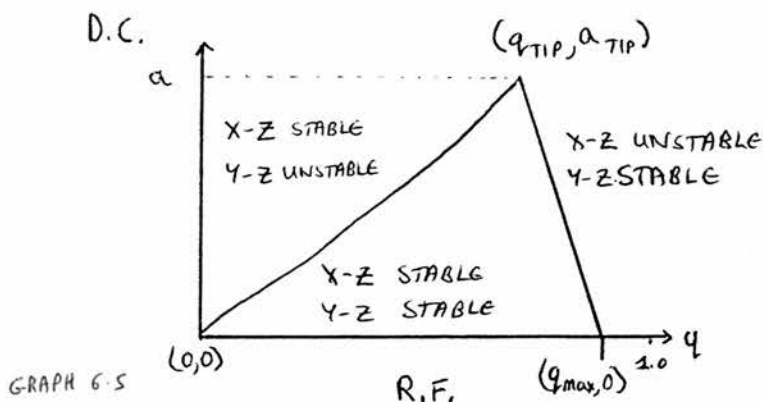
FACTORS AFFECTING THE STABILITY AND RESOLUTIONS OF IONS

IN A QUADRUPOLE

A plot of a (D.C.) against q (R.F.) where

$$a = \frac{(8eU)}{(mr_o^2\omega^2)} \quad \text{and} \quad q = \frac{(4eV)}{(mr_o^2\omega^2)}$$

yields a stability/resolution graph (6.5) in which there are three regions.



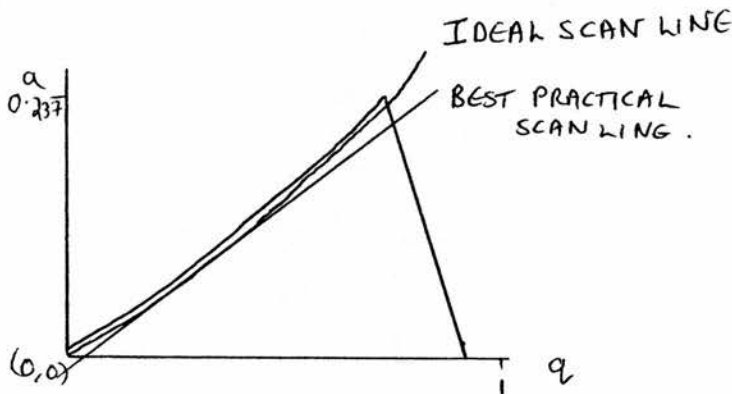
There are two stability boundaries. The curve which goes from the origin $(0,0)$ to (q_{TIP}, a_{TIP}) and the line from (q_{TIP}, a_{TIP}) to $(q_{max}, 0)$.

Any ion experiencing values of (q,a) which lie above the curve $[(0,0), (q_{TIP}, a_{TIP})]$ will have a stable X-Z motion but an unstable Y-Z motion and will not pass through the quadrupole. Similarly, any ion experiencing values which lie above the line $[(q_{TIP}, a_{TIP}), (q_{max}, 0)]$ will have a stable Y-Z motion but an unstable X-Z motion and will not pass through the quadrupole.

Any ion having values which lie within the area mapped out by these boundaries will have stable X-Z and Y-Z motion and will pass through the quadrupole. When scanning the quadrupole with no D.C. voltage applied to the rods the scan line follows the X-axis - all ions, up

to the limit q_{max} , are stable and pass through the quadrupole - this is described as Total Ion Mode and it is this mode which operates on the quadrupoles used as reaction chambers. Within the stable area the maximum resolution for an ion would occur when it is close to the curve $[(0,0), (q_{IFP}, a_{IFP})]$. The further the ion lies from this curve the purer its resolution will be.

When using the quadrupole as a mass analyser the optimum operating condition would be reached if the D.C. could change non linearly with R.F. so that the scan line would follow the curve of the resolution/stability diagram (Graph 6.6).



GRAPH 6.6

In practice a varies linearly with q so that the scan line is a straight line (Graph 6.6) starting from the point $(q = 0, a = 0 + a)$ and with a gradient of $a_2 - a_1/q_2 - q_1$ which can be reduced to

$$\frac{2(U_2M_2^{-1} - U_1M_1^{-1})}{(V_2M_2^{-1} - V_1M_1^{-1})}$$

which only involves mass and the D.C. and R.F. values.

The gradient is determined by the RESOLUTION CONTROL which selects the D.C. component.

RESOLUTION CONTROL

According to the stability diagram in the V.G. manual ²¹¹ the maximum mass of an ion that would be resolvable, M_{\max} , would occur when ($q_{\text{RIP}} = 0.706$, $a_{\text{RIP}} = 0.237$). From this we can get two equations

$$q = 0.706 = \frac{4eV}{m_{\max} r_o^2 \omega^2} \quad (6.1)$$

$$\text{and } a = 0.237 = \frac{8eU}{m_{\max} r_o^2 \omega^2} \quad (6.2)$$

rearranging these gives

$$M_{\max} = \frac{4eV}{0.706 r_o^2 \omega^2} \quad (6.3)$$

$$\text{and } M_{\max} = \frac{8eU}{0.237 r_o^2 \omega^2} \quad (6.4)$$

$$\Rightarrow M_{\max} = \frac{8eU}{0.237 r_o^2 \omega^2} = \frac{4eV}{0.706 r_o^2 \omega^2}$$

$$\Rightarrow \frac{4V}{0.706} = \frac{8U}{0.237} \Rightarrow v = \frac{1.412}{0.237} U$$

$$\Rightarrow V = 5.9578 U$$

$$\frac{U}{V} = \frac{1}{6}$$

So for maximum mass range the ratio of D.C./R.F. should be = 1/6. This should be the initial gradient. The Resolution Control will alter the ratio of D.C./R.F. and so alter the gradient of the scan line. This is shown well in the results, presented in table 6.8 and graph 6.8, of an experiment in which the D.C. on the rods was measured whilst the m/e was altered.

 ΔM

The ΔM control alters the intercept of the scan line with Y-axis by offsetting the D.C. supplied to the rods

by a fraction of 100m volts. The ΔM control is divided into 10 divisions so each division of ΔM should alter the D.C. reading by 10m volts.

The experiment described above was repeated but with the resolution set at 10 High. The results, as represented in table 6.9 and graph 6.9 show this to be the case.

An example of the effect of ΔM on the resolution of the signal was obtained by repeatedly scanning the peaks of mass 29 and 31 from dimethyl ether at M from 1 to 10. These are presented in diagram 6.4.

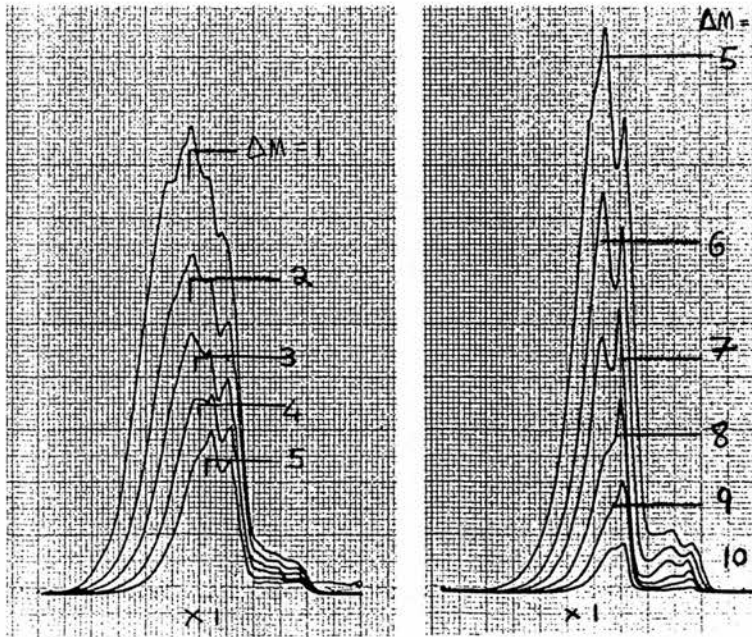


DIAGRAM 6.4

TABLE 6.8 $\frac{1}{2}$ D.C./ (MILLIVOLTS $\times 10^{-1}$) AGAINST m/e

FOR FOUR SETTINGS OF RESOLUTION CONTROL

m/e	10 High	7 High	10 Low	0 Low
0	0.394	0.419	0.394	0.34
5	1.785	1.759	1.678	1.52
10	3.563	3.478	3.318	3.03
15	5.319	5.197	4.93	4.55
20	7.073	6.94	6.57	6.08
25	8.822	8.64	8.19	7.56
30	10.54	10.34	9.83	9.10
35	12.33	12.04	11.45	10.61
40	14.07	13.78	13.05	12.11
45	15.81	15.48	14.70	13.63
50	17.54	17.20	16.32	15.14
55	19.31	18.93	17.96	16.65
60	21.08	20.63	19.58	18.16
65	22.85	22.36	21.21	19.68
70	24.60	24.08	22.85	21.20
75	26.35	25.80	24.47	22.70
80	28.10	27.54	26.11	24.22
85	29.87	29.23	27.75	25.72
90	31.62	30.94	29.37	27.26
95	33.37	32.66	30.97	28.75
100	35.12	34.39	32.62	30.26

GRAPH 6.8 $\frac{1}{2}$ D.C./ (MILLIVOLTS $\times 10^{-1}$) AGAINST m/e

FOR FOUR SETTINGS OF RESOLUTION CONTROL

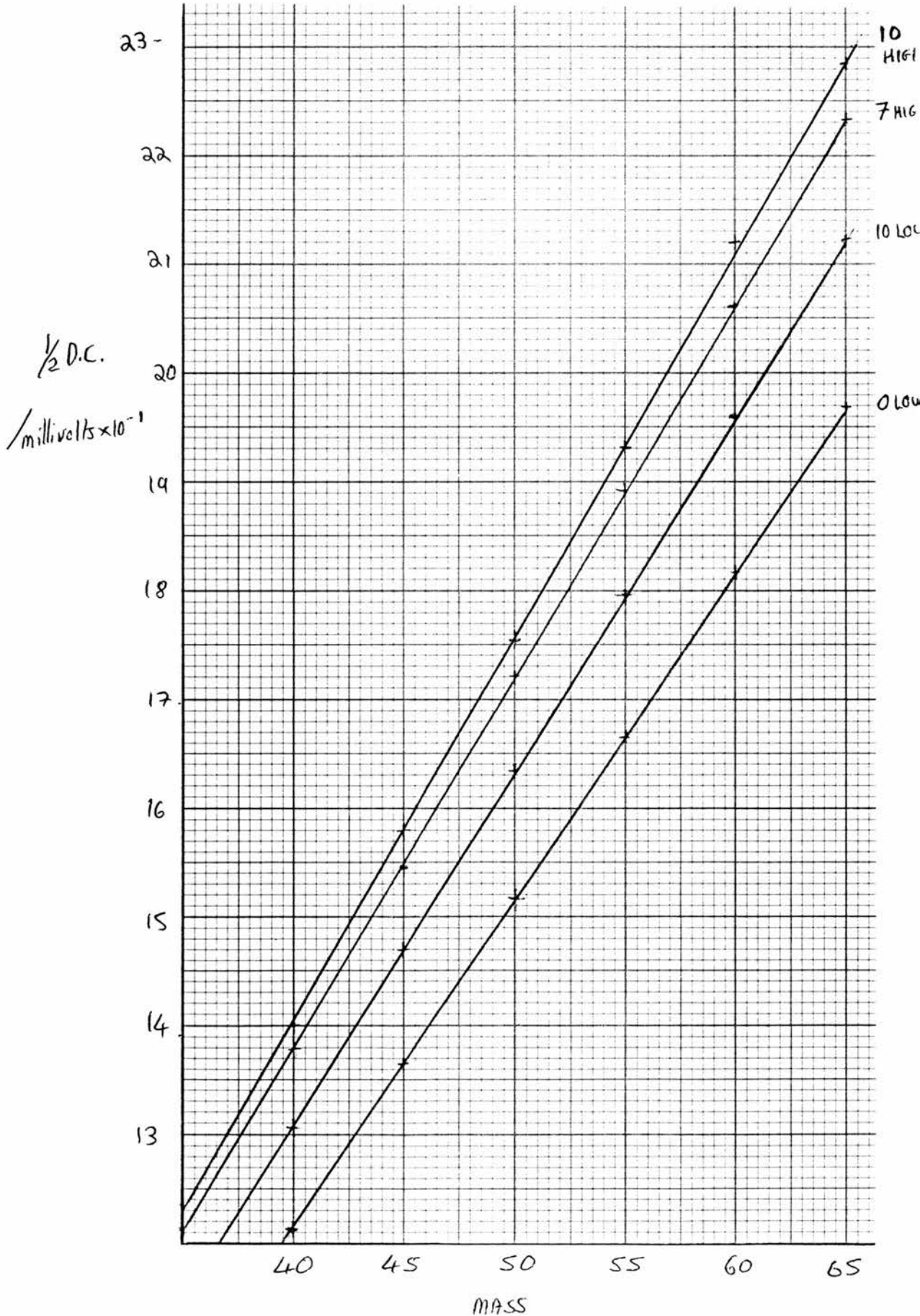


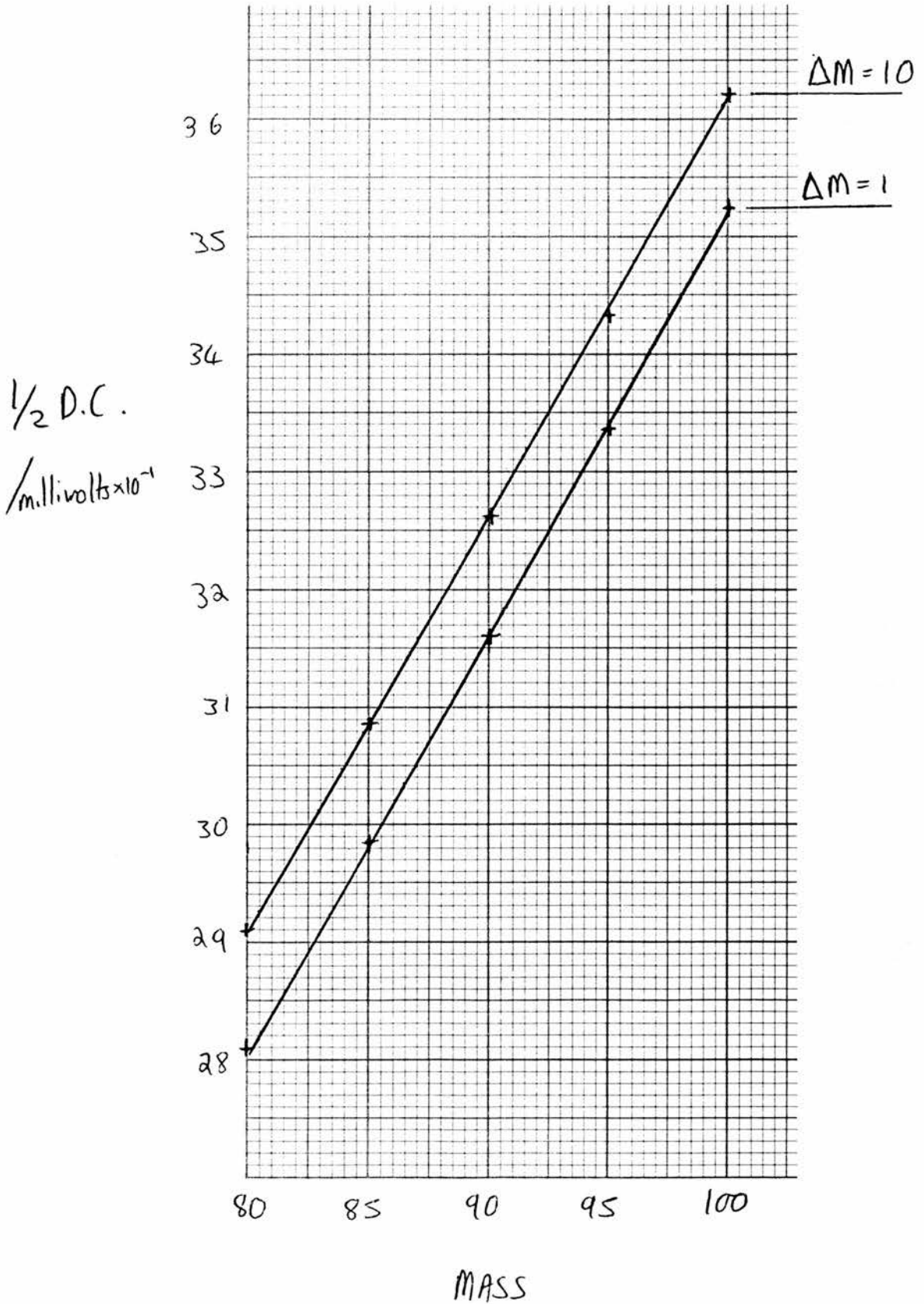
TABLE 6.9 $\frac{1}{2}$ D.C./ (MILLIVOLTS $\times 10^{-1}$) AGAINST m/e

FOR $\Delta M=1$ AND $\Delta M=10$

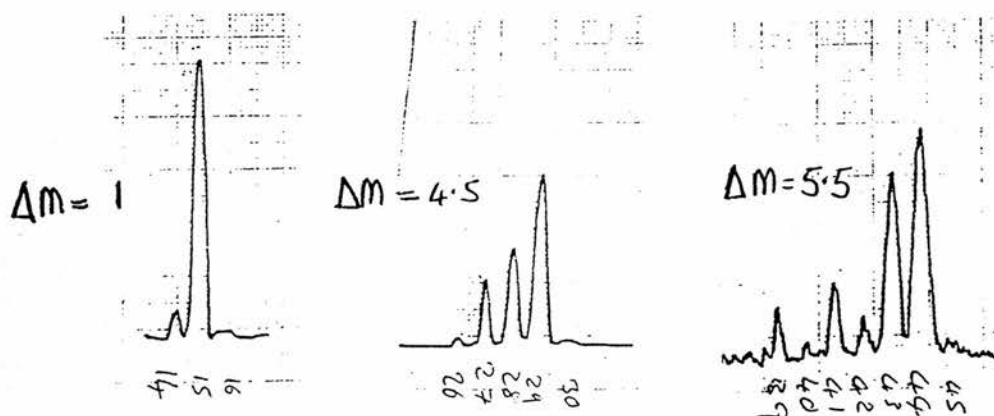
m/e	$\Delta M=1$	$\Delta M=10$	Δ (SHOULD =1)
0	0.43	1.42	0.99
5	2.20	3.18	0.98
10	3.55	4.53	0.98
15	5.31	6.29	0.98
20	7.07	8.05	0.98
25	8.82	9.79	0.97
30	10.57	11.55	0.98
35	12.32	13.29	0.97
40	14.07	15.03	0.96
45	15.82	16.79	0.97
50	17.57	18.57	1.00
55	19.32	20.32	1.00
60	21.06	22.06	1.00
65	22.83	23.81	0.98
70	24.58	25.55	0.97
75	26.34	27.32	0.98
80	28.09	29.08	0.99
85	29.84	30.84	1.00
90	31.59	32.59	1.00
95	33.34	34.31	0.97
100	35.21	36.19	0.98

GRAPH 6.9 $\frac{1}{2}$ D.C. / (MILLIVOLTS $\times 10^{-1}$) AGAINST m/e

FOR $M=1$ AND $M=10$



At various stages during the commissioning of the quinquadrupole mass spectrometer it was found that the resolution and M controls did not have sufficient power to allow complete resolution. That is to say that with M set at 10 and resolution set at 10.0 High the peaks were not completely resolved. When this occurred it was generally found that the D.C./R.F. ratio was off balance. This was either due to a maladjustment of the variable resistors or due to one of the transistors in the R.F. generator breaking. This happened quite frequently. It could be due to a deficiency in the design or the operation of the circuits which caused the transistors to be overloaded or it could be associated with the quality and life expectancy of the transistors.



On 30th May 1988 the resolution of the mass spectrum of propane was such that at $M=1$ the peak of mass 15 was resolved. The peaks around mass 27 to 29 and 39 to 44 were amorphous mounds. It was found that if the spectrum was recorded as the M was increased in stages of 0.5 from 1 to 10 the peaks of higher mass became resolved. With $M=4.5$, the peak of 15 was over resolved and was not

visible but the peaks at mass 27, 28 and 29 were perfectly resolved. The peaks around 40 were still not resolved until the M was increased to 5.5. It was also found that if the area of the amorphous mounds obtained at $M=1$ were measured and divided by the ratio of the peaks when they were resolved at higher M the resultant values for the spectrum of propane was very close to that reported in the Eight Peak Index of Mass Spectra.²¹²

TABLE 6.10

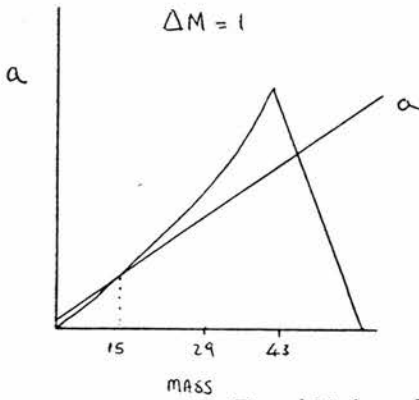
INTENSITY OF IONS FROM ELECTRON IMPACT OF PROPANE

SOURCE	ION MASS							
	29	28	44	43	27	39	41	42
REF. 211	100	60	29	23	40	18	13	-
REF. 211	100	62	40	34	32	17	15	6
Q.Q.Q.M.S.	100	36	42	33	18	11	11	-

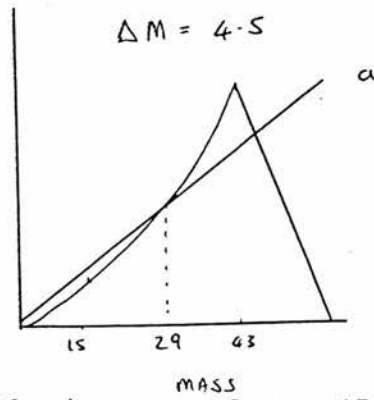
The spectrum of butane was attempted but it was found that the ions above mass 43 could not be resolved at maximum resolution.

A hypothesis was suggested to account for these failings of the spectrometer to resolve over a wide range of peaks. M alters the position at which the scan line intersects the y -axis whilst keeping the gradient constant. The results of these experiments would tie in with a situation as represented in the three stability graphs below.

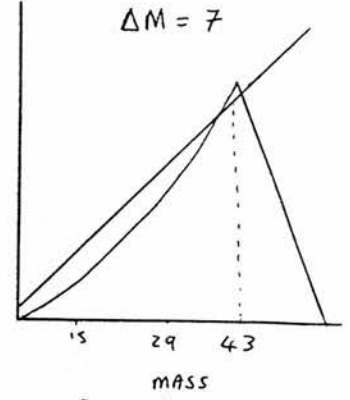
GRAPH 6.10



GRAPH 6.11



GRAPH 6.12



For $\Delta M=1$ only the ions around mass 15 are close to the resolution/stability boundary so they are resolved. The ions around mass 29 and 40 are stable but poorly resolved. As ΔM is increased from 1 to 4.5 the ions around 15 are now unstable so they are not observed. The ions of 27, 28 and 29 are now close to the resolution line and so are resolved. The ions around 40 are closer to being resolved. At $\Delta M=5.5$ the ions below 36 are on the wrong side of the stability line so they are not observed. The peaks of 39, 41, 43 and 44 are at the peak of their resolution. With the ions of higher mass from propane - 57 and 58 - they would never be close enough to the resolution curve to be resolved.

The hypothesis was that the D.C./R.F. ratio that was supplied to the quadrupoles was not correct. The D.C. component was not sufficient to give a scan line of sufficient gradient to keep close to the resolution curve for a wide range of masses. The following experiments were carried out to test this hypothesis.

The absolute D.C./R.F. values cannot easily be measured as any attempt to connect a meter to the R.F. supply will cause perturbation. The m/e value can be

measured and as the R.F. and m/e are related the values of D.C. can be plotted against value of m/e . It is also difficult, because of the geometric arrangement of the circuit board to connect a meter between the +ve and -ve rod supplies, but with the Pole Bias switched off, it can be assumed the the +ve and -ve rods are equidistant from ground and so if the meter is connected between one pair of rods and ground this will give us a reading of $\frac{1}{2}$ D.C. The table therefore has $\frac{1}{2}$ D.C. millivolts for various values of Resolution against m/e .

TABLE 6.11 $\frac{1}{2}$ D.C./ (MILLIVOLTS $\times 10^{-1}$) AGAINST m/e

FOR MAXIMUM AND MINIMUM SETTINGS OF RESOLUTION CONTROL

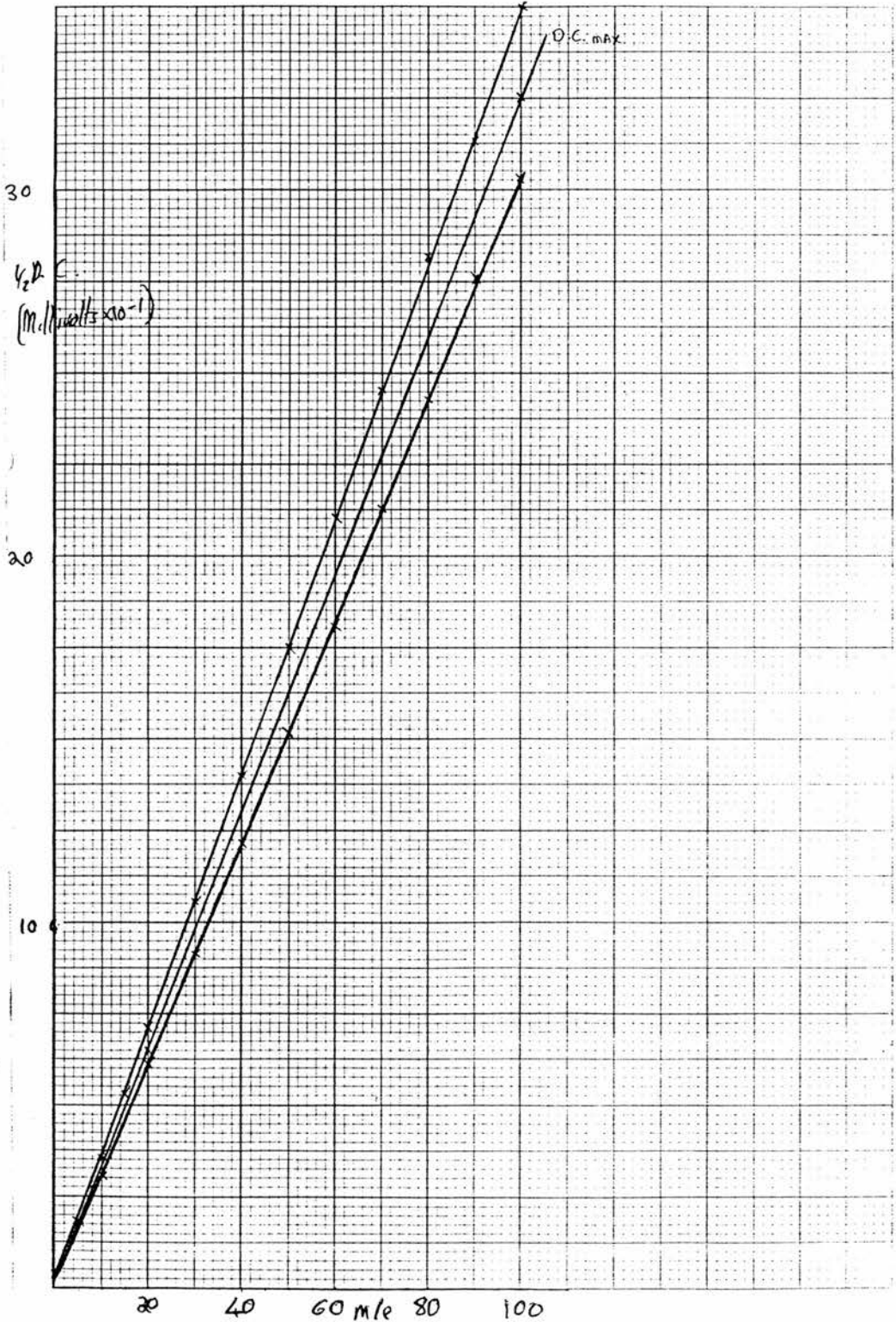
AND FOR THE MAXIMUM D.C. AT WHICH IONS WOULD BE STABLE.

m/e	10 High	0 Low	D.C. MAX.
0	0.394	0.34	0.00
5	1.785	1.52	1.63
10	3.563	3.03	3.25
15	5.319	4.55	4.88
20	7.073	6.08	6.5
25	8.822	7.56	8.13
30	10.54	9.10	9.75
35	12.33	10.61	11.38
40	14.07	12.11	13.0
45	15.81	13.63	14.63
50	17.54	15.14	16.25
55	19.31	16.65	17.88
60	21.08	18.16	19.5
65	22.85	19.68	21.12
70	24.60	21.20	22.75
75	26.35	22.70	24.38
80	28.10	24.22	26.0
85	29.87	25.72	27.6
90	31.62	28.75	29.25
95	33.37	28.75	30.88
100	35.12	30.26	32.5

TABLE 6.11 $\frac{1}{2}$ D.C./ (MILLIVOLTS $\times 10^{-1}$) AGAINST m/e

FOR MAXIMUM AND MINIMUM SETTINGS OF RESOLUTION CONTROL

AND FOR THE MAXIMUM D.C. AT WHICH IONS WOULD BE STABLE.



The results of these experiments have shown that the D.C. was varying linearly with m/e and therefore with R.F.. The theoretical maximum D.C. value required to resolve an ion of mass M to infinity can be calculated from the equation 6.5.

$$\text{D.C.}_{\text{max}} = (3.9 \times M) / 6 \quad (6.5)$$

As measurements of $\frac{1}{2}$ D.C. was measured this becomes

$$\frac{1}{2} \text{D.C.}_{\text{max}} = 0.325 \text{ volts/mass unit}$$

When values for the maximum D.C. are plotted along with the values for D.C. obtained in the experiments against m/e , as in graph 6.11, it indicates the very narrow range within which the ions of low mass must be stable.

As an example an ion of mass 55 would require a D.C. below 17.88 mV to be resolved. For resolution = 10.0 high and $\Delta M=1$ the lowest voltage measured at $m/e=55$ was 19.32 mV. This explains why the ions of mass 58 could not be resolved in the previous experiment.

The D.C. is taken from the A.C. supply. If the A.C. supply deviated from ground this might lead to the situation where the circuit was asked to supply a negative value for the D.C.. The ΔM had, therefore, been offset to + 60 mV to protect the circuits by ensuring that the D.C. supplied to the rods never became negative.

This means that at low values of m/e the ions cannot be resolved because the D.C. will be too large to allow the scan line to be below the resolution/stability curve. This should not effect the working of the quads as 60mV

will only prevent resolution of ions up to mass 5. When the ΔM offset was measured it was found to be too high by a factor of two. This could account for the failure to resolve ions of low mass in some of the quads.

The lower mass range of graph 6.11 shows how little scope there is for resolving ions around mass 15. A slight variation in the voltages could move the system above the maximum resolution line or below the minimum resolution line. In either case ions of low masses would not be able to be resolved in the mass spectrometer.

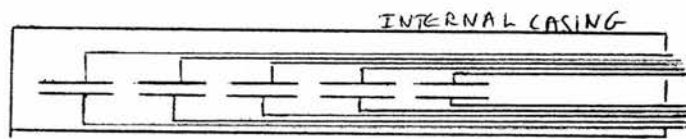
As a consequence of these results the ΔM and resolution controls were modified. This gave a much better range of masses over which the circuits were capable of resolving. A couple of experiments were done to test the range of resolution. The most comprehensive of these was to mix ethane, propane and chloromethane in the gas line because these molecules should give strong peaks at 15 CH_3^+ , 27 C_2H_3^+ and 29 C_2H_5^+ , 35 Cl^+ , 43 C_3H_7^+ , 44 C_3H_8^+ , 50 and 52 CH_3Cl . This mixture was bled into the ion source and the resultant spectrum was resolved at the one setting of M and Resolution. This experiment also showed that the system was producing a linear mass spectrum. At this point the quadrupole stopped scanning. The fault was traced back to the R.F. generator boxes where the transistor of the first quadrupole was found to have blown and a transistor in the fifth quadrupole was found to have too high a value. This is a recurring problem.

After these alterations to the resolution controls and the modifications that will be discussed in the next sections the resolution range has been much improved.

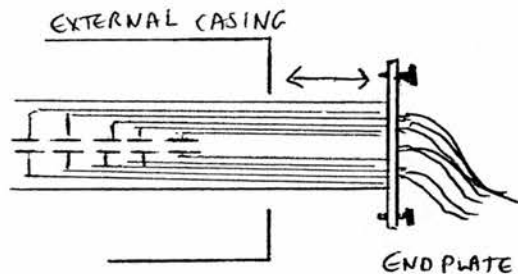
MODIFICATIONS

1) WIRES CONNECTING THE CONTROLS WITH THE QUADRUPOLES

The original design had the wires connecting the controls with the quadrupoles enclosed within the internal casing and running parallel to each other for the length of the casing.



This would allow the whole innards of the quinquapole mass spectrometer to be extracted as a whole by disconnecting the end plate only. This would make for easy maintenance.



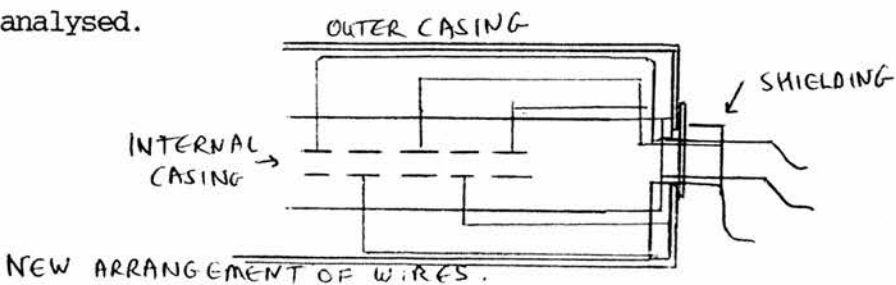
However, the current in the wires induce a field around them and it was found that the close proximity of the wires from different quadrupoles was causing interactions to occur. This problem does not manifest itself in the triple quadrupole mass spectrometer because with only three sets of wires they can be placed at 120° to each other. With the five sets of wires present in

the quinquadrupole mass spectrometer the maximum angle between them can only be 72° .



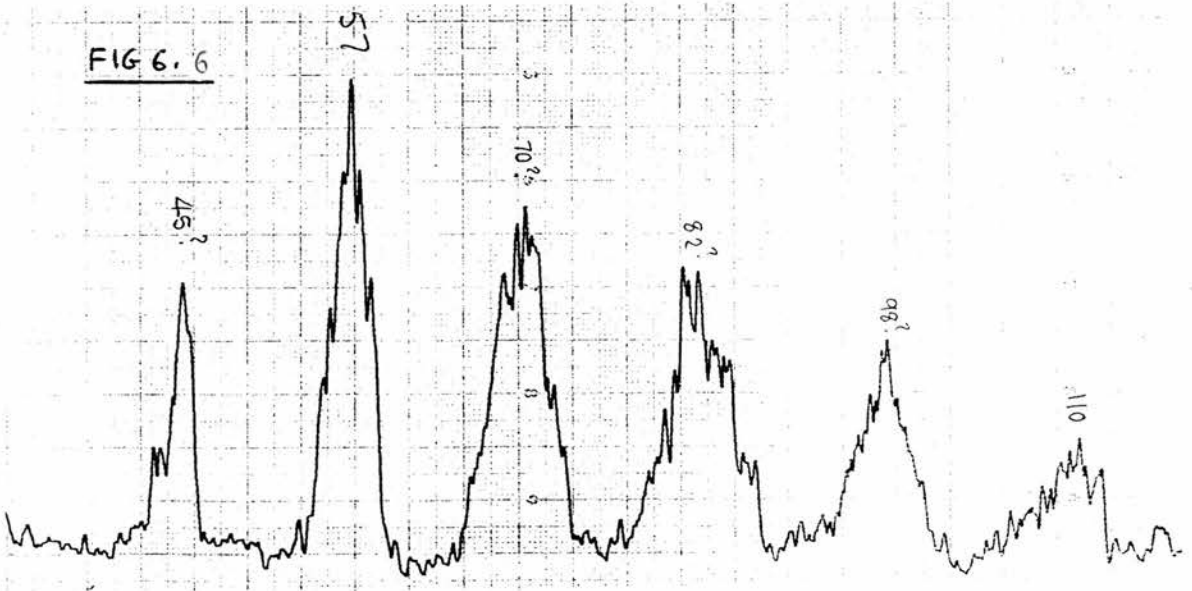
Once the quinquadrupole was in operation it was found that the quadrupoles were interacting. As the first quadrupole was scanned the second quadrupole moved in sympathy.

To counteract this undesirable effect the wires were taken out from the internal casing and placed as far apart from the others as possible. This necessitated the removal of the physical barriers between each section of the casing to make room for the wires. This succeeded in reducing the extent of interaction between the wires but it also created a problem of neutral gas flowing freely between the quadrupoles. At various times it was noted that ions were produced by the reaction of the primary ion with the primary gas which had seeped from the ionisation chamber into the subsequent quadrupoles. It is impossible - without reinstating barriers between each set of quadrupoles - to prevent the gas from the first quadrupole diffusing to the lower pressure regions. If the pressure of the primary gas is kept to a reasonable pressure - below 10^{-5} mbar - this problem can be kept to a minimum. Care must be taken at all times to ensure that this possibility is borne in mind when results are analysed.



2) LIQUID NITROGEN TRAPS

It was noticed that the background spectrum from the quinquapole mass spectrometer was extensive. This was found to arise from the oil in the rotary pumps and/or the diffusion pumps. The background spectrum was the standard hydrocarbon cracking pattern - the peaks arising in groups around 14 mass units apart. Fig. 6.6



In many of the early results it must be borne in mind that the product ions would have the same mass as those arising from the background. In the results from many experiments all of the ions that could have arisen from the reactions of the ions and molecules could also have arisen from the background.

This problem does not manifest itself with the triple quadrupole mass spectrometer. There is only one rotary pump and one diffusion pump in the triple quadrupole mass spectrometer and they are placed at a distance of 1.05 metres from the quadrupoles. There is

also a liquid nitrogen trap between the diffusion pump and the quadrupoles but it is not required.

With the quinqu quadrupole mass spectrometer there are two rotary pumps and three diffusion pumps which are positioned immediately below the quadrupoles. Maximum distance = 0.2 m. Baffles were built and placed between the tops of the diffusion pumps and the quadrupole casing. Unfortunately when the quinqu quadrupole mass spectrometer was reassembled the baffles rose up and touched the wires and shorted the transistors in the R.F. generators. The quinqu quadrupole mass spectrometer had to be disassembled to correct this. The baffles were found to have a deposit of oil on their underside indicating that the oil from the pumps was contaminating the quadrupole casing. The baffles were securely refitted. The background decreased to a great extent but not completely. It was decided to fit liquid nitrogen traps between the diffusion pumps and the main casing. This required that the whole casing be raised on eight pillars and the gas line be raised up and reconnected.

The traps were filled with liquid nitrogen. The background was measured at various times thereafter. It was considerably less than before the traps were fitted. It was found that if the traps were allowed to warm up the background increased dramatically. When the traps were refilled with liquid nitrogen the background diminished. This ratifies the decision to modify the quinquadrupole mass spectrometer. As the traps did not stay cold for longer than six hours without a refill this remained a problem throughout the subsequent experiments.

All results obtained prior to the fitting of the pumps were discarded because the product ions and background ions observed could not be differentiated.

Experiments were designed that did not require ions of the same mass as the background so as to avoid confusion. All hydrocarbons were therefore ruled out. Two alternative types of reaction were attempted. Charge exchange reactions of non-hydrocarbon compounds and protonation reactions of methanol, dimethyl ether and chloromethane. They will be discussed at the end of this chapter. These results were obtained with the minimum of background by regular filling of the traps every eight hours or so over a continuous period of days. In this way the traps were never allowed to warm up to such an extent that the background would increase.

3) THE EFFECTS OF THE PENNING GAUGE HEADS

A) TO STUDY THE EFFECT OF THE HIGH VOLTAGE AND MAGNETS IN THE PENNING GAUGE HEADS ON THE ION BEAM.

The penning heads used to determine the pressure of gas in the quadrupoles contain a large permanent magnet and use a large voltage. This set of experiments were done to investigate if either of these could be interfering with the passage of the ion beam.

The high voltage in the head could be eliminated by switching the head off. A spectrum was recorded immediately prior, and at regular intervals after, the voltage was switched off. No significant difference was detected. It can be concluded that the voltage applied to the penning heads does not affect the ion beam.

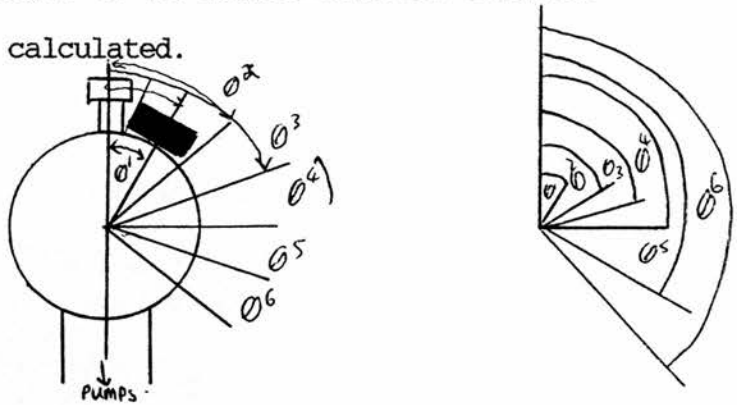
To study the effect of the magnet the magnet would have to be removed. The quinquadrupole mass spectrometer was shut down, air was allowed in and the head was totally removed to facilitate removal of the magnet. The head was replaced and the system set up as before.

Dimethyl ether was fed in to roughly the same pressure as before by monitoring on the 2nd and 3rd penning heads. The spectrum was recorded and showed a

significant decrease in size with the removal of the magnet.

A further series of experiments was done in which the size of the ion beam was measured without the magnet and then rerecorded with the magnet positioned round the circumference of the outer casing at various angles to the magnets original position.

The exact angle of the magnet from its original position can be calculated.



$$\text{Distance} = r_t + r_b + ED + 5(ID) + OB$$

$$\text{Distance} = \text{Total distance of half the circumference} = 267\text{mm}$$

$$r_t = \text{radius of the top tube} = 14.5\text{mm}$$

$$r_b = \text{radius of the bottom tube} = 8.9\text{mm}$$

$$ED = \text{External diameter of the magnets} = 60\text{mm}$$

$$ID = \text{Internal diameter of the magnets} = 29\text{mm}$$

$$OB = \text{Distance between the last placing of the magnet and the bottom tube} = 38.6\text{mm}$$

The arc for each angle can be calculated and is found to follow the general equation :-

$$\text{arc}^n = r_t + \frac{1}{2}(\text{ED-ID}) + (n-\frac{1}{2})\text{ID}$$

As $\text{arc}^n = r\theta^n$

r = distance between magnet and the centre of the quadrupoles

θ^n = angle between original position and n^{th} position of magnet

both equations can be combined to give an equation for calculating θ .

$$\theta^n = (r_t + \frac{1}{2}(\text{ED-ID}) + (n-\frac{1}{2})\text{ID}) / r \text{ in radians}$$

TABLE 6.12

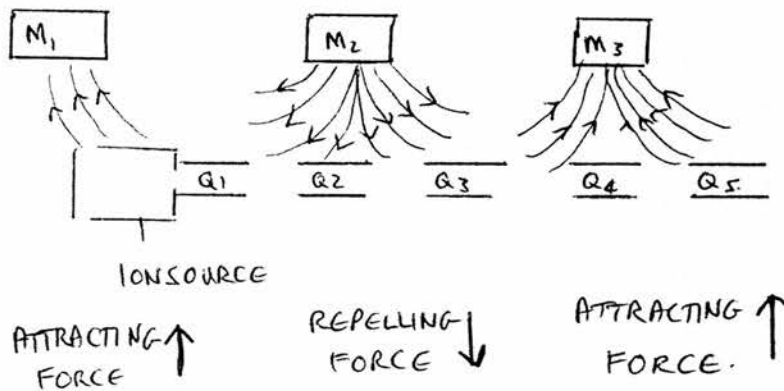
CLOCKWISE DISPLACEMENT OF MAGNET

n	θ^n rad	deg	Ratio of Peak Height with Magnet to Peak Height without Magnet
1	0.5214	29.8	3.9
2	0.692	49.3	3.3
3	0.8678	68.8	2.8
4	1.0385	88.3	1.6
5	1.209	107.8	1.5
6	1.3796	127.2	1.0

ANTICLOCKWISE

n	θ^n rad	deg	Ratio of Peak Height with Magnet to Peak Height without Magnet
1	0.5214	29.8	2.2
2	0.692	49.3	1.8
3	0.8678	68.8	1.5
4	1.0385	88.3	1.5
5	1.209	107.8	1.5
6	1.3796	127.2	1.2

From these results it can be suggested that the magnet is having a substantial effect on the ion signal. The first penning head is behind the ion source. As it attracts ions it must be drawing the ion beam away from the quadrupole. That explains why the ion energy, electron energy and pole bias have had to be at their extreme values before sufficient ions were attracted down the quadrupoles so that a signal could be observed at the detector. Further investigation revealed that the second penning head was built - by Edwards Vacuum - with the polarity of its magnets of the opposite orientation to the magnets on the first and third penning heads. Any ions that managed to leave the source in the direction of the quadrupoles would then be influenced by the magnets immediately above them and would be repelled and forced down by the second magnet and attracted up by the third magnet.



B) TO DETERMINE THE OPTIMUM DISTANCE FOR THE PENNING HEADS TO BE AWAY FROM THE QUADRUPOLES SO THAT THE EFFECT OF THE MAGNETS IS MINIMAL

A spectrum was taken of dimethyl ether when there was no magnet. This is taken as the value for the magnet at infinite distance. $D_m = \infty$. The magnet was placed over the penning head at a distance, D_m , from the external surface. The size of the peak mass 29 was recorded as the magnet was moved away from the centre of the quadrupoles.

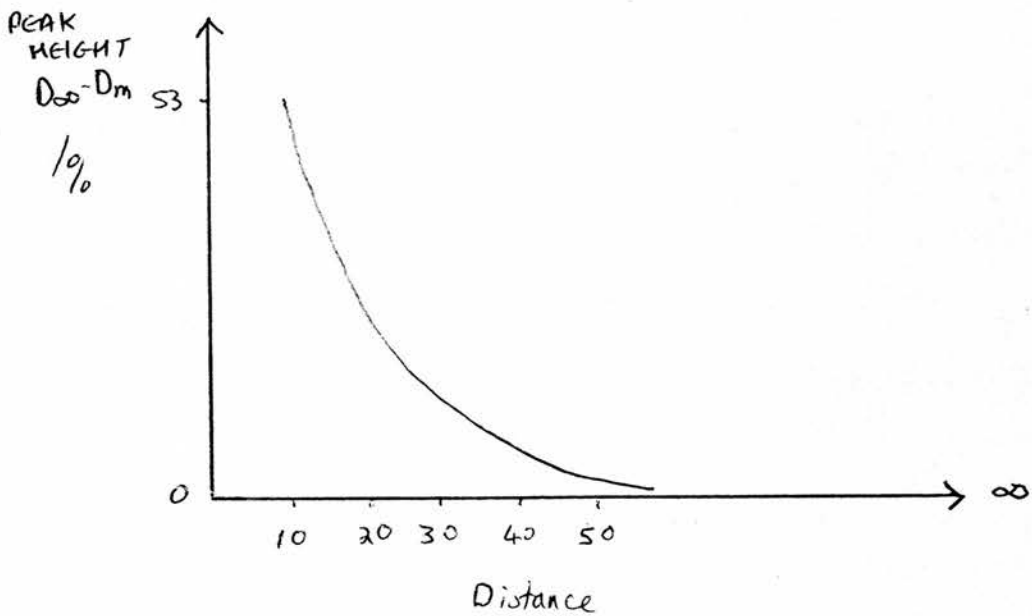
TABLE 6.13

Distance from outer casing	Distance from centre of Quads.	Peak Height	Difference % $D_\infty - D_m$	
∞	∞	38	-	-
50	58.5	39	+1	3
40	48.5	40	+2	6
30	38.5	43	+5	13
20	28.5	47	+9	24
10	18.5	58	+20	53

As can be seen from this table and graph 6.14 the size of the peak decreases dramatically as the magnet is moved away from the quadrupoles. At $D_m=50\text{cm}$ the magnet is still having an influence on the size of the ion signal but it is barely detectable.

As a consequence of these investigations it was decided to place the three penning heads on tubes 45cm long. (This length was dictated by the length of the tubing available.) This would take the magnets $55\frac{1}{2}$ cm away from the outer casing and 64 cm away from the centre of the quadrupoles.

Peak Height % $D_{\infty} - D_m$ for distance of magnet away from casing

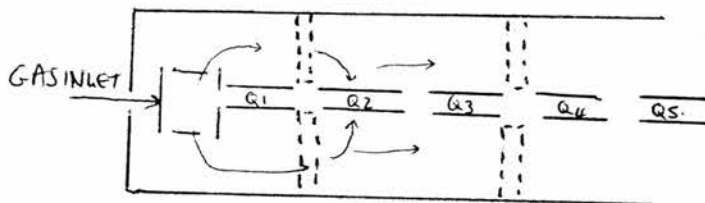


GRAPH 6.14

3) GAS INLET

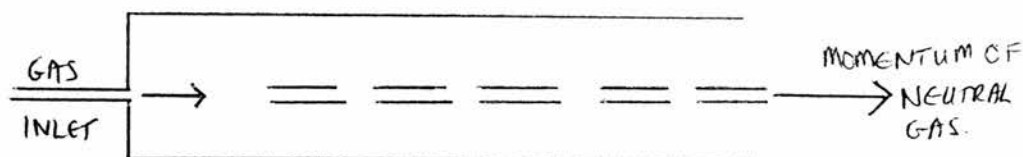
In experiments it was noticed that ions had been formed in the second quadrupole. By altering the pressure of the primary gas with respect to the secondary gas it was deduced that these ions arose from the reaction of the primary ion with primary neutral molecules. This was confirmed by removing the secondary gas completely. The ions were still present.

There are two possibilities that could explain this occurrence. 1) By removing the barriers between the sections of the casing to enable the wires to pass at a maximum distance from each other the gas in the first quadrupole can diffuse through all other areas in the casing.

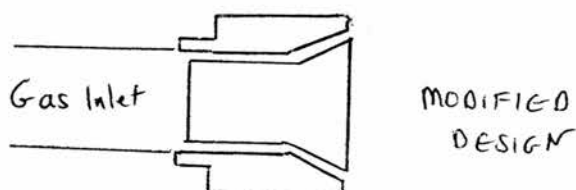
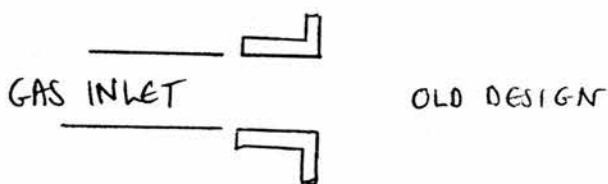


2) The alternative explanation concerns the design of the primary gas inlet. The primary gas is bled into the ionisation chamber through a stainless steel tube in the endplate. The neutral gas would have momentum in the axis of the quadrupoles and so a stream of neutral gas would flow through all the quadrupoles. In effect the primary ion selected in the first quadrupole would have

to pass through an atmosphere of the neutral gas before they reach the multiplier. In addition when a secondary gas was to be added to the second quadrupole it would have to go into an atmosphere of the primary gas. This would restrict the amount of target gas that could be present in the reaction chamber.



The gas inlet was redesigned. A dispersing nozzle was formed by combining the reshaped ceramic tube with a ceramic central core from which four cords had been cut. The gas entering the nozzle would go through the four cut out sections of the central portion. On reaching the end they would fan out. This succeeded in producing an atmosphere of primary gas in the vicinity of the filament without producing a stream of neutral molecules down the length of the quadrupoles.



This arrangement was found to produce a much larger ion signal at lower pressures than had been previously been observed. The resolution was much improved as well. Unfortunately the background was also much larger.

At high pressures it was found that some primary gas was still present in the second quadrupole. This was probably due to the seeping of gas in the casing. It was not found to be sufficiently large a problem to merit redesigning the casing to replace some form of partitioning between the quadrupoles.

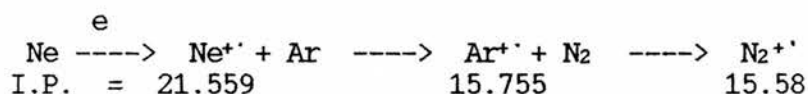
As a consequence of these modifications the quinquadrupole mass spectrometer was operating as it was designed to do. Although not at maximum capacity the quinquadrupole mass spectrometer was used to investigate ion/molecule reactions. These results are presented in the next section.

RESULTS FROM THE QUINTA QUADRUPOLE MASS SPECTROMETER

- 1) Charge exchange reactions
 - 2) The protonation Of methane
 - 3) The formation and reaction of protonated ions
- utilizing all five quadrupoles.

1) CHARGE EXCHANGE REACTIONS

A simple series of sequential charge exchange reactions - although not of great scientific significance - was useful in aiding the initialising of the quadrupole systems. Neon (Ionisation potential = 21.559eV) ²¹² in the ionisation chamber gave Ne⁺ ions of mass =20 from the first quadrupole which was put into Argon (I.P. = 15.755eV, mass = 40,38,36) in the second quadrupole giving Ne⁺ and Ar⁺ in the third quadrupole.



Ar⁺ was then isolated from the third quadrupole and put into N₂ (I.P. = 15.58eV, mass = 28) in the fourth which produced N₂⁺ as the product ions.

The great advantage of using a simple charge exchange reactions was that the product ions were not a series of ions which would dissipate the size of the signal. As the product is a single ion 100% of the signal is carried on into the next quadrupole.

The first stage of this sequence was achieved - i.e. Ar⁺ was produced - but it was only detected when the fifth quadrupole was scanned - that is using the first as an ion separator, the second, third and fourth as a reaction chamber and the fifth as an analyser.

When it was attempted to analyse the ions using the third as an analyser - and allowing the fourth and fifth to pass all ions - no product ion was observed - despite exhaustive attempts to tune the third quadrupole - to adjust the resolution, pole bias and M. That no product ion was observed from the third quadrupole whilst it was observed at the fifth quadrupole led to the suggestion of two possible explanations for this problem:-

1) the third quadrupole was not tuned and so it could not separate and resolve both the primary ion and the product ion.

or

2) the third quadrupole was isolating both primary and secondary ions but on passage through the fourth and fifth quadrupoles to the multiplier the small signal for the secondary was being lost. It is easy to appreciate on seeing the size of the primary signal with respect to the noise of the baseline how a slight mis-tuning of either the fourth or fifth quadrupole would lead to the dissipation of the peak.

It was not possible to distinguish directly which of these two possible explanations, if either, were responsible because each fault would mask the other. So in an attempt to solve the problem three things were tried:

- 1) the third quadrupole was carefully and meticulously adjusted in all of its parameters - but still no ion could be detected.
- 2) the fourth and fifth quadrupoles were likewise adjusted - again to no observable improvement.
- 3) the adjustable control box for the third and fifth quadrupoles were swapped round and adjusted to give a spectrum. A spectrum was observed on the fifth quadrupole which was controlled by the third box but no spectrum was observed on the third quadrupoles controlled by the fifth box. Therefore if there is some part of the third quadrupole controls that is out of tune it is not in the control box and so it has to be the R.F. generator.

The balance of the D.C. supplied to the third quadrupole was measured. It was found that the voltage between the negative supply and ground was +14.28 and that between the negative supply and ground was -14.26. This shows that the D.C. supply is balanced to within 0.07%.

This would seem to suggest that the third quadrupole was all right and should be capable of separating a secondary ion peak if it was present.

At this stage it was decided to change the target gas from Argon - which has a very small radius and would thus present a very small target - to Nitrogen which being diatomic would present a larger target and would

also have the advantage of being able to have an induced dipole.

Ne⁺ was put into an atmosphere of N₂ in the second quadrupole. Both Ne⁺ and N₂⁺ were detected when the fifth quadrupole was scanned. The third quadrupole was adjusted and eventually both ions were also observed when the third was scanned. The relative peak heights for the Ne⁺ and N₂⁺ ions are presented in table 6.14.1

TABLE 6.14.1 RELATIVE PEAK HEIGHTS

PRESSURE mbar x 10 ⁻⁵	4	5	6	7	8	9
Ne ⁺ m/e=20	10200	9800	8500	8000	5900	5300
N ₂ ⁺ m/e=28	56	68	81	94	107	120

The N₂⁺ peak was separated in the third quadrupole with the pressure at 9 x 10⁻⁵ mbar (6.75 x 10⁻⁵ torr) and put it into another gas in the fourth and analyse the products in the fifth quadrupole. Nitrous oxide was chosen as it has an ionisation potential of 12.6eV. The nitrous oxide cation and fragment ion at mass = 30 = NO⁺ was seen when the fifth quadrupole was scanned. The pressure of N₂O was varied and the results expressed in table 6.14.2

TABLE 6.14.2

PRESSURE mbar x 10 ⁻⁴		2	2.5	3	3.5	4
N ₂ ⁺	m/e=28	82	74	53	36	36
NO ⁺	m/e=30	trace	amount only			
N ₂ O ⁺	m/e=44	56	68	81	94	107

The Eight Peak index ²¹² lists the spectra with N₂O as in N₂O⁺ as the major peak and NO⁺ as the largest of the fragments.

The results of our chemical ionisation spectra match well in that the two largest ions were observed. The smaller ions were not seen. N₂⁺ (mass = 28) would not be distinguished from the primary ion - also N₂⁺ (mass = 28). N⁺ (mass = 14) and O⁺ (mass = 16) were not seen but it is not clear if that was because they were so small or because the quadrupoles were not tuned to analyse as low a mass as 16 mass units.

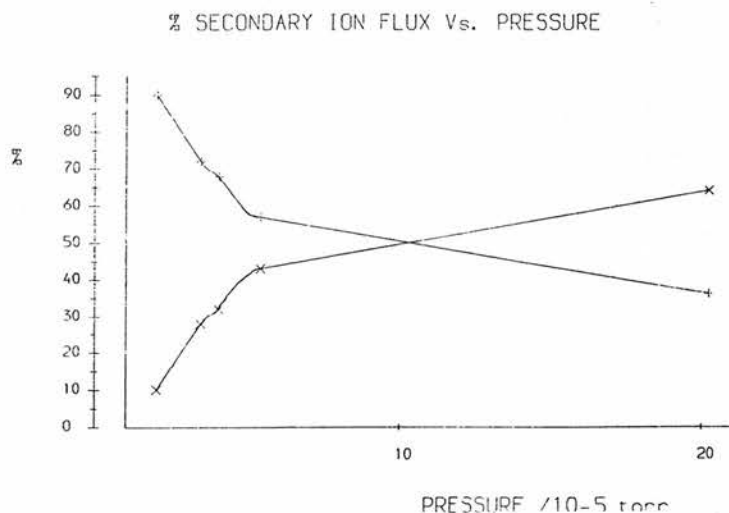
It has been shown that it is possible to take an ion from an electron ionised sample gas, separate it in the first quadrupole - analyse the products - select one of the product ions in the third quadrupole and react it with another gas in the fourth and analyse the product ions in the fifth quadrupole.

Ionistn Chamber	1st Quad.	2nd Quad.	3rd Quad.	4th Quad.	5th Quad.	m/e
			N ⁺			14
Ne -e-->	²⁰ Ne ⁺	N ₂	Ne ⁺			20
	²² Ne ⁺		N ₂ ⁺	N ₂ O	N ₂ ⁺	28
					NO ⁺	30
					N ₂ O ⁺	44

2) PROTONATION OF METHANE

One of the experiment attempted when the quinquapole mass spectrometer had a narrow resolution range was directly relevant to the work reported in chapter two :- the protonation of alkanes.

The methyleneaminylium ion, CH_2N^+ , was separated in the first quadrupole from the other ions of mono methylamine and put into methane in the second quadrupole. Analysis of the ions in the fifth quadrupole - with the second, third and fourth quadrupoles on total ion mode - produced ions of mass 15 and 17. The pressure of methane was adjusted. A graph of percentage of secondary ion for CH_3^+ and CH_5^+ against pressure was plotted.

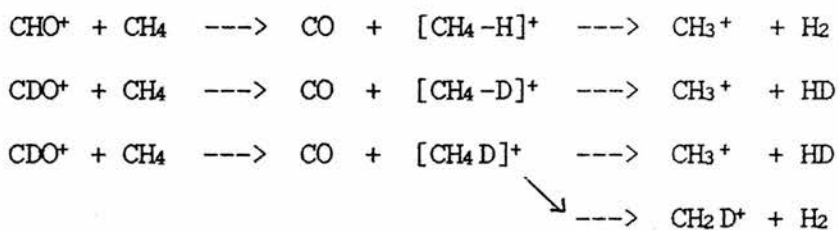


These results are comparable with the results obtained from the same experiment on the triple quadrupole mass spectrometer. Chapter 2 page 75.

After retuning the quadrupoles CH_3^+ and CH_5^+ ions were observed on analysis of the third quadrupole. The CH_5^+ was selected from the third quadrupole and were detected in the fifth quadrupole. However, when a target

gas was put into the fourth quadrupole no product ions or fragment ions were observed because the signal of CH_5^+ was not strong enough.

Had this experiment worked then the fragmentation of CH_5^+ and CH_4D^+ could have been compared to see if some indication of the structure of the protonated methane could be deduced.

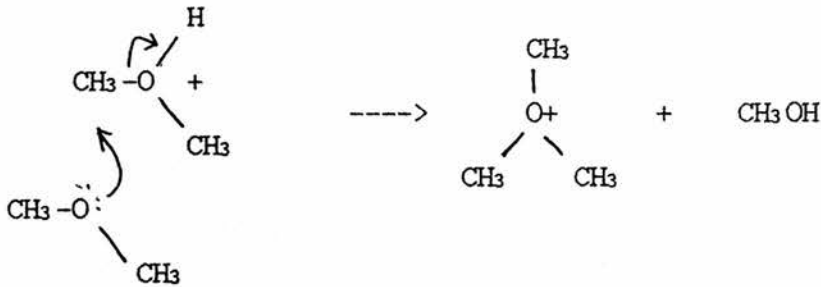


This experiment would have been repeated when the modifications had improved the strength of the signals except that the third quadrupole was found not to be resolving as low as 15 mass units.

3) FORMATION AND REACTION OF PROTONATED DIMETHYL ETHER
AND CHLOROMETHANE .

a) Following on from the experiments of chapter three the protonation of dimethyl ether was investigated in the quinquadrupole mass spectrometer.

One of fundamental steps in the reaction mechanisms proposed to account for the formation of hydrocarbons from methanol involves the reaction of dimethyl oxonium ions with dimethyl ether to produce the trimethyl oxonium ions. 7,142

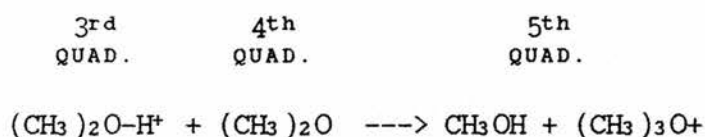
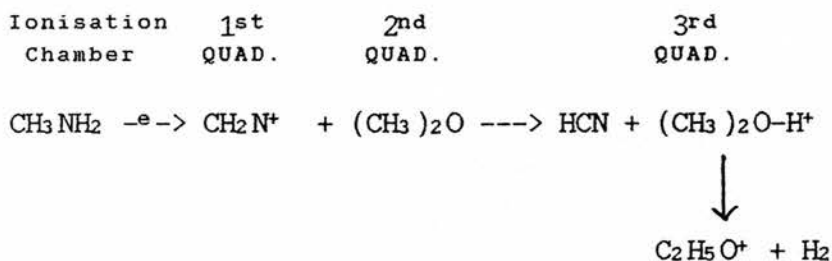


Although this reaction was thought to have occurred in the reactions of dimethyl ether in the triple quadrupole mass spectrometer it could not be investigated unequivocally.

The methyleneaminylium ion, CH_2N^+ , was isolated in the first quadrupole and put into dimethyl ether in the second quadrupole. The ions observed in the third quadrupole were dimethyl oxonium ions, $(\text{CH}_3)_2\text{-OH}^+$ mass =47 and the fragment ion $\text{C}_2\text{H}_5\text{O}^+$ of mass 45.

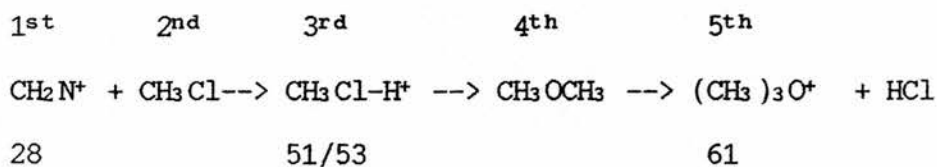
The dimethyl oxonium ion was selected from the third quadrupole and put into dimethyl ether in the fourth quadrupole. The ions produced in the fifth quadrupole

were $\text{C}_2\text{H}_5\text{O}^+$, mass =45 - a fragment of dimethyl oxonium ions- and the trimethyl oxonium ion of mass 61 $-(\text{CH}_3)_3\text{O}^+$.

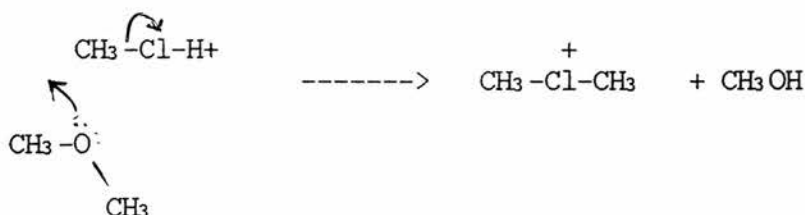


Labelled dimethyl ether could be used to prove the mechanism.

b) The following experiment was done to investigate a reaction that was relevant to the studies of chapters 3,4 and 5. It was also important as it was a reaction that involved a different gas at each stage.

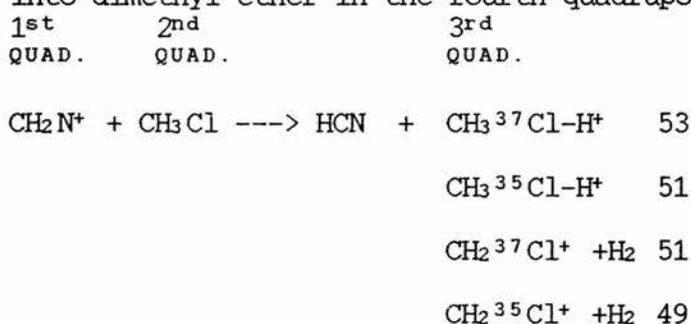


It was intended that this would show if the hydrogen chloride displacement reaction that was thought to occur could be shown to occur with the methyl chloronium ion reacting with dimethyl ether.



This experiment was not possible on the triple quadrupole mass spectrometer.

CH_2N^+ ions were put into chloromethane in the second quadrupole. Three products were detected in the third quadrupole. Ions of mass 53 - $\text{CH}_3^{37}\text{Cl}-\text{H}^+$, 51 - $\text{CH}_3^{35}\text{Cl}-\text{H}^+$ and $\text{CH}_2^{37}\text{Cl}^+$, and 49 - $\text{CH}_2^{35}\text{Cl}^+$. The majority of the peak of mass 51 was due to protonated chloromethane with the chlorine-35 isotope. This peak was separated and put into dimethyl ether in the fourth quadrupole.



The ions produced were dimethyl oxonium ions of mass 47, $\text{C}_2\text{H}_5\text{O}^+$ ions of mass 45 and trimethyl oxonium ions of mass 61.

The graph of ion percentage against pressure shows, (page 176) - that the trimethyl oxonium ions are tertiary ions and

increases as the amount of dimethyl oxonium ions decreases. The previous experiment has shown that trimethyl oxonium ions can be formed from the reaction of dimethyl oxonium ions with dimethyl ether. Because the main product of the reaction of methyl chloronium ions with dimethyl ether is dimethyl oxonium ions it is not possible, on the strength of this experiment, to show if the trimethyl oxonium ions are being formed by the addition with elimination reaction of methyl chloronium ions with dimethyl ether or of dimethyl oxonium ions with dimethyl ether. This could be resolved by using labelled dimethyl ether or labelled methyl chloronium ions. As neither of these chemicals were available this research was not taken any further.

CONCLUSIONS

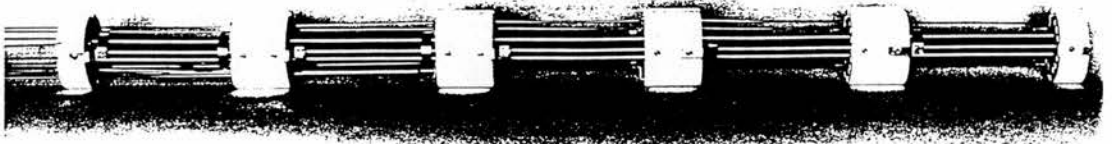
The quinquadrupole mass spectrometer has been shown to be capable of a series of sequential ion molecule reactions. Deficiencies of the original design have been removed and the 'teething troubles' have been combated. There are further improvements that could be made. The resolution range could be larger. The background spectrum could be reduced.

Despite these ongoing deficiencies several reactions have been studied which could not have been investigated on the triple quadrupole mass spectrometer. Provided that due care is taken to critically analyse the results produced from the quinquadrupole mass spectrometer to ensure that background ions are not mistaken to be product ions - the quinquadrupole mass spectrometer can be used to investigate sequential ion/molecule reactions.

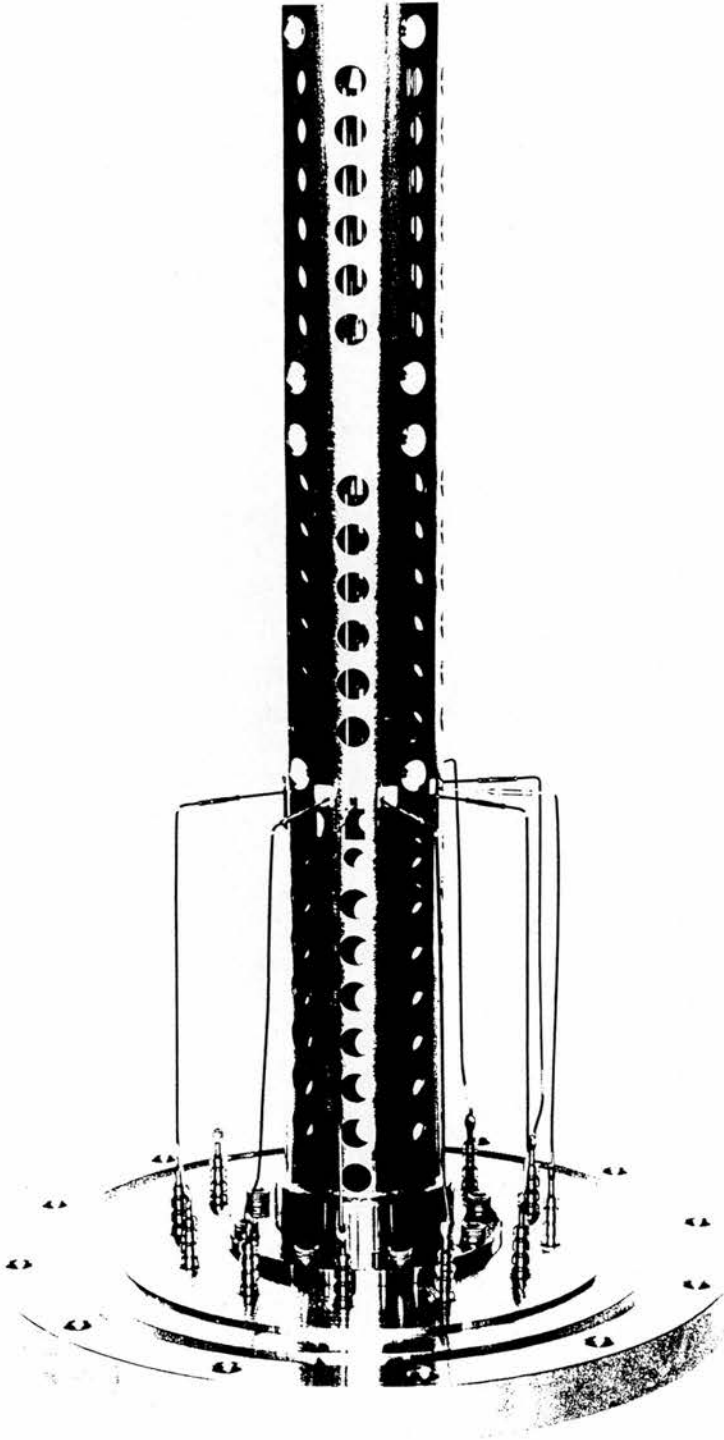
APPENDIX A

PHOTOGRAPHS OF THE QUINQUA QUADRUPOLE

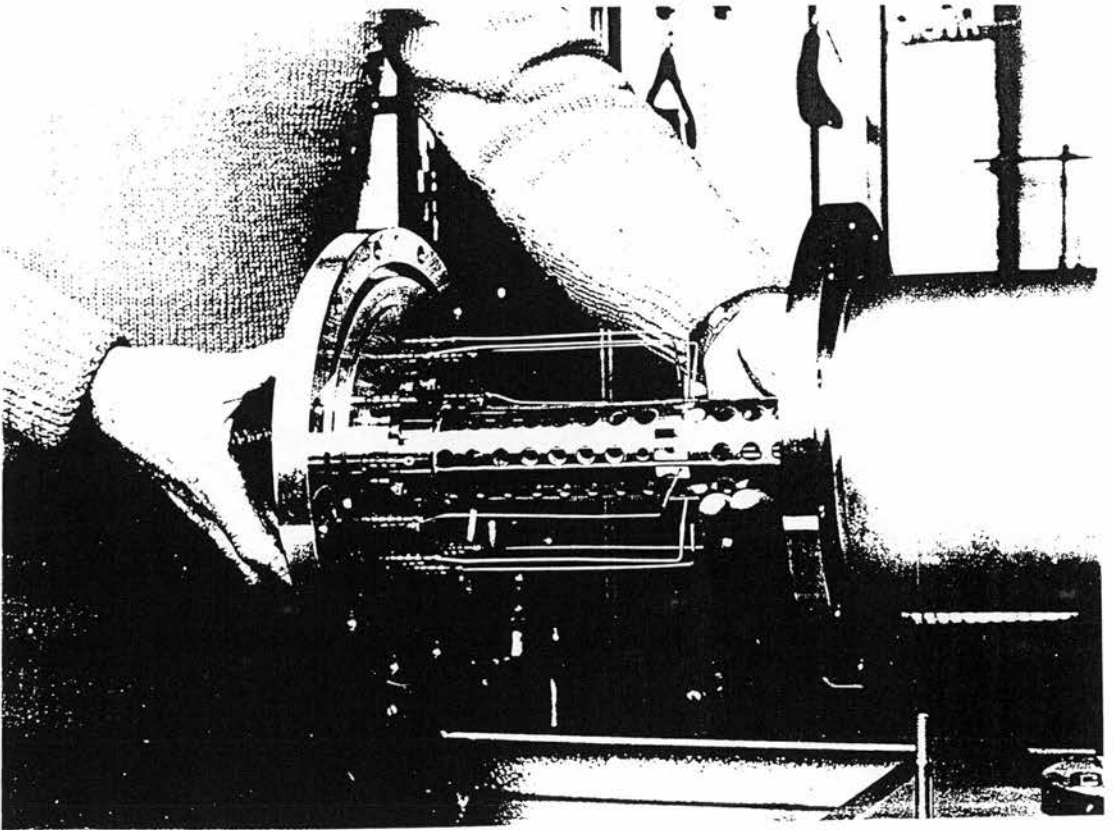
- 1) THE QUADRUPOLES - SHOWING THE INITIAL SYSTEM WITH THE WIRES RUNNING THROUGH CERAMIC HOUSING.



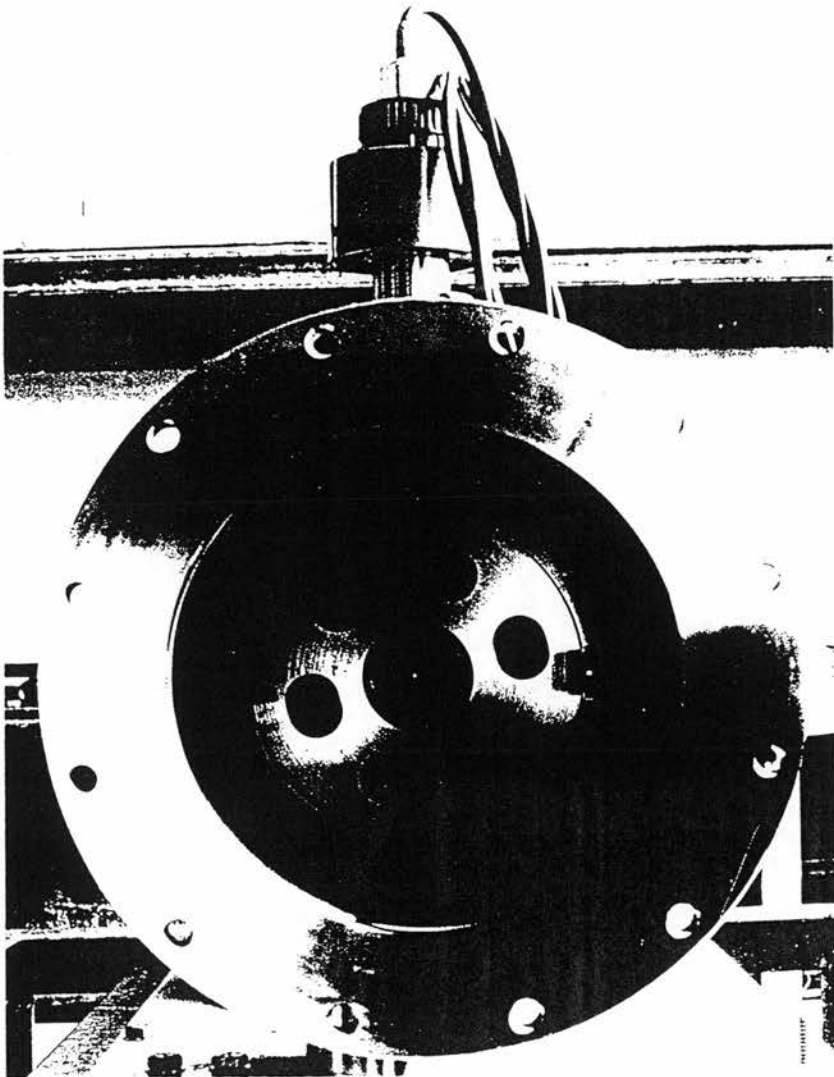
2) THE QUADRUPOLES ENCLOSED WITHIN AN INTERNAL CASING - THE WIRES ARE SEEN EXITING FROM THE CENTRAL CORE AT THE END OF THE FIFTH QUADRUPOLE. THE MULTIPLIER IS SITUATED IN THE LAST DIVISION OF THE INTERNAL CASING.



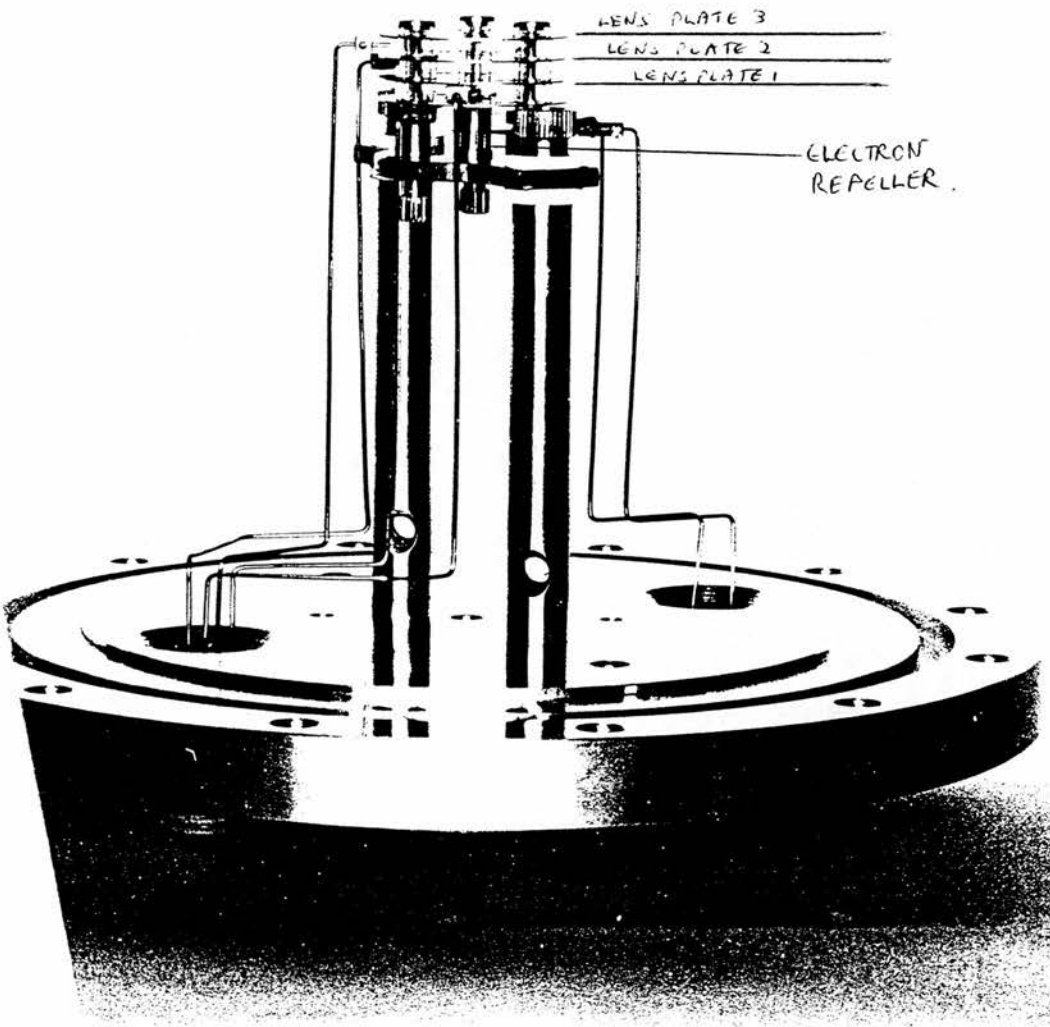
3) THE DETECTOR END OF THE QUADRUPOLES - SHOWING THE EASE WITH WHICH THE WHOLE SYSTEM COULD BE REMOVED FROM THE EXTERNAL CASING.



- 4) LOOKING UP THE CASING FROM THE DETECTOR END - NOTE :-
- a) THE DOT OF LIGHT IN THE CENTRE. THIS IS LIGHT SHINING THROUGH THE PRIMARY GAS INLET AT THE FAR END OF THE CASING.
 - b) THE METAL PLATE THAT ACTED AS ONE OF THE SUPPORTS FOR THE INTERNAL CASING AND AS A PARTIAL PHYSICAL BARRIER TO THE MOVEMENT OF GASES BETWEEN PARTS OF THE CASING. THESE HAVE BEEN REMOVED.
 - c) THE PROXIMITY OF THE MAGNET OF THE PENNING HEAD WHICH IS AT MOST 25cm ABOVE THE QUADRUPOLE RODS. THESE HAVE BEEN REMOVED TO 65cm ABOVE THE RODS.



5) THE IONISATION CHAMBER AND FOCUSING PLATES. THE FILAMENT AND CAGE ARE ENCLOSED WITHIN THE ELECTRON REPELLER.



APPENDIX BINDEX OF TABLES, FIGURES, GRAPHS AND DIAGRAMS

PAGE

- 15 Figure 1 Tandem Mass Spectrometer
- 30 Fig. 1.1 Interior of the Triple Quadrupole Mass Spectrometer.
- 32 Fig. 1.2 Exterior of the Triple Quadrupole Mass Spectrometer.
- 33 Fig. 1.3.1 Spectrum of methane.
Fig. 1.3.2 Spectrum of selected ion.
- 34 Fig. 1.3.3 Spectrum of ions from a reaction.
Fig. 1.3.4 Reaction Scheme.
- 38 Fig. 1.3.5 Graph of % of ions.
Fig. 1.3.6 Schematic Graph of ions against pressure.
- 41 Fig. 1.4 Nomenclature for quinquadrupole mass spectrometer ions and gases.
- 42 Fig. 1.5 Quinquadrupole Mass Spectrometer.
- 46 Fig. 2.1 Ions from n-hexadecane
- 53 Fig. 2.2 CH_5^+ orbitals
Fig. 2.3 Representation of CH_5^+ .
- 54 Table 2.1 Energies of CH_5^+ of various symmetries.
- 56 Fig. 2.4 Isomerisation butane.
- 58 Table 2.2 Self-protonation reactions
- 59 Table 2.3 Ratio of products
- 63 Table 2.4 Ratio of C_2D_5^+ and $\text{C}_2\text{D}_4\text{H}^+$ ions.

- 101 Graph 2.1 $\text{CH}_5^+ : ^{13}\text{CH}_4^+$ ratio
- 113 Table 2.5 $\text{CH}_3^+:\text{CH}_5^+$ Previous and present results
- 118 Fig. 2.5 C-H protonation and cleavage.
- 118 Fig. 2.6 C-C protonation and cleavage.
- 119 Fig. 2.7 Energy diagram for C_2H_7^+ and fragments.
- 128 Table 2.6 Fragments from $[\text{C}_4\text{H}_{11}^+]$
- 130 Scheme 2.1 Routes to ions from C_4H_9^+
- 131 Scheme 2.2 Routes to ions from $\text{C}_4\text{H}_{11}^+$
- 136 Table 2.7 CH_2N^+ into n-pentane
- 136 Table 2.8 CH_2N^+ into iso-pentane.
- 139 Fig. 2.8 Rearrangements of $[\text{C}_5\text{H}_{13}^+]$ ions.
- 140 Scheme 2.3 Routes to ions from $\text{C}_5\text{H}_{13}^+$.
- 147 Fig. 3.1 Channel structure of ZSM-5.
- 147 Tables 3.1, 3.2, 3.3 Product distribution from methanol conversion over ZSM-5, ZSM-11 and ZSM-4.
- 148 Table 3.4 Octane number of commercial and synthetic gasoline.
- 150 Fig. 3.2.1 Dimethyl ether production over Al_2O_3 .
- 151 Table 3.5 Product distribution from thermal analysis of aluminium alkoxides.
- 157 Fig. 3.2.2 Methyl oxonium ion
- 157 Fig. 3.2.3 Structures of solvated protons.
- 180 Graph 3.1 Amount of CHO^+ produced from $\text{CH}_2\text{OH}^+ + \text{N}_2$
- 189 Table 3.6 Isotope correction of the peak of mass 33.
- 199 Fig. 3.3 Potential energy diagram for the interconversion of $\text{C}_2\text{H}_5\text{O}^+$ ions.
- 202 Fig. 3.4 van den Berg's mechanism.
- 202 Fig. 3.5 Formation of oxonium ylid.

- 203 Fig. 3.6 Formation of methyl ethylether.
- 221 Fig. 4.1 Mechanism for the formation of ethene from dimethyl halonium ions via methylhalonium methylene.
- 225 Table 4.1 Yield of hydrocarbon products from the reaction of methanol and chloromethane over ZSM-5.
- 277 Fig. 4.2 Mechanisms for the formation of dimethyl fluoronium ions.
- 290 Diagram 4.1 The reaction pathways for the gaseous reactions of ions with methanol.
- 291 Diagram 4.2 The reaction pathways for the gaseous reactions of ions with halogenomethane.
- 298 Photographs 5.1, 5.2 and 5.3 ZSM-5 crystals magnified by 200 and 320 times.
- 300 Diagram 5.1 Fixed-bed experimental rig.
- 305 Table 5.1 Analysis of ZSM-5.
- 306 Table 5.2 Coke analysis.
- 307 Diagram 5.2 Quartz reactor tube.
- 312 Fig. 5.5 G.C. Trace.
- 313 Fig. 5.3 and 5.4 X-ray Diffraction.
- 314 Table 5.3 Selectivity for chloromethane reaction.
- 315 Table 5.4 Selectivity for bromomethane reaction.
- 316 Table 5.5 Conversion against temperature.
- 319 Graphs 5.1 and 5.2 Selectivity against temperature for chloromethane and bromomethane.
- 323 Table 5.6 Reaction of iodomethane over ZSM-5.
- 324 Fig. 5.6 Radical mechanism for production of methane.
- 343 Fig. 6.1 The quinquapole mass spectrometer

- 344 Fig. 6.2.1 and 6.2.2 Ion source configuration.
- 345 Table 6.1 Signal strength for ion energies.
- 346 Table 6.2 Signal size against electron energy.
- 348 Table 6.3 Focus voltage against setting.
- 351 Fig. 6.3 Aperture of four rods.
- 353 Fig. 6.4 Pole bias
- 355 Fig. 6.5 Multiplier.
- 355 Table 6.4 Noise to signal ratio.
- 357 Table 6.5 Peak height against emission.
- 358 Graphs 6.2, 6.3 and 6.4 Peak height against
emission.
- 359 Table 6.6 and 6.7 Peak height against emission.
- 361 Graph 6.5 Stability/resolution diagram.
- 362 Graph 6.6 Stability/resolution diagram.
- 364 Diagram 6.4 Resolution of peaks at different M
values.
- 365 Table 6.8 $\frac{1}{2}$ D.C. against m/e for resolution control
- 366 Graph 6.8 $\frac{1}{2}$ D.C. against m/e for resolution control
- 367 Table 6.9 $\frac{1}{2}$ D.C. against m/e for M = 1 and M = 10
- 368 Graph 6.9 $\frac{1}{2}$ D.C. against m/e for M = 1 and M = 10
- 370 Table 6.10 Electron impact spectrum of propane
from the quinquapole mass spectrometer.
- 371 Graphs 6.10, 6.11 and 6.12 Stability/Resolution
diagrams.
- 373 Table 6.11 $\frac{1}{2}$ D.C. against m/e for minimum and
maximum values of resolution control.
- 374 Graph 6.11 $\frac{1}{2}$ D.C. against m/e for minimum and
maximum values of resolution control.
- 380 Fig. 6.6 Background spectrum.

- 385 Table 6.12 Signal strength for various positions
of magnet round the casing.
- 387 Table 6.13 Signal strength for distance of magnet
from casing.
- 388 Graph 6.14 Peak height $D_{\infty} - D_m$ for distance of
magnet away from casing.
- 396 Table 6.14.1 Relative peak heights for charge
exchange $Ne^+ + N_2$.
- 397 Table 6.14.2 Relative peak heights for charge
exchange $N_2^+ + N_2O$.
- 406 Photograph 6.1 The quadrupoles.
- 407 Photograph 6.2 The quadrupoles enclosed within the
internal casing.
- 408 Photograph 6.3 The detector end of the quadrupoles
being removed.
- 409 Photograph 6.4 The interior of the external
casing.
- 410 Photograph 6.5 The ionisation chamber.

REFERENCES

1. B.P. Statistical Review Of World Energy, The British Petroleum Company P.L.C., (1987).
2. C.D. Chang and J.N. Miale, U.S. Patent, 4,605,803, (1986).
3. R.D. Kirkpatrick, *Chemical Engineering in Australia, ChE9*, 17, (1984).
4. C.D. Chang and A.J. Silvestri, *CHEMTECH*, 624, (1987).
5. G.J. Hutchings, *Chem. Brit.*, 23, 762, (1987).
6. as for reference 4, page 631.
7. C.D.Chang, *Hydrocarbons form Methanol*, M. Dekker, New York, 1983.
8. W. Keim, 3, *Industrial Chemicals via C₁ Processes*, American Chemical Society, New York, 1986.
9. A. Kiennemann, J.P. Hindermann, R. Breault and H. Idriss, 237, *Industrial Chemicals via C₁ Processes*, American Chemical Society, New York, 1986.
10. I. Howe, D.H. Williams and R.C. Bowen, *Mass Spectrometry - Principles and Applications*, McGraw-Hill, London, 1981.
11. M.M. Mann, A. Hustralid and J.T. Tate, *Phys. Rev.*, 58, 340, (1940).
12. F.H. Field and M.S.B. Munson, *J. Am. Chem. Soc.*, 87, 3289 and 3294, (1965).
13. J.L. Franklin, F.H. Field and F.W. Lampe, 308, *Advances In Mass Spectrometry*, Pergamon Press, London, 1959.

14. D. Price, *Chem. Brit.*, 4, 255, (1968).
15. as for reference 10, page 16.
16. M.E. Rose and R.A.W. Johnstone, *Mass Spectrometry for Chemists and Biochemists*, Cambridge University Press, Cambridge, 1982.
17. C.W. Hand and H. von Weyssenhoff, *Can. J. Chem.*, 42, 2385, (1964).
18. C.W. Hand and H. von Weyssenhoff, *Can. J. Chem.*, 42, 195, (1964).
19. S. Tsuchiya, F. Ishihara and T. Hikita, *Recent Developments in Mass Spectrometry*, Proceedings of the International Conference of Mass Spectroscopy, Kyoto, p. 1048, University Park Press, London, 1970.
20. G.C. Goode, R.M. O'Malley, A.J. Ferrer-Correia and K.R. Jennings, *Chem. Brit.*, 7, 12, (1971).
21. M.T. Bowers, D.D. Elleman and J.L. Beauchamp, *J. Phys. Chem.*, 72, 3599, (1968).
22. J.L. Beauchamp, L.R. Anders and J.D. Baldeschwieler, *J. Am. Chem. Soc.*, 89, 4569, (1967).
23. J.I. Brauman and L.K. Blair, *J. Am. Chem. Soc.*, 92, 5986, (1970).
24. F.P. Abramson and J.H. Futrell, *J. Phys. Chem.*, 72, 1994, (1968).
25. M.F. Jarrold, L.M. Bass, P.R. Kemper, P.A.M. van Koppem and M.T. Bowers, *J. Chem. Phys.*, 78, 3756, (1983).

26. D.D. Fetterolf, R.A. Yost and J.R. Eyler, *Org. Mass Spectrom.*, 19, 104, (1984).
27. T.P.J. Izod and J.M. Tedder, *Proc. R. Soc. Lond. A.*, 337, 333, (1974)
28. T.P.J. Izod and J.M. Tedder, *Int. J. Mass Spectrom. Ion Phys.*, 22, 85, (1976).
29. J.M. Tedder and P.H. Vidaud, *Chem. Phys. Lett.*, 64, 81, (1979).
30. J. Jalonen, J.M. Tedder and P.H. Vidaud, *J.C.S. Faraday I*, 75, 2040, (1979).
31. J.M. Tedder and P.H. Vidaud, *J.C.S. Faraday II*, 75, 1648, (1979).
32. J.M. Tedder and P.H. Vidaud, *J. Phys. D: Appl. Phys.*, 13, 1949, (1980).
33. J. Jalonen, J.M. Tedder and P.H. Vidaud, *J.C.S. Faraday II*, 76, 1450, (1980).
34. J.M. Tedder and P.H. Vidaud, *Chem. Phys. Lett.*, 76, 380, (1980).
35. J.M. Tedder and P.H. Vidaud, *J.C.S. Faraday II*, 76, 1516, (1980).
36. W. Paul and H. Steinwedel, *Z. Naturforsch*, 8a, 448, (1953).
37. W. Paul and M. Raether, *Z. Physik*, 140, 262, (1955).
38. G. Lawson and J.F.J. Todd, *Chem. Brit.*, 8, 373, (1972).
39. T. Kondo, S. Taya and I. Omura, *Recent Developments in Mass Spectrometry*, Proceedings of the

- International Conference of Mass Spectroscopy,
Kyoto, p. 269, University Park Press, London, 1970.
40. K. Maeda, M. Sakimura and A. Fukuda, *Recent Developments in Mass Spectrometry*, Proceedings of the International Conference of Mass Spectroscopy, Kyoto, p. 273, University Park Press, London, 1970.
41. K. Maeda, M. Sakimura and A. Fukuda, *Recent Developments in Mass Spectrometry*, Proceedings of the International Conference of Mass Spectroscopy, Kyoto, p. 277, University Park Press, London, 1970.
42. as for reference 16, page 33.
43. D.H. Smith, J.R. Walton, H.S. McKown, R.L. Walker, J.A. Carter, *Anal. Chim. Acta*, **142**, 355, (1982).
44. Promotional Booklet, V.G. Instruments plc., West Sussex, 1987.
45. C.J. Risicato, Report, 1984, *Gov. Rep. Announce. Index (U.S.)*, **85**, 184, (1985). (Chem. Abs. 102, 176130f)
46. J.D. Morrison, K. Stanney and J.M. Tedder, *J.C.S. Perkin II*, 838, (1981).
47. J.D. Morrison, K. Stanney and J.M. Tedder, *J.C.S. Perkin II*, 967, (1981).
48. J.H. Batey and J.M. Tedder, *J.C.S. Perkin II*, 1263, (1983).
49. A.L. Mitchell and J.M. Tedder, *J.C.S. Perkin II*, 667, (1984).
50. A.L. Mitchell, J.K. Conner, K. Stanney and J.M. Tedder, *Chem. Comm.*, 1529, (1984).

51. A.L. Mitchell and J.M. Tedder, *J.C.S. Perkin II*, 1197, (1986).
52. J.N. Robinson and J.M. Tedder, *Org. Mass Spectrom.* 22, 154, (1987).
53. A.L. Mitchell, J.M. Tedder and G.S. Walker, "Some Chemistry of Radical Ions." Proceedings of NATO Workshop, "Substituent Effects in Radical Chemistry", Louvain-la-Neuve, 23p, (1986).
54. P.H. Dawson, J.B. French, J.A. Buckley, D.J. Douglas and D. Simmons, *Org. Mass Spectrom.*, 17, 205, (1982).
55. P.H. Dawson, J.B. French, J.A. Buckley, D.J. Douglas and D. Simmons, *Org. Mass Spectrom.*, 17, 212, (1982).
56. G.G. Dolnikowski, M.J. Kristo, C.G. Enke and J.T. Watson, *Int. J. Mass Spectrom. Ion Processes*, 82, 1, (1988).
57. S.A. McLuckey, L. Sallans, R.B. Cody, R.C. Burnier, S. Verma, B.S. Freise and R.G. Cooks, *Int. J. Mass Spectrom. Ion Phys.*, 44, 215, (1982).
58. F.N. Preuninger and J.F. Farrer, *J. Chem. Phys.*, 77, 263, (1982).
59. W.R. Gentry, Chapter 15, *Gas Phase Ion Chemistry*, Vol.2, Academic Press, New York, 1979.
60. R.C. Dunbar, *Ion Photodissociation*, Chapter 14, *Gas Phase Ion Chemistry*, Vol.2, Academic Press, New York, 1979.
61. S.A. McLuckey, G.L. Glish and R.G. Cooks, *Int. J. Mass Spectrom. and Ion Phys.*, 39, 219, (1981).

62. F. Cacace, *Acc. Chem. Res.*, 21, 215, (1988).
63. U. von Zahn, *Rev. scient. Instrum.*, 43, 1, (1963).
64. K. Birkinshaw, D.M. Hirst and M.F. Jarrold, *J. Phys. E*, 11, 1037, (1978).
65. I.W. Griffiths, E.S. Mukhtar, F.M. Harris and J.H. Beynon, *Int. J. Mass Spectrom. Ion Phys.*, 43, 283, (1982).
66. B.E. Evans and R.W. Supple, *J. Vac. Sci. Technol.*, 8, 270, (1971).
67. P.H. Dawson and J.E. Fulford, *Int. J. Mass Spectrom. Ion Phys.*, 42, 195, (1982).
68. A.L. Burlingame, D.Malby, D.H. Russell and P.T. Holland, *Anal. Chem.*, 50, 294 R-342 R, (1988).
69. J.F.J. Todd, *Dyn. Mass Spectrom.*, 6,3,(1981)
70. I. Howe, *Mass Spectrom.*, 7, 119, (1984).
71. N.I. Sax, *Dangerous Properties of Industrial Materials*, Van Nostrand Reinhold Company, New York, 1979.
72. W.F. Edgell and L. Parts, *J. Am. Chem. Soc.*, 77, 4899, (1955).
73. D. Bethell and V. Gold, *Carbonium Ions An Introduction*, Academic Press, London, 1964.
74. M.S.B. Munson and F.H. Field, *American Petroleum Institute Proc., Division of Refining*, 46, 151, (1966).
75. A. Corma and B.W. Wojciechowski, *Catal. Rev. Sci. Eng.*, 27, 29, (1985).
76. S.E. Tung and E. McIninch, *J.Catal.*, 10, 166, (1968).

77. H. Hattori, O. Takahashi, M. Takagi and K. Tanabe, *J. Catal.*, *68*, 132, (1981).
78. O. Takahashi and H. Hattori, *J. Catal.*, *68*, 144, (1981).
79. M.L. Poutsma, in *Zeolite Chemistry and Catalysis* (J. A. Rabo, ed.), ACS Monogr, *171*, 437, (1976)
80. W.F. Pansing, *J. Phys. Chem.*, *69*, 392, (1965).
81. G.A. Olah and D.J. Donovan, *J. Am. Chem. Soc.*, *99*, 5026, (1977).
82. G.A. Olah, G.K. Surya Prakash, R.E. Williams, L.D. Field and K. Wade, p.151, *Hypercarbon Chemistry*, Wiley Interscience, New York, 1987.
83. A.F. Bickel, C.J. Gaasbeek, H. Hogeveen, J.M. Oelderick and J.C. Plattew, *Chem. Commun.*, 634, (1967).
84. H. Hogeveen and A.F. Bickel, *Chem. Commun.*, 635, (1967).
85. K. Raghavachari, R.A. Whiteside, J.A. Pople and P.R. Schleyer, *J. Am. Chem. Soc.*, *103*, 5649, (1981).
86. G.A. Olah, G. Klopman and R.H. Schlosberg, *J. Am. Chem Soc.*, *91*, 3261, (1969).
87. A. Gamba, G. Morosi and M. Simonetta, *Chem. Phys. Lett.*, *3*, 20, (1969).
88. G.A. Olah, R.H. Schlosberg, *J. Am. Chem. Soc.*, *90*, 2726, (1968).
89. G.A. Olah, G. Klopman and R.H. Schlosberg, *J. Am. Chem Soc.*, *91*, 2929, (1969).

90. G.A. Olah, G. Klopman and R.H. Schlosberg, *Ibid.*, 89, 3576, (1967).
91. G.A. Olah, G. Klopman and R.H. Schlosberg, *Ibid.*, 89, 3591, (1967).
92. K. Raghavachari, R.A. Whiteside, J.A. Pople and P.R. Schleyer, *J. Am. Chem. Soc.*, 104, 3258, (1981).
93. as for reference 82, page 4.
94. as for reference 82, page 224.
95. F.P. Abramson and J.H. Futrell, *J. Chem. Phys.*, 45, 1925, (1966).
96. F.P. Abramson and J.H. Futrell, *J. Chem. Phys.*, 46, 3264, (1967).
97. A.G. Harrison, *Chemical Ionisation Mass Spectrometry*, CRC Press, Florida, 1985.
98. A. J. Illies, M. F. Jarrold and M. T. Bowers, *J. Am. Chem. Soc.*, 105, 2562, (1983).
99. J. Berkowitz, *J. Chem. Phys.*, 69, 3044, (1978).
100. M.P. Gardner and C. Vinckier, *Int. J. Mass Spectrom. Ion Process.*, 63, 187, (1985).
101. J.H. Futrell, F.P. Abramson, A.K. Bhattacharya and T.O. Tiernan, *J. Chem. Phys.*, 52, 3655, (1970).
102. R.D. Smith and J.H. Futrell, *Int. J. Mass Spectrom. Ion Phys.*, 20, 347, (1976).
103. P. Kebarle and K. Hiraoka, *J. Am. Chem. Soc.*, 98, 6119, (1976).
104. P. Kebarle and K. Hiraoka, *ibid.*, 97, 4179, (1975).

105. D. Stahl, F. Marquin, T. Gümman, H. Schwarz, P. Carrupt and P. Vogel, *J. Am. Chem. Soc.*, *107*, 5049, (1985).
106. R. Houriet, G. Parisod and T. Gümman, *J. Am. Chem. Soc.*, *99*, 3599, (1977).
107. as for 82, page
108. D. Smith, N.G. Adams and E. Alge, *J. Chem Phys.*, *77*, 1261, (1982).
109. P. Kebarle and K. Hiraoka, *Can. J. Chem.*, *53*, 970, (1975).
110. as for reference 103, page 6124.
111. A.L. Mitchell, *Ph.D. Thesis*, University of St. Andrews. (1988)
112. J.K. Kim, V.G. Anicich and W.T. Huntress, Jr., *J. Phys. Chem.*, *81*, 1798, (1977).
113. R.D. Bowen and D.B. Williams, *J.C.S. Perkin II*, 1479, (1976).
114. I. Howe, D.B. Williams and R.D. Bowen, *Mass Spectrometry - Principles and Applications*, McGraw-Hill, London, 1981, p.90.
115. B.J. Stapleton, R.D. Bowen and D.H. Williams, *Tetrahedron*, *34*, 259, (1978).
116. R.N. Abernathy and F.W. Lampe, *J. Am. Chem. Soc.*, *103*, 2573, (1981).
117. R.D. Bowen and D.H. Williams, *J.C.S. Perkin II*, 1479, (1976).
118. J.H. Beynon, *Mass Spectrometry and its Application to Organic Chemistry*, 326, Elsevier Pub. Comp., London, 1960.

119. J.A. Lebel and W.H. Greene, *Am. Chem. J.*, *2*, 20, (1880).
120. H. Adkins and P.D. Perkins, *J. Phys. Chem.*, *32*, 221, (1928).
121. A.B. Schwartz and J. Ciric, *Adv. Catal.*, *18*, 259, (1968).
122. B.N. Dolgov, *Die Katalyse in der Organischen Chemie*, DVW, Berlin, 1963, p.439 as reported in reference 7.
123. E.G. Derouane, *NATO ASI Ser., Ser. E*, *80*, 515, (1984).
124. G.J. Hutchings, *Chem. Brit.*, *23*, 766, (1987).
125. C.D. Chang, *Mechanism of Hydrocarbon Formation from Methanol, in Methane Conversion*, Elsevier Science Publishers, Amsterdam, 1988.
126. T.R. Forester and R.F. Howe, *J. Am. Chem. Soc.*, *109*, 5076, (1987).
127. J.M. Parera and N.S. Figoli, *J. Catal.*, *14*, 303, (1969).
128. E. I. Heiba and P. S. Landis, *J. Catal.*, *3*, 471, (1964).
129. as for reference 7, page 51.
130. H. Pines and C.N. Pillai, *J. Am. Chem. Soc.*, *82*, 2401, (1960).
131. P.B. Venuto and P.S.L. Landis, *J. Catal.*, *18*, 259, (1968).
132. C.D. Chang and A.J. Silvestri, *J. Catal.*, *47*, 249, (1977).

133. T. Kotanigawa, K. Shimokawa and T. Yoshida, *J. Chem. Soc., Chem. Commun.*, 1185, (1982).
134. S. Kolboe, *On the Mechanism of Hydrocarbon Formation from Methanol over Protonated Zeolites, in Methane Conversion*, Elsevier Science Publishers, Amsterdam, 1988.
135. S. Kolboe, *Acta Chem. Scand. A*, 42, 185, (1988).
136. S. Kolboe, *ibid*, 40, 711, (1986).
137. G.A. Olah, *Acc. Chem. Res.*, 20, 422, (1987).
138. T.R. Forester and R.F. Howe, *J. Am. Chem. Soc.*, 109, 5076, (1987)
139. W. Zatorski and S. Krzyzanowski, *Acta Phys. Chem*, 29, 347, (1978).
140. J.K.A. Clarke, R. Darcy, B.F. Hegarty, E. O'Donoghue, V. Amir-Ebrahimi and J.J. Rooney, *J. Chem. Soc., Chem. Commun.*, 425, (1986).
141. R. Hunter, G.J. Hutchings and W. Pickl, *J. Chem. Soc., Chem. Commun.*, 1369, (1987).
142. J.P. van den Berg, J.P. Wolthuizen and J.H.C. van Hooff, *Proc. 5th Int. Conf. on Zeolites*, L. V. Rees (Ed.), Heyden, London, 1980, p.649.
143. G. Perot, F. Cormerais and M. Guisnet, *J. Chem. Research (S)*, 58, (1982).
144. G.A. Olah, H. Doggweiler and J.D. Felberg, *J. Org. Chem.*, 49, 2112, (1984).
145. Y. Ono and T. Mori, *J. Chem. Soc., Faraday Trans. I*, 77, 2209, (1979).
146. P. Rimmelin, H. Taghavi and J. Sommer, *J. Chem. Soc., Chem. Commun.*, 1210, (1984).

147. R. Hunter and G.J. Hutchings, *J. Chem. Soc. Chem. Commun.*, 886, (1985).
148. R. Hunter and G.J. Hutchings, *J. Chem. Soc. Chem. Commun.*, 1643, (1985).
149. as for reference p.142.
150. M.S.B. Munson and F.H. Field, *J. Am. Chem. Soc.*, 83, 1523, (1961).
151. M.S.B. Munson and F.H. Field, *J. Am. Chem. Soc.*, 87, 3289, (1965).
152. Henis, J.M.S., *J. Am. Chem. Soc.*, 90, 844, (1968).
153. R.D. Smith and J.H. Futrell, *Chem. Phys. Lett.*, 41, 64, (1976).
154. P. Kebarle, S.K. Searles, A. Zolla, J. Scarborough and M. Arshadi, *J. Am. Chem. Soc.*, 89, 6393, (1967).
155. E.P. Grimsrud and P. Kebarle, *J. Am. Chem. Soc.*, 95, 7939, (1973).
156. R. Yamdagni and P. Kebarle, *J. Am. Chem. Soc.*, 98, 1320, (1976).
157. Y.K. Lau, P.P.S. Saluja and P. Kebarle, *J. Am. Chem. Soc.*, 102, 7429, (1980).
158. R.B. Sharma, A.T. Blades and P. Kebarle, *J. Am. Chem. Soc.*, 106, 510, (1984).
159. R.B. Sharma and P. Kebarle, *J. Am. Chem. Soc.*, 106, 3913, (1984).
160. K.R. Jennings, p. 141, *Chemical Ionisation Mass Spectrometry, Gas Phase Ion Chemistry, Vol. 2*, Academic Press, New York, (1979).

161. C.D.Chang, *Hydrocarbons form Methanol*, M. Dekker, New York, 1983, p.59.
162. J.L. Beauchamp and R.C. Dunbar, *J. Am. Chem. Soc.*, *92*, 1477, (1970).
163. A.S. Blair and A.G. Harrison, *Can. J. Chem.*, *51*, 703, (1973).
164. B. Van de Graaf, P.P. Dymerski and F.W. McLafferty, *J. Chem. Soc., Chem. Commun.*, 978, (1974).
165. K. Levsen, *Fundamental Aspects of Organic Mass Spectrometry*, Vol.4, Verlag Chemie, Weinheim, 1978, p.280.
166. D.H. Williams, *Acc. Chem. Res.*, *10*, 280, (1977).
167. M.T. Bowers and D.H. Williams, *J. Chem. Soc. Chem. Commun.*, i378, (1977).
168. M.T. Bowers and P.R. Kemper, *J. Am. Chem. Soc.*, *93*, 5352, (1971).
169. M.T. Bowers, D.H. Williams and *. *. Hvistendahl, *J. Am. Chem. Soc.*, *99*, 7509, (1977).
170. F.W. McLafferty, *Anal. Chem.*, *34*, 2, (1962).
171. F.W. McLafferty, *Anal. Chem.*, *34*, 16, (1962).
172. G.A. Olah, Y. Yamada and R.J. Spear, *J. Am. Chem. Soc.*, *97*, 680, (1975).
173. G.A. Olah and J.J. Svoboda, *Synthesis*, 203, (1973)
174. G.A. Olah and J.M. Bollinger, *J. Am. Chem. Soc.*, *89*, 4744, (1967).
175. G.A. Olah, and J.M. Bollinger, *J. Am. Chem. Soc.*, *90*, 947, (1968).
176. G.A. Olah and J.M. Bollinger and J. Brinich, *J. Am. Chem. Soc.*, *90*, 2587, (1968).

177. G.A. Olah and P.E. Peterson, *J. Am. Chem. Soc.*, *90*, 4675, (1968).
178. G.A. Olah, and J.M. Bollinger and J. Brinich, *J. Am. Chem. Soc.*, *90*, 6988, (1968).
179. G.A. Olah, J.R. DeMember and R.H. Schlosberg, *J. Am. Chem. Soc.*, *91*, 2112, (1968).
180. G.A. Olah and J.R. DeMember, *J. Am. Chem. Soc.*, *91*, 2114, (1969).
181. G.A. Olah, H. Doggweiler and J.D. Felberg, *J. Am. Chem. Soc.*, 4975, (1985).
182. N.A. McAskill, *Aust. J. Chem.*, *22*, 2267, (1969).
183. N.A. McAskill, *Aust. J. Chem.*, *22*, 2275, (1969).
184. N.A. McAskill, *Aust. J. Chem.*, *23*, 893, (1970).
185. N.A. McAskill, *Aust. J. Chem.*, *23*, 2301, (1970).
186. D.K. Sen Sharma and P. Kebarle, *J. Am. Chem. Soc.*, *100*, 5826, (1978).
187. D.K. Sen Sharma and P. Kebarle, *J. Am. Chem. Soc.*, *104*, 19, (1982).
188. K. Hiraoka and P. Kebarle, *Can. J. Chem.*, *58*, 2262, (1980).
189. G. Caldwell, T.F. Magnera and P. Kebarle, *J. Am. Chem. Soc.*, *106*, 959, (1984).
190. T.B. McMahon and P. Kebarle, *Can. J. Chem.*, *63*, 3160, (1985).
191. R.B. Sharma, D.K. Sen Sharma, K. Hiraoka and P. Kebarle, *J. Am. Chem. Soc.*, *107*, 3755, (1985).
192. D.K. Sen Sharma, S. Meza de Højer and P. Kebarle, *J. Am. Chem. Soc.*, *107*, 3757, (1985).

193. C. Jortay, R. Flammang and A. Maquestiau, *Bull. Soc. Chim. Belg.*, 94, 727, (1985) - (Chem. Abs. 105:152217a).
194. T.B. McMahon and P. Kebarle, *J. Am. Chem. Soc.*, 108, 6502, (1986).
195. V.N. Romannikov and K.G. Ione, *Kinet. Kataliz.*, 25, 75, (1984).
196. G.J. Hutchings, M.V. Hall and R. Hunter, *J. Catal.*, 101, 224, (1986).
197. *Developments in Zeolite Catalysis*, Catalytica Associates, 1987, p.135.
198. C.E. Taylor, R.P. Noceti and R.P. Schehl, *Methane Conversion*, Elsevier Press, Amsterdam, 1988, p.483.
199. J. Klaus-Joachim, S. Halvorsen and E.B. Ofstad, *Methane Conversion*, Elsevier Press, Amsterdam, 1988, p.491.
200. W.E. Garwood, *Conversion of C₂-C₁₀ to Higher Olefins over Synthetic Zeolite ZSM-5*, in *Intrazeolite Chemistry*, p383, A.C.S. Symposium Series 218, (1983).
201. C. D. Chang, W. H. Lang and R. L. Smith, *J. Catal.*, 56, 169, (1979).
202. *Developments in Zeolite Catalysis*, Catalytica, California, (1987).
203. E.G. Derouane, J.B. Nagy, P.Dejaifve, J.H.C. van Hooff, B. P. Spekman, J. C. Vedrine and C. Naccache, *J. Catal.*, 53, 40 (1978)
204. W.W. Kaeding and S.A. Butter, *J. Catal.*, 61, 155, (1980)

205. F.X. Cormerais, Y.S. Chen, M. Kern, N.S. Gnep, G. Perot, and M. Guisnet, *J. Chem. Research (S)*, 290, (1981)
206. W.O. Haag, R.M. Lago and P.G. Rodewald, *J. Molec. Catal.*, 17, 161, (1982)
207. P. Dejaifve, J.C. Vadrine, V. Bolis and E.G. Derouane, *J. Catal.*, 63, 331, (1980)
208. A.E. Holme, Ph.D. Thesis, "The Quadrupole Mass Spectrometer", University of Liverpool, 1972.
209. Private communications with G.G. Dolnikowski.
210. Private communications with J.D. Morrison.
211. V. G. Manual for Quadrupole Mass Spectrometer, p. 30, V.G. Instruments Ltd.
212. Eight Peak Index of Mass Spectra, *Mass Spectrometry Data Centre*, Reading, 1970.
212. V.I. Vedeneyev, L.V. Gurvich, V.N. Kondrat'yev, V.A. Medvedev and Ye.L. Frankevich, *Bond Energies Ionisation Potentials and Electron Affinities*, Edward Arnold Publishers, London, 1966.
213. S. Ceckiewicz, *J. Chem. Soc. Faraday Trans.*, 77, 269, 1981.
214. J. Graham, C.H. Rochester and R. Rudham, *J. Chem. Soc. Faraday Trans.*, 80, 2459, (1984).
215. *Developments in Zeolite Catalysis*, Catalytica, California, (1986). p. 91.
216. Nováková, reported in *Developments in Zeolite Catalysis*, Catalytica, California, (1986). p.138.